NASA CR-179587

Space Station WP-04 Power System Final Study Report DR-15

Volume 2 Study Results

G.J. Hallinan
Rockwell International
Rocketdyne Division

January 19, 1987

Prepared for
NATIONAL AERONAUTICS AND SPACE ADMINISTRATION
Lewis Research Center
Under Contract NAS3-24666

NASA CR-179587

Space Station WP-04 Power System Final Study Report DR-15

Volume 2 Study Results

G.J. Hallinan
Rockwell International
Rocketdyne Division

January 19, 1987

Prepared for
NATIONAL AERONAUTICS AND SPACE ADMINISTRATION
Lewis Research Center
Under Contract NAS3-24666

RI/RD86-306

SPACE STATION WP-04
POWER SYSTEM

CONTRACT NUMBER NAS 3-24666

FINAL STUDY REPORT
DR-15
VOLUME 2 OF 2-STUDY RESULTS

19 JANUARY 1987

Rocketdyne Division
6633 Canoga Avenue
Canoga Park, California 91304

PREPARED FOR:
NASA LEWIS RESEARCH CENTER

PREPARED BY:
SPACE STATION SYSTEM
ENGINEERING AND INTEGRATION

APPROVED BY:

G. J. HALLINAN
PROGRAM DIRECTOR

TYPE 2

FOREWORD

During the 21-month Phase B Space Station Electric Power System study contract, Rocketdyne submitted some 56 data requirement documents in addition to regular monthly status reports. This complete set of documentation comprises the Rocketdyne-generated knowledge base for the Electric Power System.

The intent of this final report is to summarize the major study activities and results, and to provide the reader with an overview of Rocketdyne's Phase B study contract. Although the final report contains a significant amount of data to support the study conclusions, it is suggested that the reader refer to the DR in which an analysis or study was initially reported, for complete details and documentation. A complete list and schedule of all contract data requirement submittals is provided in Section 1.0, Figure 1-2.

TABLE OF CONTENTS

TABLE OF CONTENTS

FIGURES

II A

TABLE OF CONTENTS

FIGURES

III A

FIGURES

FIGURES

FIGURES

TABLES

TABLES

TABLES

TABLES

TABLES

1.0 INTRODUCTION

This is Volume II: Study Results of the two volume Final Study Report For Contract Number NAS 3-24666, Definition and Preliminary Design of Electric Power System for the Space Station and platform (WP-04). Period of performance for the contract was from 19 April 1985 through 19 January 1987.

The contract was performed by Rocketdyne with contributions from the following team members:

- Ford - batteries and PV system
- Garrett - CBC receiver/power conversion unit
- General Dynamics - 20 kHz converters
- Harris - SD concentrator
- Sundstrand - ORC receiver/power conversion unit

In addition LTV Corporation provided thermal heat rejection designs and Lockheed provided PV array information.

The study reported upon herein reflects the program requirements for the Space Station and platform as they existed prior to the recommendations of the Critical Evaluation Task Force (CETF); i.e, 75 kw station with 25 kw PV and 50 kw SD. Per NASA-LeRC direction the post - CETF change to an 87.5 kw station with 37.5 kw PV was reflected in the final DR-09 cost submittal but was not incorporated into the Phase B Preliminary Design.

This volume summarizes the study results including backup information and supporting data. The volume follows the format and order of the contract SOW and includes sections covering systems analysis and trades (Section 2.0), preliminary design (Section 3.0), advanced development (Section 4.0), customer accommodations (Section 5.0), operations planning (Section 6.0), product assurance (Section 7.0), and design and development phase planning (Section 8.0).

V2-10/1

Volume I is an executive summary and contains a summary of activities and significant achievements of the study effort (Section 1.0), a summary of results (Section 2.0), a summary of trade studies (Section 3.0), and a summary of costing activities (Section 4.0).

1.1 STUDY ACTIVITIES

The activities associated with Rocketdyne's Phase B Study Contract were performed in accordance with the objectives outlined in the contract SOW. All technical and schedule milestones were met. Figure 1-1 is an overview of the complete Phase B program showing the period of performance for each activity and the dates of key milestones and DR submittals.

Following is a brief overview of Rocketdyne's Phase B study activities:

- System Engineering and Integration - defined and conducted all SE&I activities including analysis of missions, systems, and operations requirements; conceptual system design and analysis; design-to-cost activities; system analysis and trade studies; information system analysis; man-tended option studies; automation and robotics planning; and evolutionary growth studies.
- Preliminary Design Tasks - performed the preliminary design of the baselined hybrid electric power system (EPS) including analysis of interfaces; subsystem optimization; definition of test and verification requirements; and preparation of preliminary drawings, descriptions, data sheets, ICD's, and CEI specifications at the EPS assembly level.
- Advanced Development - identified technological issues and appropriate advanced development activities; prepared an advanced development plan (DR-05) for work to be performed under the scope of the Phase B contract; implemented the advanced development plan with the completion of activities applicable to the CBC and ORC solar dynamic heat receivers, the concentrator reflective surface, and concentrator deployment/latchup mechanism; performed and reported complementary IR&D activities related to the Phase B study effort.
- Customer Accommodations - identified customer accommodation features of the EPS and reported results in DR's as required.
- Operations Planning - performed operations studies for the EPS in the areas of pre-launch and post-landing operations, orbital operations, logistics and resupply, and on-orbit maintenance.

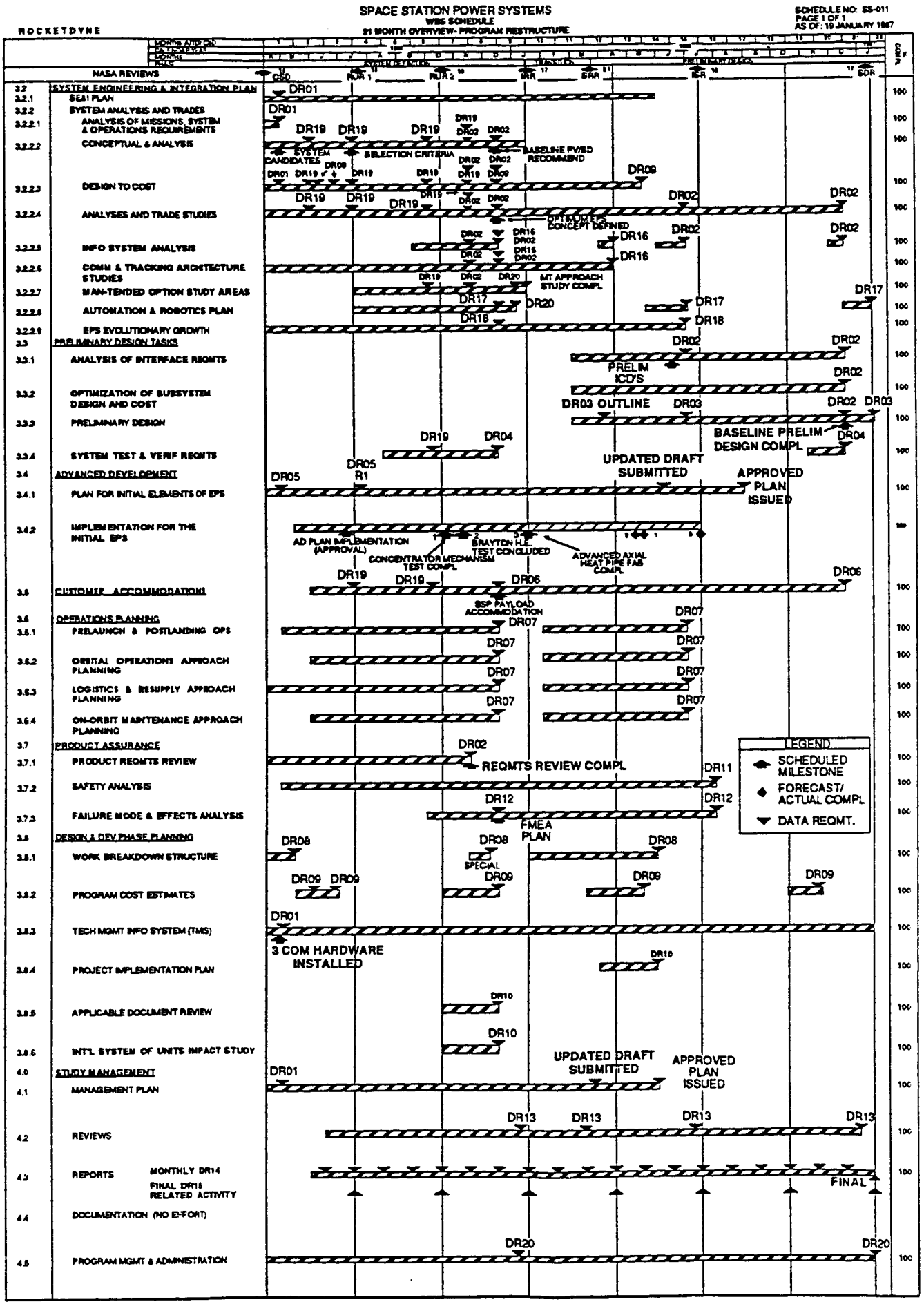

Figure 1-1 Program Overview

- o Product Assurance - performed product assurance evaluations for the EPS in the areas of safety, reliability, maintainability, and quality; prepared a preliminary safety analysis and preliminary failure mode and effects analysis for the EPS.

- o Design and Development Phase Planning - performed design and development phase planning including work breakdown structure, program cost estimates, project implementation plan (risk assessment), applicable document review, and international system of units (SI) impact study.

1.2 SIGNIFICANT ACHIEVEMENTS

Along with the successful completion of Rocketdyne's Phase B Study Contract and accomplishment of all contract objectives there were several significant achievements which merit special attention and are highlighted in the following paragraphs.

- o Conceptual Design and Reference Configuration Selection - The Phase B conceptual design effort was a major undertaking which included the definition of multiple station and platform electric power system concepts, the performance of numerous trade studies and analyses, and the incorporation of significant hardware test results. This effort led to the selection of the recommended hybrid configuration. This effort culminated in the recommendation of:

  - A hybrid station EPS with a savings of approximately $3 billion in life cycle cost compared to an all PV station,

  - Batteries for station energy storage with slightly lower costs than regenerative fuel cells and featuring commonality with the platform, and

  - Either ORC or CBC-based SD power, with a choice between these two technically feasible options being delayed while development activities continue.

- o Preliminary Design - A comprehensive preliminary design effort was completed for the baselined hybrid EPS. This effort was accomplished at the assembly level and included the preparation of preliminary drawings, descriptions, data sheets, ICDs, CEI specifications, and test and verification requirements.

- o Trade Studies - In order to provide backup data and support for the conceptual and preliminary design efforts, Rocketdyne identified and performed some 103 trade studies at the system and subsystem levels. These trade are summarized in Section 2.2 and divided into categories as follows:

System	24
PV Subsystem	17
SD Subsystem	45
PMAD Subsystem	17
Total	103

- Design to Cost - Rocketdyne's active design-to-cost effort during the Phase B Study Contract resulted in excellent consistency of WP-04 cost estimates during the EPS preliminary design. As shown below, the December 1985 cost estimate (beginning of preliminary design) and the November 1986 cost estimate (end of preliminary design), adjusted for program changes, agreed within $25 million (~2%).

		87 $ IN MILLIONS NO PRIME FEE
DEC 85 DR-09 HYBRID CONFIGURATION		1,115
37 1/2 kw PV, 37 1/2 kw SD 400 hz		
WITH PROGRAM CHANGES		
20 khz distribution vs 400 hz Power level increase (75 to 87 1/2 kw) FSE from "OR" to "C/D" FEL delay from 4-92 to 1-93	105	1,220
NOV 86 DR-09 ESTIMATE		1,195
37 1/2 kw PV, 50 kw SD 20 khz		
DIFFERENCE IN ESTIMATES		-25

- Data Requirement Submittals - During the Phase B Study Contract Rocketdyne maintained a perfect record of on-schedule data requirement submittals. In addition to monthly status reports (DR-14), a total of 55 DRs were submitted to NASA-LeRC, plus an unscheduled man-tended approach report. Figure 1-2 illustrates the Rocketdyne data requirement submittal schedule.

- Advanced Development - The following advanced development activities were performed by Rocketdyne team members during the Phase B Study Contract, leading to increased understanding and resolution of several SD technology issues. These activities were performed in accordance with our Advanced Development Plan (DR-05).

V2-10/4

ROCKETDYNE

DATA REQUIREMENT SUBMITTAL SCHEDULE

SCHEDULE NO: SS-019
AS OF: 19 JAN 1987

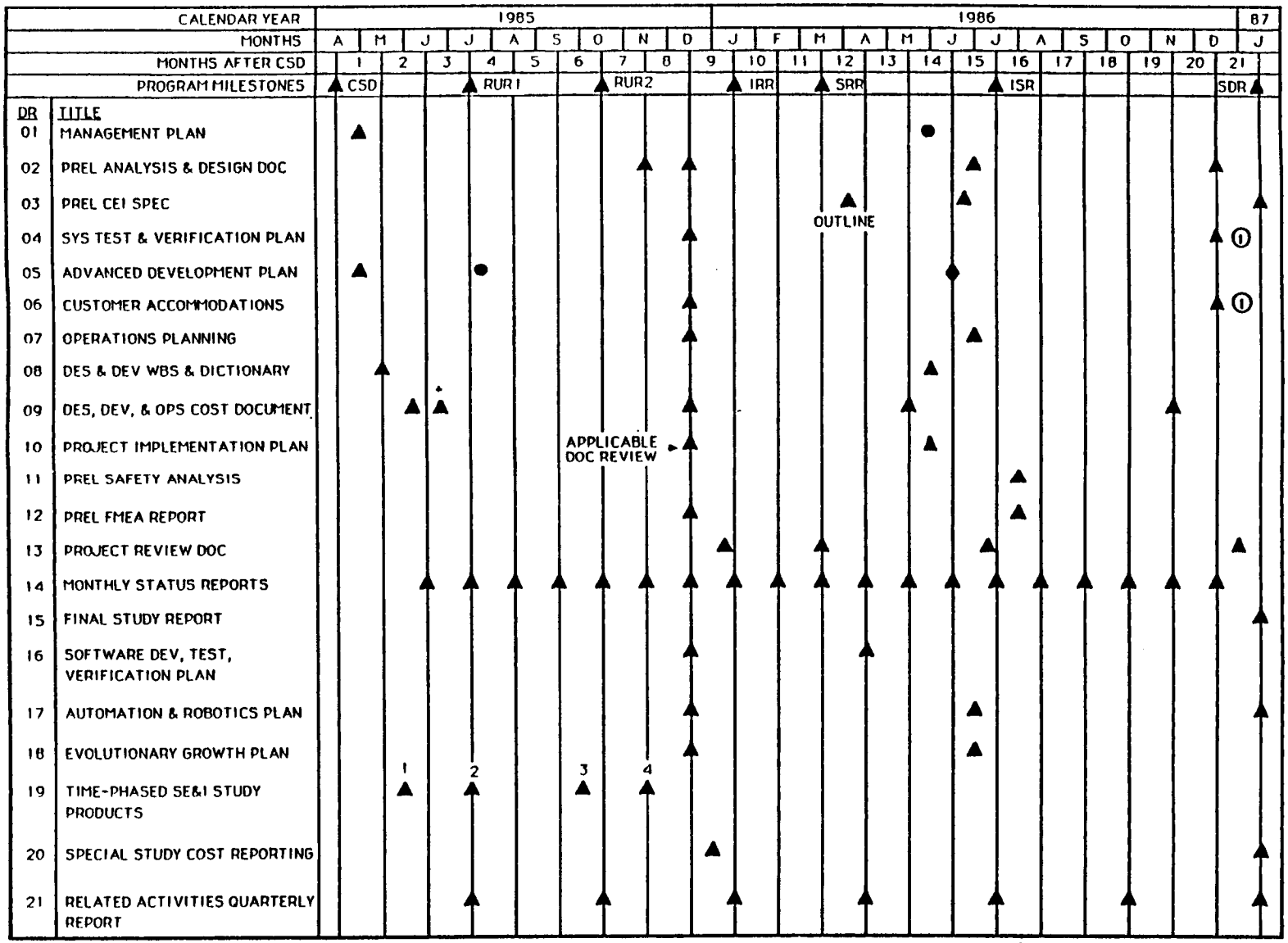

• CONSTRAINED FUNDING SUBMITTAL
O REVISION
◇ DRAFT SUBMITTED FOR APPROVAL
ⓘ INCLUDED WITH DR-02

Figure 1-2

Garrett

- Characterization of LiF-MgF_2 and LiF-CaF_2 eutectic phase change materials
- High temperature vacuum sublimination tests of candidate receiver materials
- Thermal cycling of a LiF - filled thermal energy storage device

Sundstrand

- Generation of a specification for an axial heat pipe compatible with thermal energy storage and the organic working fluid requirements
- Design and analysis to meet these requirements
- Fabrication and assembly of the heat pipe

Harris

- Characterization of the kinematics of the concentrator concept
- Evaluation of substrates, reflective coatings, and protective coatings for possible use on the concentrator

Complementary independent research and development (IR&D) activities in the SD, PMAD and PV areas were performed outside the scope of the Phase B study contract. These were reported quarterly in the related activity report.

All team members performed IR&D effort that complimented the Phase B activity. The areas addressed were as follows:

Ford

- Kapton substitute studies
- Solar array evaluations
- DC PMAD component studies
- NiH_2 batteries
- NaS batteries

Garrett

- CBC Receiver/Thermal Storage Design Fabrication and Test

General Dynamics

- AC PMAD component evaluations

Harris

- Concentrator Studies

V2-10/5

Sundstrand

- ORC receiver/storage thermal storage test
- ORC fluid evaluation
- ORC two phase fluid management
- AC PMAD studies

Rocketdyne

- ORC and CBC thermal storage media studies
- Liquid metal cooled receiver/thermal storage system for CBC and ORC
- Thermal control modeling
- Dynamic modeling of SD subsystem
- PMAD architecture studies
- Health monitoring
- Higher order language evaluation
- PMAD test bed implementation

2.0 SYSTEMS ANALYSIS AND TRADES

2.1 ANALYSIS OF MISSION, SYSTEM, AND OPERATIONS REQUIREMENTS

Requirements analysis has been a continuing task throughout the Phase B contract effort and has been an iterative process with continual refinement of parameters as the baseline EPS configurations matured. As new or changed requirements for the EPS were determined, they were reviewed thoroughly for impact on the EPS design and implemented as appropriate.

The initial analysis performed under this task item involved the review of the mission, operations, and system requirements documents (attachments C-2, C-3, and C-4) of the contract and the deriviation of a set of requirements for the manned and man-tended Space Station options as well as the platforms. The results of these analyses were reported in Rocketdyne's management plan, DR-01. The key power system drivers as derived from the documents are summarized below.

- Mission (customer) Requirements (C-2)
  - Mission Characteristics--Provides overall design criteria for power system and subsystems.
  - Standard Power Interface--Affects distribution subsystem in terms of output devices employed.
  - Transparent Power System (Friendly to users and independent of the type of power generation option chosen)--Affects design of distribution, control, and storage system chosen.
  - Power to External Payloads/Vehicles--Affects distribution subsystem interfaces.
  - Ten-Year Power Growth--Delineates the power level requirements on a yearly basis. Affects overall configuration chosen (solar dynamic versus photovoltaic).

- Operations Requirements (C-3)

  - Continuous Operation (24 h/day, every day)--System design will not constrain user.

  - Growth Capability--Affects the tradeoffs between photovoltaic and solar dynamic systems. This requirement has a large effect on life-cycle cost (LCC).

  - Operational Safety--Because of the proximity of personnel, this item affects the choice of component design margins and component arrangements to provide fail operational/safe capability. Also, working fluids and materials will be carefully evaluated.

  - User Friendly--Affects distribution subsystem and storage subsystem design.

  - Easily Maintained and Repaired--Affects commonality of power system elements and commonality of elements with other systems. Overall system design constrained by chosen repair approach.

  - Automatic Operation--Affects the controls approach to power system. (This requirement is expanded in C-4.)

Table 2.1-1 summarizes power system requirements relating to initial/growth and manned/man-tended Space Station and the platforms.

Table 2.1-1
RECOMMENDED POWER SYSTEM REQUIREMENTS

ITEM	MANNED		MAN-TENDED	PLATFORM	
	INITIAL	GROWTH	INITIAL	INITIAL	GROWTH
ORBIT, KM/INCLINATION DEG. (TABLE C-4-I) (TABLE C-5-I, C-5-III)	500/28.5	500/28.5	500/28.5*	POLAR 700/98.2	700/98.2
AVERAGE BUS POWER, KW; C-4 (2.2.3)	75	300	21.0*	8	25
VOLTAGE C-4 (2.2.3)	120 (MIN)	COMMONALITY		COMMONALITY	120 (MIN)
FREQUENCY, HZ	TBD	COMMONALITY		COMMONALITY	TBD
REGULAR POWER DURATION C-3 (2.4)	CONTINUOUS				CONTINUOUS
EMERGENCY, % LOAD DURATION, C-4 (2.3.3)	50 1 ORBIT			**	50** 1 ORBIT
SAFE HAVEN POWER, C-4 (2.2.3)	10 KW* FOR 28 DAYS		---	---	---
LIFETIME	INDEFINITE WITH MAINTENANCE AND REPLACEMENT, C-4 (2.1.4.1). 10-YEAR DESIGN LIFE BEFORE REPLACEMENT*		3-5 YEARS TO MANNED STATION, C-5 (2.4) (SEE MANNED REQMT.)	INDEFINITE WITH MAINTENANCE AND REPLACEMENT,* C-4 (2.1.4.1). 10-YEAR DESIGN LIFE BEFORE REPLACEMENT*	
RELIABILITY C-4 (2.1.10)	J8400001				
MAINTENANCE	MINIMIZE USE OF CREW, C-4 (2.1.9; DESIGN TO FACILITATE REPAIR AND REPLACEMENT, PROVIDE MONITORING CHECKOUT AND FAULT DETECTION, C-4 (2.1.9).			AUTOMATED, C-4 (2.1.9); REMOTE SERVICING C-2 (3.1.6); CHECKOUT AND RETRIEVAL, SERVICE SUPPLIED BY SPACE STATION, C-4 (2.1.2.4). 2-YEAR SERVICE INTERVAL (JSC-19989)	
ENVIRONMENTAL C-4 (2.1.3.1)	EXTERNAL PER NASA TM-86490 (J8400040)				
DESIGN FEATURES	USE MODULAR DESIGN TO FACILITATE GROWTH, C-4 (2.1.5); DESIGN FOR SAFE DISPOSAL, C-4 (2.1.4.1). FUNCTIONALLY INDEPENDENT SUBSYSTEMS. PROTECT POWER AGAINST OVERLOADS AND FAULTS C-4 (2.2.3).				
OPERATIONAL SAFETY	PROVIDE EMERGENCY CONTROL AND FAULT DETECTION CAPABILITY, C-4 (2.1.11.2). FAIL SAFE AND RESTORABLE, C-3 (2.2).			CORE POINTING WITHOUT GIMBALS (JSC-10089 *	*
PRELAUNCH OPERATIONS	COST-EFFECTIVE VERIFICATION OF READINESS FOR LAUNCH, C-3 (2.3)			*	*
	SUITABLE FOR ON-EARTH TRANSPORTATION, SUITABLE FOR INSTALLATION IN ORBITER, C-4 (2.1.3.2, 3.1). CAPABILITY TO SERVICE AND DESERVICE CONSUMMABLES, C-3 (2.3).			PLATFORM SUITABLE FOR SINGLE STS LAUNCH (JSC-19969) *	*
AUTOMATION FEATURES	AUTOMATED TO FULLST EXTENT PRACTICAL, C-4 (3.3). PROVIDE MANUAL OVERRIDE, OPERATIONS FEEDBACK, C-4 (2.1.11.4), C-3 (3.3).			AUTOMATED OPERATION TO FULLEST EXTENT PRACTICAL, C-4 (2.1.9).	
AUTONOMY	PHASED DEGREE CONSISTENT WITH COST AND TECHNOLOGY, C-4 (2.1.7)			AUTONOMOUS BETWEEN SCHEDULED SERVICING--GROUND INTERVENTION NOT PRECLUDED, C-4 (2.1.7).	
RESUPPLY CYCLE, C-4 (3.4)	90 DAYS (NOMINAL)		90 DAYS NOMINAL	POLAR: 12-24 MONTHS (NOMINAL) WITH 6 MONTHS CONTINGENCY.	
STRUCTURALS AND MATERIALS	USE OF HAZARDOUS MATERIALS TO BE MINIMIZED, C-4 (2.11.3); MEET REQUIREMENTS FOR VACUUM OUT-GASSING, (2.1.11.3); CONSIDER ATOMIC OXYGEN EFFECTS, (2.1.11.3). FACTORS OF SAFETY GIVEN BY TABLE C-4-11, C-4 (2.2.1).				
CONTROL	PROVIDE MEANS OF SELECTING, CONNECTING, AND DISCONNECTING SOURCES AND LOADS, C-4 (2.2.3).				
REDUNDANCY	DIVERSE ROUTING NO REDUNDANT WIRING AND COMPONENTS. SINGLE OPEN CIRCUIT SHALL NOT CAUSE LOSS OF BUS, C-4 (2.2.3)				
NUMBER OF ATTACHED PAYLOADS, C-4 (2.1.2)	9	18	6*	TBD	TBD
RADIATION LIMITS C-4 (2.2.10)	PROTECTION FOR CREW SUCH THAT THE MAXIMUM EXPOSURE LIMITS OF TABLE C-4-X ARE NOT EXCEEDED.				

*SELECTED FOR CONCEPTUAL DESIGN
**PROVIDE IF REQUIRED BY MISSION

2.2 CONCEPTUAL DESIGN ANALYSES AND TRADE STUDIES

2.2.1 Overview

An important part of the Phase B conceptual and preliminary design efforts was the identification and performance of analyses and trade studies to support the selection of the recommended EPS configuration, and the subsystem optimization activities during preliminary design.

The following sections provide a brief summary of the trade studies performed on the system and subsystem levels. The system trades include the major PV vs. SD trade which resulted in the recommendation of a hybrid EPS for the station. PV subsystem trades include the battery vs. RFC trade which resulted in selection of Ni-H_2 batteries for energy storage. SD subsystem trades include the ORC vs. CBC trade with a recommendation to delay the decision while development activities continue. PMAD subsystem trades are highlighted by the selection of a dual ring architecture and 20 kHz primary distribution.

2.2.2 System Trades

Numerous system level trade studies and analyses were performed in accordance with the Phase B SE&I plan. The objective of this study effort was to develop sufficient data on competing EPS designs to allow NASA and the Rocketdyne team to select the concept that best supports the Space Station and Platforms. The trade studies and analyses and their updates, which were reported in DP's 4.1, 4.2, 4.3 and 4.4 of DR-19 and the last submittal of DR-02, are listed in Table 2.2.2-1. Synthesis of these system level studies and the subsystem analyses and trade studies provided the basis for the overall system concept trade study.

Rocketdyne's overall trade study plan is illustrated in Figure 2.2.2-1. This plan required three trade study iterations prior to IRR. The first two iterations were completed prior to RURs 1 and 2, respectively, and the results were reported in DPs 4.1 through 4.3. The objectives of these iterations were to (1) develop early system evaluation results and

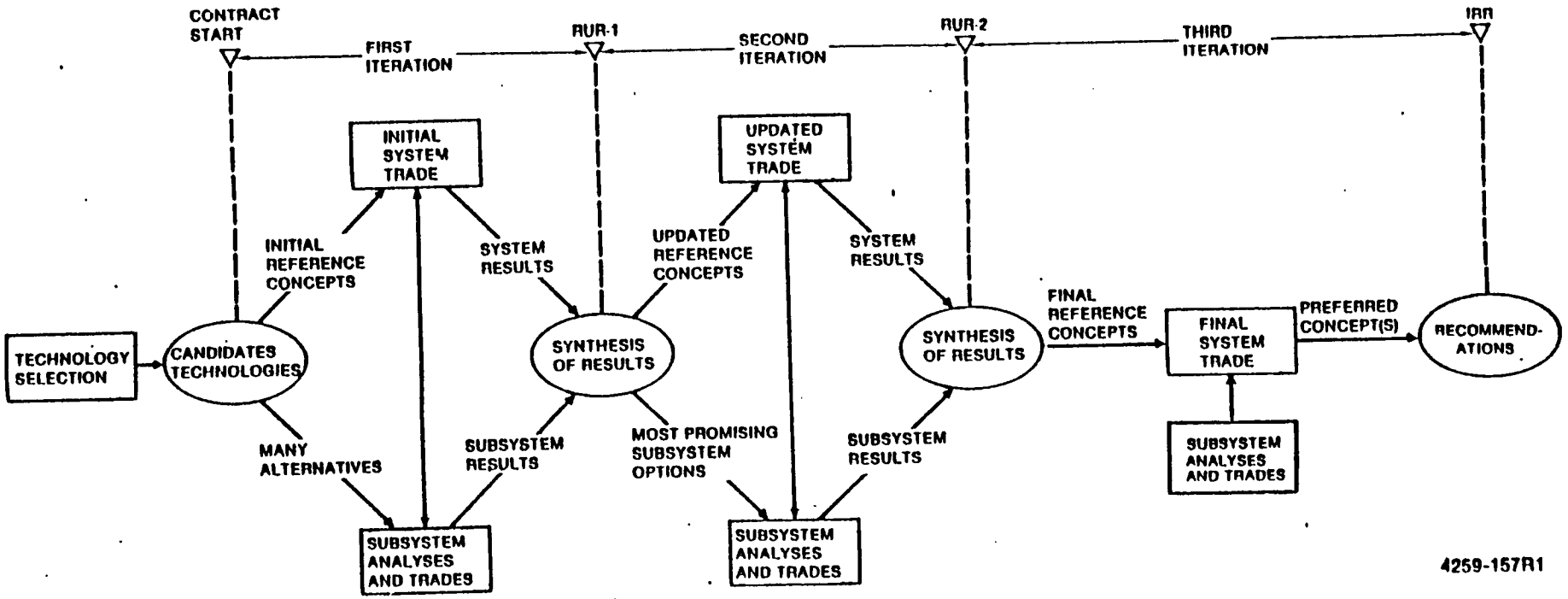

Figure 2.2.2-1 Overall Trade Study Plan

TABLE 2.2.2-1
SYSTEM ANALYSES AND TRADE STUDIES

SYSTEM ANALYSES AND TRADE STUDIES	DR -- SECTION REFERENCE DR-19, DP 4.1 6/3/85	DR-19, DP 4.2 7/19/85	DR-19, DP 4.3 10/3/85	DR-19, DP 4.4 11/19/85	DR-02 6/30/86
COMMONALITY IDENTIFICATION	8.1	10.1	5.1		
GROWTH SCENARIOS	8.2	10.2	5.2		
LOAD STRUCTURE REQUIREMENTS	8.3	10.3	5.3		
POINTING CONTROL STABILITY	8.4	19.4	5.4		
PLATFORM SIZING	8.5	10.5			
CUSTOMER INTERFACE		10.6	5.6		
MAINTENANCE APPROACH		10.7	5.7		
TEST & VERIFICATION		10.8	5.8	5.2	
AUTONOMY		10.9	5.9	5.3	
AUTOMATION		10.10	5.10	5.4	
ASSEMBLY		10.11	5.11		
SHADOWING		10.12	5.12		
SYSTEM MASS			5.5	5.1	
LAUNCH PACKAGING			5.13		
LOGISTICS			5.14	5.5	
SAFETY			5.15		
PRODUCTION				5.6	
END-OF-LIFE DISPOSAL				5.7	
PRELAUNCH ASSEMBLY INTERFACE VERIFICATION AND SERVICING				5.8	
PEAK POWER SPLIT					5.1
GIMBAL JOINTS					5.2
SYSTEM TRADE STUDY	2.0,4.0	5.0	4.0	4.0	

insights, (2) test and update the decision criteria, and (3) screen and refine the reference concepts. The third iteration of the system trade study was reported in DP 4.4, seven weeks after the submittal of DP 4.3. The objective of this iteration was to select the preferred station and platform EPS concept(s) for recommendation to NASA. The overall schedule for the trade study effort prior to IRR is shown in Figure 2.2.2-2.

Rocketdyne's trade study convergence plan is represented in Figure 2.2.2-3. The circles on the left-hand side of this figure represent the point-of-departure designs and alternatives selected prior to contact start. As the trade studies progressed through iterations, the subsystem options were progressively reduced and the reference concepts refined.

V2-22/2

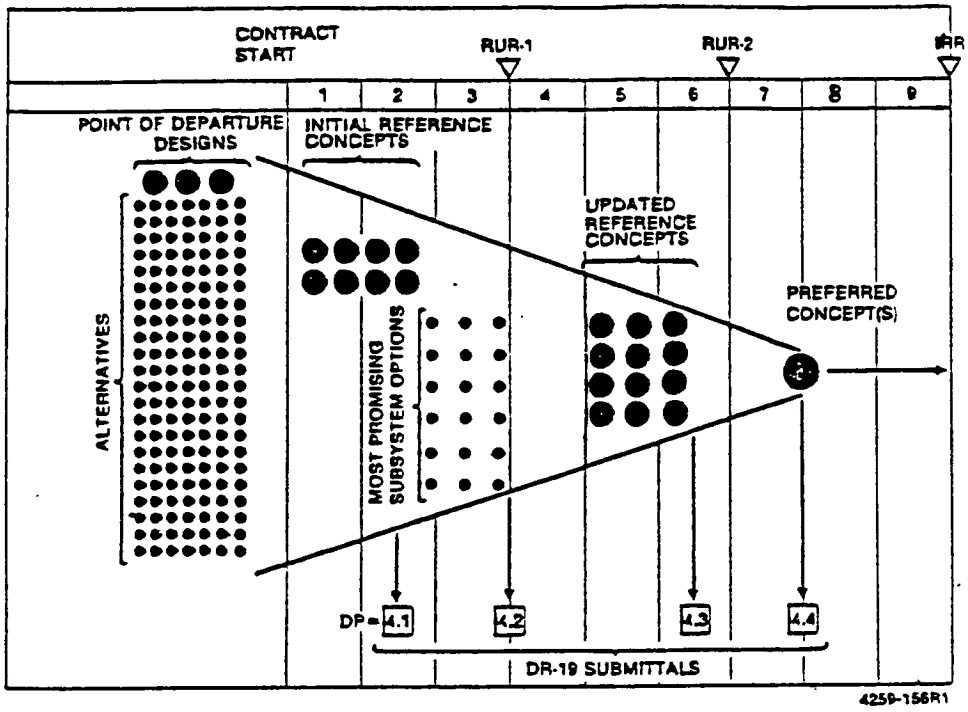

Figure 2.2.2-3 Trade Study Convergence Plan

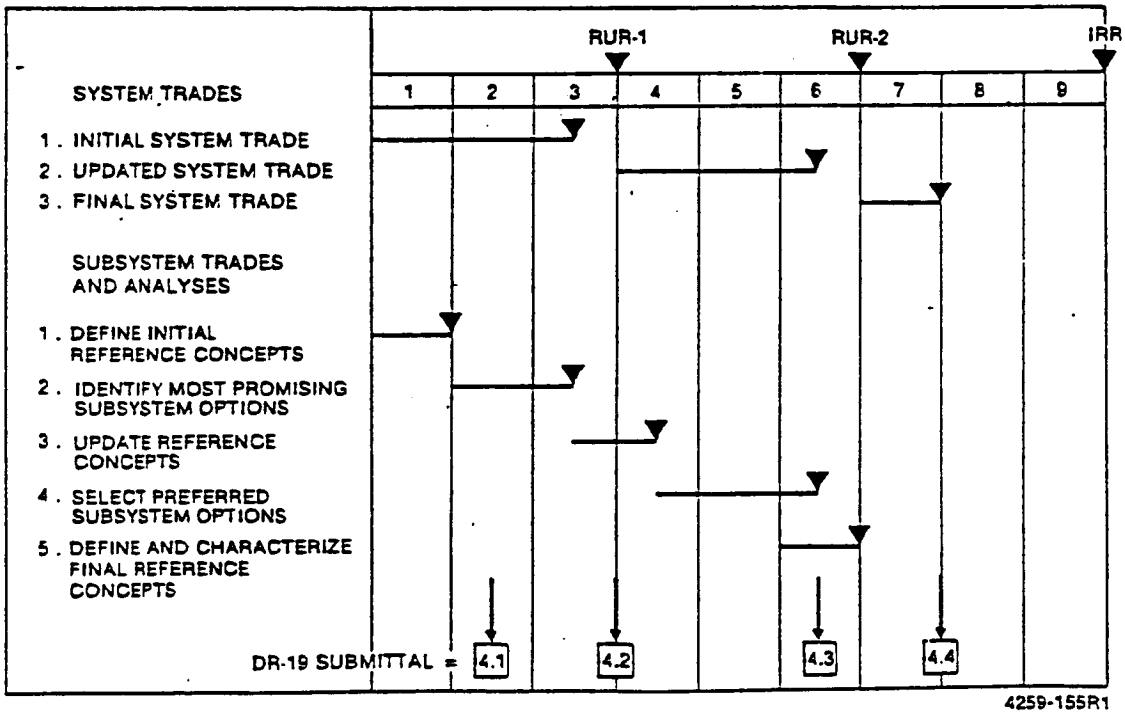

Figure 2.2.2-2 Trade Study Schedule

2.2.2.1 Initial System Trade Study

The eight initial reference concepts shown in Table 2.2.2-2 were defined and preliminarily characterized in DP 4.1. After the submittal of DP 4.1, these reference concepts were refined in several areas, including the following: (1) the Brayton turbine inlet temperature was reduced from 1500°F to 1300°F, (2) the solar dynamic platforms were changed to use small redundant power generation modules rather than single large modules, (3) the module size in the Stirling growth option was reduced, and (4) the nuclear growth option module size was decreased and its configuration rearranged. None of these refinements represented final selections but only interim results. Key design features of the refined initial reference concepts are summarized in Tables 2.2.2-3, -4 and -5.

These eight concepts were evaluated, compared and the results presented in section 5.0 of DR-19, DP 4.2. In reviewing these results, it should be remembered that the objective of this initial trade was not to select a preferred concept, but rather to develop early system evaluation decision criteria including (1) initial costs, (2) annual costs, (3) growth costs, (4) life cycle costs, and (5) subjective ratings.

2.2.2.2 System Trade Update

The reference concepts defined and evaluated in DPs 4.1 and 4.2 were purposefully kept as simple as practical to facilitate their use in the initial system and subsystem trades.

However, it was recognized from the start that a more complete set of reference concepts would be needed to evaluate the full range of viable alternatives. Therefore, for system trade update, an expanded set of reference concepts was developed based on the initial reference concepts and the initial system and subsystem trades. This expanded set of reference concepts, shown in Table 2.2.2-6 included various hybrid and growth options as well as as single technology systems. Concepts 1 through 3 use near-term PV (photovoltiac), CBC (closed Brayton cycle), and

TABLE 2.2.2-2

INITIAL REFERENCE CONCEPTS

REFERENCE CONCEPT	STATION			PLATFORM	
	IOC (75 kWe)	MAN-TENDED (37.5 kWe)	GROWTH (300 kWe)	INITIAL (8 kWe)	GROWTH (23 kWe)
PV STATION	PV	PV	PV	—	—
CBC STATON	CBC	CBC	CBC	—	—
ORC STATION	ORC	ORC	ORC	—	—
PV PLATFORM	—	—	—	PV	PV
CBC PLATFORM	—	—	—	CBC	CBC
ORC PLATFORM	—	—	—	ORC	ORC
STIRLING GROWTH OPTION	—	—	S	—	—
NUCLEAR GROWTH OPTION	—	—	N	—	—

PV = PHOTOVOLTAIC

CBC = CLOSED BRAYTON CYCLE

ORC = ORGANIC RANKINE CYCLE

S = STIRLING

N = NUCLEAR

70400-133

TABLE 2.2.2-3

REFERENCE STATION EPS CONCEPTS

Reference Concept	IOC Station (75 kWe)					Man-Tended Station (37.5 kWe)	Growth Station (300 kWe)
	PGS	ESS			PMAD		
		Eclipse Storage	Contingency	Safe Haven			
PV station	. 8 - 9.4 kWe (net) flexible deployable/ retractable solar arrays	. 4 - 18.8 kWe (net) alkaline regenerative fuel cell system (RFCS) modules		. 1 - 10 kWe (net) alkaline primary fuel cell	. 20-kHz, 440-Vac, 1Ø, primary power . Dual-ring with backbone bus distribution sized for growth station . Conversion to secondary power in 21 load centers . Distributed controllers with master processor	Same as IOC except: . Delete 4 solar arrays . Delete 2 RFCS modules . Delete safe haven fuel cells . Delete 9 PMAD load centers	Same as IOC except: . Add 24 replicated solar arrays . Add 12 replicated RFCS modules . Add 2 replicated safe haven primary fuel cells . Add 7 replicated PMAD load centers
CBC station	. 2 - 37.5 kWe (net) power generation modules . Deployable solid surface concentrators . Direct receiver with LiF-MgF_2 thermal storage . Sensible heat radiator with copper/water heat pipes	. Eclipse power is provided by thermal storage	. 4 - 9.4 kWe (net) alkaline primary fuel cells		. Same as above except ac-to-ac instead of dc-to-ac conversion	Same as IOC except: . Both PGS modules are are operated at half power with half the concentrator and radiator area . Delete ESS (safe haven is not required and eclipse and contingency power is provided by thermal storage) . Delete 9 PMAD load centers	Same as IOC except: . Add 6 replicated PGS modules . Add 12 replicated primary fuel cells . Add 7 replicated PMAD load centers
ORC station	. 2 - 37.5 kWe (net) power generation modules . Deployable solid surface concentrators . Heat pipe receiver with LiOH thermal storage . Condensing radiator with aluminum/ammonia heat pipes						

TABLE 2.2.2-4

REFERENCE PLATFORM EPS CONCEPTS

Concept	Initial Platform (8 kWe)			Growth Platform (23 kWe)
	PGS	ESS	PMAD	
PV platform	. 2 - 4-kWe (net) flexible deployable/retractable solar arrays	. 2 - 4 kWe (net) Ni-Cd batteries (eclipse storage only)	. 20-kHz, 440-Vac, 1Ø primary power . Distribution system sized for growth platform	Same as initial platform except: . Add 4 replicated solar arrays . Add 4 replicated Ni-Cd batteries
CBC platform	. 2 - 8-kWe (net) power generation modules . Deployable solid surface concentrators . Direct receiver with LiF-MgF_2 thermal storage . Sensible heat radiator with copper/water heat pipes	. Eclipse power is provided by thermal storage	. Same as above except ac-to-ac instead of dc-to-dc conversion	. Upgrade PGS modules to 11.5 kWe (net each)
ORC platform	. 2 - 8-kWe (net) power generation modules . Deployable solid surface concentrators . Heat pipe receiver with LiOH thermal storage . Condensing radiator with aluminum/ammonia heat pipes			

0024K/anm

TABLE 2.2.2-5

REFERENCE GROWTH STATION OPTIONS

Reference Concept	Growth Station (300 kWe)				
		ESS			
	PGS	Eclipse Storage	Contingency	Safe Haven	PMAD
SD-Stirling growth option	. 6 - 50 kWe (net) power generation modules . Deployable solid surface concentrator . Pumped loop receiver with LiF thermal storage . Stainless steel/mercury heat pipe radiators	. Provided by thermal storage	. 16 - 9.4 kWe (net) alkaline primary fuel cells		. Same as growth station PMAD for SD-B and SD-ORC (see Table 2-2)
Nuclear growth option	. 2 - 100 kWe (net) liquid metal-cooled reactors . 2 - 50 kWe (net) solar dynamic modules	. None required			

0024K/bjm

TABLE 2.2.2-6

UPDATED REFERENCE CONCEPTS

Concept			Station			Platform	
			Man-Tended (37.5 kW)	IOC (75 kW)	Growth (300 kW)	Initial (8 kW)	Growth (23 kW)
1.	PV station and PV platforms		PV	PV	PV	PV	PV
2.	CBC station and CBC platforms		CBC-S	CBC-S	CBC-S	CBC-S	CBC-S
3.	ORC station and ORC platforms		ORC-S	ORC-S	ORC-S	ORC-S	ORC-S
4.	CBC station and PV platforms	Large modules	-	CBC-L	CBC-L	PV	PV
5.		Small modules	CBC-S	CBC-S	CBC-S	PV	PV
6.	ORC station and PV platforms	Large modules	-	ORC-L	ORC-L	PV	PV
7.		Small modules	ORC-S	ORC-S	ORC-S	PV	PV
8.	PV/CBC hybrid[a]		-	PV/CBC-L	PV/CBC-L	PV	PV
9.	PV/ORC hybrid[a]		-	PV/ORC-L	PV/ORC-L	PV	PV
10.	CBC growth option		PV	PV	PV/CBC-L	PV	PV
11.	ORC growth option		PV	PV	PV/ORC-L	PV	PV
12.	Advanced PV growth option		PV	PV	PV/APV	PV	APV

PV---photovoltaic
APV--advanced photovoltaic
CBC--closed Brayton cycle
ORC--organic Rankine cycle
S----small (18.75 kW) modules
L----large (37.5 kW) modules
[a]These concepts provide 16 kW more power than the minimum of 75 and 300 required for the IOC and growth station, respectively, because of the extra PV panels and batteries.

ORC (organic Rankine cycle) technology, respectively, for both the stationand platform electrical power systems (EPSs). Concept 1 used planar deployable silicon arrays and regenerative fuel cells for the station and batteries for the platforms. Concepts 2 and 3 used small (18.75 kW) solar dynamic (SD) modules to facilitate station/platform commonality concepts 4 through 7 used CBC and ORC technology for the station and PV for the platforms. Concepts 4 and 6 used large (37.5 kW) SD modules, and Concepts 5 and 7 used small (18.75 kW) modules. Concepts 8 and 9 were hybrid approaches that included both PV (16 kW) and SD (75kw) for the IOC station and grow with SD technology. The PV portion of the hybrid station used two initial (8kW) platforms PGSs for commonality. Concepts 10 through 12 were growth advanced PV technology, respectively. The nuclear and Stirling growth options in Table 2.2.2-2 were dropped from consideration for reasons discussed in Section 4.1 of DP 4.3.

The key design features of the reference station and platform EPS concepts are summarized in Tables 2.2.2-7 and 2.2.2-8, respectively, and described in Section 3.0 of DP 4.3. These reference concepts were similar to those described in DP 4.2, except that they were expanded and refined in several areas, including the following: (1) small (18.75 kW) as well as large (37.5 kW) SD modules were included in the updated reference concepts to provide a basis for comparing the effect of module size; (2) the distribution system frequency was changed from 20 kHz to 400 Hz; (3) a PV/SD hybrid concept was defined with four 4-kW (net) planar deployable Si arrays and NiH_2 batteries and two 37.5-kW (net) SD modules; and (4) an advanced PV station and platforms were defined with planar deployable GaAs arrays and sodium-sulfur batteries.

The results of the system trade update iteration were reported in section 4.0 of DP 4.3. The objectives of this iteration were not to select a preferred concept, but rather to (1) develop preliminary system evaluation results, (2) update the decision criteria, and (3) refine the reference concepts. The recommended EPS concept was selected prior to IRR in the third and final iteration. It is discussed next.

2.2.2.3 Third System Trade Study Interactions

Twelve reference concepts were selected for evaluation and comparison

TABLE 2.2.2-7

REFERENCE STATION CONCEPTS

Concept	PGS	ESS			PMAD
		Eclipse Storage	Contingency	Safe haven	
PV station	9.3 kW (net) planar deployable Si arrays	18.75 kW (net) regenerative fuel cells		Primary fuel cells	400 Hz
CBC station	37.5 or 18.75 kW (net) modules Deployable solid surface concentrator Exocentric gimbals Direct receiver (CBC) Heat pipe receiver (ORC)	Thermal storage	Primary fuel cells		
ORC station					
PV/SD hybrid	Four 4-kW (net) planar deployable Si arrays	NiH_2 batteries			
	37.5 kW (net) SD modules	Thermal storage			
Advanced PV growth station	Planar deployable GaAs arrays	Sodium-sulfur batteries		Primary fuel cells	

TABLE 2.2.2-8

REFERENCE PLATFORM CONCEPTS

Concept	PGS	ESS	PMAD
PV platform	Two 4 kW (net) planar deployable arrays expandable to 11.5 kW (net)	4 kW (net) NiH_2 batteries	400 Hz
CBC platform	Two 18.75 kW (net) modules Deployable solid surface concentrator Exocentric gimbals Direct receiver (CBC) Heat pipe receiver (ORC)	Thermal storage	
ORC platform			
Advanced PV growth platform	Planar deployable GaAs arrays	Sodium-sulfur batteries	

in the third trade study iteration. These reference concepts, which are summarized in this section and described in detail in Section 3.0 of DP 4.4, include four major EPS options:

- o PV Concept: PV initial station and PV growth
- o SD concept: SD initial station and SD growth
- o Hybrid concept: PV/SD hybrid initial station and SD growth
- o PV/SD growth concept: PV initial station and SD growth.

Within these four EPS options, there are two pairs of subsystem options:

- o SD power generation alternatives: CBC and ORC
- o PV energy storage alternatives: alkaline RFCs and independent pressure vessel Ni-H_2 batteries.

The resultant 12 reference concepts are shown in Table 2.2.2-9. Their key design features are summarized in Table 2.2.2-10, and they are illustrated in Figures 2.2.2-4 through 2.2.2-7. All 12 concepts include PV platforms.

The reference concepts were designed to satisfy a common set of requirements to provide a fair basis for comparison. These common requirements, consistent with technical direction given by NASA-LeRC in a letter dated 25 October 1985, included (1) average, peak, and contingency power requirements and failure tolerance criteria shown in Table 2.2.2-11; (2) PMAD efficiency assumptions in Table 2.2.2-12; and (3) station buildup power levels in Table 2.2.2-13.

The reference concepts were similar to those described in DP 4.3, but they were updated and refined in several areas, including the following:

- o The PMAD distribution frequency was changed fro 400 Hz to 20 kHz
- o The SD concentrator approach was changed from parabolic symmetric concentrators with ecentric gimbals to parabolic offset linear-actuated concentrators with orthogonal gimbals.
- o The CBC radiator was changed from a heat pipe design to a pumped loop concept.

TABLE 2.2.2-9

REFERENCE CONCEPTS

Concept			Station			Platform	
			Man-Tended (37.5 kW)	IOC (75 kW)	Growth (300 kW)	Initial (8 kW)	Growth (24 kW)
PV	RFC		PV	PV	PV	PV	PV
	B		PV	PV	PV	PV	PV
SD	CBC		CBC	CBC	CBC	PV	PV
	ORC		ORC	ORC	ORC	PV	PV
Hybrid	RFC	CBC	PV	PV/CBC	PV/CBC	PV	PV
		ORC	PV	PV/ORC	PV/ORC	PV	PV
	B	CBC	PV	PV/CBC	PV/CBC	PV	PV
		ORC	PV	PV/ORC	PV/ORC	PV	PV
PV/SD growth	RFC	CBC	PV	PV	PV/CBC	PV	PV
		ORC	PV	PV	PV/ORC	PV	PV
	B	CBC	PV	PV	PV/CBC	PV	PV
		ORC	PV	PV	PV/ORC	PV	PV

PV = photovoltaic
RFC = regenerative fuel cell
B = batteries
SD = solar dynamic
CBC = closed Brayton cycle
ORC = organic Rankine cycle.

TABLE 2.2.2-10

KEY DESIGN FEATURES OF THE REFERENCE IOC STATION CONCEPTS

Concept		PGS	ESS	PMAD
PV	RFC	• 8-9.4 kW (net) planar deployable Si arrays	• 4-18.75 kW (net) alkaline RFCs	20 kHz
	B	• Same as above	• 4-18.75 kW (net) Ni-H_2 batteries	
SD[a]	CBC	• 3-25 kW (net) modules with nonredundant engines • Parabolic offset linear-actuated concentrator • Direct insolation receiver • Pumped loop radiator	• Thermal storage (LiF/MgF_2) integral with receiver	
	ORC	• 2-37.5 kW (net) modules with redundant engines • Parabolic offset linear-actuated concentrator • Heat pipe receiver • Heat pipe radiator	• Thermal storage (LiOH) integral with receiver	
Hybrid		• 4-9.4 kW (net) planar deployable Si arrays • 2-25 kW (net) CBC or ORC power generation modules with nonredundant engines	• 2-18.75 kW (net) RFCs or Ni-H_2 batteries Thermal storage	
PV/SD growth[b]		• 8-9.4 kW (net) planar deployable Si arrays	• 4-18.75 kW (net) RFCs or Ni-H_2 batteries	

[a]SD concepts also include 2-5 kW (net) PV arrays and 2-5 kW (net) Ni-H_2 batteries to satisfy initial station buildup, peaking, and safe-haven requirements, and hydrazine-fueled auxiliary power units to meet contingency power requirements. The PV arrays may be removed later to make room for SD growth.

[b]The PV/SD growth concept is identical to the PV concept for the IOC station. However, for the PV/SD growth concept, SD is developed in parallel with IOC station development so that it is ready for use when the station grows.

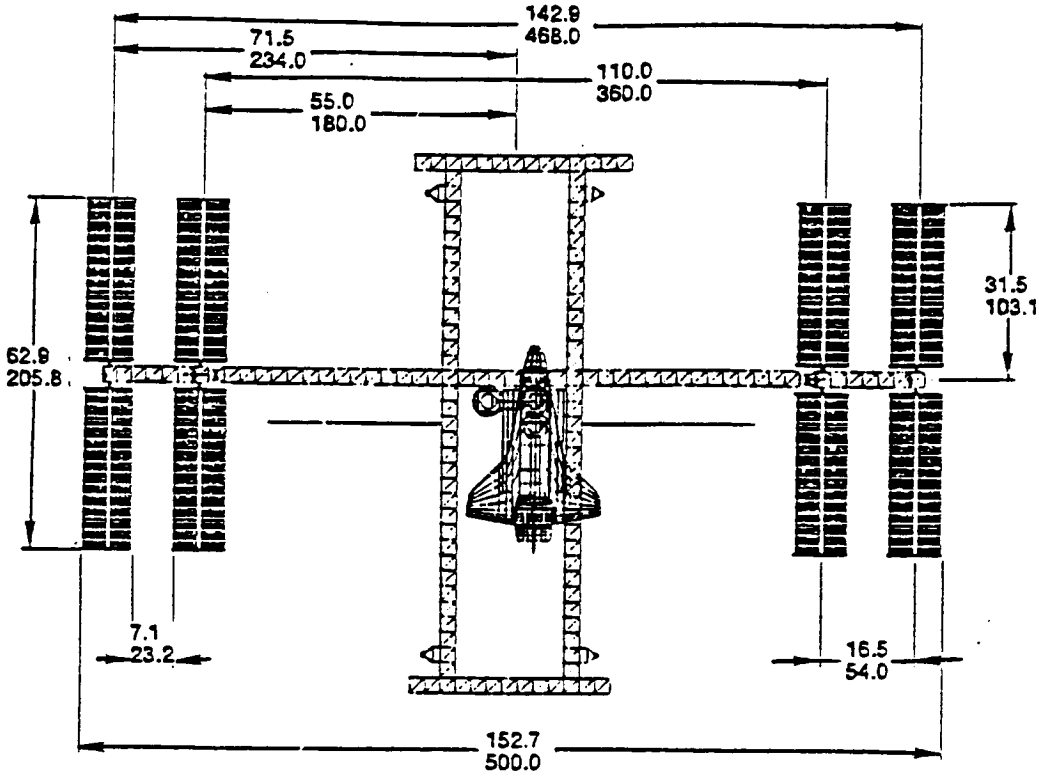

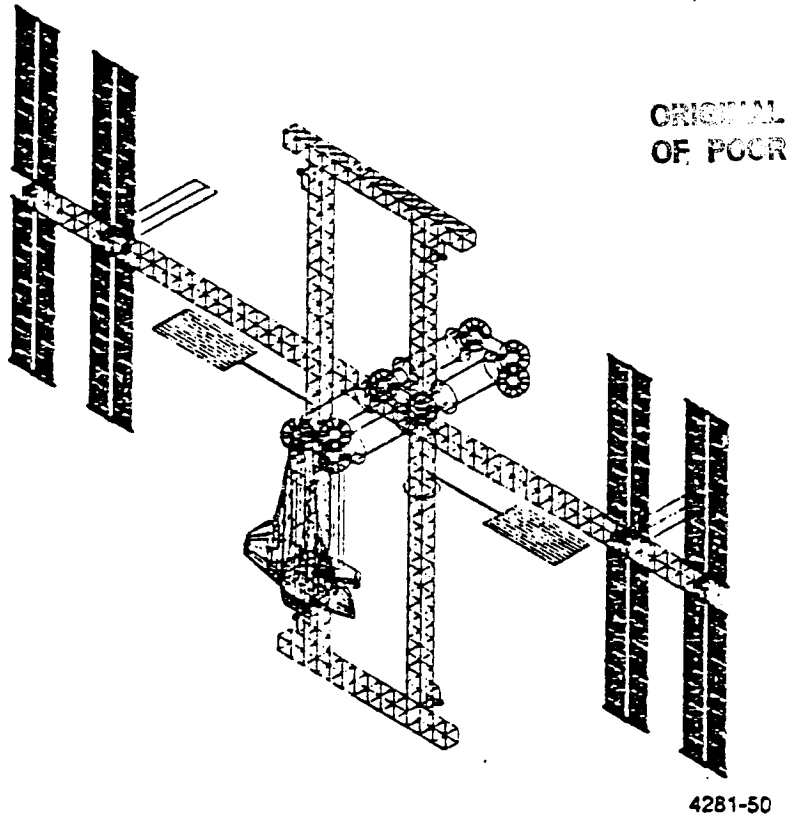

4281-50

Figure 2.2.2-4 Reference PV Station Concept

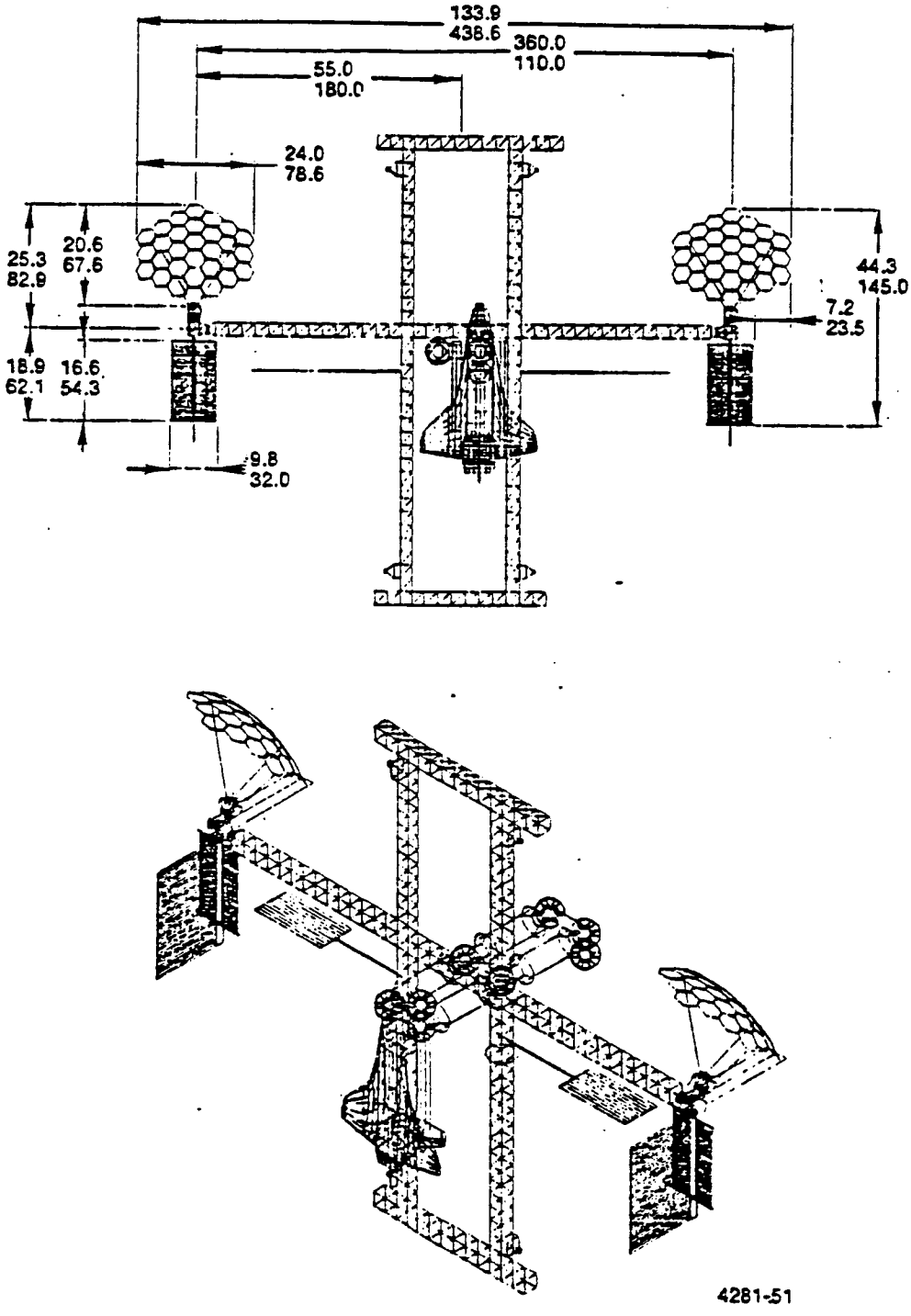

Figure 2.2.2-5. Reference ORC Concept

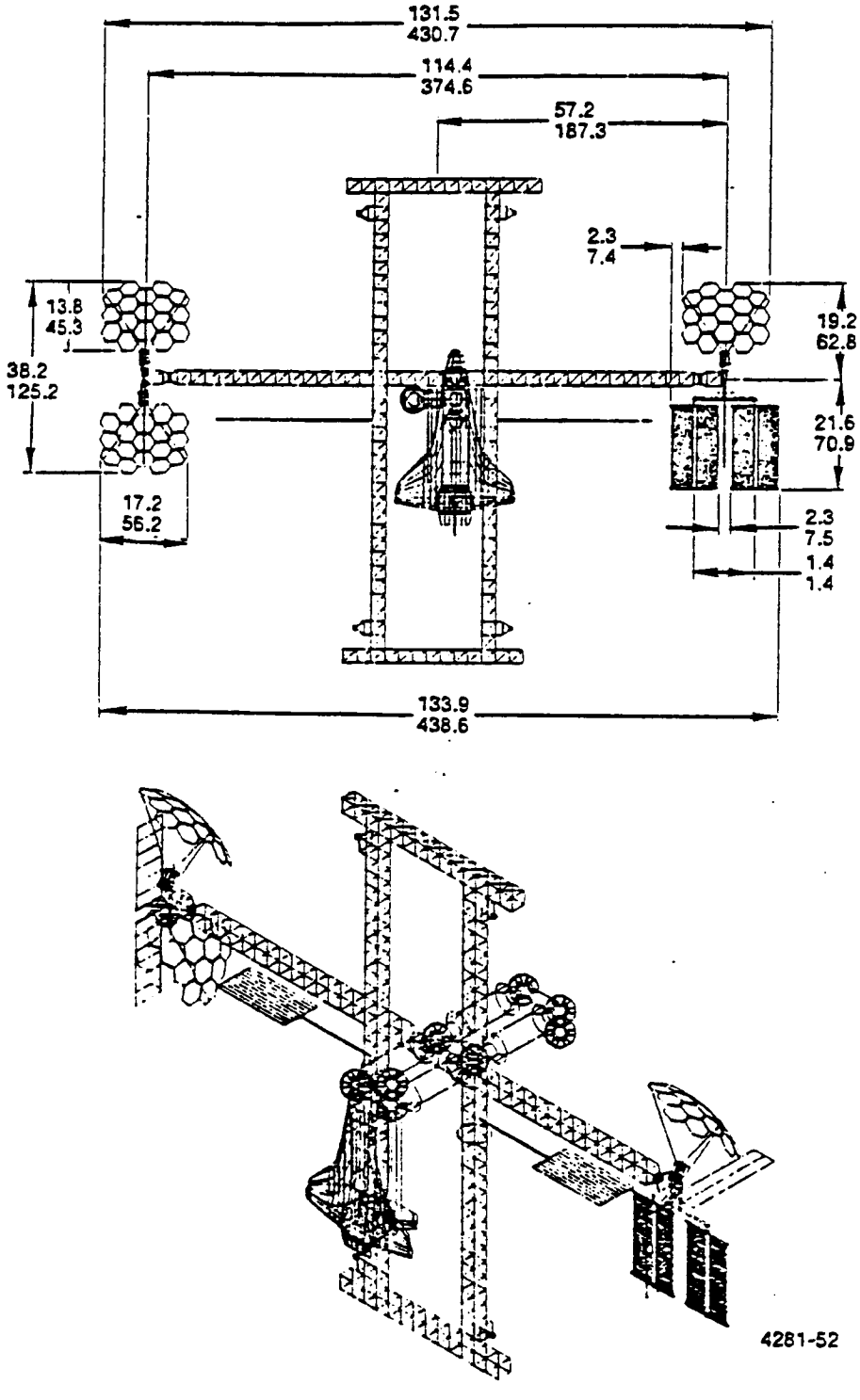

Figure 2.2.2-6 Reference CBC Concept

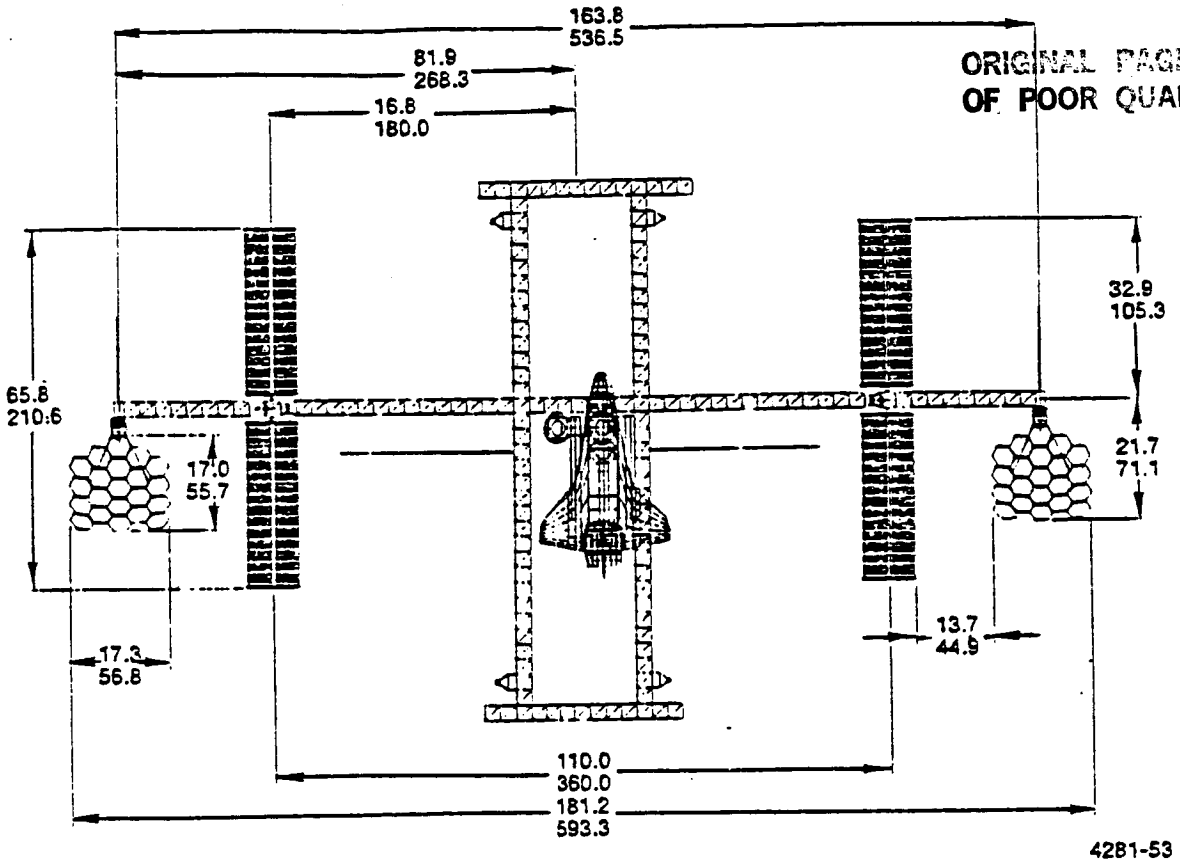

Figure 2.2.2-7 Reference Hybrid Concept

TABLE 2.2.2-11

POWER REQUIREMENTS AND FAILURE TOLERANCE CRITERIA

	Station			Platform	
	Man-Tended	IOC	Growth	IOC	Growth
Average power (kW)	37.5	75	300	8	24
Peak power (kW)	37.5	100	350	18	34
Peak power duration (minutes/orbit)					
Insolation	-	7.5	7.5	5	10
Eclipse	-	7.5	7.5	5	10
Contingency power level (kW)	18.75	37.5	150	4	12
Failure tolerance: Power level (kW) after					
One credible failure	18.75	55	-	8	24
Two credible failures	0	35	-	4	6
Three credible failures (safe haven)	0	10	-	0	0

TABLE 2.2.2-12

PMAD AND ESS EFFICIENCY ASSUMPTIONS WITH REFERENCE 20-kHz DESIGN

Item	Efficiency	
	PV	SD
Source to user	0.91	0.90
Source to storage	0.98 (RFCs) 0.92 (batteries)	-
Energy storage subsystem	0.63 (RFCs) 0.79 (batteries)	-
Storage to user	0.90	-
Other losses		
User/bulk conversion	8%	8%
PMAD peripheral loads	7%	7%
Subtotal	15%	15%

TABLE 2.2.2-13

DESIRED POWER DURING STATION BUILDUP

Flight	Power Requirement (kW)
1	2.7
2	4.3
3	6.3
4	8.1
5	8.7
6	18.2 (station is manned)
7	24.4
8	25.7
9	27.9
10	30.9
11	35.6
12	35.9 (station is complete)

- o The size and redundancy of the SD modules was modified to satisfy the failure tolerance criteria shown in Table 2.2.2-11.
- o PV arrays, batteries and auxiliary power units were added to the SD concepts to satisfy initial station buildup, peaking, contingency, and safe-haven requirements.
- o Separate safe-haven fuel cells and stored reactants in the previous reference concepts were eliminated.

The results of the their iteration are summarized here and presented in detail in Section 4.0 of DP 4.4.

2.2.2.3.1 Decision Criteria

The decision criteria used in the system trade study consisted of three elements: (1) go/no-go constraints, (2) objective measures, and (3) supplemental (subjective) ratings. The go/no-go constraints were fundamental limits that were so important that it was not worth considering concepts that did not satisfy them. The only go/no-go constraints identified were (1) STS compatibility and (2) IOC schedule. All of the reference concepts satisfied these go/no-go constraints.

The second element in the decision criteria (the objective measures) was the primary means for ranking reference concepts that satisfied the go/no-go constraints. The objective measures in our decision criteria include (1) initial cost, (2) growth cost, (3) operations cost (including maintenance and logistics), and (4) life cycle cost (LCC).

Because many station/platform requirements and costing assumptions were uncertain, five alternative station/platform scenarios and numerous sensitivities to costing assumptions were evaluated in the cost assessment.

To the maximum extent practical, all factors that affect decisions were explicitly factored into the cost.

However, since it was impractical to cost everything, supplemental (Subjective) ratings were also used in the decision criteria. The supplemental rating criteria included (1) technology readiness (schedule/cost risk), (2) reliability and availability of power, (3)

safety, (4) growth potential, (5) flexibility to accommodate lower IOC power requirements, (6) capability for larger peaks/contingency, (7) flexibility to allow lower orbit altitudes, and (8) tolerance to pointing errors.

2.2.2.3.2 Cost Assessment Results

This section summarizes the EPS cost assessment results presented in DP-4.4. Table 2.2.2-14 shows the base case cost estimates for each of the 12 reference station EPS concepts, broken down into five major cost elements. Phase C/D cost (the first row in Table 2.2.2-14) includes the cost of developing and producing IOC flight hardware. Other IOC costs (the second row in Table 2.2.2-14) include (1) hardware launch cost; (2) cost of initial spares; and (3) cost impact on other station systems, including the transverse boom and beta joints. Growth cost is the cost to grow from 75 kW to 300 kW, including hardware production and launch cost and cost impact on other station systems. Operations cost includes the cost of (1) producing and launching replacement hardware, (2) on-orbit operations (EVA and IVA), (3) ground support, and (4) reboost. LCC is the sum of the initial, growth, and operations costs.

Figure 2.2.2-8 compares LCCs for the four major EPS options. The costs shown in this figure are the averages of those for the subsystem options in Table 2.2.2-6. Figure 2.2.2-8 clearly indicates that operations cost is a major part of LCC. Figure 2.2.2-9 breaks operations cost into its constituent elements for the PV and SD concepts. This figure shows the major operations cost elements for the PV concept to be (1) PGS and ESS replacement hardware and (2) reboost. The PGS replacement costs are large for the PV concept, even though a low PV array replacement frequency of once every 25 years was used; this is so because PV arrays have large production costs. The ESS replacement costs are large because batteries and RFCs are postulated to have (high) replacement frequencies of once every 5 and 6 years, respectively. The major operations cost element for the SD concept is PGS replacement hardware. The major contributors to this cost are the concentrators and receivers, which are assumed to have replacement frequencies of approximately once every 24 years. Figure 2.2.2-10 shows the sensitivity of station EPS LCC to

TABLE 2.2.2-14

SUMMARY OF STATION EPS COSTS (1987 $M)*

	PV		SD		HYBRID RFC		PV/SD GROWTH B		PV/SD GROWTH RFC		PV/SD GROWTH B	
COST ELEMENT	RFC	B	CBC	ORC	CBC	ORC	CBC	ORC	CBC	ORC	CBC	ORC
Phase C/D cost (75 kW)	946	923	984	990	1053	1031	1028	1006	1119	1103	1088	1072
Other IOC cost **	170	176	234	256	230	235	222	227	170	170	176	176
Growth cost (75-300 kW)	1303	1283	871	863	953	951	953	951	953	951	953	951
Operating Cost (30 years)	3635	3719	1912	1813	2082	2006	2089	2014	2299	2240	2318	2258
Total (life-cycle cost)	6075	6101	4001	3922	4318	4223	4292	4198	4541	4464	4535	4457

* DP 4.4

** Includes hardware launch, initial spares and impact on other station system costs

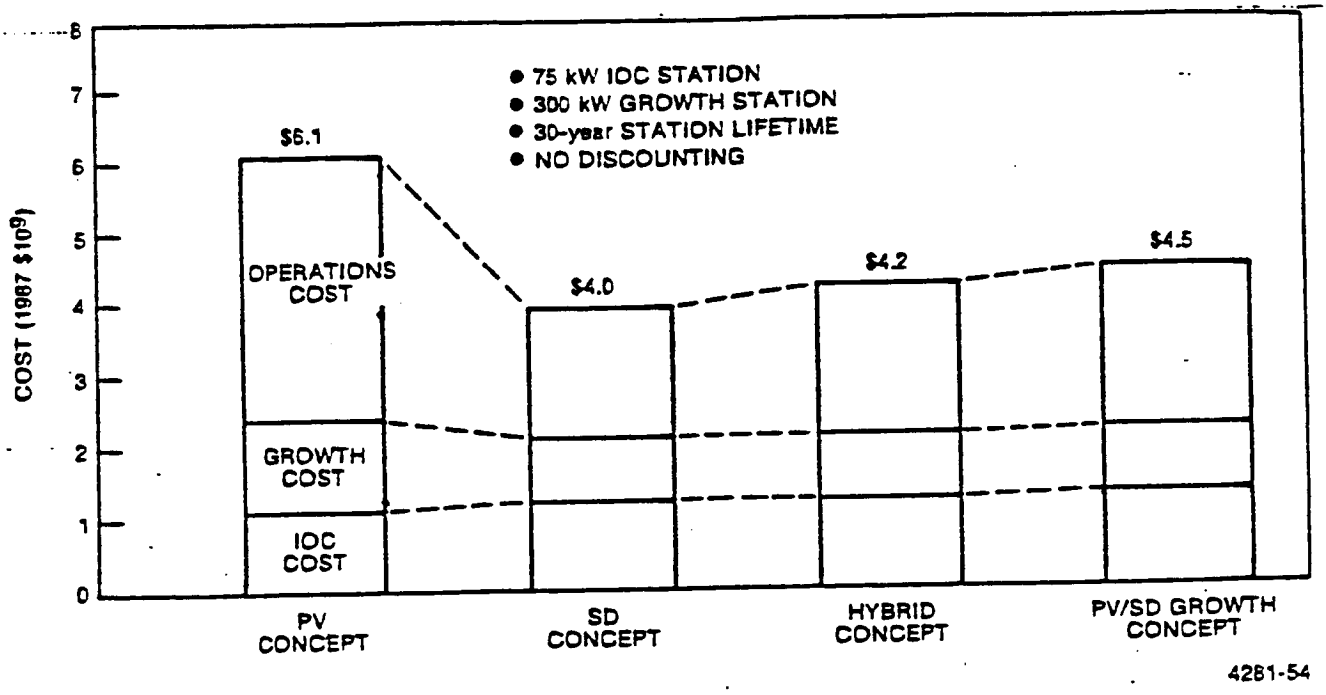

Figure 2.2.2-8 Station EPS Life-Cycle Cost Comparison

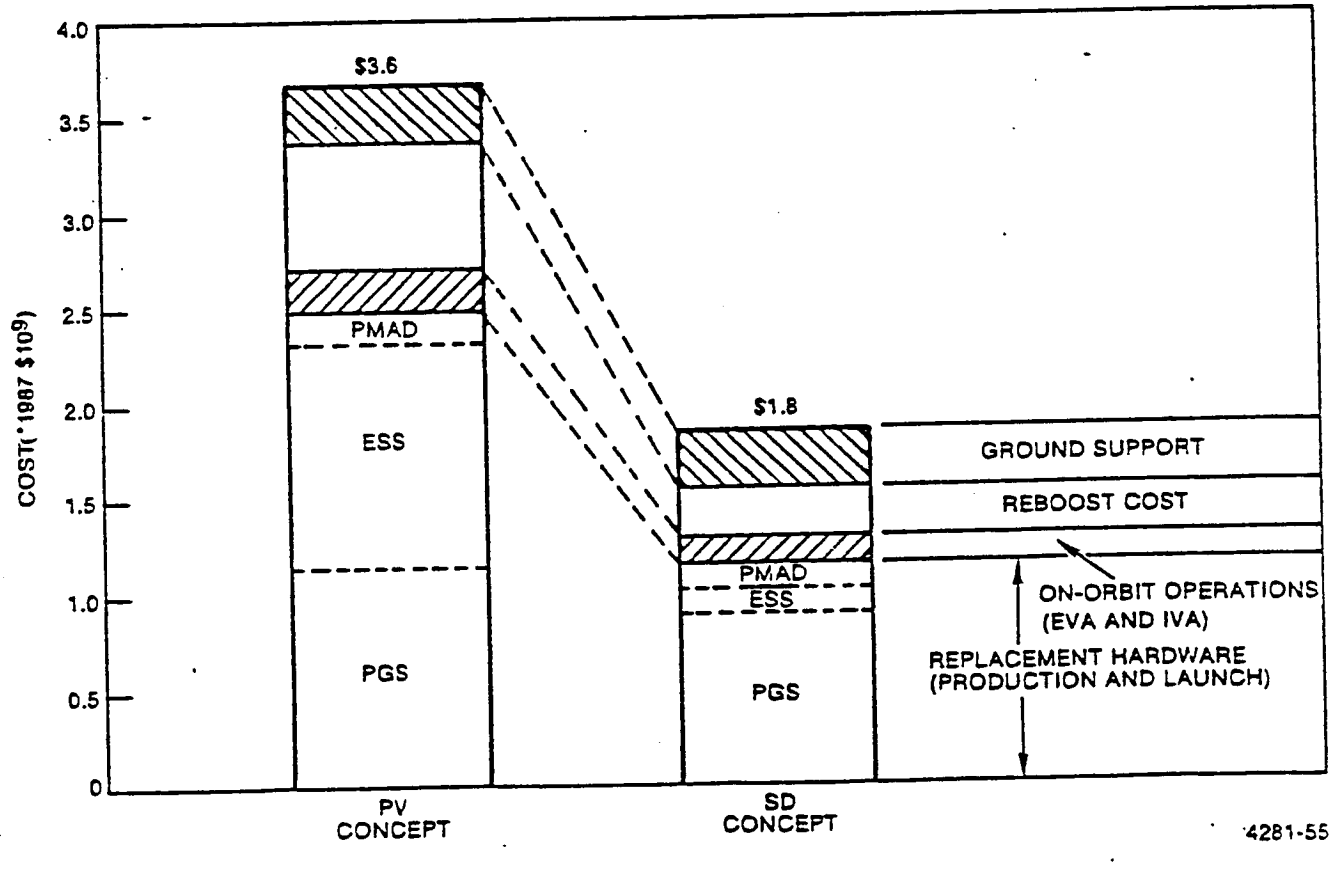

Figure 2.2.2-9 PV versus SD Operations Cost Comparison

several key assumptions in the cost assessment. For all cases examined, the PV concept has significantly higher LCC than the three other system options.

Table 2.2.2-15 compares alkaline RFCs and Ni-H_2 battery costs. The numbers in this table indicate that batteries offer a slight initial cost advantage over RFCs. However, this cost advantage could be reduced or reversed if RFC development costs can be shared with other (common) life support/propulsion system components The costs in Figure 2.2.2-7 take no credit for shared RFC development costs with other work packages. (However, both the RFC and battery radiator development costs in Figure 2.2.2-7 take into account the fact that they use technology that is common with the station thermal bus radiator.) Figure 2.2.2-11 shows ESS cost sensitivity to stored energy and contingency requirements. It may be desirable to increase stored energy requirements not only for contingency purposes, but also for peaking (to improve load factors) and possible for a scaled-down (low-cost) separate safe-haven power supply. Figure 2.2.2-11 shows that RFC costs are much less sensitive than battery costs to potential changes in stored energy requirements.

Table 2.2.2-16 compares CBC and ORC costs. Costs appear comparable for the CBC and ORC concepts.

2.2.2.3.3 Supplemental Ratings

Table 2.2.2-17 summarized the supplemental (subjective) ratings given to the 12 reference concepts. These ratings reflect our current best judgement concerning the eight supplemental criteria categories. Highlights of this table include:

- The principal strengths of the PV concepts are their technology readiness (low schedule and cost risks), tolerance of pointing errors, flexibility to accommodate lower IOC power requirements, and inherent capability to handle large peak loads. Current indications are that station control and dynamics considerations may prevent growth beyond about 225 kW (net) with PV concepts, but this should be confirmed by WP-02.

- The major strengths of the SD concepts are their growth potential and flexibility for lower orbit altitudes (due to their small drag areas). In addition to these advantages, SD offers significantly lower LCC than PV.

TABLE 2.2.2-15

COMPARISON OF ALKALINE RFC AND IPV Ni-H_2 BATTERY COSTS FOR REFERENCE PV STATION CONCEPTS

Cost Element	Cost (1987 $M)	
	Alkaline RFC	Ni-H_2 Battery
IOC cost (75 kW)		
Development	35	17
Production	37	26
Launch	21	34
Spares	9	2
PGS impact	Base	-12
PMAD impact	Base	+19
Subtotal	102	86
Annual operations cost		
Replacements	9.1	7.2
Launch	2.9	7.2
On-orbit operations	1.9	1.5
Reboost	Base	-1.0
Subtotal	13.9	14.9

Above costs do not include system-level wraps (WBS Items A-J).

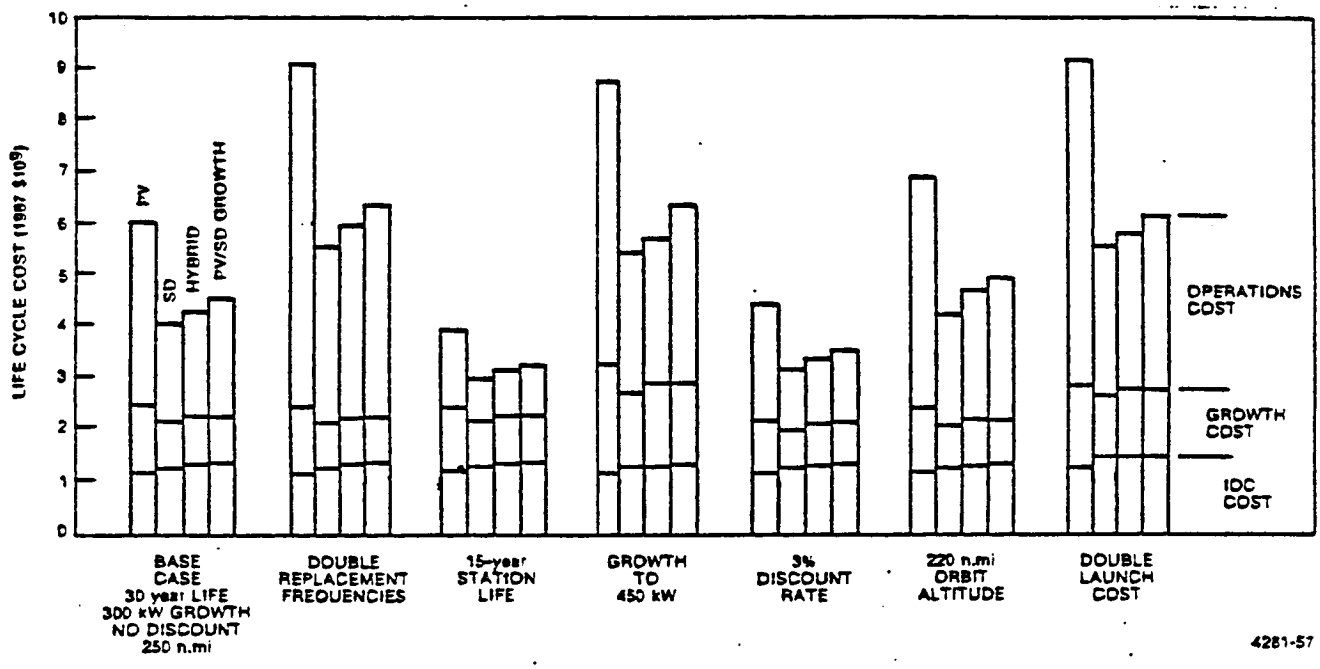

Figure 2.2.2-10 Sensitivity of Station EPS Life-Cycle Cost to Variations in Key Assumptions

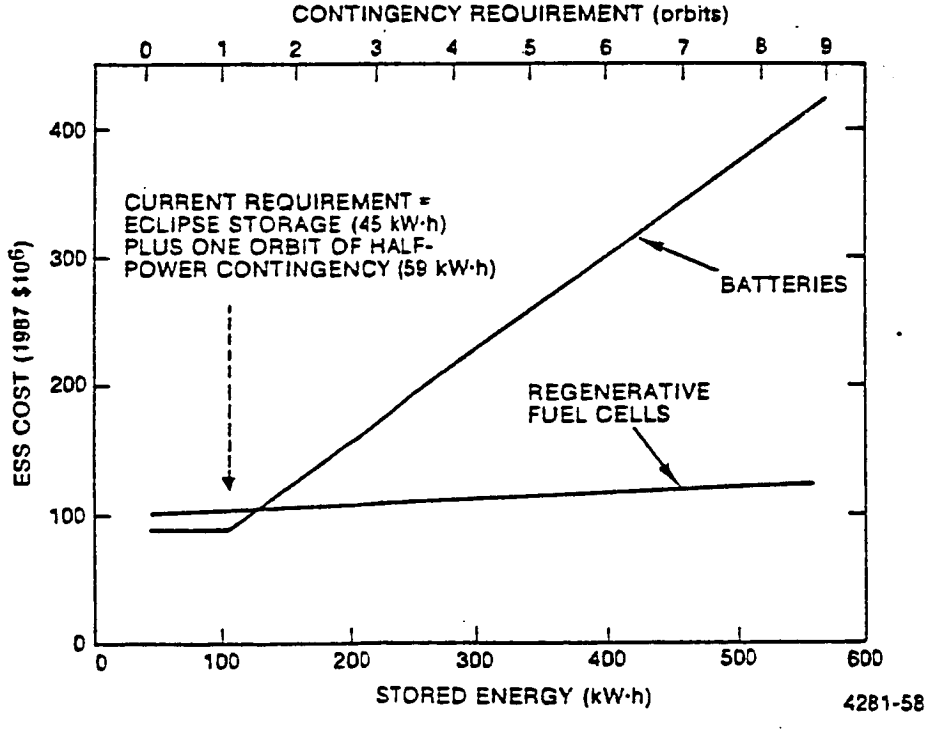

Figure 2.2.2-11 ESS Cost Sensitivity to Stored Energy Contingency Requirements for the 75-kW Reference PV Station

TABLE 2.2.2-16

COMPARISON OF CBC AND ORC COSTS FOR SD REFERENCE IOC STATION CONCEPTS

Item	CBC		ORC	
	Three 25-kW (net) Modules (Nonredundant Engines)		Two 37.5-kW (net) Modules (Redundant Engines)	
	Design Concept	Cost (1987 $M)	Design Concept	Cost (1987 $M)
Concentrator	Parabolic offset linear-actuated concentrator	75	Parabolic offset linear-actuated concentrator	77
Receiver	Direct insolation receiver with LiF/MgF_2 thermal storage salt	41	Heat pipe receiver with LiOH thermal storage salt	45
PCU	CBC with He-Xe working fluid	60	ORC with toluene working fluid	52
Radiator	Pumped loop radiator	31	Heat pipe radiator	31
Total		207		205

Above costs cover hardware development and production but not system-level wraps (WBS items A-J).

TABLE 2.2.2-17

SUBJECTIVE RATINGS

Criteria	PV		SD		Hybrid				PV/SD Growth			
					RFC		B		RFC		B	
	RFC	B	CBC	ORC	CBC	ORC	CBC	ORC	CBC	ORC	CBC	ORC
Technology development risk	B^-	B^+	C	C^+	C^+	B^-	B^-	B	B^-	B^-	B^+	B^+
Reliability and availability of power	B^-	B	C	C	B^-	B^-	B	B	B^-	B^-	B	B
Safety	B^-	B	C	C^-	C	C^-	C^+	C	C^+	C	B^-	C^+
Growth potential	C	D	A^-	A^-	A^-	A^-	B	B	C^+	C^+	C	C
Flexibility for lower IOC power requirements	A^-	A	B^-	B^-	A^-	A^-	A	A	A^-	A^-	A	A
Capability for larger peaks/ contingency	A	B^+	C^-	C	B	B^+	C^+	B^-	B^+	A^-	B^-	B
Flexibility for lower orbit altitudes	D^+	D^+	A	B^+	B^+	B^-	B^+	B^-	B	B^-	B	B^-
Tolerance of pointing errors	A	A	C	C^+	B^-	B	B^-	B	B	B^+	B	B^+

- o The subjective ratings for the hybrid concepts are generally between those of the PV and SD concepts. Hybrid advantages include good programmatic flexibility (e.g., ability to easily requirements), capability for larger peaks and contingency, and good growth path with low schedule/cost risk.

- o The PV/SD growth concepts are similar to the hybrids, but they provide less programmatic flexibility and have more problematic growth paths since SD is not included on the IOC station.

- o Batteries are rated higher than RFCs in the areas of technology readiness (schedule/cost risk) and reliability, but poorer in growth potential and the capability to accommodate larger peaks and/or contingency requirements.

- o The CBC and ORC concepts are rated almost equal.

2.2.2.3.4 Discriminators and Recommendations

The final objective of any trade study is to identify discriminators that allow one option to be selected over competing approaches. In the final trade study, the major competing options were:

- o PV versus SD
- o CBC versus ORC
- o RFCs versus batteries

Table 2.2.2-18 through 2.2.2-20 summarize the key discriminators related to those options. The discriminators in these tables are the ones that in our opinion are the most important factors to be considered in the decision process.

The conclusions and recommendations from the RFC versus battery reported in DP 4.4 trade are summarized in Table 2.2.2-21. The decision depends greatly on stored energy requirements (e.g., for contingency, peak power, load matching, safe haven) and commonality considerations that extend beyond WP-04. It was therefore recommended that requirements should be firmed up and commonality opportunities discussed with other work package centers before a selection was made. Rocketdyne's recommendations for changes to requirements was provided in DR-02 in December 1985 per the contract.

Following DP 4.4 submittal, the battery option was selected because of requirement changes and to provide commonality with the platform ESS.

TABLE 2.2.2-18

MAJOR DISCRIMINATORS BETWEEN ALKALINE RFCs AND NiH_2 BATTERIES

Concept	Advantages	Disadvantages and Uncertainties
RFCs	• Lower mass • Better growth potential • Flexibility to easily accommodate longer peaks/contingency • Potential commonality with life support/propulsion system components • Charge regulating unit probably not needed	• Many active components • Reliability and life must be proven
Batteries	• Higher efficiency • Proven reliability • Lower development risk	• Limited flexibility to accommodate changes in requirements • Life must be proven

TABLE 2.2.2-19

MAJOR DISCRIMINATORS BETWEEN CBC AND ORC CONCEPTS

Concept	Major Advantages	Uncertainties
CBC	• Higher efficiency • Lower mass • Lower area • Simpler concept • Single-phase nondegrading working fluid	• High-temperature receiver . Chromium sublimation . Material creep . LiF/MgF_2 heat of fusion . Thermal performance • Working fluid containment
ORC	• Inherent peaking/throttling capability • Low temperatures . Materials flexibility . Lower concentration ratios . Less pointing accuracy • Receiver and PCU may be separately replaceable	• Two-phase fluid management • Degradable working fluid • Receiver design . Heat pipe performance . LiOH corrosiveness

TABLE 2.2.2-20

MAJOR DISCRIMINATORS BETWEEN PV AND SD CONCEPTS

Concept	Advantages	Disadvantages and Uncertainties
PV	• Lowest development cost and risk • Good peaking capability • Tolerant of pointing errors • Lowest mass and volume	• Limited growth potential • Large drag area • Frequent ESS replacement • High PV array costs
SD	• Good growth potential • Low drag area • Low hardware cost • Lowest LCC	• Development cost and risk • Intolerant to pointing errors • Small PV system required for early station buildup
Hybrid	• Programmatic flexibility • Good growth path • Diverse power generation • Low LCC	• Cost and complexity of developing and maintaining both PV and SD systems
PV/SD	• Low schedule risk • Moderately low LCC	• Cost and complexity of developing and maintaining both PV and SD systems • Difficulty and timing of transition to SD from initial PV station

Elimination of the safe haven requirement and a reduction of contingency power requirements reduced the stored energy need and the advantage of the RFC growth potential.

TABLE 2.2.2-21

ALKALINE RFC VERSUS Ni-H_2 BATTERY TRADE STUDY
CONCLUSIONS AND RECOMMENDATIONS

Conclusions	o	Batteries offer lower initial cost with current requirements and lower development risk
	o	RFCs offer better growth potential and could cost significantly less than batteries if stored energy requirements are increased (e.g., for contingency, peaking, load matching, or safe haven) or life support/propulsion system component commonality can be achieved.
Recommendation	o	Firm up requirements and explore potential commonality before making decision. (Rocketdyne's recommendations for changes to requirements will be provided in DR-02 in December 1985 per the contract.)

The DP 4.4 conclusions and recommendations from the CBC versus ORC trade are summarized in Table 2.2.2-22. Both concepts are roughly equivalent in cost and technical performance. No overwhelming discriminators were identified.

TABLE 2.2.2-22

CBC VERSUS ORC TRADE STUDY CONCLUSIONS AND RECOMMENDATIONS

Conclusions	o	Cost and technical performance are roughly equivalent
	o	Tests are under way to demonstrate the key design features of each concept CBC: Chromium sublimation, receiver thermal performance, and LiF/MgF_2 tests ORC: Toluene degradation, two-phase fluid management, heat pipe performance, and LiOH tests
Recommendations	o	Await results from ongoing tests before making a decision

The key conclusions of the PV versus SD trade are

- PV is desirable for initial station buildup and offers advantages of lower development cost and risk, good inherent peaking and contingency capability, and tolerance of pointing errors However, it has a growth limit of about 225 kW and a LCC that is about 50% higher than SD.

- SD provides good growth potential and significantly lower LCC. Large module sizes are best for growth and low LCC>

- Hybrid concepts combine strengths of PV and SD for modest IOC cost difference

  PV panels and either RFCs or batteries support early station buildup and satisfy peaking, contingency, and safe-haven requirements.

  SD modules (either CBC or ORC) provide a low-cost means to achieve full IOC power level and growth.

- The PV/SD growth concept offers potential advantages similar to those of the hybrid concept, but require SD development in parallel with construction of a full PV station if current growth schedules are to be achieved. Also, programmatic pressure may delay SD development indefinitely, resulting in limited station growth potential and high power costs.

Based on these conclusions, we recommend the following:

- Select the hybrid concept (SD augmented with PV) as the reference for the Space Station.

- Determine the optimum sizing for PV (approximately 10 to 37.5 kW) and SD modules (approximately 20 to 40 kW) in the next 2 to 3 months as station buildup and growth requirements are finalized.

All of the above trade study recommendations were based on our evaluation of EPS options at requirements current as of DP 4.4 (e.g., 75-kW IOC station growing to 300 kW).

2.2.3 PV Subsystem Trades

2.2.3.1 PV Array Voltage

An investigation of the interaction of the space plasma and the solar array voltage in low earth orbit (LEO) has been concluded. No experimental data on large area solar arrays of the type under consideration for this mission is currently available. In addition, no flight experiments on large solar array at operating voltages beyond 100 Vdc have been made.

A literature search was made to assist in the investigation and is documented in this section. A summary of these major conclusions obtained from the search is presented in Table 2.2.3-1. The following items should be considered in selecting the PV array voltage:

- Array recommended operating voltage range is 100 to 400 Vdc
- Plasma loss estimates range from negligible at 100 V to 5% worst case at 150 Vdc
- Other factors influencing plasma loss include:
  - Array geometry
  - Array wiring layout
  - Array electrical configuration
  - Array substrate construction and rear coatings
  - Array grounding.

There is no doubt that for a given solar array design the plasma loss is dependent on the array operating voltage. Figure 2.2.3-1 shows the relationship between the maximum array power loss due to plasma effects and the array operating voltage. It is suggested that this data be used for solar array output calculations until better information becomes available.

The grounding system adopted for the solar array and the electrical distribution system will also influence the plasma potentials and losses.

V2-223/1

Table 2.2.3-1 Space Station Plasma Effects--Summary of Major Conclusions

Ref.	Suggested		Other Major Observations
	Voltage	Plasma Loss	
7	<100 Vdc	Negligible	Solar array geometry may effect losses.
8	<300 Vdc	1%	Consider geometry and wiring of array. Use isolated floating array and transformer couple array to spacecraft. Conductive coating on reary of array.
9	150 Vdc	5% max. (estimate)	Array geometry test is necessary.
10	200 Vdc	30 mA	-
11	100 Vdc 400 Vdc	<0.1% <1.0%	Arc discharges down to 300 V.
12	100/200 V	Some	Conductive coating on rear of array.
13	400 Vdc 270 Vdc	1% max.	-
14	-	-	Large area, low-voltage array reduces power loss.
15	190 Vdc	-	Tests used LMSC flexible array and 2 x 4-cm wraparound cells.
16	120/256 V	Low	-
17	400 Vdc	Heavy	Biased shield close to front of panel reduced plasma loss significantly.
18	220 Vdc	Low	Cold solar arrays have high voltage but leakage limited to >1% of capacity.

Again, no hard data is available. An initial approach would be to adopt the standard aerospace practice of bonding all metalic structure components, conductive films, etc., to form a common structure ground including hard wiring through rotating joints. All electrical circuits, including positive and return busses, are then isolated from the structure ground, i.e., no structural electrical returns. A floating array with a transformer to couple the ground into the spacecraft thereby keeping the spacecraft structure near plasma "ground." Based on the above, it would seem that comprehensive structural grounding together with electrically isolated solar arrays should form the initial approach until further data is available. Any tieing of electrical circuits to the structure can then be implemented later if found to be necessary.

The operating voltage of a large area solar array in LEO is essentially influenced by the following:

- o Plasma losses
- o Arc threshold
- o Voltage of batteries and electric component ratings
- o Array configuration
- o Array wire harness mass
- o Growth

In summary, plasma losses are estimated to be not more than 1% up to 400 v. Arcing may occur on the solar array beyond 300V. A 200V solar array system can be supported by ongoing technology and development. The large area flexible solar array developed by LMSC can be reconfigured to use 8 x 8-cm colar cells. Each panel of the array would accommodate about 200 solar cells in series to give an operating voltage of approximately 80 V. Two such panels can be connected in series to provide a 160Vdc array operating voltage. Array wire harness conductor mass is reduced with high operating voltage. However, the conductor mass sensitivity to voltage decreases substantailly beyond 150V.

The absence of hard data indicates that a conservative approach to the selection of the solar array operating voltage would be prudent. The present upper limit with acceptable losses appears to be from 250 to 300 Vdc. Therefore, it is suggested that a conservative solar array operating voltage of

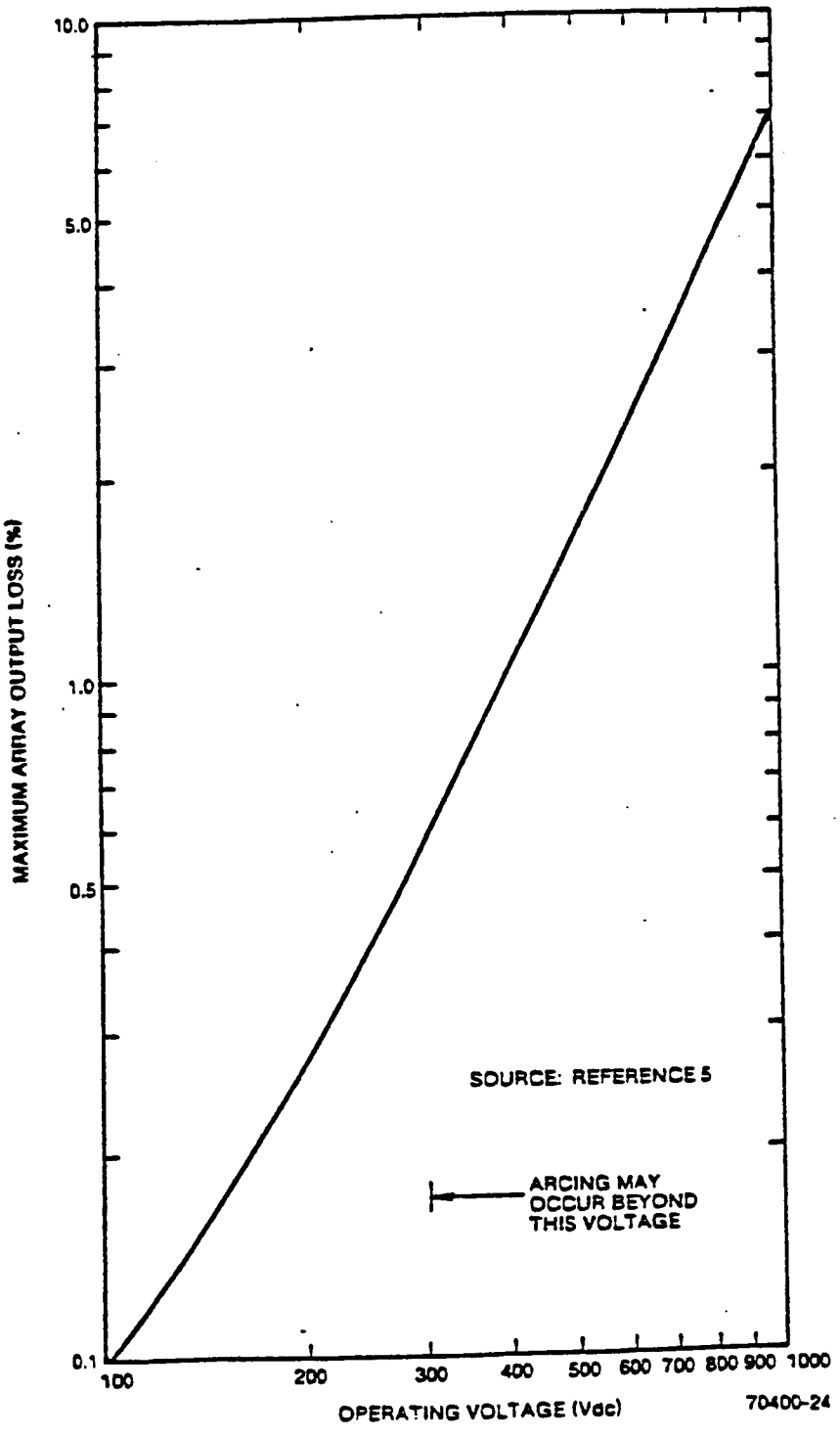

Figure 2.2.3-1 Maximum Solar Array Loss Due to Plasma in LEO

of approximately 160 Vdc be selected at this time. Such a voltage meets the requirements of the foregoing observations. If appropriate data and flight experience show that a higher array operating voltage can be tolerated, the array voltage can be increased in multiples of 80 V. Such a voltage increase can then be implemented on the growth option.

2.2.3.2 PV Cell Material

The result of the cost trade study of projected GaAs technology vs current-technology wilicon solar cells is shown in Figure 3.2.3.-2. The analysis uses the LMSC array silicon cell configuration and compares it to a similar array using higher efficiency, but heavier and more costly, gallium arsenide cells. Factors considered in determining an end-of-life cost are summarized in Table. 2.2.3-2. Inputs used for this run are summarized below:

- o GaAs cells have 300-um substrates.
- o Baseline silicon cell thickness is 200 um.
- o A 25% reduction in mechanical systems weight and cost will result from using GaAs cells.
- o One shuttle flight costs $120M.
- o One shuttle flight can carry 30,000 lb to an altitude of 270 n.mi.
- o Hardware reduction factor = 0.75.

Figure 2.2.3-2 summarizes the results of the analysis for a number of different assumed GaAs cell efficiencies and shows the relative cost of the end-of-life design as a function of the ratio of GaAs cell costs to silicon. As an example, the crossover point, in terms of cost, for a GaAs cell that is 40% more efficient than the baseline silicon cell, is at 4.5. That is to say, a gallium arsenide array would have the same end-of-life cost a a silicon array if the cost of a bare gallium arsenide cell were 4.5 times the cost of a silicon cell.

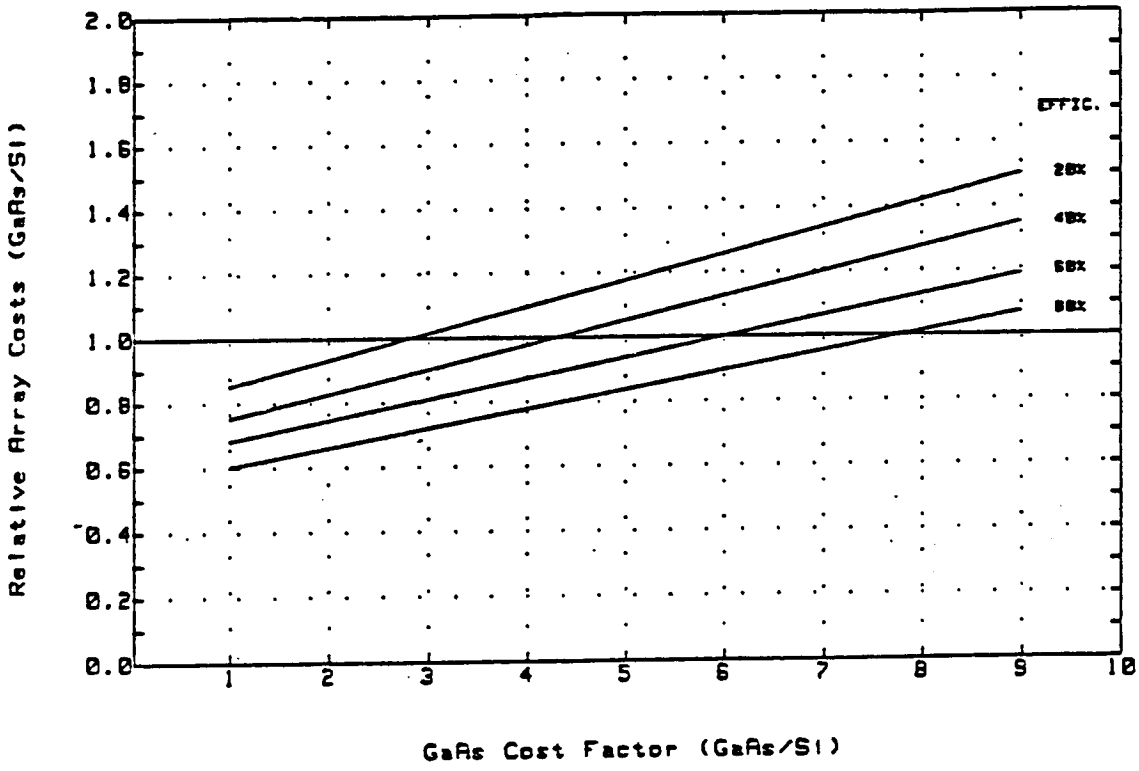

Figure 2.2.3-2 GaAs Array Cost as a Function of Efficiency

Table 2.2.3-2. Program parameters used in the GaAs Trade Study

Silicon Cells

1. Baseline cell quantity
2. Cell dimensions (cm)
3. Packing factor (%)
4. Total cost of the bare silicon cells ($)

Gallium Arsenide Cells

1. Percent increase in efficiency over silicon (%)
2. Cell thickness (cm)

General Factors

1. Shuttle launch capability (lb)
2. Cost of a shuttle launch
3. Total baseline cost of a silicon array ($)
4. Solar cell glassing costs ($)
5. Hardware reduction factor (%)
6. Total system mass for the baseline silicon array (kg)
7. Number of shuttle flights required for delivery of station-keeping fuel

In the model, the slope of the curve is driven mainly by the efficiency of the GaAs cell, and the crossover point if mainly driven by lifetime drag-fuel launch costs. As the efficiency of the GaAs (or multifunction cells, etc.) cell improves, the curve gets flatter, and the point of cost equivalence moves to the right along the abscissa.

It should be noted that no attempt has been made in this model to analyze the effects on the mechanical system and substrate material resulting from the heavier GaAs cells. Stronger and heavier materials may be required to meet substrate frequency requirements and would result in increased launch costs.

For the IOC configuration, gallium arsenide will not be cost-effective until the cells are 40% more efficient than silicon, and cost not more than 4.5 times as much as silicon cells. It is recommended to use silicon for the IOC configuration, switching to GaAs as the technology improves, and the costs decrease.

V2-223/6

2.2.3.3 Concentrating versus Planar Solar Arrays

The following summarizes the results obtained in comparing the planar baseline silicon IOC Space Station PV design to a similar design using gallium arsenide cells and high solar intensity cassengrainian reflector assemblies. A 10-year IOC design using Cassengrainian reflectors in an untruncated hexagonal design, was generated using solar cell data from GaAs production runs. In the trade, optical degradation values were used to evaluate the capability of the Cassengrainian design. GaAs cell data, and representing production lot capabilities (17.5% efficient, 1 sun) was used to determine circuit output when operated at a solar intensity of 88 suns. All known degradation factors, relative to both designs, were included to allow for a meaningful comparison of the two methods. The Cassengrainian design resuled in an array with a 0.86 packing factor, providing 80.5 W/m2 at 10 years, summer solstice. The required projected area for the Cassengrainian design is 22.4% larger than the current baseline planar design.

As a result of the above comparisions, the use of a high solar intensity, Cassengrainian reflector photovoltaic design should not be considered for use on the IOC space station. Other concentration scenarios (SLATS, Truncated Pyramidal, etc.) face similar constraints. Until GaAs cell efficiencies approach the 30% level, these designs will not be able to compete with the planar silicon design when one considers overall lifetime costs.

2.2.3.4 PV Cell Size

This trade study covers analysis of the sensitivity of the solar array recurring cost at beginning-of-life (BOL) to silicon solar cell size. The basic solar array considered for the analysis is the Lockheed deployable flexible planar solar array, whic uses a 5.9 x 5.9-cm wraparound silicon solar cell with a 150-um-thick cover slide. The major considerations used to complete the cell size study are as follows:

- Current SAFE solar array technology
- Constant array mass for constant BOL power outlet

- o Solar array recurring cost - electrical $300/W, total array $614/W
- o Exludes G&A charge on cell stack costs
- o Solar array operating temperature is +55°C (131°F) Cost of attaching cell stack to blanket is $30 per cell
- o Mechanical cost of solar array is constant for a given output power level
- o Electrical blanket cost is proportional to array area and is approximately constant for a given array output power.

The cost information for a filtered solar cell of 5.9., 8, and 10 cm square was obtained by quotation from Spectrolab, Solarex, and Applied Solar Energy Corp. A review of the cost data indicated the need to eliminate some quotes as "out-of-line" and then average the remaining quotes. These are presented in Table 2.2.3-3

Table 2.2.3-3
Sensitivity of Solar Array Cost to Solar Cell Size

Cell Stack Size (cm)	Approximate Cost ($)
5.9 x 5.9	86
8 x 8	143
10 x 10	235

The results of the analysis are shown in Figure 2.2.3-3. This Preliminary tradeoff shows that the larger size solar cells offer potential cost savings.

The major savings come from reduction of the number of piece parts which must be handled during the fabrication of the solar array.

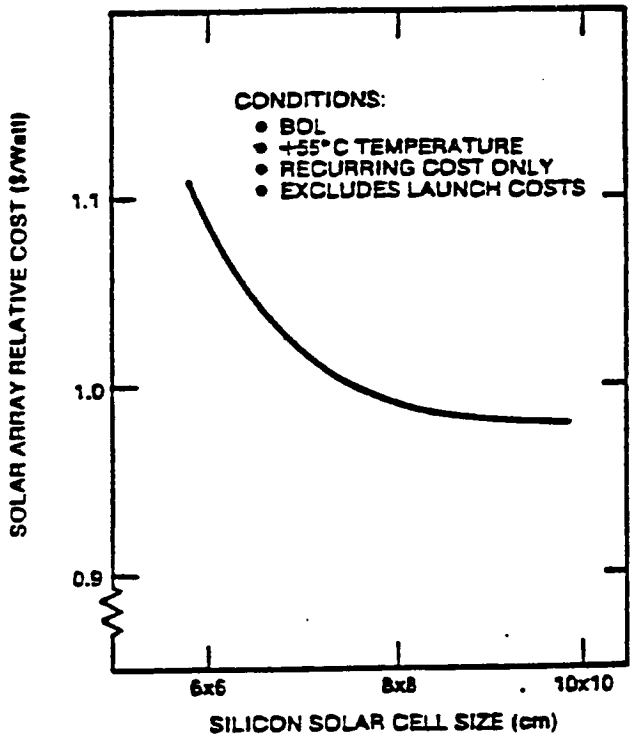

Figure 2.2.3-3 Solar Array Cost Versus Cell Size

Table 2.2.3-4 Advantages and Disadvantages of Three Solar Cell Sizes

Advantages	Disadvantages
5.9 x 5.9-cm Wraparound Solar Cell	
• Current technology • Existing solar array design • No configuration changes • Qualified array design • Flight proven array • Reduced nonrecurring costs • Current production • Low risk	• Higher total cell cost compared to larger cell sizes for a given power • More parts • Higher recurring cost
8.0 x 8.0-cm and 10.0 x 10.0-cm Pass-Through Solar Cells	
• Current technology • Fewer solar cells required for a given array power level • Reduced total array cost	• High nonrecurring costs • New design and configuration • Needs qualification • Wider panel size in both cases • Existing panel size accommodates fewer cells • Panel output voltage reduced to: 8 x 8-cm cell - ~98 V 10 x 10-cm cell - ~66 V • Not currently in production

However, variability in the manufacturer's solar cell cost data is such that any potential cost saving of the larger 10 x 10-cm solar cell versus the 8 x 8-cm cell is questionable. Table 2.2.3-4 summarizes the advantages and disavantages of the three cell sizes considered.

After a review of the advantages and disavantages presented in Table 2.2.3-4 it is recommended that the 8 x 8-cm cell be considered baseline for planar arrays. The consideration of full back contact versus gridded back transparent cell is presented in Subsection 2.2.3-3.

2.2.3.5 PV Cell Configuration

2.2.3.5.1 Solar Cell Thickness

The effect of solar cell stack thickness upon the relative in-orbit electrical cost of the solar array is shown in Figure 2.2.3-4. The solar array considered in the analysis was the LMSC deployable flexible planer array described earlier in this report. From the figure, it can bee seen that the thicker silicon solar cell comprising a 200-um-thick solar cell and 150-um-thick cover glass gives least in orbit EOL cost for a low earth orbit.

The assumptions used in performing the analysis are the following:

- Low Earth Orbit (LEO) STS Launch cost $7.5K/kg
- Solar array considered is LMSC's Space Station Design
- Solar array size is 10 kW at BOL with a 10-year orbital life operating at 55°C (131°F), active area 101 m^2 (1087 ft^2)
- Excludes nonrecurring solar array costs and all mechanical costs but included launch costs via STS.

The results of the analysis are presented in tabular form, in Table 2.2.3-5 with more detail than shown in Figure 2.2.3-4. Table 2.2.3-5 includes the intermediate cost and specific weight factors for each configuration addresses. Similar calculations for the beginning of life condition led to the same conclusions.

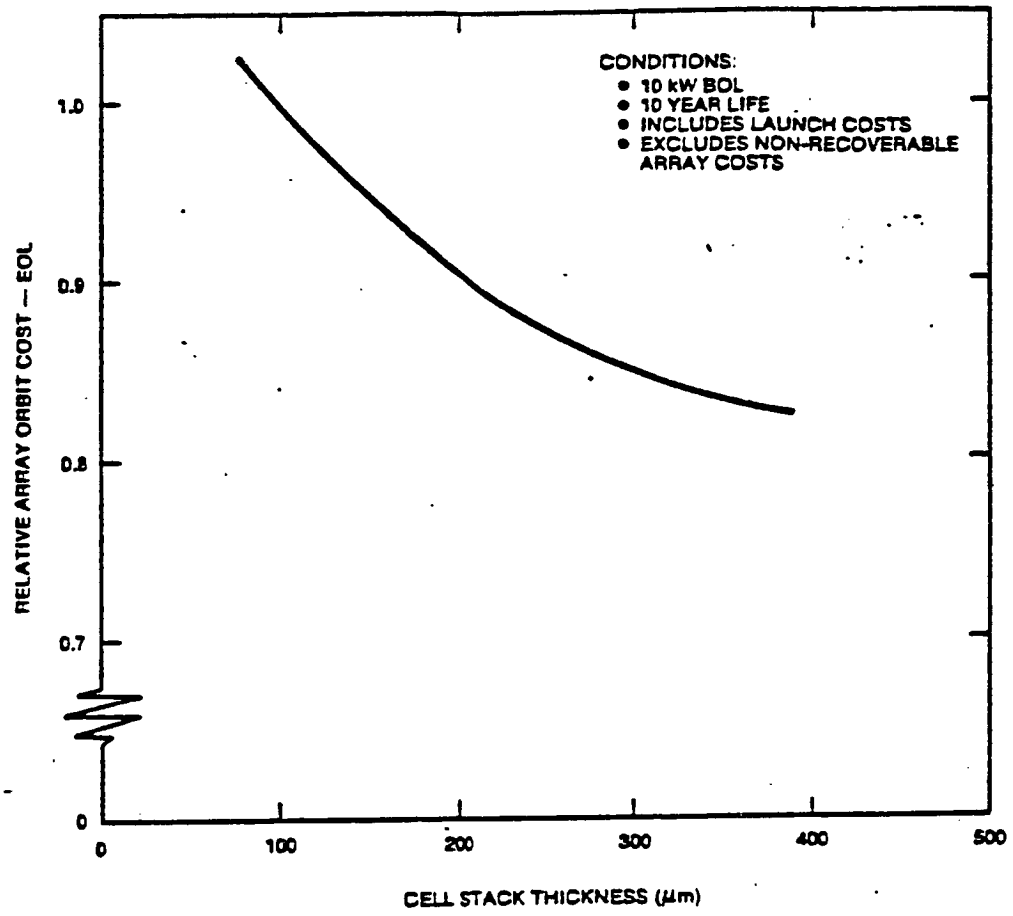

Figure 2.2.3-4 Solar Array In-Orbit Electrical Cost Versus Cell Stack Thickness

Table 2.2.3-5 Relative Costs of Varying Solar Cell Stack Thickness

Case	Solar Cell		Cover Thickness (μm)	Stack Thickness (μm)	Array Output (W/kg)	Electrical Cost ($/W)			Relative Cost
	Type	Thickness (μm)				Launch	IOC Fabrication	Total	
A	Silicon	50	50	100	116	65	500	565	1.0
B	Silicon	100	100	200	68	110	400	510	0.902
C	Silicon	200	150	350	50	150	319	469	0.83
D	Silicon	300	300	600	39	191	280	471	0.833

2.2.3.5.2 Transparent Solar Array Considerations

A trade study using two different types of 8 x 8-cm solar cells was also completed. They used a transparent (gridded back contact) solar cell on a transparent substrate (laminated apton), the other used a typical full contact cell on a nontransparent substrate such as might be used in an erectable design or in a design mandated by atomic oxygen degradation to polymer laminates. The major differences in the designs are the solar cell operating temperatures. The transparent cell bounded to a substrate that passes infrared energy operates at a lower temperature and requires fewer series cells. This design produces 0.86 W/m^2 (9.24 W/ft^2) at 160 V. A similar design using a solid substrate operates at a higher temperature and requires more solar cells in series. As a result, the power density is reduced to 0.77 W/m^2 (8.29 W/ft^2), a penalty of approximately 10% relative to projected array area.

The input parameters and assumptions are listed as two blankets per array, panel size about 0.37 x 4.6 m (1.2 by 15 ft), operating voltage nominal 160 V. The cell characteristics are listed as identical for each configuration except solar absorptance and Isc. The Isc of the transparent cell is 3% less than an equivalent BSR because of the single pass of electromagnetic radiation while the absorptance is 0.10 less.

The design factors used for the predicted end-of-life performance are typical for LEO of extended duration. The resulting designs are summarized in DR02. The lower operating temperature is, of course, the driver of the design resulting in an IOC configuration of 27,000 fewer cells, which, at $200/cell laydown, saves about $5 million.

2.2.3.6 Deployable versus Erectable Solar Array

A trade study has been performed to evaluate the advantages and disavantages of deployable and erectable solar array assemblies. In addition, various types of masts were included for the evaluation. The method used is to identify possible solar array systems that consider both rigid and flexible solar cell assemblies, deployable and retractable structures and include sequential as well as simultaneous implementation. The availability of masts from AEC Able and Astro are compared. Solar array wing assemblies are compared, costed, and four preferred systems selected.

A matrix of 16 different systems for solar array wings for the Space Station was evaluated. Options include masts, solar array substrates, construction on orbit and integration of the substrate to the mast. Many variations can be eliminated due to impractical or impossible combinations such as simultaneusly deploying a flexible blanket while erecting a boom, or erecting a felxible blanket. The remaining 9 options were studied and narrowed down to 4 candidate systems. Hardware was then chosen to best suit these systems.

Table 2.2.3-6 lists the advantages and disavantages of erectable and deployable wing systems. Generally, an erectable wing consists of a much simpler and less expensive mast but requires more EVA time to assemble or extend. The solar cells/substrate must also be integrated and extended to the mast which requires more EVA. Once operational, the wing would be very difficult to retract.

Deployable wings require minimum EVA to integrate to the main structure. Such systems are however more complex and costly to build and test. They can be deployed remotely and most can be retracted just as easily if needed.

Table 2.2.3-7 lists different methods of constructing masts on orbit and the corresponding hardware required. Construction methods range from erectable to deployable with many variations in between. At one extreme is a truly erectable boom where components are transported to space and assembled on location. This method has the advantage of very low cost parts but would required many hours of EVA to assemble. At the other extreme is a fully assembled mast which would deploy and lock upon command. Here, EVA is held to a minimum but manufacturing and test costs would be high. This method has been used extensively on spacecraft to date and is well established. Between these two extremes are variations which are possible better suited to Space Station requirements. Among these alternatives are:

- Erectable Bays--Instead of erecting or assembling a mast component by component, whole bays can be preassembled on the ground and collapsed to fit compactly in the shuttle cargo bay. On orbit, these bays could be unfolded and combined during EVA. The assembly would be much simpler and quicker than construction from individual struts and joints.

Table 2.2.3-6 Erectable Versus Deployable Solar Wings

Erectable Wings

Advantages	Disadvantages
• No deployment mechanisms	• Requires extended EVA
• Lower cost	• Requires separate installation of solar cell blanket/panels
• Lower weight	• No flight heritage
• Elimination of complex ground deployment tests	• Nonretractable
• Less complex/more reliable	
• No electronics/motors required for deployment	
• Smaller storage volume	
• Easily repairable	
• Launch load insensitive[a]	

Deployable Wings

• Can be retractable	• Larger storage volume
• Flight proven (i.e., SAFE)	• Heavier
• Can deploy solar cells simultaneously	• More complex
• Minimal EVA	• Harder to repair
	• Launch load sensitive

[a]AIAA-81-0043 "Primary Design Requirements for Large Space Structures," John M. Hedgepeth

- Extendable Mast--Taking the above concept a step further, a whole mast could be preassembled and extended during EVA or by the MSC. Even greater assembly time savings would be realized.

- Shuttle--Instead of using astronauts or the MSC to supply deployment force, a motorized deployer can be mounted in the shuttle cargo bay and used to erect each mast individually. This would reduce the complexity of EVA without dedicating costly deployment mechanism to each mast.

- Mechanism--Similar to SAFE, a motorized canister or similar mechanism deployment is built as an integral part of each mast. The stowed package is build as an integral part of each mast. The stowed package is mechanically and electrically integrated to the station structure. Deployment or retraction of each wing can then be initiated remotely.

- Two construction concepts were chosen as candidates: the erectable mast and the mechanism deployment. Mechanism-deployed masts have been used on numerous spacecraft and incorporate proven technology. To adopt existing systems to Space Station application, only minor redesigns are involved in most cases. These are also several kinds of masts which can be used with this concept. These will be discussed in detail.

Table 2.2.3-7

Construction Concepts and Associated Mast Systems

Erectable Components	Erectable Bays	Erectable Boom	Shuttle Deployment	Mechanism Deployment	Self Deployable
Tinker Toys	PACTRUSS	PACTRUSS	PACTRUSS	Articulated longeron	Continuous longeron
	Modular tower	Articulated longeron	FASTMAST	Continuous longeron	FASTMAST
			Continuous longeron	FASTMAST	
			Articulated longeron	STACBEAM	

The extendable mast concept has been chosen as the candidate for an erectable structure. Its construction on orbit is the least complex and requires the least EVA while still retaining the advantages of an erectable structure.

Based on these cost considerations, and the adequacy of performance and maturity of the continuous longeron mast, this technology is recommended for the Space Station solar arrays, to maintain a low-risk development program.

2.2.3.7 PV ORU Sizing

The solar array wing is, in general, an assembly of two blankets with a deployable mast. Although the blanket is composed of numerous panels, the replacement of individual panels is not recommended. The lowest level of replacement is the blanket box or mast canister ORU. During the preliminary design phase, the capability for removal/replacement of a stowed blanket, was determined to be an essential requirement, therefore the primary ORU was baselined. This will permit the removal and replacement of individual blanket boxes as necessary. The secondary level of replacement is the entire stowed wing. Figure 2.2.3-5 depicts the blanket and wing ORU's. The mechanical and electrical interface at the beta joint will be designed for ease of service. Major changes can most easily and safely be incorporated in ground facilities. Retractability is necessary for practical solar array replacement.

2.2.3.8 Battery Trade Studies

2.2.3.8.1 Station Battery Selection

Battery options for the Space Station were evaluated in order to arrive at a selection of the most cost-effective battery system for final comparison and trade with the RFCS. This trade was described originally in DR-19 submittal DP 4.3. Abbreviated descriptions of the battery designs are included here as background for the trade study. The candidates for IOC are:

- Ni-Cd
- IPV (individual pressure vessel) Ni-H_2
- Bipolar Ni-H_2

Designs of the key candidates at the time the trade was completed, are appended to this section.

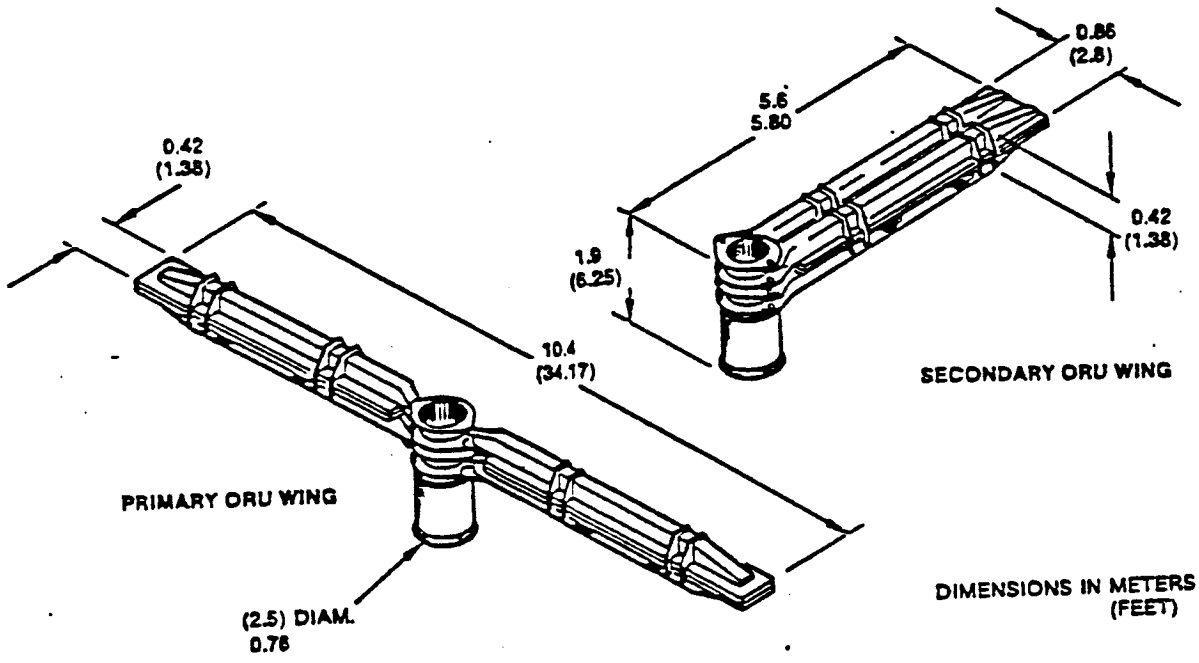

. Blanket Box (R-L) ORU

. Mast Canister ORU

Figure 2.2.3-5 PV System ORU Configuration

2.2.3.8.1.1 Technology Readiness and Development Risk

Potential technology readiness by late 1989, the expected design-freeze point prior to flight production, is a major consideration in the selection of the preferred Space Station battery options. The following discussions summarizes current and projected readiness status, and development risk.

Ni-Cd Battery. Space Ni-Cd battery technology is well-established and currently provides energy storage for the majority of spacecraft. It is produced in sizes up to 100 Ah in aerospace cell configurations. The current Space Station Ni-Cd battery design requires 125-Ah cells. Scale-up of the cell design from 100 to 125 Ah is considered a low-risk development, particularly if it is accomplished by increasing the width dimension only and leaving the height and thickness unchanged. Development of the Battery packs is also low-risk, because an extensive data base exists on the baseline pack design approach, as well as on successful scaling of this design with capacity. The battery assembly, incorporating 4 battery packs and 8 heat pipes, requires development based on current technology heat pipes and panel/heat pipe integration methods, which are considered low-risk and can be verified with mass and thermal pack simulators independent of the battery pack development. Overall, the development of the Ni-Cd battery assembly is considered low-risk, because no new technology is required and key items are developed along largely independent paths.

The only potential risk results from uncertainties about consistent Ni-Cd cell quality, which has adversely affected several space programs over the last few years. The dependance of current aerospace Ni-Cd cell production on a larger commercial production line will perpetuate a certain level of rish in this area. However, corrective actions taken by the manufacturer in response to the recent problems should reduce this risk considerably.

IPV Ni-H_2 Battery. The IPV Ni-H_2 battery is expected to be higher-risk option than the Ni-Cd battery. While development of the large 220-Ah Ni-H_2 cells is well underway and no significant problems are apparent, the scale-up being accomplished here is greater than that required for the Ni-Cd cell. The individual elements of the cell are, however, rather straight-forward extrapolations of existing components and are therefore low-risk. The

significant change is the dimensional scale-up, for which design requirements are well understood and lend themselves to adequate analysis prior to manufacture. Successful fabrication of single-stack 4.5-in diameter cells has already been completed, and dual-stack cells are expected to be complete by IRR. Prior to phase C/D start, a second genertion of cells will have been demonstrated. Life testing of smaller cells at NWSC in Crane, IN is starting this year and is expected to yield valuable data for LEO life projection and further design optimization. If IPV Ni-H_2 batteries are selected at IRR, representative full-size Space Station cells could go on test at NWSC as early as September 1986 to develop a 3-year data base by the start of flight battery production and 5.5- to 6-year data base at launch. The battery assembly is a relatively straightforward structure incorporating heat pipes and cells. The risk areas involve mechanical stability during cell pressure cycling, and thermal interface quality. Elements of this design are expected to be demonstrated in 1986 Phase B advanced development in a battery module incorporating the large cells.

Bipolar Ni-H_2 Battery. The bipolar Ni-H_2 system is currently being developed by NASA-LeRC as well as Ford Aerospace and Yardney. Demonstrations of subscale hardware and battery stacks with realistic thermal management have been accomplished, and demonstration of full-size cells in sort stacks is planned for the near future provided development funding continues. While many components are very similar to those used in IPV cells the manner in which they are used places somewhat different demands on these components in some cases. Also, the technology for full-stack thermal management and containment must be demonstrated at high voltages, as with the RFCS. At the currently planned level of funding for development of the bipolar Ni-H_2 battery it is unlikely that it will be ready for IOC. Aggressive development could result in IOC readiness, although the life test data base as a full system would be somewhat limited, and development would be more costly than that of the IPV System.

Summary. Table 2.2.3-8 summarizes in a semiquantiative and subjective manner the estimated risk associated with the development of the three systems form an expected state of readiness at the start of phase C/D. The values for individual elements represent our estimate, based on similar past developments, of the probability of not unanticipated problems occurring in that element, recognizing that no area is entirely immune. Based on this assessment one can

expect the probability of problem-free development to be about 70, 60 and 45% respectively for the Ni-Cd, IPV Ni-H_2, and bipolar Ni-H_2 systems. Contingencies may be applied to success-oriented development cost estimates based on these probabilities, in order to derive probable real costs of development.

The risk estimates for the Ni-Cd and IPV Ni-H_2 systems suggest that both systems can be developed in the required time assuming a minimum 15% risk tolerance per year. The estimate for the bipolar Ni-H_2 battery indicates that development for IOC as a sole option would entail some risk, but for growth its advantages can be realized at minimal risk.

2.2.3.8.1.2 Cost

Costs of the Ni-Cd and IPV Ni-H_2 options have been estimated for development and production. Impacts of these options on costs of other sysems (primarily PGS) and launch costs were also assessed. Assumptions are stated below. Since the bipolar Ni-H_2 battery is a high-risk IOC option has not been included in this cost comparison as it is clearly more costly to develop than the other alternatives and therefore not alikely IOC selection.

Ni-Cd Battery Development Program. The Ni-Cd battery development effort would cover the following hardware.

- Production and test of 25 development cells. Production and test of 1 prototype battery pack Production and test of 1 qualification battery pack
- Production and test of 1 prototype battery assembly with thermal/mass simulated packs.
- Production and test of 1 qualification battery assembly with 1 qualification pack and 3 thermal mass models.
- Production and test of 100 cells for NASA tests and evaluation.

Table 2.2.3-8 **Risk Assessment of Battery Option Development**

Risk Area	Ni-Cd	IPV Ni-H_2	Bipolar Ni-H_2
Cell	(0.859)	(0.759)	(0.674)
Positive Electrode	0.98	0.95	0.95
Negative Electrode	0.95	0.99	0.99
Separator/Electrolyte	0.99	0.95	0.95
Mechanical Support	0.99	0.97	0.98
Recombination Mgmt	0.99	0.95	0.90
Electrolyte Mgmt	0.98	0.98	0.90
Conduction Path	0.99	0.98	1.00
Thermal Management	0.98	0.98	0.95
Pressure Containment	(0.960)	(0.960)	(0.951)
Container	0.98	0.98	0.98
Seals	0.98	0.98	0.97
Battery. Pack/Stack	(0.970)		(0.857)
Mechanical	0.99		0.95
Thermal	0.99		0.95
Electical	0.99		0.95
Battery Assembly	(0.922)	(0.884)	(0.864)
Mechanical	0.99	0.95	0.98
Thermal	0.95	0.95	0.95
Electrical	0.98	0.98	0.98
Battery System	(0.941)	(0.941)	(0.951)
Integration	0.98	0.98	0.99
Operation	0.98	0.98	0.98
Maintenance	0.98	0.98	0.98
Overall Probability			
Problem-Free	0.694	0.606	0.476
Problems	0.306	0.394	0.524
Relative Risk	1	1.25	1.7

Ni-H2 Battery Development Program. The Ni-H_2 battery development program would cover the following hardware:

- Production and test of 40 development cells
- Production and test of 1 prototype battery assembly
- Production and test of 1 qualification battery assembly
- Production and acceptance test of 1 life test battery assembly
- Production and test of 100 cells for NASA test and evaluation

Solar Array Cost/Mass/Drag: Costs associated with solar array impacts were conservatively estimated as:

- Solar array electrical costs: $ 350/W Solar array electrical mass: 18.43 g/W Solar array drag cost: 123/W-year.

Launch Costs. The launch cost ground rule used is (to 270 n.mi orbit):

- Launch cost: &7040/kg

Cost Comparison. Table 2.2.3-9 shows that cost comparison between the Ni-Cd and IPV Ni-H_2 system is lowest in direct cost by about $30M, which primarily represents launch cost differences. Solar array IOC cost impacts are about a $10M reduction for both options with respect to a 60% efficient RFCS. Drag-related cost compared to those for a 60% efficient RFCS are about $2.5M/year lower, for a total reduction of $12.5M for the expected 5-year lifetime for these systems.

Development and production costs were estimated independent of the RCS PRICE model by a "bottoms-up" approach based on Ford Aerospace experience in developing advanced space battery systems as well as cell costs from ROM quotes by cell manufacturers or derived from manufacturer's current price lists. Costs do not include life tests conducted by NASA.

Table 2.2.3-9 Battery Option Cost Comparison

Parameter	IPV Ni-H_2		Ni-Cd	
	Value	Cost ($\$10^6$)	Value	Cost ($\$10^6$)
Mass	4370 kg		8680 kg	
Volume	12.5 m^3		9.65 m^3	
Cost				
Development[a]		14		10
Production[a]		19		28
Launch		31		61
Subtotal		64		99
IOC cost versus 60% RFCS				
Array power	(20.3 kW)			(20.6 kW)
Array mass	(374 kg)			(380 kg)
Array cost[a]		(7.1)		(7.2)
Launch cost.		(2.6)		(2.7)
Subtotal		(9.7)		(9.9)
Drag-related costs versus 60% RFCS		(2.5)/year)		(2.5)/year)
For 5-year life		(12.5)		(12.5)

[a]Costs are exclusive of prime contractor G&A and fee

The somewhat higher development risk for the Ni-H_2 battery is reflected in the higher development cost. Additional margin could be added to allow for unanticipated problems, but this margin would not remove the significant cost advantage with respect to Ni-Cd batteries.

We conclude that based on cost the IPV Ni-H_2 sysem is the preferred battery option for the Space Station.

2.2.3.8.1.3 Other Factors

Additional factors which may affect the selection of a Ni-Cd or IPV Ni-H_2 battery system for the station are performance, reliability, life, maintance, commonality, contingency capability, operations, controls and data requirements, etc. In most of these areas the systems, as configured, provide essentially equal performance.

Electrical performance is similar because of the battery string sizing and the fundamental similarity of the electrochemical behaviors. Reliability of the systems is similar due to the tolerance to cell shorting in the large series strings. The parts count in the Ni-Cd battery system is considerably higher, and therefore more random failures may be expected, but the high level of replication minimizes the impact of failures. Life expectancy is equalized by the selection of appropriate depth of discharge levels.

Maintenance of either system is essentially not required. Periodic reconditioning may be beneficial for the Ni-Cd system, but is not absolutely required. Reconditioning of the Ni-H_2 battery does not appear to be required, but may be done if desired. Both systems will have let-down reistors to permit individual assembly discharge for increased maintenance safety, and these resistors could be used for reconditioning.

Commonality between the station and the platform is desirable and can be achieved to an extent with either system. In the case of Ni-Cd some hardware commonality is practical and design commonality would be significant, although the capacities would be 124 Ah and 100 Ah, respectively. In the case of Ni-H_2 commonality can be achieved at the component design level for the cells, and for heat pipes. An additional platform Ni-H_2 battery option is

the use of the same cell as on the station in a 24-cell assembly with voltage boosted to the 16- V level. This option would achieve almost complete commonality between station and platform batteries.

Contingency capability is provided by both batteries. The Ni-Cd option provides this capability with considerably more margin, however, than the Ni-H_2 option, because its nominal DOD is low.

Operational requirements for the two systems are virtually identical. Charge management techniques are the same. The Ni-H_2system offers the potential of state-of-charge verification via pressure sensing, although the coulometry method of charge management would obviate it for normal operations. It may be of interest for special situations such as contingency.

Controls and data requirements are also similar, with a requirement of approximately twice the voltage data quantity for the Ni-Cd option because of the large number of cells. Current and thermal control sensing requirements are similar.

Impacts on other subsystems vary. The Ni-Cd options requires a larger quantity of charge and discharge regulators and associated switch gear than the Ni-H_2 system. This will increase cost of production and test of source PMAD equipment. Thermal subsystem impacts are similar, since time-averaged dissipation levels are about the same. Instantaneous dissipation for the Ni-H_2 system is somewhat higher on discharge. With the lower thermal mass this yields either a larger temperature swing or requires a slightly larger radiator.

Modularity (number of ORUs) for the Ni-Cd and Ni-H_2 batteries are 16 and 20, respectively. This means that the on-board spare requirement, if temporary operation with one battery out is undesirable, represents only 5 to 6% of the total system mass: 211 kg for Ni-H_2 and 530 kg for Ni-Cd. If on-board sparing is desired, some relative penalty accrues to the Ni-Cd system.

2.2.3.8.1.4 Summary and Conclusion

The IPV Ni-H_2 battery system is much lower in mass, much lower in 2 launch cost as a result, and is slightly less expensive to develop and produce

than the Ni-Cd system. Other factors are generally not discriminators between the systems. Development risk for the Ni-H_2 battery is somewhat higher, but is well outweighed by the cost savings resulting from its mass advantage. The Ni-H_2 battery system is therefore selected as the preferred battery option for the Space Station.

2.2.3.8.1.5 Space Station Ni-Cd Battery

The Space Station Ni-Cd battery system option consists of 16 batteries. A pair of batteries is assigned to one source bus. Each battery is comprised of a support plate on wich four assemblies are mounted, each containing 26 cells of 124-A.h capacity each. Heat pipes embedded in the honeycomb plate collect battery waste heat and transport it to a contact heat exchanger that is clamped against a cold plate in the utility center coolant loop. In each utility center, eight batteries are placed in a rack-type mounting configuration.

Table 2.2.3-10 summarizes key battery design and performance parameters for a description of the station and platform battery assembly refere to DR02.

2.2.3.8.2 IOC PV Platform Battery Option Selection

Battery options for the platforms were evaluated in order to arrive at a selection of the most cost-effective battery system for final comparison and trade with the RDCS. Battery options were described in previous DR-19 submittals DP 4.1 and DP 4.2 and DP 4.3 and DR02. Abbreviated design descriptions are included here as background for the trade study. The candidates for IOC are:

- o Ni-Cd
- o IPV (individual pressure vessel) Ni-H_2
  - Option 1: Station-derived, low voltage
  - Option 2: Platform-specific, high voltage
- o Bipolar NI-H_2

The platform-specialized (Option 2) Ni-H_2 battery is selected based on overall lower cost compared with the Ni-Cd option, the fact that it appears no

Table 2.2.3-10 Station Ni-Cd Battery Characteristics

Characteristic	Value
System configuration	
Nominal power rating (kW)	86.2
Total number of battery assemblies	16
Assemblies per utility center	8
Capacity per assembly (Ah)	125
Packs per assembly	4
Cells per pack	26
Total cells	1664
Electrical	
Average discharge voltage (V)	127.9
Average charge voltage	150.8
Average discharge current per battery (A)	42.1
Peak charge current per battery (A)	30.1
Nominal depth of discharge (%)	20
Mechanical	
Mass per cell [kg (lb)]	4.04 (8.91)
Mass per battery pack [kg (lb)]	121 (267)
Mass per battery assembly [kg (lb)]	530 (1168)
Total ESS mass [kg (lb)]	8680 (19136)
Cell dimensions [cm (ft)]	20.6 x 20.1 x 3.2 (0.68 x 0.66 x 0.10)
Battery pack dimensions [cm (ft)]	56 x 50 x 22 (1.84 x 1.64 x 0.72)
Battery assembly dimensions [m (ft)]	1.30 x 1.17 x 0.30 (4.27 x 3.84 x 1.0)
Battery system dimensions per utility center [m (ft)]	1.40 x 1.30 x 2.65 (4.59 x 4.27 x 8.7)
Total battery system envelope volume [m^3 (ft^3)]	9.65 (341)
Thermal	
Operating temperature range (°C)	0 to 20
Thermal mass (Wh/°C)	2080
Average dissipation on discharge (kW)	15.84
Average dissipation during recharge (kW)	4
Heat pipes per battery assembly	8
Heat pipe capacity (ea.) (W)	300
Total heat pipe rejection capacity (kW)	38.4

different in development risk, and the absence of any other discriminators. This selection is valid whether or not there is a parallel Ni-H_2 battery development program for the space station. The reduced assembly-level redundancy associated with the station-derived Ni-H_2 system makes it less desirable from an apparent system reliability point of view. However, it is recommended that the reliability of this option be investigated in some more detail if the Ni-H_2 battery is selected as the Station Energy Storage. For full details of the baseline platform option refer to DR02.

2.2.3.8.3 Battery and Array Size Selection

The key trade study performed in support of the PV subsystem definition was concerned with the sizing of the array power and battery capacity. The major consideration was the optimization of array and battery for the polar platform while meeting the station requirements in a cost-effective manner. Emphasis has been placed on polar platform optimization to minimize first-launch mass.

In addition to the general requirements stipulated in the Space Station Program Power System Definitions and Requirements, specific ground rules used for the battery and PV array size trade are:

- Minimize polar platform first-launch and IOC EPS mass
- Identical assemblies on platform and station for source hardware (strict commonality)
- The platform carries one redundant battery at first launch and IOC
- The platform battery DOD is 35% maximum with one battery to
- The station must have an even number of batteries, but carries no redundant batteries
- Station battery DOD is 35% maximum with all batteries working

In addition to these criteria, the following are considered as goals:

- o The IOC platform has at least three batteries plus on redundant battery
- o Station PV nominal power capability of 25 kW at user input plus 1 kW for PMAD processors at 3 years in orbit
- o Minimize PV subsystem mass on the station

2.2.3.8.3.1 Approach

Following detailed definition and refinement of array degradation factors for the worst-case altitude conditions for the polar platform and the station, the power capability of array panels for the 10-year polar orbit case and 3-year station orbit case were determined. A simple linear mass model equation was used for one array wing:

Wing mass = 181.2 kg + 5.5 kg/(panels/blanket) and for one battery:

Battery mass = 72 kg + 2.4 kg/Ah

These models have good validity in the ranges of interest

The peaking requirements on the platform permit variation of depth-of-discharge carry-over to subsequent cycles, so long as full recharge is achieved at the completion of the two peaking orbits and two make-up orbits. Larger arrays minimize this carry-over, thus reducing the battery size required to maintain a maximum 35% DOD. Smaller arrays necessitate increased battery size.

Total battery capacity requirement for the station is a function of array capability. Since the platform-optimized array may not meet the station PV power goal of 25+1 kW, the batteries are not necessarily sized to support 25+1 kW, but rather the actual capability of the PV system up to 26+1 kW.

2.2.3.8.3.2 Trade Summary

Capacity Range. Potentially viable battery capacity options cover the range of 30 to 120 Ah. However, the platform redundancy considerations result in significant penalties at the very large capacity sizes. Thus, capacities above 80 Ah were effectively eliminated from consideration. Below about 50 Ah capacity, the quantity of batteries on the station becomes quite large and this begins to present significant cost penalties. Since appropriate redundancy levels for the platform do not demand batteries smaller than 50 Ah, the lower limit was set at that level for further trades. The viable range of 50 to 80 Ah was selected.

Array/Battery Trade. Figure 2.2.3-6 shows the mass trade for 46 and 48 panel arrays and the selected parametric range of battery capacities. The mass figures represent the array wings, batteries, and the power-independent mass of the charge and discharge power converters (the power dependent part does not vary with capacity selection). The sawtooth shape of the curves reflects the modularity of the batteries; mass increases with capacity as batteries are increasingly oversized with respect to the need, until the point is reached where smaller whole number of batteries fits the requirement (a whole even number in case of the station).

Array Size Selection: Only in the case of the IOC platform would a system with a 48-panel array be potentially lighter than a 46-panel system over a small range of battery capacities. In that range, there would be overall mass penalties on the first-launch platform and the station. with the first-launch platform being particularly mass-critical, the 46-panel array was selected as common baseline for the platform and the station, even though the station PV power capability does not quite reach the output power goal of 25+1 kW.

Battery Capacity Selection: Figure 2.2.3-6 illustrates the following potential capacity selection (46-panel case):

- 55 Ah - minimal first-launch platform mass
- 58 Ah - low station mass

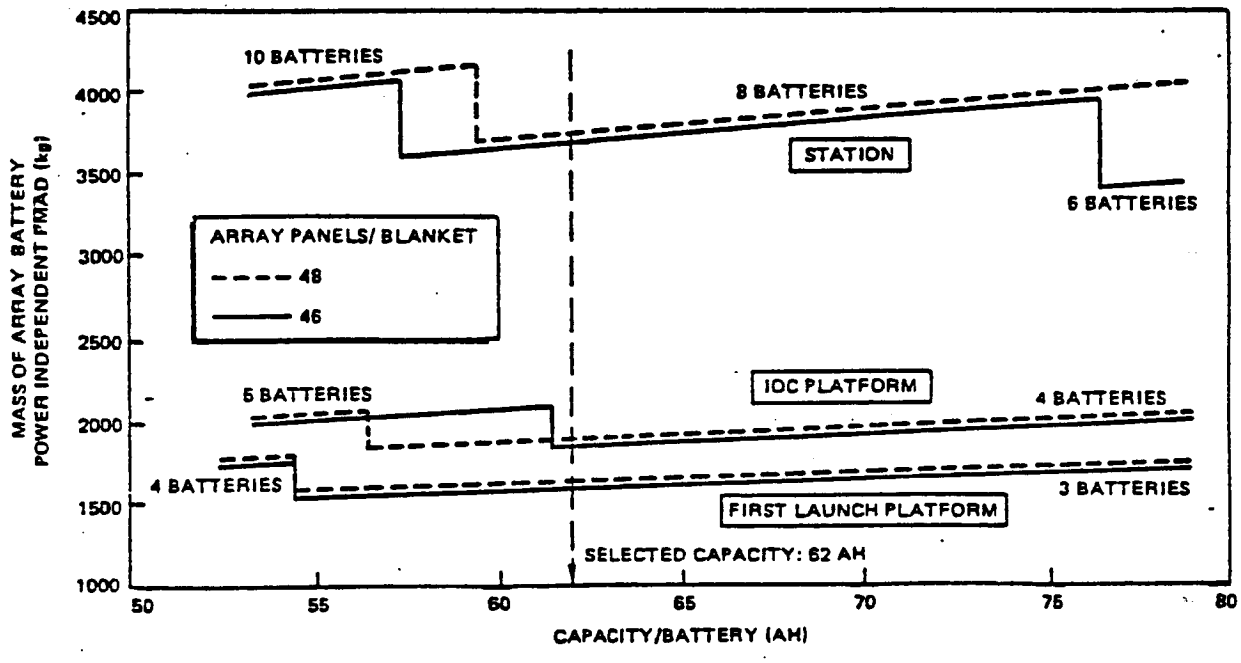

Figure 2.2.3-6 Battery Capacity Sizing Trade

- o 62 Ah - minimal IOC platform mass

- o 77 Ah - minimal station mass, minimal total installed mass

The 77-Ah option appears attractive, but the first-launch platform mass penalty is large. The 55-Ah capacity is best for first-launch but yields large penalties on IOC platform and station. The 62-Ah capacity, which provides low total installed mass with minimal added mass on the first-launch platform, is an attractive compromise. The 62-Ah batteries are therefore selected as baseline.

Battery Cell Diameter: Options are the conventional 3.5-inch diameter Ni-H^2 cells versus the more recently demonstrated 4.5-inch versions. The 4.5-inch cell, while nearly equivalent in maturity to the smaller size, is not mass-effective below about 90-100 Ah capacity. Since platform redundancy requirements force the selection of the cell capacity well below this level, the 3.5-inch diameter technology is the logical choice.

Battery Voltage and Modularity: Options are voltage levels optimally matched to the source bus voltage, and voltage levels that provide the opportunity for commonality with lower-voltage space station elements, such as the Mobile Servicing Center (MSC) and related systems such as the OMV. The former would require approximately 100 cells in series, split in two or more manageable series assemblies. The latter could be implemented with a modular battery assembly with 22 to 23 cells. Four of these in series (88 to 92 cells) would serve station and platform, and a single assembly would be compatible with low-voltage (MIL-STD-1539) systems.

The modular approach does not appear to present significant cost penalties, since practical constraints already dictate a level of physical modularity for the 100-cell batteries. Using a 23-cell modular design approach, battery development costs would be virtually eliminated for the low-voltage systems, so that the overall cost of energy storage hardware for the program could be reduced. Therefore, a 23-cell battery assembly has been baselined as the building block for the space station and associated batteries.

2.2.3.9 Capillary Pumped Loop Thermal Control System Study

V2-223/28

2.2.3.9.1 Introduction

The baseline design of the integrated thermal control (ITC) system for the PV modules is described in section 2.1.1.5 of DR-02. The mechanically pumped two phase (MPTP) thermal transport system was selected. A study was performed in order to compare the MPTP system with the capillary pumped loop (CPL) concept. Both are two phase heat transport systems using ammonia as the working fluid. The primary difference is that the MPTP design incorporates a motor driven pump, while capillary action provides the pumping power in the CPL system. The conclusion was that, although the CPL system is better from a technical standpoint, commonality with the WP-02 thermal transport system favors the MPTP design.

2.2.3.9.2 Description Of CPL System

The ITC, shown schematically in Figure 2.2.3-7, is a redundant capillary pumped loop (CPL) system which uses ammonia as the working fluid. Alternate independent capillary pump evaporators are manifold to separate, independent flow loops. The capillary pumped loop design is based on the CPL technology developed by the OAO Corporation, Greenbelt, Maryland. The OAO cold plate provides heat acquisition from the battery or PMAD electronics. Each cold plate consists of aluminum honeycomb containing the redundant axially grooved aluminum evaporators. A capillary evaporator pump is shown in Figure 2.2.3-8. A porous wick provides the required capillary pumping mechanism. The heat flow path from the batteries and PMAD electronics to the CPL cold plate is part of the system utility plate, which also contains interfaces for the transfer of data and power from the ORU's to other parts of the station.

2.2.3.9.3 Performance Definition

The thermal rejection system has been sized for the orbital average peak heat rejection requirement of the battery, despite the fact that there is considerable thermal mass in the batteries. The PMAD heat rejection is based on the maximum heat rejection of each ORU and the maximum number of ORU's that are operational at any one time. For a single module, the resulting total heat rejection required is 6.0 kW. The system is designed to reject this amount of

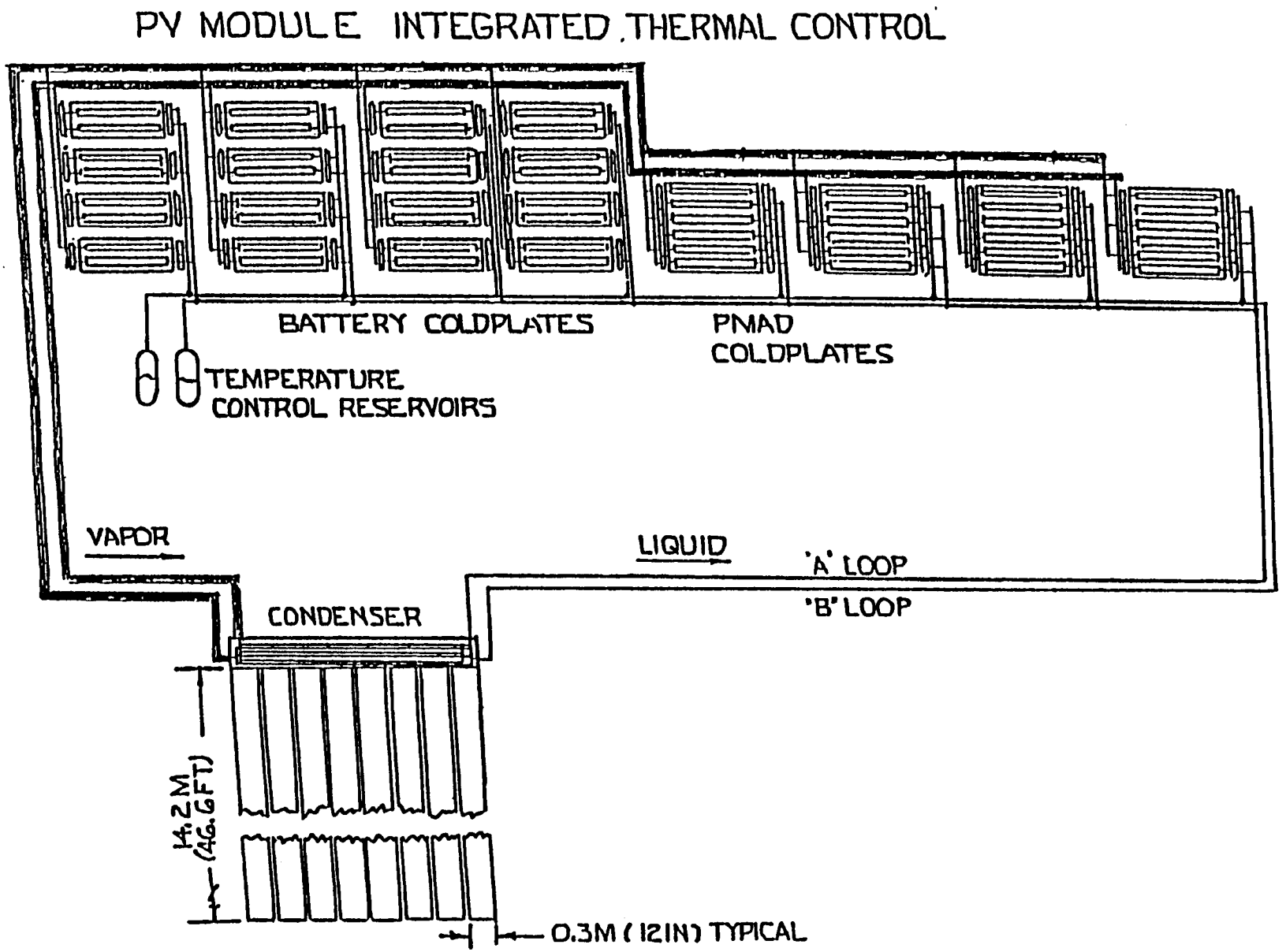
PV MODULE INTEGRATED THERMAL CONTROL
BATTERY COLDPLATES
PMAD COLDPLATES
TEMPERATURE CONTROL RESERVOIRS
VAPOR
LIQUID
'A' LOOP
'B' LOOP
CONDENSER
14.2M (46.6FT)
0.3M (12IN) TYPICAL

FIGURE 2.2.3-7

heat with the CPL cold plates at $2^{o}C$. Selection of this cold plate temperature assures that the nominal 5 ± 5 C temperature is maintained at the batteries under all but contingency or failure conditions.

A two phase capillary pumped heat transport loop using ammonia as the fluid is used to collect and transport the heat from the PMAD and battery cold plates to the radiator system.. A schematic of the capillary pumped loop design is given in Figure 2.2.3-9. This design has the advantage of requiring no moving parts and little power. The heat load on the cold plate evaporates the ammonia in a porous which structure. The vapor is then condensed in the radiator heat exchanger. The capillary forces in the porous wick provide the pumping power to return the liquid to the capillary pump where it is again evaporated. A temperature controlled reservoir provides ammonia to flood the pumps for initial start up, insures that they are constantly receiving liquid at the inlet, and controls the temperature and pressure at which the loop operates. Anisolator consisting of an annulus for liquid flow and a porous wick similar to that in the pump prevents the depriming of one pump in the parallel flow arrangement from affecting the operation of the other pumps. In the event of depriming of an evaporator pump, or of a sudden change in the thermal load on one or more pumps, the reservois control restores the CPL system to a stable operating mode. These operating characteristics have been demonstrated by OAO Corporation and NASA GSFC under both ADP programs and for WP-03 platform thermal control. Two engineering units, each capable of rejecting 6.3 kw of heat over a 10 meter transport distance, have been built and tested extensively. These tests demonstrated the transport limit, heat load sharing between evaporators, liquid inventory and temperature control by the reservoir, pressure priming under heat load, the ability of legs of the condenser to automatically shut down when they become too hot, and isolation of a single deprimed evaporator. Two smaller CPL systems have been flown on shuttle on STS 51-G (6/85) and STS 61-C (1/86). Flight test results obtained during zero-g operation were almost identical to results of the same tests performed on the ground. From experience gained with these models, a vapor line diameter of 1.0 in and a liquid line diameter of 0.5 in were selected for the CPL system in each utility center. The maximum capillary pumping head developed will be approximately 0.5 psi.

CAPILLARY EVAPO...TOR PUMP

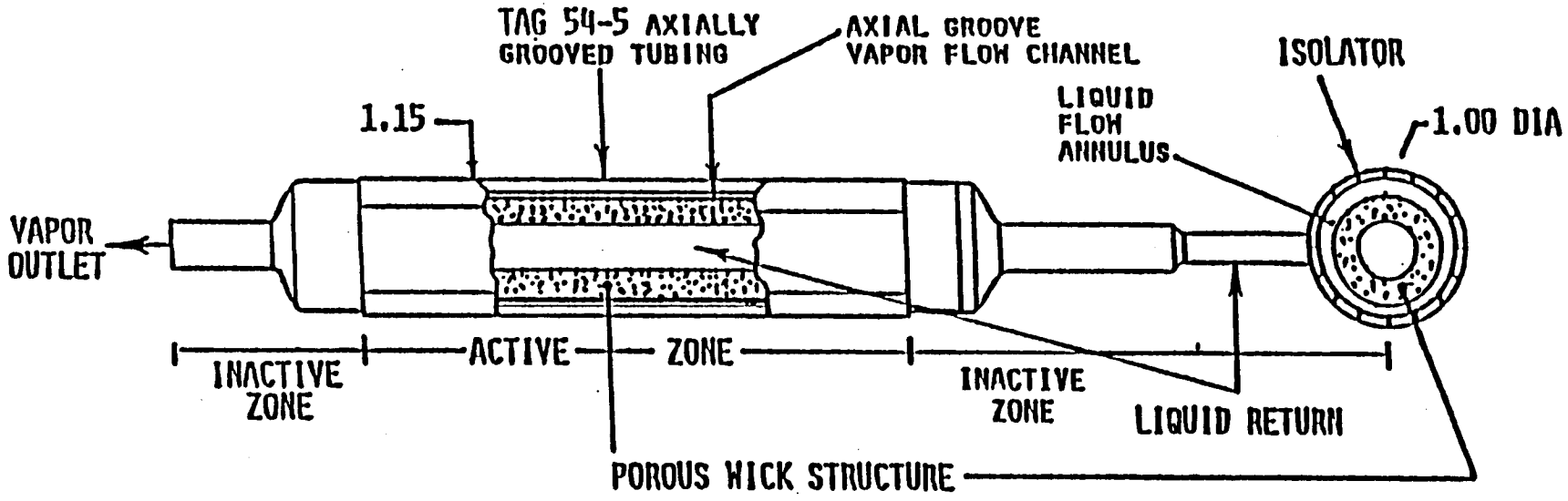

FIGURE 2.2.3-8

CAPILLARY PUMPED LOOP SCHEMATIC

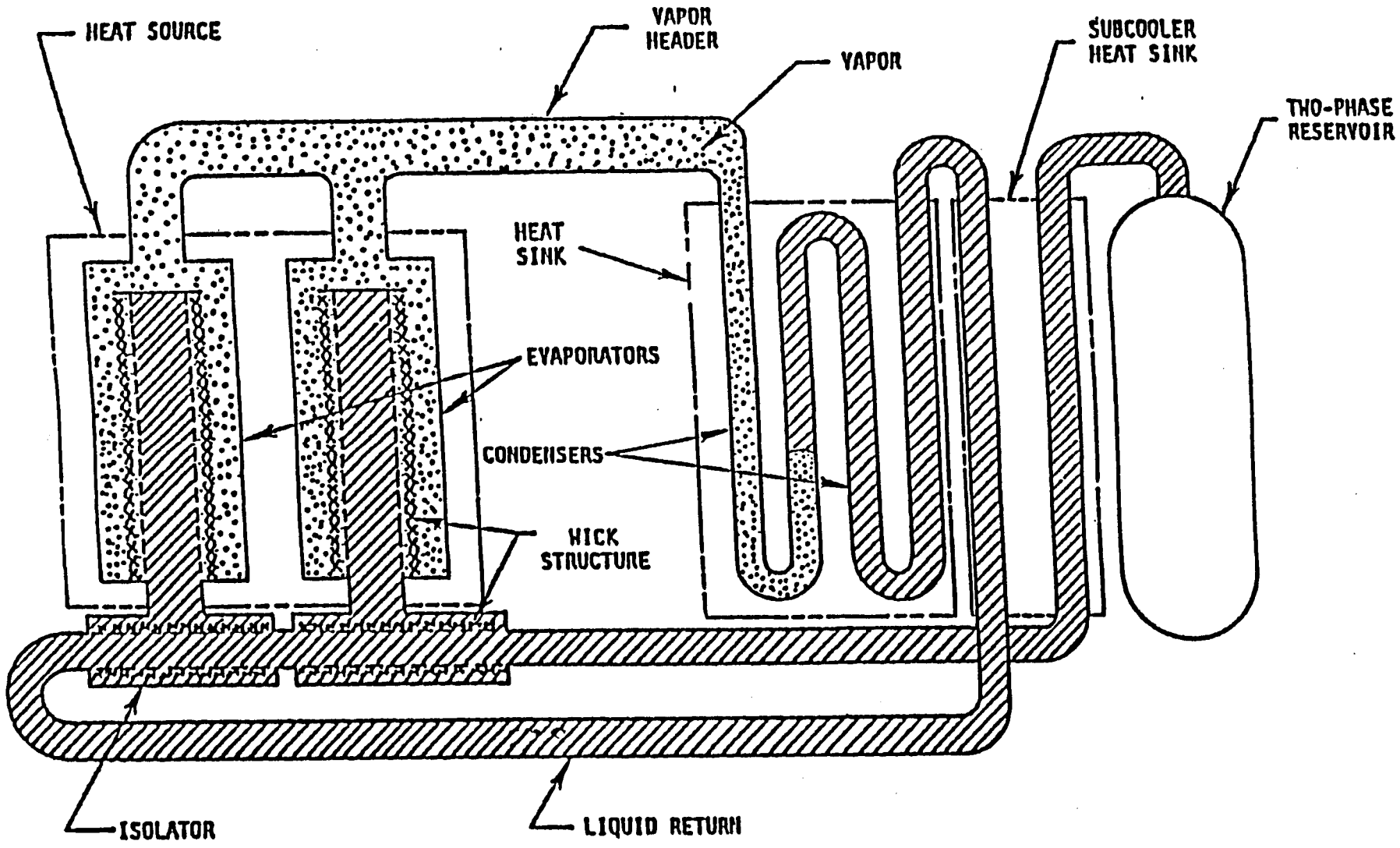

FIGURE 2.2.3-9

2.2.3.9.4 Conclusion

The performance of both the MPTP and CPL systems has been demonstrated in testing at one g. In addition,. two CPL systems have flown in the payload bay of the shuttle. These units verified that the performance of the CPL design in space is the same as on the ground. The MPTP design has yet to be flight tested. The CPL concept is inherently self controlling, and the absence of any moving parts makes it more reliable and less complex. The MPTP design has been selected as the WP-02 thermal transport system, due in part to the fact that the thermal transport distances inboard of the alpha joint are much longer than any that have been demonstrated using CPL. If the mandate to maximize commonality is overriding, the MPTP design will be favored.

V2-223/31

2.2.3.9.4 Conclusion

The performance of both the MPTP and CPL systems has been demonstrated in testing at one g. In addition,. two CPL systems have flown in the payload bay of the shuttle. These units verified that the performance of the CPL design in space is the same as on the ground. The MPTP design has yet to be flight tested. The CPL concept is inherently self controlling, and the absence of any moving parts makes it more reliable and less complex. The MPTP design has been selected as the WP-02 thermal transport system, due in part to the fact that the thermal transport distances inboard of the alpha joint are much longer than any that have been demonstrated using CPL. If the mandate to maximize commonality is overriding, the MPTP design will be favored.

2.2.3.10 Energy Storage Trade Study

The IPV NiH_2 battery system was selected over the regenerative fuel cell (RFC) for supplying EPS energy storage. The primary factors in this trade decision were lower cost, greater technical maturity, and commonality considerations. The IPV NiH_2 technology and operational risks are relatively low due to the mature technology base and the availability of back-up cell vendors who have supplied proven reliable space battery systems and have an understanding of operational requirements and techniques. A key determinant in the battery selection was the baselining of a hybrid EPS and PV platforms. Limiting the maximum quantity of PV on the station to 25 kw, with growth by addition of SD modules, nullified the advantages of RFCs which were particularly well suited to a station with PV growth. In addition, commonality with the platform was an important consideration and was maximized by selection of batteries for energy storage.

2.2.4 SD Subsystem Trades

2.2.4.1 Concentrator Trade Studies

2.2.4.1.1 Structure Trades

A preliminary structure dynamics design analysis and trade study in support of the Solar Dynamic (SD) concentrator, interface structure and fine pointing controls trades was completed. The objective of the analysis was to evaluate novel concentrator fine pointing mechanisms and interface structure concepts in terms of structural dynamic performance and system mass characteristics. Other criteria such as cost were excluded from this analysis. The specific goal was to evaluate the configurations with respect to mass and coupled structural vibration modes. Modal frequency constraints ($\geq$ 1 Hz) were derived from the desire to separate structural modes from the fine pointing control loop bandwidth (0.5Hz) by a factor of two, to preclude control/structure interaction. It was concluded from the results of this study that the dual axis fine pointing mechanism/interface structure configuration, adopted as part of the preliminary design reference concept, is both low in mass and sufficiently rigid to effectively avoid modal frequencies below one Hertz. In some, but not all of the cases studied, the lowest modes involved significant modal participation from the concentrator reflective surface. Important gains in concentrator structural dynamic performance were achieved with the incorporation of the current reflective surface and support structure design into the recommended reference configuration.

The reflective surface configuration consisted of a hex-truss modular construction using graphite-epoxy support beams for mirrored facets. Each hex-truss was modeled as 12 major beam elements, with the weight of hinges, latches, beam elements and facets lumped at the various circumferential and interior nodes.

2.2.4.1.1.1 Interface Structure And Strut Configurations

Figure 2.2.4.1-1 depicts the initial and final integrated interface structure, strut and reflective surface assembly configurations. The initial interface and strut structure is represented by a three-point space frame network, made up of a back-up truss, main mast, supporting struts and "T-brace"

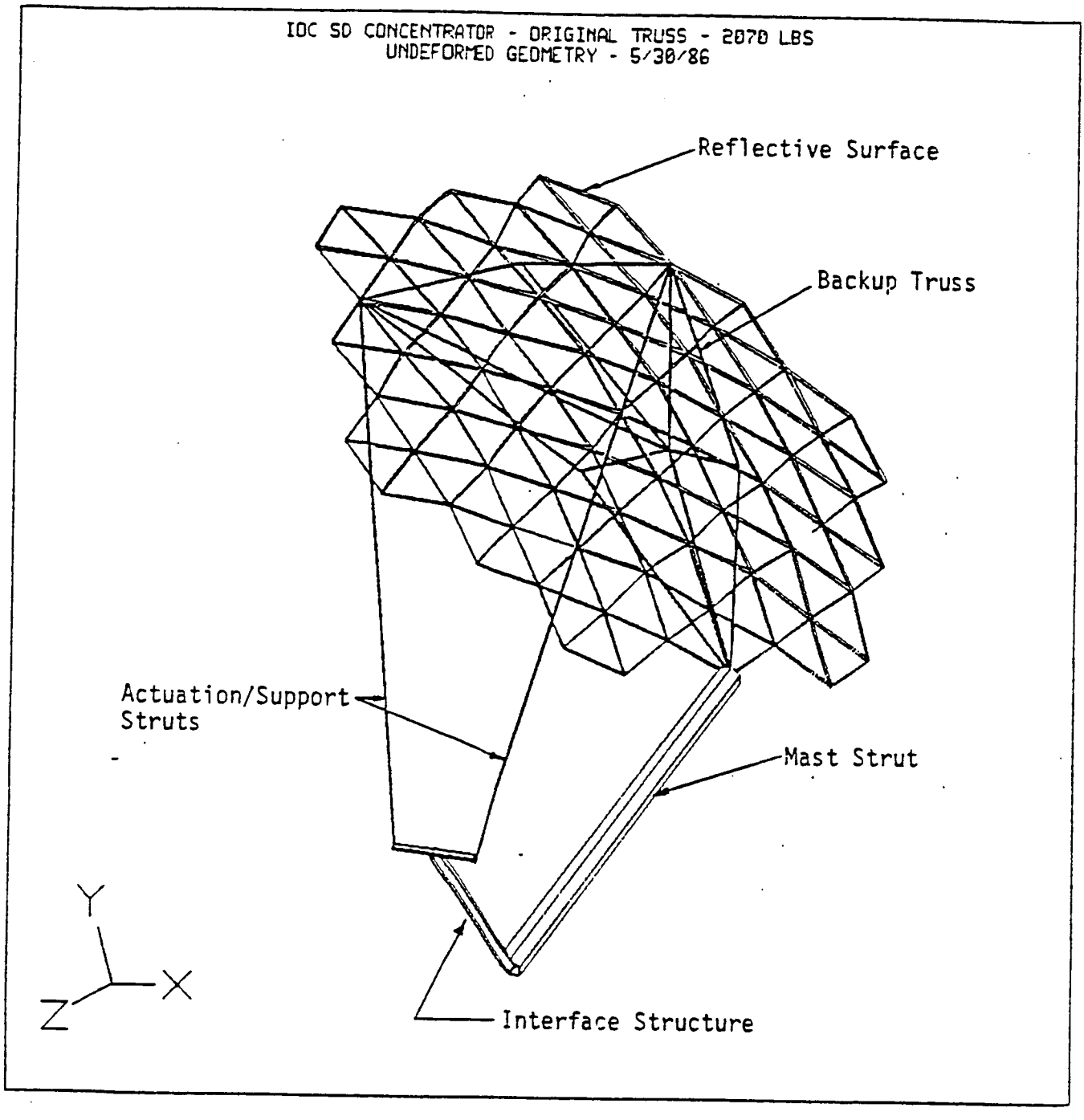

Figure 2.2.4.1-1a - Previous Concentrator Model Configuration

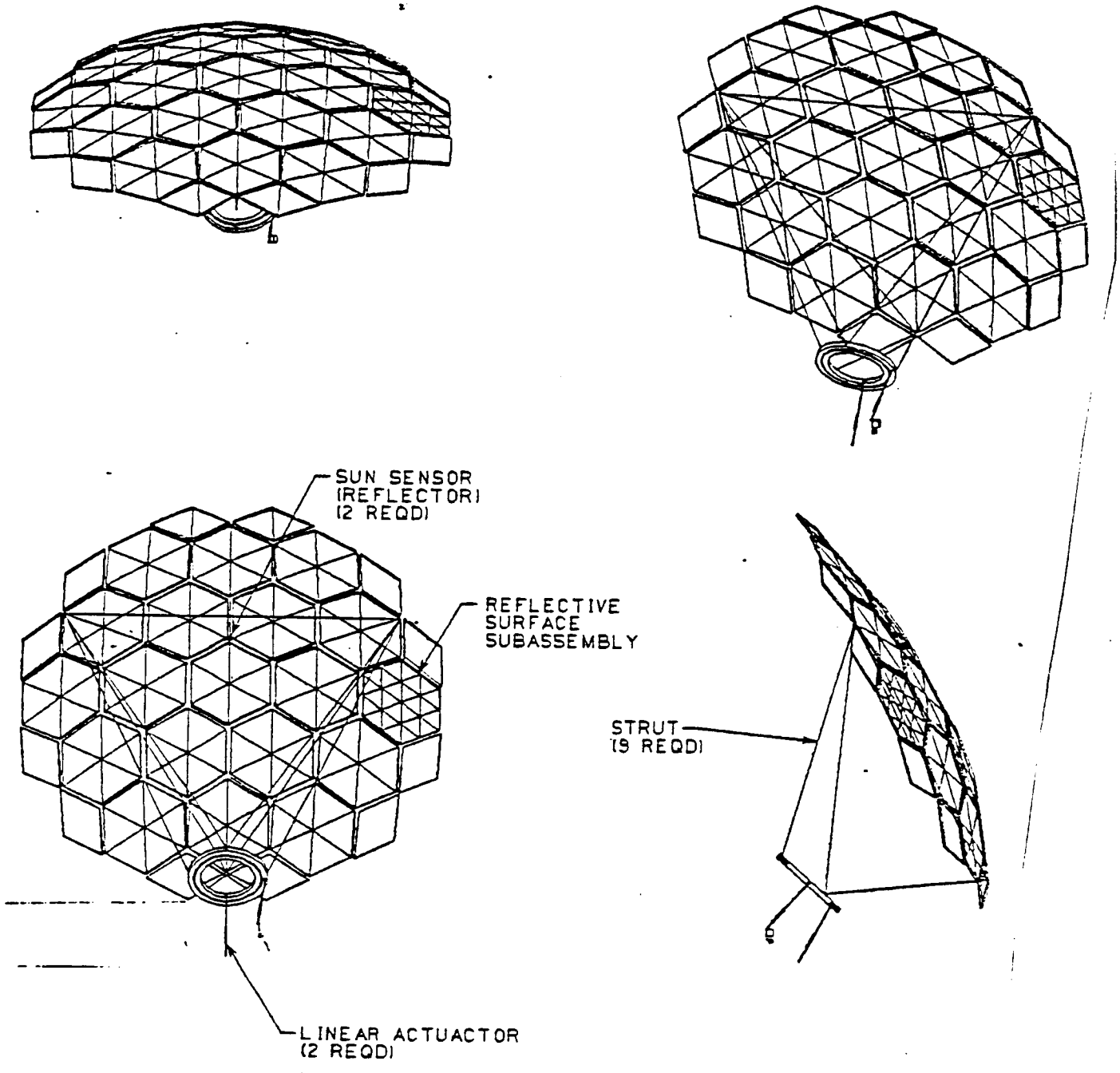

Figure 2.2.4.1-1b Current Concentrator Model Configuration

interface structure assembly for attachment to the beta joint and mounting of the PCU equipment. The final configuration of these items is represented by a prismatic truss space frame, reinforced by a triangular frame, made up of equal diameter struts; and a double ring-gimbal fine pointing mechanism, attached to a space frame interface structure superstructure mounted to a base plate. In all configurations, all frame elements are of filament-wound graphite-epoxy construction.

2.2.4.1.1.2 Analysis Results

Table 2.2.4.1-1 shows the results of the analysis. The initial configuration first vibration mode had a frequency of 0.129 Hz. The final configuration first mode frequency was 0.976 Hz. Other configurations considered had first modes between 0.5 and 1.09 Hz.

Table 2.2.4.1-1 Concentrator Structure Analysis Results

Concept	First Mode (Hz)	Second Mode (Hz)	Third Mode (Hz)
Three Strut, Front Mount Initial Configuration	0.129	0.538	0.572
Flat Frame Back Mounted	<0.5		
Parallelapiped Front Mount	<0.5		
Back Mounted Truss I	1.089	1.255	
Back Mounted Truss II	1.12		
Three Actuator Truss	1.033	1.158	1.231
Front Mounted Truss	1.063	1.276	1.359
Double Ring Gimbal, Prismatic Space Frame, Final Configuration	0.976		

A detailed description of this trade study is located in the December issue of DR02 Section 7.3

2.2.4.1.2 Concentrator Control Options

A fine-pointing concentrator control option evaluation was completed in support of the concentrator preliminary design. The objective of the study was to evaluate several fine-pointing control concepts in terms of control loop logic and suitability for this application. The optical performance of four of these concepts was also evaluated. The evaluation criteria included control simplicity, authority and error budgets, as well as optical performance. The specific objective was to identify the concentrator control requirements and to specify concentrator control performance. The control loop bandwidth was selected at 0.5 Hz, based on structural dynamics and Space Station controller bandwidths inboard of the SD subsystem. It was concluded, as a result of this study, that viable control loops for concentrator fine-pointing control can be of a simple variety and that the optical performance of the reference configuration is acceptable, based on the data obtained to date.

The initial reference concept for fine-pointing actuation employed a steerable reflector oriented by shortening or lengthening two of three struts connecting the concentrator to the interface structure. Five 2-axis universal joints were used to avoid bending moments in the struts or reflector structure. With length-positioning actuators on two of the struts, the concentrator may be pitched or tilted about the parabola vertex. Since the receiver is rigidly attached to the interface structure, it is possible to orient the reflector continuously so that its concentrated image is centered in the receiver.

This optical system, however, presents three issues: (1) At any off-axis sun angle, the focus will be displaced with respect to the receiver aperture; (2) At any off-axis angle, the focal spot will expand and distort; (3) The structural stiffness of the system is primarily limited by the stiffness of the mast strut.

In response to these issues, three major configuration options were evaluated : (1) An integrated system of the type identified by LeRC; (2) a variation on the previous reference concept with respect to strut, universal joint, and actuator arrangements, using 3 linear actuators; and (3) the concept which was ultimately selected as the final reference, wherein the fine pointing

mechanism consists of a dual ring-gimbal and two linear actuators mounted on the interface structure.

The integrated concept, avoided all three issues cited above for the initial reference concept. In trade, however, the greater inertia of the integrated concept required increased actuator loads and power, flexing of fluid lines, and perhaps, increased stiffness of the transverse boom.

Nevertheless, the integrated concept remains an attractive option and is a strong alternative to the current reference concentrator fine pointing configuration.

The second candidate was a variation on the previous reference concept. Because its struts are fixed at their bases, all participate in structural resistance to disturbances about the optical axis-- which, as discussed in Section 2.2.4.1.1, was the weakest mode for the previous reference concept. In addition, because all struts are actuated, a second deficiency of the previous reference concept is resolved; i.e., the focus can be positioned along the receiver optical axis. However, this concept can have, under some circumstances, a smeared and distorted focus which affects the solar intercept factor.

The third candidate, features a two axis fine pointing mechanism which gimbals the reflector independently of the PCU, resulting in a low gimbaled mass and modest coarse and fine pointing parasitic power requirements. The two-axis fine pointing mechanism kinematically constrains the reflector focal point and effectively eliminates translation of the focal point with respect to the receiver aperture, resulting in a simplified optical system. However, this candidate has a greater fine pointing inertia than the initial reference concept. The inertia about an axis parallel to the alpha axis is 150% of that of the initial reference concept. The inertia about an axis parallel to the beta axis is about 3 times that of the initial reference concept. However, the inertia of this concept is significantly lower than that of the integrated concept. The increased inertia of the third candidate was judged to be acceptable in terms of the linear actuator forces required. This candidate also exhibits a 300 lbm penalty with respect to the initial reference concept. In spite of these detrimental features the third candidate was selected on the

basis of superior optical performance, structural stiffness and control simplicity.

2.2.4.1.3 Concentrator Deployment Trade Study

Five alternate concepts were considered for the on-orbit assembly of the reflector subassembly. They included: a fully automatic, motorized, hinged/latched concept requiring no EVA for assembly; a fully deployable, non-motorized, hinge/latch concept requiring no EVA; a hinge/latch concept which is part EVA, part IVA assembly wherein all the panels are connected with hinges; a hinge/latch concept which is part EVA, part IVA assembly where the assembly of three groups of hex-trusses is required; and a latch only, all-EVA assembly concept. These concepts are designated A through E, respectively. They are illustrated in Figure 2.2.4.1-2. Concept D was the reference concept prior to this trade study.

The quantitative selection criteria used in the trade study are shown in Table 2.2.4.1-2. They include EVA and IVA resources required to assemble, overall program risk, and overall reflector subassembly program cost. Qualitative selection criteria were also used as discriminators. They include: ground and flight support equipment required, stowed volume and weight, deployment tooling for AICO, restow capability, NBS compatibility, deployment envelope, and structural stiffness. The weighting factors were established based on a negotiated understanding of the relative importance of the quantitatively evaluated criteria.

Each of the alternate assembly concepts was evaluated against the quantitative criteria by selecting one or more key parameters and using those as indicators. In the case of required EVA/IVA resources, a detailed timeline of EVA and IVA resource usage was developed for each concept. In evaluating the overall program risk of each concept, the key parameters were complexity of the AICO, and ground test facilities, probability of successful restow after 30 year life, Neutral Buoyancy Simulator compatibility, and EVA time allowance criticality.

CONCEPTS EVALUATED

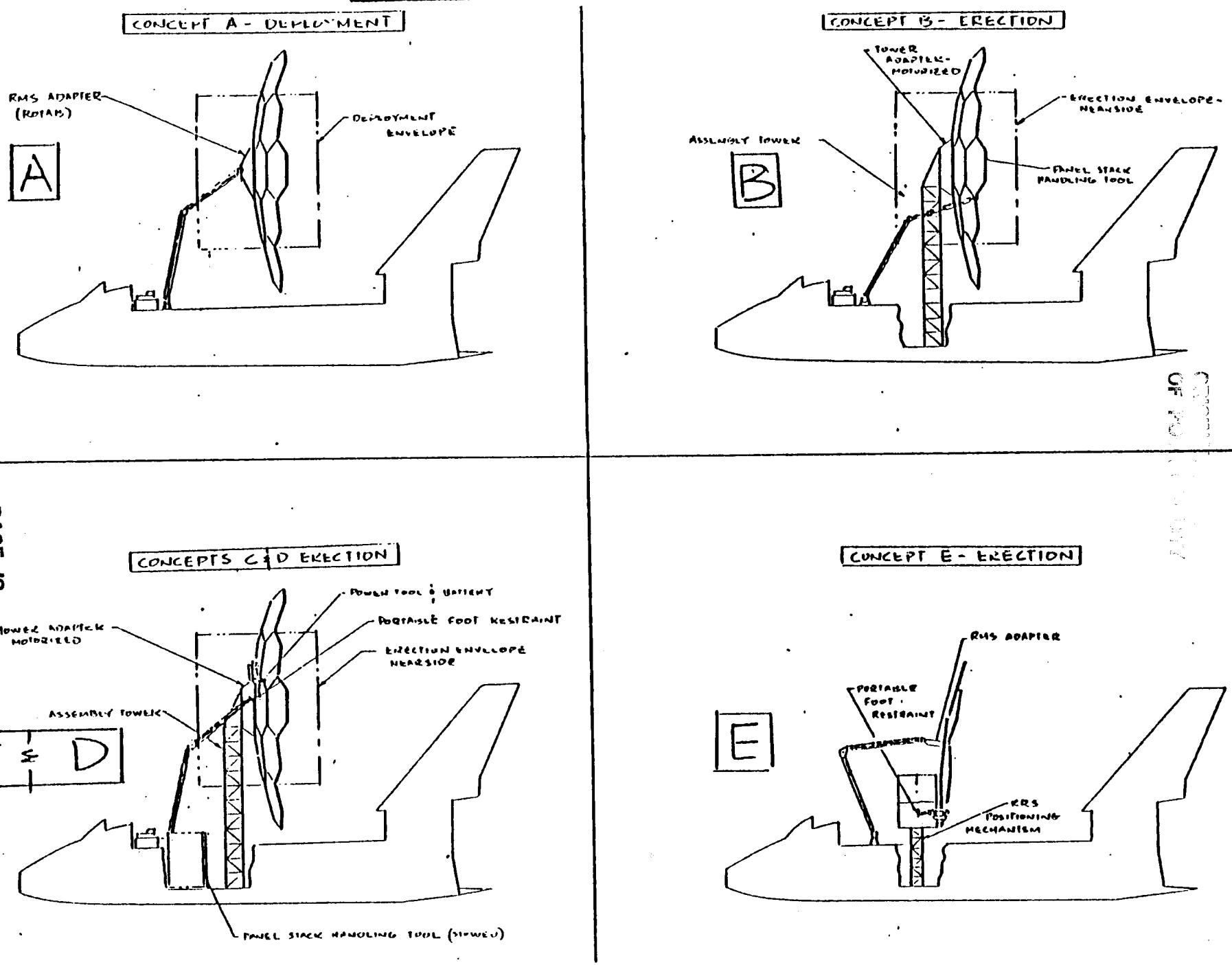

Figure 2.2.4.1-2 Alternate Reflector On-Orbit Assembly Concepts

Table 2.2.4.1-2
DEPLOYABLE/ERECTABLE REFLECTOR TRADE STUDY CRITERIA

Criteria	Weighting Factor
Quantitative Criteria	
EVA/IVA Resources Required	4
Overall Program Risk	3
Overall Program Cost	5
Qualitative Discriminators	
Ground and Flight Support Equipment Requirements	
Stowed Volume and Weight	
Deployment Tooling for Assembly, Integration and Checkout	
Restow Capability	
Neutral Buoyancy Simulator Compatibility	
Deployment Envelope	
Structural Stiffness	

The evaluation of the overall cost was based on the estimated number of drawings required for the flight, flight support and ground support equipment included in each concept. This parameter has a good historical correlation to the relative program cost of antennas produced by Harris Corp., the team member responsible for the reflector subassembly. A summary of the overall cost evaluation is shown in Table 2.2.4.1-3.

Concepts C and D are marginal with respect to existing neutral buoyancy simulation facility compatibility. Concept A is marginal with respect to restow capability. Concepts C and D are marginal with respect to EVA resource availability and allocation.

The results of the evaluation are summarized in Table 2.2.4.1-4. Each of the concepts is evaluated against each of the criteria and ranked in the matrix. In the upper right hand corner of each EVA/IVA and Program Cost matrix cell the raw evaluation results are listed. The relative ranking of each concept for each criteria is located in the middle of each matrix cell. Rankings are from 1 to 5, 1 being the highest ranking. The criteria score for each concept is located in the lower left corner of each matrix cell. The

Table 2.2.4.1-3

PROGRAM COST MATRIX

CONCEPT / PARAMETER	A	B	C	D	E
REFLECTOR	892	807	717	717	622
GROUND SUPPORT EQUIPMENT	525	460	330	330	255
FLIGHT SUPPORT EQUIPMENT	195	195	320	320	185
TOTAL	1612	1462	1367	1367	1062
RELATIVE VALUES	1.51X	1.38X	1.29X	1.29X	1X

NUMBERS ARE COMPLEXITY FACTORS BASED ON THE DRAWING COUNT FOR EACH SYSTEM.

Table 2.2.4.1-4

REFLECTOR ASSEMBLY EVALUATION MATRIX

PARAMETER \ CONCEPT	A	B	C	D	E	WEIGHTING FACTOR
EVA/IVA	0/48 1 4	0/180.2 4 16	7.2/15 3 12	110.5/29 4 16	54.5/5 2 8	4
OVERALL PROGRAM RISK	5 15	5+ 15	3 9	3 9	1 3	3
PROGRAM COST	1.5X 5 25	1.4X 4 20	1.3X 3 15	1.3X 3 15	1X 2 10	5
TOTALS	44	51+	36	40	21	

criteria score is the product of the relative ranking and weighting factor, shown on the extreme right side of the matrix. The total score is shown across the bottom of the matrix. The lowest score indicates the highest ranked concept.

The concepts were ranked E, C, D, A, and B. Concept E was clearly superior to the other concepts. Concepts A, C and D are fairly close together, and concept B is significantly lower in the ranking.

The all latch concept appears to be clearly superior to the other alternatives considered. In addition to its high quantitative ranking, it is the most flexible with respect to assembly location and method, and has a reasonable assembly timeline. The all latch design is the recommended approach and has been included in the reference preliminary design concept.

2.2.4.2 Receiver/PCU Trades

2.2.4.2.1 CBC Receiver / PCU Trades

The trade studies and analyses carried out in arriving at the design for the CBC receiver / PCU can be broken into three general categories. These are receiver trades, PCU trades, and control loop trades. Certain of the assembly trades have strong subsystem effects and the interactive nature of each trade is indicated in order to tie it to the whole.

2.2.4.2.1.1 Thermodynamic State Point Selection

This highly interactive analysis was carried out in two phases. The first phase concentrated solely on minimization of subsystem mass to optimize subsystem equipment. Approximate mass and area models for the concentrator and radiator were used in this analysis. Parametric variation of several design variables allowed selection of the most effective design by plotting all designs surveyed. (see Figure 2.2.4.2.1-1)

The second phase of thermodynamic statepoint selection was carried out with explicit recognition of three other subsystem drivers. These were receiver lifetime, packaging, and reliability enhancement.

Receiver lifetime was addressed by taking advantage of the flux tailoring capabilities of the segmented concentrator to avoid flux peaks in the receiver cavity and by lowering the turbine inlet temperature slightly. This lead to substantial enhancement of receiver lifetime at a small cost in concentrator size and mass.

Packaging constraints were explicitly incorporated by limiting the concentrator size to 19 hexagonal panels. This avoids packaging and installation complexities associated with "edge wedges". More effective use is thus made of the orbiter payload envelope and limited installation resources.

Reliability enhancement is achieved by reducing the complexity of the equipment required for cooling the SD electronics by sizing the cycle radiator

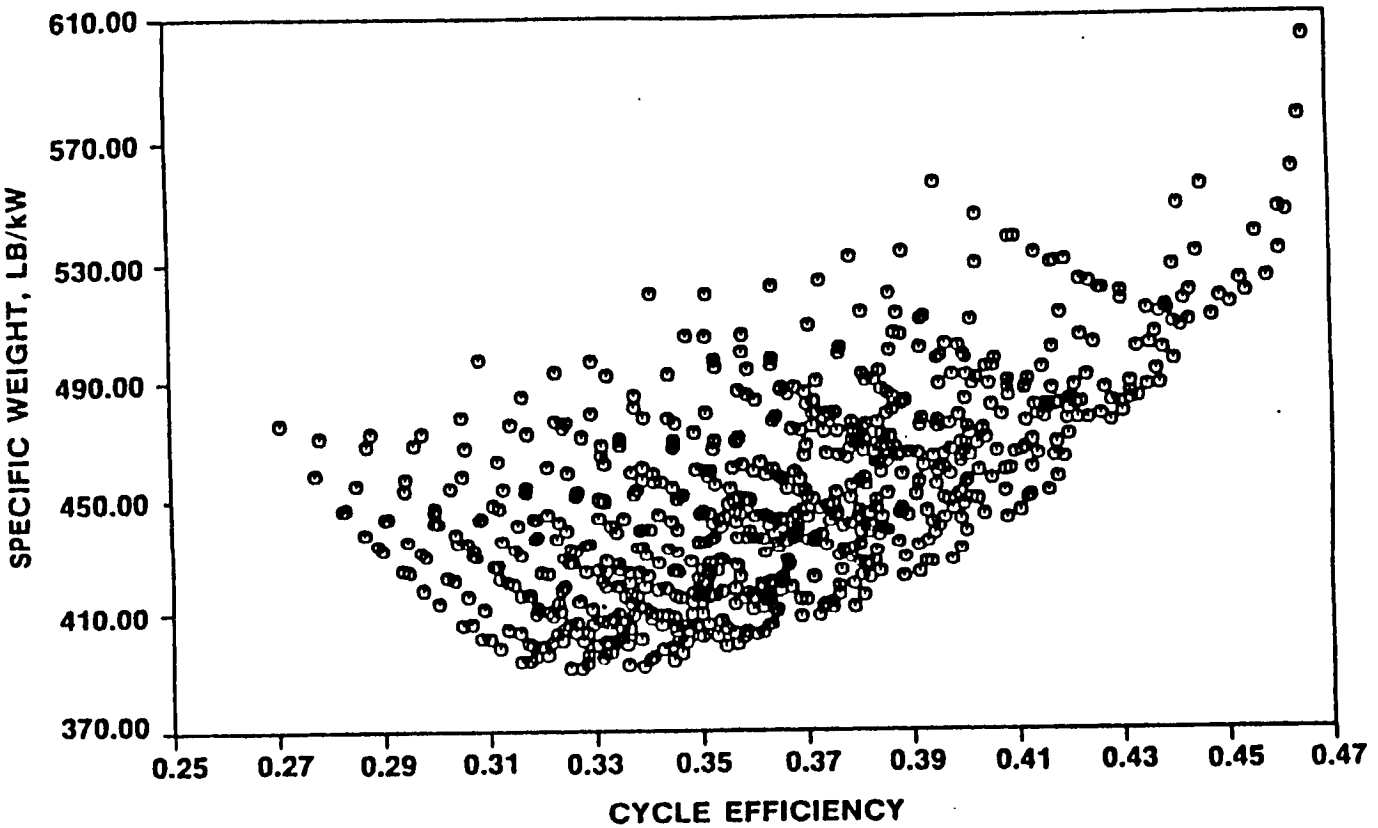

FIGURE 2.2.4.2.1-1

TYPICAL PLOT FROM DESIGN-POINT PROGRAM

to accomplish this task. The lowered radiator outlet temperature produces lower electronics operating temperatures and consequently longer electronics component life expectancy.

The options considered in the thermodynamic statepoint trade were ranges of values associated with recuperator and gas cooler effectiveness, compressor inlet temperature, pressure ratio, and specific speed, rotor speed, pressure drop ratio, and bleed gas flow ratio. Turbine inlet temperature was also varied over a small range consistent with the selected thermal storage salt.

The sensitivity of the mass and performance of each of the components to the various design parameters was used to determine a subsystem mass for each set of parametric values. The full set of subsystem mass totals was plotted, and the family of solutions at or near the minimum were used for selection of the preferred state point set. The range examined for each of the parameters is shown in Table 2.2.4.2.1-1 along with the selected value for that variable and comments on the rationale for its selection.

Table 2.2.4.2.1-1
State Point Trade Parameters

Parameter	Range	Value	Comments/Rationale
Recuperator effectiveness	0.84 - 0.97	0.94	Minimun mass
Gas cooler effectiveness	0.84 - 0.97	0.94	Minimum mass
Compressor inlet temperature	480R - 580R	520R	Minimum mass
Compressor pressure ratio	1.6 - 2.2	1.9	Compromise mass/accum. size
Compressor specific speed	0.07 - 0.10	0.093	Compromise efficiency/pressure
Rotor speed	20 - 40 (1000 rpm)	32,000	Compromise alternator/aero
Pressure drop ratio	0.90 - 0.95	0.93	Compromise mass/duct size
Bleed gas flow ratio	0.02 - 0.05	0.025	Minimum for cooling

V2-22421/2

2.2.4.2.1.2 Receiver trades

The major receiver trades carried on in the phase B activity were related to the selection of a thermal energy storage material and to the configuration of the receiver, thermal energy storage, and heat source heat exchanger. At a more detailed level, important analysis in support of the second phase of the state point selection trade was carried out in the TES canister thermal stress/lifetime study.

TES Salt selection

The options considered for the TES salt were LiF, LiF-MgF2, LiF-CaF2, Li2CO3, and a large family of other candidates which did not get much further than initial screening.

The recommended TES salt is lithium fluoride calcium fluoride eutectic (LiF-CaF2).

The rationale for this selection is as follows. The fluoride salts were known from previous experience to have very good compatibility characteristics which are essential for this application. Previous work with lithium fluoride for brayton cycle solar receivers and DOE molten salt reactor fuel formed this data base. Former Rocketdyne experience with molten carbonates also suggested lithium carbonate as a backup candidate. The uncertainty associated with LEO atomic oxygen and the economics of atmospheric versus vacuum chamber testing pointed away from use of refractory metals. The economics of ORU replacement placed a premium on long receiver life. These two factors lead to an upper temperature constraint that eliminated lithium fluoride as a candidate for this application.

The remaining set of candidates were surveyed for their thermodynamic properties and ranked in order of their heats of fusion LiF-MgF2, LiF-CaF2, and Li2CO3. However, when the lithium fluoride magnesium fluoride eutectic was examined experimentally, it was found to form solid solutions which interfered with its ability to release the full heat of fusion effectively. This phenomenon disqualified the lithium fluoride magnesium fluoride eutectic. When

the lithium fluoride calcium fluoride euctectic was examined it was found to behave as predicted. Subsequent analysis of receiver designs based on this salt confirmed that acceptable receiver lifetimes could be achieved without resort to refractory materials. Once the salt was selected the selection of thermodynamic cycle state points was possible.

Salt containment design

The options for salt containment design were those of material selection and geometry selection. The full range of high strength superalloys was examined for suitable salt containment candidates. The options for geometry were confined to large scale versus small scale encapsulation of the salt once the integrated receiver/TES/HSHX concept was chosen.

The material selected for the TES salt containment was Haynes 188. The geometry selected was small scale encapsulation.

The material selection was made primarily on compatibility and high temperature creep strength. Availability and extensive historical characterization of the material also played an important role in the selection. Issues concerning sublimation of volatile components of alloys exposed to hard vacuum at high temperature were addressed in an advanced development test which demonstrated that this was not a significant problem from the standpoint of materials strength and receiver lifetime.

The geometry selection was made in the presence of two opposing design drivers. Larger salt containers imply less fabrication and thus reduced cost, but this occurs at the expense of higher thermal and phase change expansion stresses and greater risk of freeze void migration. Smaller salt containers imply more fabrication and increased cost, but the risk of void migration is eliminated and the thermal and phase change expansion stresses are substantially reduced. The possibility of using automated production techniques for small salt canisters significantly reduces the probable cost difference between these two candidates and the advantages of risk reduction provide a great incentive toward use of the small canisters.

Receiver lifetime analysis

The receiver lifetime analysis is not a trade study, but its central role in supporting the major trade studies that have been performed makes inclusion here appropriate.

As previously described the selection of thermodynamic state points for the CBC is dependant on the selection of the salt for the thermal energy storage. Salt selection is in turn strongly influenced by the response of the receiver lifetime to the operating temperature. This issue of receiver lifetime was in fact responsible for the elimination of pure lithium fluoride as the TES salt of choice.

The initial selection of lithium fluoride calcium fluoride was made based on an estimate of receiver life that indicated that acceptable life was achievable. The tools to verify that initial estimation have now been developed and were applied to the problem of receiver design in the latest itteration of the CBC receiver and PCU design.

In addition to the increased level of receiver analysis there was an advance in the ability to predict and control the flux distribution in the receiver cavity. The GTRI work with segmented concentrator optics showed that the flux could be modified from the pattern expected from offset parabolic mirrors. The most important aspect of this development was the demonstration that the flux peak incident on a cylindrical cavity could be reduced by selective adjustment of the mirror facets to spread the energy over a wider area while maintaining good optical intercept properties. This property of segmented optics "tailorability" is key to the receiver design optimization that took place.

The CBC receiver design absorbs most of the solar energy toward the front or inlet of the receiver where the working fluid is coolest and a smaller amount of energy is absorbed at the rear where the working fluid is hottest. The receiver thermal analysis assumed that with flux tailoring there would be a 45 percent reduction in the maximum incident flux. Performance of the receiver around the minimum and maximum insolation orbits was calculated using the

tailored flux and the PCU codes to generate time varying receiver boundary conditions. The receiver was then systematically examined for the canister which experienced the most severe combination of high temperature and high stress over the entire orbit. The severity of the combined temperature and stress was determined from the Larson Miller curves for creep rupture for time at temperature and stress. This was done for both the minimum and maximum insolation orbits. The average creep damage done to the most severely stressed canister in one orbit was then used to calculate a probable minimum canister life. This was substantially in excess of the thirty year goal. The margin with which the worst canister met the life requirement was then evaluated in terms of temperature and stress conservatism. The worst canister was found to have a 90 degree F margin or a 60 percent stress margin. Subsequent evaluation of possible flux and or flow maldistribution effects showed that the margin was sufficient to accommodate simultaneous ten percent variation in these parameters. This analysis is the basis for the claim of thirty year life for the CBC receiver.

Receiver aperture size

The effects of receiver aperture size were examined over the range of 14 to 22 inches.

An aperture diameter of 43 cm (17 inches) was chosen based on concentrator size minimization and cycle economics. Smaller aperture diameters were more efficient with solar energy once it entered the receiver because there was less area for reradiation. However, reduced aperture size also implied either a more accurate and expensive concentrator or a decreased intercept factor that overcompensates for the higher efficiency with which the receiver retains heat. The selected aperture size was found to strike a balance at the cost minimum between these two competing effects.

2.2.4.2.1.3 Power conversion unit trades

In addition to the trade studies carried out in the thermodynamic state point selection several trades were pursued for the equipment in the PCU.

Alternator selection

The major candidates for the alternator type were the Rice alternator and the premanent magnet generator (PMG).

The Rice alternator was selected for the CBC power conversion unit.

The rationale for selecting the Rice alternator was that it allows better control of output voltage, it has a stiffer rotor with better dynamic characteristics, and it has a better pedigree of successful use on dynamic power systems intended for space application. The slightly higher efficiency of the PMG was not sufficient to overcome these advantages for the Rice alternator.

Alternator cooling method

The options for alternator cooling include gas cooling and a combination of gas and liquid cooling.

The selected alternator concept is to cool the rotor with a gas stream that has been prechilled by a cooled liquid and to cool the stator with a liquid that is circulated through cooling channels in the backiron.

The selected cooling concept makes use of the most compact method available to cool the generator components. This compactness reduces the mass of the alternator assembly. Gas cooling of the alternator stator would be inefficient because of the large penalties associated with either of the two options available. Partial flow cooling in which the exhaust is returned to the compressor inlet would represent too great a loss of compressor work to provide the circulation needed. Full flow cooling in which the gas is then sent to the heaters and turbine would have too great an impact on the beta ratio between the turbine and the compressor.

Gas cooler design characteristics

The heat transfer surface candidates for the gas coolers in the CBC PCU are the finned tube type and the plate fin type.

The plate fin type of heat exchanger was chosen for the cycle gas cooler and the bleed gas cooler.

The reason for choosing the plate fin type of heat exchanger was primarily because of its supperior mass properties. Plate fin heat exchangers in the heat duty and effectiveness are lighter, smaller, and have lower liquid side pressure drop characteristics. The only apparent advantage that finned tube heat exchangers have is that there is less manufactured joint between the liquid and the gas spaces. However, the demonstrated leaktightness and success of plate fin heat exchangers for the BIPS and certain dual fluid aerospace applications provides assurance that joint integrity can be achieved in this application of the plate fin technology.

Other candidate design characteristics of the gas cooler were examined in the design trades. These included the selection of number of liquid passes from the range of 2 to 8, selection of the hot and cold side fin spacing from the range 12 to 16 and 16 to 20 fins per inch respectively and the selection of the gas cooler aspect ratio from the range 0.1 to 2.

The number of fluid passes selected was 8. The hot side fin spacing was set at 12 fins per inch. The cold side fin spacing was set at 16 fins per inch. The gas cooler aspect ratio selected was 0.235.

The rationale for each of these selections was mass minimization consistent with the requirement for face matching between the recuperator and the gas cooler.

Recuperator design characteristics

The recuperator design trades were similar to those for the gas cooler in that the heat exchanger type was decided and aspect ratio value was selected from the range of 0.5 to 7.0.

The plate fin type design was selected for the recuperator. An aspect ratio of 5.0 was chosen.

The rationale for the recuperator design trade selections was minimization of component mass consistent with the requirement for face matching with the gas cooler.

2.2.4.2.1.4 Control equipment trades

The control equipment for the CBC receiver/PCU was selected through a series of design analyses and trades after a number of candidate concepts were conceptualized. The controls selection has been evolutionary during the phase B activities in response to the changing environment of requirements as various system level decisions have been made and as analytical data have been developed. The decision to use 20kHz power distribution in response to stringent EMI requirements, the requirement for a throttleable dynamic engine to provide peaking, and the development of more sophisticated optical and receiver thermal analysis tools are chief among these influences.

The control equipment trade selections are fully responsive to these requirements as they currently stand.

Receiver temperature control selection

The candidates for receiver temperature control were recuperator bypass valve, inventory control, and rotor speed control.

The selected method of receiver temperature control is inventory control by means of an accumulator and two solenoid valves. Pressurization and depressurization of the accumulator is provided by the cycle compressor.

Inventory control was selected for receiver temperature control because it is more efficient, more versatile, and probably more reliable than recuperator bypass methods, and it is more certain of success without possible GN&C impacts than rotor speed control.

The recuperator bypass valve was wasteful of usable thermal power and it controlled receiver inlet temperature by dumping turbine exhaust heat directly to the thermal rejection radiator instead of using it for recuperation. There was no opportunity to take advantage of excess thermal energy by processing it to produce extra electrical output such as needed for peaking.

Rotor speed control would provide receiver temperature control by varying mass flow rate, but it does not do it as efficiently as inventory control. This happens because it does not do as good a job of preserving the balance of high aerodynamic component efficiency and matching heat exchanger heat transfer coefficient and pressure drop ratio. In addition the rotor speed changes necessary to effect this type of control have small but perceptable impacts on the GN&C through torque imposition. These effects while small may be a nusiance.

Parasitic load radiator design

The PLR design options included switched resistance and unswitched fixed resistance banks.

The unswitched resistance bank was chosen for the CBC PLR.

Selection of a unswitched, voltage regulated, DC resistance device for a PLR was the result of EMI considerations. The selection of the optimum number of resistance elements was based on a system mass versus reliability trade described in the December 86 issue of DR02. The controller power electronics design reflects this decision to drive the PLR by modulating a DC voltage to a fixed resistance to avoid much of the EMI produced by switching resistors on and off. This concept also reduces the severity of the thermal transient experienced by individual resistance elements.

2.2.4.2.2 ORC Receiver/PCU Trades

Numerous analyses and trade studies were undertaken during the preliminary design of the Organic Rankine Cycle Solar Dynamic power generation subsystem. These studies fall into the following categories:

- o Thermodynamic State Point Selection
- o Commonality Identification
- o Pointing, Control and Stability
- o Receiver
- o PCU
- o Radiator/Condenser
- o Parasitic Load Radiator
- o Reliability
- o System

Completion of these studies resulted in an optimized, cost effective design concept for the Organic Rankine Cycle.

2.2.4.2.2.1 Thermodynamic State Point Selection

Two trade studies were performed in this area; one which considered state point effects, and one which evaluated options to maximize efficiency.

State Point Effects

The two options considered were operation with or without a back pressure relief valve (BPRV). The selected approach was to delete the BPRV as this configuration was found to improve system efficiency, reduce complexity with a corresponding increase in reliability, and reduce mass.

Efficiency Maximization

The parameters evaluated in this study were turbine inlet temperature, turbine inlet pressure, and RFMD pressure. The selected conditions were a turbine inlet temperature of 750°F, turbine inlet pressure of 610 psia, and RFMD pressure of 5 psia. These conditions were found to maximize efficiency and minimize system weight. Other criteria met by these conditions were a temperature consistent with minimal working fluid degradation, and a

supercritical inlet pressure which avoids two-phase vaporizer conditions.

2.2.4.2.2.2 Commonality Identification

Two trade studies were performed in this area; radiator heat panels, and the RFMD.

Radiator Heat Pipe Panels

Two commonality options were considered for the radiator heat pipe panels; a unique design or a design similar to the WP-02 central radiator. The selected approach uses a design similar to WP-02 which provides commonality of technical approach and also results in minimum mass.

RFMD

The options considered for the RFMD also included a unique design or a design similar to the WP-02 Two-Phase Thermal Management System (TPTMS) RFMD. The selected approach was a design similar to the WP-02 design which can be modified by deleting the temperature control feature to simplify its applicability to the ORC.

2.2.4.2.2.3 Pointing, Control, and Stability

This trade study considered the effects of pointing error on the ORC by evaluating active aperture plate cooling vs. passive aperture plate cooling. Passive aperture cooling uses the recommended approach since the flux densities on a conical aperture are within the capabilities of passive cooling.

2.2.4.2.2.4 Receiver

Eight trade studies were performed in this area including aperture sizing, type of absorber surface, heat pipe selection, type of heat pipe, circumferential flux maldistribution, type of thermal energy storage, salt selection, and type of vaporizer.

Aperture Sizing

This trade study had as it objective the minimization of reflective, reradiation, and intercept losses; maximization of tolerance to tracking errors, and accountability for orbital effects, off-design performance, and thermal transport. The recommended aperture size was 28 inches (71.1 cm) diameter resulting from a study performed using a finite difference computer model.

Type of Absorber Surface

This trade study considered direct insolation and heat pipes for the absorber surface. The recommended approach was heat pipes due to their ability to accommodate axial flux distribution, their low weight, and their simplicity.

Heat Pipe Selection

Types of heat pipes considered in this trade study included single and multiple monotube, and parallel flow. The recommended approach was multiple axial heat pipes, each including TES canisters and a working fluid vaporizer. The rationale for the selection was the light weight, best flux distribution, low manufacturing risk, possibility for solar heated startup and addition of circumferential heat pipes, and adaptability to alternate TES materials.

Type of Heat Pipe

This trade study evaluated single heat pipes vs. multiple heat pipes. Multiple heat pipes were selected since a single heat pipe would involve complex, expensive fabrication; would have no redundancy; and would not be testable on the ground.

Circumferential Flux Maldistribution

This study considered whether or not to utilize circumferential heat pipes. It was determined by a receiver math model that the expected circumferential flux maldistribution would be acceptable without circumferential heat pipes and that the working fluid temperature effect would

be minimal. Therefore, no circumferential heat pipes was the simpler and lighter choice.

Types of Thermal Energy Storage

The two options considered in this trade study were sensible heat storage and phase change storage. Phase change storage was selected due to its lighter mass and the availability of well-characterized phase change materials which meet the requirements.

Salt Selection

Over 100 alternative salts were considered with the prime candidates being LiOH, LiF-kF,and Li_2CO_3-K_2CO_3. The recommended salt was LiOH due to is high heat of fusion, high density, negligible volume change, low corrosion rate, melting temperature higher than peak cycle temperature,and experience base.

Type of Vaporizer

The two types of vaporizer considered in this trade study were the Bayonet/Return flow type vs. Through flow type. The recommended vaporizer was the Bayonet/Return flow type due to its simple interface and ease of thermal growth.

2.2.4.2.2.5 Power Conversion Unit (PCU)

This trade study considered the following list of alternator types:

- Synchronous
- Permanent magnet
- Induction
- Cascade
- DC
- Homopolar
- Rice/Lundell
- Hybrid
- Flux switch

The recommended alternator was the Rice/Lundell due to its good efficiency/

weight tradeoff and its regulated voltage to the source converter.

2.2.4.2.2.6 Radiator/Condenser

The types of radiator/condenser considered in this trade study were the annular and flat plate. The flat plate was the recommended option due to its minimal fluid joints, replaceable pressurization system, and commonality with the WP-02 approach.

2.2.4.2.2.7 Parasitic Load Regulator (PLR)

This trade study considered direct load and electrical load options for PLR design. The recommended approach was electrical with diode bridge discrete switched loads. The rationale for the selection was low EMI, acceptable speed resolution, simple circuits, low losses, fast response, and achievement of power quality requirements.

2.2.4.2.2.8 Reliability

This trade study considered the following redundancy alternatives:

- o No component redundancy
- o Controller redundant
- o PCU and controller redundant
- o PCU, controller, and tracking redundant
- o Complete redundancy

The recommended approach was controller redundant which represented the best compromise of reliability vs. complexity and mass.

2.2.4.2.2.9 System

The two system trades performed were the number of ORC engines, and the choice of working fluid.

Number of ORC Engines

This trade study considered to PGS modules with either one or two PCUs per

receiver, and four PGS modules with one PCU per receiver. The recommended approach was two PGS modules with one PCU per receiver. This option was selected on the basis of minimum life cycle cost based on the IOC power requirements and failure tolerance criteria.

Working Fluid

This trade study evaluated toluene vs. RC-1 as the working fluid for ORC. Toluene was selected due to its 100,000+ hours of ORC experience, ready availability, and lack of documentation concerning RC-1 thermal stability.

2.2.4.3 SD Radiator Trades

The trade studies described in this section were conducted in support of the ORC and CBC preliminary radiator designs. The detailed results have been reported in previous DR-19 and DR-02 documents and are referenced in Table 2.2.4.3-1. The separate trade studies are abstracted in Sections 2.2.4.3.1 through 2.2.4.3.10 of this report.

TABLE 2.2.4.3-1

SD RADIATOR TRADE STUDY REFERENCES

	DR-19 REFERENCE			DR-02 REFERENCE		DR 15 REFERENCE
TRADE STUDY TITLE	4.2	4.3	4.4	6-86	12-86	SECTION NUMBER
RADIATOR LOCATION	X			X	X	2.2.4.3.1
RADIATOR/PCU TRANSPORT LOOP	X		X			2.2.4.3.2
RADIATOR/PCU THERMAL INTERFACE	X		X			2.2.4.3.3
RADIATOR COATINGS			X	X	X	2.2.4.3.4
RADIATOR METHOD OF HEAT REJECTION			X			2.2.4.3.5
CBC CONSTRUCTIBLE RADIATOR TRADES		X				2.2.4.3.6
CBC PUMPED LOOP VS HEAT PIPE RADIATOR				X	X	2.2.4.3.7
ORC PUMPED LOOP VS HEAT PIPE RADIATOR					X	2.2.4.3.8
ORC CONSTRUCTIBLE RADIATOR TRADES		X				2.2.4.3.9
ORC RADIATOR COMMONALITY				X	X	2.2.4.3.10

2.2.4.3.1 Radiator Location

Two options were considered for the radiator location: collocated and underslung, as shown in Figure 2.2.4.3-1. The selected collocated configuration results in a less complex structure, lower mass, better deployability, and elimination of scarring for growth at the penalty of moving the center of gravity (for IOC only) off the alpha axis. The resulting micro-g effect and bending loads are considered acceptable. Table 2.2.4.3-2 summarizes the principal characteristics of the two options.

The reduced plumbing required for the collocated radiator results in many advantages. Because the plumbing length is considerably shorter, fluid pressure losses and mass are reduced. The plumbing in the underslung position requires beta joint accommodation with the potential need for quick disconnects on both ends of the bay. Collocated, it is possible to launch and deploy the receiver, PCU and radiator in a single launch package and automatically deploy. This was feasible for CBC but not for the ORC radiator boom which is still a separate launch package.

The underslung position requires scarring for growth. When the second SD power module is added at the beta joint location, the underslung radiator must be disconnected and reconnected in the collocated postion. This would require shutting down the power module during growth and require additional EVA time.

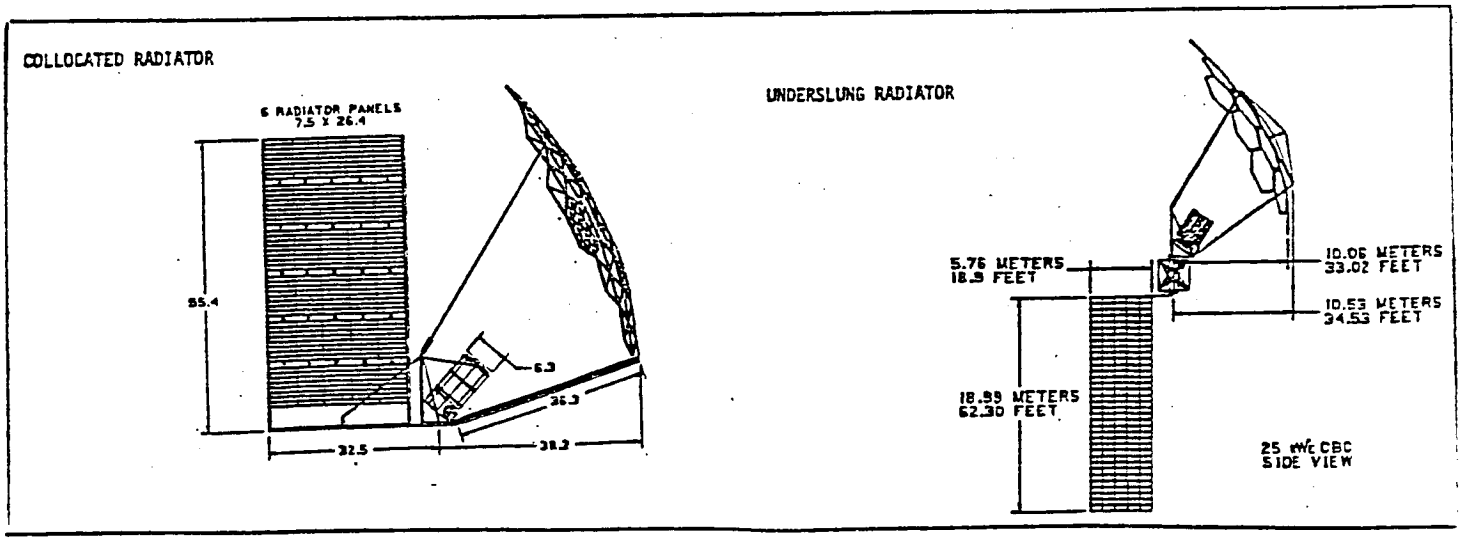

Figure 2.2.4.3-1
Radiator Location Options

TABLE 2.2.4.3-2

COLLOCATED RADIATOR VERSUS UNDERSLUNG RADIATOR

Feature	Collocated	Underslung
Plumbing	x 3m (10 ft) to radiator x Less complex	o 7.6m (25 ft) to radiator o Requires Beta joint accomodation
Parasitic Losses	x Reduced fluid pressure drop	
Mass	x Less due to less plumbing	
Deployability	x Deployable interface structure & plumbing (CBC only)	o Erectable interface structure and plumbing
Growth	x No scarring	o Growth requires moving radiator to collocated position when second module is added at Beta joint
Sink Temperature	o Higher sink temperature	x Lower sink temperature but only at IOC
Center of Mass	o CBC: 12,000 lbs located 26 ft from axis of rotation o ORC: 13,700 lbs located 24 ft from axis of rotation	x Located at and axis of rotation
Truss Bending Loads	o Increased load located at module: CBC: 0.013 lb ORC: 0.014 lb	x Base case
Micro G Effect	o Increases station microgravity by CBC: 0.59×10^{-7}g ORC: 0.62×10^{-7}g (Station allowable is 10^{-5}g)	x Base case

x Indicates Preferred Option

V2-224/3

2.2.4.3.2 Radiator/PCU Transport Loop Trade Study

Various methods can be employed to transport the waste heat from the engine working fluid to the radiator. Four different techniques were considered for the current trade study; there are many issues affecting each of these options. Reliability, maintainability, weight, parasitic power requirements, durability, and size are some of the subsystem parameters that must be considered when making this selection. Also, because the heat rejection requirements are different for each of the cycles, the engine/radiator interface selected for one many not be appropriate for the other.

Single-Phase Heat Transport Loop

The single-phase heat transport loop takes advantage of a large, sensible-heat temperature drop. This makes it a viable candidate for the Brayton cycle, which rejects heat over a 93.3°C (200°F) temperature range. Single-phase loops for spacecraft are a mature technology and are not sensitive to zero gravity. These systems may have limited component life, however, and higher power consumption. Critical components are the pump and accumulator.

Two-Phase Heat Transport Loop

A two-phase heat transport loop with a mechanical pump is a circulated fluid loop that accepts and rejects heat by a change in the phase of the working fluid. The fluid is circulated by a pump located in the liquid portion of the loop. A two-phase pumped loop, which can transport heat at near isothermal conditions, is a candidate for the ORC interface loop. Latent heat transport during phase change reduces the amount of coolant flow required, and the pump, piping, and accumulator sizes are reduced.

Two-Phase Heat Transport Loop (CPL)

A two-phase capillary pumped loop (CPL) is also an option for the engine/radiator interface. A CPL offers all the advantages of latent heat transport, with none of the disadvantages associated with the pumps or accumulators. Like a simple heat pipe, a CPL for a two-phase heat transport

system is self regulating; its pumping is always consistent with the applied heat load. The flow regulation and system stability problems common with the mechanically pumped systems do not exist. These advantages must be weighted against the potentially higher subsystem weights (because of the larger vapor headers associated with the low pumping head), limited zero-gravity experience, and limited experience with large Space Station-sized systems. A mechanically assisted CPL, which could accommodate the larger heat loads, is also an option but involves the major disadvantages of both two-phase systems.

Direct Connected Heat Transport Loop

A directed-connected heat transport loop looks very similar to a two-phase heat transport loop for the ORC and the single-phase heat transport loop for the CBC. The advantage of the direct-connected loop is the elimination of the intermediate heat exchanger and the consolidation of the transport loop pump into the engine system pump. This would result in a redundancy in weight and cost. A primary loop does not have the cooling redundancy to provide power system reliability and flow control dependability. It also exposes the engine working fluid to the meteoroid environment, and in a gas system with long piping lines, would have impact on the engine pressure drop.

The ORC with its latent heat rejection, would profit most from a direct connection. The RFMD regulates the flow and ensures high-quality toluene at the condenser inlet. Because the engine cannot function if the radiator is not operational, no reliability is gained with a secondary loop; in fact, the increased complexity would actually reduce the reliability.

The CBC, with its sensible reject heat, is best associated with a single-phase heat transport loop. Both flow regulation and pressure losses are issues in a gas thermodynamic cycle; a secondary loop is, therefore, the recommended choice.

2.2.4.3.3 Radiator/PCU Thermal Interface Trade Study

Trade studies were performed on the radiator/ORC condenser interface. The annular configuration employing condensers plumbed in parallel and interfacing with a round heat pipe was traded against a flat plate constructible version

employing a pressurized interface technique similar to the annular version. The selected flat plat configuration is slightly heavier than the annular version because of the difference in the interface conductance. The flat plate version eliminates, however, the multiple fluid joints associated with the parallel design and precludes any vapor bypass that could arise in the event that one or more of the heat pipes failed in the parallel flow version. A failure of the pressurization diaphragm of the annular configuration cannot be easily repaired, while the pressurized loading device of the flat plate configuration could be replaced in the event of a failure. Table 2.2.4.3-3 summarized the advantages and disadvantages of the two condenser radiator interface approaches.

An important factor to recognize in the ORC thermal interface design is that the selected flat plate configuration is consistent with that under consideration for the WP-02 central radiator. The final selected configuration will be the same as the central radiator concept, which will minimize DDT&E costs and development and operating risks.

TABLE 2.2.4.3-3

RADIATOR INTERFACE CONFIGURATION		
	Advantages	Disadvantages
Annular pressurized	1000 to 1500 Btu/h/ft^2^{o}F	Multiple single point failures
	Easy assembly	Failed heat pipes could cause vapor bypass flow and degraded performance
Flat plate pressurized	Failed pressurization system can be replaced	800 Btu/h/ft^2^{o}F
	Obviates bypass potential Minimum fluid joints	Better alignment needed for assembly.

2.2.4.3.4 Radiator Coating Trade Study

A trade study of radiator coatings has resulted in the selection of Z93 white paint as the baseline radiator coating for both CBC and ORC. Silver teflon is a backup option.

V2-224/6

A number of coatings were evaluated for use on both the ORC and CBC radiators; however, all the candidates were of two basic types: white paint and metallized tape. The choices were narrowed to silver Teflon tape of the type used on the Shuttle radiators and Z93 white paint used on the Apollo Service Module. The properties of each are given in Table 2.2.4.3-4.

TABLE 2.2.4.3-4

RADIATOR COATING CANDIDATES

Property	Silver Teflon Tape	Zinc Oxide Paint
End of Life		
Absorptivity	0.20	0.30
Emissivity	0.76	0.90
Weight kg/m^2 (lb/ft^2)	0.33 (0.068)	0.20 (0.04)
Maximum Use Temperature $^oC(^oF)$	121 (250)	316 (600)
Susceptibility to Contamination	low, easy to clean	medium, requires reasonable ground handling precautions
Previous Uses	Shuttle radiator Satellites	Apollo Shuttle Satellites

The Teflon tape has a lower solar absorptivity and also a lower thermal emittance. The lower absorptivity serves to reduce the environmental sink temperature and thus increase heat rejection; however, the lower emissivity reduces the emissive power and lowers heat rejection. Experimental evidence has shown that Teflon can be eroded by the atomic oxygen environment on-orbit. This would reduce the thickness and lower thermal emissivity further. The erosion of Teflon is not great, however, and could retain near initial properties for a number of years by starting with sufficient thickness. White paint with inorganic binders is not affected by atomic oxygen. White paint, however, is more susceptible to contamination by thrusters or ground handling and is not easily cleaned as is the Teflon coating. Since the physical advantages of the two candidates were subjective in evaluation, an analysis of the performance difference was conducted to select one over the other.

V2-224/7

To evaluate the coatings, a TRASYS environment model of the radiator and concentrator was constructed. Form factor and environmental flux data from this model were used to construct a SINDA thermal analysis model of the radiator and concentrator using a identical nodal breakdown. The thermal mass and front-to-back side conductance of the mirror was modeled; however, the radiator panels were input as having zero mass. The calculated temperatures therefore represent the radiator sink temperature variations around the orbit considering the natural environment and radiant interchange between the radiator and concentrator.

The analysis was conducted for orbit beta angles of 0, 52, and -52 degrees. A comparison of the calculated thermal emission values for a 327 K ($130^{o}F$) typical SD radiator surface temperature indicate the heat rejection for the Z93 to be 17.5% higher than for silver Teflon. For this reason Z93 white paint was selected for both the ORC and the CBC radiator coating.

2.2.4.3.5 SD Radiator Method of Heat Rejection Trade Study

Three different concepts of heat pipes and pumped loop radiators were traded for each of the SD subsystems. These trade study results, presented below, were made for a 37.5 kWe module size. The current preliminary designs are based upon a 25 kWe size and the radiators are accordingly smaller than those described below.

For the CBC radiator, a pumped loop heat rejection subsystem has been selected as the reference concept. Separate fluid systems provide redundancy and are additionally protected from meteoroid penetration by bumpering. Heat transfer fluid (FC 75) is pumped through the panels after picking up the rejected cycle heat in the compact engine cooler. Extruded aluminum flow tubes are inserted in the aluminum honeycomb panels. The use of pumped fluid radiators for space applications is a mature technology. combinations of redundancy and bumpered tube protection are used to enhance the CBC radiator survivability. This design provides the lightest weight structure and lowest life-cycle costs.

For the ORC radiator, a space constructible radiator consisting of 36 individual heat pipe panels was selected as the reference concept. Each panel

interfaces the ORC toluene condenser through a dry contact joint. Interface pressure is established by pressurized gas bellows that provide sufficient clamping forces between the evaporator sections of the heat pipes and the condenser. Each of the honeycomb panels contains two Lockheed tapered-artery, high-capacity heat pipes having dual evaporator sections. Similar radiator designs will be tested in the JSC Space Erectable Radiator System (SERS) program and under Contract NAS9-17327.

CBC Radiator Trade Studies

Three different CBC radiator concepts were developed and trades as shown below:

- o Deployable low-capacity heat pipe radiators
- o Constructible high-capacity heat pipe radiators
- o Deployable pumped liquid radiators

The first concept includes redundant pumped liquid heat transport loops, each of which contain redundant pairs of pumps. Two types of heat pipes are required because of the wide range of heat rejection temperatures. One-half of the panels use copper-water heat pipes, the other half uses aluminum/ammonia heat pipes. A summary of the design characteristics for the three radiator concepts is shown in Table 2.2.4.3-5.

Concept 2 is a constructable radiator using high-capacity heat pipes. The particular concept employs four different panel configurations of increasing size as the temperature decreases to maintain a near constant heat rejection per panel. A reduction in size is necessary for the higher temperature panels in order not to exceed heat pipe capacity.

Benzene is used as the heat pipe working fluid until the radiator temperature is reduced to about 338 K (150^{o}F), then ammonia fluid is used. The basic heat pipe design is the same throughout. The panels interface with the heat transport fluid loop through a round, pressurized interface now under development and being tested by LTV Aerospace and Defense for the Space Erectable Radiator System Program.

Concept 3 is a deployable radiator and consists of eight pumped liquid

radiator panels arranged in two independent systems. Each of the eight panel contain two sets of tubing and manifolds; flex hoses provide fluid transfer across the joints. The deployment mechanisms are of the scissors-type employed by the Apollo Telescope Mount (ATM) solar array on the Skylab Program. LTV Aerospace has installed similar radiator panels on an ATM fixture, and conducted thermal vacuum tests at NASA-JSC under the Self-Contained Heat Rejection Program in 1975.

The system is designed for a 0.99 probability of no penetration of both the primary and redundant system for a 10 year period. Utilization of two independent systems allows the use of a thinner wall thickness for the tubing while maintaining the desired meteoroid protection. The probability of penetration is a function of the wall thickness, time, and exposed area. Use of multiple systems reduces the exposed area in each and thus allows using thinner tube walls.

A comparison of the three CBC candidate radiators evaluated as a part of this trade study is shown in Table 2.2.4.3-5. Concept 3 is seen to have the

TABLE 2.2.4.3-5

SUMMARY OF CBC RADIATOR TRADE STUDIES

Concept	Deployable Low-Capacity Heat Pipe Radiators	Constructible High-Capacity Heat Pipe Radiators	Deployable Pumped Liquid Radiators
Area [m^2(ft^2)]	81.9 (881)	96.5 (1038)	89.3 (961)
Total mass [kg (lbm)]	1393 (3064)	1675 (3684)	988 (2173)
Panel specific mass [kg/m^2 (lbm/ft^2)]	14.2 (2.9)	8.1 (1.7)	7.3 (1.5)
Number of panels	6	52	8
Hardware cost estimates			
Nonrecurring ($M)	17.1	19.1	14.2
Recurring ($M)	7.9	11.3	8.8
Total Cost ($M)	32.9	41.7	31.8

V2-224/10

lowest hardware costs and mass. In addition, the concept is based on available technology, thereby reducing technical risks.

ORC Radiator Trade Studies

Three radiator concepts were developed and trades performed for the ORC PGS:

- o Constructible radiator with round interface
- o Constructible radiator with flat interface
- o Deployable low-capacity heat pipe radiators.

The heat pipe employed in concept 1 is the Lockheed taperd-artery design having two condenser legs for each evaporator leg. Each evaporator is formed into a round cross section to interface with a pressurized contact joint of the type developed by LTV Aerospace and Defense for NASA-JSC. The entire ORC concept 1 configuration is similar to that being developed for NASA-JSC under the Space Erectable Radiator System Program (SERS) contract. The panel configuration was selected by a cost optimazation method. A summary of the three radiator concepts traded for the ORC application is given in Table 2.2.4.3-6.

Forty-three panels are employed in concept 2; each panel consists of two high-capacity aluminum/ammonia heat pipe condensers bonded into an aluminum honeycomb matrix. The radiator panels interface with the ORC condenser through a flat heat pipe evaporator section, forced into intimate contact with the condenser by a pressurized bellows arrangement. This design provides a high contact force that is evenly distributed over the contact area and produces a high contact conductance with low mass. The bellows is pressurized by GN_2 from individual canisters outfitted with a Schrader-type valve. The concept is currently a candidate for use in the central radiator system. A development unit of a similar device will be fabricated and tested under NASA-JSC Contract NAS9-177327, Development of an Alternate High Capacity Heat Pipe and Thermal System Interface.

ORC concept 3 consists of 12 deployable, low-capacity heat pipe radiator panels., This ORC radiator design is similar to that of concept 1 in the CBC V2-224/11

trade studies. The heat pipes are thermally connected to manifolds made ofheat exchanger core. Two scissors deployment mechanisms are used to deply the 12 panels, with 6 installed on each. Flex hoses are used to provide flow across the joints and quick disconnects to allow panel removal and replacement. Provisions is made on the panels for a fully redundant system.

A comparison of the three ORC radiator concepts is shown in Table 2.2.4.3-6. Although ORC concept 3 had a slightly lower hardware cost, it was higher in weight and featured a condenser integral with the panel. ORC concept 2 was similar in cost, had lower mass, and would allow construction and assembly of the condenser into the ORC loop independently of the radiator panels, providing a simple mechanical interface between the ORC loop and the radiator system. In addition, variations in the condenser size could allow further reductions in panel weight through reoptimization. For these reasons, ORC concept 2 has been selected as the ORC reference design concept.

TABLE 2.2.4.3-6
SUMMARY OF ORC RADIATOR TRADE STUDIES

Concept	Constructible Radiators With Round Interface	Constructible Radiators With Flat Interface	Deployed Low-Capacity Heat Pipe Radiators
Area [m^2 (ft^2)]	205 (2208)	220 (2372)	165 (1770)
Total mass [kg (lbm)]	2482 (5461)	2375 (5224)	2443 (5374)
Panel specific mass [kg/m^2 (lbm/ft^2)]	8.1 (1.6)	8.1 (1.6)	12.6 (2.6)
Number of panels	69	43	12
Hardware cost estimates			
Non-Recurring ($M)	17.0	18.0	17.1
Recurring ($M)	17.8	13.4	13.0
Total cost ($M)	52.6	44.8	43.1

2.2.4.3.6 CBC Constructible Radiator Trades

Two types of constructible heat pipe radiators were considered for the CBC, one employing a high capacity copper/water heat pipe and the second an aluminum/benzene heat pipe for high temperature heat rejection. Heat transport

is accomplished utilizing a secondary pumped liquid loop with FC 75 as the fluid. Due to the rapid degradation of heat pipe performance of the aluminum/benzene heat pipe at temperatures below 333 K (140°F), aluminum/ammonia heat pipes of the same design were employed for the lower temperatures. The copper/water configuration used that design over the entire range. Both concepts utilized the OAO ATAG high capacity heat pipe design ccurrently under development by OAO for NASA-JSC. The concepts were optimized by a comparative cost formula which considered heat pipe cost, radiator cost contact heat exchange cost, launch cost, on orbit assembly cost, and cost penalty for drag.

The panel length of each concept was based on the capacity of the heat pipe. A comparison of the optimized designs for the two concepts considered is given in Table 2.2.4.3-7.

TABLE 2.2.4.3-7

OPTIMIZED CBC RADIATOR DESIGN COMPARISONS[a]

Heat Pipe Type	Copper/Water	Aluminum/Benzene Aluminum/Ammonia
Panel length	7.6 m (25 ft)	4.6 m (15 ft)
Panel width	0.3 m (1 ft)	0.3 m (1 ft)
Area	112 m^2 (1200 ft^2)	112 m^2 (1200 ft^2)
Mass	26.4 kg/m^2 (5.405 lbm/ft^2)	18.4 kg/m^2 (3.765 lb/ft^2)
Number of Panels	48	80
Fin Width	0.15 m (6 in.)	0.15 m (6 in.)
Fin thickness	2.24 mm (0.883 in.)	2.24 mm (0.883 in.)
Fin effectiveness	0.85	0.85

[a]Trades were done for radiators rated at 89 kWt.

Based on these trades, the aluminum/benzene and aluminum/ammonia heat pipe design was selected for the reference concept.

V2-224/13

2.2.4.3.7 CBC Pumped Loop Versus Heat Pipe Radiator Trade Study

Pumped loop and heat pipe radiators for a CBC power system have been compared. According to the selection criteria, a pumped loop radiator is preferable to a heat pipe radiator. The IOC cost for heat pipe radiators would be greater that the IOC cost for pumped loop radiators by 13% and the life-cycle cost would be greater by almost 40%.

The trade was made quantitatively on the bases of life-cycle cost, IOC cost, mass, area, and maintenance requirements; and qualitatively on the bases of complexity, development risk, cycle match, power module integration, and STS integration. The design shown in Figure 2.2.4.3-2 formed the basis for the pumped loop system. The heat pipe radiator design was based on a Grumman dual-slot heat pipe shown in Figures 2.2.4.3-3 and 2.2.4.3-4.

For the pumped loop radiator, life-cycle cost was minimized by optimizing the designs of the radiator and coolant management ORUs. The radiator panels were optimized by trading mass versus puncture reliability. The coolant management ORU was optimized by varying the number of redundant pumps. Life-cycle cost is minimized when a single pump is specified, but a second pump is necessary to meet fail-operational requirements.

Basic cost rates (for transportation, reboost, and EVA and IVA time) are consistent with the bases of the economic studies contained in previous DR-19 data packages. Component installation and replacement times were preliminary estimates made by Rocketdyne. Total costs for the IOC and the life-cycle are broken down to show the contributions of development, procurement, transportation, installation or mainenenace, and reboost. The Space Station is assumed to have a 30 year design (depreciation) life, with component lifetimes extended indefinetely through ORU replacement, as has been assumed in previous economic studies.

Quantitative comparisons between the two designs are presented in Table 2.2.4.3-8, while qualitative comparisons between the designs are presented in Table 2.2.4.3-9. On the basis of these selction criteria, the pumped loop radiator appears to have more advantages that the heat pipe radiator for a CBC power system.

V2-224/14

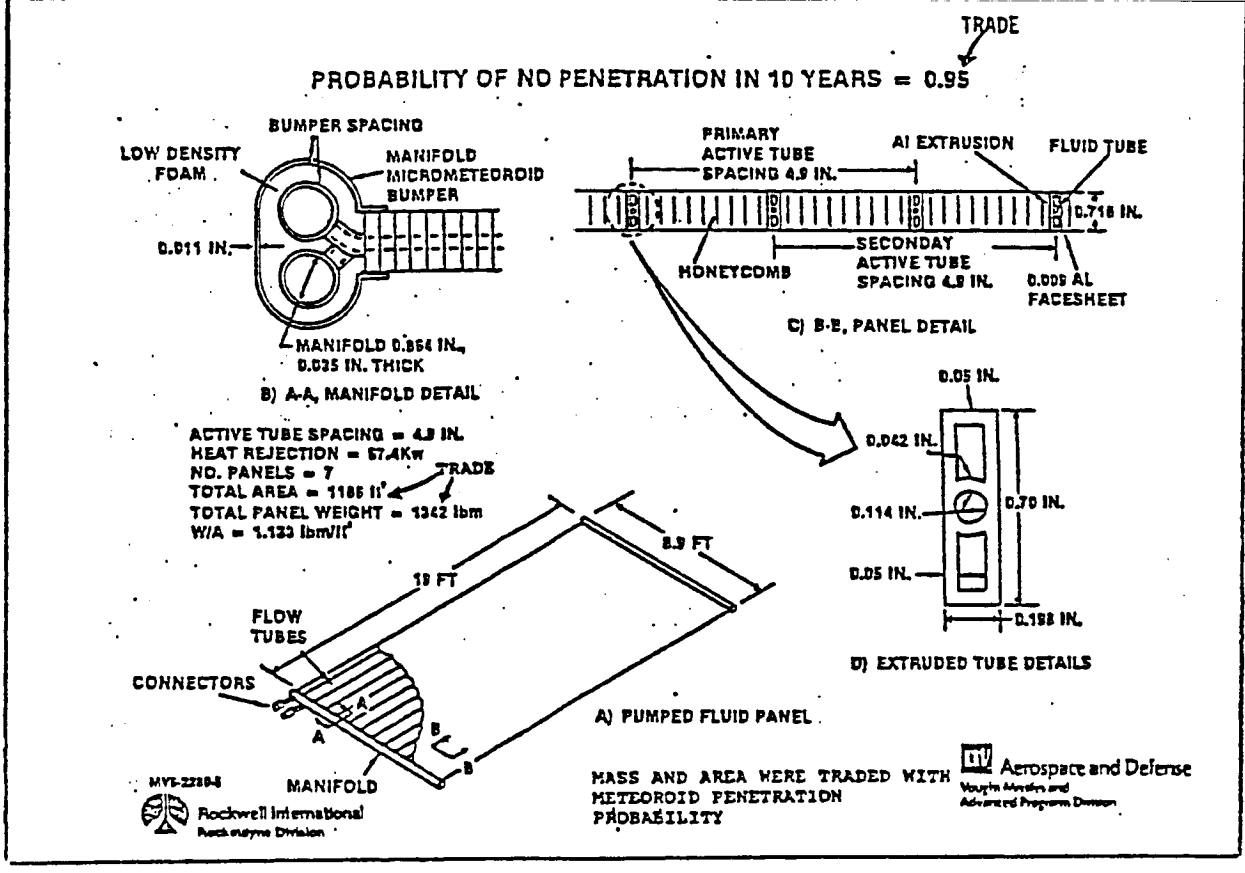

Figure 2.2.4.3-2. CBC Pumped Loop Radiator Concept

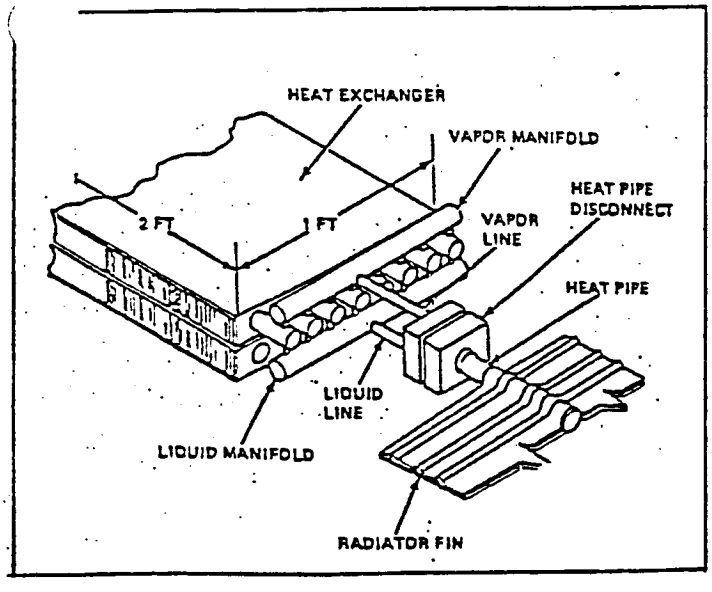

Figure 2.2.4.3-3. HRS Heat Pipe/Hx Concept

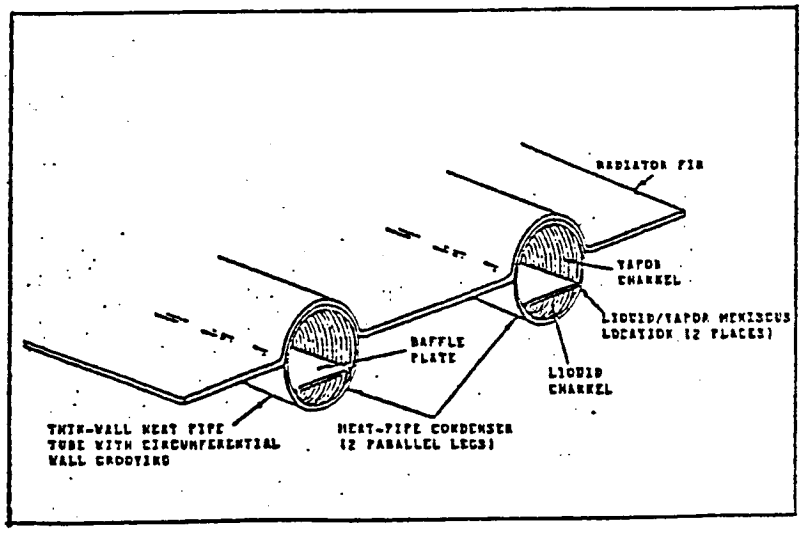

Figure 2.2.4.3-4.

Dual-Slot Heat Pipe Radiator Concept

ORIGINAL PAGE IS
OF POOR QUALITY

Only on the bases of complexity and drag area does the heat pipe radiator hold an advantage. By more significant criteria, such as life-cycle cost and life-cycle maintenance time, the advantage is in favor of the pumped loop concept, which is therefore Rocketdyne's choice at this time for the CBC power system radiator.

TABLE 2.2.4.3-8

QUANTITATIVE RADIATOR COMPARISONS

Quantity	Pumped Loop Radiator	Heat Pipe Radiator
Life Cycle Cost	$570 Million	$798 Million
IOC Cost	$68.1 Million	$76.9 Million
Mass (each) (on growth station)	1,044 kg 12,525 kg	1,496 kg 16,456 kg
Area (each) (on growth station)	152 m^2 1674 m^2	118 m^2 1293 m^2
EVA Maintenance Time	77h (154 man/hr)	817h (1634 man/hr)
Module Down-Time	521h	817h
ORU Failures	18.5*	195.6*
MRMS Maintenance Time	10.63h	471h

*Heat Pipe Failures are much less severe than Pumped Loop ORU Failures

TABLE 2.2.4.3-9

QUALITATIVE RADIATOR COMPARISONS

Quality		
Number of ORUs	3	1* (Heat Pipe Panels)
Number of Unique Part Sets	More	Fewer
Development Risk	Lesser	Greater
CBC Cycle Match	Better	Worse
CBC Puncture Risk	Lesser	Greater
Ability to Cool Power Electronics	Greater	Lesser
STS Package Volume	Smaller	Larger
STS Package Mass	Lower	Higher

*HX Boom is replaced with PCU and is not a radiator ORU

V2-224/15

2.2.4.3.8 ORC Pumped Loop Versus Heat Pipe Radiator Trade Study

A deployable pumped loop radiator concept was traded against the current ORC baseline heat pipe radiator design. The two concepts were compared quantitatively on the basis of life cycle cost, IOC costs, mass and area considerations, and on a "relative cost" basis which considered only reboost and launch costs. In addition, they were compared qualitatively on the basis of development risk, operational considerations, STS integration, commonality, reliability and cycle match. The panel design presented in Figure 2.2.4.3-5 formed the basis for the pumped loop radiator design. The heat pipe panel design on the other hand, was based on the characteristics of the Lockheed tapered artery heat pipe shown in Figure 2.2.4.3-6.

A pumped loop radiator was not included in the initial ORC trade studies described in Section 2.2.4.3.5 for several reasons. First, it requires an additional fluid system; secondly, the inefficiencies of interfacing the two phase ORC with a single phase pumped liquid system were perceived to result in additional weight and power requirements; and, thirdly, a constructable radiator system using aluminum/ammonia heat pipes was feasible thus allowing some commonality with the central radiator system. Another look at this option was taken based upon the desire to minimize on-orbit operations and to reduce the ORC condenser length.

A schematic of an ORC pumped loop radiator is shown in Figure 2.2.4.3-7. This arrangement would allow reduction in the ORC condenser size since the condenser length is set by the radiator interface rather than condensing flow criteria. Automatic deployment of the radiators such as is baselined for the CBC radiators will also greatly reduce on-orbit operations. The driving design parameter for an ORC pumped loop is the temperature drop across the radiator. The lower this value, the higher the radiator temperature, thus reducing radiator area and weight. Low temperature drops however, result in higher pumping power.

On the basis of the trade study, the pumped loop radiator provides the following advantages relative to the heat pipe concept.

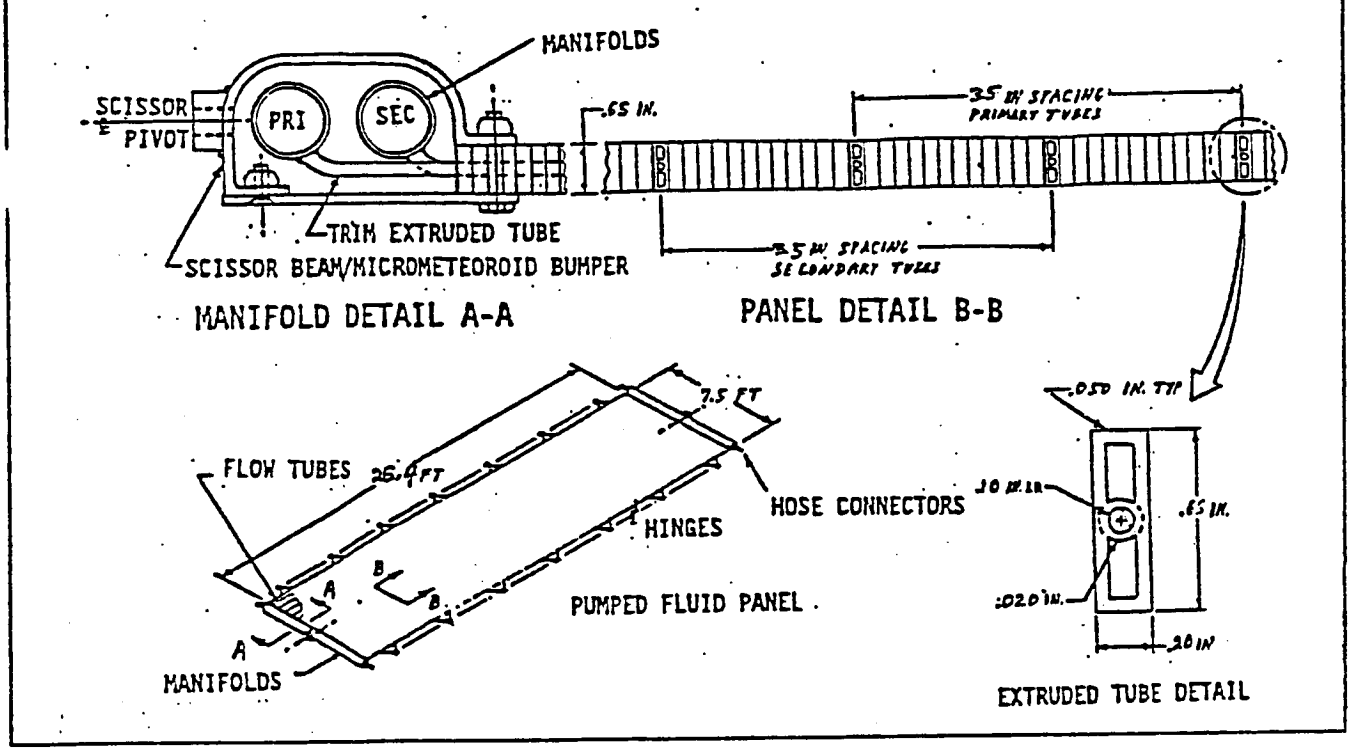

Figure 2.2.4.3-5 ORC Pumped Loop Radiator Panel Design

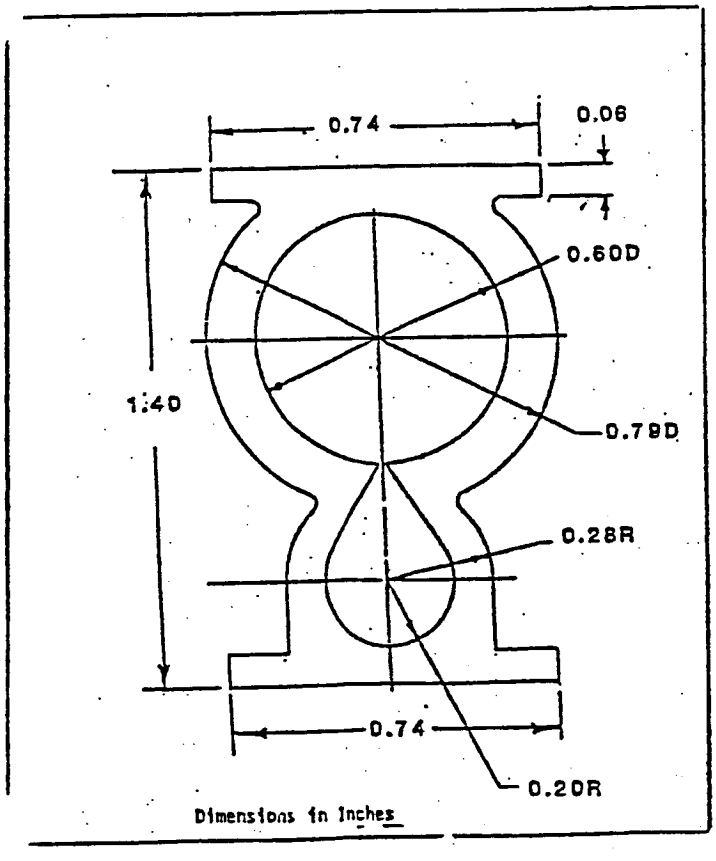

Figure 2.2.4.3-6
Lockheed Tapered-Artery Heat Pipe Design

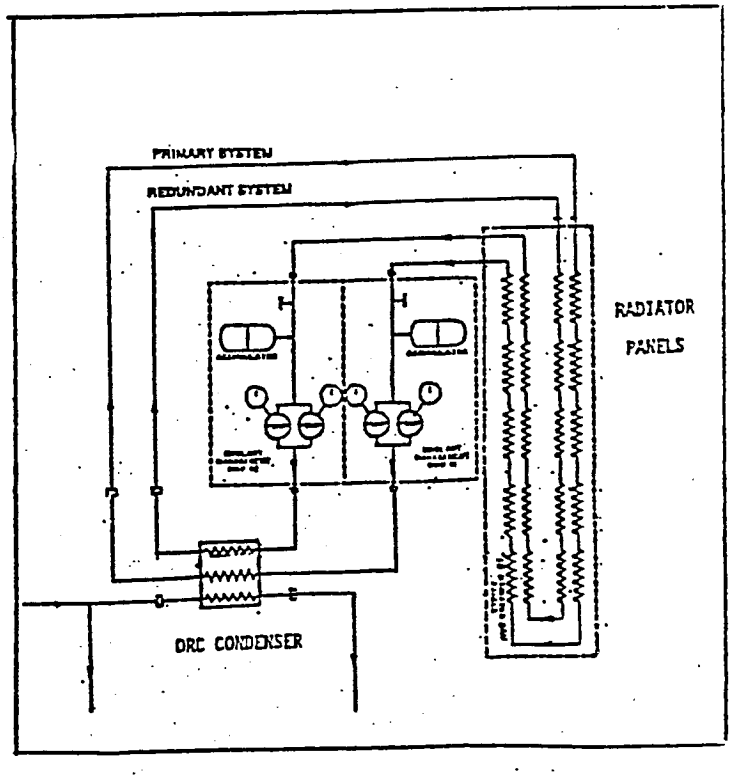

Figure 2.2.4.3-7
ORC Deployable Pumped Loop Radiator Schematic

1. Lower LCC
2. Lower IOC cost
3. Lower technical risks
4. Minimum start-up problems
5. Better packaging
6. Commonality with fluid management components
7. Lower weight

Similarly, the heat pipe radiator concept was found to have certain advantages over the pumped loop design:

1. Better overall reliability
2. No parasitic power requirements
3. Graceful degradation
4. Maximum commonality
5. Potential utilization of current ADP technology
6. Lower area
7. State point match

Although both ORC radiator concepts provide some level of commonality with the other Space Station work packages, maximum commonality would be achieved with the constructible heat pipe radiators.

Radiator area produces a cost penalty for the Space Station and is reflected in propellant reboost costs, associated with increased drag in the direction of the velocity vector. Similarly, radiator weight produces an additional penalty via increased launch costs. The sum of these two separate cost factors (reboost and launch) have been identified as "relative cost", and the calculated values plotted in Figure 2.2.4.3-8 for several specific radiator designs.

Relative cost represents some fraction of the total LCC since factors such as hardware development, procurement and on-orbit maintenance have not been included. The other parameter plotted in Figure 2.2.4.3-8 is specific weight, and is defined as the ratio of total radiator weight to its area. As shown, the magnitude of the relative cost associated with the pumped loop concept depends upon whether or not the penalty associated with the parasitic power requirement of the pump are considered. Although the pumped loop radiator panels can be fabricated with less weight, the added weight penalty must nevertheless be launched into orbit. With this penalty taken into account, the relative cost of the ORC pumped loop concept compares closely with that calculated for the heat pipe radiator with the single-sided, flat interface.
V2-224/17

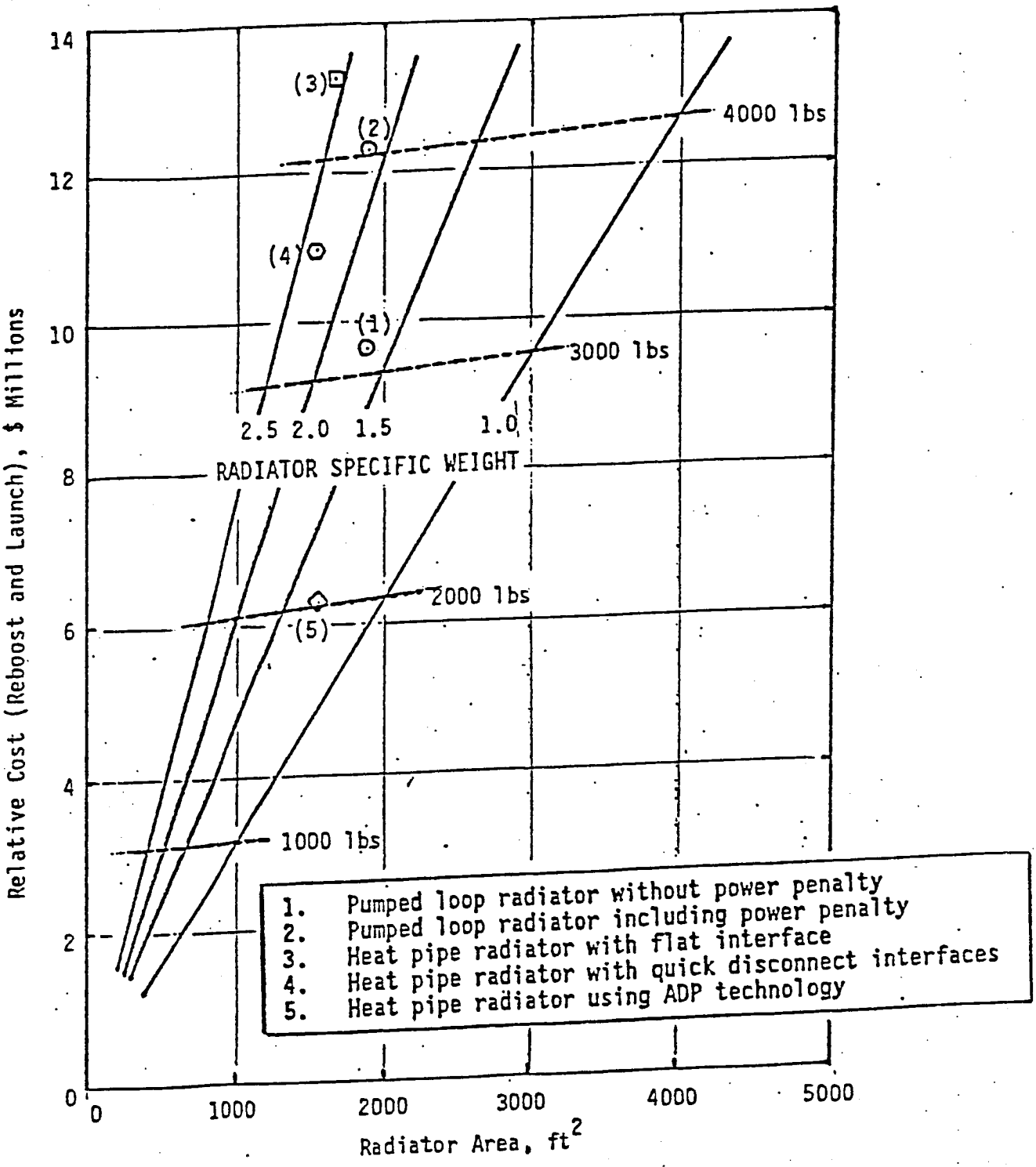

Figure 2.2.4.3-8 Relative Cost Comparison for Different ORC Radiator Concepts

The potential additionally exists to reduce the relative cost of the heat pipe radiator by replacing the pressurized, flat interface with the multiple, quick disconnect-type of interface. As shown on Figure 2.2.4.3-8, this could result in a lighter weight radiator with lower relative cost.

The last data point in this figure represents an ORC radiator design incorporating the aluminum, dual-slot heat pipe currently being evaluated under the NASA ADP. Although this design has potential advantages, it must be considered as a higher risk at this time.

The constructible heat pipe radiator approach has been retained for the Phase B preliminary design.

2.2.4.3.9 ORC Constructible Radiator Trades

Two types of heat pipes were considered for the ORC application, the OAO ATAC pipe and a tapered artery heat pipe developed by Lockheed Missiles and Space Company. Radiator designs using each of these heat pipes were generated. The separate vapor and liquid passages in the heat pipe allow use of a single evaporator with two condenser sections in the radiator panel. The low weight of the Lockheed extrusion [0.34 kg/m (0.23 lbm/ft)] promotes the viability of this concept. This configuration allows a shorter fin length and thus higher fin effectiveness and a larger radiating area per panel.

The selected reference configuration was developed for the JSC Space Erectable Radiator System. The two concepts were optimized in a manner similar to that described for the CBC using the comparative cost formula. A comparison of the optimization results are shown below in Table 2.2.4.3-10.

Based on this comparison the concept using the Lockheed heat pipe was selected for the ORC Reference design and more detailed design information developed. This design information is given in Table 2.2.4.3-11.

2.2.4.3.10 ORC Radiator Commonality Trade Study

Commonality options for the ORC radiator with the central radiators were evaluated. The trade study is preliminary in nature and is dependent upon more

OPTIMIZED ORC RADIATOR DESIGN COMPARISONS

Heat Pipe Type	DAD Heat Pipe	Lockheed Heat Pipe
Panel length	13.7 m (45 ft)	13.7 m (45 ft)
Panel width	0.3 m (1 ft)	0.4 m (16 in.)
Mass	14.7 kg/m^2 (3.010 lbm/ft^2)	8.1 kg/m^2 (1.655 lbm/ft^2)
Number of panels	54	46
Fin width	0.15 m (6 in.)	0.10 m (4 in.)
Fin thickness	1.55 mm (0.0612 in.)	0.64 mm (0.0253 in.)
Fin effectiveness	0.85	0.85

TABLE 2.2.4.3-11

ORC RADIATOR REFERENCE CONCEPT DATA FOR ONE 37.5-kW SYSTEM

Type	Constructible radiators
Heat rejection	153 kW
Heat transport loop	ORC working fluid loop
Panel size	13.7 m (45 ft) x 0.4 m (16 in.)
Evaporator length	1.2 m (4 ft)
Number of panels	46
Panel deployed area	256 m^2 (2760 ft^2)
Maximum heat pipe capacity	25,400 W-m (10^6 W-in.)
Material	Aluminum heat pipe with ammonia fluid/ aluminum fins

TABLE 2.2.4.3-12

SPACE STATION RADIATOR SYSTEMS

SYSTEM	TYPE RADIATOR	HEAT REJECTION TEMPERATURE (^{0}F)	HEAT LOAD (kW)	WORK PACKAGE
MODULE BODY MOUNTED RADIATOR	REPLACEABLE THROUGH FLUID SYSTEM DISCONNECTS	35	8 kW	1
LOW TEMP BODY MOUNTED RADIATOR	REPLACEABLE THROUGH DISCONNECTS	-20	.5 kW	1
CENTRAL RADIATORS	CONSTRUCTABLE	35 AND 70	70 kW TOTAL	2
PLATFORM ESS, PMAD AND EXPERIMENT	CONSTRUCTABLE	35 AND 70	12 kW	3
STATION ESS AND PMAD	CONSTRUCTABLE	41	9.5 kW	4
STATION SOLAR DYNAMIC	CBC-PUMPED LIQUID OR CONSTRUCTABLE	273-60	134.8 kW	4
	ORC-CONSTRUCTABLE	150	230.0 kW	

definition of detailed design requirements, cost, and test and verification plans. Initial results indicate:

- o The radiator panel design should use common technology but should be optimized for the higher heat capicity and higher temperature application
- o Use an identical contact heat exchanger
- o Incorporate a fluid charge (excess heat pipe length for low temperature startup) for the solar dynamic heat pipes only and not on the station.

Table 2.2.4.3-12 is a list of other space station radiators with their major characteristics of type, heat rejection temperature, and heat load. The central radiators are closest in requirements to the ORC radiator. The Space Erectable Radiator System (SERS) advanced development program data was used as the basis for the central radiator design comparison. The radiator elements evaluated for commonality are: 1) the heat pipe cross section for both the condenser and evaporator sections, 2) the contact heat exchanger interface, and 3) the heat pipe fluid charge (required for low temperature startup).

The following three options represent varying degrees of radiator commonality and is based upon constructable heat pipe technology.

Option 1: Use identical radiator hardware (ie. same part number) as the central radiator. Lower the ORC heat rejection temperature to remain within the heat pipe capacity.

Option 2: Use the same central radiator heat pipe design (ie. cross section) but with shortened heat pipe to obtain the design heat capacity with the higher temperature application.

Option 3: Use the same central radiator heat pipe technology (ie. same fluids, materials, and methods for panel construction, wicking, and vapor flow passages but with all dimensions optimized for the particular application) and optimize the panel design for the higher temperature application.

All three options assume an identical contact heat exchanger. A comparative cost trade was made and includes all IOC costs, including DDT&E and production hardware. These costs must be evaluated at the system level and

require more detailed test and verification requirements than are available at this time for an accurate cost comparison. For purposes of this trade, the reference configuration assume option 3 and does not consider any cost savings in DDT&E due to commonality.

2.2.4.4 SD Interface Structure

As an additional improvement in the ORC concept for cooling the SD equipment box, a direct heat pipe/cold plate configuration was examined in lieu of the CPL. The CPL Configuration is shown schematically in Figure 2.2.4.4-1, and the direct heat pipe/cold plate concept is showin in Figure 2.2.4.4-2. In this case a series of bolts is used to clamp four heat pipe radiators directly to the cold plate. On the bases of an assumed heat transfer conductance across the contact interface of 50 Btu/hr-ft^2-^{o}F, four panels, with a total radiating area of 8.06 m^2 (173.8 ft^2), were found to be sufficient. The platform is one-half this value and the total weight is approximately 91.3 kg (201 lbs). The panels would be shortened versions, but otherwise identical to the panels designed for the WP-02 central radiator. Each panel would have two heat pipes each 0.027 m high and each having three evaporator sections and one condenser section.

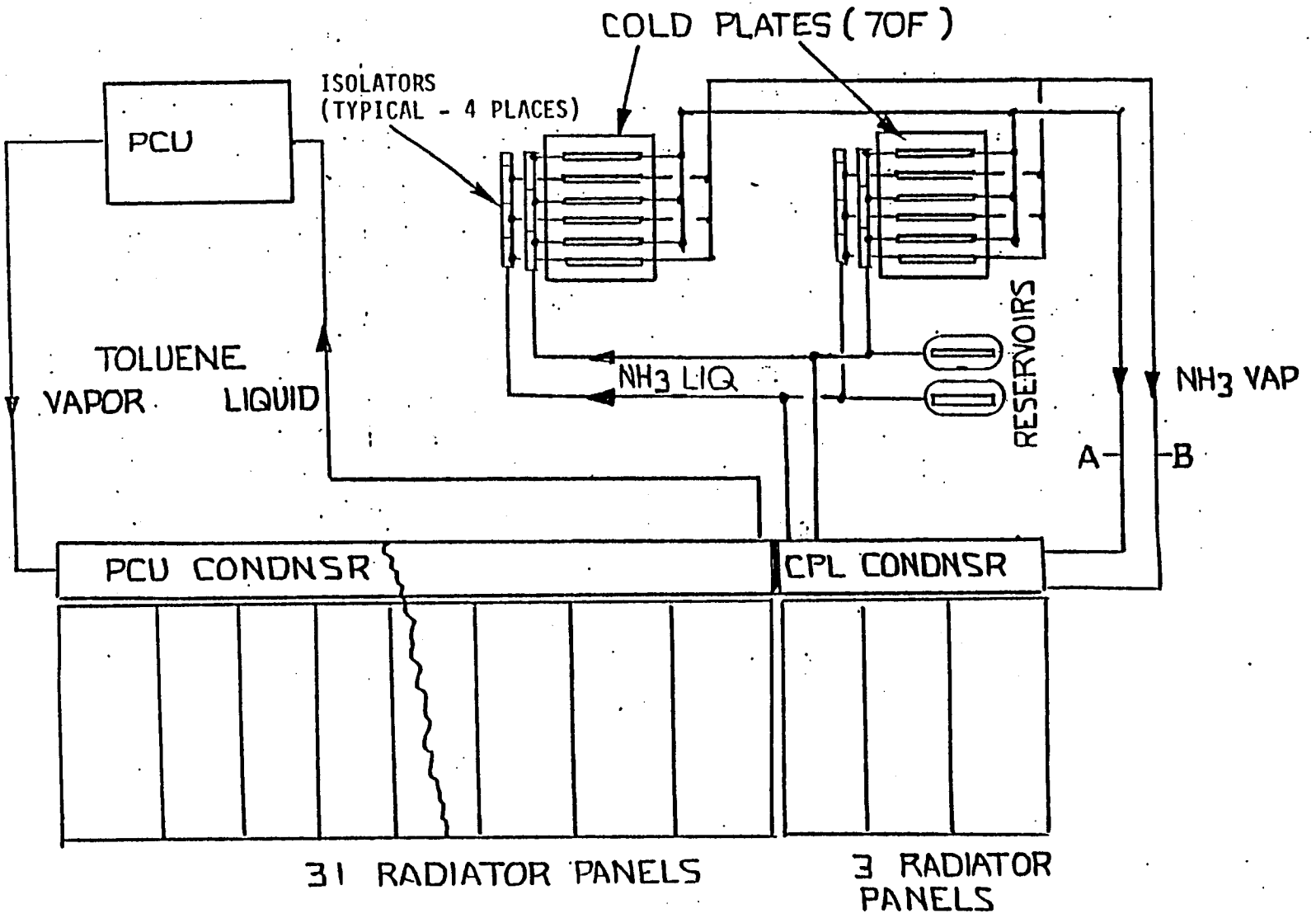

Figure 2.2.4.4-1 SD Equipment Box ORC Capillary Pumped Loop (CPL) Concept

ORC HEAT PIPE ELECTRONIC COOLING CONCEPT

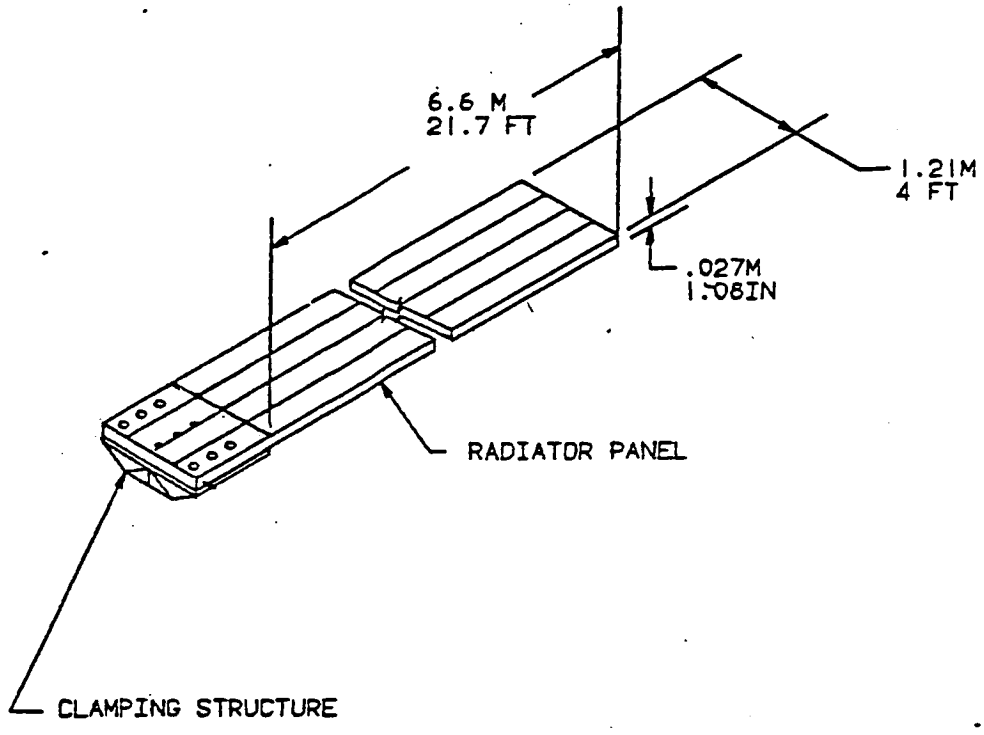

FIGURE 2.2.4.4-2

2.2.5 PMAD Subsystem Trades

2.2.5.1 PMAD Man-Tended Option Study

Various combinations of DC, low frequency and high frequency distribution architecture with PV only and SD only station power sources were compared in the option study prior to the selection of the 20 kHz distribution system. This selection brought about a simplification of the man tended options of the PV only or a form of hybrid PV-SD station with the variance being the power generation size of the PV and SD portions. For both the PV only and hybrid IOC reference, the selected man-tended option is PV only.

Further simplification in the cost reduction options is possible by reducing the growth-sized capability in such items as cabling, switch gear and feeders; however a preliminary estimate of resultant hardware savings is negated by additional operational costs including EVA time required to add full growth capability.

2.2.5.2 PMAD Evolutionary Growth Study

The purpose of the evolutionary growth study is to ensure that the PMAD design at IOC has the maximum possible growth potential. This requirement is met by including growth considerations in every design decision. All reference configurations described earlier have considerable growth potential. For example, SD controllers can easily be added as the station grows and SD software may be modified by on-board or earth-based operators.

As the station grows and evolves, advanced technology components can be incorporated in PMAD subsystems and ORU's. For example, the use of advanced technology converters could be implemented, resulting in mass savings and lower power conversion losses. The PMAD subsystem is designed for modular growth using ORU's as element building blocks in the module construction.

The power distribution network is installed at IOC and is sized for the final growth power level. Consequently, the station power capacity is fixed.

The alpha joint installed cabling and installed bus network are the growth limiting components. However, if the alpha joint and bus could be considered as ORUs then the growth of the station could evolve to any desired power level.

2.2.5.3 PMAD Health Maintenance Study

Extensive health maintenance capabilities for the electrical power system are provided by the power management processor (PMP) subsystem controllers and associated state-of-health electronics. Each processor includes software for reading and storing sensor and other measurement data, comparing current values against predefined limits, and evaluating rates-of-change for measurements where trend information is of significance. Measurement data from each processor are available to the central power management processor, and the data management system (DMS), for station level evaluations.

Where applicable, power system components will have built-in provision for current and voltage monitoring, and temperature sensing. State-of-health electronics assemblies will be provided to act as interfaces between the data processors and the temperature sensors. These assemblies will select a sensor on command from the processor and convert its output to digital form for use by the processor.

Certain parts of the electrical power system use components not solid state. Examples of these are the valves and pumps in the regenerative fuel cell system, and the generators in the solar dynamic system. State-of-health monitoring for these types of components will include additional measurements beyond voltage, current, and temperature. Examples of these measurements include pressure, flow rate, vibration, acceleration, and strain. Many of these measurements will be used for both control and status monitoring purposes.

State-of-health monitoring will initially and primarily be used for diagnostic purposes (i.e., to identify faults as they happen). Growth scenarios will include prognostic and advanced failure detection techniques.

2.2.5.4 PMAD Load Analysis

In order to properly size the distribution equipment capacity for the external (non-manned module) station areas, knowledge of the expected loads is required. Preliminary information has been generated by the other centers working on payloads and housekeeping (subsystem) loads. Based on information from C&A Panel Meetings for utility ports, and station baseline data, a loads analysis for the electric power system was done.

After reviewing load information, it becomes apparent that a PDCA capacity of 50 kW (or 25 kW/PDCU) is needed to serve the external station loads. All of the PDCA's would not be loaded to their maximum value at the same time since this would exceed the generation capacity of the station, however, it is possible and probable that one PDCA would be delivering its maximum load while the others were very lightly loaded. In order for the space station EPS to serve as a utility, the PDCA's must be designed to meet these changing conditions and sized for their maximum expected loading.

Maximum demand loading that could be expected on the lower ring feeder network and the upper ring feeder network was determined. The values indicate that 50 kW feeders will be necessary to deliver the required power under maximum demand loading conditions This will also require that the PDCU power buses that are in series with the feeders be sized at 50 kW, which is greater than that needed to serve the loads connected to the PDCU.

To summarize, the loads analysis indicates that the ring feeder capacity should be 50 kW for each feeder cable and the PDCU bus size should also be 50 kW.

2.2.5.5 PMAD Primary Power Quality

The primary power will be distributed at 440 V, 20 kHz, single phase. Bulk load conversion can be used wherein standard power voltages will be available to the loads. The standards being considered are 120 V, 400 Hz, single phase, 28 Vdc, and 50 Vdc. Bulk conversion has a distinct advantage in that the distribution system has control over the loading of the raw 20-kHz

bus. Primary power at 20 kHz can be used directly for some heating and lighting loads, but for all other loads it must be rectified and/or converted and processed as required. To ensure the least distortion of the 20-kHz sine wave, rectification should be of the inductive input filter type. This type results in loading the primary sine wave throughout the cycle. To avoid a high value of di/dt, a radio frequency low-pass filter must be used to prevent rapid rise to the rectified current thereby reducing electromagnetic interference. Use of this approach should reduce distortion of the 20-kHz sine wave to less than 2%. For practical considerations of cable weight and mass, a worst case of 5% (±2.5%) voltage regulation will be allowed for system feeders.

Power factors poorer than 0.5 can be tolerated in the system without damage to converters; however, such power factors will result in high losses. Normal power factors are expected to be 0.90. About 13% of final load use is estimated to be at 15 Vdc and about 7% will be at 5 Vdc. These two voltages require regulation of better than 1%. In this case, post regulators whose efficiencies approach 90% will be used. The bulk method shows further advantage here in that the cost of regulation is paid only where it is needed.

2.2.5.6 PMAD Primary Distribution Power Type

Primary distribution power type trade studies ranged from DC to to kHz with detailed analysis and comparisons of DC, 400 Hz and 20 kHz. The selected baseline primary power distribution throughout the station will be 440 VAC, single phase at 20 kHz. The NASA selection of 20 kHz power frequency allows use of small, efficient load isolation and voltage step down transformers. Selective use of these transformers throughout the station will simplify the task of designing ground-loop free signal and control cables. Another benefit of 20 kHz is that potential EMI problems diminish at higher frequencies. In addition, the use of 20kHz resonate power converters ensures the prevention of catastrophic fault currents since controlled fault current shut down and rapid current limiting is an intrinsic beneficial property of these power converters.

2.2.5.7 PMAD Distribution Architecture Study

The PMAD power distribution system can be configured in various ways to

take the power generated and transmit the power to the user loads. The PMAD Distribution Architecture Study was performed to quantify the merits of various configuration methods. The initial study in DR-02 of December 1985 compared ring with radial configurations. A more complete study with additional configurations of STAR and NETWORK was added in the DR02 submittal of December 1986.

The evaluation factors considered in the trade studies included cable mass, system efficiency, fault protection methods, switchgear requirements, voltage levels, and EMI. The configurations were constrained by load location, load level, fault tolerance requirements, cable parameters. Computer programs were written to calculate load flow, mass, and losses for each configuration. The results indicated that the ring configuration had the least mass, good efficiency, low switchgear count, and flexibility making it the best choice - for the baseline Space Station.

2.2.5.8 PMAD Feeder Study

A preliminary design and evaluation cable study was performed by team member General Dynamics to establish and verify key trade-off cable parameters to optimize power distribution characteristics with minimum acceptance cable loss. A typical Space Station cable was designed, fabricated and tested to verify theoretical power distribution characteristics such as characteristic impedance, shunt current losses, power losses and EMI emissions. The results of this effort established specific design requirements to produce a practical cable with acceptance power loss for minimum mass and satisfactory EMI emissions. A Litz wire in woven stripline configuration was tested and meets the requirements for a practical cable with acceptable power loss and EMI emissions.

2.2.5.9 PMAD Computer Fault Tolerance and Redundancy Study

The PMAD Fault Tolerance and Redundancy Management and Control Study addressed the processors used in the PMAD subsystem recognizing the fact that the "standard computer" ultimately would be chosen by the Work Package 02 contractor. The study was undertaken to explore the basic features required for PMAD in the hopes of being able to influence the choice of these features.

The study compared standby and active redundant configurations and potential restart mechanisms after a restored failure. The study addressed Error Detection and Correction (EDAC) for single-event upsets and compared the use of self-checking pairs and triple module redundancy (TMR) as the primary architecture. It also looked at cross-strapping of inputs and outputs for improved probability of mission success by elimination of single point failures. The need for on-orbit repair/replacement was studied. Sample scenarios for each type of system were generated to provide practical considerations. The need for and topology of redundancy of the data links connecting controllers was addressed briefly. The prime conclusions and recommendations were:

1. Use a basic processor with a redundant configuration such as self-checking pairs or triple module redundancy.
2. Provide automatic autonomous redundancy switching with manual intervention capability.
3. Use EDAC memory to eliminate most single event upsets.
4. Use dual sensors and actuators in critical functions to eliminate single-point failures.
5. Provide for on-orbit repair capability.

Recommendation for further study were provided.

2.2.5.10 PMAD Bus Alternative Study

The Space Station PMAD Bus Alternative Study looked at different means of communicating between PMAD controllers and their controlled devices. Several means of communicating with the numerous RPCs and RBIs were considered and the MIL-STD-1553B interface was selected primarily based on power consumption. The controller-to-controller communication interface was studied and included the CSMA/CD-type bus, the 1553B, and the IEEE 802 type of bus. The use of a dedicated net controller was considered. Response time requirements and performance for each type of network were determined. The use of a common versus a separate net with DMS was explored including the possible use of a broad-band network. Considerations in the use of fibre-optics versus co-ax for inter-controller communications were examined. Recommendations were made to

continue the study for survivability and the incorporation of redundancy. The main conclusions and recommendations were:

1. Use MIL-STD-1553B as a local area network to communicate with the RPCs and RBIs.
2. Use MIL-STD-1553B or TBD to communicate between controllers.
3. Use a dedicated net controller to unload the system controllers.

2.2.5.11 PMAD Subsystem/Component Optimization

Purpose

The purpose of this study was to determine the PMAD component optimization for the PV station Energy Storage Subsystem (ESS) interface with the PMAD.

Decision Factors

Two options were considered: one connecting the ESS to the DC source bus and the other connecting the ESS to the AC source bus beyond the source power converters. An ESS connection comparison between the two options was made as follows:

Component	DC Connection	AC Connection
Source Converters	8 to 25 kW, 692 lbs	8 to 50 kW, 1384 lbs
ESS Converters	N/A	4 to 25 kw, 384 lbs
Total mass	692 lbs	1748 lbs

From this comparison it is evident that the quantity and capacity of converters is greatly increased for the ac-connection option. Increased power conversion losses and reduced reliability are also the result of the addition of ESS power converters. And the increased conversion losses result in an increase in the PV array size. Thus the cost of the ac-connected ESS is greater because of the increased mass of the converters, array size, and quantity of converters and controls.

Conclusions

Based on the above considerations, it was recommended that the dc-connected ESS option be used because it meets the requirements at a much lower cost.

V2-225/7

2.2.5.12 PMAD Higher-Order Language Selection

Purpose

The purpose of this study was to select of a higher-order language (HOL) for use in programming the general purpose computers on the Space Station project. Specifically omitted was the selection of an object-oriented language for use in knowledge-based systems, which are planned for growth capabilities.

Decision Factors

The following three factors were considered in selecting the HOL:

a) Effectiveness/ease of use during software development
b) Effectiveness/ease of use during software maintenance
c) Project management considerations

The effectiveness/ease of use during software development was judged on the basis of previous experience and the information available describing the generated code of the compilers studied. Both the amount of generated code and its execution time were considered. Resources to conduct benchmark tests on which to make comparisons were not available. However, it was felt that the qualitative information available was adequate to make conclusions.

The effectiveness/ease of use during software maintenance was judged on the basis of the software development environment available during software development since the same environment will be used for both activities.

The primary project management consideration was the availability of project status reporting tools as part of the software development environment. These tools are sometimes provided as part of the software development environment.

Comparisons of Candidate Languages

The languages chosen for the study were Ada, C, Fortran, Pascal, and PL/M. HAL/S and Jovial were not considered since Ada is intended to replace them. Fortran was eliminated because of its lack of a modern software development environment, Pascal because of its deficiencies in embedded applications, and PL/M because it is restricted to use in a limited set of processors. Thus, Ada and C were the HOL's studied in depth.

Conclusions

Based on a detailed evaluation of the factors listed previously, it was concluded that Ada is the best choice for the standard Space Station high-order language. C is recommended as an acceptable backup.

2.2.5.13 Software Development Environment Centralization

Purpose

The purpose of this study was to identify the possible software development environments and to compare them.

Decision Factors

Four types of software development environments were identified as follows:

a) Fully centralized, with all software to be used residing on a single, time-shared computer, accessed via local and/or remote terminals by all developers

b) Centralized control, with developers at different sites using the hardware and software specified by a central authority, the hardware and software being the same at all sites

c) Decentralized hardware with specified software, wherein each site may choose its own hardware with the restriction that it support the software development tools that form a specified standardized software development environment

d) Fully decentralized hardware and software, but with the restriction that project-wide standardization and communication requirements be met. Unique tools would be made compatible with respect to language, syntax and data base format with the common tools, either directly or through the use of translators.

A table was constructed showing, for each option, its advantages and disadvantages.

Conclusions

It was recommended that software support environment standards be set for the entire Space Station project and that standard tools be made as widely available as possible. Also, that consideration be given to a time-varying degree of centralization, with considerable freedom during the earlier stages of software development and stricter standards enforced as system integration approaches.

V2-225/9

2.2.5.14 SSIS/DMS Interface with the PMAD

Purpose

The purpose of this study was to determine the manner in which the EPS controllers should interface with the DMS.

Decision Factors

The factors considered in determining the type of physical interface between the DMS and the EPS controllers were as follows:

a) development time and cost
b) additional load effect on the DMS
c) security of PMAD from other systems on the DMS
d) network costs

The three basic physical interfacing options considered were as follows:

a) an independent PMAD network configuration in which only the Power Management Controller would interface with the DMS

b) a shared DMS network configuration in which all communications between PMAD controllers would be through the DMS

c) a distributed PMAD configuration in which there is no central power management controller, each individual PMAD controller operating in an autonomous manner under control of the DMS central computing system.

Conclusions

It was recommended that an independent PMAD network configuration be used with only the Power Management Controller interfacing with the DMS. Only data would be provided to the DMS by PMAD, and both data and control flow would be accepted by the PMAD from the DMS.

2.2.5.15 PMAD Control - Centralized Versus Distributed Processing

Purpose

The purpose of this study was to identify the types of processing networks associated with centralized and distributed processing systems and determine their applicability for use in the Space Station project.

Decision Factors

In resolving use of centralized and/or distributed processing systems, three network structures were identified: centralized, federated, and hierarchical. A centralized network is one in which a single controller supervises the entire system through the use of local dumb controllers. A federated network consists of many controllers, each of which performs a specific task and communicates with others for data transfer or control purposes. A hierarchical network is one in which controllers have different levels of authority, with higher level controllers supervising lower level controllers.

The choice of which type of network to use for the Electrical Power System (EPS) was centered on its performance requirements. The primary consideration was that the Power Management and Distribution System (PMAD) be receptive to changing needs, robust enough to effect changes in EPS topology without human intervention, and sufficiently knowledgeable to correct any previously inefficient configuration changes. This requires a network in which several levels of analysis are being performed concurrently. At the lowest level, responses to local changes would be immediate to provide the best possible response time. The jurisdiction of this controller would be sufficiently narrow to service user's needs in real time. Higher level controllers whose domain encompasses several lower controllers need a broader range of authority. Here, system integrity was of major concern, with efficiency of the EPS topology in regards to source power generation, power availability, and load schedules having major consideration.

Conclusions

The hierarchical network structure was recommended for the EPS and the federated network structure was recommended for the Data Management System (DMS). The feasibility of the other network structures will continue to be evaluated.

V2-225/11

2.2.5.16 PMAD Data Transmission - Optical Versus Wire

Purpose

The purpose of this study was to determine the advantages and disadvantages of fiber optics and wire as the communication media between PMAD controllers in a hierarchical network structure.

Decision Factors

The relative advantages and disadvantages of fiber optics and wire were tabulated as follows:

Attribute	Fiber Optics	Wire
Technology Maturity	Relatively new	Very Mature
Power Requirements	More power	Less Power
Weight	Less weight	More weight
External Noise Immunity	Better immunity	Less immune
Data Rate	Higher	Lower

Conclusions

Wire was recommended as the communication media between PMAD controllers in a hierarchical network structure because it was felt that its advantages outweighed those of fiber optics.

2.2.5.17 PMAD Local Power Control - Hardware Versus Software

Purpose

The purpose of this study was to determine which power management and distrubution control functions should be performed by hardware and which by software.

Decision Factors

Since software has the over-riding advantage of being much more easily modified than hardware or firmware, it was determined that the hardware/firmware approach should be considered only under the following conditions:

a) the task can be expected to be invariant unless other major hardware changes are made which require its modification
b) the task requires a response time that cannot be met by software

Conclusions

It was recommended that only two types of PMAD components use the hardware/firmware approach: switchgear and remote power controllers. In these two cases, the required fast response time for quick fault detection and isolation, and for over-current protection cannot be met by the software. It was also recommended that the current limits for the remote power controllers be programmable so that their limits can be set/reset by the PMAD software.

2.2.6 Beta Joint Trade Study

The beta gimbal joints, used on the Space Station, and the alpha gimbal joint on the platforms, all perform the same function; positioning of the PV solar arrays, and the SD power modules. This analysis supports and documents the selection of the gimbal joint design. A description of our gimbal joint design concept is contained in Section 3.3.5 of Volume II.

The design aspect requiring a trade-off study was the degree of commonality among the station PV joints, SD beta joints, and the platform alpha joint. Elements of design such as the number of main bearings in the beta joints, and the type of joint drive motors, were resolved as part of the design process.

The following approaches were considered as to the possible degree of commonality.

A) Individual tailored design for the station SD, the station PV and the platform.

B) Commonality of joints for the station SD & PV and a special one for the platform.

C) Commonality among the station PV, SD and the platform joints.

A systematic evaluation of the alternatives or options with respect to the various relevant criteria was completed and is summarized in Tables 2.2.6-1 through 2.2.6-3.

The element of cost is implicit in all the elements listed. Explicit cost data was not available and is not be expected to change the order of the recommended alternatives.

Table 2.2.6-4 summarizes the comparison of the approaches evaluated.

TABLE 2.2.6-1

INDIVIDUALLY TAILORED DESIGN FOR THE STATION SD, PV AND THE PLATFORM (OPTION A)

ELEMENT	COMMENT	RATING
Design Effort	This will require the maximum design effort.	0
Procurement	While components for these different joints are required, still there are 4 each for PV, and 12 each for SD on the station.	7
Manufacturing	Same as for Procurement.	7
Assembly and Testing	Different tools and fixtures are required, although some commonality is expected.	3
Packaging for the NSTS	Three different types are required.	0
Weight	With individual design the weight is kept to a minimum.	10
Reliability	With oversizing and weight kept to a minimum some relative loss of reliability is expected.	5
Maintainability (EVA)	A simple design is expected.	10
Spares (ORU)	Requires the maximum variety and quantity of spares. However, consideration should be given to the actual number of each joint.	3
Interfacing	Requires the maximum variety. Still considerations are given to the number of each joint.	7
	TOTAL	52/100

TABLE 2.2.6-2

COMMONALITY OF JOINTS FOR THE STATION SD & PV AND A SPECIAL ONE FOR THE PLATFORM - (OPTION B)

ELEMENT	COMMENT	RATING
Design Effort	Two different designs are required.	5
Procurement	16 out of 18 joints have the same elements.	9
Manufacturing	Some slight difference between the Station PV & SD.	8
Assembly and	Number of different tools and fixtures is low.	6
Packaging for the NSTS	Two different package types are required.	5
Weight	Some weight growth is expected on the station and the platform joint.	6
Reliability	Reliability should increase with the slight overdesign of the station PV joint.	7
Maintainability (EVA)	Same as Option A.	10
Spares (ORU)	The number of spares are low.	8
Interfacing Hardware	There is a high interface uniformity	9
	TOTAL	73/100

TABLE 2.2.6-3

COMMONALITY AMONG THE STATION SD & PV AND THE PLATFORM JOINTS (OPTION C)

ELEMENT	COMMENT	RATING
Design Effort	Single design is required with some minor differences.	9
Procurement	Single - uniform effort.	10
Manufacturing	Only slight differences.	9
Assembly and Testing	Uniform tools and fixtures with slight differences.	9
Packaging for the NSTS	Uniformity maximized - some differences still exist	8
Weight	The overall weight is highest.	2
Reliability	With overdesign for the Station PV and the platform, the reliability improves.	8
Maintainability (EVA)	Same as Option A.	10
Spares (ORU)	The number of spares are the minimum possible.	10
Interfacing Hardware	Maximum uniformity, with slight differences.	9
	TOTAL	85/100

TABLE 2.2.6-4

COMPARISON MATRIX

APPROACH	PRO	CON	RATING
A. Individually designed joints	Minimum weight.	Everything else particularly ORU spares are the maximum.	52
B. Station beta joint same, platform joint unique	All elements are above average.	No one particular elements.	73
C. All joints are practically the same	Spares minimized reliability maximized. All advantages of commonality are maximized.	Weight will be the highest.	85

The advantage of approach B over approach A is pronounced. The case for commonality is not as strong when comparing approaches C and B, for the following reasons:

1) There are six beta joints on the IOC station, which after growth expand to sixteen, of which twelve are for the SD and four are for the PV. There are only two joints on a platform. Hence, commonality of the beta joints on the station affects 22% of the joints, while the alpha joint on a platform affects only 11% of the joints.

2) The contribution of platform joints to the overall commonality is balanced by the expected increase in weight of the platform joint. This is not the case on the station, i.e., no significant weight penalty to the station PV beta joints, due to its commonality with the SD joint is expected.

Roll rings were included in all joints. A case can be made for flexible cables in the beta joints for the station. However, it was assumed that roll ring reliability will be equal to or better than flexible cable reliability. Furthermore, it was assumed that less spares are required, and that the ORU maintenance for the roll rings is no more difficult than that for flexible cables. Furthermore, roll rings, slip rings or some other non-rewindable means of transferring power and signals across the joints will facilitate manual maintenance since no mechanical position limitation is placed on the joint.

It is recommended that: 1) full commonality for the station beta joints and the platform alpha joint be employed; 2) the platform alpha joint design and commonality be reevaluated when the exact alpha joint to platform interface is known; and, 3) roll rings be utilized throughout the station and platform joints.

2.3 DESIGN-TO-COST

The design-to-cost (DTC) program for the EPS during Phase B was dedicated to minimizing IOC cost and life-cycle cost (LCC). The primary activities consisted of cost modeling and data base generation, trade study cost analyses, and identification of cost drivers.

Initially, a cost estimate was made for the Phase C/D program. Subsequently, both IOC cost and LCC were estimated in the trade studies cost analyses. Cost drivers were identified to show where to concentrate cost optimization efforts. A high level of cost visibility was maintained. Cost activities and results were reported in all submittals of DR-09, DR-02, and DR-19.

2.3.1 Trade Study Cost Analyses

Cost assessments were made for each trade study configuration in two steps. The first step estimated the cost of hardware (for PV, SD, and PMAD), software; and level-of-effort (LOE) WBS items (e.g., work package management, system engineering and integration, ground support equipment, etc.) for development, IOC production, growth production, and initial spares. The second step incorporated the other costs (e.g., launch, EVA and IVA, replacement hardware, station reboost,etc.) to obtain a total life-cycle cost (LCC).

For the first step, four cost models were used for estimating the cost of hardware and software, namely, PRICE H, FAST, EPSCM, and PRICE S. These are described in Table 2.3-1. The PRICE H model was used for all of the hardware development and production cost estimates. The other two hardware models were used for limited independent checks on the PRICE model. The generic forms of the PRICE input are shown in Table 2.3-2. Input data for the PRICE runs were obtained from Rocketdyne engineers and the Rocketdyne team members. Costs were specific in constant 1987 dollars.

"Bottoms up" engineering cost estimates, received from the team members for particular configurations were used to calibrate the PRICE model. Costs

Table 2.3-1
SUMMARY OF COST MODELS USED FOR WP-04 COST ANALYSES

COST MODELS	DESCRIPTION	UTILIZATION
	COST MODELS (ROCKETDYNE)	
PRICE H	Parametric Cost Prediction Model (for hardware) Programmed review of information costing and evaluation. Predicts development and production costs for proposed electromechanical systems or devices while they are still in the concept stage. Two-step process in conducting an analysis with PRICE: (1) Creation and storage of the hardware parametric data, and (2) Using PRICE model with data file to estimate cost.	Used extensively for all PV, SD, and PMAD system subsystem level trades involving cost
FAST-E	Frieman Analysis of System Technique (for hardware costs) Similar to PRICE except code calibration can be done if weights and performance of the references cannot be determined.	Limited use as a check on PRICE for PV, SD, and PMAD system and subsystem level trades involving cost.
EPSCM	Electric Power System Cost Model (for hardware) EPSCM predicts LCC of candidate PV and SD EPSs with various component options based on cost estimating relationships for the various cost categories.	Limited use as a check on PRICE for PV, SD, and PMAD system and subsystem level trades involving cost. Rocketdyne developed proprietary code.
PRICE S	Parametric Cost Prediction Model (for software) Predicts development cost for software including systems engineering, programming, configuration, QA, documentation and program management.	Used for system and subsystem level software trades involving cost

Table 2.3-2
INPUT DATA FOR PRICE COST ESTIMATES

- Quantity of equivalent prototypes (PROTOS)
- Quantity of production units (QTY)
- Mass of electronics portion (WE)
- Mass of structure portion (WS)
- Factors for structure and electronics portion
  - Integration with other assemblies (INTEGS, INTEGE)
  - Manufacturing complexity (MCPLXS, MCPLXE)
  - New design (NEWST, NEWEL)
  - Design repeat (DESRPS, DESRPE)
- Engineering complexity factor (ECMPLX)
- Schedule
  - Start of development (DSTART)
  - Start of production (PSTART)

for the numerous other trade study configurations were estimated with the calibrated PRICE model. PRICE S was used for software development cost estimates. PRICE H was also used for estimating the cost of the WBS element Installation, Assembly and Checkout, and the WBS element Test. The other WBS elements were direct estimates of time-phased man-loading. The estimates were based on the DR-08 WBS dictionary definitions of the type of effort included in each level 5 element, prior programmatic experience, and the overall schedule estimated for the EPS.

LCC Evaluation Methodology

Step two used the cost assessment logic and information flow shown in Figure 2.3-1. To accomplish the cost assessment, worksheets and data tables were completed for each concept evaluated. These worksheets and data tables were the heart of the evaluation methodology. They assured that the evaluation was based on as much factual data as practical and provided a documented record of their bases.

The information was generated on a concept modular basis to facilitate the various growth scenarios and EPS concept configurations considered for evaluation. An electronic spreadsheet (LOTUS 1-2-3) was used to generate and document the cost assessment data. The cost assessment spreadsheet contained several levels of worksheets and data files. Lower levels, such as the

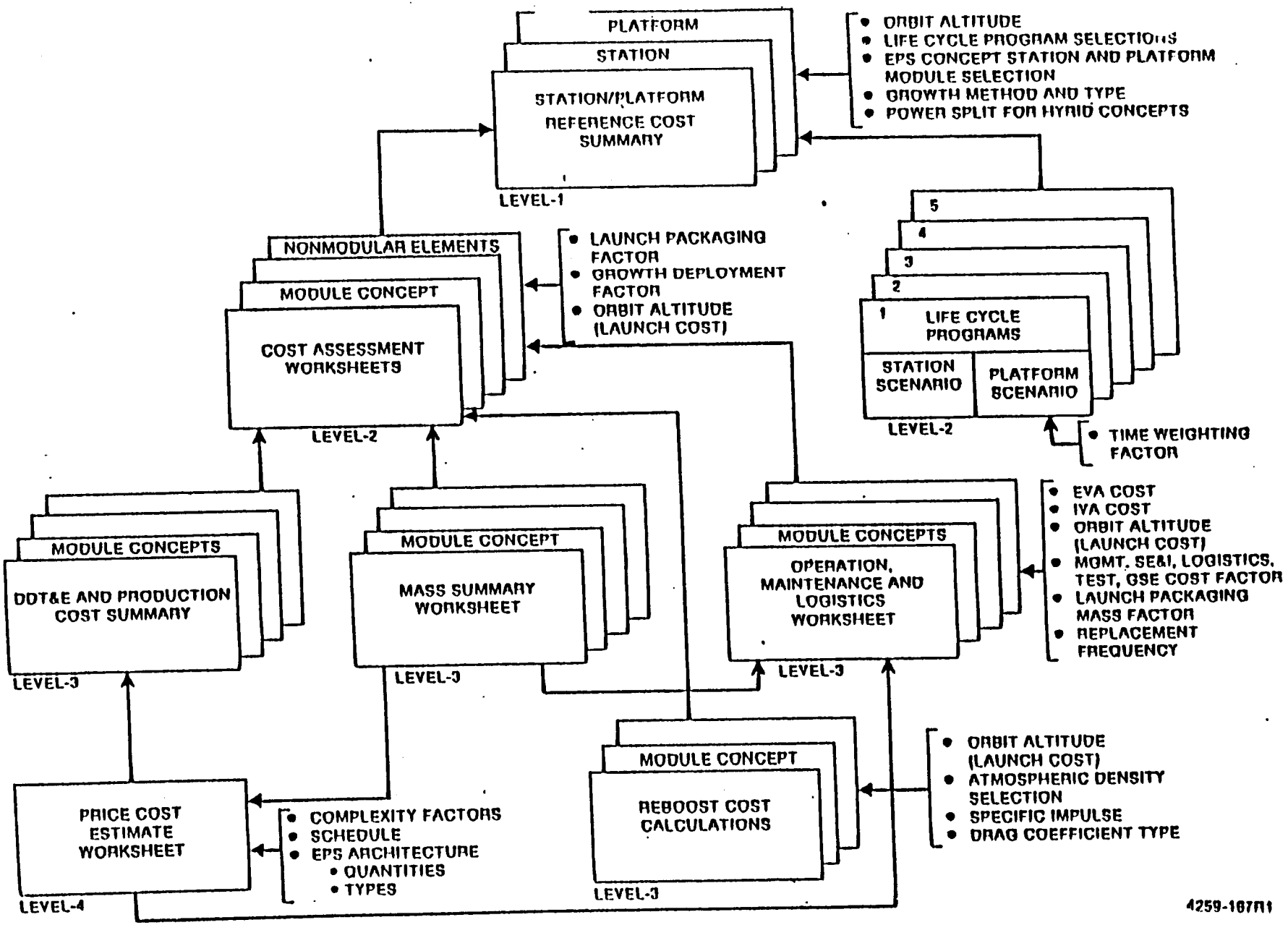

Figure 2.3-1 Cost Assessment Logic and Information Flow in Rocketdyne LCC Estimating Code

reboost cost calculations spreadsheet (example shown in Table 2.3-3) were used as inputs to upper level spreadsheets, such as the cost assessment worksheet (example shown in Table 2.3-4). The cost assessment worksheet information was, in turn, collected in the reference concept (level 1) cost summary worksheet, which was used in conjunction with the life-cycle scenario file to generate the LCC for each of the reference concepts. Any change in data files or their input worksheets automatically updated the entire cost assessment. This approach accurately and rapidly accommodated changes in concept, life-cycle scenario, discount rate, cost data, etc.

Postulated EPS Life-Cycle Programs

There were five life-cycle programs. Each program comprised a station and platform time-power schedule. There were three station scenarios (nominal, man-tended, and high power) and three platform scenarios (no platforms, platforms starting at IOC, and delayed platforms). The computer code combined the platform and station scenarios (as instructed) to form the desire life-cycle program. Both the combination of scenarios and time-power schedule could be varied as desired.

Cost Assessment Worksheet

The cost assessment worksheet and EPS life-cycle program data were used to calculate the EPS concept cost elements appearing in the reference concept cost summary. There were three groups of cost data listed for each defined concept module, initial cost, growth cost, and annual cost. Cost items such as DDT&E, initial spares, and ground support were not a function of the number of concept modules. There were other cost elements that do not grow as a function of number of modules, such as portions of PMAD. The cost assessment worksheet "pulled the data" from the operations, maintenance, and logistics (OML) worksheet, mass summary worksheet, and reboost cost calculations worksheet. The DDT&E production, and initial spares cost data were directly inputted based on PRICE-generated data.

Reboost Cost Calculations

The factors that affected the reboost cost were physical surface area,

MODULE LOCATION	DRAG COEF. TYPE	DRAG COEF. (CD/CDN) VALUE	FUEL MASS/ AREA(WF/A) (lb mass/ ft^2	UNIT REBOOST COST ($/m^2/yr)	EPS MODULE PHYSICAL AREA(SQUARE METERS)							
					START PV-2 12.5KW 1	CDC-4 25KWe 2	ORC-4 25KWe 3	4	5	PV-3 8KWe 6	7	8
PV ARRAY	4	0.5677	0.0876	2751	289.00					223.00		
SD CONCENTRATOR	4	0.5677	0.0876	2751		194.60	231.90					
FRONTAL	2	0.6282	0.0969	3045		20.70	26.30					
PROFILE												
PGS RADIATOR	5	0.6282	0.0969	3045								
PARALLEL TO TRNSVERSE BOOM	6	0.2314	0.0357	1121		92.00	200.50					
NORMAL TO TRANSVERSE BOOM	6	0.2314	0.0357	1121		0.67	0.67					
PARASITIC LOAD RADIATOR	1	1.0000	0.1543	4847	23.90	7.80	6.00			19.96		
EPS STRUCTURE												
PGS SUBTOTAL					312.90	315.77	464.87			242.96		
ESS RADIATOR(ECLIPSE AND CONTINGENCY)	2	0.6282	0.0969	3045	35.00					0.00		
ESS RADIATOR(SAVE HAVEN AND CONTINGENCY)	2	0.6282	0.0969	3045								
ESS RADIATOR(SAVE HAVEN)	2	0.6282	0.0969	3045								
ESS SUBTOTAL					35.00	0.00	0.00			0.00		
PMAD RADIATOR	2	0.6282	0.0969	3045	0.00	0.00	0.00			0.00		
TOTAL MODULE PHYSICAL AREA(SQUARE METERS)					347.90	315.77	464.87			242.96		
ANNUAL MODULE REBOOST COST(MILLION)										1.21		

(a) TWO WING ASSEMBLIES PER MODULE
(b) DRAG CALCULATIONS DO NOT INCLUDE SHADOWING EFFECTS
(c) THE DENSITY VALUES ARE BASED ON THE 2 SIGMA,MEAN AND -2 SIGMA VALUES OF PREDICTED SOLAR FLUX

H-SPACE STATION ORBIT ALTITUDE(n.mi)	250
DENSITY SELECTION NUMBER	2
RHO-ATMOSPHERIC DENSITY(Kg/m^3)	8.00E-13
LC-LAUNCH COST($/lb mass)	2920
IPS-SPECIFIC IMPULSE(lb-s/lb mass)	230
CDN-MAXIMUM DRAG COEFFICIENT(SURFACE NORMAL TO VELOCITY VECTOR)	2.30
WF/(A(CD/CDN))-ANNUAL FUEL MASS/ UNIT AREA-DRAG COEF PROD(lb mass/ft^2)	0.1543

LAUNCH COST(LC) AND ATMOSPHERIC DENSITY(RHO) MEMO

H (n.mi)	LC ($/lb mass)	AVERAGED FROM 1991-2001(c) +2SIGMA (97.7%) (Kg/m^3) 1	MEAN (50%) 2	-2SIGMA (2.3%) 3	RANGE MAX. 4	MIN. 5
175	2400	2.20E-11	1.10E-11	6.00E-12	4.25E-11	3.30E-12
200	2550	1.05E-11	4.50E-12	2.15E-12	2.20E-11	1.00E-12
220	2690	5.50E-12	2.20E-12	1.11E-12	1.35E-11	9.20E-13
250	2920	2.26E-12	8.00E-13	3.00E-13	6.30E-12	1.16E-13
270	3100	1.38E-12	4.23E-13	1.38E-13	4.25E-12	5.55E-14

DRAG COEFFICIENT MEMO

TYPE	BETA0 (DEG)	THETA (DEG)	DESCRIPTION	CD/CDN VALUE
1	90	0	FIXED NORMAL (VELOCITY) SURFACE	1.0000
2	0	90	TRANSVERSE BOOM PARALLEL SURFACE, ALPHA JOINT FOLLOWING	0.6282
3	0	0	TRANSVERSE BOOM PERPENDICULAR SURFACE, ALPHA JOINT FOLLOWING	0.0734
4	90	0	SUN POINTING SURFACE, ALPHA AND BETA JOINT FOLLOWING	0.5677
5	0	90	NON SUN POINTING SURFACE PARALLEL TO, TRANSVERSE BOOM,ALPHA AND BETA JOINT FOLLOWING	0.6282
6	0	0	NON SUN POINTING SURFACE PERPENDICULAR TO, TRANSVERSE BOOM,ALPHA AND BETA JOINT FOLLOWING	0.2314
7	90	0	SAME AS TYPE 4 EXCEPT SURFACE PARALLEL TO THE VELOCITY VECTOR DURING ECLIPSE(e)	0.4285
8	0	0	SAME AS TYPE 6 EXCEPT SURFACE NORMAL TO THE VELOCITY VECTOR DURING ECLIPSE(e)	0.2130
9	0	90	SAME AS TYPE 5 EXCEPT SURFACE NORMAL TO THE VELOCITY VECTOR DURING ECLIPSE(e)	0.8100
10	0	90	SAME AS TYPE 2 EXCEPT SURFACE NORMAL TO	0.8100

Table 2.3-3 Example of Reboost Cost Calculations Spreadsheet (Values Not Current)

Table 2.3-4 Example of Cost Assessment Worksheet

COST ASSESSMENT WORKSHEET

ORBIT ALTITUDE: 250 n.mi DS: 2

MODULE COSTS(1987 $MILLIONS)

	MODULE NO.	STATION 1	2	3	STATION 4	STATION 5	PLATFORM 6	PLATFORM 7	8
	TYPE	PV	CBC	ORC	COM PMAD	COM PMAD	PV	COM. PMAD	NO GROWTH
	POWER(KWe)	12.50 (a)	25.00	25.00	IOC	250.00 DELTA GROW	0.00	NO GROWTH	
IOC-DDT&E FIXED									
PV MODULE(W/PV SOURCE PMAD)									
SD MODULE(W/SD SOURCE PMAD)									
COMMON PMAD									
SOFTWARE									
PSF HARDWARE									
BETA JOINT									
ALPHA JOINT									
PMAD USER LOAD CONVERTERS									
SUBTOTAL DDT&E FIXED									
IOC-PRODUCTION FIXED									
ALPHA JOINT									
PROTOFLIGHT CREDIT									
SUBTOTAL PRODUCTION FIXED									
IOC-OTHER FIXED(INITIAL SPARES)									
TOTAL FIXED									
IOC-PRODUCTION VARIABLE									
PV MODULE(W/PV SOURCE PMAD)									
SD MODULE(W/SD SOURCE PMAD)									
COMMON PMAD									
BETA JOINT									
PMAD USER LOAD CONVERTERS									
SUBTOTAL PRODUCTION VARIABLE									
IOC-OTHER VARIABLE									
SYSTEM IMPACTS									
LAUNCH LAUNCH PKG FACTOR: 1.20									
DEPLOYMENT									
SUBTOTAL OTHER VARIABLE									
TOTAL VARIABLE									
GROWTH-DELTA PRODUCTION VARIABLE($M/KW)									
GROWTH-DELTA TOTAL VARIABLE($M/KW)									
ANNUAL-FIXED(GROUND SUPPORT)									
ANNUAL-VARIABLE									
REPLACEMENT HARDWARE & LAUNCH									
ON-ORBIT OPERATIONS & MAINTENANCE									
REBOOST & OTHER SYSTEM IMPACTS(b)									
SUBTOTAL ANNUAL VARIABLE									
GROWTH-DELTA ANNUAL VARIABLE($M/KW/YR)									

(a) TWO WING ASSEMBLIES PER MODULE
(b) DRAG CALCUL[illegible]S DO NOT INCLUDE SHADOWING EFFECTS

surface orientation, reboost fuel specific impulse, and orbit altitude. The reboost cost was directly proportional to atmospheric density and drag coefficient and inversely proportional to reboost fuel specific impulse. The surface orientation and location determined the drag coefficient. For the same physical area, orientation and location could have a large impact on reboost cost. The values appearing in the drag coefficient menu were derived by relating the surface angle of attack to the alpha and beta angles and then averaging the pressure and shear contribution to the drag coefficients over the number of Space Station orbits that occur in one year (5640).

The fuel launch cost and atmospheric density were functions of the orbit altitude. A predicted mean value (for a 10-year period) of atmospheric density was used in the cost assessment. The uncertainty in predicting the solar flux and geomagnetic index, which affect atmospheric density, could result in a large uncertainty in reboost cost. Selection of the orbit altitude, drag type, and density selection number automatically entered the appropriate values from the menus into the spreadsheet calculations. The reboost fuel specific impulse, module physical area, and maximum drag coefficient were entered directly.

Operation, Maintenance, Logistics (OML) Worksheet

An OML worksheet was prepared for each EPS concept. The OML worksheet calculated the ORU (orbital replacement unit) replacement hardware cost and its launch and maintenance costs for each ORU and totaled them for the module based on the following inputs: (1) number of ORUs per module, (2) ORU unit cost, (3) ORU mass, (4) MTBF, (5) live, and (6) EVA and IVA maintenance times. The factors appearing in the worksheet were also inputs to these calculations and could be varied to perform cost sensitivity studies. The EVA and IVA times for module deployment were estimated, thus, providing EPS deployment cost data. The calculated data from the OML worksheet and the other module OML worksheets was collected in the OML worksheet summary (example shown in Table 2.3-5). From there, the information was extracted and placed into the cost assessment worksheet.

Table 2.3-5 Example of OML Worksheet Summary

COST ASSESSMENT STUDY INDEPENDENT INPUT PARAMETERS

OML WORKSHEET(OML SPREADSHEET)	
LAUNCH PACKAGING MASS FACTOR:	1.20
EVA COST($K/man-h):	103.00
IVA COST($K/man-h):	15.20
SUBCONTRACTOR AND RK G&A FACTOR:	1.50
MGMT.,SE&I,LGSTCS.,TEST & GSE FACTOR:	1.50
OVERALL REPLACEMENT FREQ. FACTOR:	1.00
SPECIFIC REPLACEMENT FREQ. FACTOR:	1.00
POSTULATED LIFE CYCLE PROGRAM	
TIME RATE FACTOR:	.00%
LIFE CYCLE TIME(yr):	30
MAXIMUM POWER GROWTH(KWe):	300

COST ASSESSMENT WORKSHEET	
LAUNCH PACKAGING MASS FACTOR:	1.20
GROWTH DEPLOYMENT FACTOR:	1.00
DEPLOYMENT ALTITUDE(n.mi):	220
PSF HARDWARE INCLUDED(Y=1,N=0):	0
USER LOAD CONVERTERS INCLUDED(Y=1,N=0):	0
SYSTEM IMPACTS INCLUDED(Y=1,N=0):	0
REBOOST COST CALCULATIONS	
ORBIT ALTITUDE(n.mi):	250
DENSITY SELECTION NUMBER:	2
IPS-SPECIFIC IMPULSE(lb-s/lb mass):	230
CDN-MAXIMUM DRAG COEFFICIENT:	2.30
LAUNCH COST FACTOR:	1.00
REBOOST FUEL PALLET FACTOR:	1.70

COST ASSESSMENT STUDY DEPENDENT INPUT PARAMETERS

LCD-LAUNCH COST DEPLOYMENT($/lb mass):	26
LC-LAUNCH COST($/lb mass):	29
RHO-ATMOSPHERIC DENSITY(Kg/m^3):	8.00E-
WF/A*CD-ANNUAL FUEL MASS/AREA-DRAG COEF(lb mass/ft^2):	0.15
NUMBER OF PLATFORMS	

FILE NO: DP46OML
REVISION DATE: 18-Jun-86
ROCKETDYNE
R.PASCHALL X4796

OPERATION, MAINTENANCE, LOGISTICS WORKSHEET SUMMARY

COST ELEMENTS	MODULE NO.	STATION 1	2	3	STATION 4	STATION 5	PLATFORM 6	PLATFORM 7	8
	TYPE	PV	CBC	ORC	COM PMAD	COM PMAD	PV	COM. PMAD	NO GROWTH
	POWER(KWe)	12.50	25.00	25.00	IOC	250.00 DELTA GROW	0.00	NO GROWTH	
RPLCMNT HARDWARE/CONSUMABLES(lb mass/yr)									
RPLCMNT HARDWARE/CONSUMABLES COST($M/yr)									
RPLCMNT HARDWARE/CONSUMABLES LAUNCH COST($M/yr)									
COST SUBTOTAL($M/yr)									
EVA TIME(h/yr)									
IVA TIME(h/yr)									
OPERATIONS AND MAINTENANCE COST($M/yr)									
DEPLOYMENT($M)									

ORBIT ALTITUDE (n.mi):	250.
LAUNCH COST($/lb mass):	2920.
LAUNCH PACKAGE MASS FACTOR:	1.
EVA COST($K/h):	103.
IVA COST($K/h):	15.
*SUBCONT. & RK G&A FACTOR:	1.
*MGMT.,SE&I,LOGISTICS,TEST AND GSE FACTOR:	1.
LAUNCH COST FACTOR:	1.
OVERALL RPLCMNT FREQ. FACTOR:	1.
SPECIFIC RPLCMNT FREQ. FACTOR:	1.

ORIGINAL PAGE IS OF POOR QUALITY

Mass Summary Worksheet

The mass summary worksheet (example shown in Table 2.3-6) listed masses by subsystem, assembly, and component (if available) for each concept module and nonmodular element. These data were used to calculate the EPS mass for the reference concepts as input to the cost assessment worksheets (to calculate launch cost), to the OML worksheets, and to PRICE.

2.3.2 Cost Drivers

In order to determine EPS cost drivers, the Rocketdyne life-cycle cost (LCC) model was run to identify the more significant costs and the factors contributing to them. The model was run using the following assumptions and ground rules.

One station plus one platform
Station power: 75 kW IOC, 300 kW growth
Platform power: 8 kW IOC, 15 kW growth
IOC station has 2-12.5 kW PV modules and 2-25 kW SD modules
Station growth is by replication of SD modules
Station and platform commonality for PV arrays and Ni-H_2 batteries
Beta joints are included
PMAD frequency: 20 kHz station, 20 kHz platform
User load converters are included.
All costs include estimates for subcontractor and contractor G&A and fee and other WBS items (management, SE&I, GSE, IACO, Test, Ops, Maint., etc.)

Costs were estimated for the latest PMAD architecture (including 20 kHz equipment on both the station and platform) and include user load converters.

Station reboost cost was omitted for the latest determination of cost drivers. The reason for omitting station reboost cost was that the station propulsion system now uses hydrogen-oxygen fuel, and the fuel source for reboost is already on the station (i.e., water). The only reboost cost could

Table 2.3-6 Example of Mass Assessment Worksheet Summary (Values Not Current)

EPS COMPONENT	MODULE NO. TYPE POWER(KWe)	STATION 1 PV 12.50	2 CBC 25.00	3 ORC 25.00	STATION 4 COM PMAD IOC	STATION 5 COM PMAD 250.00 DELTA GROW	PLATFORM 6 PV 8.00	PLATFORM 7 COM. PMAD NO GROWTH	8 NO GROWTH
		MASS ASSESMENT SHEET							
		MODULE MASS (lb mass)							
PGS-PV		1808.00	0.00	0.00	0.00	0.00	1808.00	0.00	
PGS-SD(CBC/ORC)									
CONCENTRATOR		0.00	1948.00	2181.00	0.00	0.00	0.00	0.00	
RECEIVER		0.00	3367.00	2624.00	0.00	0.00	0.00	0.00	
POWER CONVERSION UNIT		0.00	1527.00	652.00	0.00	0.00	0.00	0.00	
RADIATOR		0.00	1927.00	3457.00	0.00	0.00	0.00	0.00	
SUBTOTAL PGS-SD		0.00	8769.00	8914.00	0.00	0.00	0.00	0.00	
BETA JOINT ASSY		1300.00	650.00	650.00	0.00	0.00	0.00	0.00	
PGS TOTAL		3108.00	9419.00	9564.00	0.00	0.00	1808.00	0.00	
ESS TOTAL NI-H2 BATTERY		2792.00	0.00	0.00	0.00	0.00	1005.00	0.00	
PMAD-STATION PV SOURCE		559.00	0.00	0.00	0.00	0.00	0.00	0.00	
PMAD-STATION SD SOURCE		0.00	109.00	109.00	0.00	0.00	0.00	0.00	
PMAD-STATION COMMON		0.00	0.00	0.00	10299.20	9579.60	0.00	0.00	
PMAD-PLATFORM PV SOURCE		0.00	0.00	0.00	0.00	0.00	895.00	0.00	
PMAD-PLATFORM COMMON		0.00	0.00	0.00	0.00	0.00	0.00	1016.10	
PMAD TOTAL		559.00	109.00	109.00	10299.20	9579.60	895.00	1016.10	
TOTALS		6459.00	9528.00	9673.00	10299.20	9579.60	3708.00	1016.10	

be for (1) the extra electrolysis units required to electrolyze water into hydrogen and oxygen and (2) the power to operate the units. An estimate showed these costs to be small, and they were not included since they did not significantly affect the cost drivers. The only reboost cost included was for the platform.

A detailed breakdown of cost distribution is provided in Table 2.3-7. It shows costs as a percentage of total LCC. The primary cost drivers can be obtained from this table.

The largest cost driver is replacement hardware cost during 30-years of operations (36% of the total LCC for station + platform). The factors in this cost are:

Quantity of each ORU
Mean time between replacement (MTBR) for each ORU
Cost of each ORU (for hardware cost)
Weight of each ORU (for launch cost)

For the station, launch costs are about 40% of the total replacement hardware cost and are dependent on the orbital altitude.

Shown below are: (1) the ORUs that are the primary contributors to replacement hardware costs, (2) the contribution to the subsystem life-cycle cost (LCC), (3) the important cost factors.

SUBSYSTEM	ORU	% CONTRIBUTION TO SUBSYSTEM LCC	PRIMARY FACTORS THAT CONTRIBUTE TO COST
PV MODULES	SOLAR ARRAY WING	52%	ORU COST
	Ni-H2 BATTERY	20%	ORU QTY,WEIGHT,MTBR
		72%	
SD MODULES	CONCENTRATOR SURFACE	26%	ORU COST & WEIGHT
	RECEIVER/PCU	14%	ORU COST & WEIGHT
	RADIATOR PANEL	39%	ORU QTY & WEIGHT
		79%	
PMAD	POWER DISTRIBUTION & CONTROL UNIT (PDCU)	89%	ORU QUANTITY

V2-23/7

TABLE 2.3-7 EPS COST DRIVERS -- % OF TOTAL LCC

	STATION				I PLATFORM			
	IOC POWER(75KW)		ADDED POWER(225KW)		IOC POWER(8KW)		ADDED POWER(8KW)	
HARDWARE COST		32.94		18.49		2.04		1.33
DDT&E		20.10		0.00		0.09		0.00
PV MODULE		5.40		0.00		0.05		0.00
PV WING ARRAY	1.27		0.00		0.02		0.00	
NI-H2 BATTERY	0.77		0.00		0.02		0.00	
THERMAL CONTROL	0.49		0.00		0.00		0.00	
PV PMAD	2.36		0.00		0.00		0.00	
BETA JOINT	0.52		0.00		0.00		0.00	
SD MODULE		8.38		0.00		0.00		0.00
CONCENTRATOR	2.40		0.00		0.00		0.00	
RECEIVER/PCU	2.67		0.00		0.00		0.00	
RADIATOR	1.51		0.00		0.00		0.00	
SD PMAD	1.80		0.00		0.00		0.00	
PMAD		4.90		0.00		0.04		0.00
SOFTWARE		1.42		0.00		0.00		0.00
PRODUCTION		7.41		10.55		1.45		1.08
PV MODULE		2.45		0.00		1.08		1.08
PV WING ARRAY	1.27		0.00		0.64		0.64	
NI-H2 BATTERY	0.49		0.00		0.25		0.25	
THERMAL CONTROL	0.11		0.00		0.00		0.00	
PV PMAD	0.59		0.00		0.16		0.16	
BETA JOINT	0.08		0.00		0.04		0.04	
SD MODULE		1.60		8.73		0.00		0.00
CONCENTRATOR	0.40		2.86		0.00		0.00	
RECEIVER/PCU	0.17		1.22		0.00		0.00	
RADIATOR	0.76		3.42		0.00		0.00	
SD PMAD	0.23		1.05		0.00		0.00	
BETA JOINT	0.04		0.18		0.00		0.00	
PMAD		3.35		1.82		0.38		0.00
OTHER		5.44		7.94		0.49		0.25
INITIAL SPARES		1.92		0.00		0.15		0.00
PV MODULE	0.96		0.00		0.00		0.00	
SD MODULE	0.82		0.00		0.00		0.00	
PMAD	0.14		0.00		0.15		0.00	
LAUNCH		2.86		6.41		0.32		0.25
PV MODULE	0.86		0.00		0.25		0.25	
SD MODULE	1.30		5.83		0.00		0.00	
PMAD	0.69		0.57		0.07		0.00	
DEPLOYMENT		0.07		0.26		0.02		0.00
PV MODULE	0.01		0.00		0.02		0.00	
SD MODULE	0.06		0.26		0.00		0.00	
SYSTEM IMPACTS		0.59		1.28		0.00		0.00
PV MODULE	0.31		0.00		0.00		0.00	
SD MODULE	0.28		1.28		0.00		0.00	
30-YEAR OPERATIONS COST		37.50						7.69
REPLACEMENT HARDWARE & LAUNCH				30.34				5.74
PV MODULE			9.55				5.37	
SD MODULE			17.06				0.00	
PMAD			3.73				0.37	
ON-ORBIT OPERATIONS & MAINT				5.28				0.38
PV MODULE			0.54				0.28	
SD MODULE			3.28				0.00	
PMAD			1.46				0.10	
REBOOST				0.00				1.26
PV MODULE			0.00				1.26	
SD MODULE			0.00				0.00	
PMAD			0.00				0.00	
GROUND SUPPORT				1.88				0.31

On-orbit operations and maintenance is about 5% of the total LCC. Its primary factors are the MTBR for each ORU combined with the number of EVA and IVA hours and the cost of those hours. Any significant change to these factors could make an appreciable difference in LCC.

While DDT&E is a large part of the IOC cost, it is only 20% of the total LCC. Here is the area where relatively minor expenditures could possibly lead to major cost savings in production and 30-year operations costs, especially if ORU cost and weight can be reduced or the mean time between replacement can be increased.

For instance, an increase of 5 years in MTBR for PV arrays would reduce 30-year replacement hardware costs by about 70 million dollars. Similarly, increasing battery MTBR by 5 years would save about 180 million dollars in total LCC.

Operations costs for 2-12.5 kW PV modules is approximately 20 million dollars per year compared to 5 million dollars per year for a 25-kW SD module. The two PV modules could be replaced with one SD module for about 80 million dollars which could be recovered in operations cost savings in less than 6 years.

2.4 SPACE STATION INFORMATION SYSTEM (SSIS) ANALYSES

2.4.1 System Architecture and Requirements Definition

Work Package 04 will utilize as much as possible hardware and software which will be designed by work package 02 and provided as GFE for the Space Station program. Hardware and software which will be used to implement PMAD controllers is listed in Table 2.4.1-1.

PMAD communicates with other PMAD controllers by means of its own dual redundant PMAD control bus. Thus PMAD will not require the use of the DMS global data bus network for normal operations between PMAD controllers. However, the DMS global data bus will be utilized to obtain the required tracking data from the C&T Station System for PV and SD pointing functions.

The EPS is expecting to use the crew MPAC work stations services for EPS manual control and monitorig when required. The use of these work stations will be minimal since the PMAD system is designed for automatic and autonomous operation with minimum operator interaction.

During the design effort, work package 04 will require the use of a DMS simulator to design and checkout the DMS/PMAD interface. A simulator will also be required for C&T/PMAD interface design and checkout. These simulators are expected to be furnished to work package 04 by work package 02.

Table 2.4.1-1

Work Package 04 Hardware/Software Requirements

EXPECTED GFE HARDWARE TO WP-04	PMAD CONTROLLER (1)		
	PMC	PSC	PDC, MBC PVC, SDC
HARDWARE			
EMBEDDED DATA PROCESSOR	-	X	X
STANDARD DATA PROCESSOR	X	-	-
NETWORK INTERFACE UNIT	X	-	-
BUS INTERFACE ADAPTOR	X	X	X
MULTIPLEXER/DE-MULTIPLEXER	-	-	X
DATA LINKS	X	X	X
SOFTWARE			
OPERATING SYSTEM KERNEL	X	X	X
STANDARD SYSTEM SERVICES	X	-	-
OPERATING SYSTEM	X	-	-
NETWORK OPERATING SYSTEM	X	X	X
DATA BASE MANAGEMENT SYSTEM	X	-	-
USER INTERFACE LANGUAGE	-	-	-
SSE SOFTWARE	X	X	X

NOTE:
(1) PMC = POWER MANAGEMENT CONTROLLER
PSC = POWER SOURCE CONTROLLER
PDC = POWER DISTRIBUTION CONTROLLER
MBC = MAIN BUS CONTROLLER
PVC = PV CONTROLLER
SDC = SD CONTROLLER

V2-241/2

2.4.2 Software Development Environment

The Software Development Environment (SDE) is the collection of software tools (programs) used for the specification, development, testing, configuration control, and documentation of computer programs.

At Rocketdyne, the SDE activities will be supervised and directed by a software manager, as specified by the combined Level A/B Software Management Plan. Agency coordination and direction for the EPS software development effort will be provided by a NASA Software Manager at the Lewis Research Center (LeRC).

2.4.2.1 Language Processors

In selecting a language for the SDE, consideration should be given to the associated support software: linkers, syntax-directed editors, executive systems, library of math functions, etc. The PDL chosen should provide cross-referencing and a module invocation tree.

2.4.2.2 Simulators

A simulation environment unique to the Power System will be used for software development and testing. Consideration should be given for using EASY5, IGSPIIE, SIMSCRIPTII.5, and NETWORKII.5. Consideration should also be given to developing DMS, PMC, PDCU, MBSU, PSC, PVC, and SDC simulators so that software development of each of those controllers can proceed in parallel.

2.4.2.3 Data Base Management Systems

The requirements for local data base tools are specified in the Requirement and Design Tools section.

2.4.2.4 Requirement and Design Tools

2.4.2.4.1 Requirement Tools

2.4.2.4.1.1 Synthesis Tools

These tools help an analyst find or generate the requirements for a software task since the requirements may not always be explicit and need to be derived. Tools that can assist in this process are:

a) A word processor to scan system specifications for "shalls."

b) An interactive, graphical, structured analysis package that can help an analyst "think through" the requirements.

c) An environment that would allow rapid prototyping, simulation, and testing of requirements.

2.4.2.4.1.2 Analysis Tools

Analysis tools measure the quality of requirements and are used iteratively with the synthesis tools to develop the final requirements. However, these tools have, to date, two major drawbacks: They require mathematical expressions to be entered in a formal requirements statement language (RSL), which too many reviewers do not understand, and secondly, the RSL processors have not been able to deal with the so-called "fuzzy" requirements that tend to be prevalent during the early stages of a project. For this reason, the synthesis tools and requirements reviews are used for checking for completeness and consistency.

2.4.2.4.1.3 Documentation Tools

The documentation tool is a word processor that contains, as a minimum, the following features: automatic paragraph numbering; text copy and move operations; deletion/insertion of characters/words; automatic page, figure and table numbering; and automatic indexing and table of contents, figures and tables generation.

2.4.2.4.2 Design Tools

Design tools are necessary to help identify the interfaces between the functions in a program. One such tool is the N-squared chart, in which the function names are placed in squares that are along the diagonal of a page, from top left to bottom right. Outputs from one function to another are

described in squares that are in the horizontal rows of a function. Inputs to a function are in the squares that are in the same column as the function. See Figure 2.4.2-1 for an example. Note that this is a manual tool.

2.4.2.5 Test and Analysis Tools

These tools help describe test sequences in a high level test language, translate them to test transactions, use the transactions to drive a system under test, monitor and record the test results, and produce reports of interest from the recorded results.

2.4.2.5.1 Source Program Static Analysis Tools

These programs perform the following analyses/checks: code analysis, program structure analysis, proper interface checks, event sequence checks, and syntax analysis.

2.4.2.5.2 Source Program Dynamic Analysis

These programs are used for automatic test case generation, run time monitoring, and assertion checking.

2.4.2.5.3 On-orbit Maintenance

These programs are used for documentation and for validating modifications.

2.4.2.5.4 Performance Enhancement (On-orbit Upgrade)

These programs allow program restructuring and validate parallel operation.

2.4.2.6 Build and Delivery System

This "program" is a set of system commands that cause a PMAD operating system to be built from source code. The system can then be run or delivered to the customer.

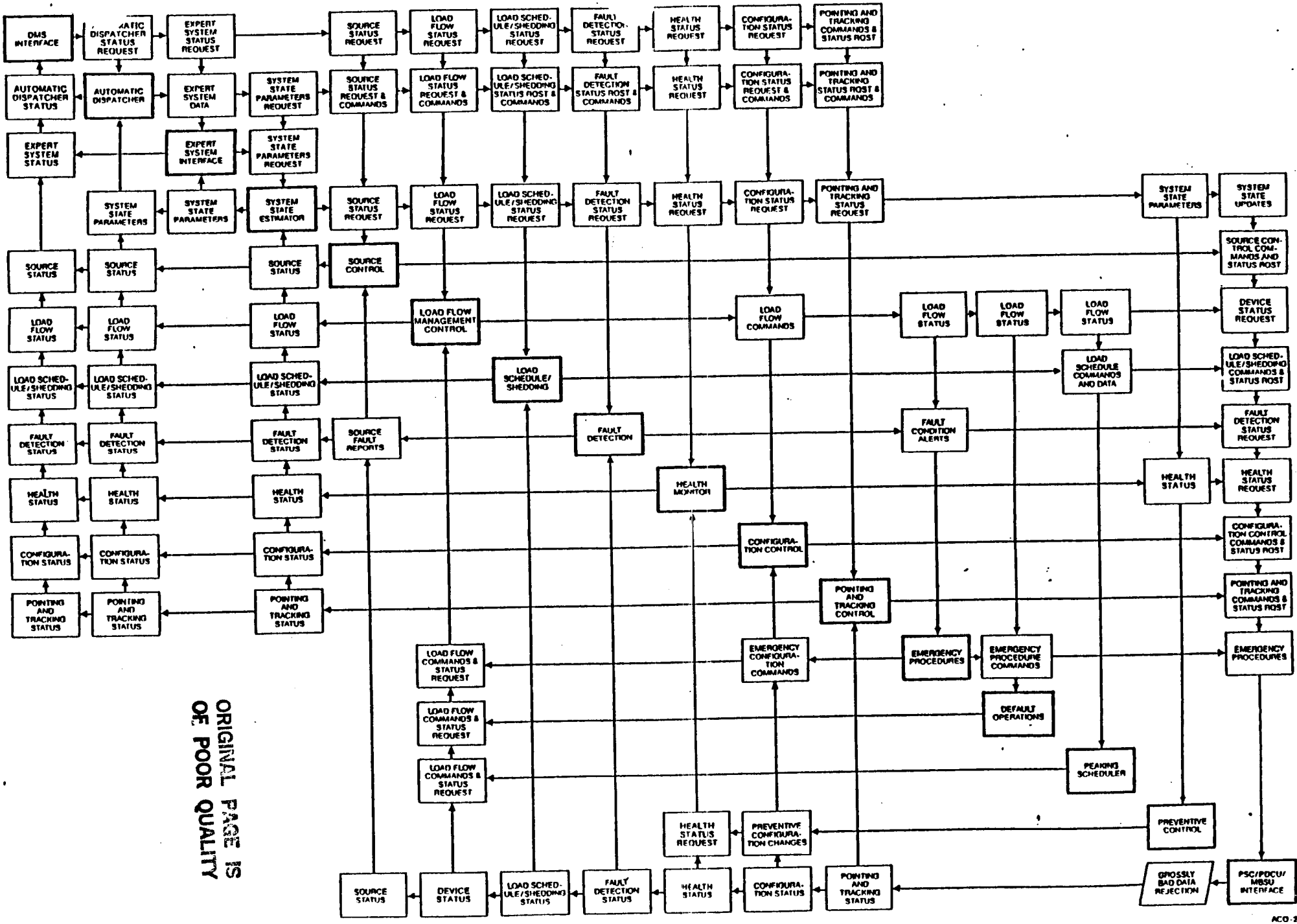

ORIGINAL PAGE IS
OF POOR QUALITY

Figure 2.4.2-1 U-squared Chart Example

2.4.2.7 Operating Systems

There will be two operating systems for the PMAD: a ROM-based system which performs minimum functions and a RAM-based system which supports communication to the DMS and all other controllers and I/O devices (sensors included). It also supports the scheduling of the various tasks in the controller.

2.4.2.8 Business Support System

This system monitors the status of program design, coding, test, and integration.

2.4.2.9 Support Facilities

The SDE must support a local multi-user (up to 50) environment at each facility.

2.4.2.10 Configuration Management Tools

A program, such as the DEC Code Management System (CMS) can assist the configuration management function.

2.4.2.11 Quality Control

The PMAD software requirements will be subjected to a quality review to verify compliance with system specifications and project standards. The outputs of the design phase will be verified against the requirements and the output code phase will be checked against the design. Automated tools to help in this process would improve productivity and quality.

2.5 MAN-TENDED OPTION

2.5.1 Background and Approach

The electric power system (EPS) for a man-tended approach (MTA) Space Station was studied by Rocketdyne as a potential phase in the development and buildup of a permanently manned capability (PMC) station. This study was documented in a Man-Tended Approach Study submitted to NASA-LeRC on 17 January 1986. The study focused on a hybrid EPS which had already been recommended by Rocketdyne at that time, RFC's or batteries for energy storage, and CBC or ORC for SD Power. The hybrid configuration begins as a MTA station with 37.5 kW of PV and RFCs or batteries for energy storage. Growth to PMC is accomplished with the addition of two 25-kW SD modules (CBC or ORC) to 87.5 kW total. The following general guidelines were used for the MTA study.

a. The MTA is not a substitute for the permanently manned Space Station but a potential phase in its development and buildup. The man-tended station will evolve to a permanently manned capability (PMC) at the end of the man-tended phase, and will be scarred as needed for such evolution.

b. The MTA shall be designed to operate in a man-tended mode for a period of from three to five years after initial deployment.

c. Polar and co-orbiting platforms are to be retained as part of the Space Station Program. Polar platforms are assumed not to be affected by the MTA.

d. The first assembly launch of the man-tended station will be planned for the same year as that planned for the first assembly launch of the permanently manned station.

e. The MTA will make no special provisions, over and above those included in the PMC, against loss of user operating time or data resulting from Space Station malfunctions.

f. The MTA reference configuration includes one man-tended multipurpose laboratory module (MML), one interconnect node and one airlock. Truss bay size is assumed to be nine feet.

g. MTA average electrical power will be 37.5 kW, or half of the reference PMC power level. 25 kW are available to users, with a preliminary allocation of 20 kW to the MML and 5 kW to attached payloads.

h. Minimum MTA station altitude is 250 n.m. for operations and 220 n.m. for assembly, the same as baselined for the manned station.

i. The automation and robotics state of the art utilized for the MTA will be no more advanced than that planned for the PMC. The amount of automation and robotics provided for users by the station will be no more than that provided in the PMC: any additional automation required will be provided by the user.

j. NSTS launch cost is assumed to be $100M per launch.

2.5.2 Reference Configuration

The reference man-tended approach (MTA) configuration is a PV electric power system (EPS) providing 37.5 kW average electrical power. Either RFCs or batteries are used for eclipse and contingency power. The reference EPS consists of the following subsystems:

PGS - Deployable and retractable flexible planar solar arrays utilizing silicon solar cells

ESS - RFCs or batteries for energy storage and eclipse and contingency power

PMAD - DC and AC source management and regulation equipment for PV and DC/AC conversion and management equipment and AC distribution equipment for the SD growth to PMC.

Figure 2.5-1 illustrates the configuration and dimensions of the reference MTA station.

After three to five years of operation the MTA station will evolve into a permanently manned capability (PMC) station. The reference PMC configuration described herein is an 87.5-kW hybrid EPS, developed by adding two 25-kW SD modules to the existing 37.5-kW PV MTA station. In addition, batteries (battery option) or additional reactant tankage (RFC option) must be added to meet the PMC station peaking and contingency requirements.

Figure 2.5-2 illustrates the configuration and dimensions of the reference PMC station.

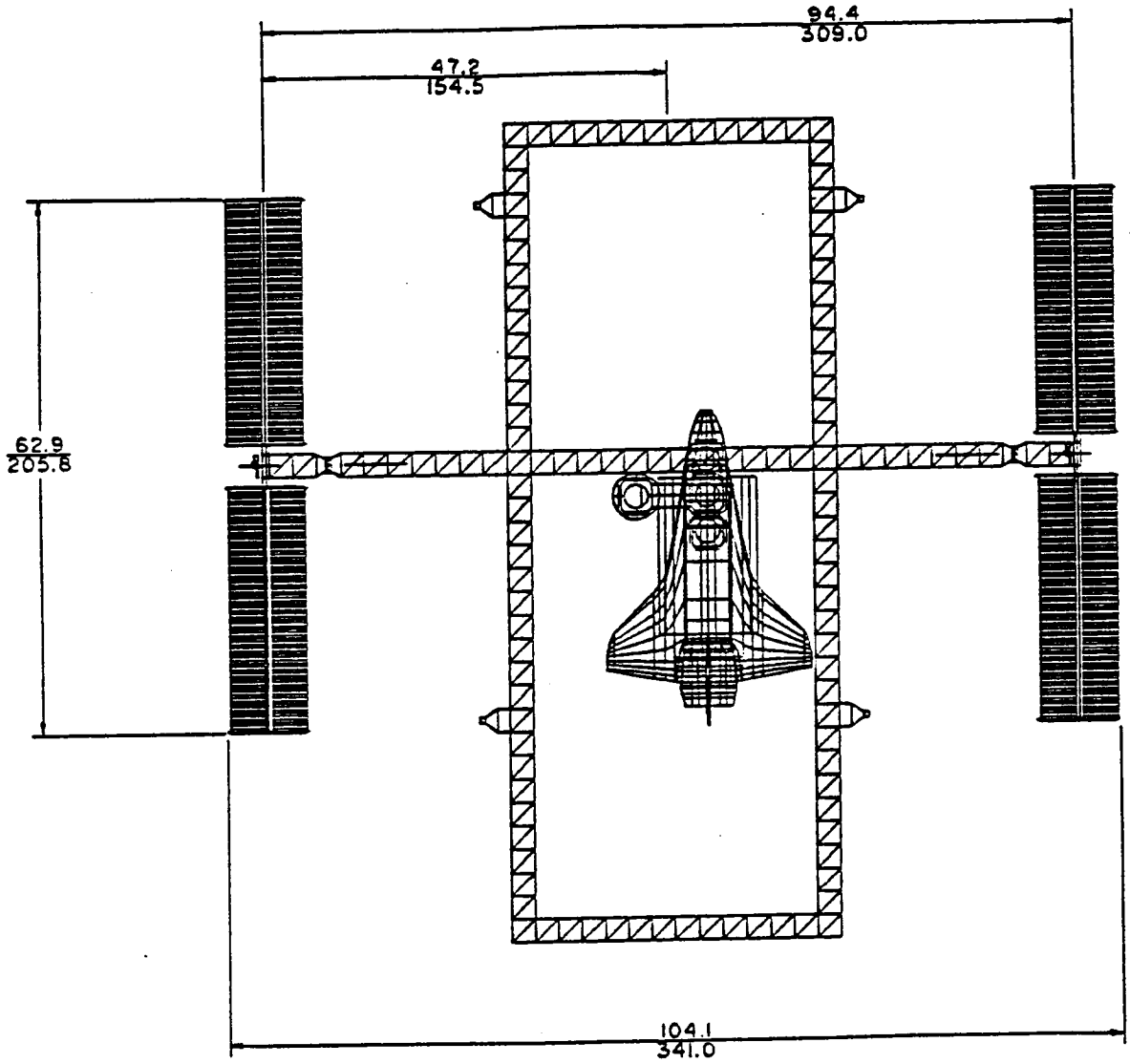

Figure 2.5-1 Reference Man-Tended Station Configuration

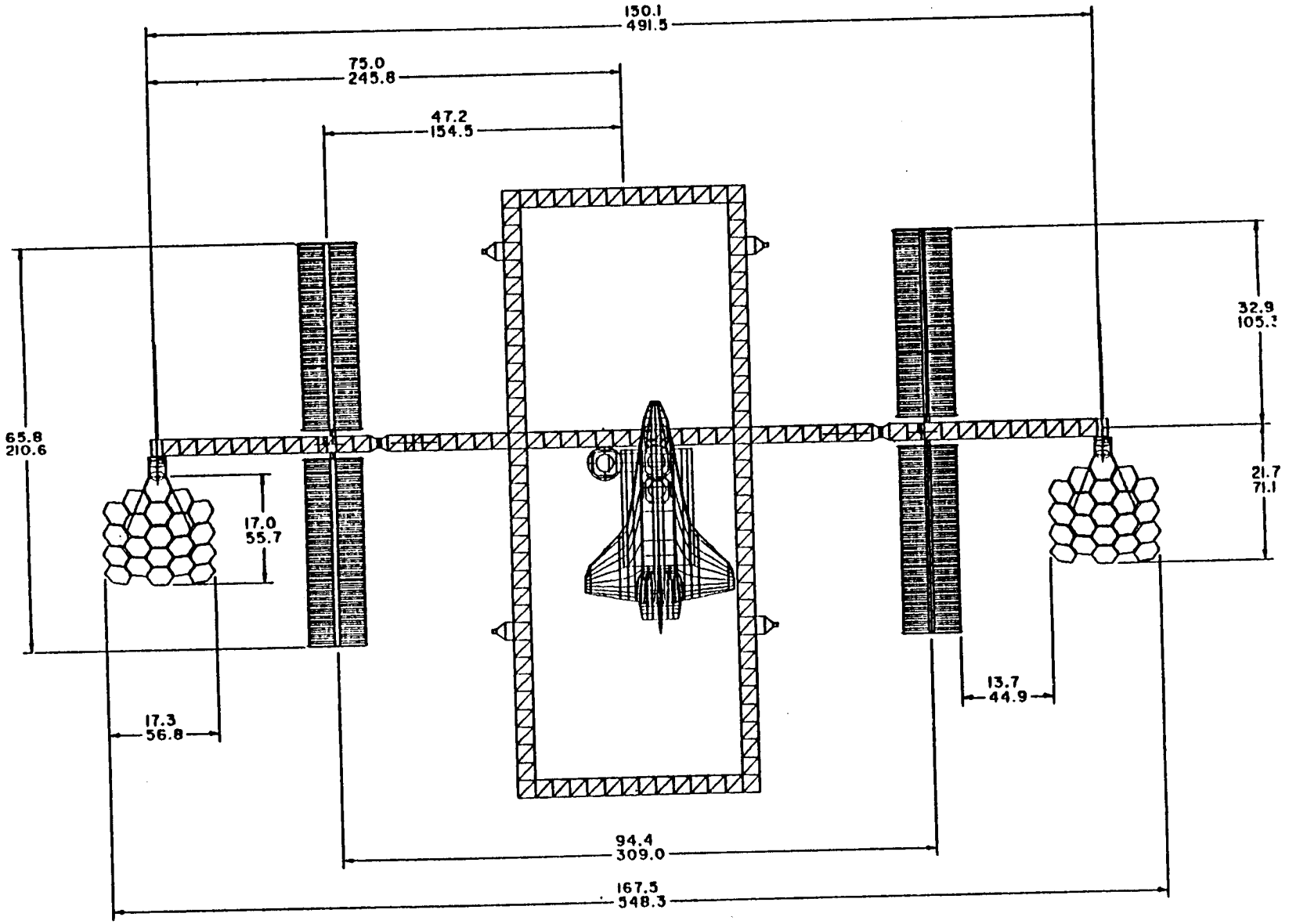

Figure 2.5-2 Reference PMC Station Configuration

2.5.3 Cost Assessment

Cost assessments for each of the options investigated were evaluated in detail for the specific operating scenarios of three years MTA operation (1992-1994) followed by two years of PMC operation (1995-1996), compared with five years PMC operation (1992-1996).

A cumulative cost comparison between MTA and PMC stations from 1987 to 1996 is given in Table 2.5-1. The cost data includes platform costs. Figures 2.5-3 through 2.5-6 present this information graphically. The comparison shows MTA cost savings of from $186M to $199M at time of first launch (1992). However, this MTA savings decreases thereafter until in 1996 the MTA savings becomes a deficit of about $33M average.

2.5.4 Conclusions and Recommendations

Rocketdyne's man-tended study analyzed in considerable depth the impact of a man-tended approach (MTA) on the Space Station electric power system (EPS). The study focused specifically on Rocketdyne's recommended EPS configuration for the permanently manned capability (PMC) station, the hybrid option.

The hybrid option is readily adaptable to the MTA. Beginning as an MTA station with 37.5 kW of PV and RFCs or batteries, growth to PMC is easily accomplished by the addition of two SD modules. Additional batteries or RFC reactant tankage would be added to the ESS for peaking and contingency requirements, and only minor additions are required by the PMAD subsystem since most of the components are already present on the MTA station. Two launch packages are sufficient to complete the EPS for the MTA station, with one additional launch required to add the elements needed for growth to a hybrid PMC station.

The cost savings that could be realized with an MTA station was evaluated in detail for the specific operating scenarios of three years MTA operation (1992-1994) followed by two years PMC operation (1995-1996), compared with five years PMC operation (1992-1996). Although the results are somewhat dependent on the station and platform options they are consistent for each option and lead to a definite conclusion.

Table 2.5-1 CUMULATIVE COST COMPARISON OF EPS OPTIONS * ($M)

	RFC-CBC		RFC-ORC		BATTERY-CBC		BATTERY-ORC	
YEAR	MTA	PMC	MTA	PMC	MTA	PMC	MTA	PMC
1987	11	13	11	12	10	12	10	12
1988	110	132	110	129	103	126	103	122
1989	327	393	327	384	309	375	309	366
1990	757	899	757	879	729	872	729	852
1991	933	1084	930	1059	901	1052	898	1028
1992	1232	1431	1219	1405	1209	1408	1192	1381
1993	1397	1501	1370	1474	1368	1477	1337	1451
1994	1469	1569	1439	1543	1433	1545	1405	1519
1995	1667	1630	1635	1604	1640	1604	1609	1579
1996	1723	1686	1691	1659	1695	1660	1664	1635

*Platforms are assumed to use same ESS technology as stations.

MTA/PMC CUMULATIVE COST COMPARISON

(RFC – CBC)

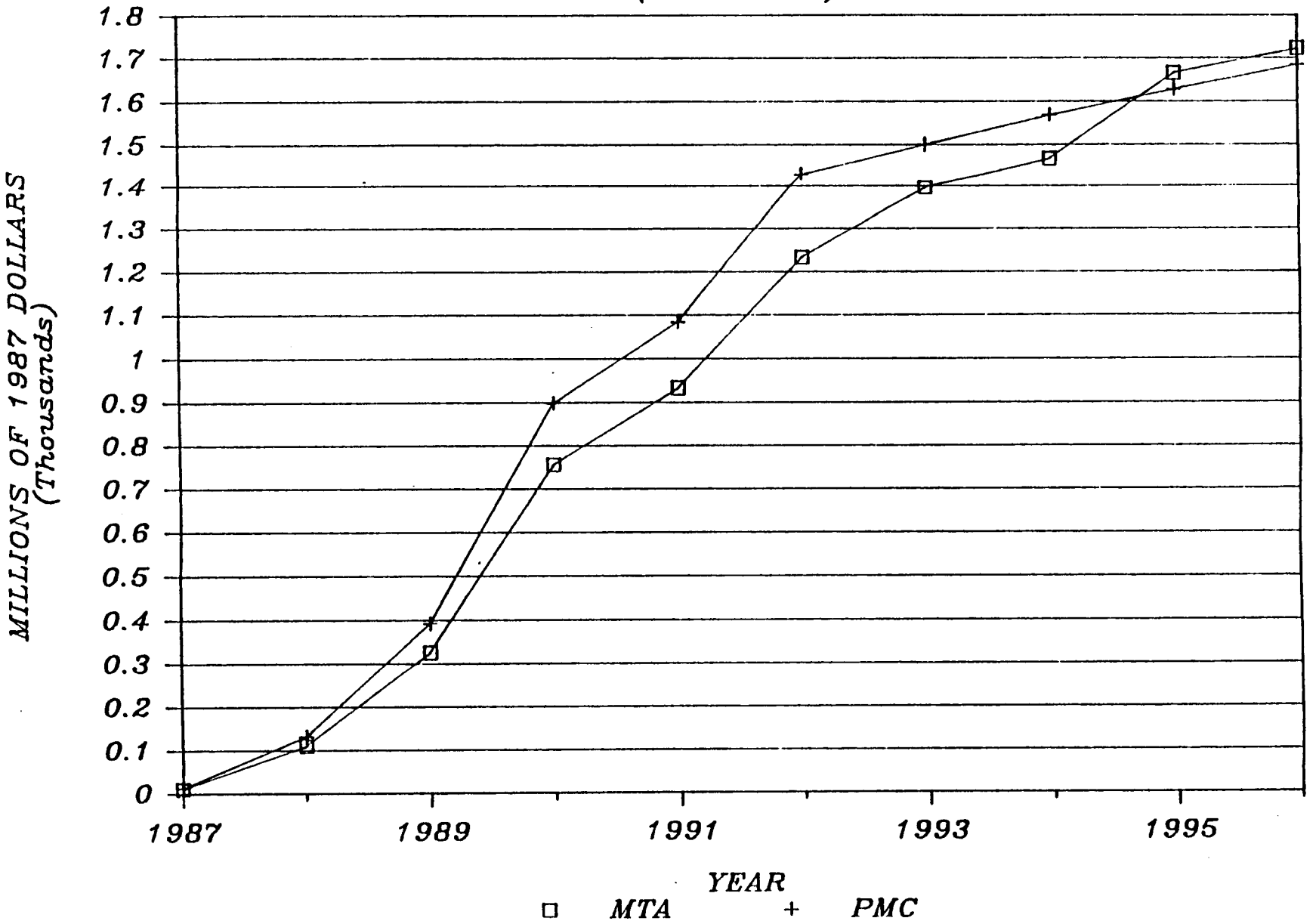

Figure 2.5-3

MTA/PMC CUMULATIVE COST COMPARISON

(RFC – ORC)

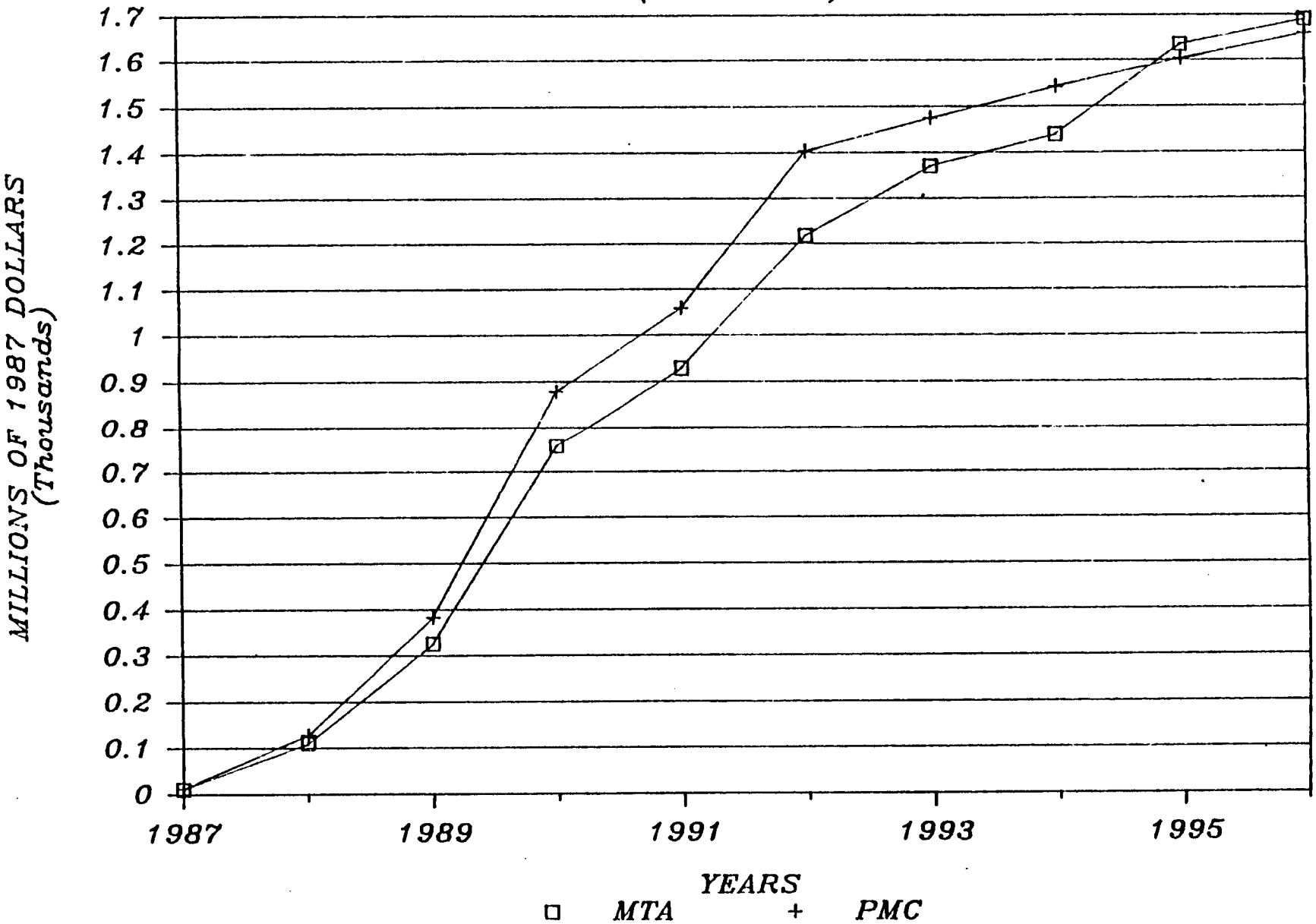

Figure 2.5-4

MTA/PMC CUMULATIVE COST COMPARISON

(BATTERY – CBC)

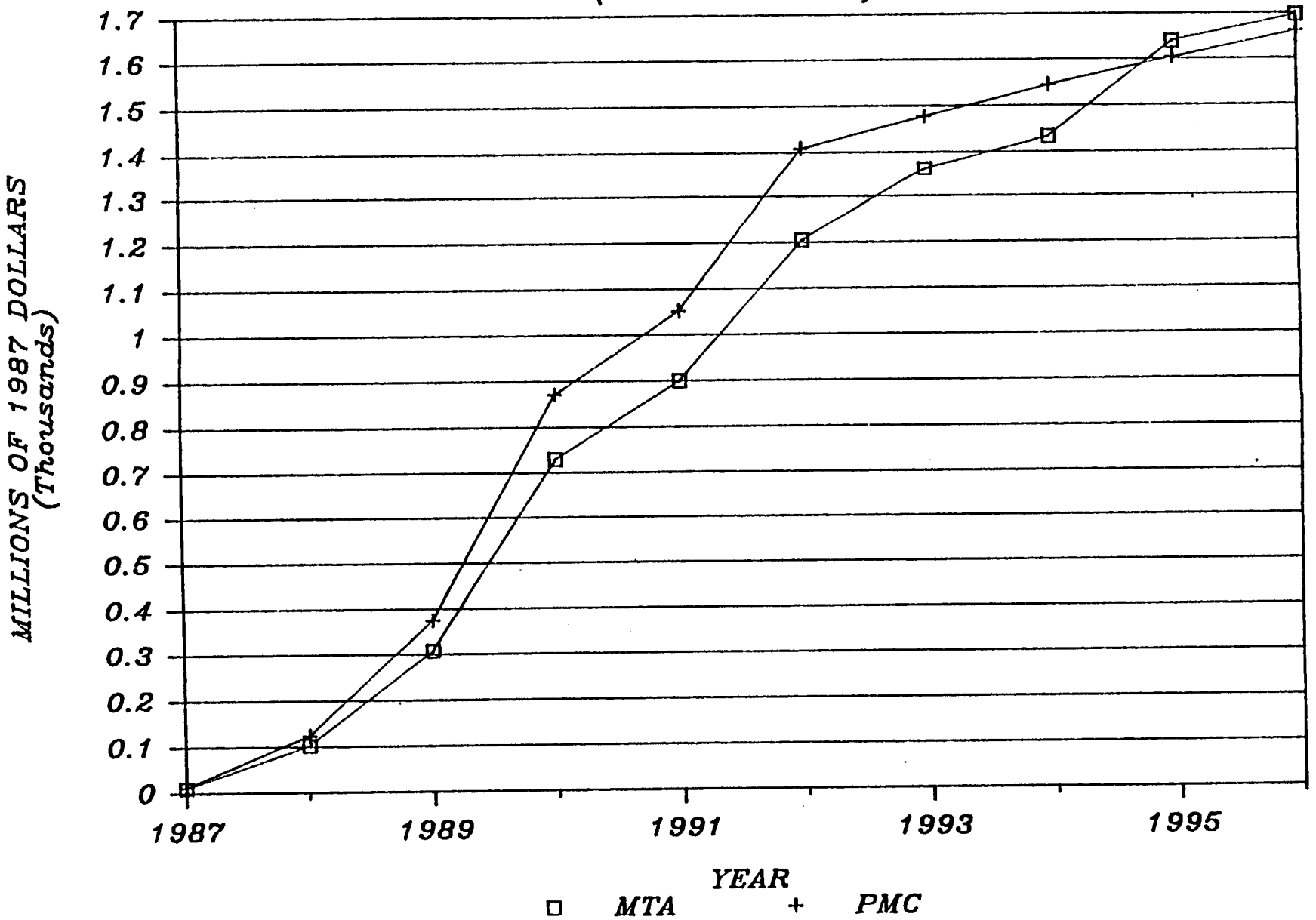

Figure 2.5-5

MTA/PMC CUMULATIVE COST COMPARISON

(BATTERY – ORC)

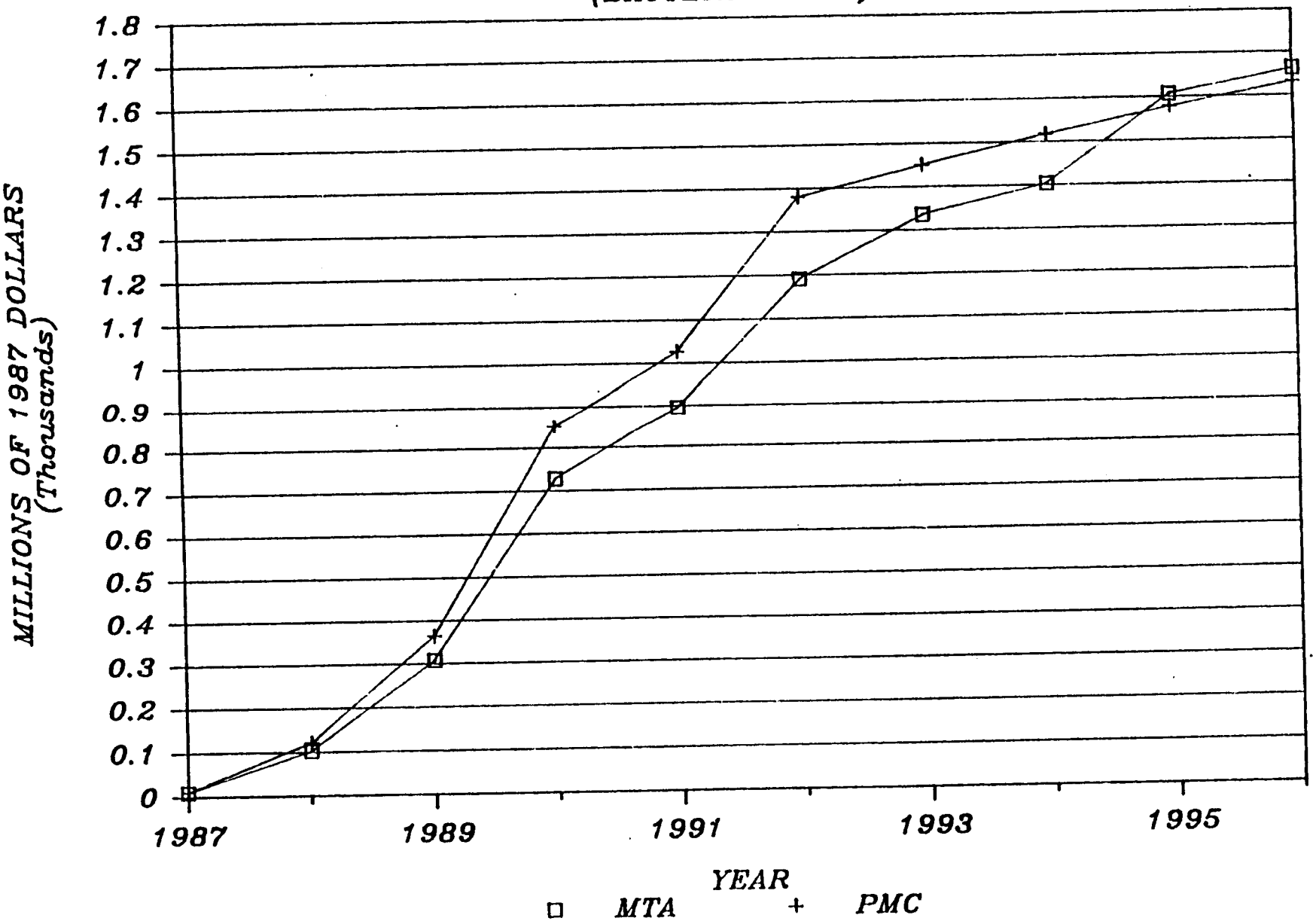

Figure 2.5-6

The average cumulative cost savings for the MTA increases steadily through 1992, the year of initial station operation. At this point, cumulative savings average $193M, due to DDT&E and productions cost savings, as well as operations and additional savings during the first year of operation. However, beginning in 1993, DDT&E and production costs for the MTA growth to the PMC are charged and the savings begin to evaporate. By the end of 1995, first year of PMC station operation (for the MTA scenario), all savings are gone and the MTA in fact, has cost an average of $33M more than the initial PMC scenario. This is explained by noting that the savings in operations and operational costs obtained by operating an MTA station for three years, is smaller than the added cost of building a PMC station in two phases instead of one.

In order to draw meaning from these results, the budgetary limitations of the Space Station Program must be determined, along with an evaluation of the user impact of the reduced power availability for three years. Only then can the advisability of the MTA be determined.

V2-25/4

Conclusions

It was recommended that only two types of PMAD components use the hardware/firmware approach: switchgear and remote power controllers. In these two cases, the required fast response time for quick fault detection and isolation, and for over-current protection cannot be met by the software. It was also recommended that the current limits for the remote power controllers be programmable so that their limits can be set/reset by the PMAD software.

2.6 AUTOMATION AND ROBOTICS

2.6.1 Introduction and Summary

One of the significant Space Station challenges is to incorporate advanced automation and robotics to increase man's productivity in space. Achievements in this technology can also have a wide range of effects on our national goal to increase terrestrial productivity and make our country more competitive. Our approach began with the ATAC Committee recommendations documented in NASA TM87566 as applied to the electric power generation system and has evolved during the Phase B effort.

Automation is an integral part of the Space Station Electric Power System. The IOC station power system will be designed for flexibility so that increasingly sophisticated software and its associated hardware can be added in orbit. The goal at IOC is for the system to automatically operate, reconfigure itself in case of failure, adequately monitor health, and provide a diagnostic expert system to assist with maintenance, failure isolation and ORU replacement. The evolutionary approach to automation will encourage the development and implementation of advanced technology to reduce human intervention and thus increase man's productivity. Beyond IOC, increasing expert system capability, health monitoring, artificial intelligence, and advanced sensors will be a vital extension of our current technology, their possible application to the Space Station will provide a clear focus for automation research and advanced development.

The development of the Rocketdyne and NASA LeRC power test beds and their associated control software and hardware provides an excellent testing capability for advanced control, health monitoring, failure detection, isolation, and reconfiguration as well as expert system/artificial intelligence. Such development resources will provide valuable data prior to IOC and beyond.

For the assembly and early operation of the Space Station, teleoperation and EVA are expected to be available. Based on the expected national effort in robotic development, it is anticipated that this technology will be

increasingly utilized during the growth and subsequent timeframes. The Electric Power System is comprised of Orbital Replacement Units each of which is capable to interface with the end effector of a robotic system. Potential robotic applications were shown in the previously submitted DR17 and are not repeated herein.

2.6.2 Automation

In order to implement realistic goals both for IOC and beyond, the approach will be to establish a basic level of automated control and diagnostics for the initial station, with explicit provisions and plans outlined for expanded capabilities. This strategy calls for 3 phases of automation development:

1) IOC - Initial hardware and software for diagnostics and control

2) Growth - Increased software sophistication and autonomy, including greatly increased use of expert systems for diagnostics, maintenance, and control.

3) Advanced - Addition of new diagnostic and computational hardware, with expanded use of artificial intelligence for all software applications.

An important aspect of this automation strategy is the research and development necessary to provide cost-effective implementation of advances in computer capability, artificial intelligence, diagnostic sensors, failure mode analysis, state estimation, and control theory. Work in these, and related, areas will proceed during all phases of space station development and operation, with both theoretical and experimental efforts. This research will be supported by the Rocketdyne and NASA LeRC power system test beds which will be utilized to test new ideas, and to prove design concepts.

By working from this solid base of applications research it will be possible to continuously upgrade the station and platform power systems, as advancements in automation become affordable and practical. In this manner the station power system will become increasingly autonomous, and consequently will steadily improve the productivity of man in space.

The initial phase of the automation plan incorporates a level of control and sensor monitoring that frees the station crew from direct involvement with routine EPS operations. Features that will be tested and implemented to the fullest extent possible include:

1) Automatic power generation and balancing.

2) Power distribution and management, including state estimation and load flow analysis.

3) Fault detection, isolation, and reconfiguration (FDIR).

Beyond IOC the automation plan calls for a program of phased research, testing, and implementation of advanced hardware and software capabilities. Even during the various stages of implementation of the IOC configuration, the following areas of advanced development are planned to be in progress:

1) Expert systems for trend analysis, state estimation, and fault reconfiguration.

2) Networking techniques for combining multiple expert systems.

3) Use of space-qualified symbolic processors, as well as Ada-based expert systems which will operate on space station standard data processors (SDPs).

4) Advanced diagnostic hardware and instrumentation techniques.

2.6.2.1 IOC Power System Architecture

The IOC EPS design consists of solar dynamic and photovoltaic power generation systems, energy storage systems, and power distribution and management systems. A diagram of the overall EPS architecture is shown in Figure 2.6.2-1.

The control system for the platforms is almost identical, except that the SD subsystem and main bus switching assemblies are absent.

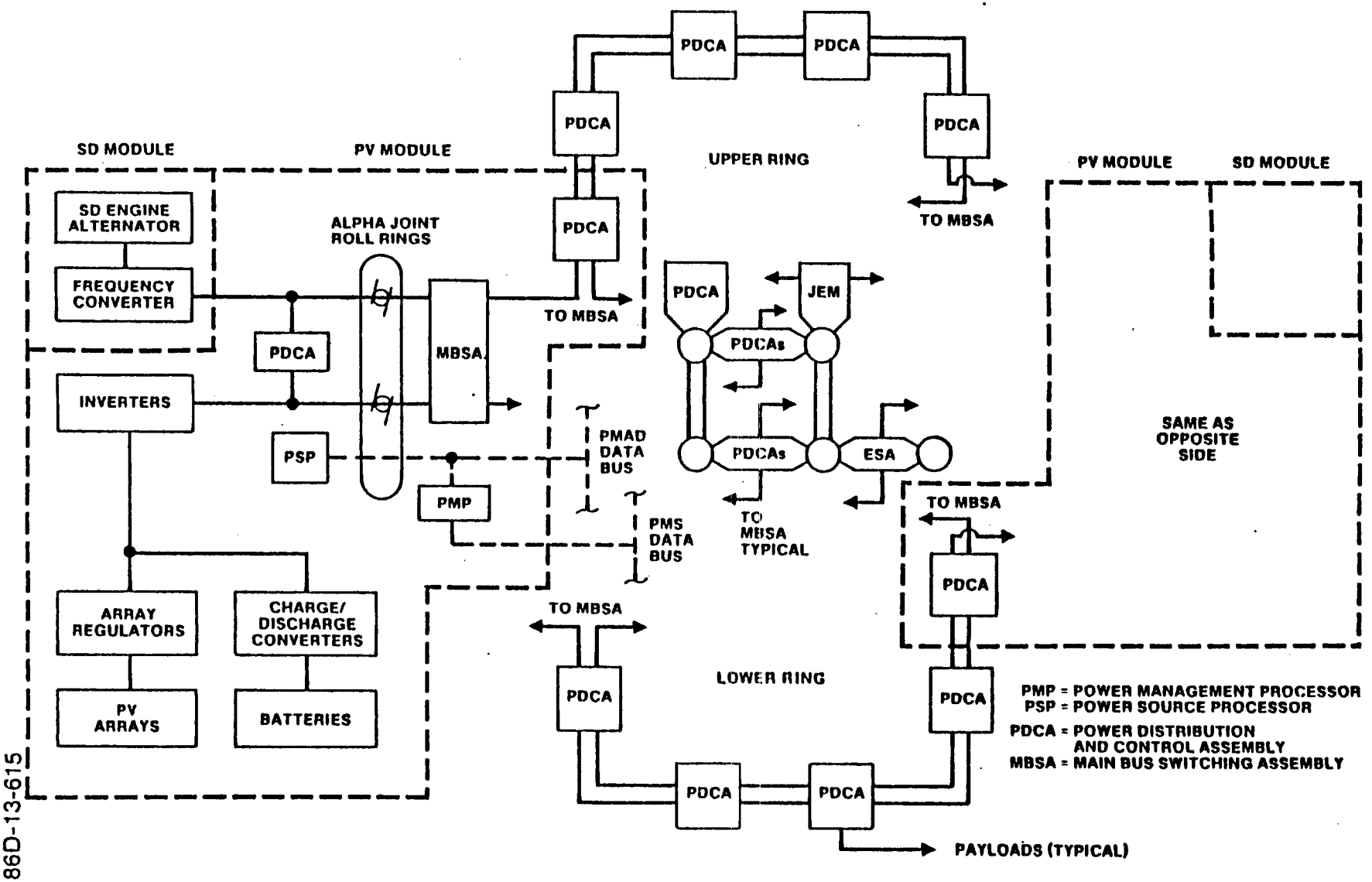

Rockwell International
Rocketdyne Division

Figure 2.6.2-1. Electrical Power System Architecture

2.6.2.2 IOC Automation Capability

Initial automation capability for the EPS will be a function of the complexity of the control software, and digital programmability of the system hardware. Capabilities of the present, preliminary design include:

1) Programmable set points for currents and voltages

2) Basic isolation and recovery from hard faults.

3) Hardware switch status reporting

4) Current, voltage, temperature, and pressure sensor reports

5) Load shedding based on priorities which have been input from the Operations Management System (OMS).

6) Automatic load adjustment and energy balance

To facilitate a structured plan, the automation features that could be implemented at IOC are divided into the following categories:

1) Baseline Autonomous Routine Operation - This includes steady state operations, load and bus switching, basic status monitoring, and double failure responses.

2) Enhanced Contingency Operations - This includes advanced evaluation of possible operating modes, and response to multiple, complex faults.

3) Trend Analysis in Health Monitoring - Trend analysis involves the statistical evaluation of historical sensor data over a long period of time to determine if a given component is beginning to malfunction. It includes failure prediction, and maintenance recommendations.

4) Advanced Artificial Intelligence - Use of expert systems for health monitoring, and non-deterministic response decisions. This represents a more advanced approach than a basic rule-based system, and would undergo extensive, parallel ground-operations testing and evaluation prior to on-orbit implementation.

The automation plan provides for these four categories to be developed in parallel, as funding is available, for implementation at IOC. This approach is shown in Figure 2.6.2-2, and reflects the distinction between the baseline level of automation and the more advanced options enumerated as items 2,3, and

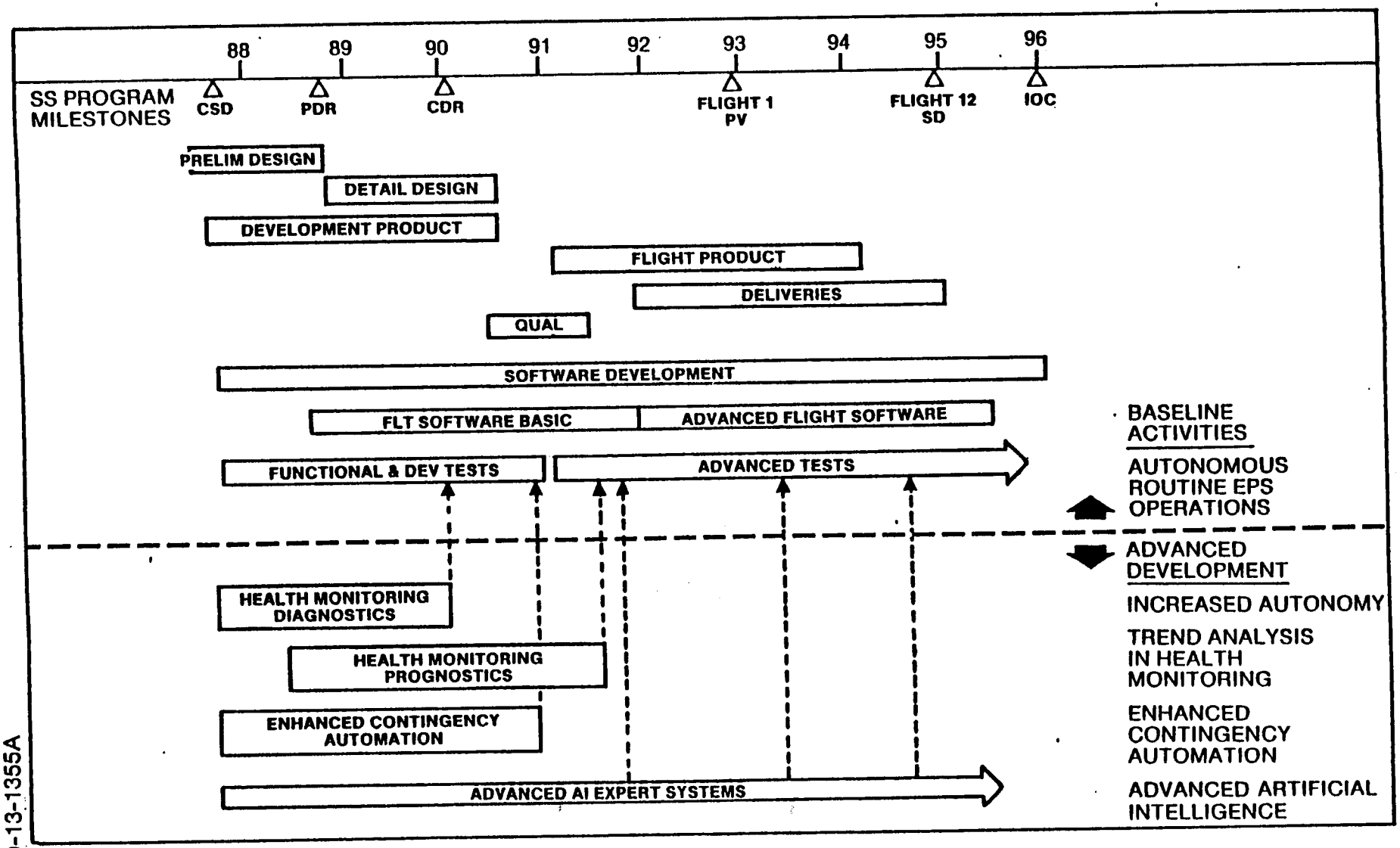

86D-13-1355A

Figure 2.6.2-2 Automation Plan

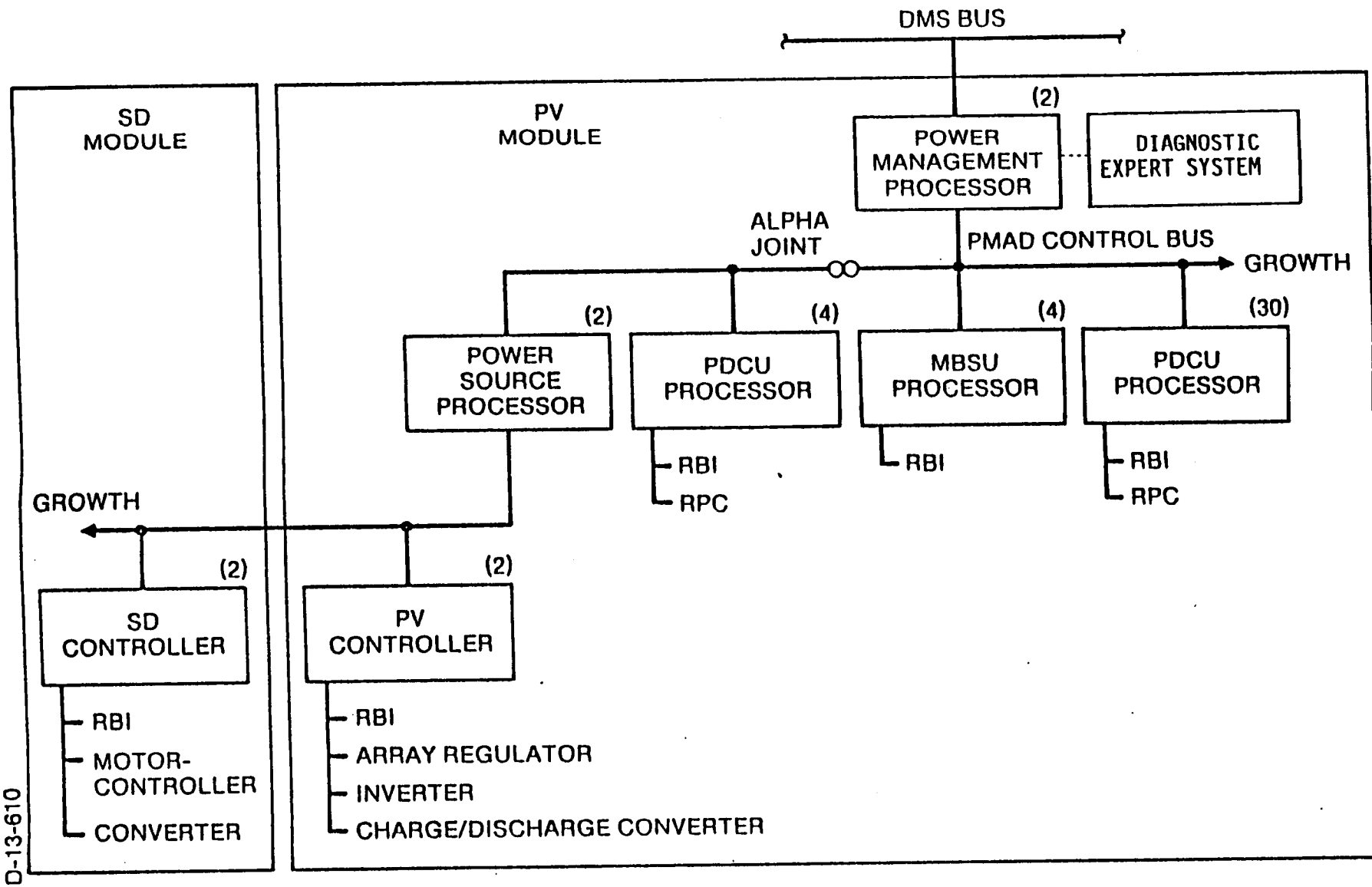

86D-13-610

Rockwell International
Rocketdyne Division

Figure 2.6.2-3. EPS Processor Functional Hierarchy

4 above. Baseline autonomous operation includes all of those functions which are necessary for the basic, safe operation of the power system. The additional features, either for IOC, or beyond can either be developed as an early parallel effort or later as part of the time-phased automation plan. In either case, the time-phased plan remains essentially the same, with adjustments only in the degree of enhancement at each step.

2.6.2.3 Automation Architecture

The current design for the EPS control configuration incorporates a set of standard station processors operating in a functional hierarchy as shown in Figure 2.6.2-3. The processor software and EPS hardware combine to form an automated system which functions within a limited and pre-defined scope of circumstances for IOC operation.

Power Management Controller (PMC) - The PMC is the highest level controller in the hierarchical network of the EPS system. As the coordinating processor for the entire EPS its primary functions are to coordinate the global power generation and distribution operations. It conducts all state estimation, load flow management, and high-level fault reconfiguration functions, and handles all communication with the station data management system (DMS).

Power Distribution and Control Unit (PDCU) Controller - The PDCU controller will be an integral part of each Space Station module or other load center, and controls all switching and load shedding operations for the loads under its jurisdiction. Each PDCU controller maintains an internal data base consisting of:

1. The current load configuration
2. Component failure status
3. Operational voltage and current levels at test points
4. Operational load voltages and currents
5. operational state-of-health sensor information

The PDCU controller automates the operations for load management at its level, and communicates directly with the PMC for commands and status.

Main Bus Switching Assembly (MBSU) Controller - The purpose of the MBSU controller is to act as the interface between the power management processor and the switch controllers (e.g. RBI's and RPC's) for the main power buses. It removes some overhead from the central processor by performing routine operations associated with the main power distribution system.

Power Source Controller (PSC) - The power source controller (PSC) is located in the same area as the power generation and energy storage processors and provides local functions not performed by those processors. The processor functions include:

1. Coordination of power generation and energy storage between the PV and SD modules
2. Power conversion controls such as inverter synchronization
3. Coordinates with a local PDCA to provide power to itself and other equipment in the region beyond the alpha joint.

SD and Photovoltaic Module Controller (SDC and PVC) - The SDC and PVC controls the elements of SD and PV power generation. The PVC also controls the energy storage subsystem to optimize performance during charge and discharge operations. To accomplish these functions, the controllers receive command and status information from the PMC via the PSC and use this information in conjunction with internal status data. The status data from the SD and PV controllers will be used by a ground-based or Space Station based expert system at IOC for trend analysis.

IOC Expert System - Preliminary design plans call for implementation of a diagnostic expert system interacting with the power management processor in an advisory capacity. While, due to cost or hardware constraints, a space-based expert system may not be feasible at IOC, it will certainly be possible to have such a system operating on the ground with a telemetry link to the station.

The configuration for these two cases. and their related issues are summarized as follows:

1) Space based expert system - Because symbolic processors, which are best suited to artificial intelligence applications, are not likely to be space qualified by IOC, any expert system onboard the station would have to be executing on a standard data processor (SDP). One option would be to have a separate physical SDP hosting the expert system with a direct link to the PMC. The other option would be to allocate a portion of the PMCs memory for the expert system which would run on a non-interfering basis. Current work at Rocketdyne is focused on implementing and evaluating an Ada-based inference engine which would enable this initial expert system to run on an SPD.

   The merits of these two options will be evaluated as preliminary design progresses.

2) Ground based expert system - If it is decided not to fly an EPS expert system at IOC, development work, testing, and evaluation would still proceed utilizing a lab-based system which would receive data from the station. If the ground system proves its value it could be moved later to a space implementation.

In either case, data obtained from the PMC will be utilized for testing the response and recommendations of the expert system, so that its performance can be evaluated during the course of actual station operation. Initially the expert system responses will be compared against PMC, crew, and ground-based decisions. As the system improves and confidence is gained in its recommendations, it will be used to increase the autonomy of the EPS.

2.6.2.4 Growth and Advanced Automation Plan

The growth and advanced automation portions of this plan build on the configuration established for IOC. Earliest growth and upgrades to the EPS automation capability will be primarily software oriented. Later phases will include utilization of advanced sensors instrumentation, and on-board computers.

The elements of the advanced plan are:

1) Continued research and development, for both hardware and software, using data from operating station as well as other sources for guidance.

2) Modification and expansion of software programs functioning as part of the then-current station configuration.

3) Addition of new or modified EPS hardware, sensors, instrumentation, and computers.

2.6.3 Robotics

The availability of robotics at IOC and subsequent periods play a major role in the definition of the requirements from these devices. Information available to date indicates that the following robotics capabilities can be expected during various phases of the Space Station Program:

- Remote manipulator system (RMS), utilized during the assembly phase as an integral part of the NSTS.
- Flight telerobotics servicer (FTS), utilized during the assembly phase from within the NSTS bay.
- Space Station transporter, capable of carrying about the station and RMS, launch packages and ORUs. It is expected to be available for service after flight number three. The complete mobile service center (MSC), will be available after flight number 24.

The fundamental ground rules utilized by the EPS designers are:

- EVA by astronauts should be minimized to the extent practical
- The requirements imposed by the designer shall not exceed the RMS capabilities
- In all cases astronauts EVA capabilities shall be provided, at least as a back-up.

2.6.3.1 Assembly Phase

During assembly of the PV module (flights 1 and 2) the STS remote manipulator system (RMS) , will be utilized to perform the following:

a) Unstow equipment from launch package.

b) Lift equipment from STS payload bay.

c) Support and stabilize the beta gimbal joint/solar array assembly while the EVA crew attaches the assembly to truss.

d) Position, support and stabilize the PV equipment box while the EVA crew attaches the box to the truss.

e) Assemble radiator heat pipe panels into the PV box condenser.

During assembly of the SD module the STS remote manipulator system (RMS) and the mobile service center (MSC) will be utilized to perform the following:

a) Unstow equipment from the launch package.

b) Lift equipment from the STS payload bay.

c) Transport equipment from the STS to the assembly location on the station.

d) Position, support and stabilize gimbal joint while the EVA crew attaches joint to truss.

e) Position, support and stabilize the PCU/receiver assembly while EVA crew attaches assembly to beta joint.

f) Assemble radiator heat pipe panels into condenser.

g) Support and rotate concentrator while EVA crew attaches hex panels.

h) Position and support concentrator assembly while EVA crew attaches support struts.

2.6.3.2 Operational Phase

During the operational phase the MSC will be utilized during maintenance to remove and install ORUs. All EPS ORUs are designed for interface with the MSC remote manipulator arm end effector and end effector adapters. The ORU/end effector interface design shown in Figure 2.6.3-1 is typical for all PMAD ORUs and other system ORUs as applicable. However, not all ORUs will be replaceable by the MSC without EVA crew assist.

This ORU concept features:

1. Single-action attachment.
2. Operable by EVA, RMS, and OMV automated equipment.
3. Capable of transferring electrical power, electrical/optical data, fluid (for cooling) or conductive heat transfer.

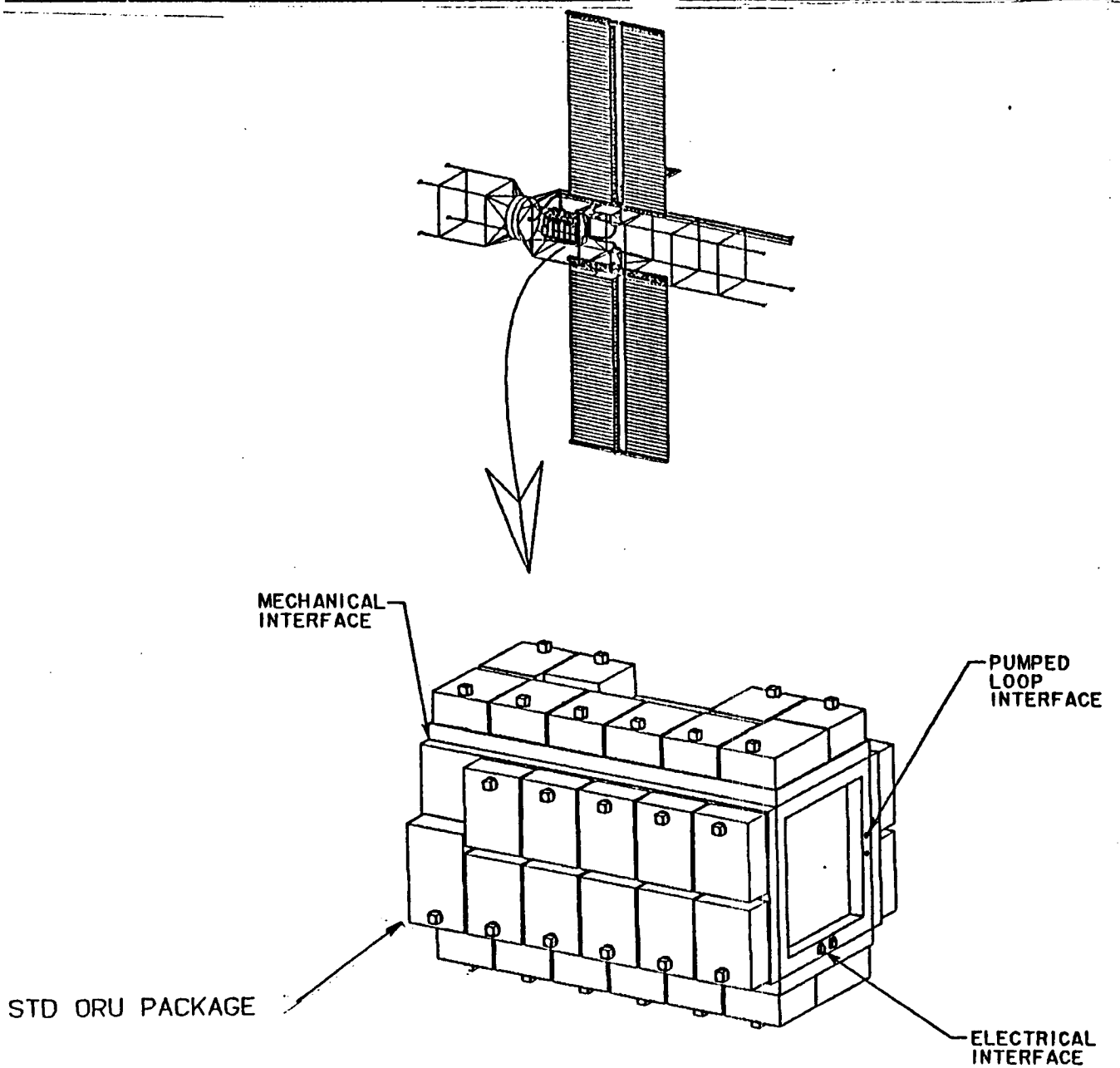

Figure 2.6.3-1

Rockwell International Corporation
Rocketdyne Division

COMPONENT LOCATIONS
PV EQUIPMENT BOX

SIZE C | DWG NO. 7R070045 | REV NO. 02602

SCALE NONE | DO NOT SCALE PRINT | SHEET

DWG NO. 7R070045 SH

4. All force necessary for attachment/detachment are resolved at the handle.

5. Interfaces with standard module servicing tool (MMS).

2.7 EVOLUTIONARY GROWTH

2.7.1 Subsystems Growth

2.7.1.1 Power Generation Growth

The hybrid concept baselined for the Space Station EPS combines the SD and PV power generation sources. This combination provides the station with a reliable and diverse source of power. The hybrid EPS will begin with 23.5 kWe of PV on the first two launches and will grow to a 75 kWe IOC station by addition of two 25.75 kWe SD modules. The station can continue to grow by adding two 25.75 kWe SD power modules at a time. Energy storage for the hybrid station is provided by batteries sized to support 23.5 kWe nominal load at the user interface with a peaking capability of 42.5 kWe. Eight Ni-H_2 batteries are employed at IOC with a nominal capacity of 62 A·h each.

2.7.1.2 PMAD Growth

The PMAD configuration has been designed for growth to a nominal 300 kWe (e.g., 332 kWe) station. However, the power distribution cabling at IOC is sized for growth to 175 kWe. Several major PMAD components which are installed at IOC and intended to remain throughout station life are sized to accommodate the growth station. These include the alpha joint roll rings, main bus switching assembly (MBSA), and the interconnecting power cabling between the MBSA and alpha joint. Since the MBSA serves as the point of paralleling and synchronization of all power sources on its respective side of the station, the MBSA must have adequate capacity at IOC to handle a nominal 166 kWe of source power. Likewise the alpha joint has similar capacity since all of the eventual source power must flow through the roll rings. Cabling between these two items is also installed at IOC to eliminate complex and time-consuming EVA field wiring downstream of the MBSA. The distribution cabling is scarred for a nominal 175 kWe capacity. The distribution cabling to the external points on the station (upper and lower keels and booms) is sized for the final growth station loading which is estimated at approximately 100 kWe. This eliminates field wiring on this part of the structure which is not expected to change over the station life. The manned module area however, is where the bulk of

structural growth is expected and is the area where field installation of new cabling (over the 175 kWe scar) is planned. As new manned modules are added to the station, new feeders from the MBSA to the modules are required.

2.7.1.3 Platform Growth

The polar platform has a continuous power requirement of 8 kWe at IOC. The power is provided by two PV arrays controlled by sequential shunt units (SSUs). The platform is capable of growing to 15 kWe with a peak power requirement of 24 kWe. The growth is accomplished by replication of the PV arrays and addition of batteries. The platform PMAD growth is accommodated by the extension of the DC and AC power buses and the addition of power distribution and control assemblies (PDCAs).

2.7.1.4 Estimated Costs

Table 2.7-1 shows the estimated total (design, development, test, engineering and production) and annual EPS costs for the station man-tended, IOC, and growth configurations; and the platform IOC and growth configurations. Additional data which illustrate the incremental production and annual cost for each growth block is presented in Section 2.4.

2.7.2 Mission Scenarios and System Requirements

The mission scenarios for Space Station EPS growth are shown in Figure 2.7-1. Three different scenarios are shown; (1) low growth beginning with a 23.5 kWe man-tended station and growing to 178 kWe; (2) base growth beginning with 75 kWe and growing to 332 kWe; and (3) high growth beginning with 75 kWe and growing to 487 kWe. Growth by replication of SD power modules is assumed for all three cases, with each 51.5 kWe growth block consisting of two 25.75 kWe modules.

Alternate growth methods which could be employed include scaled-up modules, technical improvements, and addition or replacement of modules with advanced technology modules. It is estimated that the incorporation of the five meter truss design has stiffened the structure sufficiently to allow growth by SD module replication to continue as high as 1 MWe or beyond, if necessary.

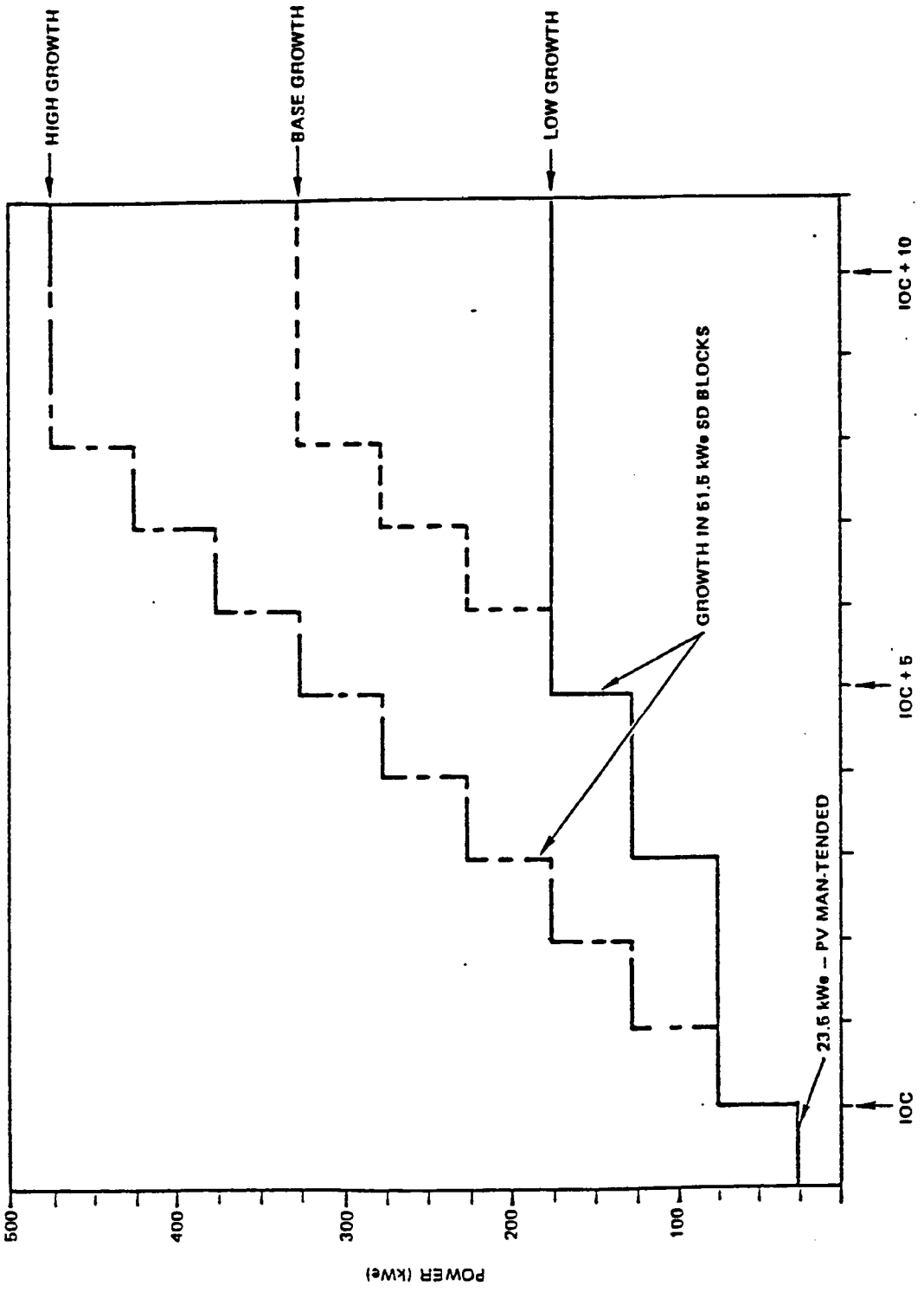

Figure 2.7-1 EPS GROWTH PATH SCENARIOS

TABLE 2.7-1

ESTIMATED EPS COSTS

	CAPACITY (kWe)	TOTAL COST(1) (1987 $M)	ANNUAL COST(2) (1987 $M)
STATION			
Man-Tended	23.5	770	17
IOC	75	813	20
Growth	332	1293	40
2 PLATFORMS			
IOC	8	78	9
Growth	15	137	17

(1) DDT&E and production; includes beta joints and load converters
Does not include transportation or installation cost or spares

(2) Includes ground support cost
Does not include transportation or installation cost

System requirements which led to the selection of the growth block size have been discussed in Section 1.2. Appendix A includes CAD-drawn figures showing the station configuration for each block change, from 75 kWe through 487 kWe in 51.5 kWe increments.

2.7.3 Design Concepts

As stated earlier, replication of SD modules is the proposed method for EPS growth. Several different size modules were studied and reported upon in DR-19, DP4.3 and DP4.4. Among those evaluated were 18.75 kWe, 25 kWe, and 37.5 kWe modules for both the SD and PV sources. Factors such as parasitic losses, station drag and mass, symmetry, ORU replacement, and commonality between the platform and station were considered. The selection of 23.5 kWe of PV and the resulting 51.5 kWe SD blocks was discussed in Section 1.2. Due to the thermal

energy storage capability of the SD designs and the inherent peaking capability of the PV and SD modules, no additional batteries are required for growth.

Additional details of the PV, SD, and PMAD design concepts are presented in the Preliminary Analysis and Design Document, DR-02, dated 30 June 1986.

2.7.4 Incremental Costs

The incremental costs for each block change are attributed only to the SD modules and the required PMAD components. The PV modules including batteries are installed only for IOC, and no more are added during EPS growth (not including replacement of solar arrays and batteries during the life of the station). The PMAD subsystem does not lend itself to simple block changes, and several different components have to be added for each block change during growth.

The estimated incremental production and annual cost for each block change of SD modules and PMAD components added to the system in 1987 dollars is shown in Table 2.7-2.

TABLE 2.7-2
COST OF BLOCK CHANGES

	Production Cost (1987 $ M)	Annual[1] Cost (1987 $ M)
Two 25.75 kWe SD modules (including source PMAD)	83.8	3.52
Common PMAD components to support block change of 51.5 kWe	12.1	0.43
Total	95.9	3.95

(1) Does not include transportation or installation cost

2.7.5 Capability at Each Block Change

The hybrid EPS IOC configuration has two PV modules (11.75 kWe each) and two SD modules (CBC or ORC, 25.75 kWe each). The PMAD architecture controlling the hybrid source configuration consists of dedicated PV and SD controllers and software which interface with the power source processor via a local control bus. The power source processor interfaces with the power management processor which processes DMS information. Power distribution cabling is provided for growth to 175 kWe nominal. With each block change, the EPS capability increases by 51.5 kWe.

Source PMAD growth is planned to coincide with the addition of the SD modules. Each module addition brings its associated PMAD equipment which consists of a frequency converter, remote bus isolators, and cabling. Also included is the SD controller which controls the SD module and interfaces with the power source processor via the local control bus.

The station has the flexibility to use other advanced technology SD modules such as Stirling cycle engines or PV technology such as GaAs, by replacing SD-ORC/CBC or Si arrays respectively. Section 2.10 covers flexibility in more detail.

2.7.6 Growth Schedule

Potential growth schedules are shown in the growth path scenarios of Figure 2.7-1. The power capability is plotted as a function of years from IOC. The low and base growth cases operate at 75 kWe for three years. Growth then takes place in blocks of 51.5 kWe by adding a pair of 25.75 kWe SD modules at a time. These blocks could be added at any frequency desired with limitations imposed by STS flight availability and available space in each flight. The high power scenario shows the power growing in one 51.5 kWe block per year, reaching 487 kWe in eight years.

2.7.7 Design Trade-Offs

The growth potential of a number of candidate concepts was studied at length during the conceptual design stage of the Phase B study contract. Some of the features traded-off were: physical size of modules, power losses, voltage requirements, conductor mass, structural requirements, station stability, and cost. The recommendation and subsequent baselining of the hybrid concept resulted from consideration of all the above. Details of the many system analyses and trades performed are presented in Section 5 of DR-19, DP4.3 and DP4.4.

The growth scenario costs reported in DR-19, DP4.4 illustrated that while IOC costs for the four principal concepts are roughly comparable, there is a wide disparity in life-cycle costs. For all three growth scenarios considered, the SD option has a significant life-cycle cost advantage over PV, with moderate increases noted as the amount of PV on the IOC station increases. The difference is primarily attributable to the much higher replacement cost of PV hardware, as as well as the higher reboost costs caused by the higher drag area.

2.7.8 Limiting Factors

2.7.8.1 Technical

The limiting technical factors that constrain the design of growth concepts are the following:

a) boom length,
b) shuttle constraints,
c) power losses,
d) voltage requirements,
e) module size,
f) drag,
g) shadowing,
h) conductor mass,
i) structural factors,
j) weight, and
k) scar.

The boom length limitation was reduced with the new five meter truss design. However, other practical considerations such as flight dynamics, conductor mass, voltage requirements and power loss still limit the boom length. The module size and weight are limited by the shuttle load capacity and available space. As indicated, selection of the SD module size was influenced by the shuttle capability to transport two modules in one mission. Increasing the module size and reducing the total number of modules would reduce the built in redundancy. Drag and shadowing are also serious constraints as the reboost cost increases with the increase in drag and weight, and the module efficiency is reduced due to concentractor shadowing.

The PMAD growth constraints were addressed in Section 2.1.2. The scarring of the distribution cabling for a nominal 175 kWe capacity and the alpha joint roll ring for a nominal 300 kWe capacity are obvious constraints. Growth beyond the 175 kWe power level would require routing of new cables and or cable splicing. Growth beyond 300 kWe is limited by the alpha joint roll ring size. One potential solution is to use transformers on the outboard side of the joint to increase the voltage to approximately 600 volts. This would increase the power capacity of the roll rings by 36% allowing station power growth to 410 kWe. A step down transformer would then be required on the inboard side of the alpha joint to return the voltage to 440 volts for distribution thus permitting the continued utilization of existing equipment. However, the roll rings must be initially designed for the highest voltage anticipated. Growth to higher power than above would require replacement of or additions to the alpha joint roll ring, the MBSA, and interconnecting power cabling between the alpha joint and the MBSA.

2.7.8.2 Schedule

The growth scenarios include growing to a 332-kWe or even 487-kWe capability in 10 years, placing a limit on the technological advancement that can be employed for EPS growth. Long-lead-time items reduce the 10 years available to incorporate advances into the growth design. Phase B studies have therefore been limited to existing technologies and those advances anticipated during the preliminary design allocation of 21 months.

2.7.8.3 Program

The principal limiting factor imposed on growth by programmatic considerations is the limit on the cost of the entire Space Station program. This limit places financial constraints on growth that favor the least expensive growth scenario.

2.7.9 Assumptions

The principal assumptions made for assessing the station growth scenarios are:

a) The Space Station operating altitude is 180-250 nmi,
b) Maximum orbiter payload mass at 220 nmi is 38,245 lbs,
c) Available orbiter cargo bay length with design docking module installed is 45.5 feet, and
d) Modification of existing hardware and resupply flights are not considered growth flights.

2.7.10 Growth Flexibility and Constraints

The ability of the Space Station to grow is limited by the capability of the STS to support dedicated Space Station flights. It is presently planned to deliver two 25.75 kWe solar dynamic units on one STS flight for Space Station growth. The number of flights that will be available for Space Station growth depend on:

a) Number of orbiters available (size of fleet),
b) Number of resupply flights required annually,
c) Number of mission (customer) payload flights,
d) Number of (maximum) orbiter flights per year available to NASA,
e) Number of flights available for Space Station support,
f) IOC assembly launch cradles available for growth flights, and
g) Crew availability for growth assembly.

Allowing the station orbit altitude to decay to a minimum altitude for resupply and other required servicing flights could reduce the required number of yearly flights.

The conceptual design studies of the EPS covered eight reference concepts which included PV and SD options for the station and platform and Stirling and nuclear options for station growth. In subsequent studies some concepts were expanded to allow consideration of various alternatives, and others were eliminated, as only those considered practical for use at IOC were retained. The finalists were several SD, PV, and hybrid concepts and they are presented in Reference 3. The Stirling and nuclear growth options were evaluated during the conceptual design phase in DR-19, DP's 4.1 and 4.2 and subsequently addressed in more detail in sections 3.9 and 3.10 of DR-19, DP4.3.

Both the nuclear and Stirling options were dropped from further consideration because their disadvantages at IOC were judged to outweigh their potential advantages. Space nuclear power systems are very attractive for repetitive, unmanned applications requiring large amounts of electrical power. However, for the Space Station, the need for a large man-rated shielding mass results in nuclear having no cost advantage over alternative concepts while having significant safety and technology development cost/risk disadvantages. The Stirling engine has a slight potential mass and area advantage over alternative SD concepts because of its greater efficiency and higher heat rejection temperature (reduced by conversion losses of the Stirling reciprocating motion into rotary motion). This potential is offset by its less mature development status.

It is recognized, however, that in future years, significantly increased power requirements, utilization trends, and/or changing priorities for the Space Station, may occur. Under these circumstances, the use of all available technologies should be reconsidered. Nuclear power for space missions, at the present state of the art, presents safety and technological problems for use on a manned Space Station. However, further technolgocial advancement in the areas of safety, cost, and shielding mass, should not be discounted. With such advances, or for location on an unmanned station or platform, nuclear power could become a viable option for future evolutionary growth. Employment of a new Space Station or platform would probably be the most practical course of action under these circumstances, although integration onto an existing station could be studied and evaluated if necessary.

The Stirling option has no human safety problems and is more viable for near/moderate term use on the station. However, a suitable module must be developed capable of being transported into orbit and integrated with existing station systems and components.

The EPS has the flexibility to accommodate new or modified SD modules, or possibly larger modules. The initial silicon PV arrays could be replaced with more advanced and higher capacity GaAs arrays and the Ni-H_2 batteries by Na-S batteries. This would be applicable on both the station and platform. Advanced PV growth is addressed in DR-19, DP4.3. The station flexibility also permits the use of other hybrid splits of PV and SD. The constraints for utilization of new technologies are:

a) Cost effectiveness.
b) Human health and safety considerations,
c) Availability of proven hardware, and
d) Transport limits due to size,
e) Physical and functional interfaces with existing station.

3.0 PRELIMINARY DESIGN

3.1 ELECTRIC POWER SYSTEM OVERVEIW

The Electric Power System (EPS) for the Space Station program consists of a combination photovoltaic (PV) and solar dynamic (SD) power generation subsystem and a power management and distribution (PMAD) subsystem.

The solar power generation module concept for the EPS consists of two 12.5 kWe rated PV modules and two solar dynamic power modules. Each PV module consists of two solar arrays. Table 3.1-1 summarizes how the solar dynamic modules combine with the photovoltaic modules to provide IOC and growth station power requirements of 75 and 300 kWe net, respectively.

Table 3.1-1
SUMMARY OF SOLAR DYNAMIC/PV POWER MODULE CAPABILITIES

	IOC	GROWTH
SD nominal module design power (kWe)	25	25
SD minimum power/module (kWe)	26	26
SD maximum power/module (kWe)	30	30
Number of SD modules	2	12
SD minumum power (kWe)	52	312
PV minimum power (kWe)	23.5	23.5
Station minimum power (kWe)	75.5	335.5
SD maximum power (kWe)	60.0	360.0
PV maximum power (kWe)	42.5	42.5
Station maximum power (kWe)	102.5	402.5

The PMAD subsystem consists of that hardware and software necessary to control power generation from all sources and distribute it to the variable load centers throughout the Space Station structure and manned modules. Figure 3.1-1 is an overview of the EPS components at IOC and Figure 3.1-2 is an overview of the PMAD architecture.

As an overvew, the following tables detail the items that comprise the power generation system (WP-04). Table 3.1-2 lists the PV module major assemblies; Tables 3.1-3a and 3.1-3b list the SD module major assemblies of ORC and CBC, respectively; Table 3.1-4 lists the platform major assemblies; Table 3.1-5 lists the PMAD ORUs and Table 3.1-6 lists the specific assembly required for each launch. Module launch masses are

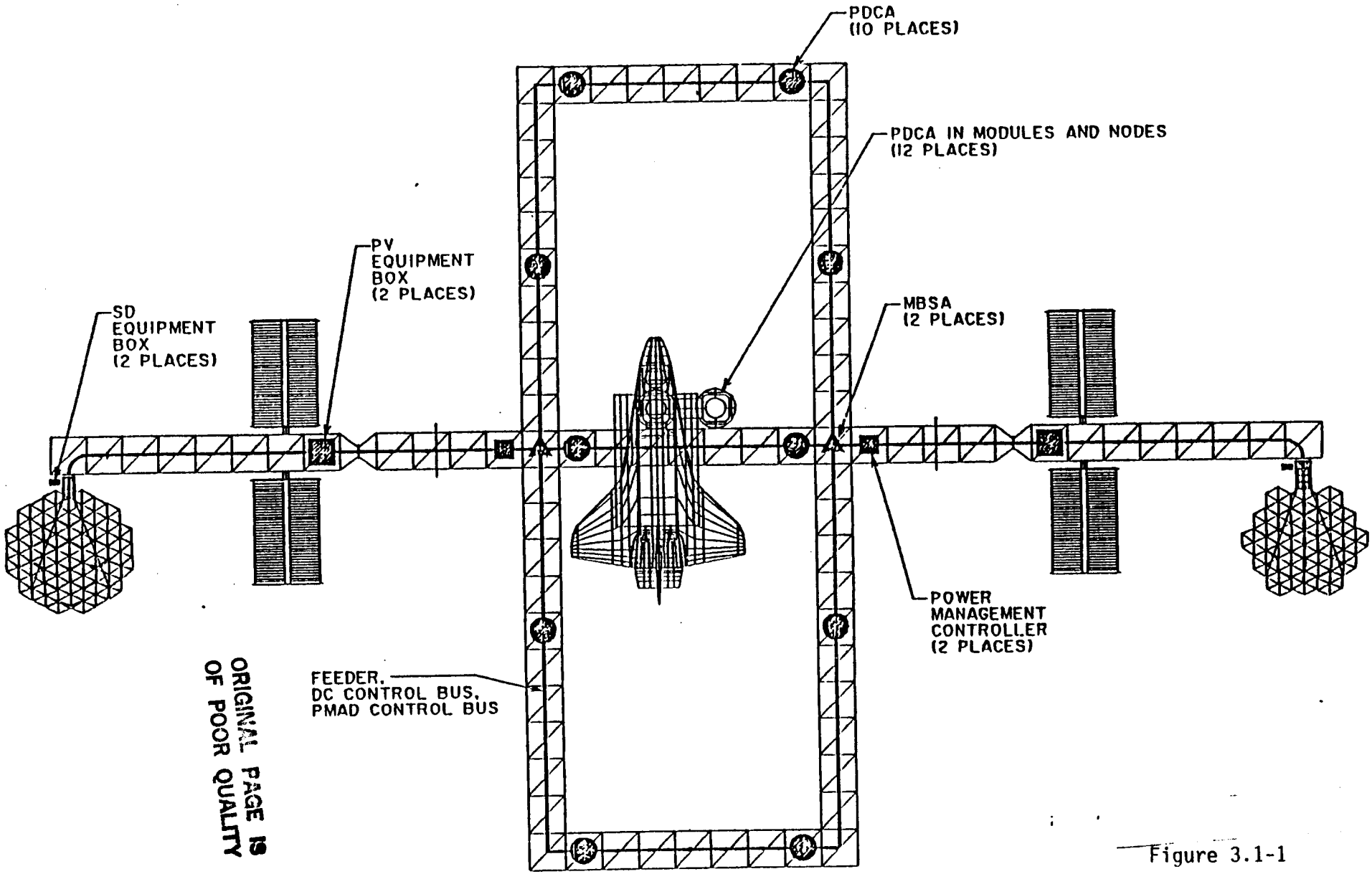

Figure 3.1-1

Rockwell International Corporation
Rocketdyne Division

SPACE STATION EPS COMPONENT LOCATIONS

SIZE C | FSCM NO. 02602 | DWG NO. 7R070021

SCALE NONE | DO NOT SCALE PRINT | SHEET

EPS SYSTEM DIAGRAM

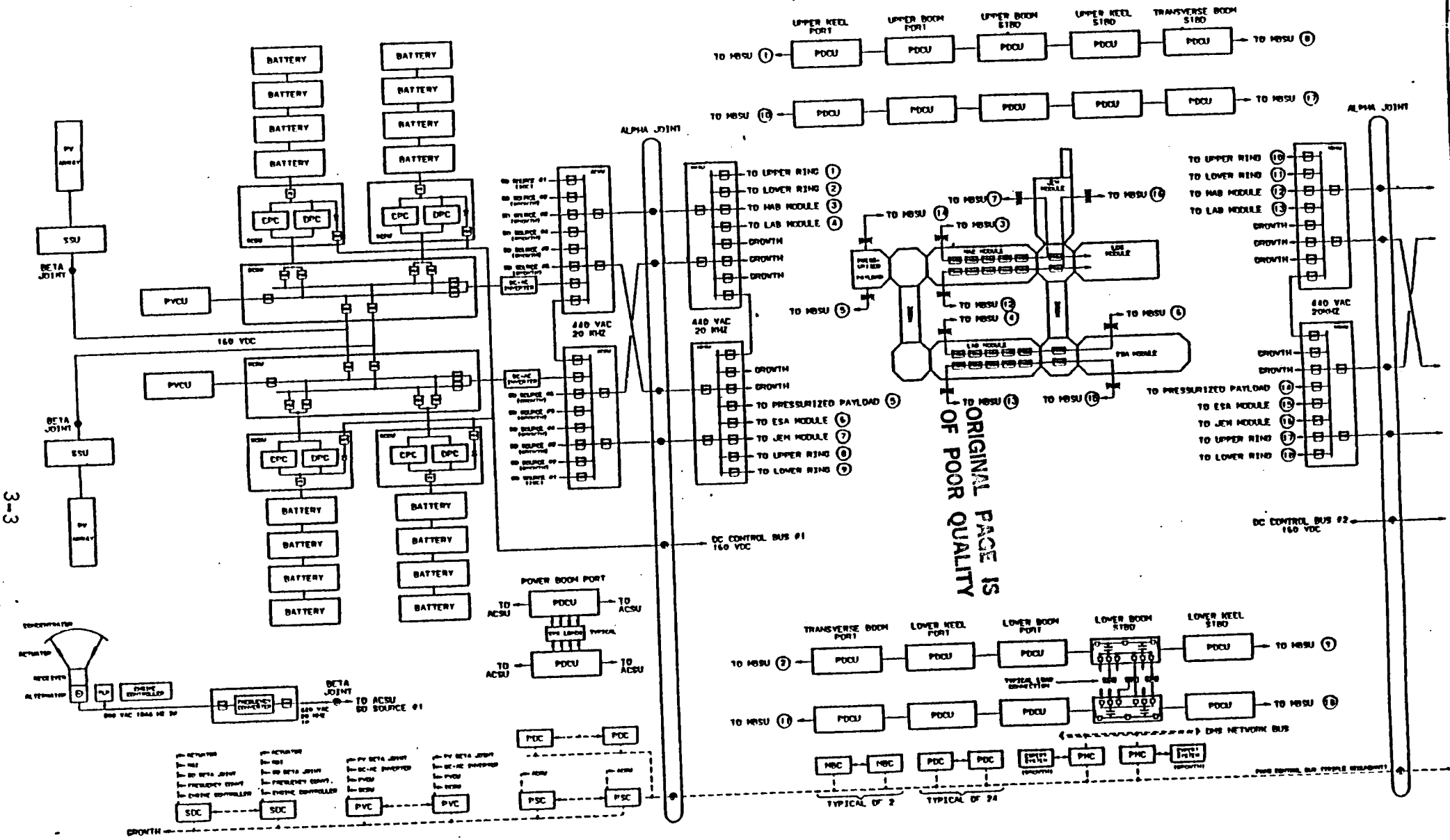

LEGEND

AC - ALTERNATING CURRENT
ACBU - AC SWITCHING UNIT
BCDU - BATTERY CHARGE/DISCHARGE UNIT
CPC - CHARGE POWER CONVERTER
DC - DIRECT CURRENT
DCSU - DC SWITCHING UNIT
DMS - DATA MANAGEMENT SYSTEM
DPC - DISCHARGE POWER CONVERTER
EPS - ELECTRICAL POWER SYSTEM
ESA - EUROPEAN SPACE AGENCY
FI - FAULT ISOLATOR
HAB - HABITAT MODULE
JEM - JAPANESE ENGINEERING MODULE
KHZ - KILO HERTZ
LAB - LABORATORY MODULE
LOG - LOGISTICS MODULES
MBC - MAIN BUS CONTROLLER
MBSU - MAIN BUS SWITCHING UNIT
PVCU - PHOTOVOLTAIC CONTROL UNIT
PDC - POWER DISTRIBUTION CONTROLLER
PDCU - POWER DISTRIBUTION AND CONTROL UNIT
PLR - PARASITIC LOAD RESISTOR
PMAD - POWER MANAGEMENT AND DISTRIBUTION
PMC - POWER MANAGEMENT CONTROLLER
PSC - POWER SOURCE CONTROLLER
PV - PHOTOVOLTAIC
PVC - PV CONTROLLER
RBI - REMOTE BUS ISOLATOR
SD - SOLAR DYNAMIC
SDC - SD CONTROLLER
SSU - SEQUENTIAL SHUNT UNIT
VAC - VOLTS ALTERNATING CURRENT
VDC - VOLTS DIRECT CURRENT

2. VOLTAGE INSIDE ALL PRESSURIZED MODULES AND TO ALL LOADS IS 208 VAC 20 KHZ 1Ø.

1. COMPONENTS OUTBOARD OF THE STBD ALPHA JOINT ARE THE SAME AS COMPONENTS OUTBOARD OF THE PORT ALPHA JOINT.

NOTE: UNLESS OTHERWISE SPECIFIED

EPS SYSTEM DIAGRAM

E 02602 7R07000

Figure 3.1-2

TABLE 3.1-2 PV MODULE BREAKDOWN

PV MODULE CONTENT:	2 PV Wings and Wing PMAD 2 Beta Gimbals 4 Batteries and Battery PMAD PV Source PMAD PV Thermal Control PV Equipment Box Structure PV Module Cabling
PV MODULE ORUs	
PV Wing:	1 PV Array Blanket and Box (L) 1 PV Array Blanket and Box (R) 1 Deployable Mast and Canister
Wing PMAD:	1 Sequential Shunt Unit
PV Battery:	4 Battery Subassemblies
Battery PMAD:	1 Battery Charge/Discharge Unit
PV Source PMAD:	2 AC Switch Units 2 DC Switch Units 2 DC-AC Inverters 2 Power Distribution and Control Units (Truss) 2 PV Control Units 2 PV Controllers 2 Power Source Controllers
PV Thermal Control:	8 Utility Plates 2 Pump Units 1 Condenser/Interface 8 Radiator Panels 8 Pressurization Units 8 GN_2 Canisters
Beta Gimbal:	1 Beta Joint Subassembly 1 Beta Roll Ring Subassembly 2 Beta Joint Drive Motors 1 Station Beta Joint Transition Structure 1 Insolation Meter (Mounted on Moving Section)
PV Equipment Box Structure	

TABLE 3. 1-3a SD MODULE BREAKDOWN
ORC OPTION

SD MODULE CONTENT:	Concentrator
	Receiver/PCU
	Condenser/Radiator
	SD Equipment Box
	Beta Gimbal
	SD Interface Structure
	SD Module Cabling
SD MODULE ORUs	
Concentrator:	Reflective Surface Subassembly
	Two Axis Gimbal Subassembly
	2 Linear Actuators
	Sun Sensor Subassembly - Mounted on Reflector
	Strut Set
Receiver/PCU:	Receiver
	PCU
	PCU Controller
	PLR
Condenser/Radiator:	Condenser
	32 Radiator Panels
	32 Pressurization Units
	32 GN_2 Canisters
SD Equipment Box:	2 SD Controllers
	Frequency Converter
	Utility Plate
Beta Gimbal:	Beta Joint Subassembly
	Beta Joint Roll Ring Subassembly
	2 Beta Joint Drive Motors
	Station Beta Joint Transition Structure
	Insolation Meter (Mounted on Moving Section)

TABLE 3.1-3b SD MODULE BREAKDOWN
CBC OPTION

SD MODULE CONTENT:	Concentrator Receiver/PCU Radiator SD Equipment Box Beta Gimbal SD Interface Structure SD Module Cabling
SD MODULE ORUs	
Concentrator:	Reflective Surface Subassembly Two Axis Gimbal Subassembly 2 Linear Actuators Sun Sensor Subassembly (Mounted on Reflector) Strut Set
Receiver/PCU:	Receiver/PCU Engine Controller PLR
Radiator:	Radiator/Deployment Unit 2 Hot Interconnect Lines 2 Cold Interconnect Lines
SD Equipment Box:	2 SD Controllers Frequency Converters 2 Fluid Management Units Utility Plate
Beta Gimbal:	Beta Joint Subassembly Beta Joint Roll Ring Subassembly 2 Beta Joint Drive Motors Station Beta Joint Transition Structure Insolation Meter (Mounted on Moving Section)

TABLE 3.1-4 PLATFORM EPS BREAKDOWN

PLATFORM EPS CONTENT:	2 PV Wings and Wing PMAD 2 Alpha Gimbals 4 Batteries and Battery PMAD Platform PMAD Platform EPS Cabling
PLATFORM EPS ORUs	
PV Wing:	PV Array Blanket and Box (L) PV Array Blanket and Box (R) Deployable Mast and Canister
Wing PMAD:	Sequential Shunt Unit
Battery:	4 Battery Subassemblies
Battery PMAD:	Battery Charge/Discharge Unit
Platform PMAD:	2 AC Switch Units 2 DC Switch Units 3 DC-AC Inverters 4 Power Distribution and Control Units (Truss) 2 PV Control Units 2 PV Controllers 2 Power Management Controllers
Alpha Gimbal:	Beta Joint Subassembly Beta Joint Roll Ring Subassembly 2 Beta Joint Drive Motors Platform Alpha Joint Transition Structure

listed in their respective sections of this report. The major WP-04 launches are identified as MB-1 and MB-2, launch of PV modules and Power Conversion Modules in nodes; P-1, polar platform EPS launch; MB-9, launch of SD modules; MB-16, distribution on upper and lower keels' launch; P-3, coorbit platform EPS launch.

Table 3.1-5
Summary of PMAD ORUs

ORU	IOC QUANTITY STATION	EACH PLATFORM
Sequential Shunt Unit (SSU)	4	2
Photovoltaic Control Unit (PVCU)	4	2
Battery Charge/Discharge Unit (BCDU)	12	4
DC-AC Inverter	4	3
Photovoltaic Controller	4	2
DC Switching Unit (DCSU)	4	2
AC Switching Unit (ACSU)	4	2
Power Source Controller	4	-
Frequency Converter	2	-
Solar Dynamic Controller	4	-
Main Bus Switching Unit (MBSU)	4	-
Power Distribution & Control Unit (PDCU) Truss	24	4
Power Distribution & Control Unit (PDCU, Module	24	-
Power Management Controller (PMC)	2	2
Transformer	10	-
Node Bus Switching Unit (NBSU)	2	2
NSTS Power Converter	2	2

TABLE 3.1-6 NUMBER OF ORUs

ORIGINAL PAGE IS
OF POOR QUALITY

WORKSHEET: FLIGHT 25kW
REVISION: 1
DATE: 21 NOV 86

SUB SYST.	NAME OF ORU	NUMBER OF ORUS MANIFESTED PER FLIGHT - 25 kW OPTION												
		FLIGHT NUMBER												
		MB-1	MB-2	MB-3	P-1	MB-5	MB-6	MB-7	MB-9	MB-10	MB-11	MB-16	P-3
IH	BETA JOINT DRIVE MOTOR ASS'Y	4	4		4				4				4
IH	BETA JOINT ROLL RING ASS'Y	2	2		2				2				2
IH	BETA JOINT SUBASS'Y	2	2		2				2				2
IH	COORBIT PLATFORM ALPHA JOINT TRANS'N STRUC.												2
IH	POLAR PLATFORM ALPHA JOINT TRANS'N STRUCT				2								0
IH	PV EQUIPMENT BOX STRUCTURE	1	1										
IH	STATION BETA JOINT TRANS'N STRUC.	2	2						2				
PMAD	AC SWITCH UNIT	2	2		2								2
PMAD	BATTERY CHARGE/DISCHARGE UNIT	4	4		4								4
PMAD	CABLESET- PLATFORM				1								1
PMAD	CABLESET- STATION PMAD	0.1	0.1			0.1	0.1	0.1				0.5	
PMAD	CABLESET- STATION PV MODULE	1	1										
PMAD	CABLESET- STATION SD MODULE								2				
PMAD	DC SWITCH UNIT	2	2		2								2
PMAD	DC-AC INVERTER	2	2		3								3
PMAD	FREQUENCY CONVERTER								2				
PMAD	MAIN BUS SWITCHING UNIT (MBSU)	2	2										
PMAD	NODE BUS SWITCHING UNIT (NBSU)	2	2					4					
PMAD	NSTS POWER CONVERTER		1	1	2								2
PMAD	PHOTOVOLTAIC CONTROL UNIT (PVCU)	2	2		2								2
PMAD	PHOTOVOLTAIC CONTROLLER	2	2		2								2
PMAD	POWER DISTRIBUTION AND CONTROL UNIT (MODULE)					10	10	4					
PMAD	POWER DISTRIBUTION AND CONTROL UNIT (TRUSS)	4	4		4							16	4
PMAD	POWER MANAGEMENT CONTROLLER	1	1		2								2
PMAD	POWER SOURCE CONTROLLER	2	2										
PMAD	SD CONTROLLER								4				
PMAD	SEQUENTIAL SHUNT UNIT (SSU)	2	2		2								2
PMAD	TRANSFORMER					2	2			2	2		
PV	BATTERY ASS'Y	16	16		16								16
PV	DEPLOYABLE MAST & CANISTER	2	2		2								2
PV	GN2 CANISTER	8	12										
PV	PV ARRAY BLANKET & BOX (L)	2	2		2								2
PV	PV ARRAY BLANKET & BOX (R)	2	2		2								2
PV	PV CONDENSER/INTERFACE SUBASS'Y	1	1										
PV	PV ITC PUMP UNIT	2	2										
PV	PV PRESSURIZATION UNIT	8	12										
PV	PV RADIATOR PANELS	8	12										
PV	PV UTILITY PLATE	8	8										

TABLE 3.1-6 NUMBER OF ORUs (Continued)

WORKSHEET:FLIGHT 25kW
REVISION: 1
DATE: 21 NOV 86

SUB SYST.	NAME OF ORU	NUMBER OF ORUS MANIFESTED PER FLIGHT - 25 kW OPTION												
		FLIGHT NUMBER												
		MB-1	MB-2	MB-3	P-1	MB-5	MB-6	MB-7	MB-9	MB-10	MB-11	MB-16	P-3	
SD-CBC	2-AXIS CONCENTRATOR GIMBAL SUBASSEMBLY								2					
SD-CBC	CBC ENGINE CONTROLLER								4					
SD-CBC	CBC INTERFACE STRUCTURE								2					
SD-CBC	CBC PARASITIC LOAD RADIATOR (PLR)								2					
SD-CBC	CBC RADIATOR FLUID MANAGMENT UNIT								4					
SD-CBC	CBC RADIATOR / DEPLOY'T MECH'M								2					
SD-CBC	CBC RECEIVER/PCU								2					
SD-CBC	COLD INTERCONNECT LINES								4					
SD-CBC	HOT INTERCONNECT LINES								4					
SD-CBC	INSOLATION METER SUBASSEMBLY	1		1					2					
SD-CBC	LINEAR ACTUATOR								4					
SD-CBC	REFLECTIVE SURFACE SUBASS'Y								2					
SD-CBC	STRUT SET								2					
SD-CBC	SUN SENSOR SUBASSEMBLY								2					
SD-CBC	UTILITY PLATE								2					
SD-CBC	VALVE ACTUATOR								2					
SD-ORC	2-AXIS CONCENTRATOR GIMBAL SUBASSEMBLY								2					
SD-ORC	GN2 CANISTER								64					
SD-ORC	INSOLATION METER SUBASSEMBLY	1		1					2					
SD-ORC	LINEAR ACTUATOR								4					
SD-ORC	ORC CONDENSER/INTERFACE STRUC. SUBASS'Y								2					
SD-ORC	ORC ENGINE CONTROLLER								4					
SD-ORC	ORC INTERFACE STRUCTURE								2					
SD-ORC	ORC PARASITIC LOAD RADIATOR (PLR)								2					
SD-ORC	ORC POWER CONVERSION UNIT (PCU)								2					
SD-ORC	ORC PRESSURIZATION UNIT								64					
SD-ORC	ORC RADIATOR PANEL								64					
SD-ORC	ORC RECEIVER								2					
SD-ORC	ORC UTILITY PLATE								2					
SD-ORC	REFLECTIVE SURFACE SUBASS'Y								2					
SD-ORC	STRUT SET								2					
SD-ORC	SUN SENSOR SUBASSEMBLY								2					

3.2 PV SUBSYSTEM

The PV Subsystem consists of photovoltaic array wings, batteries, PMAD equipment for conditioning and conversion of source power as well as control and management of the PV source power elements, and local thermal control hardware. The update to this subsystem includes descriptions of the baselined mechanically pumped loop thermal control system as opposed to the previously presented capillary pumped loop system. Refer to the trade study section for an updated description of the CPL. The PV equipment box has been incorporated to reflect Rocketdyne's concept of packaging the energy storage and PMAD components. This section focuses on the power source elements: the arrays and batteries, and the PV equipment box with thermal control. Source PMAD equipment design is described in more detail in Section 3.4.

The design of the PV subsystem has been guided by the principle of commonality between the hardware designs for the station and the platforms. This approach is appropriate since the station PV power elements are sized to provide nominal output power of about 25 kWe at the user interface and are not expected to grow in the current baseline hybrid power system, while the platform power level, served by a PV exclusively, starts at 8 kWe and grows to 24 kW. The similarity between the power levels suggests that commonality should be practical and beneficial. Specific considerations, such as polar platform first launch weight volume constraints and the operating voltage requirement (28 VDC) of the Mobile Service Center (MSC) power system have influenced the selection of the NiH_2 IPV cell capacity size and the design of the low series voltage (28V) battery (ORU) package assemblies. Where differences in detailed requirements between station and platform were encountered, the approach was taken to let the platform considerations drive the design in the absence of significant overall program penalties or feasibility problems on the station. For details of the PV platform subsystem refer to Section 2.1.2. of DR-02.

3.2.1 Station PV Module

The station PV Power Subsystem contains two PV Power Modules, each located just outboard of an alpha joint on the transverse boom. Each PV Power Module consists of two photovoltaic array wings, two beta joints and a PV equipment box containing four batteries, associated source power control, conditioning and management equipment, and local thermal control equipment. The nominal source bus voltage is 160 V.

The subsystem provides the following power levels at a 3-year end-of-life design point under worst-case orbit and seasonal conditions.

- o Nominal constant power operation
  - 23.5 kWe to the user load input
  - 1 kWe share of the PMAD processor load
- o Peaking operation
  - 23.5 kWe average power to user load input
  - 1 kWe continuous share of PMAD processor load
  - 42.5 kWe peak power to user load input
  - 7.5 minute peak in eclipse and/or sunlight

3.2.1.1 PV Module Overview

A PV power module for the IOC Station shown in Figure 3.2-1 provides 11.75 kWe to the input of the user load converters plus 1 kWe for PMAD processor loads. The IOC station includes two of these modules. Each module consists of two solar array wings, NiH_2 storage batteries, PV electronics, thermal control and heat rejection for energy storage and PMAD losses, required truss structure, roll rings, and beta joints. The PV electronics, energy storage and the thermal control/heat rejection systems are contained in the PV equipment box outboard of the alpha joint. The module also includes a main bus switching assembly (MBSA), a power distribution and control assembly (PDCA) and a power management controller (PMC) located inboard of the alpha joint.

Two solar array wings supply an average 12.25 kWe to the loads during the sun portion of the orbit. In addition the arrays supply the power to charge the NiH_2 batteries which supply the 12.25 kWe to the loads during the eclipse portion of the orbit.

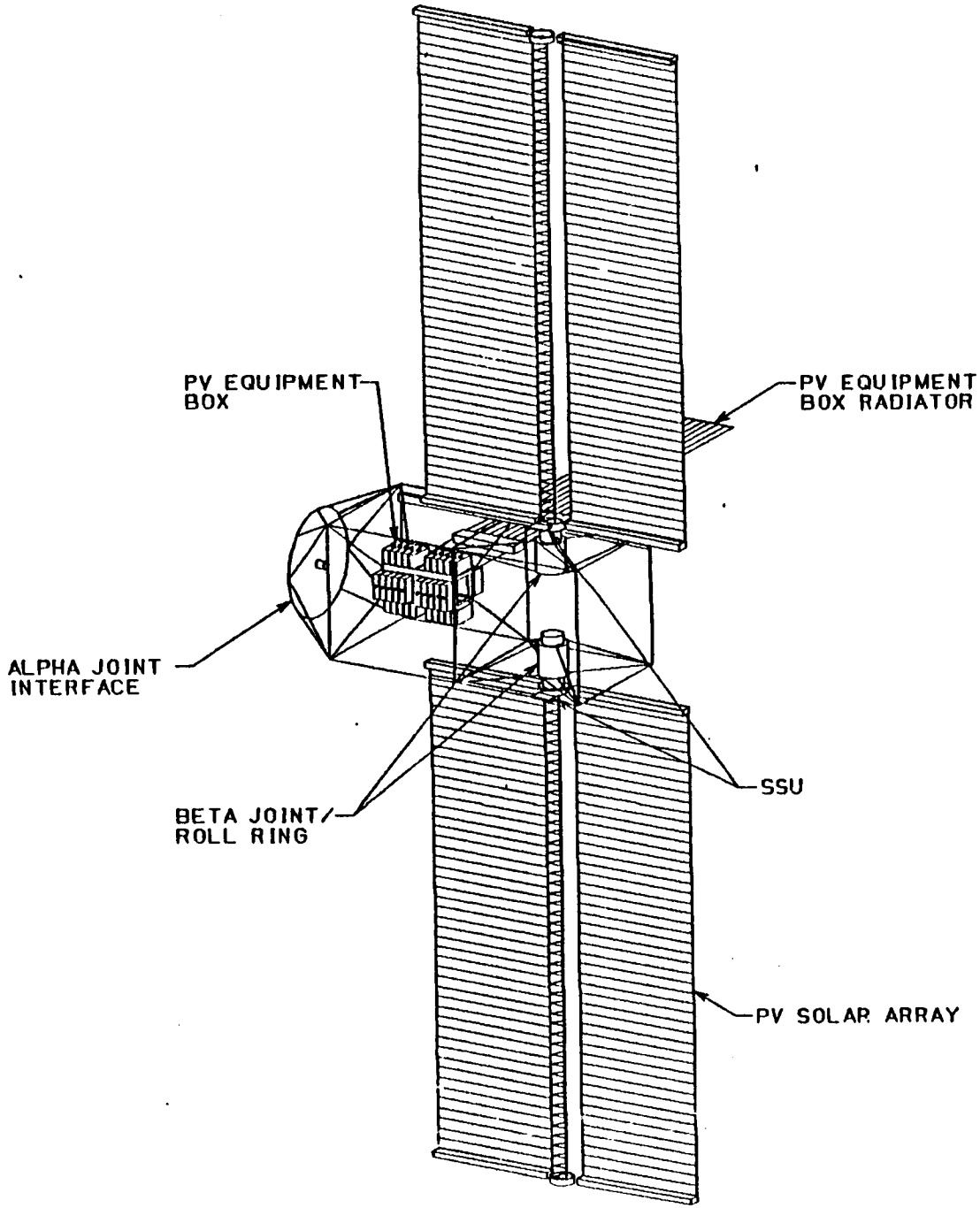

Figure 3.2-1

	Rockwell International Corporation Rocketdyne Division Canoga Park, California
	SPACE STATION EPS
	PV MODULE
	SIZE C | FSCM NO. 02602 | DWG NO. 7R070048
	SCALE NONE | DO NOT SCALE PRINT | SHEET

DWG NO. 7R070048

The array wings extend from the transverse boom through a beta joints outboard of an alpha joints on each side of the dual keel. The alpha and beta joints maintain the solar orientation of the wings. Each wing uses one deployable mast to support two identical solar blanket assemblies.

3.2.1.1.1 PV Module Layout Drawing

Refer to Figure 3.2-1 for the PV module layout drawing.

The PV equipment box (Figure 3.2-2) is within the PV module truss structure. It will contain a rack and structure for battery assemblies, PMAD equipment, and an active thermal control system. The ORUs within the equipment box will be easily accessible for replacement. The Space Station truss structure will provide the mechanical support and electrical interfaces will be at both the alpha and beta joints.

3.2.1.1.2 PV Module Mass Properties

The PV Module Mass Summary is shown in Table 3.2-1. The mass estimates are shown for the module subassemblies, PMAD associated with the PV module the alpha and beta joint target weights.

3.2.1.1.3 PV Module Performance

The PV Module contains the energy storage, integrated PV subsystem, thermal control and PMAD hardware, and structural support elements. The performance of the system as a whole is described in this subsection. More detailed performance data on the individual elements are provided in the assembly subsections.

The functional block diagram of the PV subsystem is shown in Figure 3.2-3. The subsystem contains two common source power buses, each

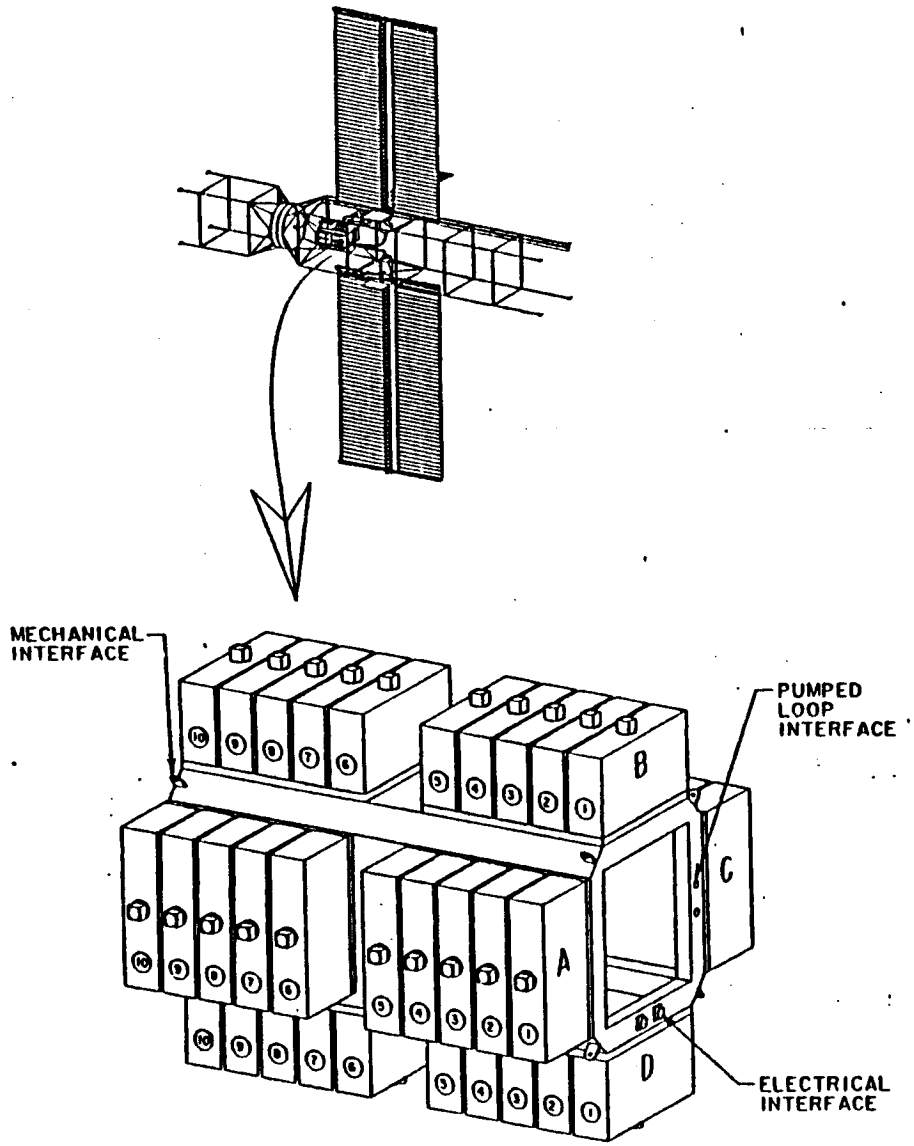

Figure 3.2-2

A1 BATTERY ASSEMBLY
A2 BATTERY ASSEMBLY
A3 BATTERY ASSEMBLY
A4 BATTERY ASSEMBLY
A5 BATTERY CHARGE/DISCHARGE UNIT
A6 SPARE
A7 SPARE
A8 PHOTOVOLTAIC CONTROLLER
A9 POWER DISTRIBUTION AND CONTROL UNIT
A10 AC SWITCH UNIT
B1 BATTERY ASSEMBLY
B2 BATTERY ASSEMBLY
B3 BATTERY ASSEMBLY
B4 BATTERY ASSEMBLY
B5 BATTERY CHARGE/DISCHARGE UNIT
B6 DC SWITCH UNIT
B7 SPARE
B8 POWER SOURCE CONTROLLER
B9 PHOTOVOLTAIC CONTROL UNIT
B10 DC-AC INVERTER
C1 BATTERY ASSEMBLY
C2 BATTERY ASSEMBLY
C3 BATTERY ASSEMBLY
C4 BATTERY ASSEMBLY
C5 BATTERY CHARGE/DISCHARGE UNIT
C6 SPARE
C7 SPARE
C8 PHOTOVOLTAIC CONTROLLER
C9 POWER DISTRIBUTION AND CONTROL UNIT
C10 AC SWITCH UNIT
D1 BATTERY ASSEMBLY
D2 BATTERY ASSEMBLY
D3 BATTERY ASSEMBLY
D4 BATTERY ASSEMBLY
D5 BATTERY CHARGE/DISCHARGE UNIT
D6 DC SWITCH UNIT
D7 SPARE
D8 POWER SOURCE CONTROLLER
D9 PHOTOVOLTAIC CONTROL UNIT
D10 DC-AC INVERTER

Rockwell International Corporation
Rocketdyne Division
Canoga Park, California

COMPONENT LOCATIONS
PV EQUIPMENT BOX

SIZE C | 02602 | DWG NO. 7R070045
SCALE NONE | DO NOT SCALE PRINT | SHEET

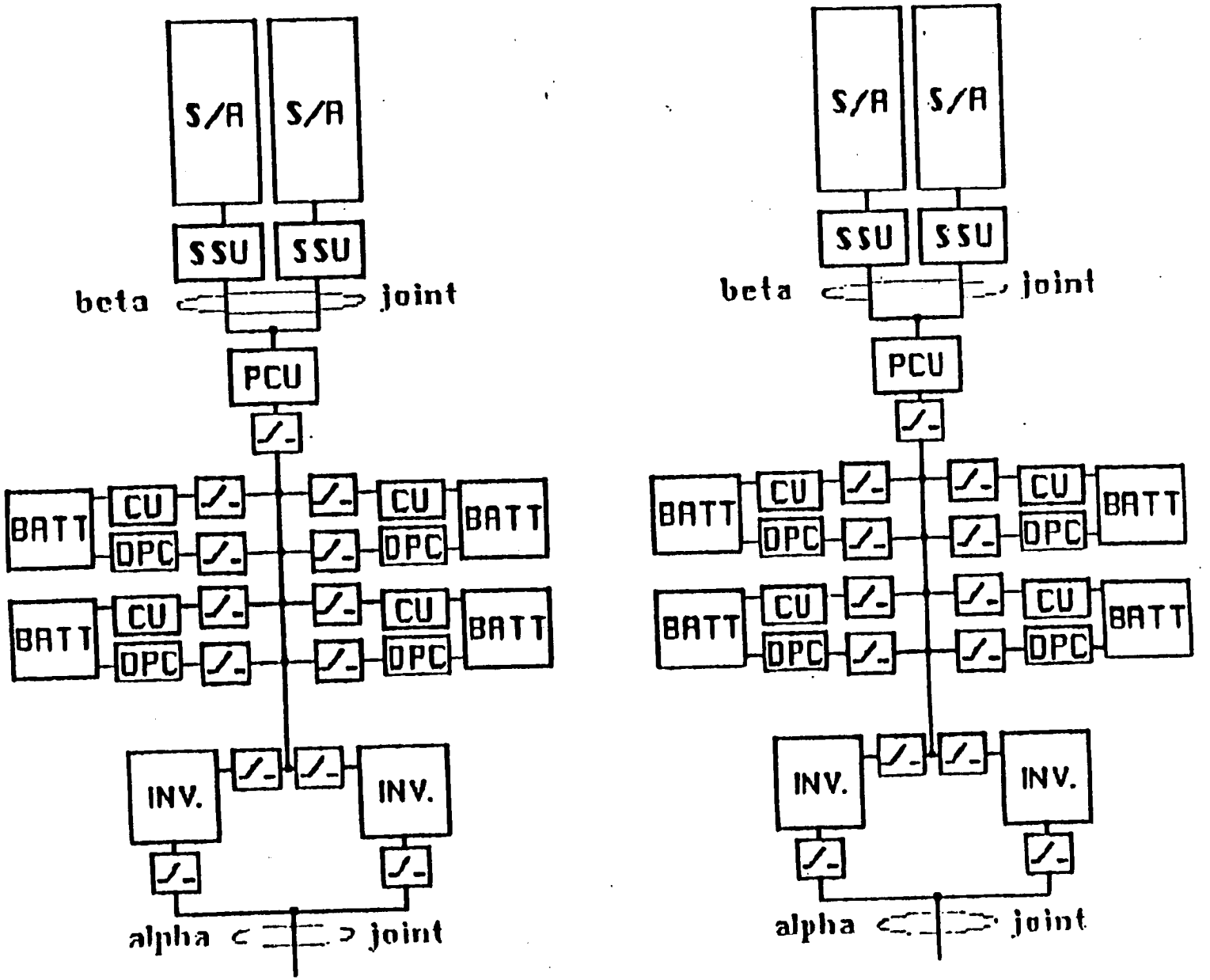

Figure 3.2-3 PV Source PMAD Architecture

TABLE 3.2-1 PV MODULE MASS SUMMARY

	MASS kg	lb
Solar Arrays + SSU (2 wings)	1004	2213
Energy Storage System (4 units)	880	1940
Thermal Control	486	1071
Source PMAD	1294	2853
Beta Joint	524	1155
PV Equipment Box	266	498
Truss structure	59	130
Alpha Joint	1182	2606
Module Total 12.5 kWe net-to-user	6255	13790

served by two deployable/retractable flexible, planar, silicon-cell solar array wings, two switching sequential shunt units (SSU), one power control unit (PCU), four nickel-hydrogen (Ni-H_2) batteries with associated charge power (buck) converters (CPC) and discharge power (boost) converters (DPC), and switchgear and cabling. Resonant inverters convert source power to 20 kHz, 440 V single phase AC distribution power.

Operation and performance of the system is as follows. During the sunlight portion of the orbit the array generates power which is provided to the inverters and CPCs. Voltage regulation of the source bus is provided by the PCUs and SSUs. The PCU senses bus voltage across a capacitor bank and drives a pulse-width modulation (PWM) circuit based on the difference between bus voltage and a reference voltage. The SSUs contain switching circuits that can shunt individual solar cell strings in the array in response to load

requirements; in the baseline design each of the four SSUs has 46 such circuits. Some of these are off, allowing array string power to flow to the bus; some are on, continuously shunting excess power to ground, and one active circuit is being switched on and off, driven by the PWM signal. The mix of on and off circuits and which circuit is active at any given time is determined by the load requirements and reference to voltage setting.

The CPC provides charge power to a battery by buck regulation of source bus power to the voltage required by the battery as a function of state of charge and charge rate. The current provided to the batteries is determined by a coulometry algorithm implemented in the PV source processor. Charge current level and end-of-charge taper profile and timing are based on measured discharge capacity on the previous eclipse discharge. Individual charge control of the batteries ensures balanced operation and control in the event that batteries have different health status.

During eclipse the batteries provide power in accordance with the demand. Discharge power from individual batteries is regulated with individual DPCs to provide balanced battery operation in case of health status differences. The regulators boost voltage to the nominal source bus voltage of 160 V.

The inverters use a resonant topology to convert DC power at a nominal 160 V to 20 kHz distribution power at 440 V. Vectoring of parallel inverter circuits provides the ability to closely control both voltage and frequency of distribution power.

The baseline SSU-regulated source bus approach also provides excellent and inherent protection of the array to high voltages which would occur on eclipse emergence of a cold array, and could lead to plasma interactions, electromagnetic interference (EMI) and corona discharge problems. The SSU maintains the voltage on array cell strings in a range from nominal bus voltage to zero at all times. Protection of crew during installation and maintenance operations is derived from a SSU default feature that shorts all cell strings when the system is unpowered.

More detailed information on the operation of individual elements of the PV subsystem is provided in the applicable subsections below.

3.2.2 Photovoltaic Array

The photovoltaic array system for the station is based on the Lockheed design of a large area, deployable/retractable planar, flexible panel substrate array. The design is similar to the array technology demonstrated in the OAST-1 flight experiment on STS-41D in September 1984.

The solar array system is composed of four wings. Each wing has two identical blanket assemblies, each stowable in a container/cover assembly. The two container/cover assemblies are hinged to a mast assembly which is structurally tied to the Space Station. The major components are:

- Blanket Assembly. The blanket assembly consists of a flexible substrate assembly which supports the solar cells and the Flat Conductor Cable (FCC) which conducts the electrical current to the base of the array.

- Container/Cover Assembly. The container/cover assembly provides the environmental protection and structural support for the stowed solar cell blankets during launch and transfer orbit. The container/cover interfaces to the mast assembly and the Space Station structure.

- Mast Assembly. The mast assembly extends, retracts and provides the structural rigidity for the extended solar array blankets. The main elements of the mast assembly are boom, canister, drive assembly and control electronics.

- Blanket Support-Tension System. The support-tension system maintains the blanket assembly in a plane and provides blanket proper tension and stiffness for array bending and torsional stabilities and controls. The major components of the system are the blanket assembly tension bars, guide wires, and the negator spring mechanisms.

Key requirements to which the solar arrays have been designed for the station are as follows:

- o Provide 23.5 kWe continuous power to the user for three years.
- o Provide 1 kWe of power for PMAD processors
- o Orbit: 250 nm, 28.5 deg inclination
- o Arrays must be retractable
- o Arrays during operation will be oriented normal to the solar vector
- o Deployed array natural frequency must be > 0.1 Hz
- o The structure must accommodate loads from RCS reboost firings

The power requirements shown were not design drivers for the station array; the design was constrained by the platform first launch, IOC and 10 year EOL power requirements for which the array was optimized. Power capability of the PV subsystem on the station was determined based on the platform array design, resulting in the power requirement definition above. The design presented in this section is fully consistent with the listed requirements and with commonality with the platform.

3.2.2.1 PV Array Layout Drawings

Figure 3.2-4 shows a layout of a solar array wing in the fully deployed configuration. The wing consists of two blanket subassemblies of 48 hinged panels, which carry the solar cells and the harness, an extendable mast subassembly, cover and container subassemblies, and tensioning mechanism hardware.

Figure 3.2-5 shows the wing in the stowed configuration with blanket containers and mast assembly integrated prior to deployment. Stowage for launch will be as separate blanket container and mast ORUs.

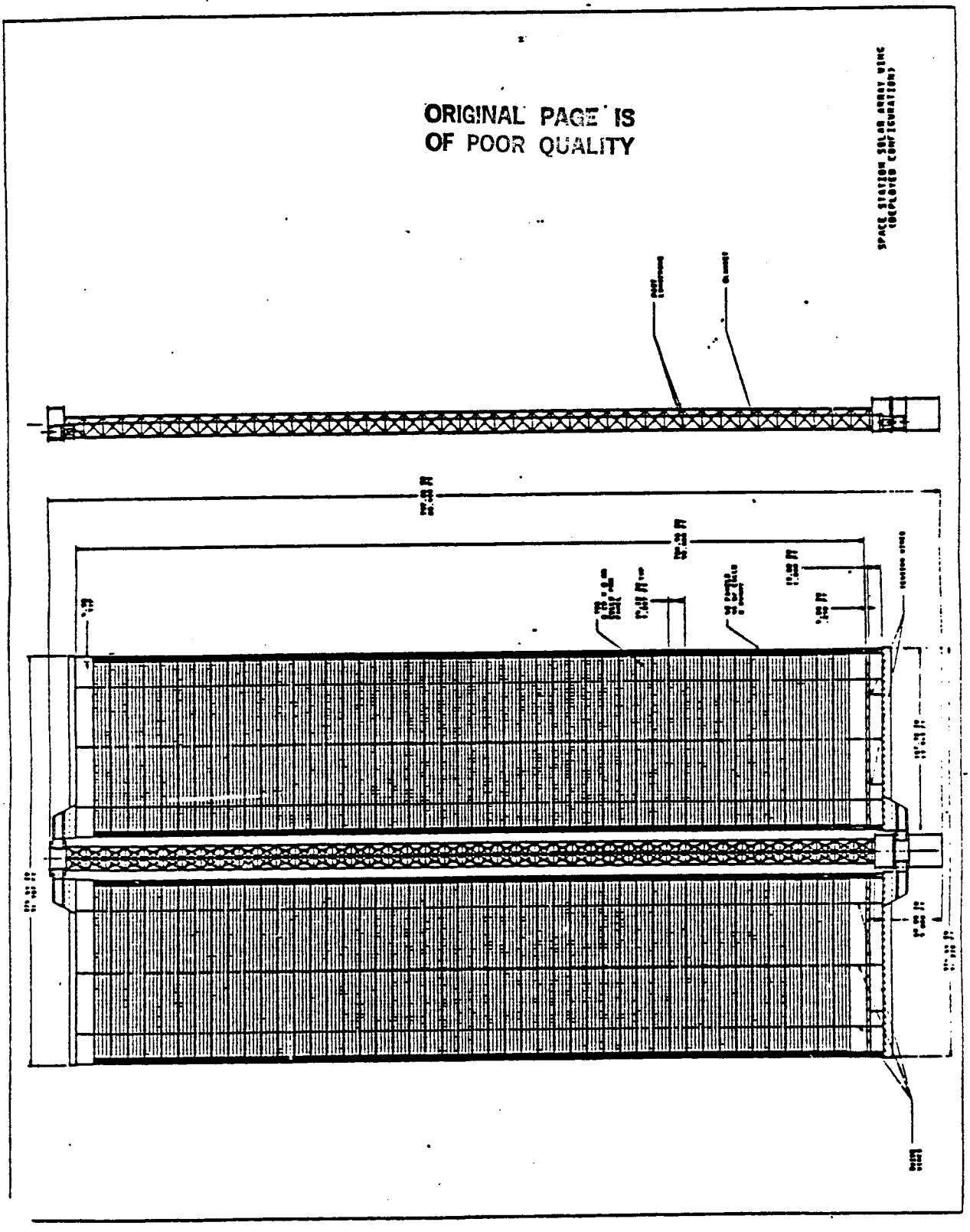

Figure 3.2-4 PV Array Wing (Deployed Configuration)

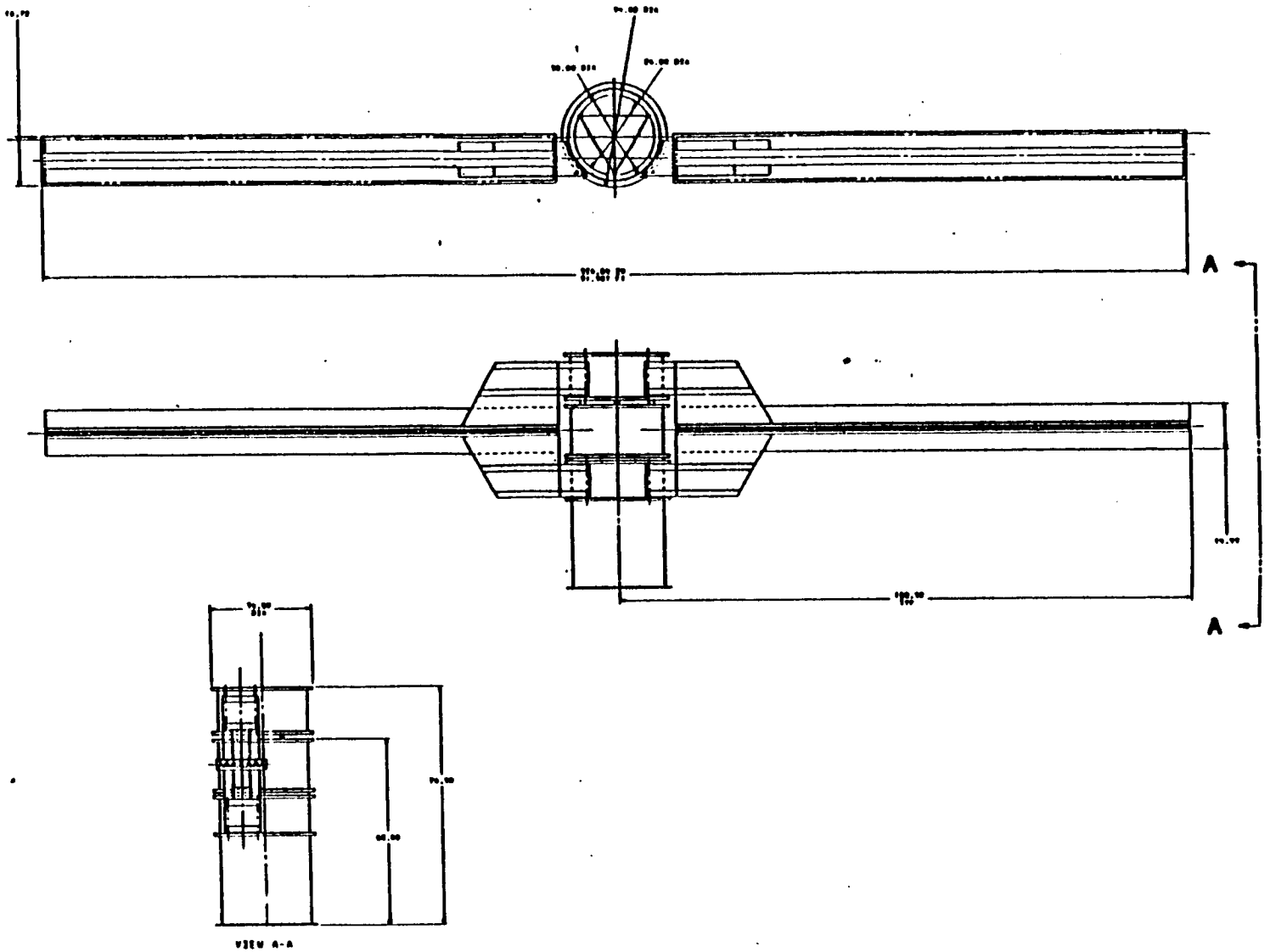

Figure 3.2-5 PV Array Wing (Stowed Configuration)

Figure 3.2-6 is a layout of a typical array panel, indicating the location of the 196 cells and 26 bypass diodes. The panel is the basic subassembly building block of the array blanket.

Figure 3.2-6 is Lockheed's concept of a 196 cell panel (4 x 19 = 196). The 196 cells are a product of the polar platform 80V/panel design requirement. This 196 cell panel is manufactured by Lockheed in two sections, one comprised of 96 cells (4 x 24) and the other has 100 cells (4 x 25). The two sections are then connected in series at the near mid-point panel stiffener to achieve the required 80V. The two sections containing an unequal number of cells will not pose any manufacturing process problems to Lockheed.

3.2.2.2 Electrical Performance

Electrical performance of the array is a function of design, seasonal, orbital and age parameters. The functional design is based on several trade studies performed under Phase B, while sizing is based on the requirements for the polar platform array.

Cell performance projection is based on the curve shown in Figure 3.2-7. This curve was measured on a cell judged representative of expected mass production cell quality, rather than ideal laboratory cell quality. Performance of the cell as degraded by assembly and environmental factors is summarized in Table 3.2-2. Values used for maximum power point voltage and current under worst-case orbital and seasonal conditions after three years in orbit are 0.438 V and 1.801 A.

The plasma and UV radiation factors will be the same for the 3 year and 10 year designs because plasma losses are a function of voltage and orbital atmospheric density and independent of mission lifetime. UV radiation loss occurring within the first to second year of the mission life then stabilizing, so a 3 and 10 year mission would show the same losses.

Micrometeoroid losses are expected to be 1% per 10 years in orbit; therefore 0.8% is used for a 3 year orbit (a large fraction of which is at a lower assembly orbit).

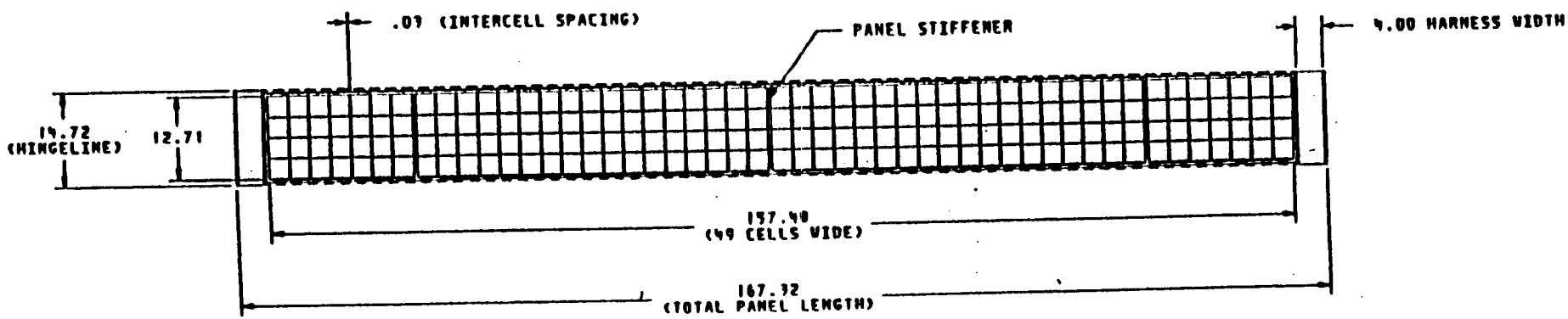

Dimensions in inches

Figure 3.2-6 Space Station Solar Array Panel Layout Drawing

Figure 3.2-7 8 x 8 Solar Cell Performance Curve

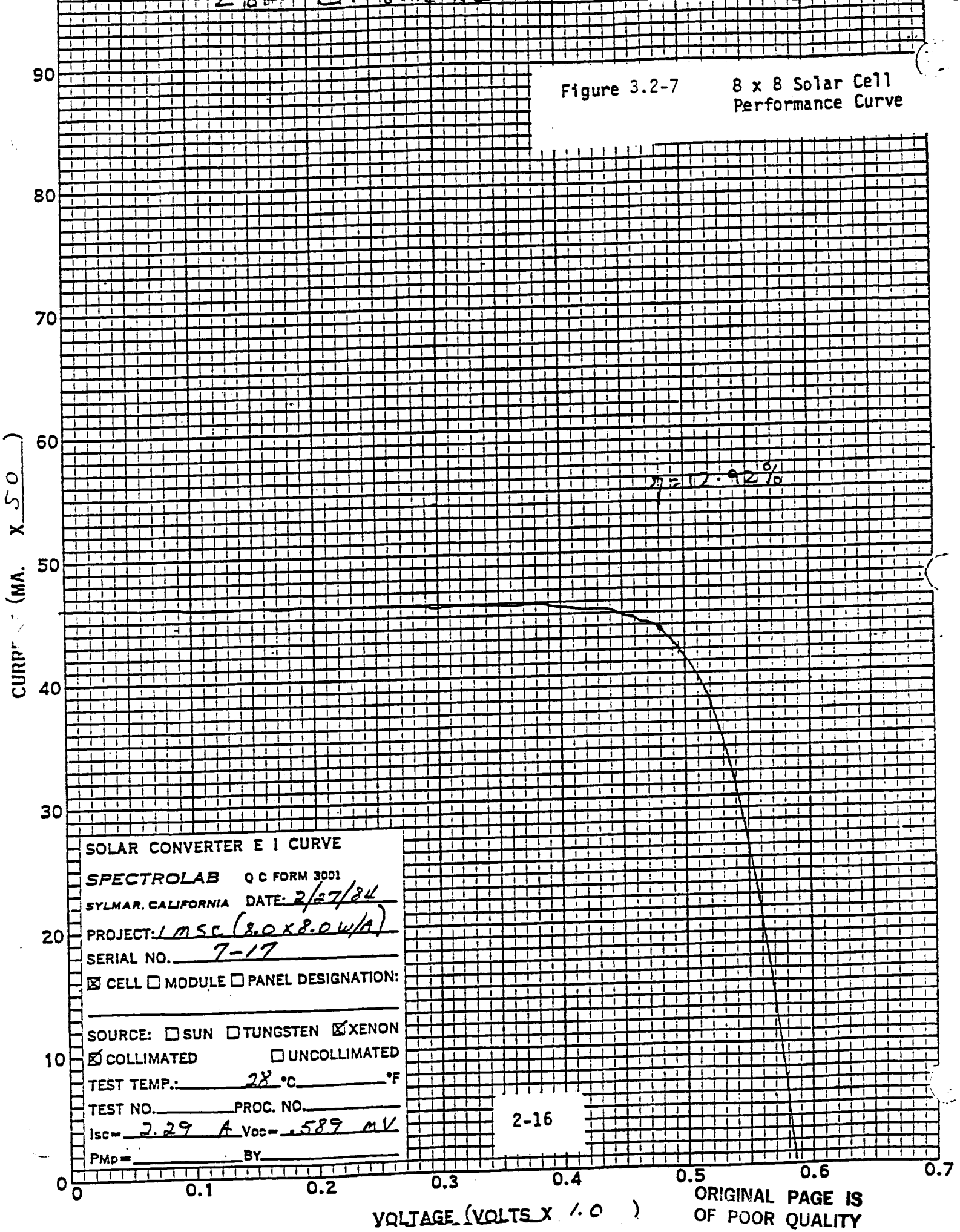

EOL STATION POWER ANALYSIS
TABLE 3.2-2

PARAMETER		FACTOR x	Isc AMPS	Voc mV	Imp AMPS	Vmp VOLT
BARE CELL @ C	25	x	2.303	0.596	2.135	0.495
COVERSLIDE		0.990	2.280	X	2.114	X
I CIRCUIT LOSS		0.980	2.234	X	2.071	X
V CIRCUIT LOSS (V)		0.010	X	0.586	X	0.485
RADIATION DEGRADATION						
RImp		0.995	X	X	2.061	X
RIsc	FLUENCE	0.998	2.230	X	X	X
RVmp		0.995	X	X	X	0.482
RVoc	6.28E12	0.998	x	0.585	x	x
ENVIRONMENTAL						
MICROMETEROIDS		0.992	2.213	x	2.045	x
PLASMA		0.990	2.191	x	2.025	x
UV RADIATION		0.980	2.147	x	1.984	x
THERMAL CYCLING		0.990	2.125	x	1.964	x
HARNESS IR LOSS		0.970	2.062	x	1.905	x
CONTAMINATION		0.955	1.970	x	1.821	x
INTENSITY FACTOR		0.978	1.926	x	1.781	x
TEMPERATURE @C						
I TEMP CORRECT	41	0.021	1.947	x	1.801	x
V TEMP CORRECT	45	-0.044	x	0.541	x	0.438
3 YEAR DESIGN-POINT TOTALS			1.947	0.541	1.801	0.438

V2-32A/11

A 2% power loss due to thermal cycling was allocated to the 10 year mission whereas a 1% loss was allocated for the 3 year mission. As the station and platform configurations are more understood, a thermal analysis will be run using appropriate payload view factors to determine the array temperature range and subsequent thermal cycling losses.

The contamination losses are the same for the SS+PP but for different reasons. The 4.5% power loss on the station was the conservative allocation used due to the STS, station and platform reboost RCS firings (assuming hydrazine propellant) over a 3 year period. The platform contamination loss is also a 4.5% but predominantly due to a 10 year mission at lesser potential contamination levels.

The contamination power loss is difficult to accurately access due to the uncertainties involved in the study. We believe the conservative value of 4.5% for the station and platform is adequate until the choice of RCS propellant is formalized and a contamination survey is undertaken to determine the type of contamination expected (solid and/or volatile), the effect of surface temperature and the effect of atomic oxygen on surface contaminants over various orbits.

3.2.2.3 Structural Performance

The selected coilable longeron boom of 0.67 m (26 in) diameter offers a minimum bending strength of 2900 ft-lb, 3500 ft-lb ultimate, surpassing the RCE reboost load requirements. The selected combined blanket and guide wire tension of 667 N (150 lb) yields a first mode natural frequency of 0.17 Hz, according to analysis by Lockheed. Adjustments in mass for atomic oxygen protection materials reduces the natural frequency to approximately 0.16 Hz bending and 0.356 (torsion).

3.2.2.4 PV Array Assembly Definition

The baseline solar array system for the space station is a four-wing configuration providing 56.89 kWe of gross power under worst-case orbital and seasonal conditions at 3 years. Each wing is composed of two fold-up solar cell blankets, a central mast assembly, the blanket containers and interface hardware. The overall size of one wing is 9.57 m (31.39 ft) wide by 20.3 m (66.5 ft) long. The area of the two blankets is 152 m2 (1636 ft2), 608 m2 (6544 ft2) for the 4 wings. The mass of one complete wing is 485 kg (1,069 lb) as shown in the breakdown in Table 3.2-3. The Station photovoltaic array design summary is shown in Table 3.2-4 and Table 3.2-5.

The baseline design of 196 cells in series produces an operating voltage of about 80 V per panel or 160 V for 2 panels in series. The 160 V nominal voltage represents a reasonable compromise between plasma interaction losses and harness losses. Eclipse emergence voltage of 270-300 V on an unregulated array would probably be safe with respect to avoiding potentially damaging plasma EMI and arcing effects; however, the sequential shunt regulation approach used will maintain array voltages at 160 V regardless of the cycle operating temperature extremes.

3.2.2.4.1 Solar Cell

The baseline solar cell is a 200 um silicon cell, 8 x 8 cm (3.15 x 3.15 in) square with cropped corners and with wrap-through contacts. They are optically infrared (IR) transparent and the back contact uses the gridded configuration to maximize IR-transparency. Cell performance as well as circuit integration, temperature, and degradation factors were covered in Section 3.2.2.2. The performance characteristics of the flight cells will reflect the results of a current NASA-LeRC-funded large cell advanced development program with a 14.5% efficiency goal. The cover slide is 150 um thick ceria doped CMX glass that covers the entire surface of the cell. The baseline adhesive is Dow Corning DC93-500.

TABLE 3.2-3
SPACE STATION/ I O C PLATFORM SOLAR ARRAY MASS

	BLANKET LEVEL			WING LEVEL	MODULE	STATION
	QUAN	UNIT MASS	TOTAL KG'S	TOTAL KG's	TOTAL KG's	TOTAL KG's
CELLS PER PANEL (8 x 8 cm)	196					
DIODES PER PANEL	14					
PANEL LENGTH - M	0.373			2 BLANKETS	2 WINGS	4 WINGS
PANEL WIDTH - M	4.250			PER WING	PER	
AREA PER PANEL - SQ M	1.5825			MODULE		
BLANKET ASSEMBLY						
PANELS PER BLANKET48	1.845	88.56	177.12	177.12		
HARNESS	2	7.16	14.32	28.64		
----TOTAL---			103.31	205.76	411.52	823.04
BLANKET BOX						
CONTAINER BASE	1	14.94	14.94	29.88		
CONTAINER COVER	1	14.94	14.94	29.88		
----TOTAL----			29.88	59.76	119.52	239.04
TENSION GUIDE WIRE ASSY						
GUIDE WIRES	3	0.62	1.86	3.72		
FINAL TENSIONER	1	2.32	2.32	4.64		
----TOTAL----			4.18	8.36	16.71	33.43
LATCH ASSEMBLY	1	12.70	12.70	25.40	50.79	101.59
SUPPORT STRUCTURE						
UPPER FITTING	1	2.72	2.72	5.44		
LOWER FITTING/CABLING	1	3.99	3.99	7.98		
----TOTAL----			6.71	13.42	26.85	53.70
EXTENSION MAST/ASSEMBLY	1					
BOOM				71.2		
CANISTER AND CABLING				50.16		
MAST CAP				2.36		
DRIVE ASSEMBLY				11.34		
DRIVE ELECTRONICS				1.59		
---- TOTAL ----				136.67	273.3	546.6
ATOMIC OXYGEN PROTECTION (1 MIL ORGANIC)				35.70	71.40	142.8
---- TOTAL SOLAR ARRAY ----				485.20	970.04	1940.0

V2-32A/10

Table 3.2-4 Station Photovoltaic Array Design Summary

Active panels per blanket	46	
Circuits per panel	0.5	
Circuits per blanket	23	
Blankets per wing	2	
Wings per station	4	
Cells per panel	196	
Cells per circuit	392	
Cells per blanket	9016	
Cells per wing	18032	
Cells per station	72128	
Operating Voltage	160 V	
Solar Cell		
- Type	Silicon, N on P, shallow junction	
- Size	8 cm x 8 cm, cropped corners 200 um thick	
- Active Area	60.14 sq cm	
- Base Resistivity	2 ohm-cm	
- Coverglass	150 um thick CMX	
- Coatings	Dual system, TiO/Al203	
- Contact Pattern	Wrap through	
Electrical Configuration		
- each panel	1 parallel x 196 series cells	
- each circuit	1 parallel x 392 series cells	
- each blanket	46 parallel x 392 series cells	
Number of blankets per wing	2	
Number of panels per wing	96	(48 per blanket; 46 celled)
Number of cells per wing	18032	(196 per panel)
Number of bypass diodes per wing	2392	(26 per panel)
Wing power - kW	14.2	(3 years on orbit)
Wing mass - kg	485	
Wing length - m	20.3	
width - m	9.57	
area - sq m	194	(Outline)
	152	(Blanket)
Natural frequency - Hz	0.16	(Bending)
	0.356	(Torsion)
Allowable acceleration - g	0.090	(Maximum ultimate; Wing perpendicular)
Stowed volume - cu m	2.96	(2 blanket boxes Plus mast canister)

V2-32A/14

TABLE 3.2-5

STATION ARRAY PERFORMANCE SUMMARY

	Blanket	Wing	Module	Station
BOL GROSS POWER - kWe	8.23	16.47	32.94	65.9
3 YEAR GROSS POWER - kWe	7.1	14.2	28.4	56.9
NET-TO-USER - kWe	2.9	5.9	11.7	23.5

V2-32A/12

3.2.2.4.2 Panel Assembly

The cells are integrated into a 392-cell circuit that covers two panels. The 196 cells per panel are arranged into a 4 x 49 cell array (Figure 2.1.1-5 showed the panel layout). The panel substrate consists of two layers of 25 um thick Kapton, between which a photo-etched copper interconnection pattern is sandwiched. The layers are bonded together with 25 um of polyester adhesive. Cutouts in the Kapton expose the copper circuit where it is to be welded to the solar cell contacts and flat conductor cable interface. Attachment of the cells is accomplished through both these welds and adhesive tape bonded to the substrate and the cell backs. For a description of the solar cell and solar array assembly refer to Figure 3.2-8

The electrical circuit includes bypass diodes: one redundant pair is wired in parallel with each group of up to 16 cells, for a total of 26 diodes per panel. The diodes have a flat-pack configuration compatible with panel stowage thickness requirements. Each panel measures about 0.373 x 4.25 m (1.2 x 13.9 ft), and has hinge lines formed by folding and bonding the substrate at its long sides.

The exposed Kapton surface of the panel is protected from atomic oxygen (AO) attack by an integral protective layer. One AO candidate coating is silicon dioxide with a 4% Teflon admixture to improve flexibility and integrity of the protection under sharp bending of the Kapton, such as occurs at the hinge lines. Final selection of protective coating materials will be made during Phase C/D following completion of 1986 advanced development tasks on materials and verification testing sponsored by NASA LeRC. Pending this resolution, a mass allocation has been added to the wing weight analysis based on a worst-case AO protection method. A 1 mil coating of CV1144 is applied to 100% of the front 25% of the and back surface areas of the Kapton blankets.

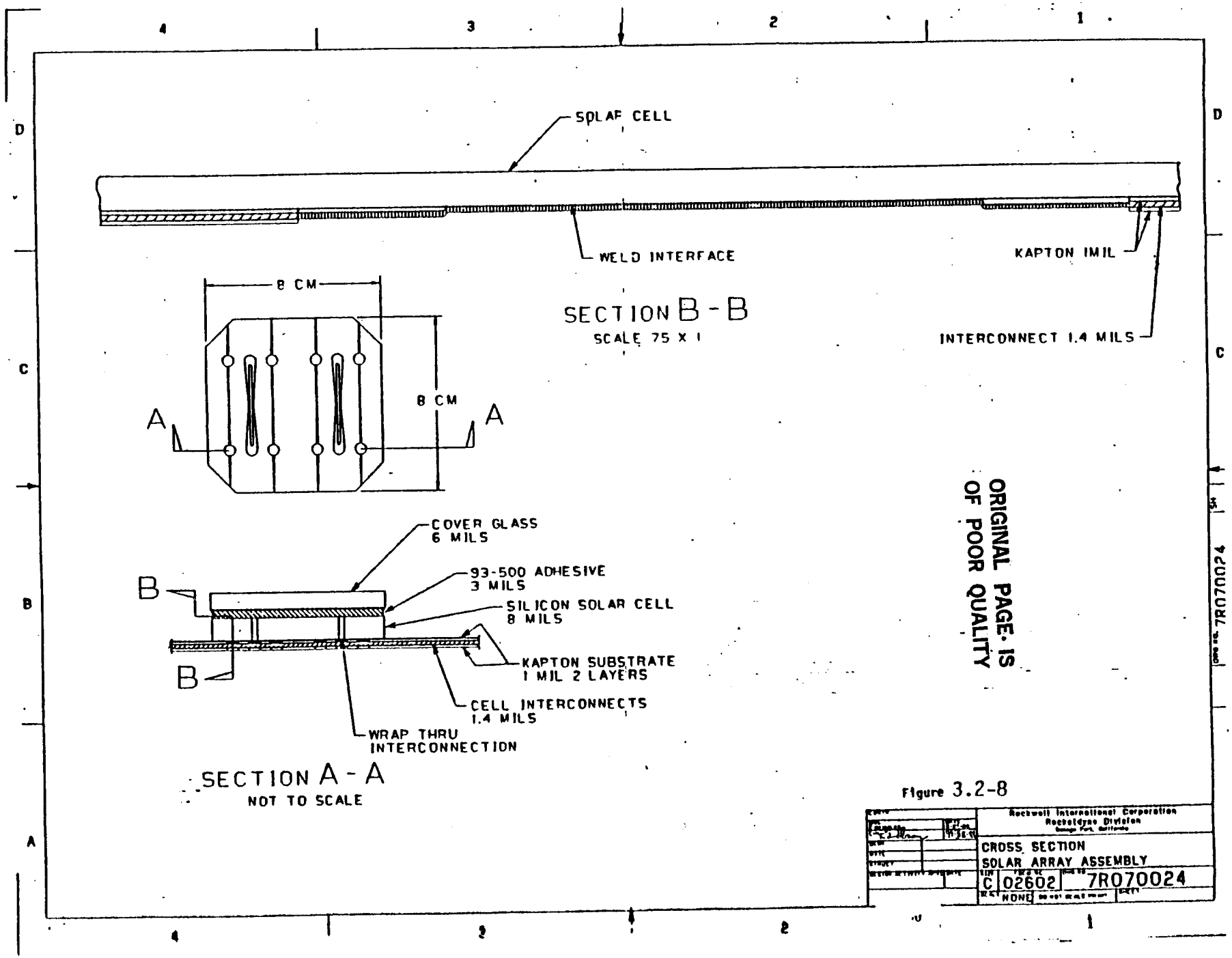
SOLAR CELL
WELD INTERFACE
KAPTON IMIL
INTERCONNECT 1.4 MILS
SECTION B-B
SCALE 75 X 1
8 CM
8 CM
A
A
B
B
COVER GLASS
6 MILS
93-500 ADHESIVE
3 MILS
SILICON SOLAR CELL
8 MILS
KAPTON SUBSTRATE
1 MIL 2 LAYERS
CELL INTERCONNECTS
1.4 MILS
WRAP THRU
INTERCONNECTION
SECTION A-A
NOT TO SCALE
ORIGINAL PAGE IS
OF POOR QUALITY
Rockwell International Corporation
Rocketdyne Division
CROSS SECTION
SOLAR ARRAY ASSEMBLY
C
02602
7R070024
NONE

Figure 3.2-8

3.2.2.4.3 Blanket Assembly

The blanket assembly is made of 46 identical panels with solar cells and leading and trailing panels without cells at the cover and container attachment areas. These two panels carry no cells and serve primarily to offset the active panels sufficiently far from the cover and container to minimize shadowing, which is a consideration more important for the polar platform than for the station. Adjacent panels are hinged to each other to form the full blanket.

A flat conductor cable is located along the two long sides of each blanket. The cable conductors are welded to the appropriate contacts on the panels. Series connection between two panels to form a full circuit is made using a segment of the flat cable. Adjacent panel pairs are wired in mirror image to cancel magnetic fields.

3.2.2.4.4 Structural Support

Structural support of the blankets in the deployed configuration is provided by the mast assembly and the container/cover assembly, which incorporates the tensioning mechanisms. In the stowed configuration, each folded blanket is contained in its container box, which is detachable from the mast assembly as an ORU.

The mast assembly uses a 3-legged coilable-longeron boom, shown in Figure 3.2-9. The continuous longerons are S-glass/epoxy rods. In the stowed condition they are elastically coiled into a flat helix within the boom canister. As the boom is deployed, the longerons are released from the canister retention and become straight. Structural connections between the longerons are made by S-glass/epoxy battens and steel cable diagonals. The boom is double-laced for enhanced stiffness. The selected boom diameter is 0.67 m (26 in).

The canister, shown in Figure 3.2-10, containing the stowed boom and the deployment drive also forms the attachment point to the station structure via

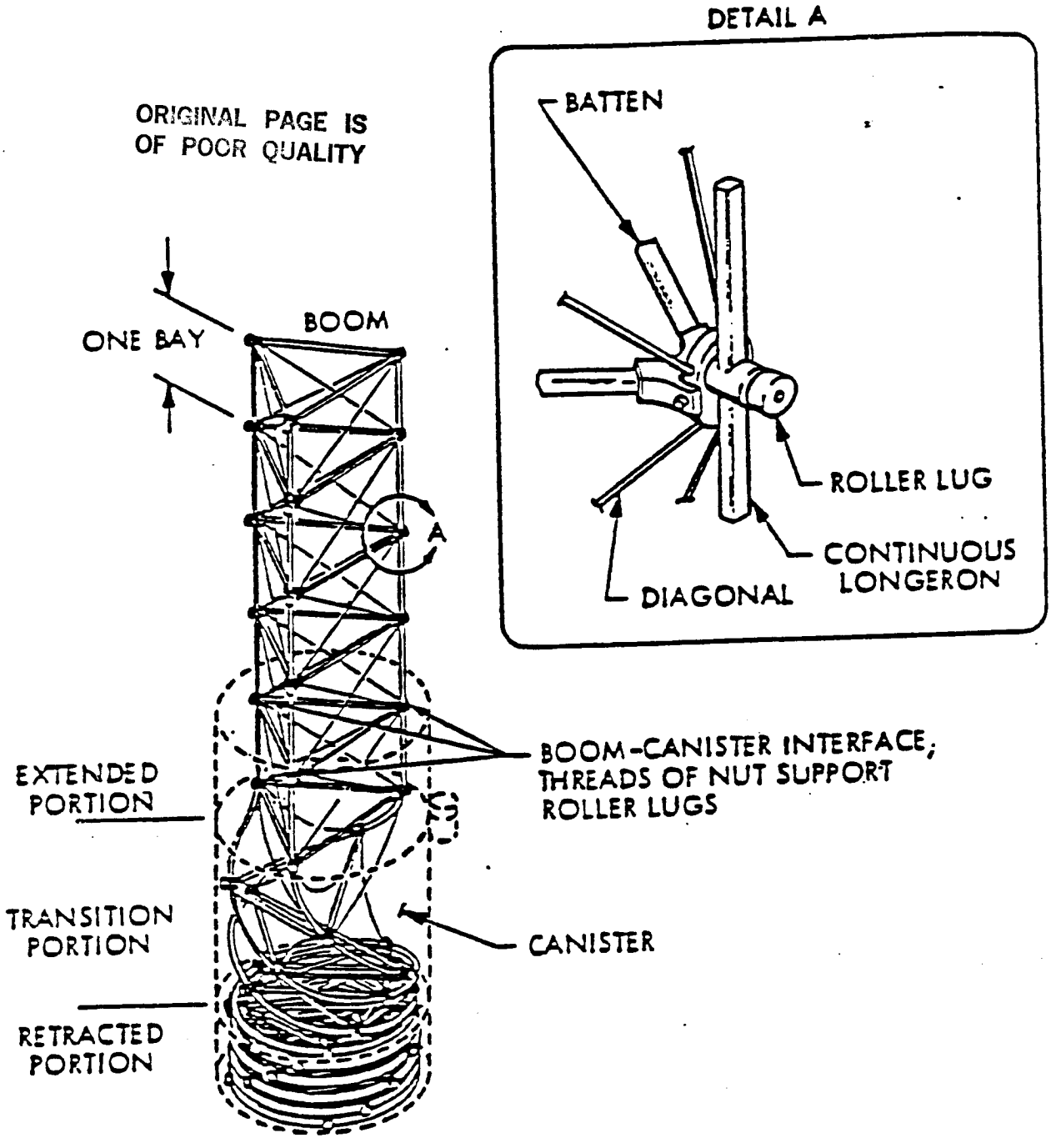

Figure 3.2-9 Mast Assembly

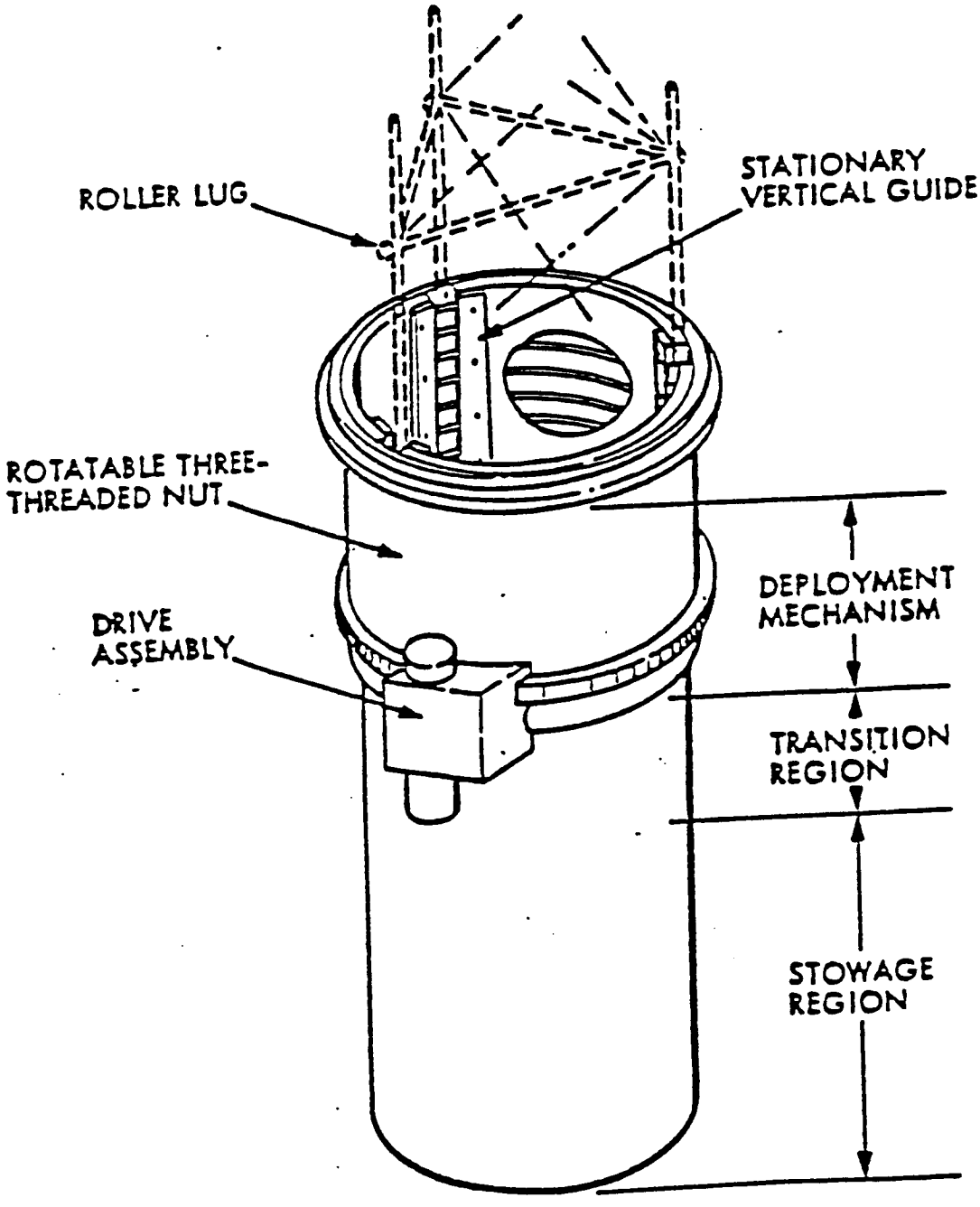

Figure 3.2-10 Mast Canister Assembly

the beta gimbal. Its main structure is an aluminum cylinder of 0.76 m (30 in) diameter. The drive assembly provides the torque to extend the boom and control the extension process. A full-diameter rotatable nut constrains the boom roller lugs to release the boom in an orderly fashion. Stationary guides maintain proper positioning and structural support of the extended portion of the boom.

The blanket box, consisting of the blanket container and the cover, holds the stowed blanket under moderate compression to provide support during launch. The folded blanket of 48 (46 celled) panels forms a stack about 3.2 cm (1.25 in) thick, while the harness stack is 6.2 cm (2.4 in) thick. This difference in stack height is accommodated with a flexible transition section within the container. Polyurethane foam padding of appropriate thickness is located on the inside of the cover to distribute the compressive load evenly. The cover latching mechanism provides the compressive load. The container is the main attachment for the tensioning mechanisms and guide wires, and provides the load path to the canister. The cover provides attachment for the guide wires and the structural load path to the mast cap. Both components are made of aluminum perforated-core honeycomb with graphite/epoxy facesheets.

The blanket tension assembly contains negator motors which provide constant blanket tension independent of differential thermal expansion between mast and blankets. Guide wires are also maintained at low, near-constant tension during extension and retraction operations and at full extension by similar negator motors. The guide wires primarily serve to provide relatively even deployment of the blankets, and guide the panels to proper positions during retraction. To satisfy the required array natural frequency > 0.1 Hz a combined blanket and guide wire tension of 667 N (150 lb) was chosen with a resultant first mode natural frequency of 0.16 Hz.

The boom, container/cover assembly, guide wires and possibly other components of the structural support system will require protection against atomic oxygen attack. Boom longerons and battens may be wrapped with thin aluminum foil to prevent epoxy erosion. The guide wires require a flexible,

low-friction, insulating surface finish; and will probably be coated with the same material selected for protection of the blankets. The container and cover may be protected with metal foil, or at a moderate mass penalty the graphite/epoxy face sheet may be replaced with aluminum.

3.2.2.5 PV Array Equipment List

The equipment list for the station PV array assemblies is provided in Table 3.2-6.

Table 3.2-6 PV Array Equipment List

COMPONENT	DESCRIPTION	SIZE
Cell Cover	Ceria-doped	150 micron nom. (6 mil)
Cover Adhesive	DC 93-500	50 micron max. (2 mil)
Solar Cell	Silicon, 2 Ohm-cm Gridded back Rear Contacts, Solderless	8 x 8 cm (60.14sq cm) 200 microns thick (8 mil)
Interconnect	OFHC Copper Photo-etched	36 microns thick (1 oz/sq ft)
Substrate	Integral Interconnect Kapton laminated with polyester adh.	25 micron Kapton, 2 sheets each, 12 micron adh
Harness	Flat Conductor	Conductor thickness 75 microns (3mil)
Mast		66 cm diameter (44gm/cu cm)
Longerons	S-Glass/Epoxy	0.99 cm/side
Battens	S-Glass/Epoxy	0.76 cm/side
Diagonals	7 x 7 Steel Cable	0.24 cm/side
Canister	Aluminum	0.76 m diameter
Blanket Box Cover	Perforated Al Honeycomb Core with Graphite/ Epoxy Face Sheets	
Base	Perforated Al Honeycomb Core with Graphite/ Epoxy Face Sheets	

V2-32A/18

3.2.3 Energy Storage - Batteries

The space station and platform use nickel-hydrogen (Ni-H2) batteries for energy storage associated with the PV subsystem. In order to achieve commonality between the station and platform applications, a moderate capacity of 62 Ah was selected. This capacity provides a close fit to station battery capacity and symmetry (even number of batteries) requirements, and accommodates the platform capacity needs with minimal mass. The trade study resulting in this selection is reported in Section 5.14.

Each battery consists of 92 Ni-H2 cells in series and is divided into four assemblies with 23 cells each. A single assembly can serve as a complete battery on systems within the space station program that may use a 30 V bus, such as the MSC, and associated vehicles such as the OMV and OTV.

Eight batteries are used on the station the PV power subsystem, four per PV module.

3.2.3.1 Battery Layout Drawings

Figures 3.2-11 and 3.2-12 provide a layout drawing of a battery assembly. A full battery consists of four of these assemblies electrically connected in series to form a string of 92 cells. The layout shows a battery pack, which is an arrangement of 23 cells with necessary harness and mechanical components, mounted on a thermal control plate consisting of a honeycomb panel with embedded heat pipes.

Figure 3.2-13 shows a preliminary cross-sectional drawing of the 62-Ah cell. It uses a dual stack arrangement within a conventional 3.5-inch diameter pressure vessel.

Figure 3.2-1 and Figure 3.2-2 show an overall location of equipment in the PV equipment box including the battery location and thermal control radiator.

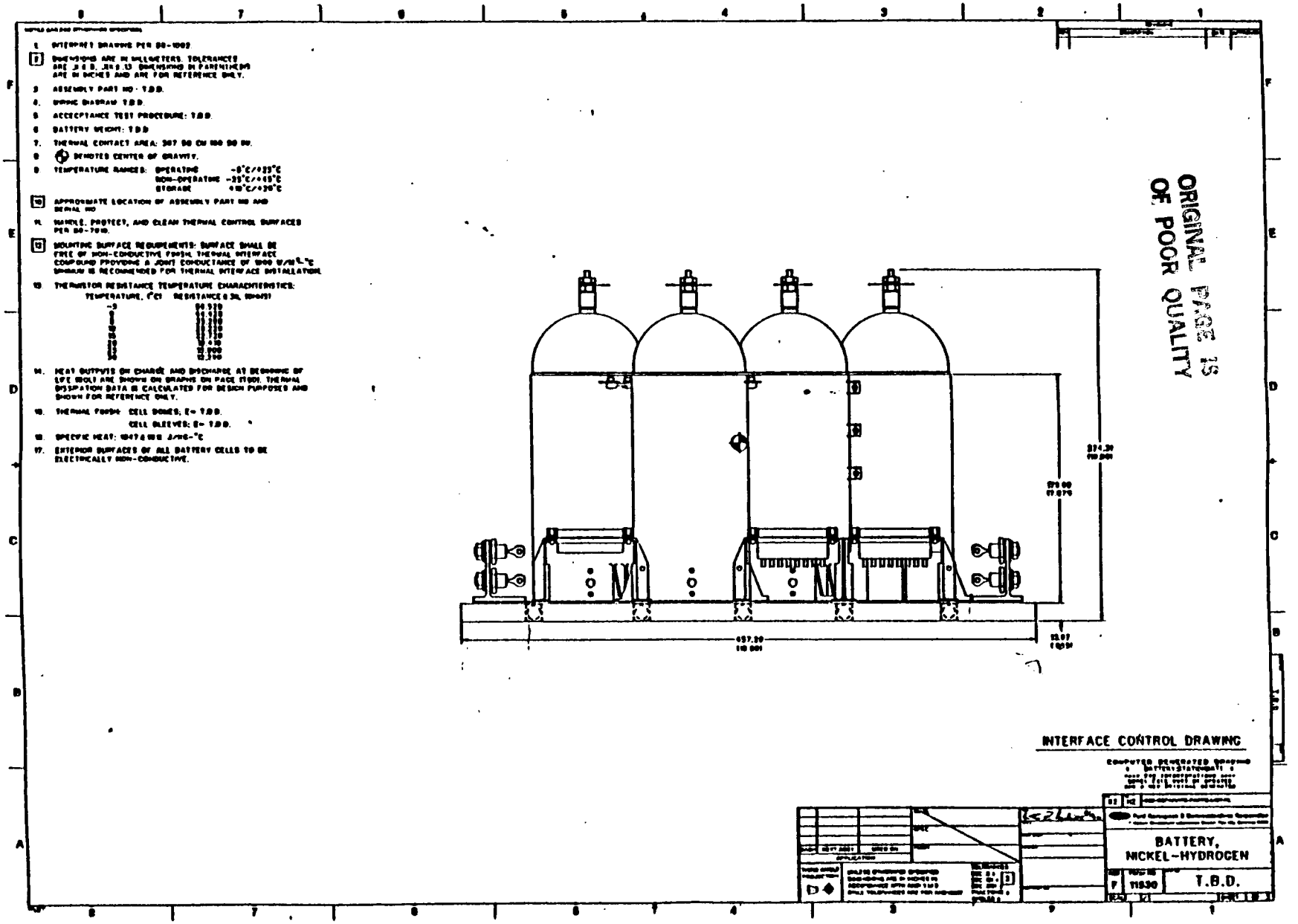

Figure 3.2-11 Battery Assembly Layout Drawing - View 1

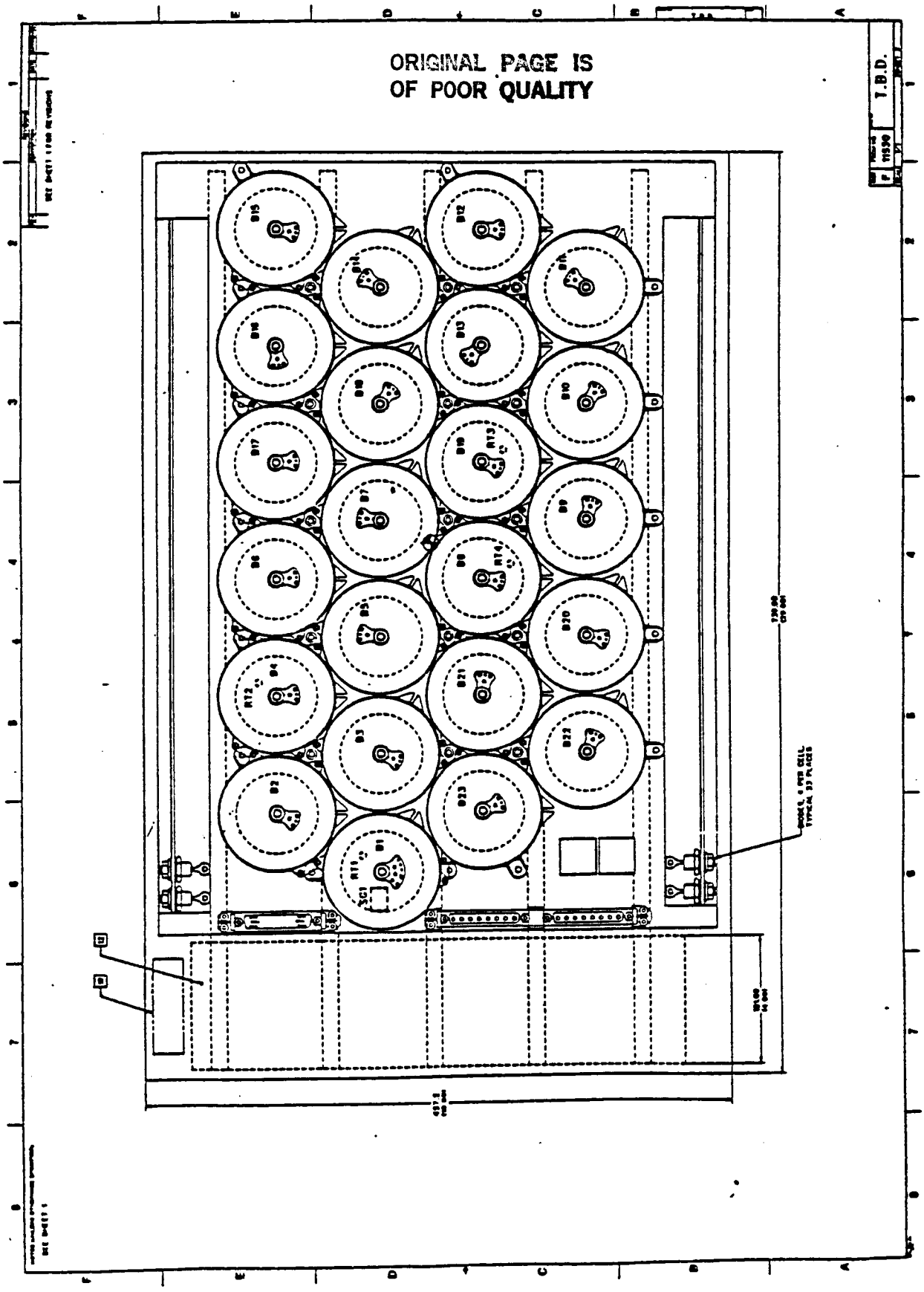

Figure 3.2-12 Battery Assembly Layout Drawing - View 2

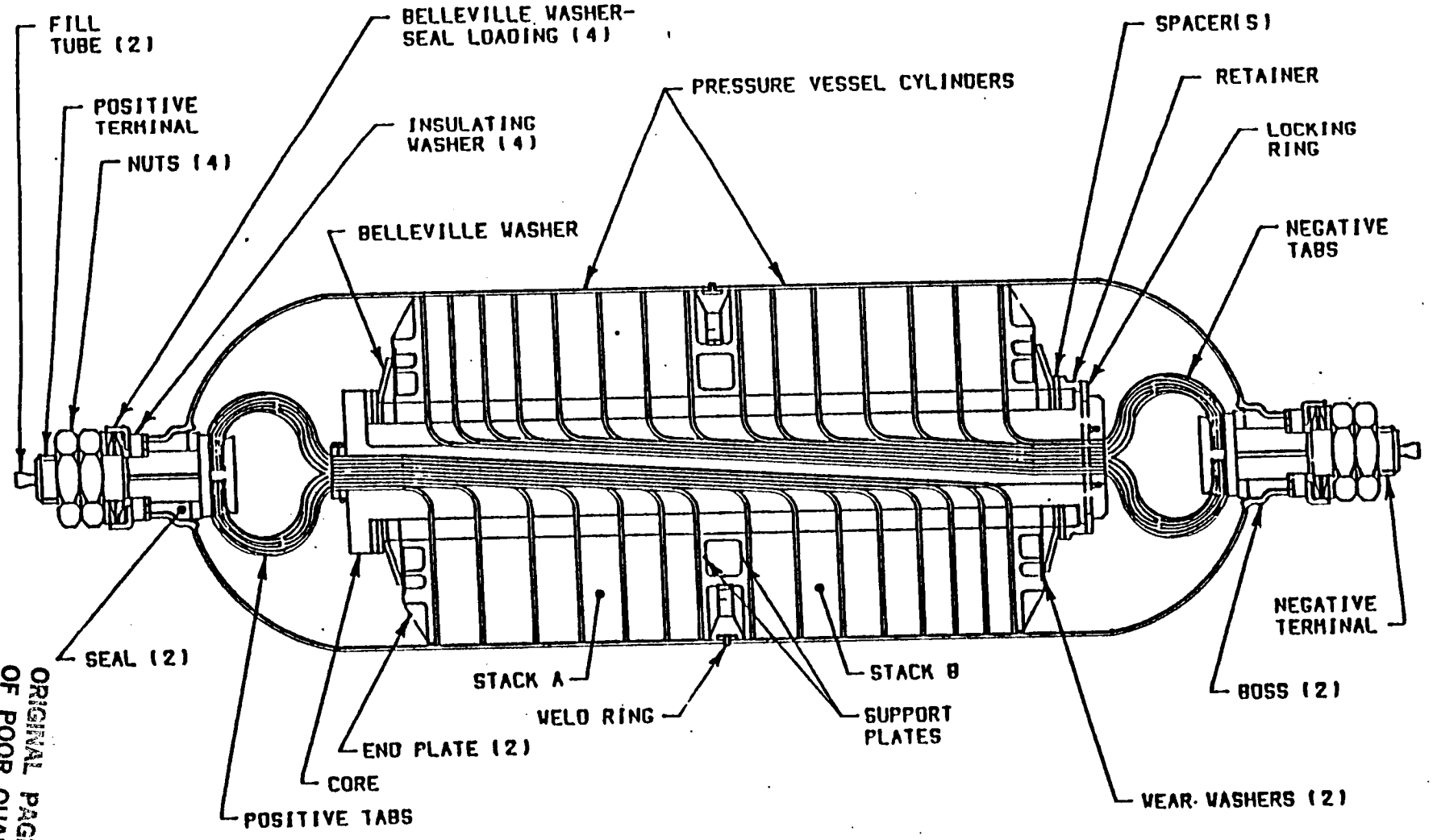

FIGURE 3.2-13 PRELIMINARY CROSS SECTION OF 62-AH $Ni-H_2$ CELL

3.2.3.2 Battery Mass Properties

Table 3.2-7 provides a preliminary mass breakdown for a single battery assembly. The packaging factor, total assembly mass divided by cell mass, is about 1.45. The center of gravity of the assembly is as indicated in Figure 3.2.3-1.

Table 3.2-8 gives the total mass of the battery system for the station.

Table 3.2-8. Station Ni-H_2 Battery System Mass Summary

Assembly Level	Mass
Mass per Cell	1.66 kg (3.66 lb)
Mass per Battery Assembly	55.3 kg (122 lb)
Mass per Battery	221 kg (487 lb)
ESS Mass per Module	880 kg (1940 lb)
Total ESS Mass	1760 kg (3880 lb)

3.2.3.3 Battery Assembly Performance

Performance of the battery system is characterized by voltage, capacity, depth of discharge (DOD), life, thermal dissipation behavior, and operational control. The important conditions are nominal eclipse and sunlight operation, peaking support, and contingency support.

Basic performance parameters are summarized in Table 3.2-9

Voltage. Battery voltage performance for nominal operation is projected to be an average of 1.27 V/cell as a result of the relatively low DOD, for a total battery voltage of 116.8 V. Actual discharge voltage will vary from about 124 V at the beginning of eclipse to about 114 V at the end of eclipse. For a discharge including a worst-case eclipse followed by contingency operation at 10 to 14 kW for one orbit, the average cell voltage is expected to be 1.20 V, for a battery total of 110 V. Cells produce useful energy down to about 1.0 V, or 92 V for the battery. Thus, the DPC should be able to accommodate input voltages from 92 to 130 V.

Table 3.2-7 Nickel-Hydrogen Battery Assembly Mass Breakdown

ITEM	QUANTITY	UNIT MASS (kg)	TOTAL MASS (kg)
CELL	23	1.660	38.18
SUPPORT SLEEVE	23	0.310	7.13
INSULATORS	23	0.038	0.87
CLAMP HARDWARE	23	0.005	0.11
HEATER RESISTORS	23	0.003	0.07
UPPER SUPPORTS	45	0.004	0.18
BASEPLATE	1	0.660	0.66
MOUNTING HARDWARE	lot	0.120	0.12
INTERCONN HARDWARE	22	0.020	0.44
INTERCONNECTS	22	0.012	0.26
TERMINAL WIRING	2	0.035	0.07
POWER CONNECTORS	2	0.030	0.06
DIODE BRACKETS	2	0.250	0.50
DIODES, DISCHARGE	23	0.035	0.80
DIODES, CHARGE	69	0.025	1.73
DIODE HARNESS	23	0.018	0.41
RELAYS	2	0.040	0.08
INSTRUMENTATION HARNESS	1	0.040	0.04
INSTRUM CONNECTOR	1	0.030	0.03
THERMISTORS	4	0.003	0.01
STRAIN GAGES	1	0.015	0.02
BONDING MATERIALS	lot	0.050	0.05
CONFORMAL COATING	lot	0.100	0.10
MISCELLANEOUS	lot	0.050	0.05
TOTAL BATTERY PACK			51.98
HONEYCOMB PLATE	1	1.600	1.60
HEAT PIPES	5	0.330	1.65
MOUNTING HARDWARE	lot	0.060	0.06
TOTAL THERMAL PLATE			3.31
TOTAL BATTERY ASSEMBLY			55.29

Table 3.2-9. Station Ni-H_2 Battery System Performance

Performance Parameter	Value
CONFIGURATION	
Total Number of Batteries	8
Capacity per Battery	62 Ah
Cells per Battery	92
ELECTRICAL	
Nominal Power Rating	27.5 kW
Peak Power Capability	48.9 kW
Nominal Average Discharge Voltage	116.8 V
Average Charge Voltage	135.2 V
Nominal Depth of Discharge	29.6%
Peak Orbit Depth of Discharge	32.5%
10 kW Contingency Depth of Discharge	67 %
85 % DOD Contingency Support Capability	15.2 kW
MECHANICAL	
Total ESS Mass	1760 kg (3880 lb)
Total Battery System Envelope Volume	4.58 m3 (162 ft3)
THERMAL	
Operating Temperature Range	0 - 10 C
Off-Nominal Temperature Range	0 - 25 C
Nominal Dissipation - Discharge	5330 W
Peak Orbit Avg Dissipation - Discharge	6360 W
Dissipation - Charge	500 W
LIFE	
Cell Cycle Life (LEO, 30-35% DOD)	50,000
Battery Calendar Life	5 - 8 years

Figure 3.2-14 shows a typical discharge voltage curve for the nominal conditions and rate projected for this application, representing a 35% DOD discharge in 36 minutes. Also shown is a "cumulative average" voltage, which is the time average of the instantaneous voltage curve to the particular point in time. This curve can be used for first-order estimating of average voltage for shallower discharges. The average shown at 20 minutes, for example, is a reasonable estimate of the average voltage for a 20% DOD cycle.

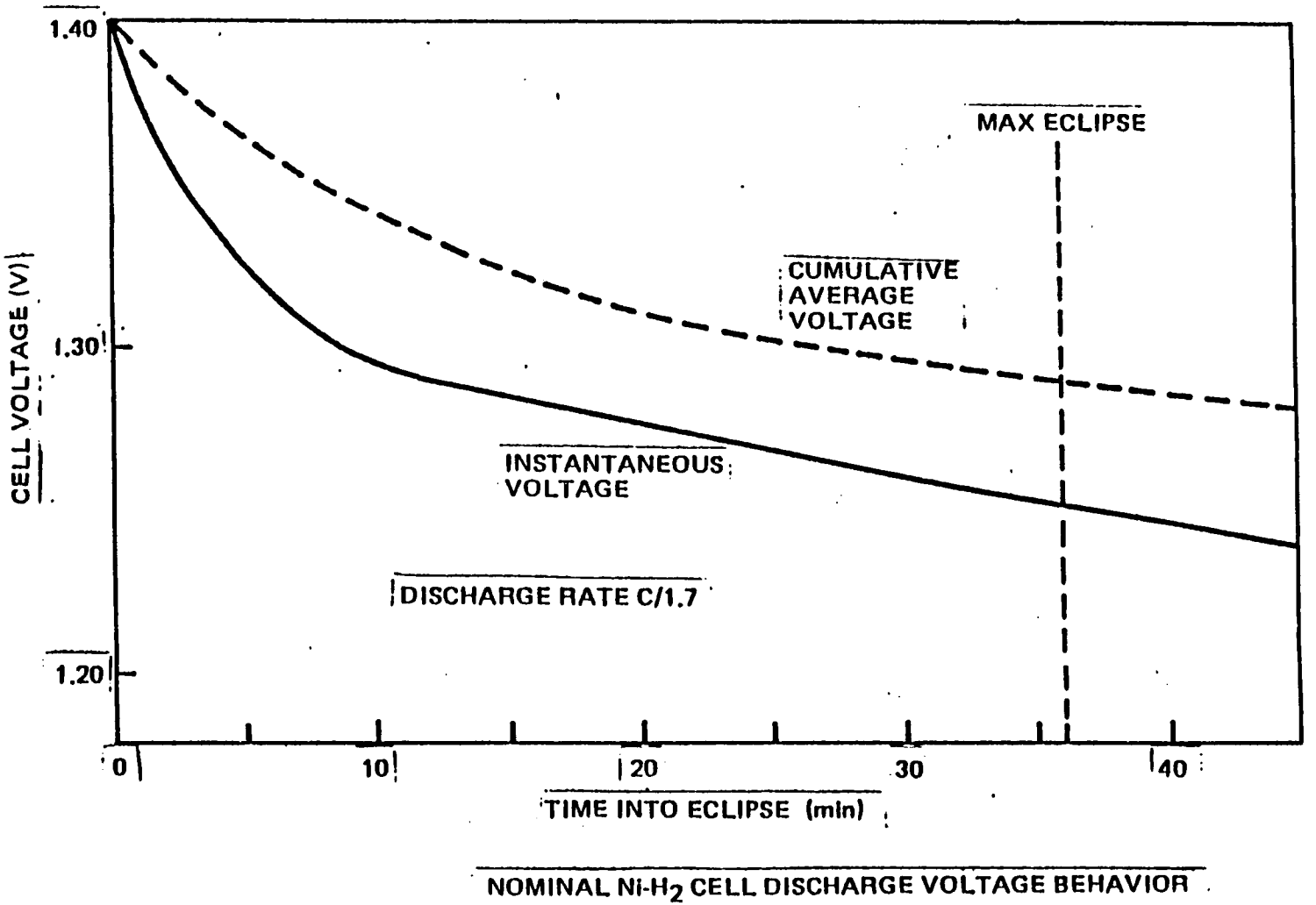

NOMINAL Ni-H_2 CELL DISCHARGE VOLTAGE BEHAVIOR

FIGURE 3.2-14

The nominal design voltage for purposes of battery sizing is the EOL expected value based on degradation from the BOL condition. This average, for the low DOD used on the Station and particularly Platform, is estimated to be 1.27 V/cell. The curve provides an illustration of typical BOL data, which clearly show a higher voltage than the system sizing voltage. The figure was included to illustrate the profile, rather than specific design point data, since 5-year LEO test data are not available as yet.

The average charge voltage is expected to be 135.2 V for nominal conditions, with a perk requirement of 139 to 143 V. Actual charge voltages at the beginning of charge following a complete discharge are very low; the CPC should therefore be able to provide output voltages of 0 to 145 V at regulated current.

Capacity The capacity of the battery is a minimum of 62 Ah at the nominal operating temperature range of 0 to 10 C. Actual expected capacity because of producibility design factors is expected to be about 66 to 69 Ah. At the reduced operating rate of the contingency situation an additional few ampere-hours can be obtained.

Depth of Discharge The DOD has been defined as a maximum of 35% for the worst-case peaking condition, with DOD conservatively based on nominal capacity. Selection of a capacity slightly higher than needed, based on the platform commonality considerations, reduces the station peaking DOD to 32.5%, and yields a DOD of 29.6% when operation is at the nominal power condition without peaking. The DOD selected for conservative contingency power capability is 85%. The batteries can support a 15 kW contingency power level for one orbit following a worst-case eclipse.

Life At the selected DOD, the life capability of the batteries is projected to be in excess of 5 years. Individual cell mean cycle life based on the extrapolation of available experimental data of similar capacity cells should be about 50,000.

The 50,000 cycle life is the expected mean cell cycle capability at the conservative DOD levels used on the Station and Platform. The battery-level life is lower due to the statistical distribution of cell cycle life. Depending on the Weibull coefficients selected, battery life capability of 5 to 8 years is projected.

Thermal Dissipation Behavior Heat dissipation during a station peak orbit eclipse averages 167 W. This yields a bulk temperature rise of approximately $4^{o}C$ during discharge depending on heat removal rate by the ITCA. Charge dissipation averages only 16 W, but most of the dissipation occurs towards the end of the charge period. Temperature gradients along the support sleeve are estimated to not exceed $6^{o}C$. Further analysis is in process to define the temperature profiles and distributions.

Operational Control Battery system operation on-orbit is fully automatic. A charge power controller (CPC) and a discharge power converter (DPC) are incorporated for each 92-cell battery. Current flow to the load is monitored and integrated during eclipse or other discharge periods by the PV subsystem processor. At discharge completion the recharge capacity requirement is determined by applying a recharge factor (nominal 1.05) to the capacity removed. The processor then controls the current output of the CPC to provide the required amount of recharge, leaving time for tapering the current near the end of charge to minimize overcharge stresses. Full charge is verified by a check of voltage and temperature behavior, followed by a reset of the capacity counter to zero prior to the next discharge.

3.2.3.4 ESS Battery Definition

The station Ni-H_2 battery system is comprised of 8 batteries, each consisting of 4 assemblies with 23 cells. Cells have a nominal 62 Ah capacity, with an expected measured value of about 66 to 69 Ah. The assemblies contain heat pipes for heat transport to a thermal system interface.

Key design and performance parameters are discussed in the following subsections. The overall system configuration is summarized in Table 3.2-10.

Table 3.2-10. Station Ni-H2 Battery System Configuration

Characteristic	Value
Total Number of Batteries	8
Total Number of Battery Assemblies	32
Capacity per Battery	62 Ah
Cells per Battery	92
Cells per Assembly	23
Total Cells	736

3.2.3.4.1 Electrical Design

Major electrical design and performance values of the battery system are identified in Table 3.2-11.

Table 3.2-11. Station Ni-H_2 Battery Electrical Design

Characteristic	Value
Nominal Power Rating (at battery)	27.5 kW
Peak Power Demand (at battery)	48.9 kW
Nominal Average Discharge Voltage	116.8 V
Average Charge Voltage	135.2 V
Nominal Discharge Current per Battery	30.2 A
Peak Discharge Current per Battery	53.1 A
Peak Charge Current per Battery	24.6 A
Nominal Depth of Discharge	29.6 %
Peak Orbit Depth of Discharge	32.5 %
10-kW Contingency Depth of Discharge	67 %
85 % DOD Contingency Support Capability	15.2 kW

The PV subsystem power level of the station is 23.5 kW at the user load inputs, plus a 1 kW allocation for PMAD processors. Accounting for a 0.89 efficiency chain from battery to load yields the battery load of 27.5 kW for a nominal orbit. The station peaking PV support is 42.5 kW at the load for 7.5 minutes in eclipse and 7.5 during sunlight, with the off-peak load adjusted to

yield an average power level of 23.5 kW for PV, 75 kW for the entire station. Batteries support the eclipse peaks at 48.9 kW, and battery charging is reduced temporarily to the minimum extent required during sunlight peaks. The worst case for battery design is the condition where only an eclipse peak occurs, since absence of a sunlight peak reduces the off-peak compensation.

The battery system is sized to operate at 35% maximum DOD under this worst-case condition. The minimum required capacity of 58 Ah for each of the eight batteries does not provide optimal platform sizing, however, and a 62-Ah capacity was baselined to accommodate this. The 62-Ah batteries will operate at a worst-case DOD of 32.5% on the station. For nominal non-peaking conditions the DOD will be just under 30%.

Contingency support at a 10 kW level can be provided at a moderate DOD of 67% for a full orbit following a worst-case eclipse. For an acceptable maximum DOD of 85%, over 15 kW of contingency load for one orbit is feasible.

The electrical design of the battery assemblies includes cell bypass diodes to ensure that the full battery system is invulnerable to the unlikely condition of an open-circuit cell failure. A load resistor network is also included in the electrical design for off-line discharging. Voltage monitoring harness will be included for all cells, although individual cells need not be monitored continuously.

3.2.3.4.2 Mechanical Design

The major mechanical design characteristics of the station battery system are summarized in Table 3.2-12.

Table 3.2-12 Station Ni-H_2 Battery Mechanical Design

Characteristic	Value
Mass per Cell	1.66 kg (3.66 lb)
Mass per Battery Assembly	55.3 kg (122 lb)
Mass per Battery	221 kg (487 lb)
Battery System Mass per Module	880 kg (1940 lb)
Total ESS Mass	1760 kg (3880 lb)
Cell Dimensions (L x DIA)	25.7 x 8.9 cm (10.1 x 3.5 in)
Battery Assembly Dimensions (L x W x H)	0.737 x 0.457 x 0.274 m (29.0 x 18.0 x 10.8 in)
Battery Dimensions (L x W x H)	(0.79 x 0.51 x 1.42 m) (31 x 20 x 56 in)
Battery Rack Dimensions-1 Module (L x W x H)	0.79 x 2.04 x 1.42 m (31 x 80 x 56 in)
Total Battery System Envelope Volume	4.58 m^3 (162 ft^3)

Each battery consists of four battery assemblies, each containing 23 cells. As was indicated in Figure 3.2.3-1 the cells are arranged in a close-packed pattern on a baseplate, and then to a honeycomb support plate. Heat pipes are embedded in the honeycomb panel and located so that each cell has access to two heat pipes. In the baseline design, a thermal interface is provided at the end of the panel. A mechanically pumped two-phase (MPTP) transport loop heat exchanger is mated to this interface.

The battery assembly and its thermal control design allows a high level of flexibility for a variety of applications within the space station program and associated vehicles such as the OMV. The universal 23-cell battery pack with its own integral base plate can be mounted on a honeycomb thermal control plate of any configuration suited to a specific application. The pack can also be mounted directly on a cold plate, if desired. This may allow some tailoring of the thermal interface configuration to differences in station and platform interface constraints, while maintaining battery pack commonality. However, the current baseline uses identical battery assemblies for both the station and platform applications.

The basic battery pack design uses flight-proven cell support technology from the INTELSAT V program, scaled up as appropriate to fit the specific capacity of the space station cells. Cells are contained in cylindrical split sleeves made of aluminum, isolated electrically and connected thermally to the cell by a silicone rubber layer reinforced with fiberglass. The sleeves have a bottom flange and mounting feet for mechanical and thermal contact with the base plate support structure. Near the top edge of the sleeves additional mechanical connections are made to form a relatively rigid overall structure. The sleeve and insulating layer thicknesses are 1.8 mm (0.070 in) and 0.5 mm (0.020 in), respectively.

The battery pack is designed with the structural integrity to withstand all STS launch and flight operational environments when mounted to a relatively rigid panel. When fastened to the honeycomb thermal panel, the overall assembly can withstand those environments while supported at panel edges. The heat pipes are integrated into the panel using a bonding approach that maximizes the strength of the honeycomb.

The estimated mass of each battery assembly of 55.3 kg includes cells, support sleeves, diodes, panel, heat pipes and interface, harnesses, blankets, switch gear, etc. Mass of the support structure is allocated to the PV equipment box and is estimated at 43.6 kg per utility center. Battery interconnect and instrumentation harness mass is projected to be 14.8 kg per equipment box.

3.2.3.4.3 Thermal Design

Major battery thermal design parameters are listed in Table 3.2-13. The recharge thermal dissipation numbers were based on approximate energy balance calculations, using average discharge voltage end current, average charge voltage, and recharge factor into account. The average recharge dissipation is the output of this calculation, without generating detail about the profile of heat dissipation through the charge period. As part of detailed design, the precise profiles will be evaluated, and this will also provide a more accurate average dissipation. For purposes of thermal subsystem sizing, the recharge dissipation is not a significant driver, and thus is typically not detailed until other design parameters are more solidly defined.

Table 3.2-13 Station Ni-H2 Battery Thermal Design

Characteristic	Value
Operating Temperature Range	0 - 10°C
Off-Nominal Temperature Range	0 - 25°C
Non-operating Temperature Range	-25 - 45°C
Storage Temperature Range	10 - 20°C
PER ASSEMBLY:	
Thermal Mass	16 Wh/°C
Nominal Avg Dissipation - Discharge	116 W
Nominal Avg Dissipation - Recharge	16 W
Dissipation - Eclipse Peak Discharge	317 W
Peak Orbit Avg Dissipation - Discharge	199 W
Peak Orbit Dissipation - Recharge	16 W
Heat Pipes	5
Heat Pipe Capacity (each) (140 Wm)	225 W
Total Heat Pipe Rejection Capacity	1125 W
TOTAL SYSTEM:	
Thermal Mass	510 Wh/°C
Nominal Dissipation - Discharge	5330 W
Nominal Dissipation - Recharge	500 W
Dissipation - Eclipse Peak Discharge	10140 W
Peak Orbit Avg Dissipation - Discharge	6360 W
Peak Orbit Dissipation - Recharge	500 W
Heat Pipes	160
Heat Pipe Capacity (each) (140 Wm)	225 W
Total Heat Pipe Rejection Capacity	36000 W

The battery thermal design relies on the cell sleeves and the heat pipes to transport heat to the thermal system interface. Cell sleeves have a 1.8-mm minimum thickness and surround the cylindrical portion of the cell over the full length of the electrode stack. The sleeves conduct heat to the flanges at their base, which interface the cell/sleeve assembly thermally to the base plate. This generic design has been flight proven in applications with similar operating rates (70% DOD in 72 minutes GEO versus 35% DOD in 36 minutes LEO).

The thermal plate can be tailored in configuration to any interface and access constraints for a particular application. For the station batteries, the plate contains heat pipes parallel with the long dimension, and extends beyond the battery pack base plate. The heat pipe condenser sections are located in this extension, where an interface area of about 10.2 x 38.1 cm (4.0 x 15.0 in) is available for cold plate mounting.

The heat pipe pattern is arranged so that each cell has access to two heat pipes so that adequate thermal control is maintained in the highly unlikely event of a heat pipe failure. The pack base plate and the honeycomb face skin act a thermal doublers to distribute heat to the heat pipes with low resistance.

The heat pipes are Al/NH_3 constant conductance devices with a square external cross section of 1.02 x 1.02 cm (0.4 x 0.4 in). The internal design uses a simple rectangular groove wick. Pipes of very similar configuration have been used by Ford Aerospace in honeycomb panel integration development and flight hardware for INTELSAT V FM-15. The pipes are bonded between the face skins for maximum thermal contact performance.

Each battery assembly includes a heater circuit that can be powered from external or internal sources to maintain battery cell temperatures above $-25^{o}C$ as required during storage of the assembly or during thermal control loop outages. Temperature sensors will be located on several cells and near the heat exchanger interface to allow the ESS or utility center processor to check for out-of-limit conditions and monitor performance.

Heat dissipation of each assembly during discharge averages 200 W under nominal peaking conditions. Average dissipation under charge conditions is about 16 W. Preferred operating temperatures are from 0 to 10 C, for optimal charge efficiency and capacity performance. Operation within the range 0 to 25 C is acceptable for off-nominal conditions. Non-operating temperatures should be maintained between -25 and 45 C, and long-term storage should be at 10 to 20 C.

3.2.3.4.4 Cell Design

The cell design for the battery is a high-rate, tandem stack Air Force MANTECH type cell with a 3.5-in diameter and a 62-Ah capacity. Cells of similar construction are baselined for MILSTAR and a LEO-specialized high-rate version has been built at 70 Ah. The 62-Ah cell will thus have many off-the-shelf features and require no high-risk or extensive, costly development. The design presented here is based on a combination of estimates and designs from several potential vendors; further convergence and design refinement is in process.

The overall cell design uses the Air Force type stack configuration with electrode tabs fed through the central core as was indicated in the cell cross-section in Figure 3.2-13. The dual stack design was chosen because the single stack approach would require extending stack length beyond demonstrated and qualified values. For long stacks, the relatively high stack compressibility can lead to dimensional distortions and local overcompression under high vibration loads. Splitting the stack into two equal, smaller sections using the tandem stack approach avoids this compression regime. The support of each stack is virtually identical to that used for single stacks and the cell is structurally and dynamically better balanced. It is typically felt that an overlong single stack represents a riskier technology that the rather simple mechanical design device of using two smaller tandem stacks. The local compressive overload concern was one of the key factors that led to the generation of the tandem stack approach. A back-to-back nickel electrode design is baselined, with a dual separator system and otherwise conventional MANTECH stack components. Oxygen recombination catalyst will be located on the wall wick on the inside surface of the pressure vessel.

The design of the 44 nickel electrodes is based on design parameters developed by the space nickel battery industry over the last decade for long life electrodes. Relatively thin electrodes are used to provide the LEO high-rate capability, with sinter porosity, pore size distribution, and loading levels yielding minimized stress levels during operation. Typical discharge current density will be no greater than 21 mA/cm^2. These parameters are consistent with those derived in the NASA-LeRC funded electrode research at Hughes Research Laboratories. The hydrogen electrodes are a proven design using a moderately low level of platinum catalyst loading in a Teflon matrix on a porous-Teflon backed photo-etched nickel grid. This basic design is flying on several spacecraft. The baseline separator is a two layer Zircar-asbestos system. The knit Zircar provides excellent electrolyte reservoir characteristics, while the thin, beater-treated asbestos layer serves as an effective barrier against direct oxygen transfer through the separator. It is expected that the approximately 200 kg (includes 50% attrition) of asbestos required for the Space Station and Platform cells will not be a problem and that sufficient material will be set aside at contract start date. The critically of the character of the raw material is reduced by reconstitution as beater-treated asbestos. The risk assessment for the initial battery production would not be affected.

Personnel safety in the use of asbestos is indeed an important concern. It is not clear what specific restrictions will be placed on its use at the different potential cell suppliers. The primary impact of these restrictions would be cost, with the magnitude dependent on the degree of protection, which may range from assembly and processing on a laminar flow bench and use of dust masks to conducting all operations in glove boxes.

Depending on the perceived long-term supply situation, an Advanced Development program on replacement barrier-type separator materials could be initiated to support production of replacement batteries. Potassium titanate is an alternative that should be readily adaptable. Early Ni-H2 cells used a separator matrix based on this material with reinforcing binders, but temporary unavailability led to exploration of other materials such as asbestos, which now has a much greater data base.

Two types of gas screens are used: a relatively thick one to provide for gas access to the back of the hydrogen electrodes, and a thin one between the back-to-back nickel electrodes. The latter provides a low-resistance oxygen path during overcharge. Electrolyte is baselined at 31% by weight KOH solution. However, the potential life enhancing benefit of a slightly lower electrolyte concentration and a low level LiOH substitution are being considered.

The mechanical design of the cell is derived from the demonstrated Air Force 3.5-in cell technology. It also incorporates features developed under the MANTECH program and additional improvements to provide more uniform stack support. The stack components are supported on a central core which attaches to the weld ring. Each stack is held between two support/end plates, one of which can move with respect to the core against a Belleville washer, to maintain constant compressive force over the life of the cell. Electrode tabs are fed through the central core.

The pressure vessel is 8.9 cm outside diameter, 0.05 cm wall and made of Inconel 718 with a nominal 3:1 safety factor based on an operating pressure of 900 psi and a burst pressure of 2700 psi as demonstrated on similar length vessels. The two hydroformed and age hardened shells are joined by electron-beam welding to the Inconel 718 weld ring. The electrical feedthroughs incorporate hydraulic cold-flow Teflon seals.

The optimal thermal design of the cell is achieved by minimizing the gap between electrodes and the vessel wall, and on proper selection of the core diameter. In addition, the cells have recombination sites for oxygen located on the inside pressure vessel wall. Heat generated during overcharge thus is removed very effectively without thermal burden on the stack.

Oxygen management is achieved by recombining oxygen generated on overcharge on the vessel wall which is coated with a porous zirconia wall wick, on which zones of platinum/Teflon catalyst are deposited. The water formed is returned to the stack by the wall wick via the separator edges in contact with

it. The wall wick also serves as electrolyte concentration and inventory equilibrator, and as a reservoir.

The wall wick in current tandem stack cells covers most of the internal vessel area, but stops short of the girth weld zone to avoid interference with the weld interface in terms of contamination and fit. The weld area is cleaned very carefully before final pressure vessel dome installation and electron-beam welding. Bridging of the wall wick across the weld ring is not necessary, since wicking interaction between the tandem stacks is not required. Sustained significant imbalances in electrolyte concentrations are avoided through vapor transport and slow surface film transport over the metal surface between the wall wick segments.

3.2.3.5 Battery Equipment List

The battery system consists of batteries, assemblies, cells and components as indicated in the hardware tree in Table 3.2-14. This is equivalent to a master equipment list at the battery level.

3.2.4 Source PMAD

Source PMAD equipment design is described in Section 3.4.

Table 3.2-14 IOC Polar Platform Nickel-Hydrogen Battery Hardware Tree

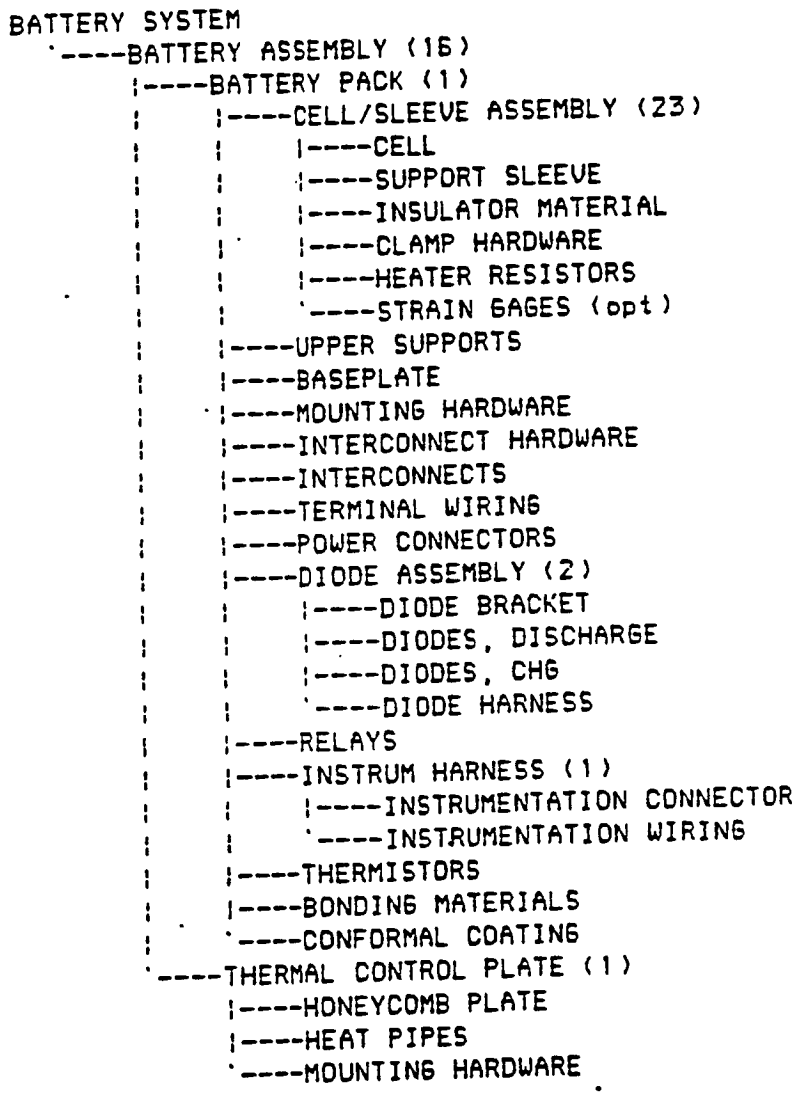

3.2.5 Integrated Thermal Control (ITC)

The Integrated Thermal Control (ITC) assembly is designed with capability to acquire and transport excess heat from the batteries and PMAD to dedicated electrical power system (EPS) radiators for rejection to space. It maintains a $5\pm5^{o}C$ temperature at the battery cells and the PMAD components under nominal conditions and 5 +20/-5^{o}C under off-nominal conditions. The ITC, shown schematically in Figure 3.2-15, is a redundant mechanically pumped two phase (MPTP) system which uses ammonia as the working fluid. Alternate, independent cold plates are manifolded to separate, independent flow loops. Similar, alternately manifolded, independent flow paths exist in the condenser. Each loop can carry the entire cooling load so that loss of fluid in a single loop will not effect battery or PMAD capability. Two ITC assemblies are used on the station, one for each PV module. Each assembly rejects heat through 8 radiator panels identical to those being developed for WP-02 central radiators under the NASA JSC Space Erectable Radiator System Program. Similar radiators are utilized for the ORC Solar Dynamic Power Concept. Additional commonality exists with the MPTP equipment being developed by WP-02 for the central thermal bus.

3.2.5.1 ITC Layout Drawings

Radiator - A space-constructible, high-capacity heat pipe radiator design, similar to the ORC radiator, is utilized as the heat rejection device for the ITC reference concept. As shown in Figure 3.2-16, each radiator panel interfaces with the MPTP condenser through a flat heat pipe evaporator section. The panels are forced into intimate contact with the condenser by means of a pressurized bellows that provides a high contact force evenly distributed over the contact area. This design provides high thermal contact conductance and low mass. The bellows are pressurized by individual GN_2 canisters. Each radiator panel consists of two high-capacity aluminum/ammonia heat pipe condensers bonded into an aluminum honeycomb matrix. These panels

PV MODULE INTEGRATED THERMAL CONTROL

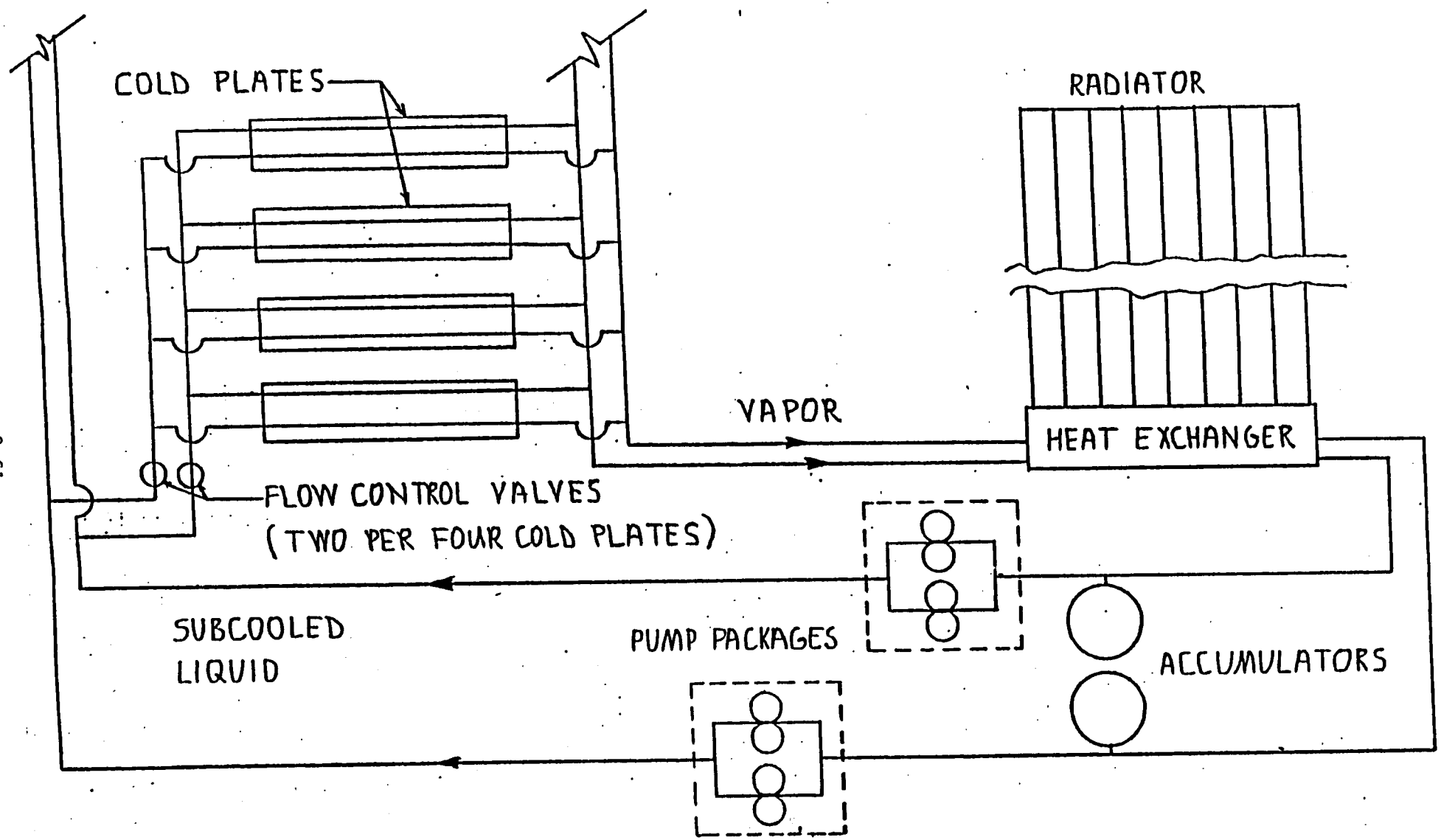

FIGURE 3.2-15

RADIATOR INTERFACE DETAIL

SHEET 2 OF 2

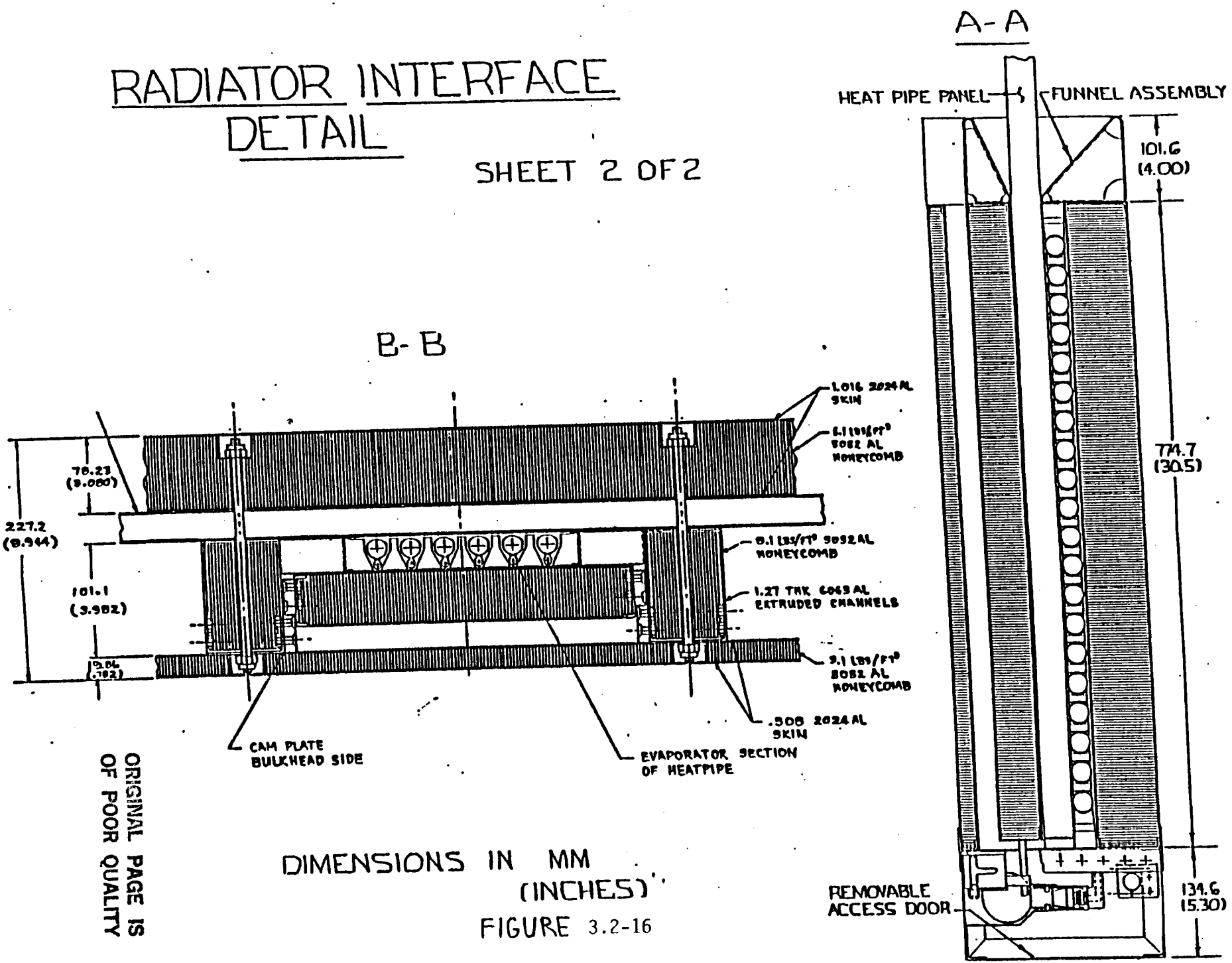

DIMENSIONS IN MM
(INCHES)

FIGURE 3.2-16

are slightly over 1 in. thick with 0.3-mm (0.012-in.) aluminum face sheets bonded on 4.8-mg/cm^3 (3-lbm/ft^3) aluminum honeycomb. Each of the two heat pipe condensers branches into three heat pipe evaporator legs. The condenser and evaporator heat pipe cross sections differ since the heat fluxes transmitted into and out of the pipes differ.

MPTP - The mechanically pumped two phase loop design is based on evaporative cold plate technology developed by Grumman, and the shear flow condenser technology developed by Sundstrand and Boeing. Component details are contained in Section 2.1.1.5 of DR-02. The Grumman cold plate provides heat acquisition from the battery or electronics, and the Sundstrand/Boeing-type shear flow condenser provides heat rejection to the radiator panels. Each cold plate consists of a number of monogroove extrusions welded together in parallel along the flanges. A wick draws liquid to the top of the extrusion where it is evaporated in the circumferential grooves. A sensor detects the presence or absence of liquid in the plate and controls a solenoid valve that resupplies liquid to the plate. The control scheme is designed so that only single phase vapor exits the plate. The batteries and PMAD electronics are packaged into electronics boxes as orbital replacement units (ORU's). The individual battery cells are mounted on a chassis that contains a number of heat pipes. These heat pipes collect the heat dissipated by the cells and transfer it to the edge of the chassis. Section 2.1.1.3 of DR-02 describes the battery physical configuration in more detail. Each ORU chassis is itself an aluminum honeycomb structure, and it contains embedded heat pipes which transfer heat from the components to the chassis edge. The generated heat is then transferred from the heat pipe condensers to the MPTP cold plate across a dry, bolted interface. The MPTP cold plate is part of the system utility plate, which also contains interfaces for the transfer of data and power from the ORU's to other parts of the station. Eight utility plates are mounted in the PV equipment box, which is shown in Figure 3.2-17.

3.2.5.2 ITC Mass Properties

The mass of the integrated thermal control assembly and major components is shown in Table 3.2-15.

PV EQUIPMENT BOX

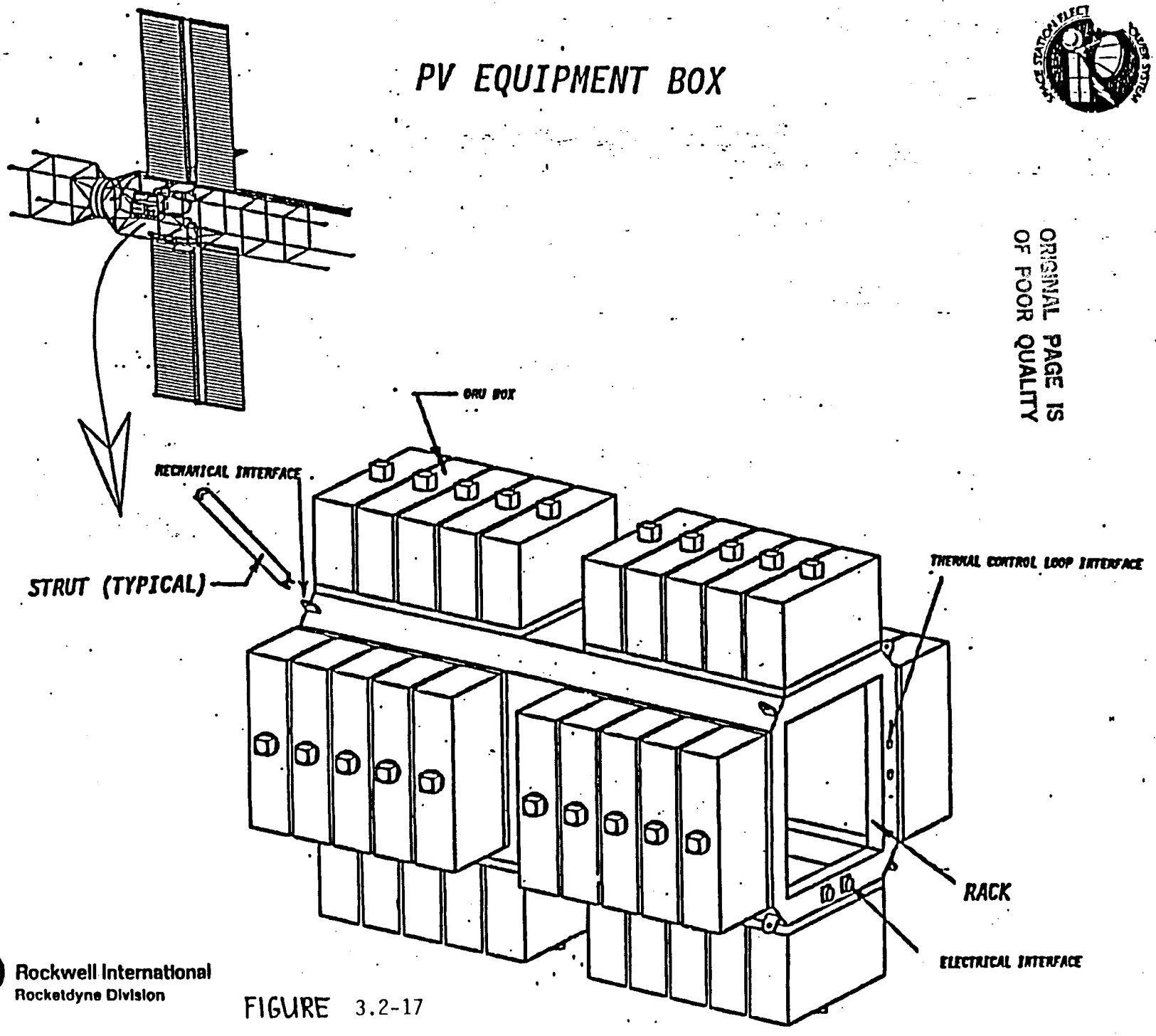

ORIGINAL PAGE IS
OF POOR QUALITY

Rockwell International
Rocketdyne Division

FIGURE 3.2-17

Table 3.2-15

INTEGRATED THERMAL CONTROL

MASS PROPERTIES

COMPONENT	INTEGRATED THERMAL CONTROL ASSEMBLY SINGLE MODULE MASS (KG)	(LBM)	INTEGRATED THERMAL CONTROL ASSEMBLY TOTAL IOC STATION MASS (TWO MODULES) (KG)	(LBM)
RADIATOR PANEL	316	696	633	1392
CONDENSER COMPONENTS				
CONDENSER INTERFACE	15	33	30	66
CONDENSER	14	30	27	60
NCG TRAP	2	4	4	8
PRESSURIZATION UNIT	2	5	5	10
GN_2 CANISTER	2	5	5	10
UTILITY PLATE COMPONENTS				
PLATE	2	5	5	10
RESERVOIR	2	5	5	10
EVAPORATOR	14	30	27	60
FITTINGS	5	10	9	20
FLOW CONTROL VALVES	18	40	36	80
ELECTRICAL CONNECTORS	2	5	5	10
PUMP UNIT COMPONENTS				
ORU HOUSING	4	9	8	18
CIRCULATION PUMP	14	31	28	62
FLUID ACCUMULATOR	11	24	22	48
CONTROLLER	36	80	73	160
PLUMBING AND SENSORS	13	29	26	58
AMMONIA	14	30	27	60
TOTALS	486	1071	975	2142

3.2.5.3 ITC Assembly Performance/Definition

The design heat rejection requirements for the batteries are shown in Table 3.2-16, and for the PMAD electronics in Table 3.2-17. Because there is considerable thermal mass in the batteries, the thermal rejection system has been sized for the peak orbital average heat rejection requirement of the battery. The PMAD heat rejection is based on the maximum heat rejection of each ORU and the maximum number of ORU's that are operational at any one time. For a single module, the resulting heat rejection required is 6.0 kW. The system is designed to reject this amount of heat with the MPTP cold plates at $2^{o}C$. Selection of this cold plate temperature assures that the nominal 5 ± 5 C temperature is maintained at the batteries under all but contingency or failure conditions. Table 3.2-18 summarizes ITC design features and performance.

A mechanically pumped two phase heat transport loop using ammonia as the fluid collects and transports the heat from the PMAD and battery cold plates to the radiator system. The heat load on the cold plate evaporates the ammonia in the grooved vapor channels of the plate. The vapor is then condensed in the radiator heat exchanger. A constant speed mechanical pump provides for the recirculation of fluid back to the cold plates. A sensor in each liquid inlet line, which supplies liquid to a group of four cold plates, causes a flow control valve to be actuated. This control is needed to insure that the cold plates neither dry out nor flood. Screen wicks in the liquid channel of the cold plate supply fluid to the vapor channel grooves. An accumulator in the liquid line contains the extra fluid needed in the system when it is transporting a small amount of heat.

Table 3.2-16

INTEGRATED THERMAL CONTROL

TOTAL EPS BATTERY HEAT REJECTION (2 MODULES)

	NOMINAL (KW)	PEAK (KW)	DURATION (MIN/ORBIT)
BATTERY CHARGE	1.26	----	55
	----	1.38	55
BATTERY DISCHARGE	5.39	----	36
	----	9.03	7.5

ORBITAL AVERAGE HEAT DISSIPATION = 3.27 KW

Table 3.2-17

INTEGRATED THERMAL CONTROL

TOTAL EPS PMAD HEAT REJECTION (2 MODULES)

ORBITAL REPLACEMENT UNIT	MAX NO OF ORU'S ON AT ONE TIME	MAX POWER PER ORU (WATTS)	TOTAL POWER (WATTS)
PHOTOVOLTAIC CONTROL UNIT	2	54	108
BATTERY CHARGE/DISCHARGE UNIT	8	254	2032
DC/AC INVERTER	2	640	1280
PHOTOVOLTAIC CONTROLLER	4	120	480
DC SWITCH UNIT	2	569	1118
AC SWITCH UNIT	2	500	1000
POWER SOURCE CONTROLLER	4	60	240
POWER DISTRIBUTION AND CONTROL UNIT	4	606	2424
		TOTAL	8682

TABLE 3.2-18

INTEGRATED THERMAL CONTROL CHARACTERISTICS

TYPE: Constructable radiators with flat interface - MPTP transport loop

PEAK HEAT REJECTION: 6.0 kW per module

HEAT TRANSPORT LOOP: Mechanically Pumped Ammonia

RADIATOR PANEL SIZE: 46.6 ft x 12 in.

RADIATOR EVAPORATOR LENGTH: 2.54 FT (3 legs each evaporator)

NUMBER OF RADIATOR PANELS: 8 (Includes one extra panel for oversizing)

PANEL DEPLOYED AREA: 373 Ft^2

MAX RADIATOR HEAT PIPE CAPACITY: 350,000 Watt-Inches (includes 30% margin)

TEMPERATURES	^oC	(^oF)
MPTP Condenser	-4.2	(24.5)
Heat Pipe Evaporator	-11.6	(11.2)
Effective Radiator Surface	-21.3	(-6.3)
Sink	-62.0	(-80.0)

FIN EFFECTIVENESS: 62.80%

3.3 SD SUBSYSTEM

Two concepts were studied extensively for the SD subsystem: closed brayton cycle and organic rankine cycle. One concept will be selected as part of the Phase C/D proposal process.

The SD subsystem consists of the assemblies shown in Figure 3.3-1 or 3.3-2. design drawings and descriptions for these assemblies are presented in the Preliminary Analysis and Design Document DR02. The major assemblies are the concentrator, the receiver, the power conversion unit (PCU), the radiator, and the interface assembly.

The concentrator captures and focuses incoming solar flux with a reflective concave surface and sends it through the receiver aperture. It includes pointing equipment to maintain proper solar orientation. The receiver accepts and absorbs the incoming concentrated solar flux in a cavity. Some of the power is transferred to the PCU be heating a working fluid, and the balance is stored as thermal energy in a phase change salt where it can be retrieved later for use during eclipse. The PCU takes energy from the receiver in the form of heated working fluid, converts some of the energy to electrical power in a heat engine, and sends the rest of the energy to the radiator as waste heat. The heat engine works by extracting useful work from the difference in the shaft power supplied by pressurized heated working fluid expanding through a turbine and the shaft power required to drive a pump or compressor operating on the cooled low pressure working fluid with a similar flowrate and pressure ratio. The radiator receives waste heat from the PCU via mass transport and heat exchange. It then dissipates the waste heat to space by thermal radiation. The interface assembly consists of an interface structure and a solar dynamic equipment box. The interface structure provides load carrying capability between the various assemblies and the solar dynamic beta joint which connects the SD subsystem to the balance of the station. The equipment box provides a protected mounting point for the majority of the solar dynamic subsystem electronics and serves as a central point for cabling interconnections.

V2-331/1

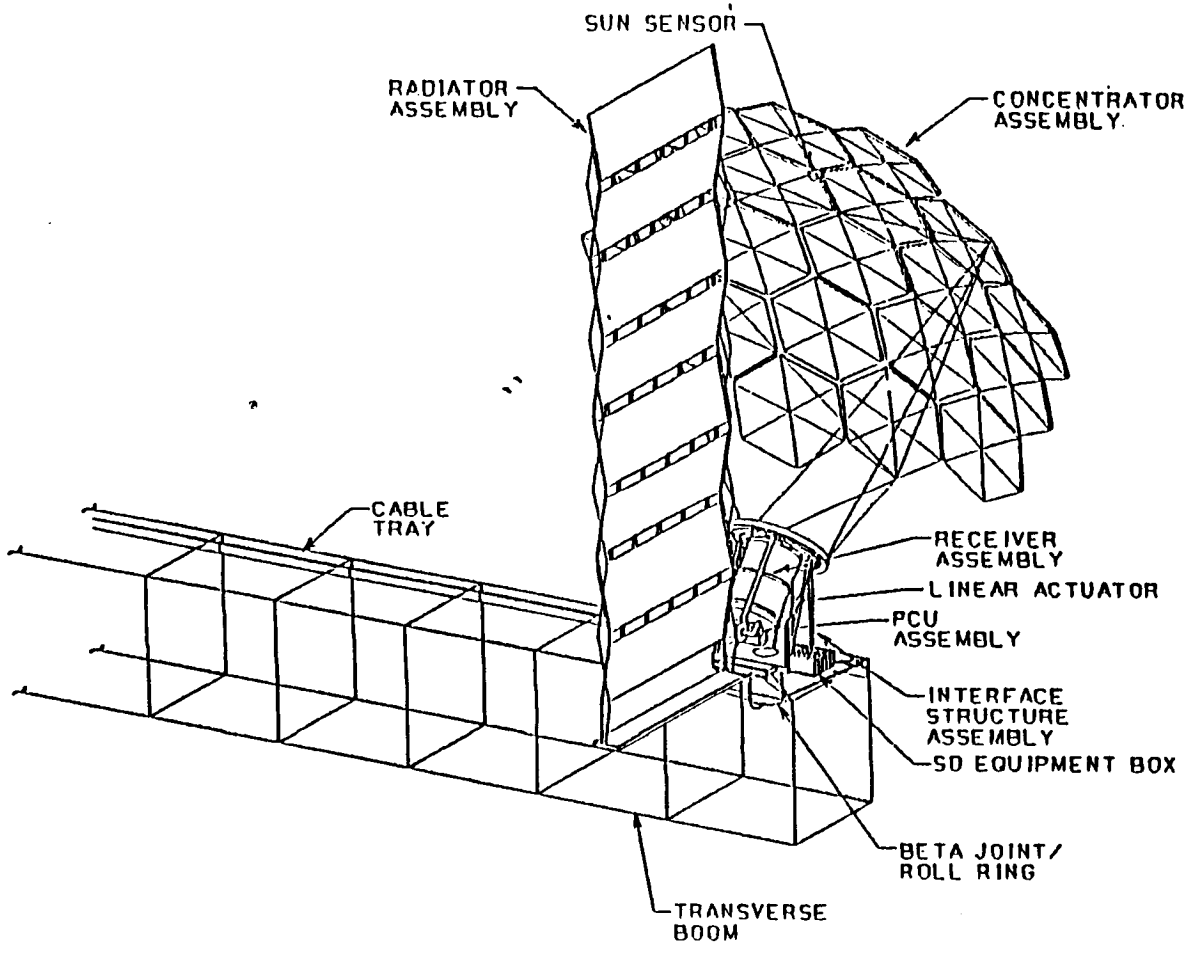

ORIGINAL PAGE IS OF POOR QUALITY

Figure 3.3-1

Rockwell International Corporation Rocketdyne Division	
SPACE STATION EPS SD POWER MODULE (CBC)	
C	02602 7R070063
NONE	

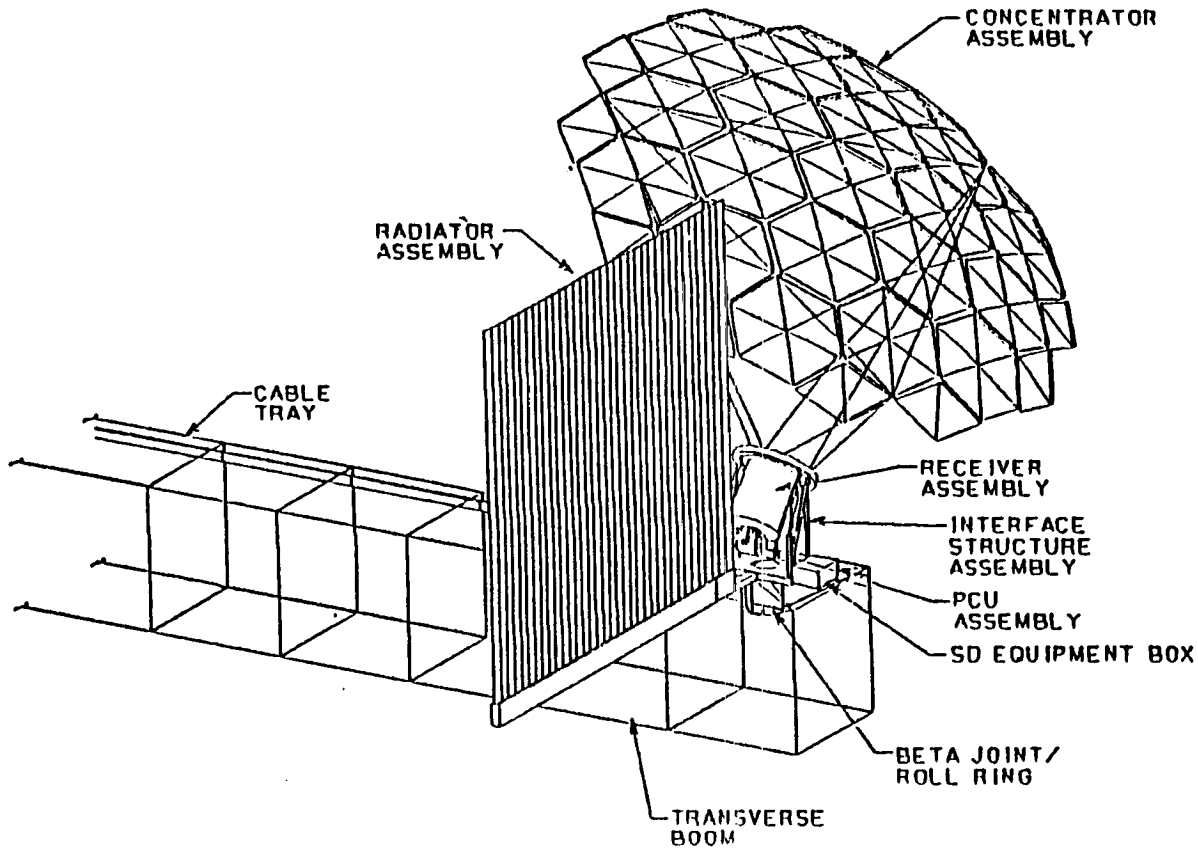

ORIGINAL PAGE IS OF POOR QUALITY

Figure 3.3-2

Rockwell International Corporation Rocketdyne Division	
SPACE STATION EPS	
SD POWER MODULE (ORC)	
C	02602 7R070064
SCALE NONE	SHEET

3.3.1 Concentrator

3.3.1.1 Layouts/Drawings

Layout drawings of the 25 kWe Solar Dynamic (SD) concentrators are shown in Figures 3.3.1-1 and-2 for the ORC and CBC modules, respectively. In each case the concentrator configuration is the offset Newtonian reflector, gimbaled about the receiver aperture center. Fine pointing is provided by two linear actuators located between a two-axis fine pointing mechanism and the interface structure. This configuration is known as The Parabolic Offset Linear Actuated Reflector, or POLAR concept. The concentrator assembly consists of four subassemblies including: reflective surface, structure, mechanisms, and controls and instruments. A detailed description of each of these subassemblies is contained in section 3.3.1.4. The ORC concentrator requires 19 full size hex truss and 12 edge wedge panels to provide the required receiver power to the ORC receiver during all projected operating environments and modes. The CBC concentrator requires 19 full size hex trusses to provide the required receiver power to the CBC receiver during all projected operating environments and modes.

3.3.1.2 Mass Properties

Tables 3.3.1-1 lists the mass breakdowns for the ORC and CBC concentrator assemblies. The mass of the ORC concentrator is 4.4% greater than that of the CBC concentrator due to the difference in performance between the two PCU cycles.

3.3.1.3 Solar Dynamic Concentrator Performance

Table 3.3.1-2 provides performance data for the ORC and CBC concentrators. In general this data includes: efficiencies, power absorbed, power delivered to the receiver, concentrator surface area, performance margins, pointing accuracies, flux distributions and other pertinent data. It can be seen that the ORC receiver requires greater input power than the CBC due to lower cycle efficiency.

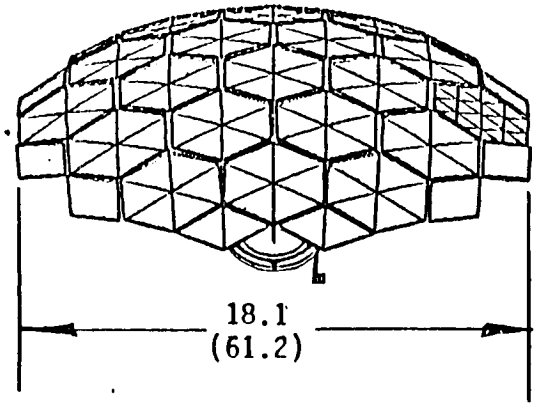

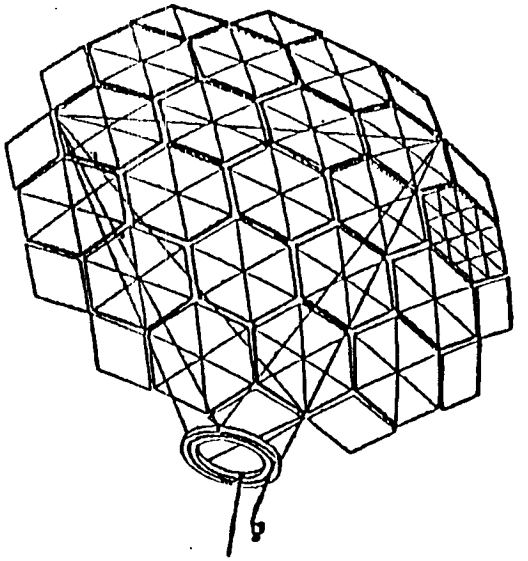

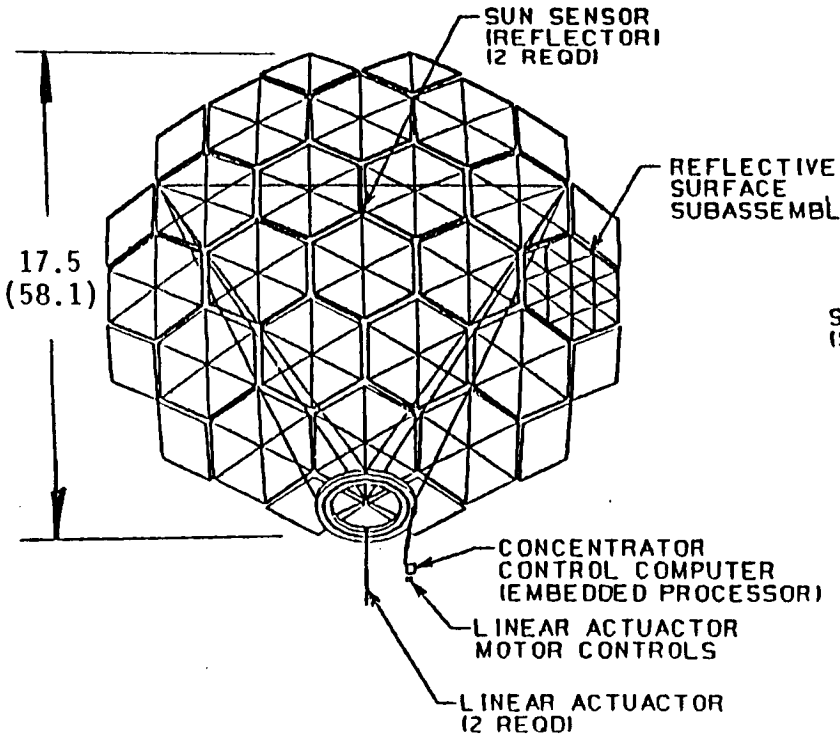

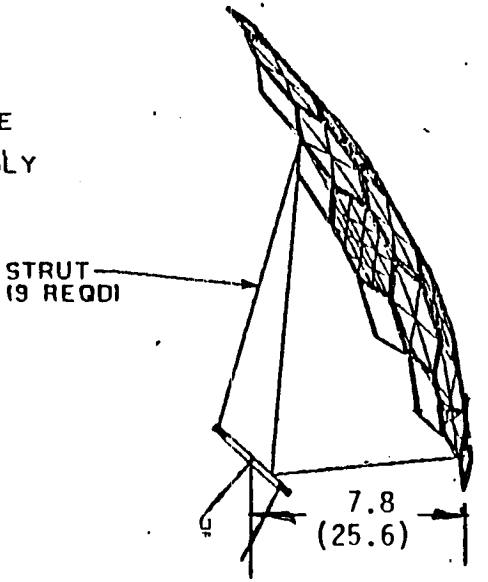

NOTE: INTERFACE STRUCTURE AND WIRING HARNESS NOT SHOWN

ORIGINAL PAGE IS
OF POOR QUALITY

Figure 3.3.1-1

	Rockwell International Corporation Rocketdyne Division
	ORC CONCENTRATOR ASSEMBLY PRELIM LAYOUT
	SIZE C | 02602 | 7R070016
	SCALE NONE | DO NOT SCALE PRINT | SHEET

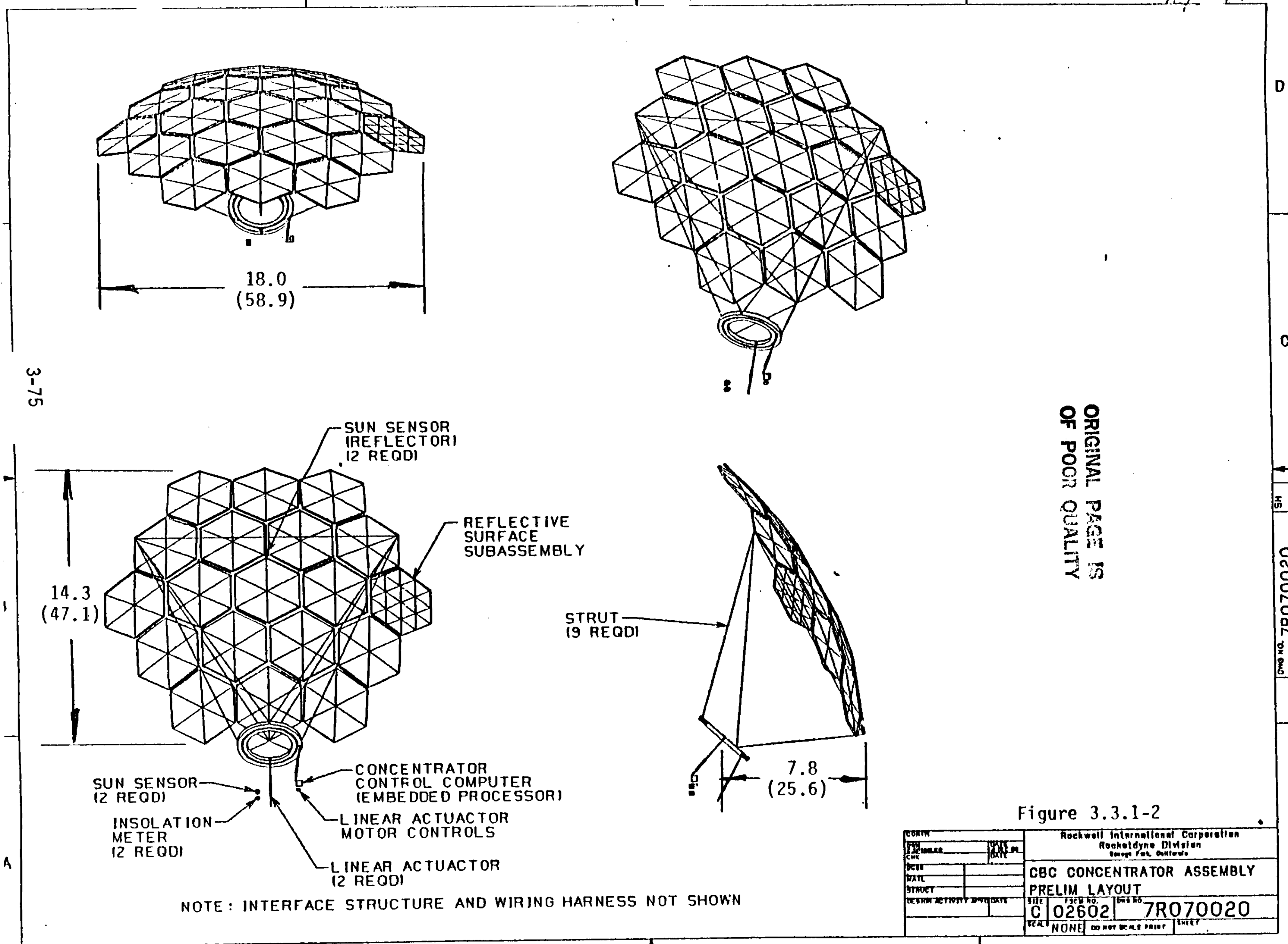

Figure 3.3.1-2

Table 3.3.1-1

POLAR SOLAR DYNAMIC CONCENTRATOR MASS/MODULE BREAKDOWN [kg (lbm)]

ITEM	kg	(lbm)	kg	(lbm)
	ORC		CBC	
Reflective Surface Subassembly				
Reflective Surface (Facets)	361	(794)	298	(657)
Hex Truss Panels	302	(665)	302	(665)
Edge Wedge Panels	79	(175)	0	(0)
Dep./Retract. Mech.	72	(158)	56	(123)
Attachment/Alignment	18	(40)	10	(23)
Insulation& Misc. Ref. Surf.	50	(110)	50	(110)
Subtotal	882	(1,943)	716	(1,575)
2 Axis Fine Pointing				
Linear Actuators (2 ea)	20	(44)	20	(44)
Motors	inc.	inc.	inc.	inc.
Position Sensors	inc.	inc.	inc.	inc.
Actuators	inc.	inc.	inc.	inc.
Limit Switches	inc.	inc.	inc.	inc.
Two-Axis Pointing Mech.	407	(897)	512	(1,127)
Subtotal	427	(941)	532	(1,171)
Structure				
Struts				
Type A	10	(21)	10	(21)
Type B	6	(12)	6	(12)
Type C	6	(12)	6	(12)
Type D	3	(7)	3	(7)
Strut I/F Fitting	31	(69)	31	(69)
Strut End Fitting	6	(12)	6	(12)
Subtotal	62	(133)	62	(133)
Controls				
Conc. Control Comp.	23	(51)	23	(51)
Sun Sensors (2 ea)	3	(6)	3	(6)
Motor Controllers	9	(20)	9	(20)
Wiring Harness	5	(11)	5	(11)
Subtotal	40	(88)	40	(88)
Misc. Hdwre. & Equip.	38	(84)		
TOTAL MASS	1,449	(3,189)	1,388	(3,051)

V2-331/2

Table 3.3.1-2
POLAR SOLAR DYNAMIC CONCENTRATOR PERFORMANCE PARAMETERS

PARAMETER	VALUE ORC		CBC	
User Power kWe	25		25	
Receiver Aperture to User Conversion Efficiency %	18.49		21.50	
Cavity Temperature K (F)	744	(880)	1050	(1,430)
Effective Sink Temp. K (F)	255	(0)	255	(0)
Receiver Aperture Dia. m (ft)	0.71	(2.3)	0.43	(1.42)
Intercept Factor %	95.7		97	
Concentrator Design Reflectivity*, %	92		92	
Solar Constant W/sq M (Btu/h-sq ft)	1323	(419.5)	1323	(419.5)
Solar Multiple	1.617		1.617	
Required Receiver Thermal Input kWt (BTU/h)	218.6	(746,067)	188	(641,644)
Required Concentrator Aperture Area sq m (sq ft)	187.7	(2,020)	159.2	(1,713)
Number of Equivalent Hexes	23		19	
Number of Full Hex Panels	19		19	
Number of Edge Wedges	12		0	
Number of Facets	552		456	
Hex Flat-Flat m (ft)	3.63	(11.90)	3.63	(11.90)
Hex Point-Point m (ft)	4.19	(13.75)	4.19	(13.75)
Facet Side Length m (ft)	1.02	(3.33)	1.02	(3.33)
Estimated Cosine Loss %	13.4		10.12	
Maximum Effective Area sq m (sq ft)	213.1	(2,290)	182.8	(1,967)
Block/Shadow Area sq m (sq ft)	21.3	(229)	20	(215)
Effective Aperture sq m (sq ft)	191.8	(2,064)	162.8	(1,751)
BOL + 3 Years Margin %	2.2		2.01	
Equivalent Dia. of Effective Area, m (ft)	15.6	(51.2)	14.4	(47.2)
Focal Length m (ft)	7.8	(25.6)	7.8	(25.6)
Estimated Global Beam Deflection+, cm (in)	0.13	(0.05)	0.13	(0.05)
Estimated Pointing Error+, degrees	0.009		0.009	
Circumferential Flux Deviation, %	<10		<7	
First Reflector Deployed Mode, Hz	2.03		2.03	
First Concentrator Deployed Mode, Hz	0.97		0.97	

* Beginning of Life + 3 Years
\+ Proportional Only, Ideal Controller

The ORC Concentrator parameters are based on the receiver configuration described in Section 3.3.2.2. This receiver and its operating temperature impose modest requirements on the ORC concentrator. Specifically, the 99% confidence level tracking requirement is 3 times less stringent than the requirement imposed on the CBC concentrator. Also, the slope error required to achieve the target interception of the ORC receiver is relaxed for ORC when compared to that for CBC.

A detailed optical performance analysis of the ORC reflector, on-target, concentrated incident flux pattern inside the receiver was completed. The results indicate that by re-aiming each of the hexes and edge wedges slightly as units, the flux inside the receiver can be tailored such that the heat-pipe to heat-pipe total incident power does not vary from the mean heat-pipe power by more than 10%.

The CBC Concentrator parameters are based on the receiver configuration described in Section 3.3.2.1. This receiver and its operating temperature impose tight requirements on the CBC concentrator. Specifically, the 99% confidence level tracking requirement is 3 times as stringent as the requirement imposed on the ORC concentrator. The slope error required to achieve the target interception of the CBC receiver is tighter for CBC than for ORC.

A detailed optical performance analysis of the CBC reflector, on-target, concentrated incident flux pattern inside the receiver was completed. The results indicate that by re-aiming selected facets, the flux inside the receiver can be tailored such that the tube to tube total incident power does not vary by more than 7% from the mean tube power.

3.3.1.4 Assembly Definition

The ORC and CBC concentrator assemblies have many common elements. The structure, mechanisms, and controls and instrument subassembly concepts for each are nearly identical. The reflective surfaces differ only in the required surface area and the slope errors of the facets.

The reference SD concentrator configuration features the parabolic offset linear actuated reflector (POLAR) concept. The reflector concept is shown in Figure 3.3.1-3, for the ORC concept, and Figure 3.3.1-4 for the CBC concept. The ORU's for these concepts are listed in Table 3.3.1-3. The function of the concentrator is to deliver concentrated solar insolation to the receiver cavity walls within prescribed flux distribution limits in a cost effective manner. As described in DR-19, DP 4.3, the concentrator is driven by the temperature of the receiver cavity, the PCU and PMAD efficiencies, the minimum solar insolation, the duration of the orbital eclipse period, STS compatibility, PGS structural requirements, Space Station GN&C stability, and the LEO environment.

The POLAR configuration was selected on the basis of minimum total cost as well as reasonable risk and low moment of inertia, a major GN&C stability driver. The trade study that selected the POLAR concept is documented in DR-19, DP 4.4, Section 7.1.6. In the POLAR concept, the reflector is a segment of a large parent paraboloid and is offset from the transverse boom. The focal point of the resulting optical system is the same as that of the parent paraboloid and is located close to the transverse boom. This allows a compact SD module configuration with minimum optical blockage and a low moment of inertia. The compact POLAR configuration enhances concentrator structural stiffness and has very low mass and launch volume. The POLAR concept also incorporates an innovative linear-actuated reflector that is gimbaled independently of the PCU, resulting in a low gimbaled mass and modest coarse and fine pointing parasitic power requirements. The two-axis fine pointing mechanism kinematically constrains the reflector focal point and effectively eliminates translation of the focal point with respect to the receiver aperture, resulting in a simplified optical system.

A detailed description of the ORC and CBC concentrator ORU's, on-orbit assembly, master equipment list, spares, refurbishment activities, risk assessment, alignment and contamination is located in section 2.2.3 of the December 1986 issue of DR02.

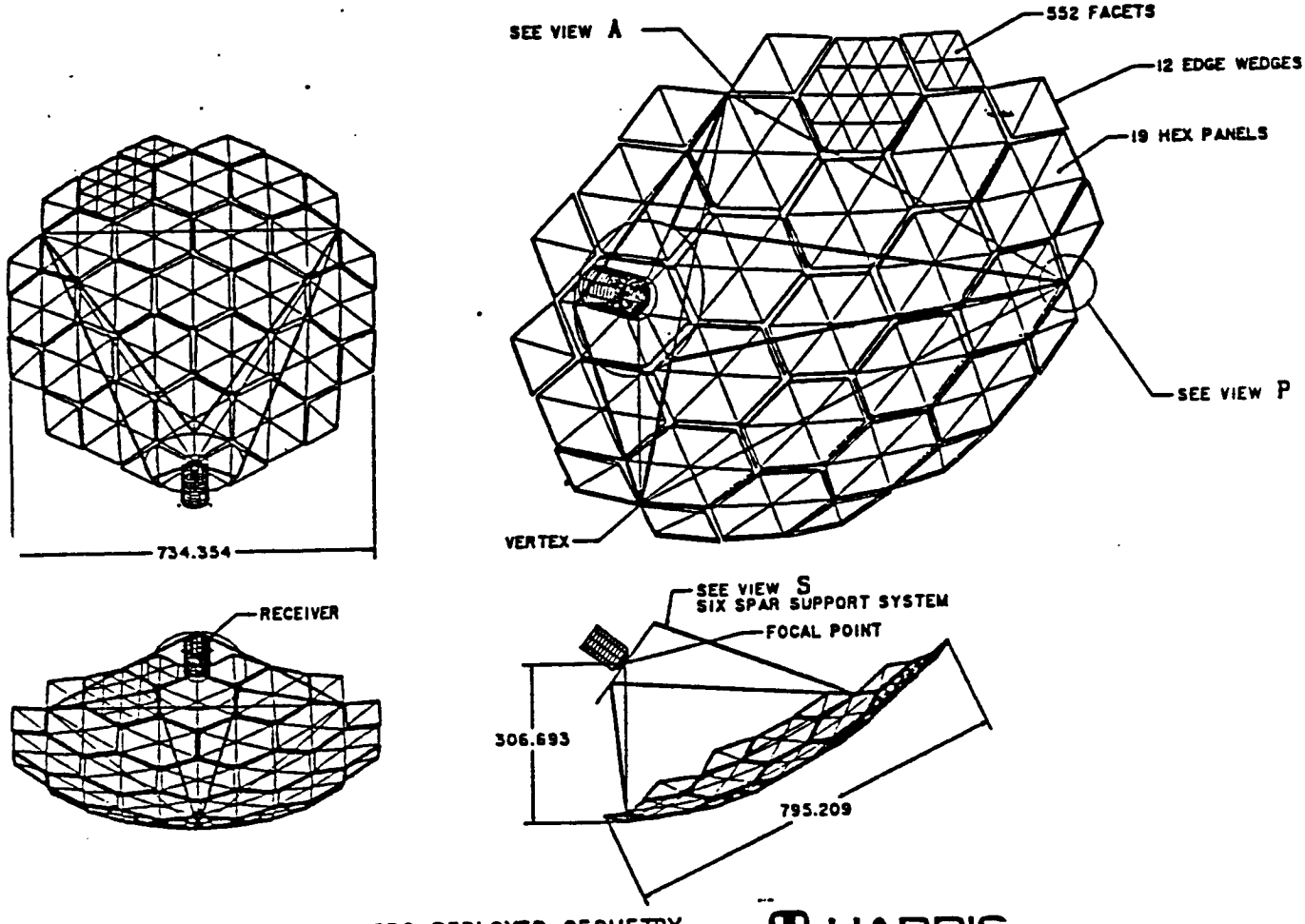

Figure 3.3.1-3 ORC Reflector Plus Structure Subassemblies

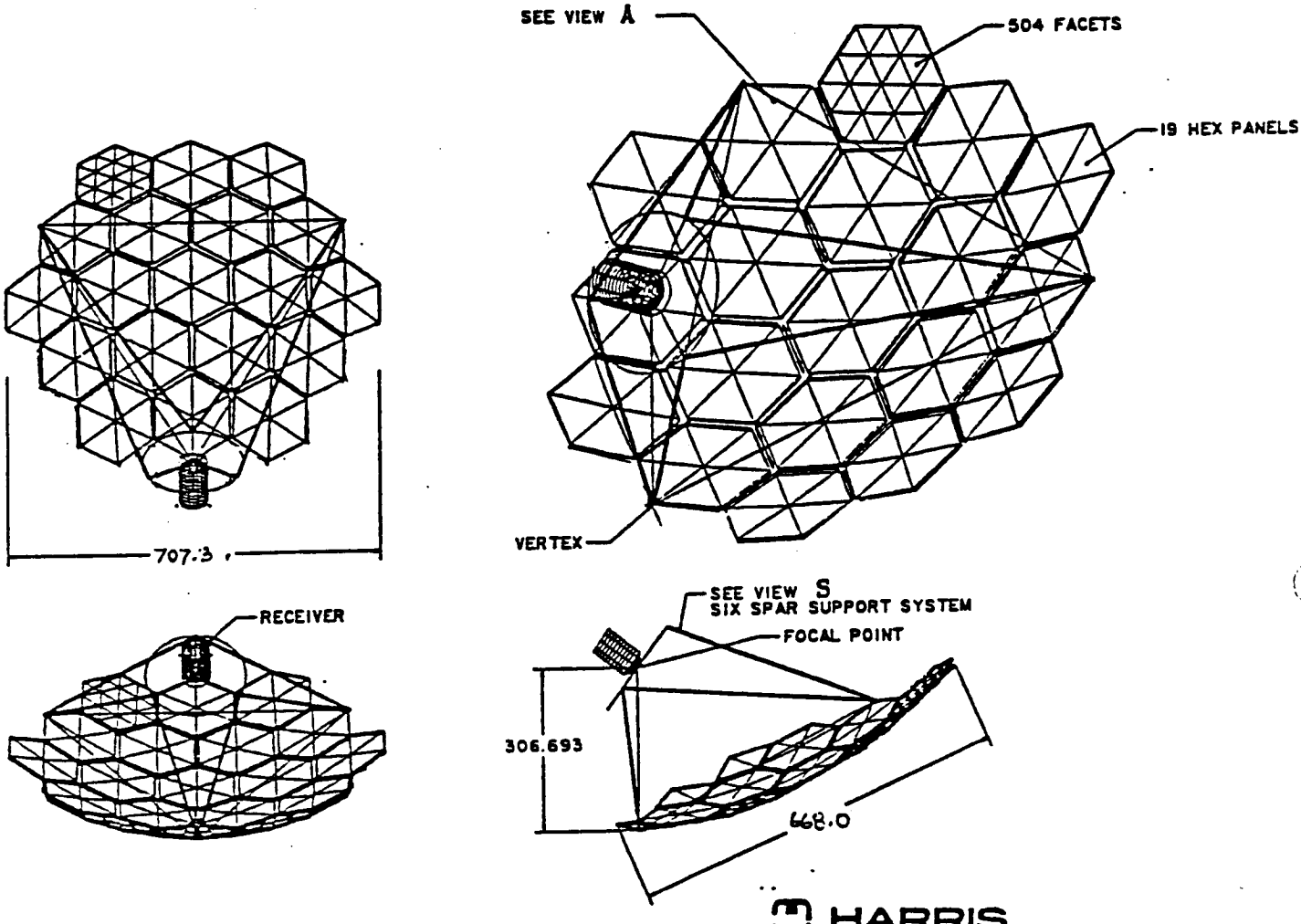

Figure 3.3.1-4 CBC Reflector Plus Structure Subassemblies

Table 3.3.1-3
CONCENTRATOR ORUs/MASTER EQUIPMENT/INITIAL SPARES

Item	Number Per Module	Approximate Dimensions+ (L x W x D) (m)	Estimated Mass+ [kg (lbm)]
*Linear actuator	2	3 x 0.15 OD	9.1 (20.1)
*Concentrator control computer (embedded processor)	2	0.5 x 0.25 x 0.25	11.4 (25.1)
*Sun sensor	2	0.5 x 0.1 OD	1 (2.2)
*Motor controller	4	0.3 x 0.1 x 0.1	2.3 (5.1)
Two-Axis Fine Pointing Mech.	1	a) 0.23W x 2.9 OD b) 0.23W x 3.6 OD	407 (897) 512 (1127)
Reflective Surface Subassy.	1	a) 2.63 x 4.58 OD b) 2.40 x 4.58 OD	882 (1943) 716 (1575)
Structure (Strut Set)	1	5.0 x .46 x .36	62 (133)

[a] ORC Dimensions and Masses
[b] CBC Dimensions and Masses
* Initial spares.
+ Excludes Launch Cradles

V2-331/8

3.3.2 Receiver/Power Conversion Unit (PCU)

3.3.2.1 CBC Receiver/Power Conversion Unit (PCU)

The CBC receiver/PCU assembly (see Figure 2.1.3.2.1-1) consists of three major elements. These are the receiver, the power conversion equipment, and the engine electric control loop equipment. Table 3.3.2.1-1 shows the operational requirements. Table 3.3.2.1-2 summarizes the CBC option. A mass and drag summary of this equipment in Tables 3.3.2.1-3a through 3.3.2.1-3c is followed by descriptions of each major element.

3.3.2.1.1 CBC Receiver

The CBC receiver incorporates three major functional elements. These are the heat absorbing surface, the CBC heat source heat exchanger (HSHX), and the thermal energy storage (TES).

The design (Figure 3.3.2.1-1) comprises a cylindrical receiver cavity lined with a series of tubes running the length of the cavity. The CBC working fluid from the recuperator flows through an external duct to a toroidal manifold at the aperture end of the receiver. The manifold distributes the fluid to the individual tubes. The flow is collected in the outlet manifold and is sent to the turbine. Thermal storage place change material (PCM) is contained in a series of metal canisters. The individual containment canisters are filled with the PCM and hermetically sealed by welding under vacuum.

The containment canisters are stacked and bonded to the working fluid tube, as shown in the figure. The canisters are not bonded to each other, but are separated by ceramic fiber spacers. The use of individual containment canisters for the PCM is a key characteristic of the receiver design. This configuration affords a readily fabricable and highly reliable design. A failure of a canister would only affect the one failed canister and have minimal impact on receiver operation. Compartmentalization of the salt also reduces the chance of stress failure by localizing the formation of freezing voids.

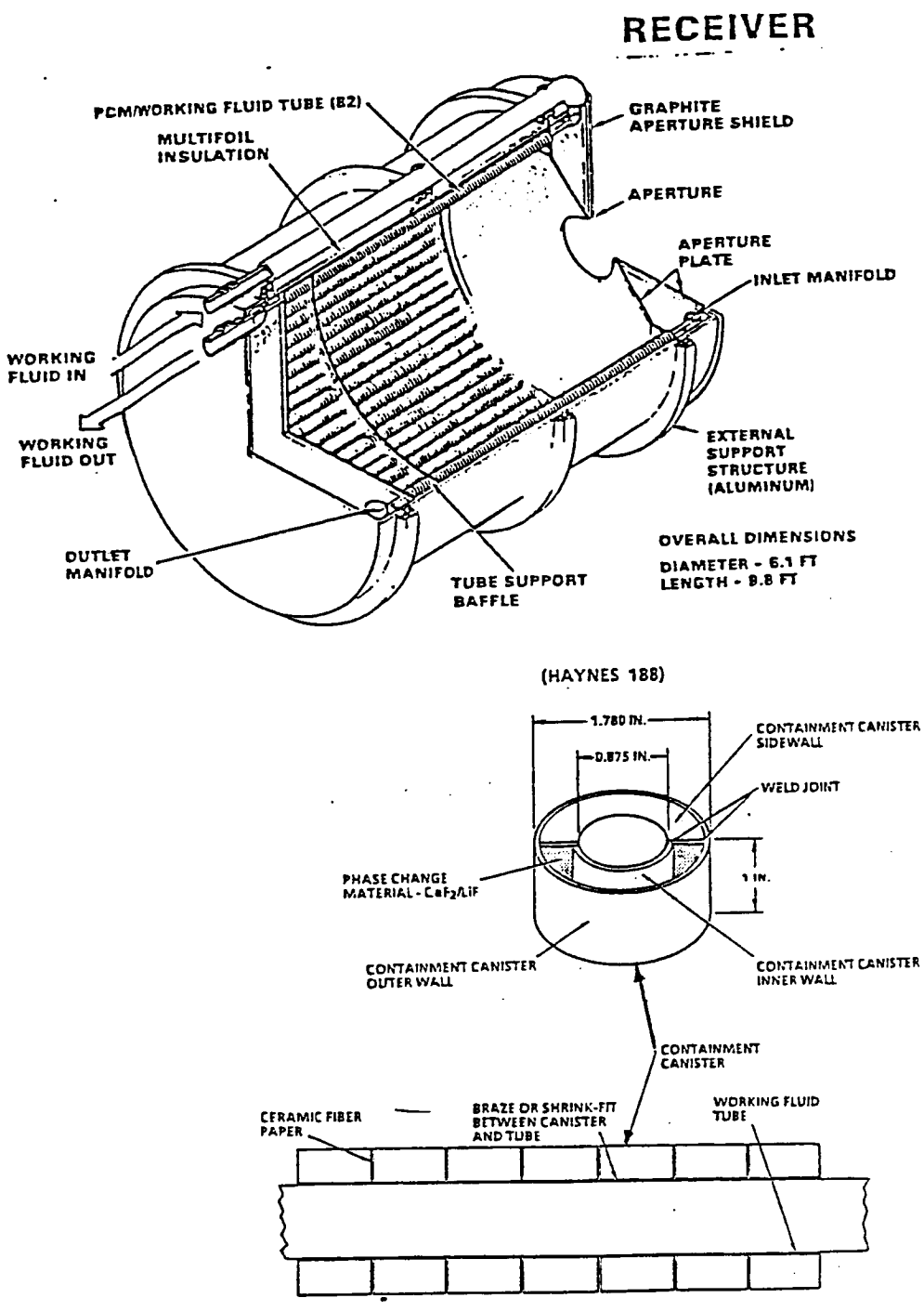

Figure 3.3.2.1-1. Receiver

TABLE 3.3.2.1-1
SOLAR DYNAMIC POWER GENERATION
SUBSYSTEM OPERATIONAL REQUIREMENTS

POWER GENERATION REQUIREMENTS

REQUIREMENT	IOC NET POWER KwE	GROWTH NET POWER KwE
o NOMINAL REQUIREMENTS		
IOC STATION POWER REQUIREMENT	75.0	300.0
NOMINAL PV POWER CAPABILITY	-23.50	-23.5
SOLAR DYNAMIC POWER REQUIREMENT	51.50	276.5
o SD PEAKING REQUIREMENT		
115% OF NOMINAL POWER	59.23	318.0

OTHER REQUIREMENTS

o ALTITUDE	
MAXIMUM	250 NM
MINIMUM	180 NM
NOMINAL	250 NM
o INSOLATION	
MAXIMUM	1.419 KW/M^2
MINIMUM	1.323 KW/M^2
o PMAD EFFICIENCY	88.82%
o PMAD PARASITIC	2.0 KW
o PEAK POWER DURATION/ORBIT	
ECLIPSE	7.5 MINUTES
SUN	7.5 MINUTES

V2-3321/3

TABLE 3.3.2.1-2
SUMMARY OF SOLAR DYNAMIC
CLOSED BRAYTON CYCLE OPTION

Key Characteristics	
Working Fluid	Helium/Xenon mixture @ MW = 40
Maximum Fluid Temperature	1034 K (1402 F)
Heat Rejection Temperature Range	447 K (346 F) to 265 K (18 F)
Primary Thermal Storage Medium	Lithium fluoride/calcium difluoride
Receiver Cavity Temperature Range	967 K (1280 F) to 1083 K (1490 F)
Receiver Heat Transport	Cavity Reradiation & conduction
Radiator Heat Transport	Coolant transport, space radiation
Radiator Surface	Z93 White Paint
Reflective Surface	Magnesium Fluoride/Alumina/Silver

System Design Performance		Efficiency (%)
PMAD (effective) (0.882 eff & 1 kWe)		85.0
SD Controls & Parasitic		96.2
Alternator	93.4	
Thermal Cycle	36.4	
Power conversion unit (Subtotal)		34.0
Cavity (optical & thermal)	92.0	
Receiver surface loss effects	92.8	
Receiver (Subtotal)		85.4
Interception	97.0	
Reflectivity	90.0	
Concentrator (Subtotal)		87.3
Sun-to-Bus (Minimum Insolation Orbit) (@ PLR load = 0)		20.8

Around the entire min insolation orbit

*Expected value at BOL + 3 years without replacing failed radiator panels.

V2-3321/4

Table 3.3.2.1-3a

CDC SUBSYSTEM MASS AND DRAG AREA SUMMARY

ASSEMBLY	MASS (KG)	MASS (LBM)	EQUIV. NORMAL DRAG AREA (M2)	EQUIV. NORMAL DRAG AREA (FT2)	DRAG FACTOR APPLIED
CONCENTRATOR	1352	(2980)	129	(1384)	Composite
RECEIVER	1752	(3862)	5.6	(60)	1.0
PCU &CONTROLS	790	(1742)	3.6	(39)	Composite
RADIATOR	1145	(2524)	40	(430)	Composite
INTERFACE EQUIPMENT	583	(1285)	4.6	(50)	1.0
BETA JOINT	275	(607)	NA	NA	NA
TOTAL	5897	(13000)*	182	(1963)	

*NOTE that 237 kg (522 (lbm) of SD electrical equipment is accounted in PMAD.

Table 3.3.2.1- 3b

CBC RECEIVER MASS PROPERTIES

ITEM	MASS (KG)	MASS (LBM)	MASS (KG)	MASS (LBM)
HEAT SOURCE HEAT EXCHANGER (SUBTOTAL)			162	(357)
HEAT EXCHANGER TUBES	109	(240)		
INLET MANIFOLD	15	(33)		
OUTLET MANIFOLD	20	(44)		
DUCTS	18	(40)		
THERMAL ENERGY STORAGE CANISTERS			698	(1538)
INSULATION MATERIALS (SUBTOTAL)			199	(438)
FORMED INSULATION MANDREL	81	(179)		
MULTIFOIL INSULATION (N1 & A1)	117	(259)		
STRUCTURAL ELEMENTS (SUBTOTAL)			315	(694)
BACKWALL SUPPORT PLATE	41	(91)		
ALUMINUM OUTER SHELL	147	(325)		
BAFFLES & SUPPORTS	45	(100)		
APERTURE PLATE	81	(178)		
APERTURE SHIELD			39	(85)
TOTAL MASS (DRY)			1412	(3112)
LITHIUM FLUORIDE-CALCIUM DIFLUORIDE EUTECTIC SALT			340	(750)
TOTAL MASS			1752	(3862)

Table 3.3.2.1-3c

CBC POWER CONVERSION UNIT & ENGINE CONROL MASS PROPERTIES

ITEM	MASS (KG)	MASS (LBM)	MASS (KG)	MASS (LBM)
TURBOALTERNATOR (SUBTOTAL)		104	(229)	
ROTOR	23.1	(22.6)		
FOIL BEARING ASSEMBLIES	4.1	(9)		
STATOR ASSEMBLY				
STATOR BACK IRON	6	(13)		
TEETH	1	(3)		
WINDINGS	2	(5)		
FIELD COILS	9	(20)		
END BELLS AND FRAME	14	(30)		
CORE SPACER	1	(3)		
COMPRESSOR AND TURBINE WHEELS	13	(28)		
SCROLLS	28.6	(63)		
BALANCE OF UNIT	14.5	(32)		
RECUPERATOR			162	(357)
GAS COOLER (DRY SUBTOTAL)			85	(188)
BLEED COOLER (DRY SUBTOTAL)			2	(4)
GAS LOOP CONTROLS (DRY SUBTOTAL)			115	(254)
DUCTS (INCLUDING INSULATION)	100	(220)		
GAS ACCUMULATOR	11	(25)		
ACCUMULATOR VALVE	4.2	(9.3)		
ELECTRIC LOOP CONTROLS (SUBTOTAL)			151	(334)
ELECTRONIC CONTROL UNIT (SUBTOTAL)				
PRIMARY (ORU)	23	(50)		
SECONDARY (ORU)	23	(50)		
JUNCTION BOX	22	(48)		
WIRING HARNESS	19	(42)		
COLD PLATE	5	(12)		
PARASITIC LOAD RADIATOR (ORU)	60	(132)		
PCU MOUNTING STRUCTURE			120	(265)
TOTAL (DRY MASS)			740	(1631)
COOLANT INVENTORY (FC75) INVENTORY			49	(107)
HELIUM-XENON INVENTORY			2	(4)
TOTAL (WET MASS)			790	(1742)

The cavity wall consists of a thin layer of high-temperature formed insulation. The wall acts to reradiate the incoming flux that passes between the tubes to the back side of the tubes providing a relatively uniform flux circumferentially around the tubes. The cavity walls also act as a mandrel to wrap sheets of very low conductivity multifoil insulation.

During sunlight periods, heat is transferred through the PCM to the CBC working fluid. The PCM is also heated and melted by the solar flux. During eclipse periods. the PCM gives up its heat to the CBC working fluid and is cooled and frozen.

The insulated cavity is enclosed in an aluminum support structure. The tubes are supported by baffles, which are, in turn, connected to reinforced regions of the support structure. The tubes fit loosely in the baffle holes and are free to expand. The back wall of the cavity moves as the tubes expand. Tube expansion is accommodated by two external bellows.

3.3.2.1.2 Power-Conversion Unit (PCU)

The PCU (Figure 3.3.2.1-2) consists of turboalternator, recuperator/ gas cooler, bleed cooler, ducts, and accumulator. These components are discussed in the following paragraphs.

Turboalternator: The turboalternator consists of a single-stage, radial-flow compressor; a single-stage, radial inflow turbine; and a straddle-mounted, Rice alternator. The rotating speed is 32,000 rpm. The design features radial aerodynamic components integrated with a high-speed, solid-rotor Rice alternator supported by foil gas bearings. This concept results in a very rugged, combined rotating unit (CRU) which is the only continuously moving part in the CBC receiver/PCU.

Recuperator: The recuperator is a pure counterflow plate-fin unit, with cross-flow triangular end sections providing fluid access to the core. It is designed for 94% thermal effectiveness. The counterflow section uses 0.153-inch high offset fins on the low-pressure side and 0.125-inch offset fins

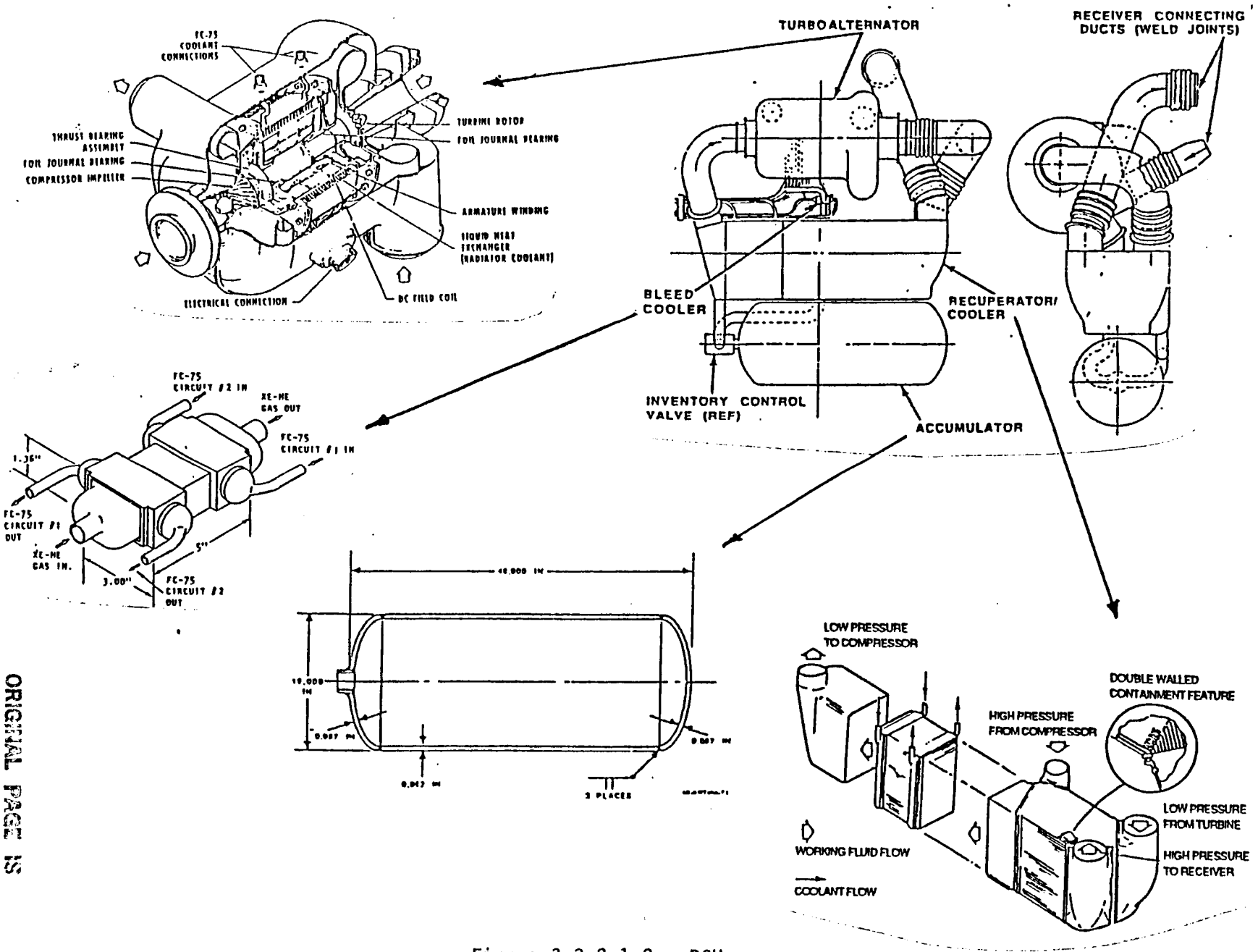

Figure 3.3.2.1-2. PCU

on the high-pressure side. The offset fin is used to promote turbulence, which in turn enhances heat transfer.

Gas Cooler: The gas cooler is an eight-pass, cross-counterflow, plate-fin heat exchanger. The fin sandwiches are rectangular offset, 0.089-inch high on the gas side and 0.075-inch high on the liquid side in a single sandwich arrangement on both sides. The gas cooler has a redundant alternating sandwich design that connects to independent fluid loops and results in double sandwich gas side passages.

Bleed Cooler: The bleed cooler is a small, counterflow, plate-fin heat exchanger similar to the gas cooler. The fin sandwiches are rectangular offset, 0.77-inch high on the gas side and 0.100-inch high on the liquid side in a single sandwich arrangement on both sides. The bleed cooler contains redundant liquid sandwiches. In this case, only 3 of the 6 liquid sandwiches are active at any given time.

Accumulator: The amount of xenon-helium inventory in the Brayton cycle control loop is varied to limit receiver temperature and provide for peaking power requirements. This is accomplished by storing or extracting working fluid from an accumulator. The accumulator is constructed of formed and welded aluminum alloy. The accumulator volume is 13.452 in^3.

3.3.2.1.3 Closed Brayton Cycle Controller (CBCC)

The Closed Brayton Cycle controllers in conjunction with the parasitic load radiator, the inventory control valve actuator, and cabling for the CBC engine control equipment form the CBC engine control loop equipment.

The CBCC consists of two redundant controller channels. Each channel is an ORU and contains a microprocessor-based electronic control unit (ECU) and a power electronic unit (PEU). The ECU communicates with the solar dynamic control microprocessor in managing the solar energy input at the receiver. The general control objective during operations is to maintain constant alternator speed (frequency), to maintain alternator output line voltage at 208 volts RMS,

and to manage receiver thermal conditions in the face of variations in user load including peaking demands and varying receiver heat input rates.

This function is performed by the CBC controller hardware which is depicted in Figure 3.3.2.1-3. Two CBC control channels share the controller load. If one channel fails, the other channel automatically assumes the full controller load. A schematic of the power electronics appears in Figure 3.3.2.1-4.

Thermal Design: The ECU contains both low-power logic and high-power control-type electronics. The ECU dissipates up to 1800W to a liquid-cooled cold plate. The cold plate has a fluid supply of FC-75.

Parasitic Load Radiator: The parasitic load radiator (PLR) assembly is designed to absorb and dissipate a part or all of the 42-kilowatt peak electrical power generated by the alternator to keep the operating speed of the CRU constant. With the selected PLR concept, the generated AC electrical power is rectified before being fed into the PLR.

The PLR assembly consists of an array of multiple ceramic supports and insulators for helical resistance wire spirals (see Figure 3.3.2.1-5). Each ceramic cylinder supports a single resistor element; all elements are parallel connected between the DC bus.

Inventory Control Valve: The dual solenoid diverter valve, shown in cross section in Figure 3.3.2.1-5, consists of two two-way solenoid valves which are spring loaded closed. The solenoids are installed in a line-mounted housing which is ported such that the combination provides a closed center, three-way diverter valve design. When solenoid 1 is de-energized, it shuts off the flow of xenon-helium gas from the compressor discharge into the accumulator. When solenoid 2 is de-energized, it shuts off the flow of xenon-helium gas from the accumulator to the compressor inlet. When both solenoids are de-energized, the accumulator is isolated from the compressor, allow pressure to be stored until needed for peak power operation.

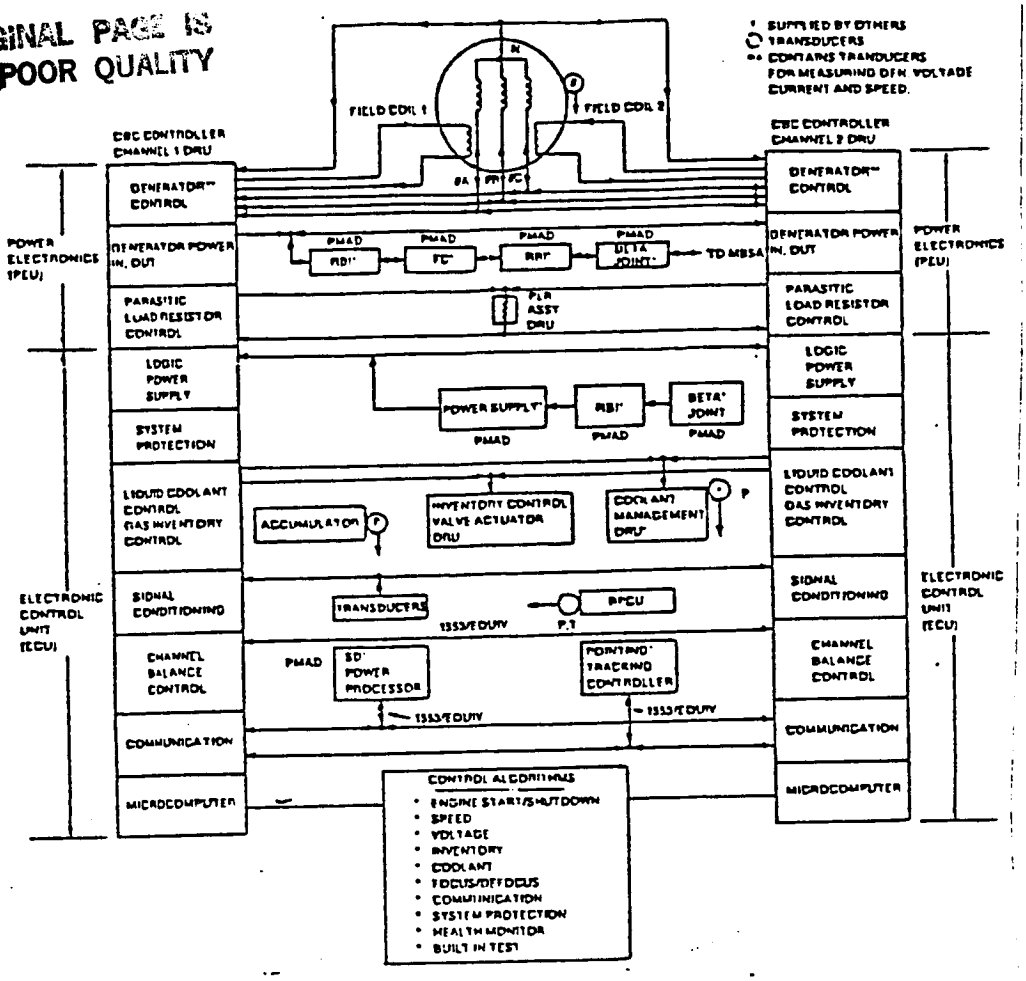

Figure 3.3.2.1-3. DUAL CHANNEL CBC ENGINE CONTROLLER INTERFACES (BY MODULE)

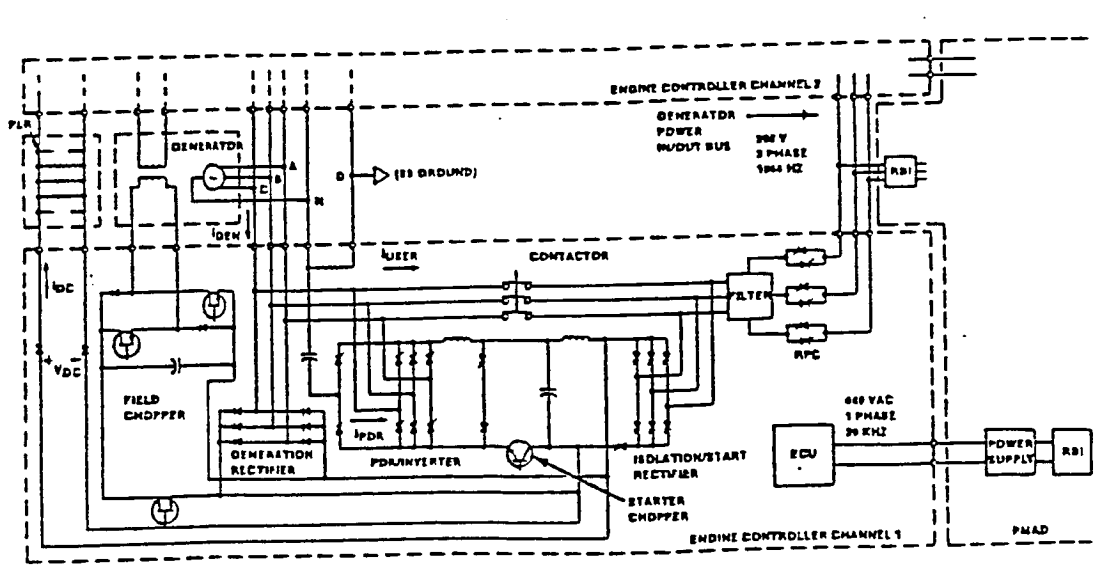

Figure 3.3.2.1-4. CBC POWER ELECTRONICS UNIT (PEU) SCHEMATIC

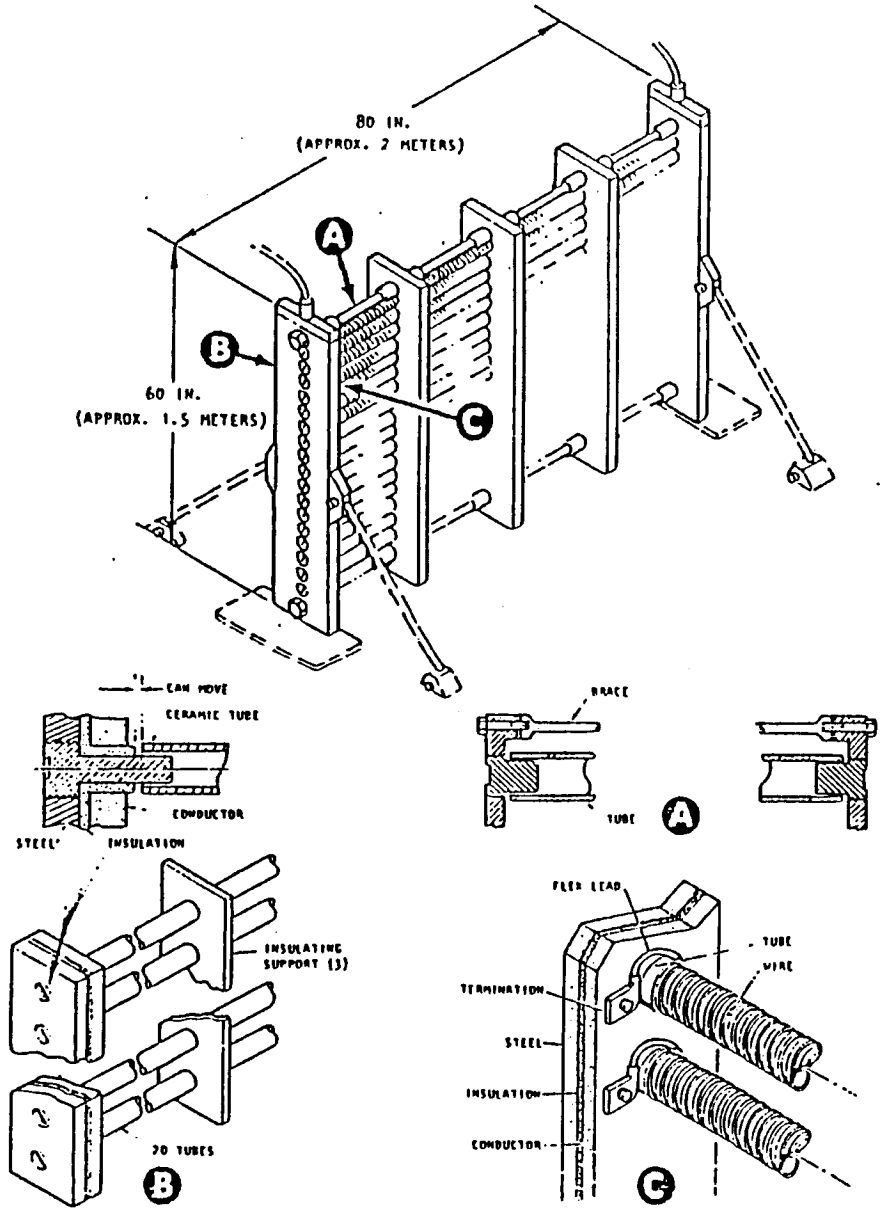

Figure 3.3.2.1-5. PARASITIC LOAD RADIATOR DESIGN CONCEPT

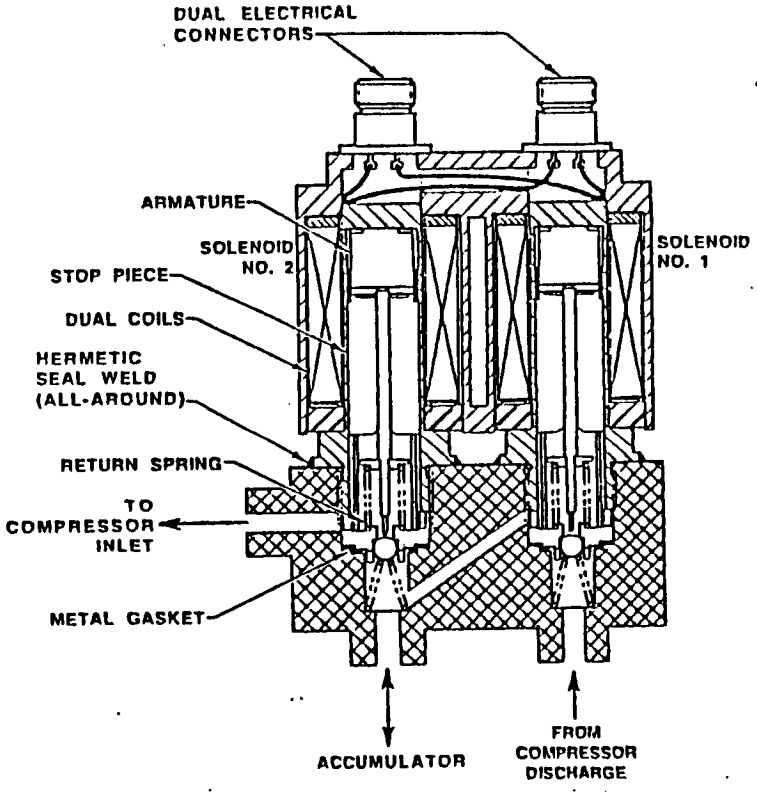

Figure 3.3.2.1-6. CBC INVENTORY CONTROL VALVE AND ACTUATOR CROSS SECTION

3.3.2.2 ORC Receiver/Power Conversion Unit (PCU)

The reference concept for the SD-ORC consists of a hybrid power system of two SD modules and two 12.5 kWe rated photovoltaic modules. Because of commonality, the photovoltaic module arrays and batteries are sized for polar orbiting platform requirements. When used on the station, the two photovoltaic modules then provide nominal power of only 23.5 kWe rather than the rated 25 kWe. As shown in Table 3.3.2.2-1, the resulting nominal SD power requirement for the IOC station is 51.5 kWe. Station growth is accomplished by adding solar dynamic modules only. Consequently, when the station nominal power requirement grows to 300 kWe, the SD requirement become 276.5 kWe. Peak power for the SD modules has been defined as 115% of the nominal power requirement. (The photovoltaic system is capable of meeting man-tended station and contingency requirements without SD and so these are not part of the SD requirements.)

The solar dynamic power generation requirements are achieved using ORC modules designed for 25 kWe nominal power. Because these modules are designed to operate with varying insolation (1.323 kW/m^2 to 1.419 kw/m^2) and with orbital/eclipse ranges corresponding to 180 to 250 nm orbital parameters, the actual power generation capability is expected to be 26.1 to 29.7 kWe at the three year design point. As Table 3.3.2.2-2 shows, two ORC modules combined with the photovoltaic modules provides the IOC station with 75.7 kWe nominal power and 101.9 kWe peak power. Adding ten additional ORC modules then allows the growth station requirements to be achieved with margin. Table 3.3.2.2-2 also shows key characteristics and design efficiencies for the ORC module.

The SD-ORC module consists of the assemblies shown in Figure 3.3.2.2-1. Detailed design drawings and descriptions for these assemblies are presented in DR-02, the Preliminary Analysis and Design Document. The major assemblies are the concentrator, which focuses incoming solar energy, the receiver which converts the solar energy to heat energy by vaporizing the working fluid and stores solar energy for vaporization during eclipse periods, the power conversion unit (PCU) which converts the heat energy to electrical energy, and the radiator which rejects heat from the thermodynamic cycle to space. Minor assemblies are the parasitic load resistor (PLR) which matches PCU electrical

TABLE 3.3.2.2-1
SOLAR DYNAMIC POWER GENERATION
SUBSYSTEM OPERATIONAL REQUIREMENTS

POWER GENERATION REQUIREMENTS

REQUIREMENT	IOC NET POWER KwE	GROWTH NET POWER KwE
o NOMINAL REQUIREMENTS		
IOC STATION POWER REQUIREMENT	75.0	300.0
NOMINAL PV POWER CAPABILITY	-23.50	-23.5
SOLAR DYNAMIC POWER REQUIREMENT	51.50	276.5
o SD PEAKING REQUIREMENT		
115% OF NOMINAL POWER	59.23	318.0

OTHER REQUIREMENTS

o ALTITUDE	
MAXIMUM	250 NM
MINIMUM	180 NM
NOMINAL	250 NM
o INSOLATION	
MAXIMUM	1.419 KW/M^2
MINIMUM	1.323 KW/M^2
o PMAD EFFICIENCY	88.82%
o PMAD PARASITIC	2.0 KW
o PEAK POWER DURATION/ORBIT	
ECLIPSE	7.5 MINUTES
SUN	7.5 MINUTES

TABLE 3.3.2.2-2
SUMMARY OF SOLAR DYNAMIC
ORGANIC RANKINE CYCLE OPTION

	IOC	GROWTH
Module Design Power (kWe)	25.0	25.0
Minimum Power/Module (kWe)*	26.1	26.1
Peak Power/Module (kWe)*	29.7	29.7
No. of Modules	2	12
ORC Minimum Power (kWe)	52.2	313.2
PV Minimum Power (kWe)	23.5	23.5
Station Minimum Power (kWe)	75.7	336.7
ORC Peak Power (kWe)	59.4	356.4
PV Peak Power (kWe)	42.5	42.5
Station Peak Power (kWe)	101.9	398.9

Key Characteristics	
Working Fluid	Toluene
Maximum Operating Temperature	399°C (750°F)
Effective Heat Rejection Temperature	60.4°C (140.7°F)
Thermal Storage Medium	LiOH
Receiver Operating Temperature	482°C (900°F)
Receiver Heat Transport	Potassium Heat Pipes
Radiator Heat Pipes	Aluminum/Ammonia
Radiator Surface	Z93 White Paint
Reflective Surface	Magnesium Fluoride over $Al_2O_3/Ag/Al_2O_3$

System Design Performance		Efficiency (%)
PMAD (effective) (88.2% less 1 kWe)		85.1
Controls		96.8
PCU		
Alternator	91.7	
Thermal Cycle	29.9	
Subtotal		27.4
Receiver		
Absorptivity	95.8	
Reradiation	94.7	
Subtotal		90.7
Concentrator		
Reflectivity	90.0	
Interception	99.7	
Subtotal		89.7
Sun-to-Bus (Nominal case, PLR load = 0)		18.3

*Expected value at BOL + 3 years without replacing failed radiator panels.

V2-33/9

ORGANIC RANKINE CYCLE SOLAR DYNAMIC POWER MODULE

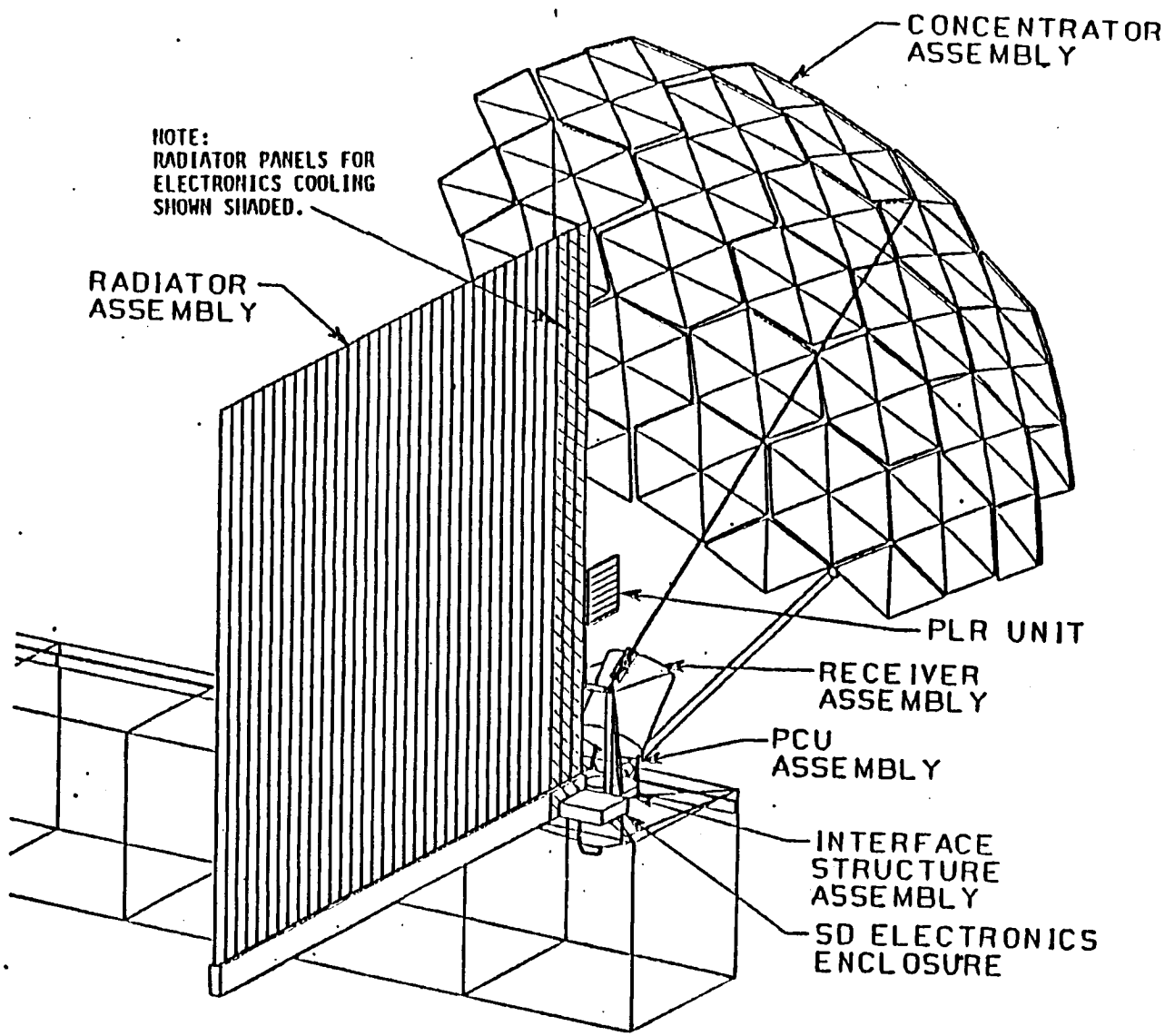

Figure 3.3.2.2-1

output to user requirements, the interface structure which connects the major components to the station beta joint and the electronics enclosure which contains the electronic controls.

3.3.2.2.1 Mass Properties

The Weight Breakdown, Table 3.3.2.2-3 presents weight by component for the 25 kW module. Radiator mass and area is shown for both the 31 radiator panels which are dedicated to cooling the PCU and the 3 panels for electronic cooling. The total raditor contains 34 heat pipe panels.

3.3.2.2.2 Receiver

The receiver must be capable of absorbing the solar input reflected by the concentrator, storing enough energy to supply the PCU during the eclipse and transferring the heat to the toluene working fluid throughout the orbit. The ORC receiver, shown in Figure 3.3.2.2-2, utilizes heat pipe technology to meet these requirements.

Due to the geometries of the concentrator and receiver, large variations in solar flux can exist. These variations are further accentuated by mirror surface inaccuracies and concentrator pointing errors. To allow for these variations, the receiver makes use of the load leveling characteristics of heat pipes. Incident solar flux is first absorbed by the heat pipes which contain integral TES canisters and a toluene vaporizer plumbed in parallel. Potassium lining the heat pipe interior wick structure is then evaporated and the resultant vapor flows to the colder surfaces of the TES canister and the vaporizer where it condenses. The condensate flows back to the evaporating surface by capillary pumping in the wicks with arteries being used to reduce the axial flow pressure drop. During eclipse, the TES is the hottest surface and potassium evaporation occurs from this surface. Condensation occurs on the vvaporizer tube. This process assures a virtually uniform heating rate for both the TES and vaporizer, during all portions of the orbit and under all anticipated incident flux distributions.

TABLE 3.3.2.2-3
ORGANIC RANKINE CYCLE
SUBSYSTEM
CHARACTERISTICS

		INDIVIDUAL MODULE		IOC STATION (2 Modules)		GROWTH STATION (12 Modules)	
--MASS--							
COMPONENT		KG	LBm	KG	LBm	KG	LBm
REFLECTIVE SURFACE		881	1943	1763	3886	10576	23316
2 AXIS FINE POINTING		427	941	854	1882	5122	11292
STRUCTURE (STRUTS)		60	133	121	266	724	1596
CONTROLS		8	17	15	34	93	204
MISC. HDWRE. & EQUIP.		38	84	76	168	457	1008
CONCENTRATOR	SUB TOTAL=	1414	3118	2829	6236	16972	37416
CRU		67	147	133	294	800	1764
RFMD		32	70	64	140	381	840
REGENERATOR		181	400	363	800	2177	4800
HOUSINGS		16	36	33	72	196	432
ACCUMULATOR		83	182	165	364	991	2184
TOLUENE		110	243	220	486	1323	2916
CONTROLLER		14	31	28	62	169	372
PLR		49	108	98	216	588	1296
PLUMBING		15	32	29	64	174	384
POWER CONVERSION UNIT	SUB TOTAL=	567	1249	1133	2498	6799	14988
HEAT PIPES/VAPORIZERS		513	1130	1025	2260	6151	13560
THERMAL ENERGY STORAGE		828	1825	1656	3650	9934	21900
STRUCTURE		32	71	64	142	386	852
INSULATN/MICROMET. SHLD		45	100	91	200	544	1200
MISC		8	17	15	34	93	204
RECEIVER	SUB TOTAL=	1426	3143	2851	6286	17108	37716
HEAT PIPE CONDNSR+FINS		1461	3220	2921	6440	17527	38640
HEAT PIPE EVAPORATOR		160	353	320	706	1921	4236
TOLUENE CONDENSR+PLBG		204	450	408	900	2449	5400
CONTACT HT EXCHG DEVICE		357	786	713	1572	4278	9432
PCU RADIATOR/CONDENSER	SUB TOTAL=	2182	4809	4362	9618	26175	57708
ADAPTER SUBASSY		264	581	527	1162	3162	6972
SUPERSTRCT. SUBASSY		106	233	211	466	1268	2796
SD EQUIPMT. BOX		120	264	239	528	1437	3168
CPL COOLING SUBASSY		217	479	435	958	2607	5748
INTERFACE STRUCTURE	SUB TOTAL=	707	1557	1412	3114	8474	18684
BETA JOINT		275	606	550	1212	3299	7272
BETA JOINT	SUB TOTAL=	275	606	550	1212	3299	7272
TOTAL MASS	TOTAL=	6571	14482	13137	28964	78827	173784
--PLANFORM AREA--		M2	FT2	M2	FT2	M2	FT2
CONCENTRATOR		213	2290	425	4580	2553	27480
PCU RADIATOR		160	1719	319	3438	1916	20628
CPL RADIATOR		15	166	31	332	185	1992
--DRAG AREA--		M2	FT2	M2	FT2	M2	FT2
CONCENTRATOR		156	1677	312	3354	1869	20124
PCU RADIATOR		37	398	74	796	444	4776
CPL RADIATOR		4	38	7	76	42	456
TOTAL DRAG AREA		196	2113	393	4226	2355	25356

Receiver Isometric

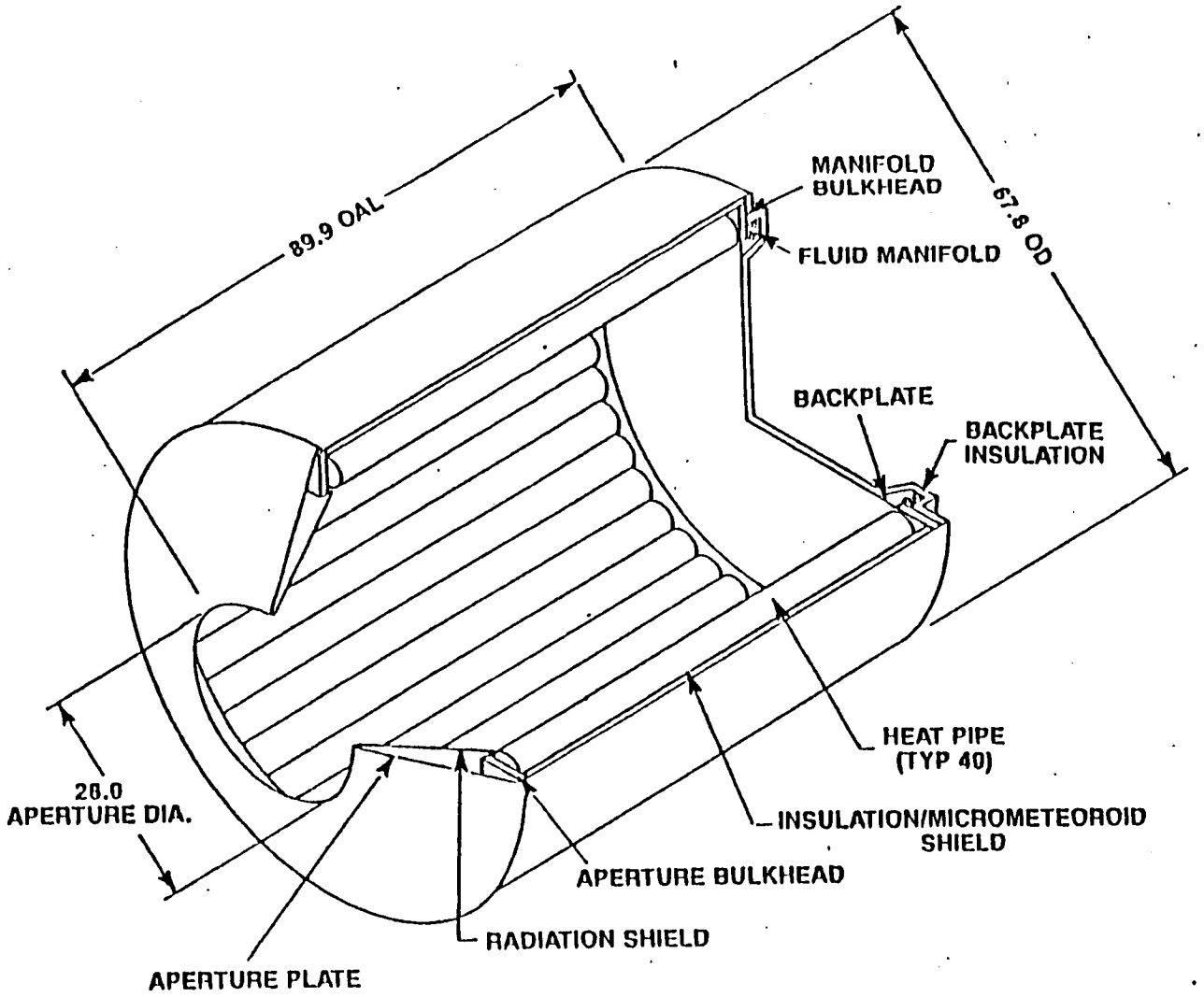

Figure 3.3.2.2-2

The ORC receiver uses the latent heat of LiOH for the TES approach. LiOH was selected because it is readily available, stable, is not a eutectic, has a very high latent heat (397 btu/lb), and has an almost constant volume during phase change. The LiOH is stored in canisters inside the receiver heat pipes. The relatively low conductivity of the LiOH is enhanced by the addition of internal nickel fins to minimize cyclic variations during the charge/discharge process.

The receiver structure is optimized to account for the thermal environment. The aperture plate material, Nextel, was selected to eliminate the need for an active cooling system if the focused solar flux is located directly on its outer surface. No special materials are required for the heat pipes. Since the receiver temperature is low (485 C/900 F) and the heat pipes eliminate hot spots, low cost, readily available 316 stainless steel is suitable. However, the heat pipe attachments must account for thermal elements of the receiver as shown in Figure 3.3.2.2-3. These heat pipes have one end cap with a ball joint connection and the other end bolted firmly to the manifold end bulkhead. The remaining 37 heat pipes are also bolted to the manifold end but have guide pins on the aperture end. This structural approach allows the aperture plate to "float" and avoid any thermal stress in the heat pipes.

3.3.2.2.3 Power Conversion Unit

The power conversion unit (PCU) converts the heat energy of the toluene working fluid to electrical energy.

The PCU, shown in Figure 3.3.2.2-4, consists of:

- o Combined rotating unit (CRU)
- o Rotary fluid management device (RFMD)
- o Regenerator
- o Accumulators
- o Valves and start pump
- o Plumbing and electrical lines
- o Working fluid (Toluene)

Receiver Structural Configuration

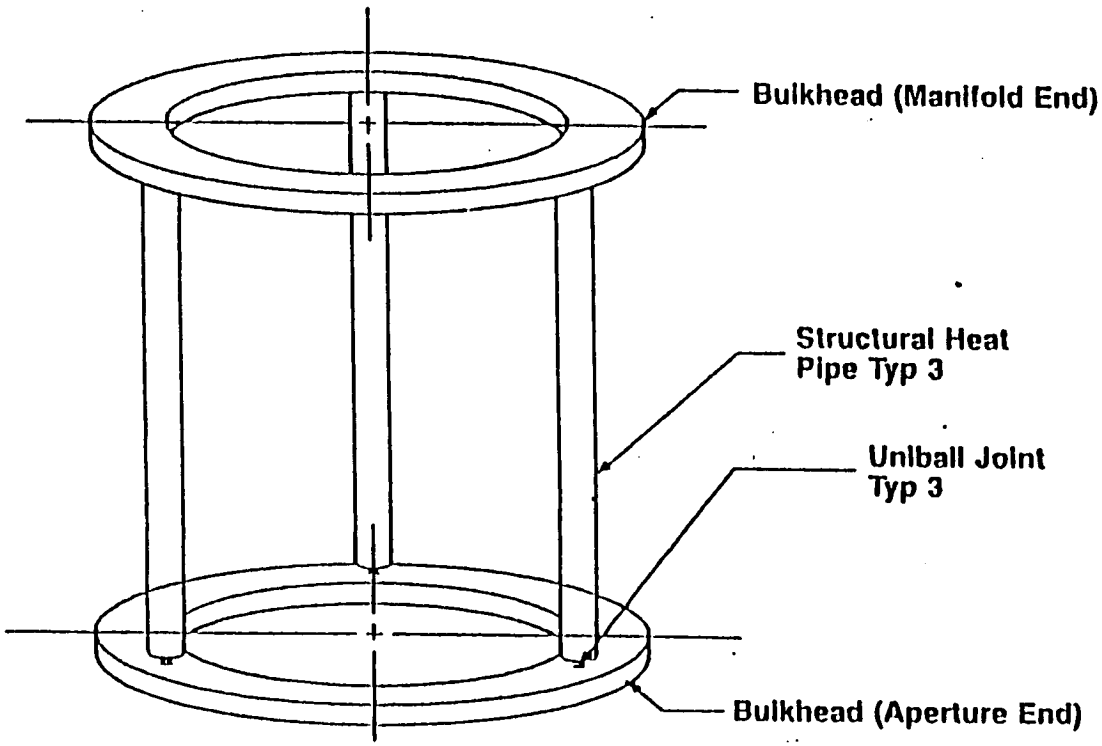

Figure 3.3.2.2-3

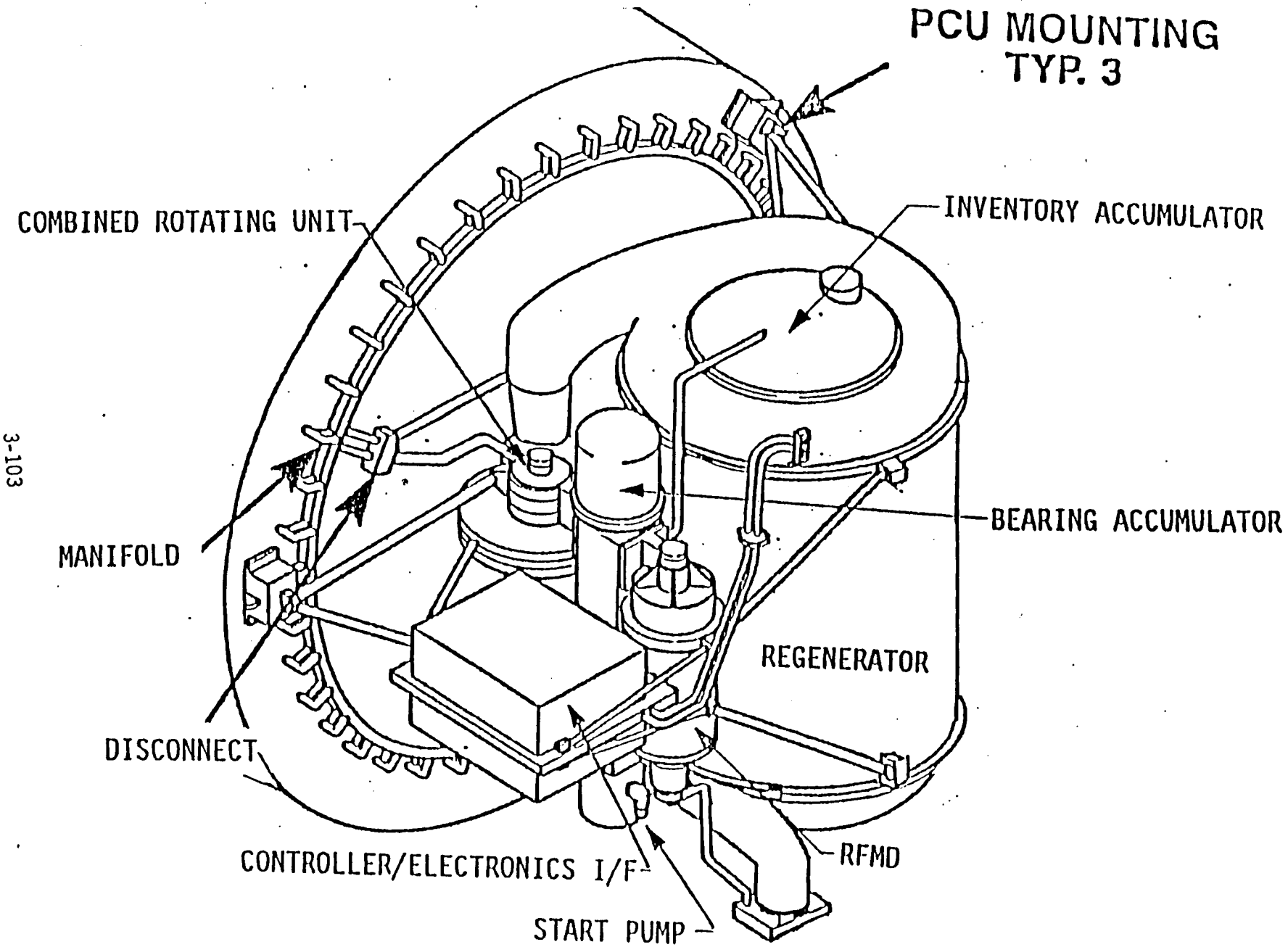

Figure 3.3.2.2-4

CRU

The combined rotating unit (CRU) is comprised of an axial impulse turbine that extracts shaft work from expanding toluene working fluid, an alternator that converts the turbine shaft work into electrical power and a feed pump that pressurizes the toluene to a supercritical state. These components are all connected on a single shaft. Designed for long life and high reliability, the CRU features a single rotating part supported on fluid film bearings. The design has been employed on the several previous successful applications.

Special attention has been given to reducing points of external leakage of the toluene. The CRU is joined to the RFMD on a common manifold for mounting to the receiver.

Turbine

The single stage axial impulse turbine driven by the working fluid, turns the alternator and system feed pump. The aerodynamic components consist of the inlet plenum, nozzles, turbine, and exhaust diffuser.

The turbine provides high efficiency at moderate temperatures and speeds. Toluene vapor at 610 psia and 750 F is expanded through nine supersonic nozzles to high velocity streams which impinge on the turbine blades to rotate the shaft. The exhaust is routed to the regenerator through a diffuser. The turbine design employes supersonic converging-diverging blading for an overall efficiency of 73.9 percent.

Alternator

A Lundell-Rice alternator converts shaft power from the turbine into electrical power. A stationary fixed coil is employed to excite the magnetic field and control output voltage. The rotor is a single piece composed of overlapping plies of magnetic material separated by a non-magnetic spacer.

V2-3321/21

The Lundell-Rice alternator design is particularly rugged due to the absence of rotor windings and commutator. It is less sensitive than other designs to temperature variations and produces high quality power. Voltage is regulated by field control, preventing over voltage during accidental over speed.

Pitot Pump

The pitot pump uses shaft power from the turbine to pressurize the system fluid in a simple low risk, low cost manner. It takes low pressure fluid from the RFMD and converts it to high pressure fluid before it goes to the receiver.

CRU Assembly

The rotating unit is fully enclosed in a static housing, thus dynamic leakage, if it were to occur, would not result in loss of working fluid. Nevertheless, dynamic shaft seals separate areas of different pressure along the CRU rotor to eliminate internal leakage which could reduce performance.

The CRU accommodates both radial and thrust loads by using tilting pad radial journal bearings and a Rayleigh step thrust bearing. Both types create a hydrodynamic film to support their loads and eliminate contact and wear between surfaces.

RFMD

The RFMD is low speed pitot pump which performs the following functions:

- o Controls flow rate for power excursions (peaking)
- o Controls toluene inventory
- o Provides for accumulation and separation of non-condensible gasses
- o Provides resaturation of subcooled condenser outlet flow

The RFMD is mounted with its rotational axis parallel to the axis of the CRU. It is composed of two pitot probes, radial and thrust bearings, a motor, two shafts, a rotating housing and a hermetically sealed stationary housing. The rotating housing is supported on radial bearings attached to the shafts

which are cantilevered from the stationary housing. The motor turns the rotating housing to provide the pumping by the pitot tubes.

Regenerator

The regenerator is a counterflow coiled finned tube design of the same configuration and materials and having similar size and has been verified on other ORC systems. The integral tube/fins are machined from solid tube stock and require no bonding, minimizing the cleanliness control problem associated with brazing, welding, etc. It provides more repeatable heat transfer effectiveness and eliminates the concern present with other types of heat exchangers about uninspectable bonded joints. The regenerator cross-section is a hollow cylinder with ring shaped inlet and exhaust plenums on the ends. The inlet plenum is directly connected to the turbine exhaust diffuser.

Condenser

The condenser is a shear-controlled design utilizing converging passages to maintain adequate velocity. The design ensures the presence of a stable liquid-vapor interface in zero gravity and causes non-condensible gases to flow through the condensor and into the RFMD.

Accumulator

The accumulator is located in the regenerator's cylindrical core and its supported from the plenum flanges, reducing the PCU package volume as well as line lengths. The accumulator is sized to start the system initially and restart it under normal and most fault shutdown conditions. The design is a simple bellows accumulator based on experience with other fluid programs.

PLR

The parasitic load resistor (PLR) matches the power produced by the SD module to user requirements. The module output is designed for maximum user power. Therefore, when use loads are less than design, excess power is radiated

to space by a bank of identical value resistors controlled by corresponding individual switch modules. Each resistor dissipates approximately 1 kW which gives sufficient resolution for control. MOSFETS are selected for their high reliability and low gate drive requirement. Sufficient modules and parasitic load resistors are provided to account for full generator output with not user load. During control, sufficient loads are switched on incrementally in a digital manner by signals from the frequency control loop of the controller. The switch modules are housed separately from the controller and near the resistors to minimize electromagnetic interference.

Engine Controller

The ORC engine controller is a microprocessor-based device that controls startup sequences, regulates electrical power dissipation in the parasitic load to maintain constant speed, manages the thermal storage condition, and monitors receiver and PCU microprossor. It receives operational command from and passes status to the PCU microprossor. The controller is cooled by liquid toluene at 92.8^{0}C (181^{0}F) which flows through the cold plate that also serves as the mounting structure for both the redundant controllers, on on each face.

3.3.3 SD Radiator

Separate design concepts were generated for the ORC and CBC radiator assemblies. A constructible, heat pipe radiator using a flat contact interface was selected for the ORC preliminary design. For this concept, commonality was maintained, to the maximum extent practical, with hardware being developed for other thermal control systems on the Space Station. A deployable, pumped fluid loop radiator was chosen for the CBC preliminary design. This concept provides a minimum weight and cost design to interface with the relatively high temperature, single phase CBC working fluid. Details of the preliminary design follow.

3.3.3.1 CBC Radiator Preliminary Design Description

The design condition for the CBC radiator is derived from the power flow and state point diagrams for the case where the heat load is greatest and the sink temperature is at its most severe (warmest) condition during the orbit. A design data sheet (Table 3.3.3-1) summarizes the design conditions and characteristics of the CBC pumped loop radiator that meets these requirements.

Radiator Panel The CBC radiator panel design is illustrated in Figure 3.3.3-1. Each of the eight panels is 8.0 x 2.3 m (26.4 x 7.5 ft) and 1.6 cm (0.63 in) thick. The panels are constructed by incorporation of tube extrusions into a honeycomb structure which is sandwiched between sheets of aluminum. The structure is bonded together using Hysol EA 9649 adhesive.

This design provides a probability of no penetration for ten years of 0.90 for each system and a probability of no penetration of both the primary and standby system of 0.99. The probability of achieving zero failures in the CBC radiator assembly is 0.967 in 10 years.

TABLE 3.3.3-1

CBC RADIATOR PRELIMINARY DESIGN CHARACTERISTICS

MODULE SIZE: 25kWe
TYPE: Deployable pumped liquid
HEAT REJECTION: 99.0 kWt
HEAT TRANSPORT LOOPS: (primary and redundant loops used)
FLUID - FC 75
FLOWRATE - 4498 lbm/hr
DELTA P - 12 psi through panels
POWER USE - 100 watts (based on Moog 50-498 Pump)
PANEL SIZE: 2.3 m (7.5 ft) x 8.0 m (26.4 ft)
NUMBER OF PANELS: 8
PANEL PLANFORM DEPLOYED AREA: 147.2 m^2 (1584 ft^2)
MATERIAL: Extruded bumpered aluminum flow tubes with aluminum fins
MASS:

PANEL SET ORU	1145 kg (2524 lbm)
PUMP PACKAGE ORUs	64 kg (141 lbm)
INTERCONNECT LINE ORUs	36 kg (80 lbm)
TOTAL	1245 kg (2745 lbm)

COATING: Z93 Zinc Oxide Paint
T-ENV: 213 K (-76F) (sink temperature)
T-COOL INLET: 449 K (348.5°F)
T-COOL OUTLET: 284 K (52.9°F)

Deployment Mechanism. The scissors deployment mechanism was selected over other candidates on the basis of previous trades conducted in 1980-81. This was done by LTV Aerospace as part of the 25 kW Power System program conducted for NASA MSFC. The mechanism selected is an adaptation of the Skylab Apollo Telescope Mount (ATM) solar array deployment mechanism which successfully deployed four solar panel arrays on-orbit. In 1975 LTV Aerospace installed radiator panels on a spare ATM frame and tested the configuration under thermal vacuum conditions at NASA JSC. During this test, successful deployment was demonstrated. These tests were conducted under the NASA JSC (NA9-14408) Self Contained Heat Rejection Module Program.

The adaptation of this design for the CBC radiator deployment uses gear drives with dual motors at the ends of the radiator panels to rotate the lower scissors arms from horizontal to a 97^0 position thus deploying the entire array in accordion fashion. Rotary stops at the base halt the motion. The first 15^0 of rotation is assisted by spring moments created by the flexible

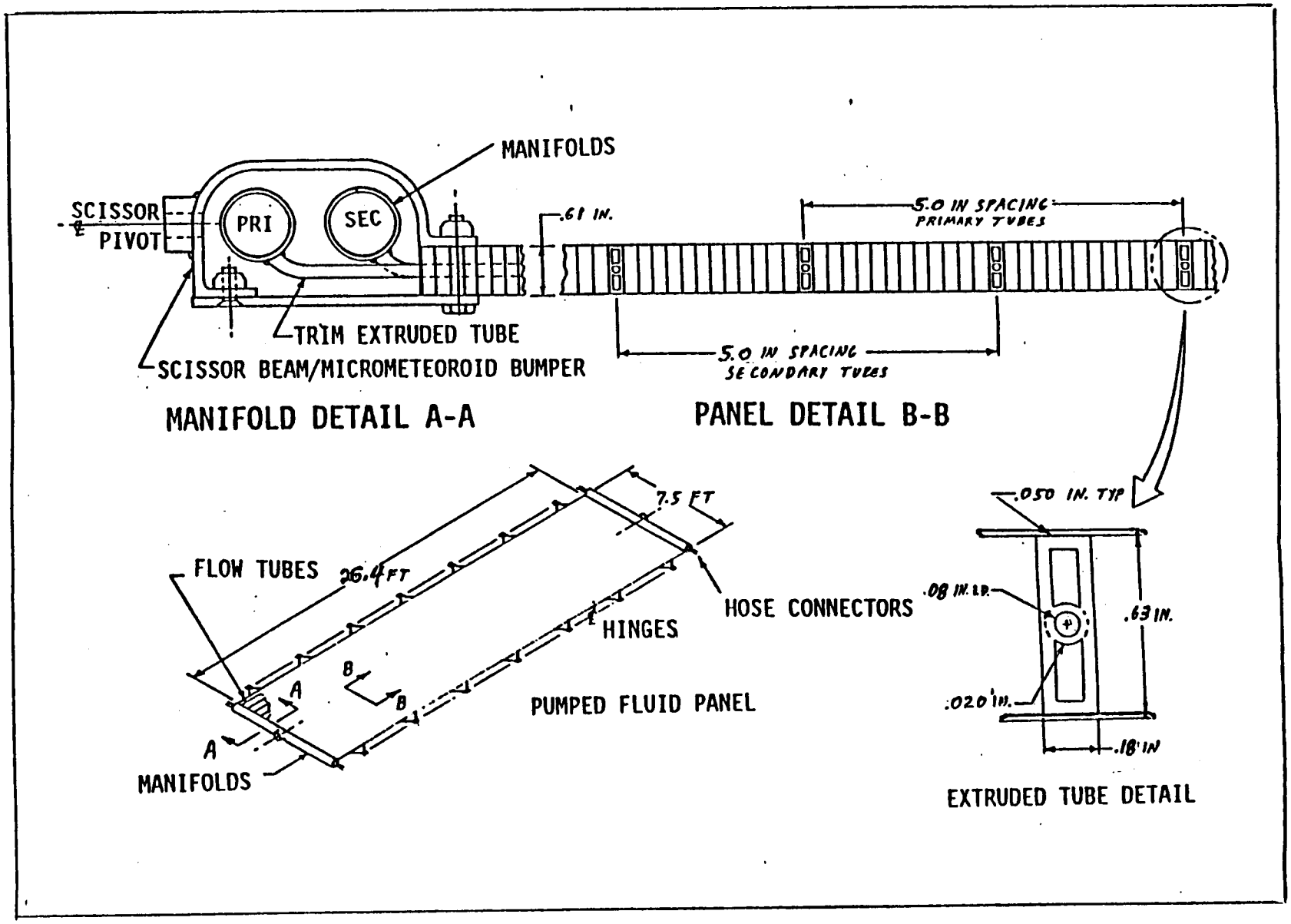

Figure 3.3.3-1

CBC Radiator Panel Design

metal hoses used to transport fluid across the rotating joints. On retraction the low mechanical advantage plus friction and the spring moments will prevent full retraction by use of the gears. For this reason a dual cable retraction system is employed to pull the top radiator panel down at both ends and compress the stack of panels against fold stops. The cable system would be locked down during transport then released to free wheel during deployment. Cable tension will be limited by a slip clutch or resettable multiple detents to prevent over stressing of the mechanism when fully folded.

Adaption for use of a MRMS or EVA tool to deploy and retract the panels will be provided. As an option these mechanisms could replace the deployment motors if this proves desirable. The motor system will provide automatic radiator deployment without EVA and MRMS support.

3.3.3.2 ORC Radiator Preliminary Design

The ORC radiator design was selected to provide an optimum design that meets the ORC cycle requirements while maintaining a maximum amount of commonality with hardware being developed for the Work Package-02 central radiator system. A summary of the preliminary design is given in Table 3.3.3-2. This design consists of 31 panels, each of which are 13.7 m (45 feet) long and 40.6 cm (16 inches) wide. The radiators are of the constructible, high capacity heat pipe design being developed for the central radiator system. The panels utilize the Lockheed tapered artery heat pipe of aluiminum material using ammonia working fluid. The panels are interfaced with the ORC condenser by means of a flat, pressurized contact interface which allows on-orbit assembly and replacement of each panel. This interface design is being developed under a NASA-JSC ADP program.

Radiator Panel. The radiator panel assembly is shown in Figure 3.3.3-2. Each panel consists of a radiator/heat pipe condenser section which is 12.7 m (41.6 ft) long and 40.6 cm (16 in) wide, a 30.5 cm (12 in) long adiabatic section and an evaporator section 69.8 cm (27.5 in) long and 22.9 cm (9 in) wide. The panel is 3.61 cm (1.42 in) thick and the total length is 13.7 m (45 ft). The panel incorporates two separate heat pipe assemblies, as shown in the drawing, each having one condenser leg and three evaporator legs.

TABLE 3.3.3-2

ORC RADIATOR PRELIMINARY DESIGN CHARACTERISTICS

MODULE SIZE: 25 kWe
TYPE: Constructible radiator/with flat interface
HEAT REJECTION: 113.3 kWt (maximum power condition)
HEAT TRANSPORT LOOP: ORC working fluid loop (toluene)
PANEL SIZE: 12.7 m (41.6 ft) x 40.6 cm (16 in)
HEAT PIPE EVAPORATOR LENGTH: 77.4 cm (2.54 ft) (3 legs each section)
NUMBER OF PANELS: 31 (includes two extra panels for reliability)
PANEL PLANFORM DEPLOYED AREA: 159.8 m^2 (1719 ft^2)
MAX HEAT PIPE CAPACITY: 514,500 Watt-Inches (includes 30% margin)
MATERIAL: Aluminum heat pipe with ammonia fluid/aluminum fins
WEIGHT:

Panel fins + heat pipe condenser	1464 kg (3220 lb)
Heat pipe evaporator	160 kg (353 lb)
Heat exchanger contact device	357 kg (786 lb)
TOTAL WEIGHT	1981 kg (4359 lb)

COATING: Z93 Zinc Oxide Paint

DELTA-T WORKING FLUID TO RADIATOR: 271K (28.4°F)
T-ENV: 213 K (-76 F) (maximum sink temperature)
T-RAD AVG: 326 K (127.6F)
T-COND INLET: 370 K (207 F)
T-COND OUTLET: 331 K (137 F)
T-SAT INLET: 345 K (162 F)
T-SAT OUTLET: 342 K (156 F)

The two condenser (one for each heat pipe) legs are incorporated into an aluminum honeycomb matrix consisting of a sandwich of two 2.5 mm (0.010 in) facesheets bonded to a core of 3.1 lbm/ft^3 honeycomb. This type of structural assembly was used in fabrication of the STS Orbiter radiators. The assembled face sheets comprise the panel fins. For this panel configuration, a total of four fins is available for radiant heat exchange per heat pipe, or eight fins per panel. Each fin is 10.2 cm (4 in.) wide. The honeycomb matrix provides the structural strength. The structure is bonded together in an autoclave using Hysol EA 9649 adhesive. This adhesive was previously qualified by Rockwell International in 1981 for use on the Orbiter.

The heat pipe evaporator section consists of the six evaporator legs (three for each heat pipe) with 1.5 mm (0.060in.) thick fins attached to each. The 30.5 cm (12 in) adiabatic section is used to manifold the three

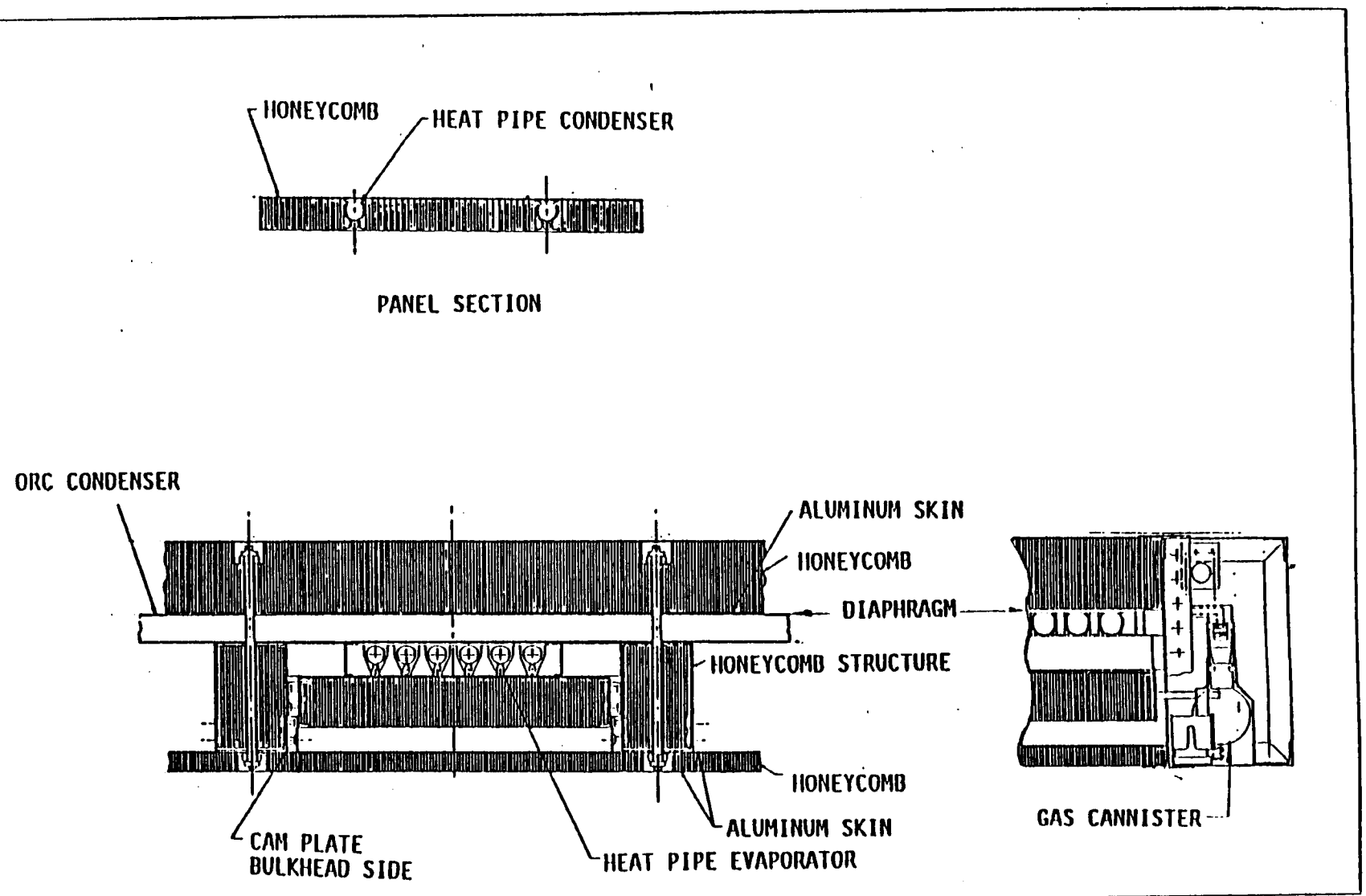

Rockwell International
Rocketdyne Division

Figure 3.3.3-2

ORC Radiator Panel Assembly Details

evaporator legs into the single condenser leg and provides a length for guiding the panel into the interface assembly.

The heat pipe extrusion is 3.6 cm (1.40 in) thick and a maximum of 2.0 cm (0.79 in) wide. It contains circumferential threaded grooves at 200 grooves per inch length in the evaporator section and 60 grooves per inch in the condenser section of the heat pipe. Ammonia fluid is wicked from the tapered, nominal 1.0 cm (0.40 in.) diameter liquid space, into the grooves and up the walls of the vapor space where it is evaporated by heat from the ORC condenser. The vapor in the evaporator passes into the heat pipe condenser due to the higher pressure in the evaporator section where it is condensed on the walls of the vapor space and wicked back into the artery by the grooves. The difference in the capillary forces at the condenser and evaporator result in a higher pressure in the liquid at the condenser and thus cause the liquid to return to the evaporator where the process is repeated.

The Lockheed tapered-artery heat pipe, has a theoretical performance limit of 735,000 watt-inches at 327 K (130^{O}F) temperature. A margin from theoretical of 30% was adopted as good design practice and a heat pipe performance requirement of 514,500 watt-inches established.

The radiator (with two panel oversizing) has a 0.999 probability of not requiring maintenance for at least ten years while maintaining 100% heat rejection. The effect of panel oversizing on radiator reliability is shown in Table 3.3.3-3.

TABLE 3.3.3-3

ORC RADIATOR RELIABILITY VERSUS OVERSIZING

PANELS REQUIRED FOR 100% HEAT REJECTION	NUMBER EXTRA PANELS	TOTAL PANELS	PROBABILITY OF 100% HEAT REJECTION IN 10 YEARS
29	0	29	0.830
	1	30	0.984
	2	31	0.999

V2-33/5

Interface Structure. The flat, pressurized contact interface design developed for use in the Space Station central radiator system is employed to interface the radiator with the ORC condenser. The design consists of a honeycomb backing structure which is continuous along the entire length of the condenser. The movable honeycomb section for each panel has a thin walled, titanium diaphragm mounted on the lower surface. An activation device at the rear of each segment is used to raise and lower the moveable section providing a 1.3 cm (0.5 in) clearance for insertion of a radiator panel when in the "up" position and to provide a snug fit when in the "down" position. The "up-and-down" movement is provided by cam plates on each side of the moveable section. The cam plates translate the linear movement into vertical movement. When in the "down" position these cam plates rest on mating flat surfaces which support the pressurization loads. A nitrogen gas pressurization device is included consisting of a small canister with a Schrader type valve and a receptacle which will open the valve when the canister is inserted. A tube connects the receptacle to the diaphragm. This tube contains a flexible section to allow the relative movement between the canister and the diaphragm.

To assemble on-orbit, the pressure plate activation device is rotated causing the moveable plate to rise. A panel is inserted through the funnel assembly at the end which provides sufficient capture volume to allow MRMS assembly. After insertion, the activation device is rotated, causing the plate with the diaphragm attached to contact the top of the panel. A gas canister is then screwed into the receptacle, opening the valve and pressurizing the d3aphragm to 3.0 mp (200 psi). The pressurized diaphragm forces the radiator panel evaporator section into intimate contact with the ORC condenser providing a high contact conductance. Triple redundant seals are provided to prevent gas leakage from the diaphragm or canister.

V2-33/6

3.3.4 Design Data for the Interface Assembly

3.3.4.1 Layouts/Drawings

The interface assembly is comprised, in the case of the CBC concept, of two subassemblies. One is the interface structure subassembly and the other is the SD equipment box subassembly. For the ORC, the interface assembly consists of three subassemblies: The interface structure, the SD equipment box, and the capillary pumped loop heat rejection subassembly. A conceptual layout drawing of the isolated interface assembly is shown in Figures 3.3.4-1 and 3.3.4-2 for the CBC and ORC, respectively. The interface structure subassembly, in turn, consists of two components: the adaptor and the superstructure. The SD equipment box subassembly, for the CBC concept, consists of six components: the utility plate, an SD control box, a redundant SD control box, an AC-to-AC frequency converter, a pump accumulator package, and a redundant accumulator package. The SD equipment box subassembly for the ORC concept consists of the same components except that the pump accumulator packages, in the CBC case, are replaced by capillary pumped loop packages.

The SD equipment box contains the electronic components necessary (1) to control the SD subsystem and (2) to convert the AC alternator power to 20 kHz AC for distribution, in addition to components that handle the heat load created by the first two items. Each SD equipment box contains six ORUs of which one is the utility plate component and its enclosure, if any. The box has been attached to the adaptor plate where access is good for maintenance purposes.

3.3.4.2 Mass Properties

Tables 3.3.4-1 and -2 list the mass breakdowns for the CBC and ORC interface assemblies, respectively. The original approach of cooling the electronic components by flowing toluene through the utility plate has been changed to incorporate a capillary pumped loop (CPL) and a separate condenser

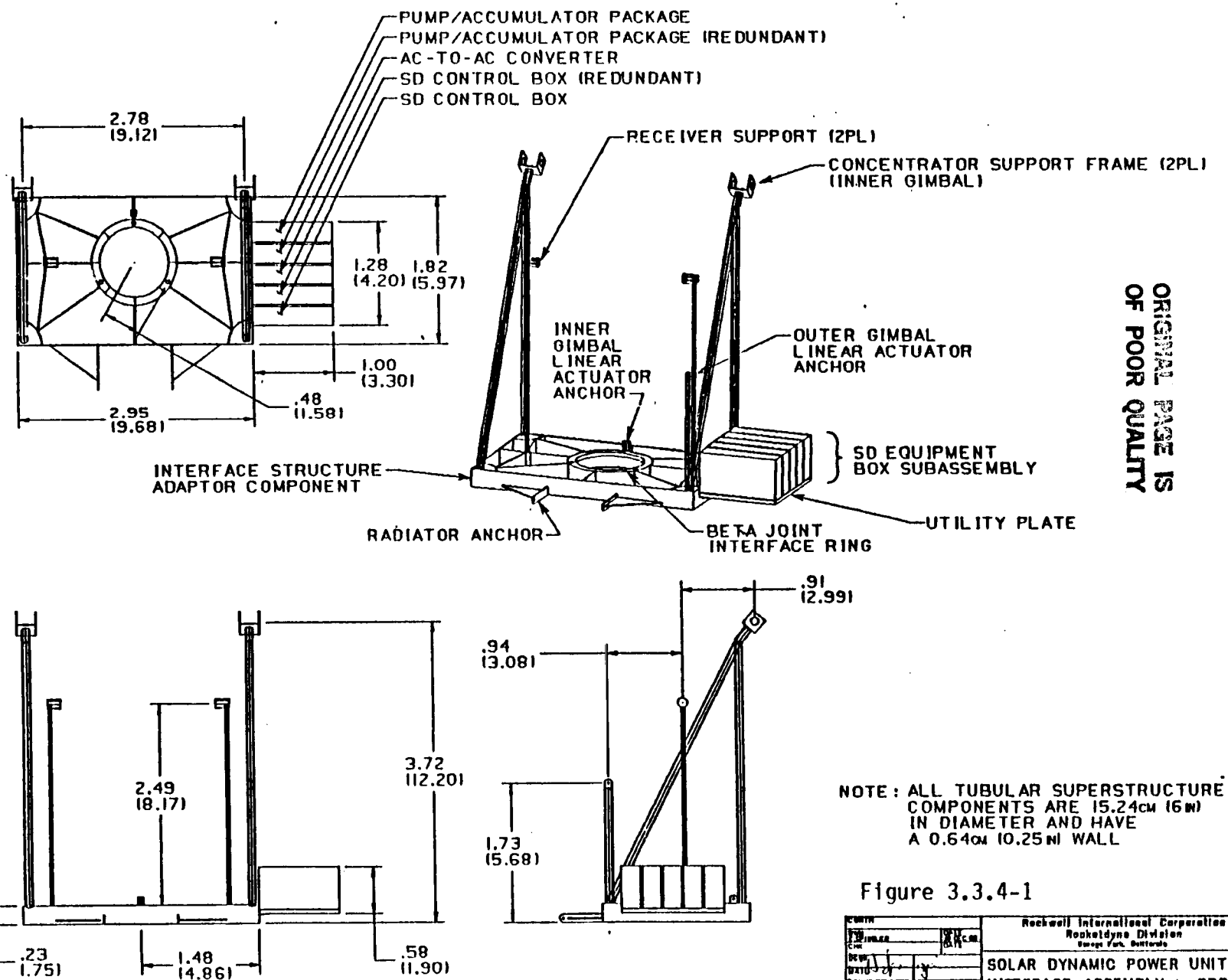

ORIGINAL PAGE IS OF POOR QUALITY

NOTE: ALL TUBULAR SUPERSTRUCTURE COMPONENTS ARE 15.24CM (6IN) IN DIAMETER AND HAVE A 0.64CM (0.25IN) WALL

Figure 3.3.4-1

	Rockwell International Corporation Rocketdyne Division
	SOLAR DYNAMIC POWER UNIT INTERFACE ASSEMBLY - CBC
SIZE C	FSCM NO. 02602
SCALE NONE	DWG NO. 7R070062
DO NOT SCALE PRINT	SHEET

DWG NO. 7R070062 SH

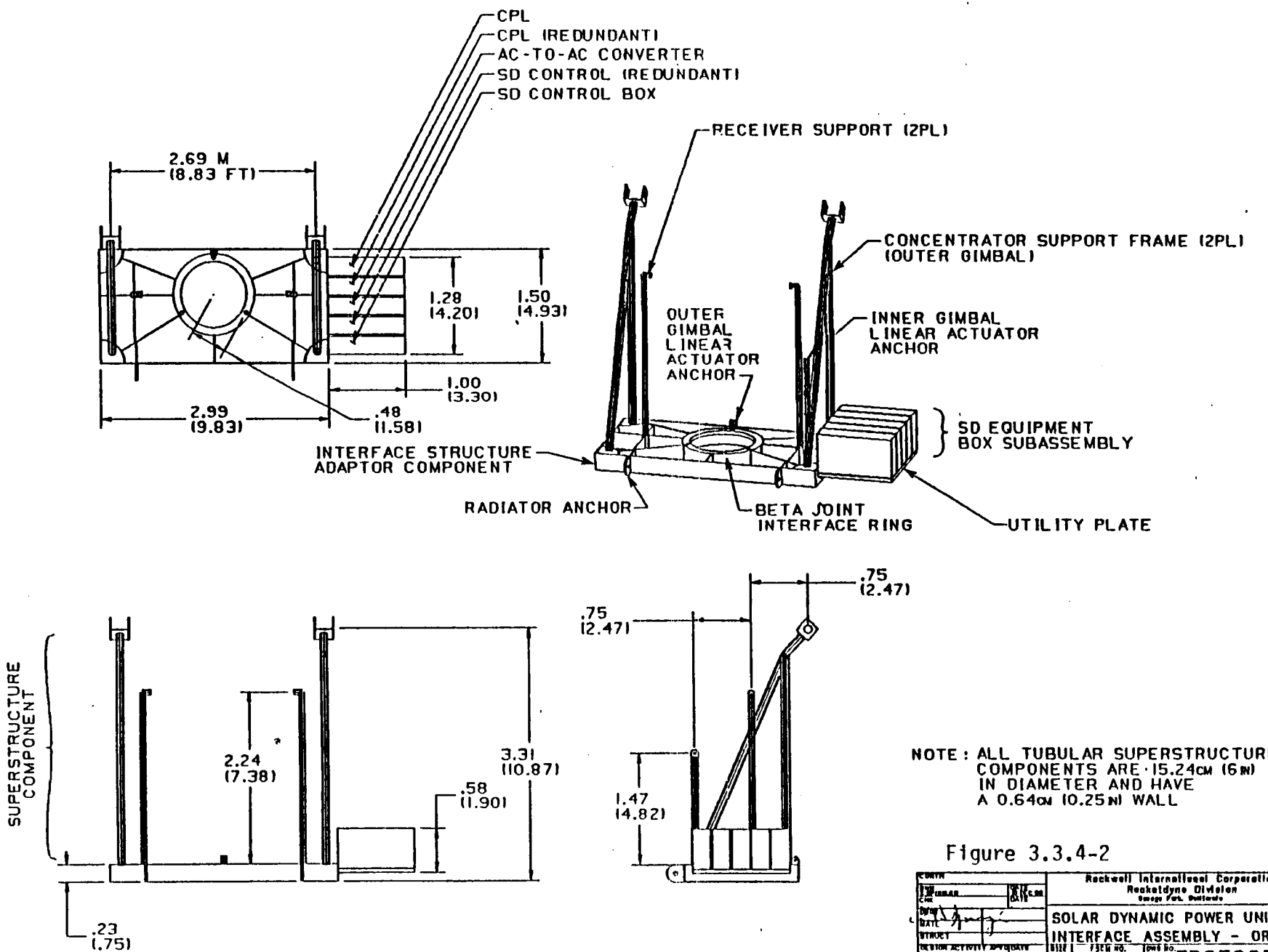

NOTE: ALL TUBULAR SUPERSTRUCTURE COMPONENTS ARE 15.24CM (6 IN) IN DIAMETER AND HAVE A 0.64CM (0.25 IN) WALL

Figure 3.3.4-2

	Rockwell International Corporation Rocketdyne Division
	SOLAR DYNAMIC POWER UNIT INTERFACE ASSEMBLY - ORC
SIZE C	FSCM NO. 02602
SCALE NONE	DWG NO. 7R070055
	SHEET

DWG NO. 7R070056 SH

and heat pipe radiator. Although the direct toluene loop has not been definitely eliminated as a feasible approach to cooling the electronics components (the PMAD AC-to-AC frequency converter, in particular), the current requirement for maintaining the utility plate at 20°C (68°F) cannot, per se, be achieved. Thus, a CPL approach has been adopted as the reference case. The condenser and radiator panels for the CPL are located adjacent to and in the same plane as are the condenser and heat pipe radiator panels for the thermodynamic cycle heat rejection assembly. However, since the electronic cooling system is a completely separate loop, its mass, including its condenser and radiator, is accounted for as part of the interface assembly in this section of the DR. Table 3.3.4-2 reflects this fact.

A backup to the CPL approach, which might result in less complexity and slightly lower mass, is one in which the heat pipe radiators are clamped directly to the utility plate, thereby eliminating the CPL section. This approach was not analyzed in detail, although some sizing calculations were performed. See Section 2.2.4.4 for additional information.

Insofar as the CBC electronic cooling system is concerned, the pumped loop radiator area has now been increased (and, therefore, its mass has been increased) to accommodate the additional heat load, and the cycle state points have been chosen in order to have the FC-75 coolant at or below 20°C (68°F) as it exits the utility plate. This change is reflected in a change in the mass of the radiator as described previously, but does not change the basic cooling concept proposed conceptually in DR-02.

(An increase in the radiator size has accomplished one other objective in the CBC system --- namely, an improvement in the overall cycle efficiency. This factor permitted the concentrator size to remain at or below that of a full 19-panel assembly. Thus, no edge wedges are necessary.)

TABLE 3.3.4-1
CBC SOLAR DYNAMIC INTERFACE ASSEMBLY MASS BREAKDOWN [kg (lbm)]

ITEM	kg		(lbm)	
Interface Structure Subassembly	376		(828)	
Adaptor Component (Aluminum)		270		(595)
Adaptor Plate		234		(515)
Fittings*		18		(40)
Attachment Hardware*		18		(40)
Superstructure Component (Composite)		106		(233)
Structural Tubes		67		(148)
Tube Joint Fittings*		14		(30)
Deployment Mechanisms*		5		(11)
Attachment Hardware*		20		(44)
SD Equipment Box Subassembly	207		(456)	
Utility Plate Component		143		(316)
Cold Plate		57		(126)
Attachment Hardware		20		(44)
Interconnect Lines (Loop 1)*		18		(40)
Interconnect Lines (Loop 2)*		18		(40)
Wiring Harness*		30		(66)
SD Control Box		**		**
SD Control Box (Redundant)		**		**
AC-to-AC Converter		**		**
Pump Accumulator Package*		32		(70)
Pump Accumulator Package (Redundant)*		32		(70)
TOTAL INTERFACE ASSEMBLY	583		(1284)	

*Values indicated by an asterisk are estimated.
**SD Control Box (and its redundant unit) and the AC-to-AC frequency converter masses on covered in PMAD section.

V2-334/3

TABLE 3.3.4-2
ORC SOLAR DYNAMIC INTERFACE ASSEMBLY MASS BREAKDOWN [kg (lbm)]

ITEM	kg		(lbm)	
Interface Structure Subassembly	369		(814)	
Adaptor Component (Aluminum)		263		(581)
Adaptor Plate		227		(501)
Fittings*		18		(40)
Attachment Hardware*		18		(40)
Superstructure Component (Composite)		106		(233)
Structural Tubes		67		(148)
Tube Joint Fittings*		14		(30)
Deployment Mechanisms*		5		(11)
Attachment Hardware*		20		(44)
SD Equipment Box Subassembly	127		(280)	
Utility Plate Component		120		(264)
Cold Plate		49		(108)
Attachment Hardware*		20		(44)
Interconnect Lines (Loop 1)*		6.5		(14)
Interconnect Lines (Loop 2)*		6.5		(14)
Wiring Harness*		30		(66)
CPL Isolator*		4		(9)
CPL Evaporator*		4		(9)
SD Control Box		**		**
SD Control Box (Redundant)		**		**
AC-to-AC Converter		**		**
CPL Package*		3.5		(8)
CPL Package (Redundant)*		3.5		(8)
Capillary Pumped Loop Rejection Subassembly	211		(463)	
Heat Pipe Radiator Panels***		157		(346)
Contact Device*		35		(76)
Condenser*		12		(26)
Ammonia*		7		(15)
TOTAL INTERFACE ASSEMBLY	707****		(1557)****	

*Values indicated by an asterisk are estimated.
**SD Control Box (and its redundant unit) and the AC-to-AC frequency converter masses on covered in PMAD section.
***Includes heat pipes, honeycomb panel and face sheets
****These values are not directly comparable with similar total for CBC in previous table since the CBC radiator size increases required to handle electronic cooling are accounted for elsewhere (see Section 2.2.4).

V2-334/4

3.3.4.3 Solar Dynamic Interface Structure Performance

3.3.4.3.1 Adapter Subassembly and Superstructure Subassembly

The adapter component and the superstructure component for both CBC and ORC are passive devices subject to dynamic loads imposed by accelerations from the operation of the two-axis-gimbal fine-pointing mechanism, from the operation of the beta joint, and from other sources on-orbit. In addition, there will be launch loads and deployment forces acting on these two components.

Although the on-orbit dynamic loads have not been analyzed in detail, a mathematical representation of the stiffness of these two components has been assumed in the analysis report in Section 7.3 of DR-02 on the concentrator structure. The designs depicted in Figures 3.3.4-1 and -2 are judged to be at least as stiff as that assumed previously, and are therefore expected to perform satisfactorily in this regard.

Since the two components will have additional supporting structures to attach them to the shuttle during launch, there is no reason to expect the current design will not be sufficient for launch purposes.

3.3.4.3.2 SD Equipment Box - CBC

The utility plate in the equipment box provides cooling for all ORUs attached to it. The total thermal loads for nominal, peaking, and maximum insolation (zero load, faulted case) are 2599 watts, 3165 watts, and 4070 watts, respectively. The engine controller, which is located elsewhere, has a maximum thermal load of 1600 watts for the maximum insolation case. The FC-75 fluid pumped through the utility plate is sufficient to maintain the required temperatures (as noted above) at 20°C (68°F). The overall performance of the FC-75 loop (including the pump/accumulator package), as well as the performance of the SD control box ORU is described in DR-02.

3.3.4.3.3 SD Equipment Box - ORC

The utility plate in the equipment box provides cooling for all ORUs attached to it. The total thermal loads for these ORUs for nominal, peaking, and maximum insolation (zero load and faulted) are 1950 watts, 2230 watts, and 3180 watts, respectively. The performance of the SD control box is described (as noted above) in DR-02.

The CPL cooling concept is described in detail in section7.16 of DR-02. The working fluid, NH_3, is evaporated at the cold plate. The vapor is "pumped" via capillary action to the CPL condenser where it becomes a subcooled liquid. The heat energy given up is carried away by a set of three radiator panels, one of which is redundant. Total radiating area required to meet the heat load is calculated to be 18.2 m^2 (196 ft^2). With one extra panel (each radiator panel is identical to each of those used in the heat engine waste-heat assembly), the total radiating area becomes 30.8 m^2 (332 ft^2). This area provides adequate redundancy and some excess active area as well.

3.3.4.4 Assembly Definition

The CBC and ORC interface structure subassemblies have many common elements. The structures and mechanisms are similar, but not identical, in configuration. The wiring harness and electronic equipment mounts would be expected to be the same except for the number of wires and size of the mounts and electrical connectors.

The reference SD interface assembly configuration features a high rigidity interface structure to which all other SD assemblies are ultimately attached. The function of the interface assembly is to support the receiver assembly, the PCU assembly and the radiator assembly, as well as the equipment box subassembly. The interface assembly also provides part of the interface between the receiver/PCU/radiator launch package and the shuttle.

The interface structure subassembly design is driven by the stiffness requirements of the concentrator and the launch load requirements of the receiver/PCU package.

The interface structure subassembly configuration was selected on the basis of low SD subsystem moment of inertia, a major GN&C stability driver. The trade study that selected the POLAR concentrator concept, which includes the interface structure general configuration, was documented in DR-19, DP 4.4, Section 7.1.6.

The CBC interface structure subassembly concept is different from the ORC interface structure subassembly in that it is slightly larger and has a different radiator interface dimension. The receiver/PCU support tabs on the adaptor component are also slightly different for each concept.

3.4 PMAD SUBSYSTEM

3.4.1 System Overview

The Power Management and Distribution (PMAD) Subsystem includes that hardware and software necessary to control power generation from all sources photovolatic arrays, batteries and solar dynamic engine-alternators and to distribute that power to variable loads throughout the Space Station structure and manned modules. The overall PMAD subsystem functions (see Figures 3.4.1-1 and 2) as a dual power bus system with independent sources for each bus. Each Main Bus Switching Assembly (MBSA) functions as the independent source feeding its own network of ring feeders. Electrical loads are served from the Power Distribution and Control Assemblies (PDCA) located throughout the station. The PDCAs contain Remote Power Controllers (RPC) that serve as the electrical interface with each load. The RPCs function to protect the electrical power system from load faults. RPCs are also used for load shedding operations during system overload situations.

The PMAD control system is designed for automatic and autonomous operation with minimum routine operator interactions. Operators may, however, interact with the PMAD control system though the DMS interface with the power management controller whenever necessary or desired. The PMAD control system is designed to control all power sources and distribution equipment to ensure maximum power availability to subsystem and payloads in accordance with mission priorities. This control includes source paralleling and synchronization, real and reactive load sharing between sources, voltage and frequency regulation, harmonic distortion monitoring, load management (shedding, balancing, scheduling), fault detection and isolation, and system health monitoring. Loads are monitored and RPCs are designed to protect the system from load faults. The control of the distribution network is designed to detect faults and isolate the smallest segment of the system necessary to clear the fault thus maintaining power availability to the maximum number of loads.

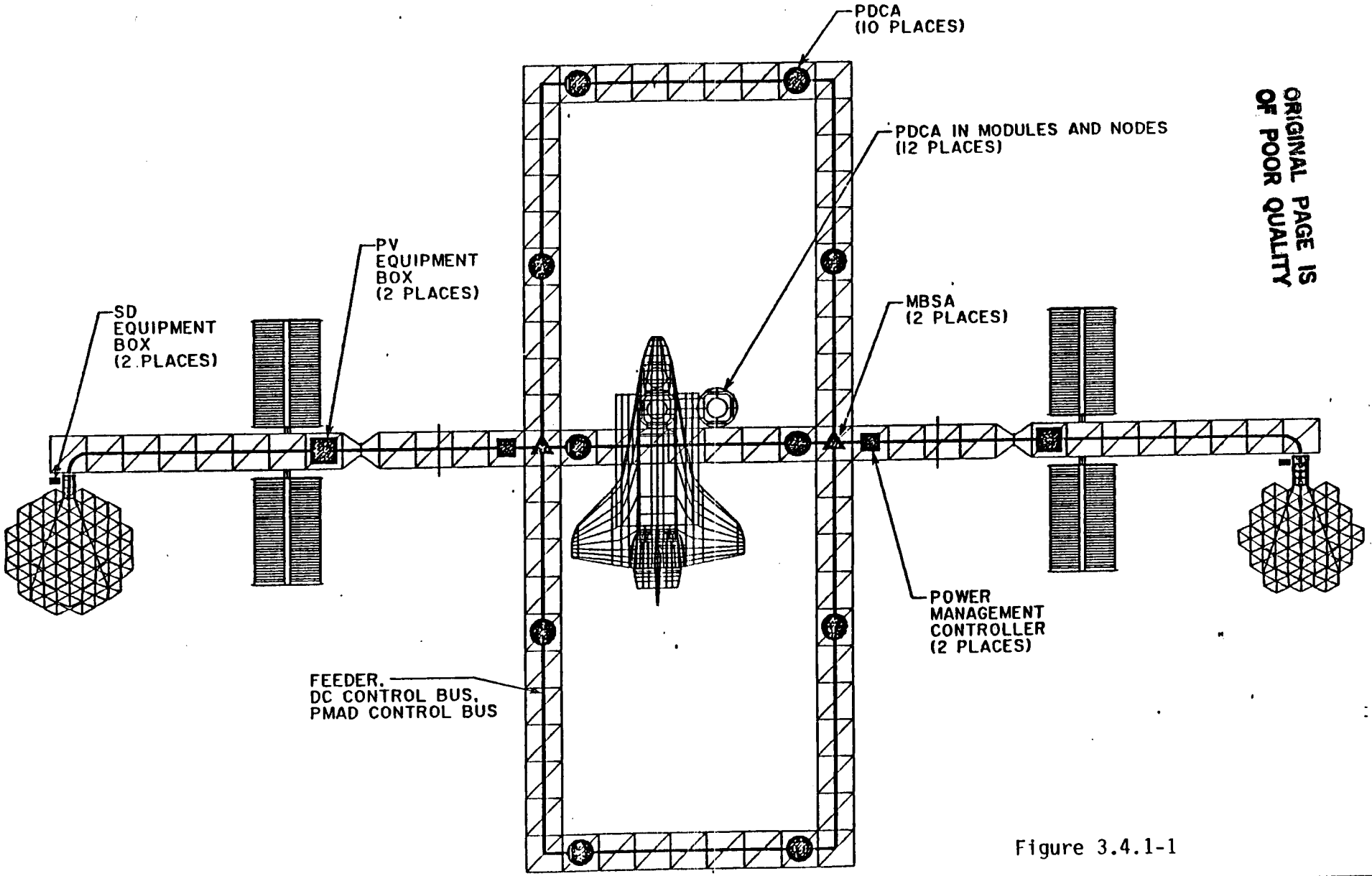

ORIGINAL PAGE IS
OF POOR QUALITY

Figure 3.4.1-1

Rockwell International Corporation
Rocketdyne Division

SPACE STATION EPS COMPON
LOCATIONS

SIZE C | FSCM NO. 02602 | DWG NO. 7R07002

SCALE NONE | DO NOT SCALE PRINT | SHEET

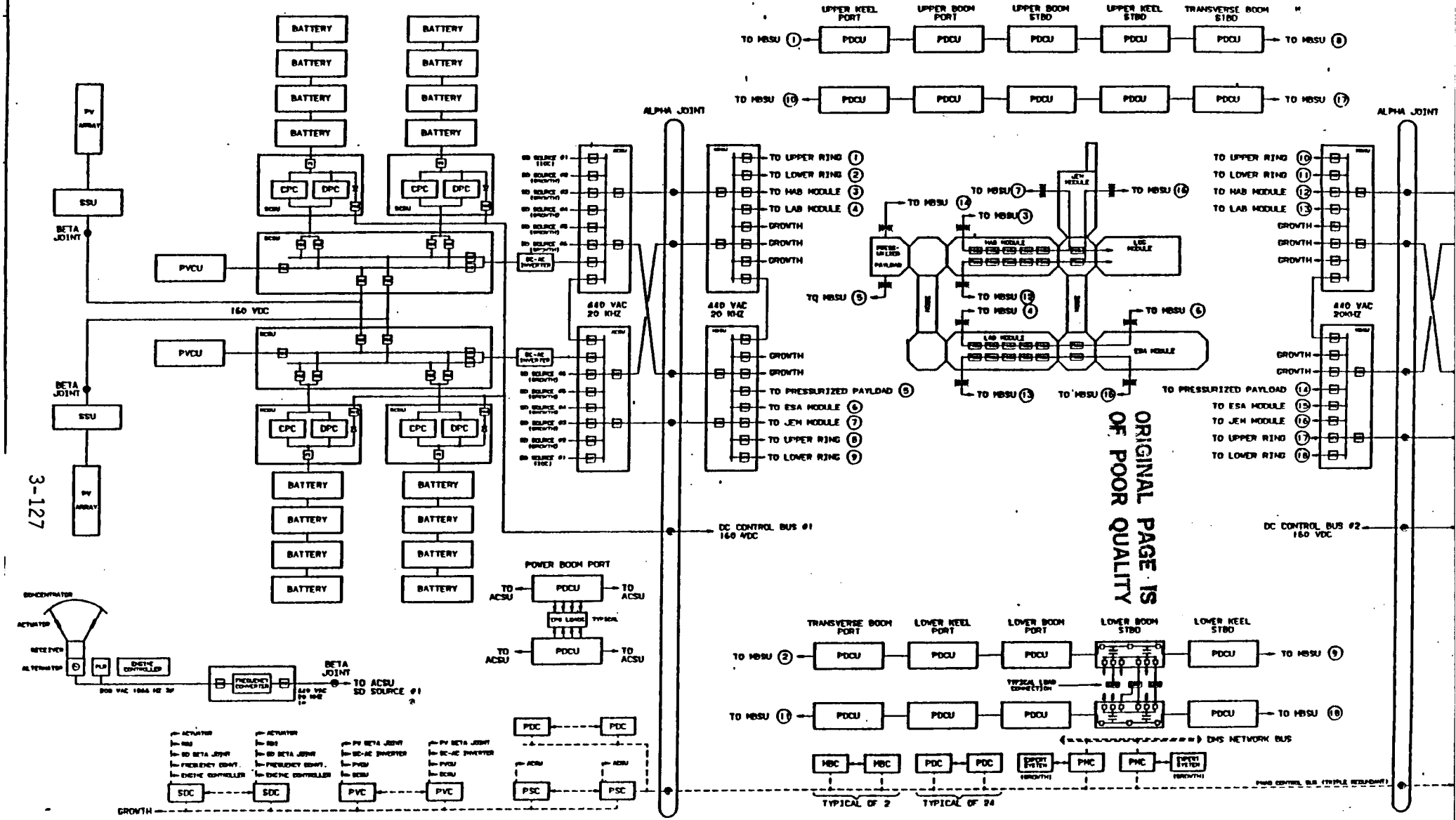

3-127

LEGEND

AC - ALTERNATING CURRENT
ACSU - AC SWITCHING UNIT
BCDU - BATTERY CHARGE/DISCHARGE UNIT
CPC - CHARGE POWER CONVERTER
DC - DIRECT CURRENT
DCSU - DC SWITCHING UNIT
DMS - DATA MANAGEMENT SYSTEM
DPC - DISCHARGE POWER CONVERTER
EPS - ELECTRICAL POWER SYSTEM
ESA - EUROPEAN SPACE AGENCY
FI - FAULT ISOLATOR
HAB - HABITAT MODULE
JEM - JAPANESE ENGINEERING MODULE
KHZ - KILO HERTZ
LAB - LABORATORY MODULE
LOG - LOGISTICS MODULES
MBSU - MAIN BUS SWITCHING UNIT
PVCU - PHOTOVOLTAIC CONTROL UNIT
PDC - POWER DISTRIBUTION CONTROLLER
PDCU - POWER DISTRIBUTION AND CONTROL UNIT
PLR - PARASITIC LOAD RESISTOR
PMAD - POWER MANAGEMENT AND DISTRIBUTION
PMC - POWER MANAGEMENT CONTROLLER
PSC - POWER SOURCE CONTROLLER
PV - PHOTOVOLTAIC
PVC - PV CONTROLLER
RBI - REMOTE BUS ISOLATOR
SD - SOLAR DYNAMIC
SDC - SD CONTROLLER
SSU - SEQUENTIAL SHUNT UNIT
VAC - VOLTS ALTERNATING CURRENT
VDC - VOLTS DIRECT CURRENT

2. VOLTAGE INSIDE ALL PRESSURIZED MODULES AND TO ALL LOADS IS 208 VAC 20 KHZ 1Ø.

1. COMPONENTS OUTBOARD OF THE STBD ALPHA JOINT ARE THE SAME AS COMPONENTS OUTBOARD OF THE PORT APLHA JOINT.

NOTE. UNLESS OTHERWISE SPECIFIED

Figure 3.4.1-2

EPS SYSTEM DIAGRAM

E 02602 7P070009

3.4.2 PV Source PMAD

3.4.2.1 System Overview

Figure 3.4.2-1 shows the PV source PMAD block diagram. The system is comprised of two solar array wings each with a sequential shunt unit (SSU) assembly. Two photovoltaic control units (PVCUs) are attached to the DC bus (via the DC switching unit). The output of the solar arrays wings powers a redundant DC bus. This DC bus is regulated during the insolation phase by the SSU/PVCU to 160 VDC nominal. There are four batteries attached to the DC bus which are individually charged by Charge Power Converters during the insolation phase. The DC bus is powered and regulated during the eclipse phase by battery Discharge Power Converters. The charge and discharge rates are determined by the PV Processor. Utility power is generated using two DC-AC Inverters. One inverter operates at full power while the other is in standby for peaking. This method is used to maximize inverter efficiency and keep the PV source size to a minimum. DC RBIs, AC RBIs and Fault Isolators are used in various parts of the subsystem to protect and isolate faults should they occur. These components can also be used during maintenance to isolate an ORU for removal and replacement.

3.4.2.2 Sequential Shunt Unit (SSU)

Array regulation is accomplished with a sequential shunt approach, which provides a low dissipation method of shunting excess power to match power delivery to demand, while maintaining voltage regulation. The specific implementation selected for the Space Station program is a pulse width modulated (PWM) sequential shunt. This design was chosen for optimal compatibility with a 20 kHz distribution frequency, in particular with regard to EMI. In the pulse width modulated mode the operating frequency is fixed at 20 kHz and is synchronized with the main inverters. This allows EMI filters to be designed for a fixed frequency of operation, for efficient filtering of the system power bus.

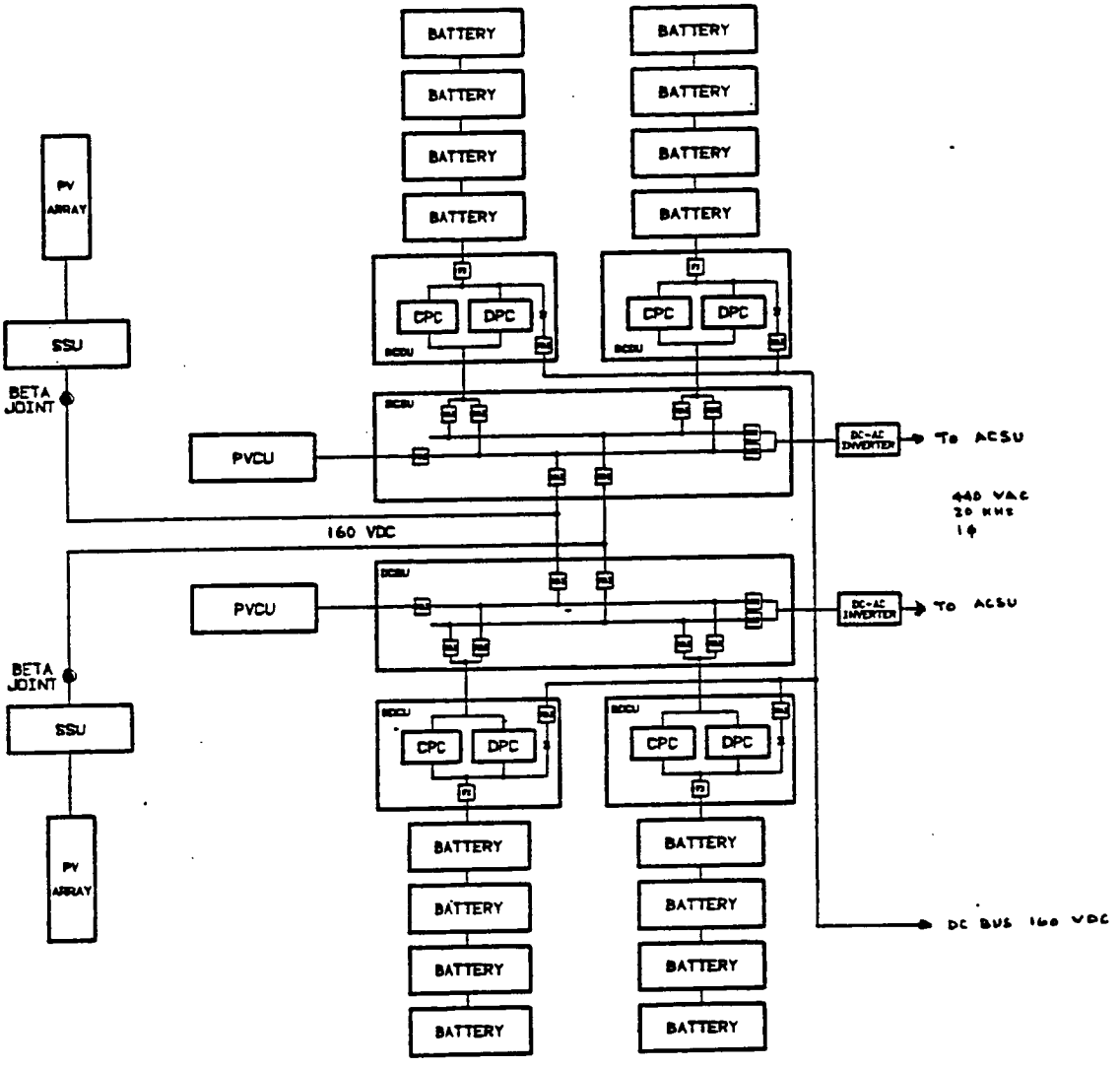

Figure 3.4.2-1 PV Source PMAD Block Diagram

3.4.2.3 Photovoltaic Control Unit (PVCU)

The photovoltaic control unit (PVCU) generates the PVCU error signal required by the SSU. The PVCU contains the error amplifiers and reference voltage circuits. Array bus voltage is sensed across the PVCU capacitor bank. The error amplifiers generates a PWM signal which relates to the difference between bus voltage and reference voltage. The capacitor bank is used to stabilize array bus voltage.

3.4.2.4 DC-AC Inverter

The main DC-AC Inverter will have regulating capability so that the AC bus voltage and frequency is regulated to the required point for AC system operations. Load sharing is also controlled by the inverters. The inverters are sized to deliver the entire nominal array output to the AC primary distribution network during peaking operations. The inverter size is thus directly related to the array size which is determined from platform system optimization.

3.4.2.5 Battery Charge/Discharge Unit (BCDU)

The Battery Charge/Discharge Unit (BCDU) is an ORU comprised of the charge power converter, discharge power converter, fault isolators, control power bus RBI, and data interfaces. One ORU is required for each battery.

A battery charge/discharge unit (BCDU) is provided for each battery. This approach is required since batteries may have varying states of health and age, which will affect their voltage. If the batteries were all connected to the DC bus without a discharge regulator, the stronger batteries would provide most of the power until their voltage fell to the level of the weaker battery, leading to depth of discharge differences. A similar mismatch would exist during charging. Consequently, in order to maximize battery performance and life, control of the charging and discharging of each individual battery is necessary and has the additional benefit that it provides for maximum flexibility in DC system operation.

3.4.2.6 DC Switch Unit

The DC Switch Unit (DCSU) consists of a dual DC power bus and DC RBIs. Connected to the DC power bus are the PV arrays, Battery Charge/Discharge Units and the DC-AC inverters. Each power input or output line is connected to a DC Remote Bus Isolator (DC RBI) which can isolate each line from the bus in the event of a failure or during maintenance. The DC RBI design is similar to the AC RBI design as described in paragraph 3.4.5.6.1, but uses a single SCR for power control. The status of the DC RBIs are monitored and can be manually opened or closed by commands from the PV controller. The DCSU is packaged into two ORUs so that PV power would not be interrupted should one DCSU fail.

3.4.2.7 PV Controller

The PV controller is an embedded data processor used to control the Energy Storage System (ESS) charge and discharge rates, the outputs of the DC-AC inverters and SSU/PVCU operation. The controller is also used to monitor the 150 VDC bus and the DCSU. The controller is connected to all PV power components by means of a local network. Details of the PV Controller are described in paragraph 3.4.7

3.4.2.8 PV/ESS Electronics Box

The PV/ESS electronics box provides the mounting points and the cold plates to mount the PV source ORUs (PVCU, BCDU, PV controller), the AC switching unit and the power source controller.

3.4.3 SD Source PMAD

3.4.3.1 System Overview

Figure 3.4.3-1 shows the SD source PMAD block diagram. The SD block diagram remains the same regardless of the ORC or CBC engine selection. The PMAD system components found in the diagram are: SD Controller, Frequency Converter and AC RBIs.

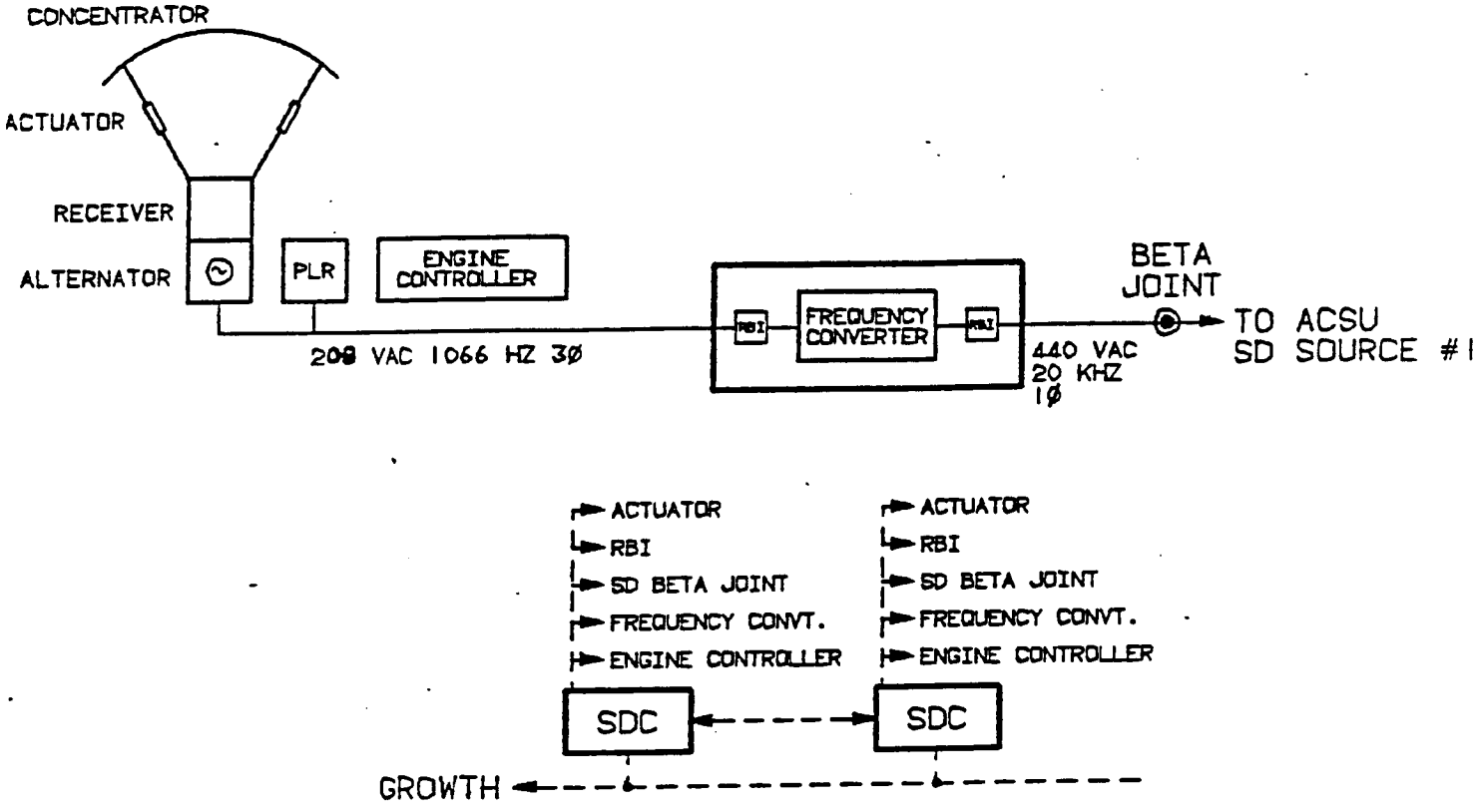

Figure 3.4.3-1 SD Source PMAD Block Diagram

The power output of the alternator is converted to utility voltage and frequency in the frequency converter. Synchronization of the SD source with other sources is accomplished by this converter. Each SD module is connected to independent alpha joint channels. If necessary, the SD source can be isolated from the rest of the system by commanding the AC RBI open.

The SD system is designed to deliver 75 kW less the photovoltaic capacity to the Space Station users. Nominally, this is 50 kW. In addition, peaking capability of 15% is also required of the SD modules. PMAD power components are designed to handle this peaking capability.

3.4.3.2 Frequency Converter

The solar dynamic alternators which supply a nominal 50 kW of power to the Space Station have a 3-phase, AC output with a frequency between 400 and 1200 Hz. For primary distribution, a frequency converter is used to convert the 3-phase low frequency power to single phase, 20 kHz. The frequency converter is designed to tolerate input frequency variations on the order of ± 10%, while maintaining a constant output frequency of 20 kHz. It has both line and load regulation capability to insure constant primary bus voltage and is capable of parallel operation with DC-AC inverters and other frequency converters.

3.4.3.3 SD Controller

The SD Controller is an embedded data processor which acts as an interface with the PMAD system and the Engine Controller. It also is used to pass the necessary pointing and tracking information that is required to control the beta joint and the linear control actuators. Any necessary signals to the frequency changer and the AC RBIs are also controlled by this processor. More detailed functions of the SD Controller is found in paragraph 3.4.7.

3.4.3.4 SD Control Assembly

The SD electronic enclosure provides the mounting points and the cold plates to mount the SD controller and frequency converter. The enclosure is located on the outboard side of the SD beta joint.

3.4.4 Hybrid Source Control

Since the primary distribution bus will be powered from both frequency converters and inverters simultaneously, the drivers must be synchronized and connected in parallel. To adjust for peak demand periods, inverters are switched on and off the bus. These inverters and frequency converters are ideal for multiple driver/parallel operation. They are easily synchronized, inherently load share when connected in parallel, and are easily switched in and out of service without presenting any transients to the primary distribution bus.

3.4.4.1 AC Switching Unit

The ACSU serves as the power bus where all AC sources on one side of the station are connected. All connections to the bus are made through RBI's so that sources can be isolated when necessary. In addition, power is distributed across the alpha joint through 4 large feeders to the MBSA. This is necessary to limit the quantity of roll rings needed in the alpha joint. All RBIs in the ACSU are controlled by the PSC.

3.4.4.2 Power Source Controller

The power source controller (PSC) is an embedded data processor that is used to coordinate the settings of the various AC sources on one side of the station. In addition it functions to control the configuration of the ACSU which is the point where all AC sources on a side of the station are paralleled prior to distribution across the alpha joint. See paragraph 3.4.7 for a detailed description of the PSC.

3.4.5 Power Distribution System

3.4.5.1 Primary Distribution

Utility power is generated by the PV and SD subsystems outboard of the alpha joint and is parallel and synchronized at the ACSU. The output at the ACSU is passed through the alpha joint to Main Bus Distribution Assemblies (MBSA). The MBSAs are located at the transverse boom and keel crossing within

each PV Module. The MBSA then places this utility power onto the station's primary distribution network. The network common consists of upper ring feeders, lower ring feeder and feeders to each module. The ring and module feeders are powered from independent sources from opposite sides of the station as shown in Figure 3.4.5-1.

The upper and lower ring follows the perimeter of the space station truss structure. About every 100 feet, a Power Distribution and Control assembly (PDCA) provides a primary/secondary distribution tie point where station and user loads can attach. Each ring consists of a series of five PDCAs. Both ends of the rings are connected to the MBSA so that during normal operation each PDCA has four sources of power. The maximum power delivered to a ring is 52 kW. The primary distribution network feeders are sized at 13 kW.

Power is provided to each common module and pressurized payload by a line from each MBSA. Before utility power enters the module it is transformed to 208 VAC. Within each module there are five PDCAs. The power lines from adjacent modules are connected so that each module has at least four sources of power (two power lines from the MBSAs and at least two from adjacent module or modules). The maximum power delivered to each module is limited to 60 kW. The primary distribution network feeders that connects each module to MBSAs are sized at 30 kW.

3.4.5.2 Main Bus Distribution Assembly

Figure 3.4.5-2 shows a block diagram of an MBSA. As seen in this figure, the MBSA consists of a power bus which source power attaches onto and also has primary distribution network lines going to the upper ring, lower ring and to each common module. Each input source and output line is connected to a Remote Bus Isolator (RBI) which can isolate that line from the rest of the bus. An embedded data processor controls the assembly. The processor can detect, locate, isolate and reconfigure the primary distribution network through its control of the MBSA's remote bus isolators. More detailed functions of the MBSU controller are found in paragraph 3.4.7. It can be seen in the block diagram that the MBSA is packaged in two identical parts. Each part is called a Main Bus Switching Unit (MBSU) which is an Orbital Replacement Unit (ORU). The MBSU can be replaced in orbit without the loss of power to any ring or

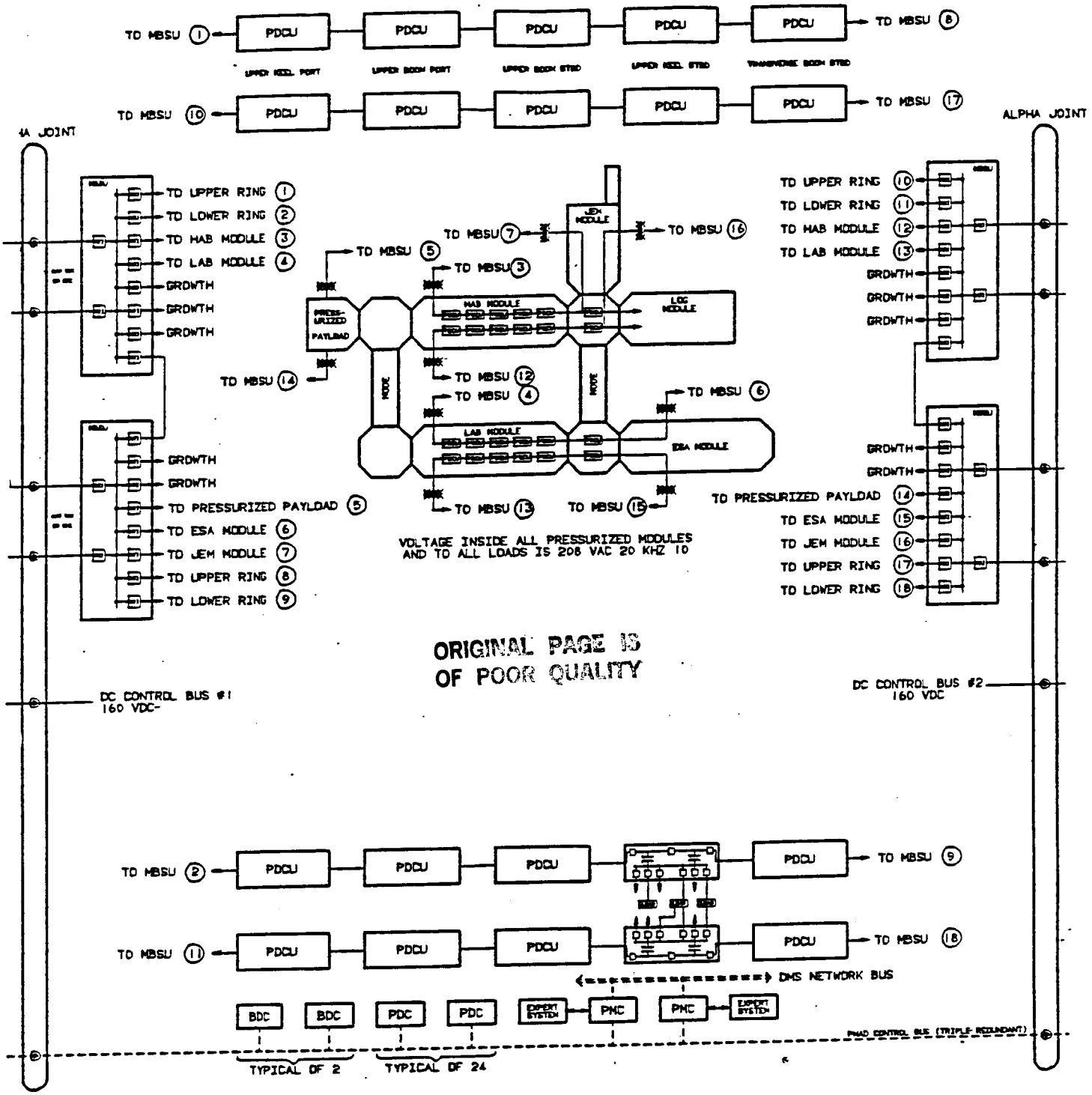

Figure3.4.5-1 Primary Distribution

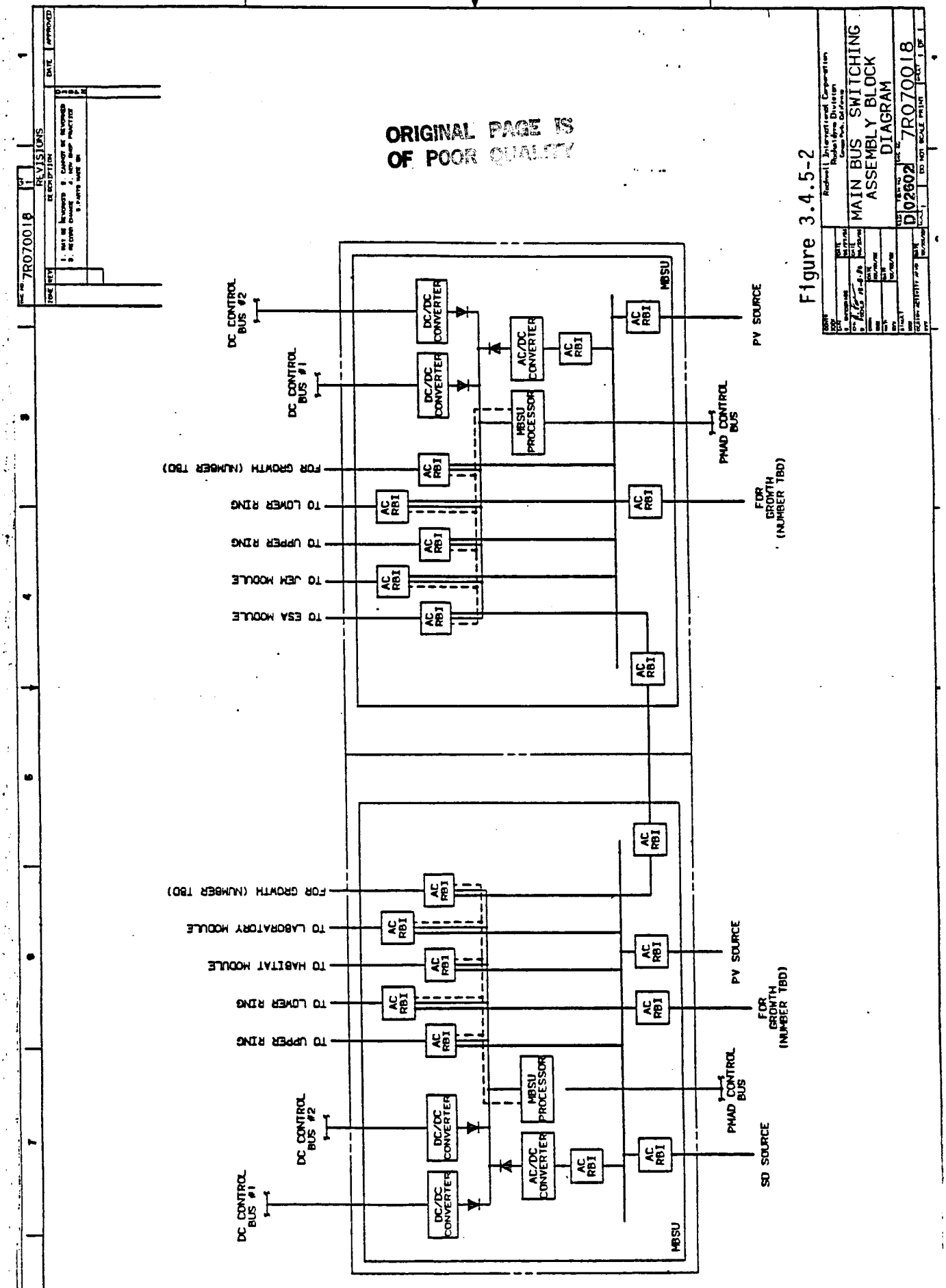
ORIGINAL PAGE IS
OF POOR QUALITY
MAIN BUS SWITCHING ASSEMBLY BLOCK DIAGRAM
D02602 7R070018
MBSU
DC CONTROL BUS #2
DC CONTROL BUS #1
DC/DC CONVERTER
AC/DC CONVERTER
AC RBI
MBSU PROCESSOR
PV SOURCE
PMAD CONTROL BUS
FOR GROWTH (NUMBER TBD)
TO LOWER RING
TO UPPER RING
TO JEM MODULE
TO ESA MODULE
TO LABORATORY MODULE
TO HABITAT MODULE
SD SOURCE

Figure 3.4.5-2

manned module. The busses within the two MBSUs are normally connected together but can be isolated from one another by opening up either RBI between them. The MBSA will have adequate capacity at IOC to handle the nominal 167.5 kW of source power which is expected for growth. Hardware and software within the MBSA will be sufficiently sized to handle all the manned modules which are expected to be installed onto the station during the growth phase.

3.4.5.3 Power Distribution and Control Assembly

The PDCA serves as a primary/secondary distribution tie point. The PDCA design goals were to: provide uninterruptable power to station and life critical loads at any location, have the ability to isolate a failed load from the rest of the system, be able to isolate the PDCA should it fail, shed loads in overloaded situations and to have commonality between all truss, common modules and platform mounted PDCAs. Figure 3.4.5-3 shows a block diagram of a PDCA. The features that can be seen in the design are: dual primary buses each with two independent sources of utility power thus provides a quad redundant source of power.

It can be seen in the block diagram that the PDCA is packaged in two identical parts. Each part is called a Power Distribution and Control Unit (PDCU) which is an Orbital Replacement Unit (ORU). The PDCU is designed so that it can be replaced in orbit without loss of power to critical loads.

The interface between the primary and secondary lines are through the Remote Power Controller (RPC) which can monitor, limit and disrupt if necessary the flow of power into the secondary lines which go to the station and user loads. Redundant RPCs can be used to insure a continuous source of power. One RPC can be used for a non-critical load and up to three RPCs can be used in parallel to service a critical load when desired. Each PDCA contains up to 36 RPCs, each with the capacity of controlling a load requiring 5, 25, or 75 amps.

Dual primary buses have RBIs on the input, output and in the middle of each primary bus which can isolate all or half of a primary bus within the PDCA if required. An embedded data processor controls the assembly. The processor functions are described in paragraph 3.4.7.

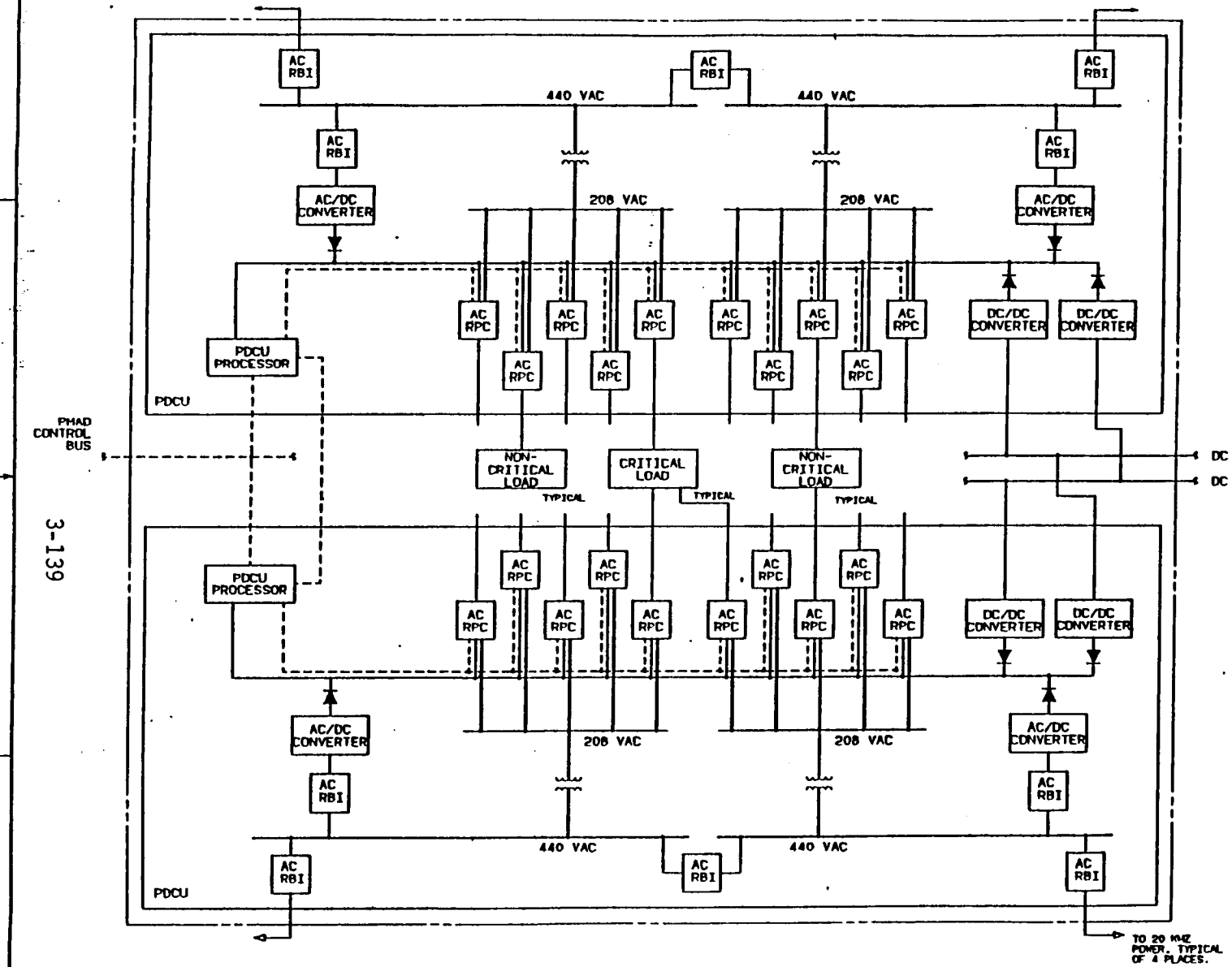

NOTE:
EACH PDCU CONTAINS:

(5) AC RPC (5A)
(4) AC RPC (25A)
(9) AC RPC (75A)

Figure 3.4.5-3

ORIGINAL PAGE IS
OF POOR QUALITY

REVISIONS

ZONE	REV	DESCRIPTION	DATE	APPROVED
		1. MAY BE REVERSED 2. CANNOT BE REVERSED 3. RECORD CHANGE 4. NOV SHOP PRACTICE 5. PARTS MADE ON		

Rockwell International Corporation
Rocketdyne Division
Canoga Park, California

POWER DISTRIBUTION AND CONTROL ASSEMBLY

ID 02802 7R070017

DO NOT SCALE PRINT

3.4.5.4 DC Control Power Bus

The Space Station contains a DC Control Bus which provides a limited source of uninterruptable power to PMAD's processors and control components. This bus is needed during initial start-up procedures of the PMAD system or during the unlikely event of loss of all AC power when all the SD and PV sources are off or failed. The DC Control Bus obtains its power from the PV Module's batteries. This power is then distributed using dual buses to all EPS equipment throughout the station as shown. The voltage on the bus is 160 VDC. Within each PMAD ORU are redundant DC-DC Converters which provide low voltage DC power that processors and control components require. Normally, PMAD ORUs will not use this bus and its associated DC-DC Converters as a source of power. Under normal operation, ORUs are powered from redundant AC-DC converters using utility AC power.

3.4.5.5 Alpha Joint Roll Rings

Electrical power from PV and SD sources are paralleled outboard of the alpha joint at the ACSU. The output of the ACSU must pass through alpha joint roll rings to the MBSA which is located inboard of the alpha joint. In addition, DC control power and PMAD control bus must also pass through the alpha joint roll rings.

3.4.5.6 Power Distribution System Components

3.4.5.6.1 Remote Bus Isolator

Remote Bus Isolator (RBI) consists of an embedded microprocessor controlled high-power "smart switch" that is used to protect the primary feeder lines. A simplified block diagram of a RBI is shown in Figure 3.4.5-4. Each RBI unit contains a hybrid switch in which a semiconductor makes or breaks the current and a parallel fast-acting mechanical contact provides low loss during switch conduction. The semiconductor switch is implemented with a pair of SCRs. Several switch elements are interconnected to provide a switch function having high internal fault tolerances. The RBI also contains a current limiter circuit which will limit fault current to three times the maximum bus current.

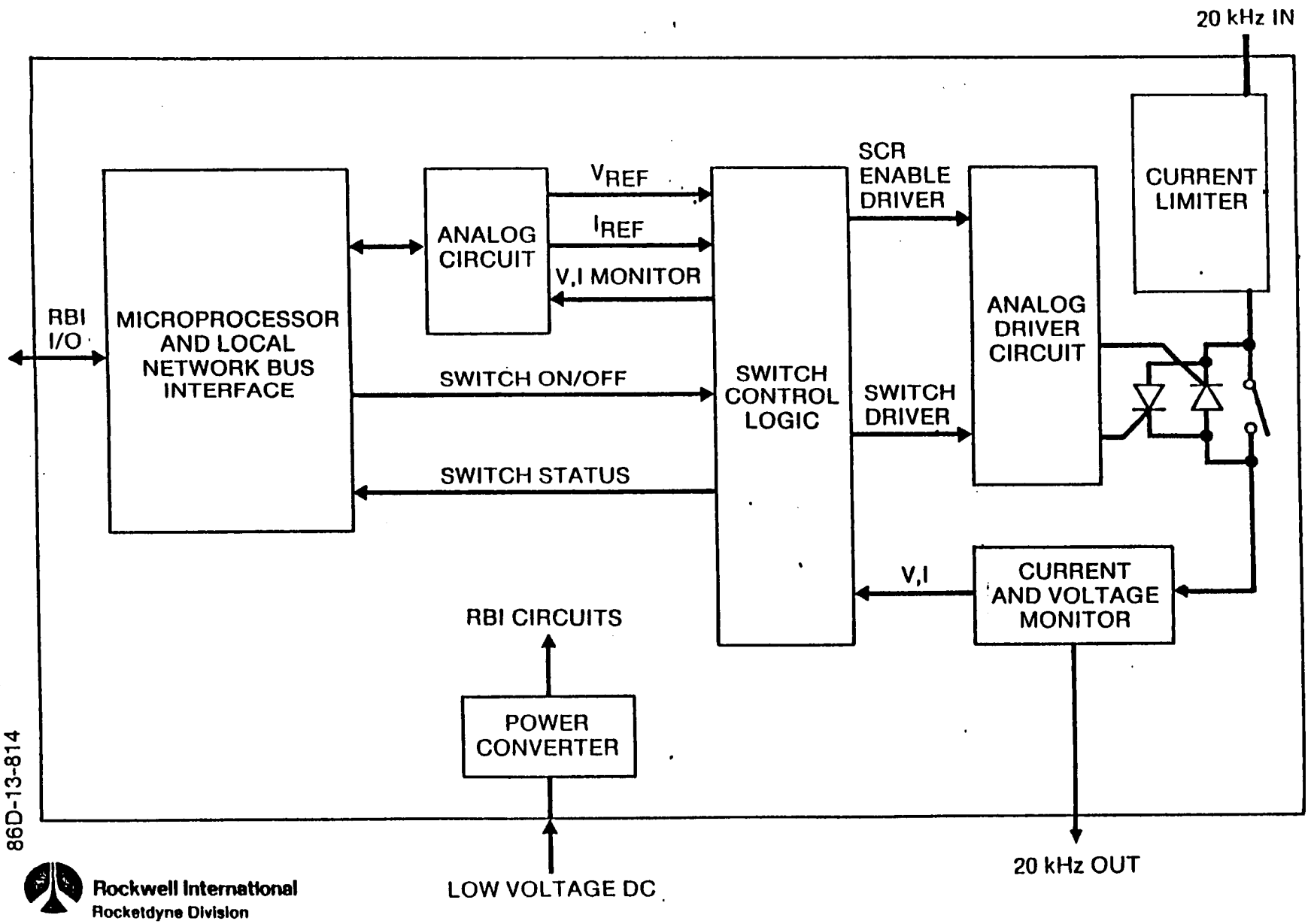

Figure 3.4.5-4. Remote Bus Isolator Block Diagram

If a fault occurs the RBI will sense the fault current over programmed levels and for ten milliseconds this current will be limited. While the current is being limited, the mechanical switch is commanded to open. The mechanical switch will fully open within 10 milliseconds. Then the SCRs will stop conducting, thus terminating current flow and preventing arcing across the mechanical switch contacts. The microprocessor is used to control the switch, using voltage and current data to provide bus fault isolation. All digital information to and from the RBI is processed by the respective PMAD processor. Five RBI control signals are transferred over the RBI/MBSU or PDCU processor local network bus. They are:

1. voltage
2. current
3. phase angle by which the current leads or lags the voltage
4. on/off commands
5. status of the RBI (on/off)

The periodically measured values of current, voltage, and phase angle are transmitted from the RBI to the MBSU/PDCU processor for use in the State Estimator or Load Flow. The phase angle is measured by the RBI using an isolated voltage sensing winding and the current signal in a phase comparator circuit.

3.4.5.6.2 Remote Power Controller

Remote Power Controllers (RPC) are microprocessor-controlled "smart switches" that are used in PDCAs as fault detectors both to protect the load and to protect the PDCA equipment. Figure 3.4.5-5 is a block diagram of an RPC. Each RPC contains a fast acting switch implemented electronically with a pair of SCRs. Within the RPC are voltage and current monitors, switch control logic, analog circuits and a microprocessor. During use, the microprocessor monitors the voltage across and the current through the load. If the load current exceeds preset programmable limits, the switch control logic will disable the switch and the load fault can be isolated from the 20 kHz power in 25 microseconds. This makes fault isolation inherently quite safe and because a solid state switch is used no arcing will occur. Over/under voltage protection is implemented the same way.

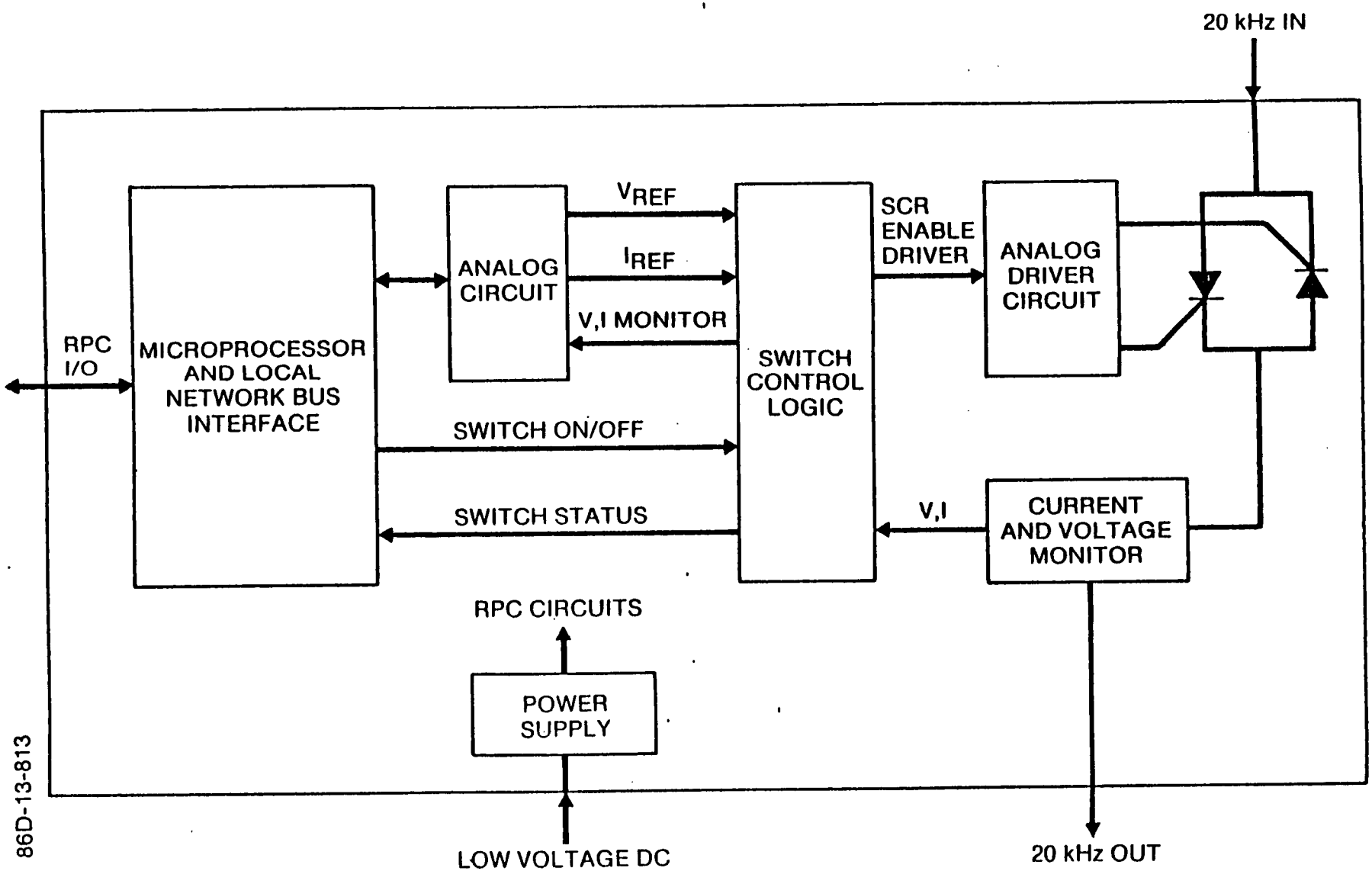

Rockwell International
Rocketdyne Division

Figure 3.4.5-5. Remote Power Controller Block Diagram

Current limiting is not required since the switch isolates the fault as fast as it takes to switch in a current limiting inductor. All digital information to and from the RPC is processed by the PDCU processor. RPC control signals are transferred over the RPC/PDCU processor interface local network. They are: voltage and current parameters, trip setpoints, on/off commands, status of the RPC (on/off) and an interrupt indicating a trip has occurred.

3.4.6 Power Management and Control System

3.4.6.1 System Overview

The power management and control system is designed for automatic and autonomous operation to control the overall electrical power system (EPS) with minimum operator interaction. The control system functions include:

- Startup and shutdown operations,
- Source paralleling and synchronization
- Peaking operations
- Energy storage management
- Real and reactive load sharing between sources
- Voltage and frequency regulation
- Load management (balancing, scheduling, shedding)
- Fault detection and isolation
- System health monitoring

The implementation of the various functions will use closed loop analog controls in local areas or ORUs where appropriate which are further controlled by the overall EPS control system.

At the heart of the EPS control system is a hierarchical set of communicating processors and controllers which manage, coordinate, and control each part of the EPS. See Figure 3.4.6-1. At the top of the hierarchy are the dual redundant power management controllers (PMC) which are the EPS's interface with the data management system (DMS) global data bus which provides data access to other Space Station subsystems. The PMC communicates with other controllers by means of a dual redundant PMAD control bus. These other controllers include power source controller (PSC), power distribution control unit (PDCU) controller (PDC), main bus switching unit (MBSU) controller (MBC).

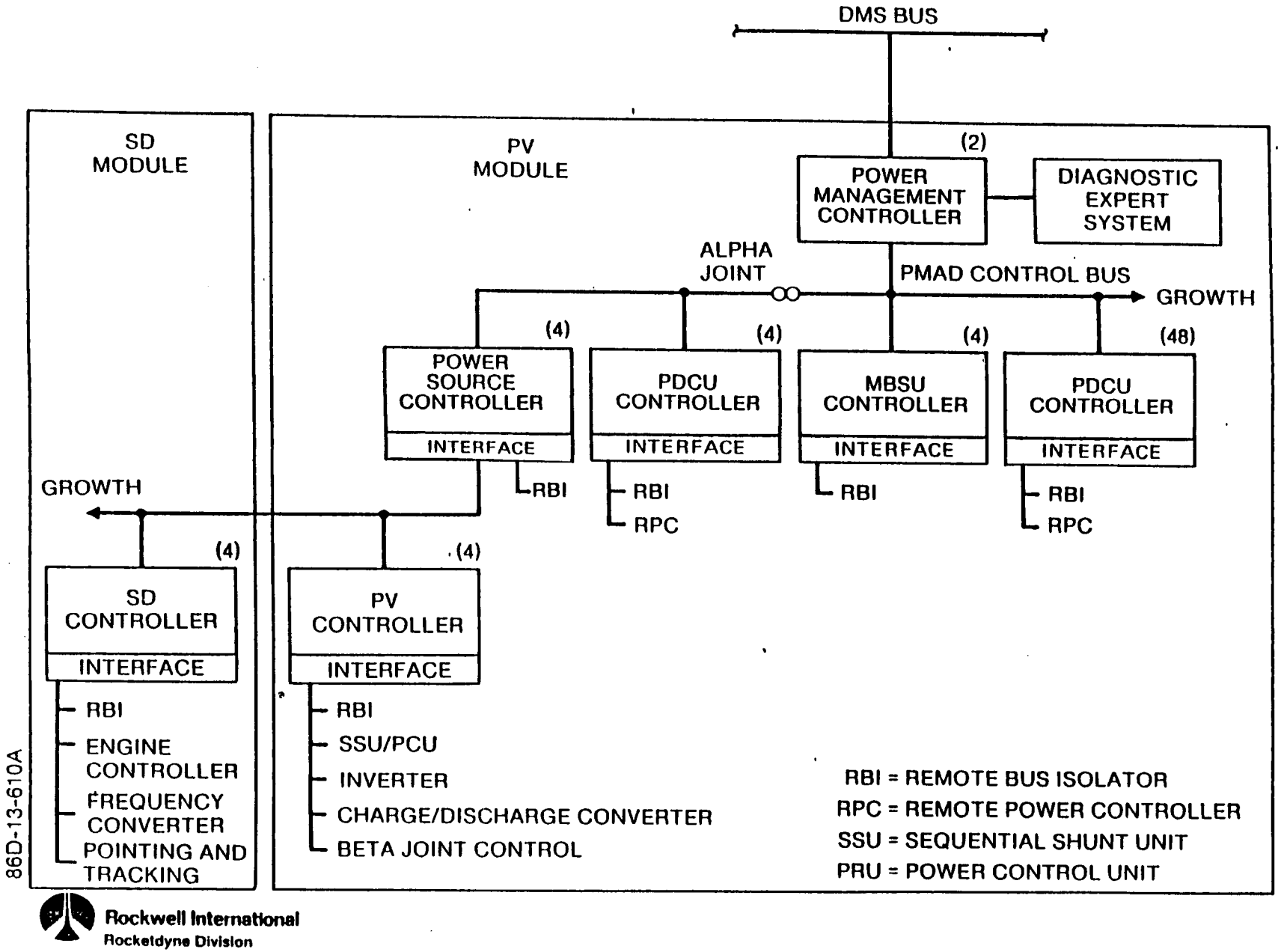

Figure 3.4.6-1. PMAD Control System

The PMC collects EPS data on operating parameters and is sized to eventually grow to include expert system capability. The PSC controls and communicates with all of the PV and SD power generation modules on a local data network outboard the alpha joint. The MBC controls and manages the primary distribution network. The PDCs each control a group of 18 RPCs and 3 RBIs in each PDCU. Two PDCUs are located together to form a PDCA and each PDC is capable of controlling the entire PDCA.

The hierarchical network of controllers used in the system, along with the monitoring capability of the EPS, allows for extensive use of control system analyses and algorithms that will maximize electrical power availability to Space Station users. Maximizing power availability is the main purpose of PMAD.

The following sections will describe the various control system functions and analyses that will be used, where the algorithms and input/output will be performed, and a description of the hardware that will be used. Associated software is described in Section 3.4.7.

3.4.6.2 Power System Control and Analyses

From one point of view, the EPS is basically an electric utility system, similar in many ways to terrestrial utility networks. Many of the methods of power system analysis that have been applied to land-based systems can and will be used on the Space Station EPS. These analyses will be modified and adapted appropriately to incorporate the unique features of the EPS.

The Space Station differs from terrestrial systems in that two independent sources of power are available at each load center area (PDCA). These sources are single phase, 20 kHz, operate independently, and are controlled separately. Instead of rotating machines, the Space Station AC sources are electronic power supplies which strongly limit available fault current. Each load circuit is also controllable by the EPS via RPCs, a luxury not enjoyed by land-based utilities. These special features complicate the load management functions but allow much improved load prediction and scheduling. Power generation and control is complicated by the sunlight-eclipse orbit cycles which introduce energy storage requirements.

The Space Station EPS will be designed with centralized system control. The overall system control program has been designated as the Automatic Dispatcher and it will use many of the same power system analysis programs used by the human dispatcher on land-based utility system. The Automatic Dispatcher will perform normal monitoring functions and take action for load and generation control As a system evaluation tool, the dispatcher will rely on various other programs as required to make system decisions.

Some of the power analyses that will be utilized include state estimation, load flow, and contingency analysis. The following subsections will describe these areas as they apply to the Space Station. In addition, load control, fault protection, and system voltage control is described.

3.4.6.2.1 State Estimation

The State Estimator (SE) program will be used to monitor the power system, detect bad measurements, and will provide reliable data input needed by other control functions. The State Estimator, for either the port or starboard power system, will utilize power flow measurements from:

28 transmission lines, 2 measurements each	= 56
24 PDCU load measurements (injections)	= 24
4 redundant PV and SD (injection) measurements	= 4
Total power measurements	= 84

For every scan cycle, real and reactive power flow measurements will be calculated from RBI data transmittal to the appropriate PMAD processor. With each measurement it is essential to determine the phase angle between voltage and current or their equivalent products (measured real and reactive power), so that the SE may estimate the power system phase angles.

Transmitting RBI current, voltage and their relative phase angle difference allows this data to be used in the Network Fault Protection and voltage monitoring programs in addition to the SE.

The State Estimator will output

- Periodically, e.g. every 3 minutes
- On demand by operator or Expert System
- In the event of a status change of any source, line, or device on the power system
- In the event of fault protection circuit operation.

3.4.6.2.2 Load Flow Analysis

The load flow analysis is used as a redundant back-up program to the state estimator program to calculate the state of the power system and as an on-line study tool for operators of the space station and for the automatic dispatcher.

The input quantities to the load flow analysis are the network connection file (topology), the transmission line parameters of each line (R,L,C,G), and the measured power injections at each load point. From this information, the Load Flow Analysis program calculates the state of the power system - i.e. the voltage magnitude and phase angle at every load point (Bus) of the power system. With the calculated state, the Load Flow then calculates line current flows. The bus voltage magnitudes and line flows are compared to nominal (rated) values and alarms triggered if there is a violation of operating limits.

Because it uses only measured power injections and line parameters, the Load Flow employs a small subset of the measurements which drive the State Estimator. Therefore, the Load Flow Analysis can be used to verify the State Estimator output or conversely, the State Estimator estimated injections may be used to calculate the state. If there is a failure in the State Estimator (non-convergence, or software problems), the Load Flow program can supply the state information for contingency analysis and other performance monitors.

The study mode is another way the Load Flow program is employed. The Space Station operator or automatic dispatcher can ask the Load Flow to calculate the exact effect of adding or subtracting another load or transmission line for the present operating conditions of the power system. There are also stored data files which may be part of the Load Control, either automatically called or

called by the operator, modified as desired, then executed by the Load Flow. These files may represent future cases. The Load Flow results of these studies are more accurate than linearized contingency results.

For the space power system, the following conditions hold:

1. At 20 kHz operating frequency, the power system transmission lines have a 1:1 ratio of line resistance to inductive reactance
2. There may be 10:1 ratios of long line lengths to short line lengths connected to the same bus (load point).
3. The power system topology (inter-connection of power transmission lines) may change from a ring type to a radial type during operation.

Each of these conditions may cause convergency problems during the solution by the load flow algorithms, and are best dealt with by using the Newton Raphson method. The Newton Raphson iterative algorithm is quite robust, in that it will converge quickly from inaccurate starting conditions.

3.4.6.2.3 Contingency Analysis

The Contingency Analysis and Configuration Control (CACC) is a periodically executed program in the PMC computer. The purpose of the CACC is to set options within the Automatic Dispatacher depending upon the present state of the power system.

The state of the power system voltage and phase angle at each bus is obtained from the State Estimator program. The topology, or present configuration of the power system is also obtained from the State Estimator.

A list of single, double and triple contingencies is used to determine the loads presented to each generating source, high or low voltages, and excessive current flow in a network branch. A list of single contingencies might begin with:

- Loss of port SD
- Loss of port PV
- Open port line MBSU to Hab module
- Loss of load in pressurized payload

The double contingencies list might begin as:

- Loss of port SD and PV
- Loss of both port lines to Hab module

The results of the contingency calculations are passed to the Automatic Dispatcher which implements a reconfiguration of the power system topology if the contingency should occur at this time.

3.4.6.2.4 Power System Monitoring and Data Acquisition

In order to perform the various power system analysis, system parameters must be monitored and passed on to the power management controller (PMC) for storage in a data base to be used by the analysis programs.

All data points scanned by the PMC shall be subdivided into 5 programmable scan groups. The scan priority and the individual scan frequency should be programed and assigned on an individual level. The following groups are essential:

- Group 1 Status Data Examples are RBI open/closed, voltage high/low, current high/low. Data base updated each cycle.
- Group 2 Analog Data PV & SD sources, frequency changer, converter
- Group 3 Analog Data Examples are current flows, voltages, and other variables which have alarm thresholds activated before shut-down point.
- Group 4 Integrated Data Variables such as watt-hr from batteries, generator watt-hr
- Group 5 Non-essential status and analog points

Each scan point will have the capacity of being removed from the scan cycle when it is out of service or not being used. Critical scan points such as status of PV and SD, etc. will be verified for change commands and will have time delays to allow check by other programs.

Analog points scanned will be converted to other engineering units as necessary and stored in the database. The following limits will be checked:

1. High and low reasonability limits representing normal operation.

2. Alarm limits, outside of category (1), these are limits which activate alarms. Display and logging of the alarm will take place and a counting cycle will be started. If the analog point remains out of limits for a programmed number of cycles, corrective action will be initiated. Notice that switching transients or other noises can cause a false alarm that disappears.

3. Rate-of-change limits could be imposed on some date points to detect catastrophic failures. The change over a number of scan cycles would establish the criterion.

This data processing is called a SCADA system for ground-based power systems (Supervisory Control and Data Acquisition). On the Space Station, the PMC will store the database of the existing system, update it each scan cycle, and will call the automatic dispatcher or other programs.

The PMC sets system alarms in a priority list:

1. Immediate action by opening switches to load or line

2. Call automatic dispatcher for corrective action. In decreasing order of importance they are:

    a. Switch excessive load to another source (load balance)
    b. De-energize the excessive load (load shed)

3. Implement other automatic dispatcher actions.

4. Warn the space station operators.

3.4.6.2.5 Load Control

Since each side of the space station is normally operating independently, the loads must be evenly divided up between these two power sources. At a given power level, the feeders from the sources suppling a common area should also be loaded evenly to minimize line losses, thereby making more power available to users.

During emergencies or casualty conditions when power sources or sections of the distribution system are lost, loads must be shed to correspond to the generating capacity and then rebalanced.

Load scheduling is necessary so that the system is balanced and power is made available to the appropriate loads at the proper time to correspond with the space station activity schedule.

3.4.6.2.6 Fault Protection

System fault protection and isolation is one of the most important functions of the overall EPS control. Sound design of an EPS must be predicated on the assumption that equipment will fail, people will make mistakes, and that "acts of God" will occur. The function of system protection is to minimize damage to the system and its components and to limit the extent and duration of service interruption whenever equipment failure, human error, or the incredible occur on any portion of the system. Since the Space Station EPS is a critical system that is needed for life safety and mission success, the protection system must be designed to provide the highest possible degree of reliability and availability. The system must be designed to protect against any system abnormalities which could reasonably be expected to occur in the course of system operation. There are several methods available to minimize the effects of abnormalities on the system itself or on the utilization equipment (loads) which it supplies. The protection system design should include features which will:

a) Quickly isolate the affected portion of the system while maintaining normal service for the rest of the system and minimizing damage to the affected portion.

b) Minimize the magnitude of the available short circuit current to minimize potential damage to the system, its components, and the utilization equipment it supplies.

c) Provide alternate circuits, automatic thowover devices, and automatic reclosing devices where applicable to minimize the duration and extent of supply and utilization equipment outages.

Protection of the EPS is designed with the following objectives:

a) prevent injury to personnel

b) prevent or minimize damage to equipment

c) minimize interruption of power

d) minimize the effect of the disturbance on the uninterrupted portion of the system, both in extent and duration

e) minimize the effect on the power sources

Protective equipment is used to detect system abnormalities and then to promptly remove the affected portion from the system. This equipment consists of remote bus isolators (RBIs) and remote power controllers (RPCs) which function to both detect system parameters and to switch open or closed, as required, to isolate the circuit affected. Power management controllers (PMCs), power source controllers (PSCs), photovoltaic (PV) controllers, solar dynamic (SD) controllers, main bus switching unit (MBSU) controllers (MBC), and power distribution and control unit (PDCU) controllers (PDC) are used to monitor and control RPCs and RBIs and the overall system operation. The protection system should be as simple as possible in order to maximize reliability. This will dictate that the protection system should be hardware implemented and reliance on the processors and associated software kept to a minimum. The method used for the protection is also dependent on the distribution system configuration or on the particular portion or zone of the system being protected. Figure 3.4.6-2 indicates some typical fault protection zones for the PMAD system. Each zone overlaps so that the total system is protected. Each should have a primary and a backup method for fault detection.

Differential protection methods are expected to be used in several areas on the Space Station. The differential method measures and sums currents flowing into and out of the protected zone. If the net current is not zero (or the expected leakage current) then the protective devices for that zone would operate to isolate that portion of the system. This method is effective in detecting and isolating both hard faults (low impedance) and soft faults (high impedance) that are greater than the differential current setpoint. This method is sensitive, high speed, and permits complete overlapping of protective zones. Differential protection will be used for most power distribution orbital replacement units (ORUs) such as the MBSA and PDCA. These zones are relatively compact and hard wiring of the differential sensors and the RBIs will be utilized.

The power feeder network will also utilize differential protection since the Space Station power distribution architecture is the ring network type With the ring network, currents can flow in parallel paths and can also change direction of the power flow making a differential type protection scheme appropriate. Typical radial feeder protection methods would not be selective in isolating only the affected portion of the network. For example,

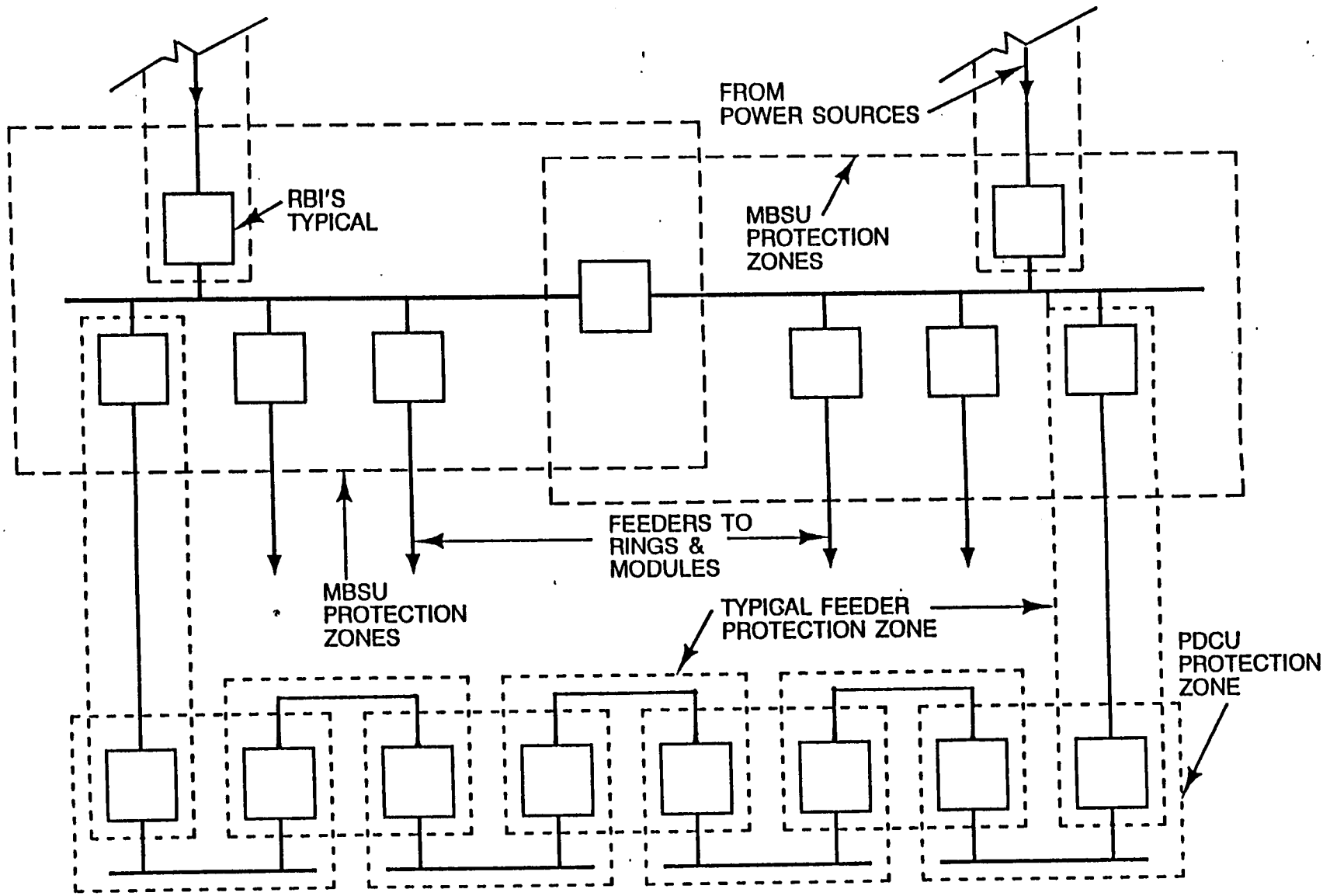

Figure 3.4.6-2. Zones of Protection

overcurrent methods used on the ring network would cause all RBIs on the ring to open when fault currents are present thus causing power outages on the non-faulted sections. The feeder protection system will also be a hard wired system. The necessary control wires will be integrated into the feeder cables. The backup protection for feeders will be the impedance method which detects a change in line impedance due to a fault. Appropriate time delays would be designed to permit the primary differential protection to act fast.

Fault protection methods must also include consideration for the source characteristics. Inverters and frequency converters are used to supply 20 kHz power to the power distribution network. As mentioned in the inverter and frequency converter sections, this equipment can respond to a hard fault condition in approximately half a cycle or 25 micro-seconds. This may be too fast for detection of down stream faults so that they can be isolated. The converters will be operated such that upon detection of a fault condition by the converter, the converter would shift to a constant power mode allowing the voltage to drop and currents to continue to flow thereby allowing the system time to detect and isolate the affected portion. This mode of operation would be limited to less than the required 50 milli-seconds specified in power quality. If the condition lasted longer than 50 milli-seconds, it would be indicative of a protective system malfunction and the converter would shutdown to protect the system.

3.4.6.2.7 Voltage Control

Voltage control of the overall distribution network of the EPS is a combination of local closed loop control and system wide digital control loops. The DC source bus voltage is maintained (during sunlight) by the closed loop control of the SSU/PVCU combination. During eclipse, the DC source bus voltage is regulated by the discharge converter in the BCDU. The voltage reference maintained by these control loops is received from the PV controller via the data interface in the PVCU and BCDU. The voltage setpoint will be determined by the PV controller and is dependent upon scheduled loading conditions (peaking), energy storage state, location in the orbit, and array state.

The SD alternator also employs a closed loop voltage control on its output. This voltage is maintained to a setpoint received from the SD controller and will be relatively constant but can be adjusted as necessary.

The AC system voltage is dependent upon the output voltage of the AC sources, i.e., the DC-AC inverters and the frequency converters. Each of these units employs closed loop control on its output voltage. The system reference voltage is computed by the power management controller (PMC). Voltage at each bus (PDCU) in the system is monitored and maintained within specification by adjusting voltage at the MBSA via the source converters setpoint. Figure 3.4.6-3 is a block diagram of the voltage control scheme. The reference voltage computed by the PMC can use actual voltage measurements or values from the state estimator. The computed reference voltage is then sent to the power source controller (PSC) and a reference voltage setpoint for each of AC converters is computed. This individual reference voltage setpoint is passed on to the units via the PV controller and the SD controller appropriately. The PSC also receives the output current data of each converter and adjusts the reference voltage setpoint as required for load sharing between the converters. The load sharing between converters will be dependent upon the load schedule, energy storage state, location in the orbit, engine state, and array state.

Voltage at each bus (PDCA) will vary according to the load applied and the network configuration. These parameters will be changing slowly (i.e. not milliseconds) thus the data speed requirements are not critical. Bus voltage data updates can be accomplished routinely as part of the PMC normal functions. Severe voltage fluctuations which would indicate a problem would be detected and will interrupt the PMC normal routine and correction action taken when detected.

3.4.6.3 Health Monitoring System

Special sensors will be located through the Space Station to monitor the operational performance of key components and subsystems. The purpose of this instrumentation is to assist PMAD in maintaining the operational health of the power generation and distribution systems. In this role, the health monitoring instrumentation and associated processors will be used for line fault

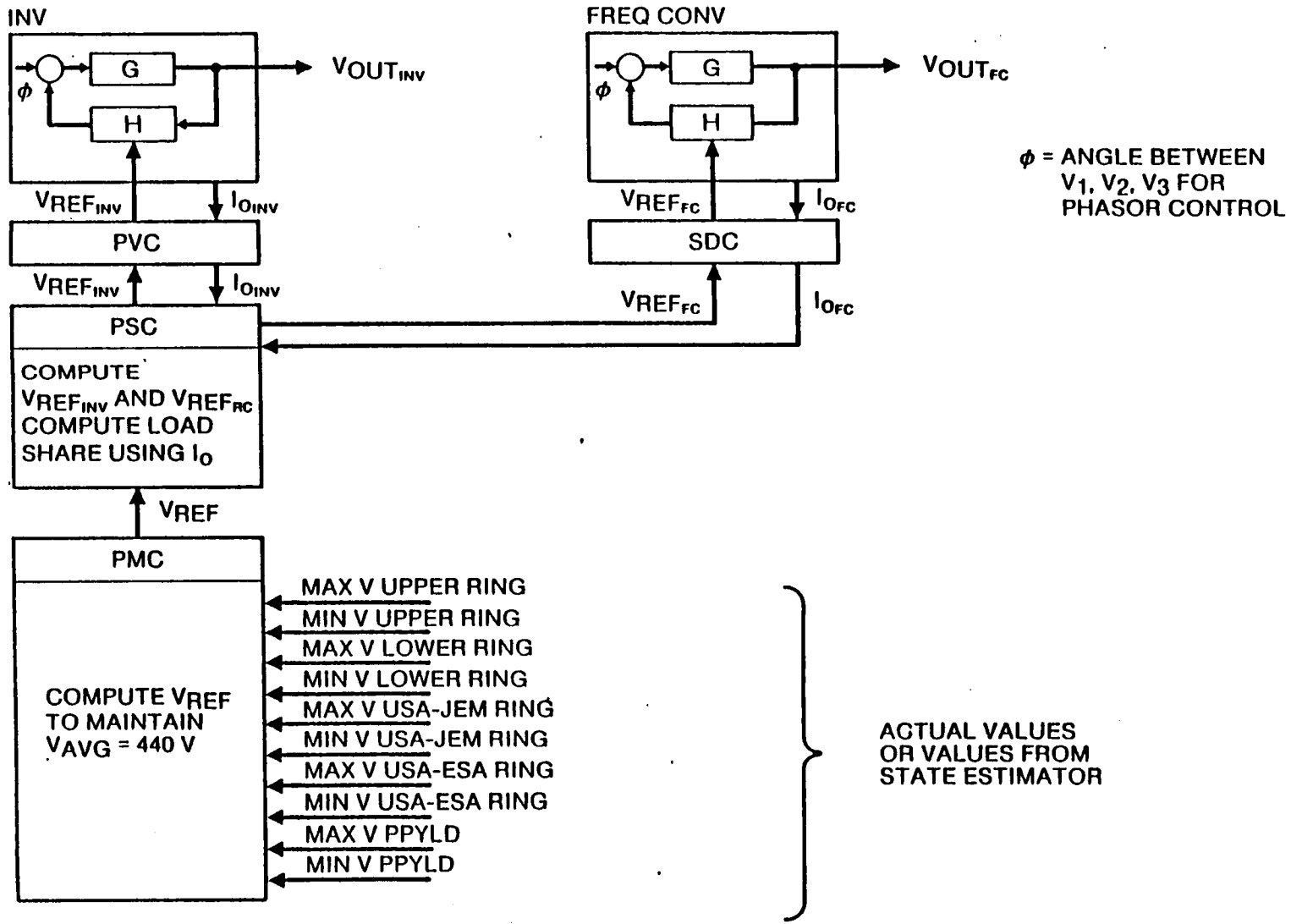

Figure 3.4.6-3. Voltage Control Block Diagram

troubleshooting/identification and, where possible, point the way to corrective action required to restore normal station operation and power distribution for the IOC. In the growth option, the diagnostic function of the health monitoring system will be expanded to include a prognostic role with trend analysis to predict component/subsystem performance and remaining useful life.

Provision to measure node currents and voltages in all remote programmable controllers and main line feeder switch gear for power management and control offers additional performance data to the off-line fault identification/ troubleshooting and maintenance requirement of health monitoring. For example, an open solid-state circuit in the hybrid switch of a remote programmable controller would result in contact degradation after a few on-off cycles.. The degraded contact condition would be noted by a rapid increase in the voltage across the contacts. The Power Management Controller (PMC) would be informed of the contact status.

Monitoring of potential ground fault currents with associated bus line interrupt if set limits are exceeded will be used to provide crew-safety and equipment protection. Since an open ground line would defeat the safety features of the line.fault monitor, verification of ground line continuity will be provided.

A log of peak power and overvoltage conditions indicating magnitude, time, and duration will be taken to provide a data base for safe, efficient power management and control. These data will also be used to assist in determining a cause in fault and failure analysis as well as provide a guide to appropriate corrective action.

The Space Station power generation and distribution reliability will be improved with the addition of an effective health monitoring prognostic system that has access to pertinent trend data on overall line power quality and a history of specific environmental conditions that components/subunits have experienced. For example, power system limit exceedances of line harmonics, oscillations, transients, power factor, and regulation will be measured and stored during limit exceedances. These data will be used for trend analysis because component life is generally degraded when subjected to excessive transient/oscillatory currents or voltages. In addition, temperature sensors

will provide a thermal stress history that key components/subunits experience. An improvement in overall reliability is due to the fact that operational trend data will be used to provide decision criteria to replace a part due to a change in system performance or predicted component/subunit failure.

These trend data together with a history of other environmental data affecting the operational life of the hybrid switch could be used in an expert-type monitoring system that would automatically analyze, evaluate, and determine the remaining useful switch life.

3.4.6.4 Power Management and Control System Hardware

The Power Management and Control System hardware consists of a standardized set of components which will be designed by Work Package 02. Details of Work Package 02 design is not well known at this time. However, the Architectural Control Document for the Space Station Data Management System does specify that the following hardware will be provided to all work packages:

Standard Data Processor
Embedded Data Processor
Network Interface Unit
Bus Interface Unit
Multiplexer/de-multiplexer
Dedicated Control Bus
Local control bus

The standardized set of components will probably be fabricated using CMOS technology and will use VSLI circuits to reduce printed circuit board size and increase reliability. All components will be cold plate cooled, will have I/O protection and include built-in test equipment (BITE).

3.4.7 Software

The PMAD software was designed to operate in a hierarchical network structure with the Power Management Controller (PMC) at the highest level, the Power Distribution Control Unit (PDCU), the Main Bus Switching Unit (MBSY), and the power Source Controllers (PSC) at the next lower level, and the Photovoltaic (PVC) and Solar Dynamic Controllers (SDC) at the lowest level.

The PMC is the only controller in this network that can communicate with the Data Management System (DMS). Figure 3.4.7-1 shows the hardware configuration for this hierarchical structure.

3.4.7.1 General Software Design

The software in each controller falls into two general categories: executive software and PMAD application software.

The executive software is the same in all controllers and contains the functions necessary for booting/loading programs and/or data and for scheduling the various PMAD application functions. It also provides the interface handlers that allow each controller to communicate with its higher and/or lower level controllers and the I/O devices attached to it.

The PMAD application software is controller specific. Each controller contains only those PMAD application functions that have been allocated to it to allow it to perform its assigned tasks. Some of these functions are the same for all controllers, some are very similar, and some are unique. Figure 3.4.7-2 shows the allocation of the PMAD functions by controller.

3.4.7.1.1 PMC Functional Description

This controller provides the overall power management control and data reduction for the station-wide electrical power system. It accepts both flow control and data from the DMS. It provides only data to the DMS.

3.4.7.1.2 PDCU Functional Description

This controller performs local load balancing and scheduling/shedding operations. In general each PDCU controller data base will include but not be limited to the following information:

a) the present load configuration
b) component failure status
c) history of voltage and current levels at test points

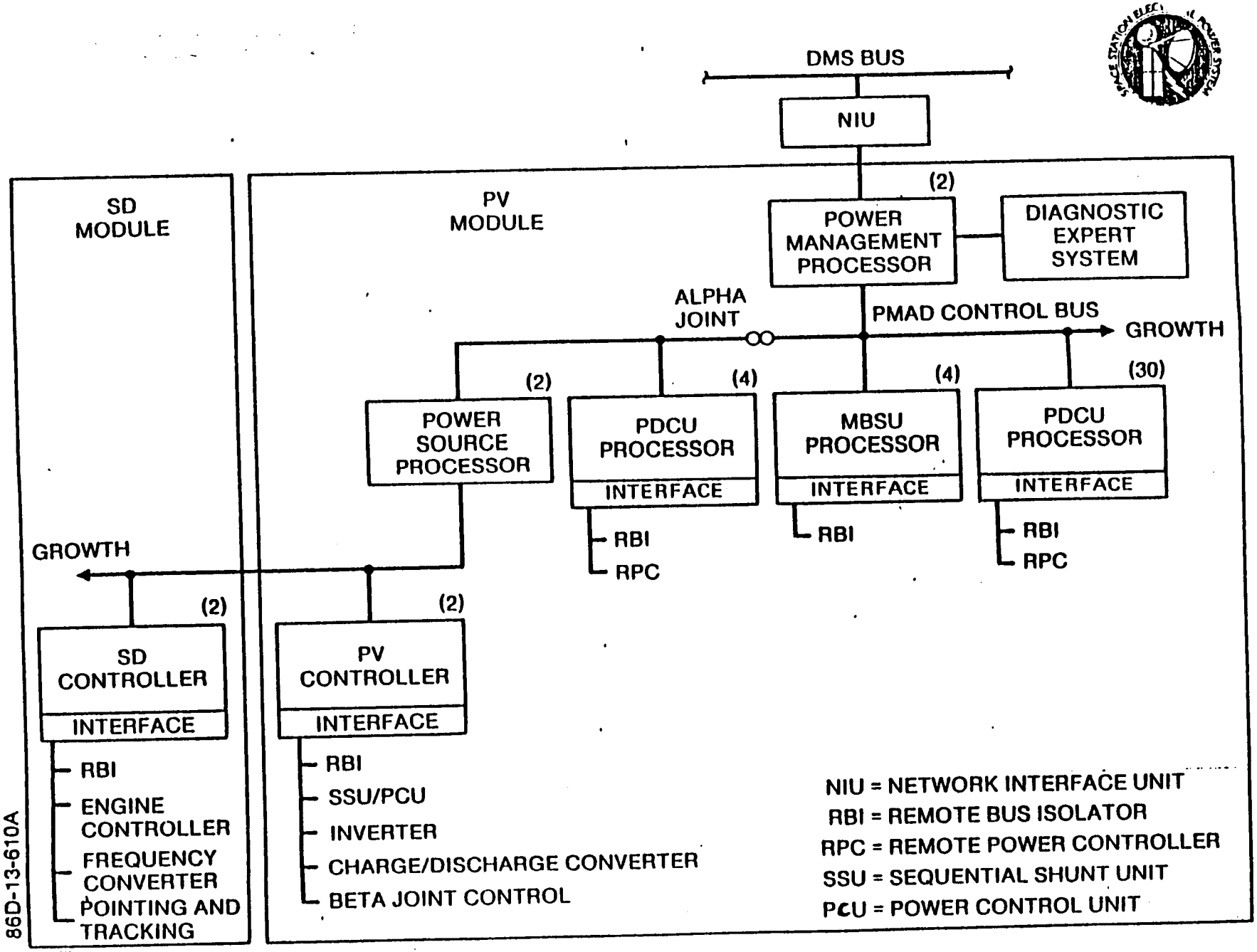

Rockwell International
Rocketdyne Division

Figure 3.4.7-1. EPS Controller Hierarchical Network Structure

	<-------CONTROLLER------->					
PMAD FUNCTION NAME	PMC	PDCU	MBSU	PSC	PVC	SDC
Array Control					X	
Automatic Dispatcher	X					
Battery Control					X	
Configuration Control	X	X	X	X	X	X
Data Base Updater		X	X	X	X	X
Default Operations	X	X	X	X	X	X
DMS Interface Handler	X					
Emergency Procedures	X	X	X	X	X	X
Engine Control						X
Expert System Interface	X					
Fault Detection	X	X	X	X	X	X
Health Monitor	X	X	X	X	X	X
Internal Redundancy Management	X	X	X	X	X	X
Load Flow Management Control	X					
Load Flow Management Support		X	X	X	X	X
Load Scheduling/Shedding	X			X	X	X

Figure 3.4.7-2a. Allocation of PMAD Functions by Controller

	<-------- CONTROLLER -------->					
PMAD FUNCTION NAME	PMC	PDCU	MBSU	PSC	PVC	SDC
Local Load Balance		X	X			
Local Load Scheduling/Shedding		X	X			
Operational Executive/Utilities	X	X	X	X	X	X
Peaking Scheduler	X			X	X	X
PMC/MBSU Interface Handler			X			
PMC/PDCU Interface Handler		X				
PMC/PSC Interface Handler				X		
Pointing and Tracking Control	X			X	X	X
Preventive Control	X	X	X	X	X	X
PSC/PDCU/MBSU Interface Hdlr	X					
PSC/PVC Interface Handler					X	
PSC/SDC Interface Handler						X
PVC Device Interface Handler					X	
RBI/RPC Device Handler		X	X			
ROM Executive & Utilities	X	X	X	X	X	X
SDC Device Interface Handler						X
Source Control	X			X	X	X
System State Estimator	X					

Figure 3.4.7-2b. Allocation of PMAD Functions by Controller (concluded)

d) history of load voltages and currents
e) history of diagnostic sensor information
f) default configuration settings in case of abnormal conditions

3.4.7.1.3 MBSU Functional Description

This controller acts as the interface between the PMC and switch controllers (e.g. RBI's and RPC's) for the main power buses. It removes some overhead from the central controller by performing routing operations associated with the main power distribution system.

Two MBSU's combine to form a main bus switching assembly (MBSA) and within the MBSA's data base will be information:

a) the current active power bus configuration
b) component failure status
c) voltage and current levels at test points
d) other data determined to be useful for configuration selection

3.4.7.1.4 PSC Functional Description

This controller performs the following functions:

a) coordinates power generation and energy storage between the PV and SD modules
b) routes pointing and tracking data to the PVC and SDC
c) coordinates power switching and utilization outboard the alpha joint.

3.4.7.1.5 PVC Functional Description

This controller provides control of the actuators, relays, and sensors connected with the PV beta joint, power generation, thermal control, and energy storage. It provides the interface between the power source controller and all PV control/data components.

3.4.7.1.6 SDC Functional Description

This controller coordinates all power generation operations, associated thermal control, beta joint position, fine pointing actuators, and monitoring of sensor data.

3.4.8 PMAD On-Orbit Assembly

3.4.8.1 PV Module (IOC)

The launch package for flight one consists of one PV Module. This package is capable of generating and distributing 4 kW of power and includes a fully operational sources PMAD subsystem.

Special Shuttle/PV module connections are required during on-orbit assembly. These connections consist of a data link and a power line. The data link will connect a command console within the Shuttle to the PMAD control bus. This link will provide communication to the PMAD controllers until the DMS is operational. The power line (160 VDC 500 watts) will provide initial PMAD start-up power until the energy that is stored within the PV modules batteries can be utilized.

Once deployed, the PMAD requires special initial start-up procedures. The batteries within the PV module are charged before launch. The DC Control Bus provides the initial power to operate PMAD system's processors, MBSA, PDCAs, discharge converters, and DC-AC inverters. Power will begin to flow from the batteries, through the discharge converters and into the DC-AC inverter where it will be converted into utility power. This utility power is then placed onto primary feeders to serve the PV module's loads. The start-up command is then given to the Power Management Processor and the PV arrays will extend and start generating power. At this time, the PV subsystem can now operate in its normal insolation/eclipitic cycles.

Flight two launch package is identical to that of fight one and is started up the same way. At the end of flight two, PMAD is capable of generating and distributing 8 kW of power. The system will not realize its full generation

potentional of 25 kW until flight four when the alpha and beta joints begin tracking the sun.

3.4.8.2 Distributed PMAD (IOC)

The Space Station structure and manned modules are deployed during flight three through eleven. PMAD equipment (PDCAs and Cables) will be integrated into the structure, and manned modules by other work packages. These PMAD components will be placed on-line by entering the appropriate PMAD configuration into the Power Management Processor which will in turn, run a self test to verify the installation. After self-check verification, the newly deployed distribution hardware is now ready to provide utility power to loads.

3.4.8.3 SD Module (IOC)

The IOC assembly flight eleven will deploy two SD modules. The modules will be integrated into EPS system by connections at the alpha joint MBSAs. The module will be verified using the SD Processors self check function to insure proper connections. If the self test is successful, the SD Engine will be started up using its start-up procedure and will be brought on-line.

3.4.8.4 Station Growth

The PMAD configuration has been designed for growth to a 300 kW station. However, the initial power distribution cabling will be installed to accept growth to only 175 kW without the major addition of new cabling.

Major PMAD equipments which are installed at IOC and planned to remain throughout station life are sized to accommodate the 300 kW growth station. This equipment consists of the alpha joint roll rings, MBSA, and the interconnecting power cabling between the MBSA and alpha joint. Since the MBSA serves as the point of paralleling and synchronization of all power sources on its respective side of the station, the MBSA must have adequate capacity at IOC to handle a nominal 167.5 kW of source power. Likewise the alpha joint has similar capacity since all of the eventual source power must flow through the roll rings. Cabling between these two items is also installed at IOC to

eliminate complex and time consuming EVA field wiring. Downstream of the MBSA, the distribution cabling is scarred for a nominal 175 kW capacity. The distribution cabling to external points on the station (upper and lower keels and booms) will be sized for the final growth station loading which is estimated at approximately 100 kW. This will eliminate field wiring on this part of the station structure which is not expected to change over the station life. The manned modules area however, is where the bulk of structure growth is expected and is the the area where field installation of new cabling (over the 175 kW scar) is planned. As new manned modules are added to the station, new feeders from the MBSA to the modules will be required. The feeders will be sized to accommodate the module loading which will be better defined in the future.

Source PMAD growth is planned to coincide with the addition of the SD source modules. Each module addition includes it associated PMAD equipment which consists of a frequency converter, RBIs and cabling. Also included is the SD controller which controls the SD module and interfaces with the Power Source Processor via the local control bus.

3.4.9 Platform

The platform PMAD system simular to that of the station. Common ORUs from the Space Station will be used to the greatest extent possible. Although the hardware will be oversized, in many cases this is a cost-effective approach that also allows growth by upgrading solar arrays and the batteries without modifying or making significant additions to the PMAD equipment. Figure 3.4.9-1 shows platform topology.

The platform's PV source PMAD system is nearly identical to that of the station except that three DC-AC inverters will be used. Due to the small size of the platform compared with the station, the dual rings approach to the primary distribution system is not practicable; therefore, a triple bus is used. The primary/secondary tie points on the platform is accomplished by two PDCAs which are common to the station. The four power connections to the PDCA will be connected to the platform's triple bus. The platform's control architecture is similar to the station's except that no SD controller, power

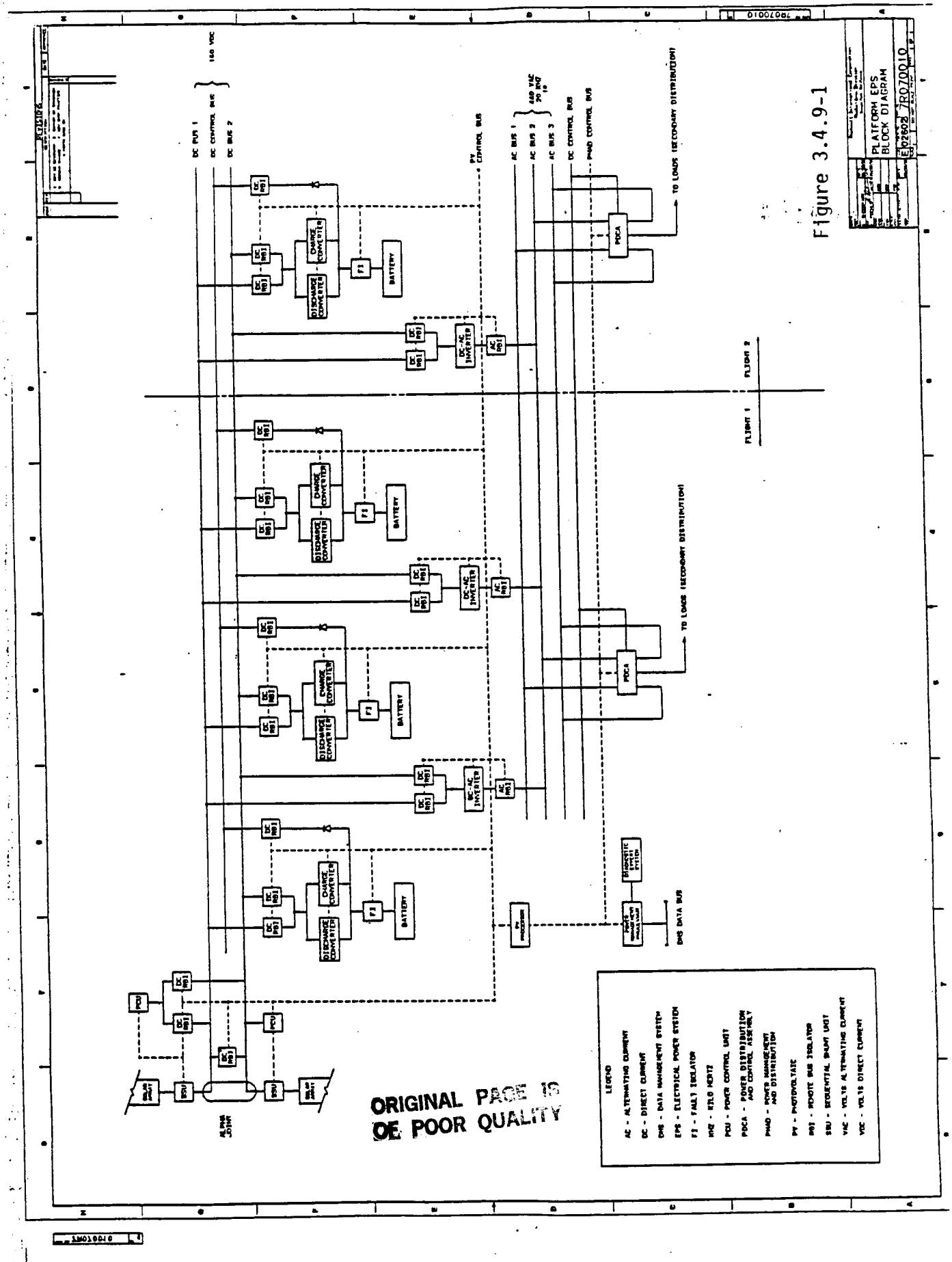

Figure 3.4.9-1

source controller or MBSA controller is required. The platform architecture is also designed to permit the platform to be operational on the first flight thought at lower power. The second flight brings additional battery capacity and an additional PDCA for additional loads. This arrangement also allows for future platform additions.

3.5 BETA JOINTS

The gimbal joints provide single-axis pointing for the station and platform PV solar arrays and SD modules to maximize solar insolation interception. They also feather the arrays and modules when required, to minimize drag resistance, and position the arrays and modules for maintenance.

Each PV solar array or SD module requires one beta joint. A total of four PV beta joints and two SD module beta joints are required for the IOC station. When the SD growth is complete there will be twelve SD beta joints total.

The platform has two alpha joints, one for each PV solar array.

3.5.1 Layouts/Drawings

A layout drawing of the common station beta/platform alpha joint is shown in Figure 3.3.5-1. The joint features a single wire race bearing of sufficient inside diameter and stiffness to: support the station or platform PV mast canisters nesting inside the bearing, which reduces the station transverse boom or platform spacecraft inertia; or attach the SD module to the interface flange. The figure illustrates a PV mast canister installation, however, the joint concept is the same for an SD module installation. Commonality between the SD and PV station beta joints, and to a slightly lesser extent, extending to the platform alpha joint was selected on the basis of a trade study documented in Section 2.2. Figure 3.5.2 shows an exploded view of the joint.

3.5.2 Mass Properties

Table 3.5-1 lists the mass breakdowns for station beta/platform alpha joint assemblies. The mass of a common station beta/platform alpha joint is 275 kg (605 lbm).

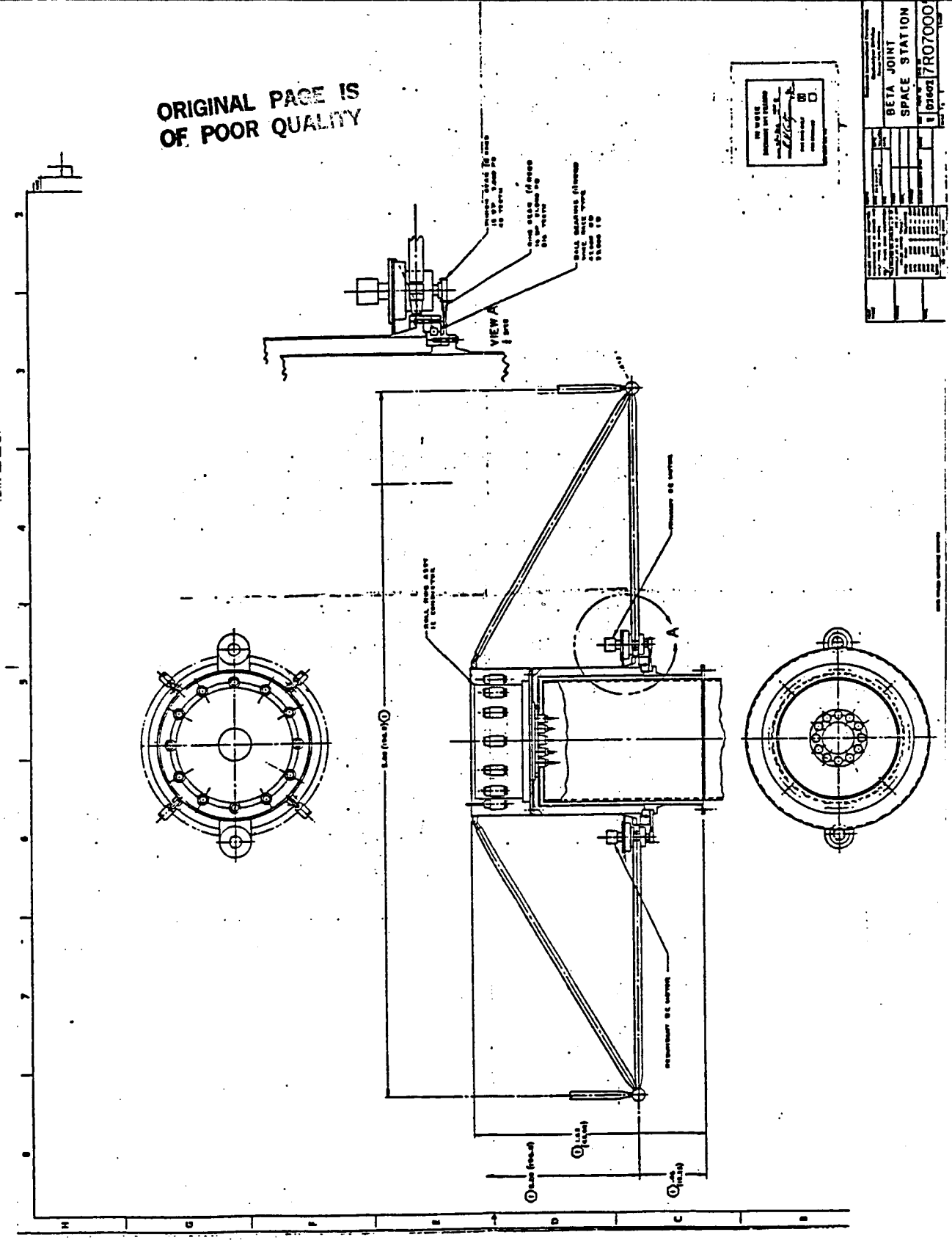

Figure 3.5-1 Station Beta/Platform Alpha Joint Layout

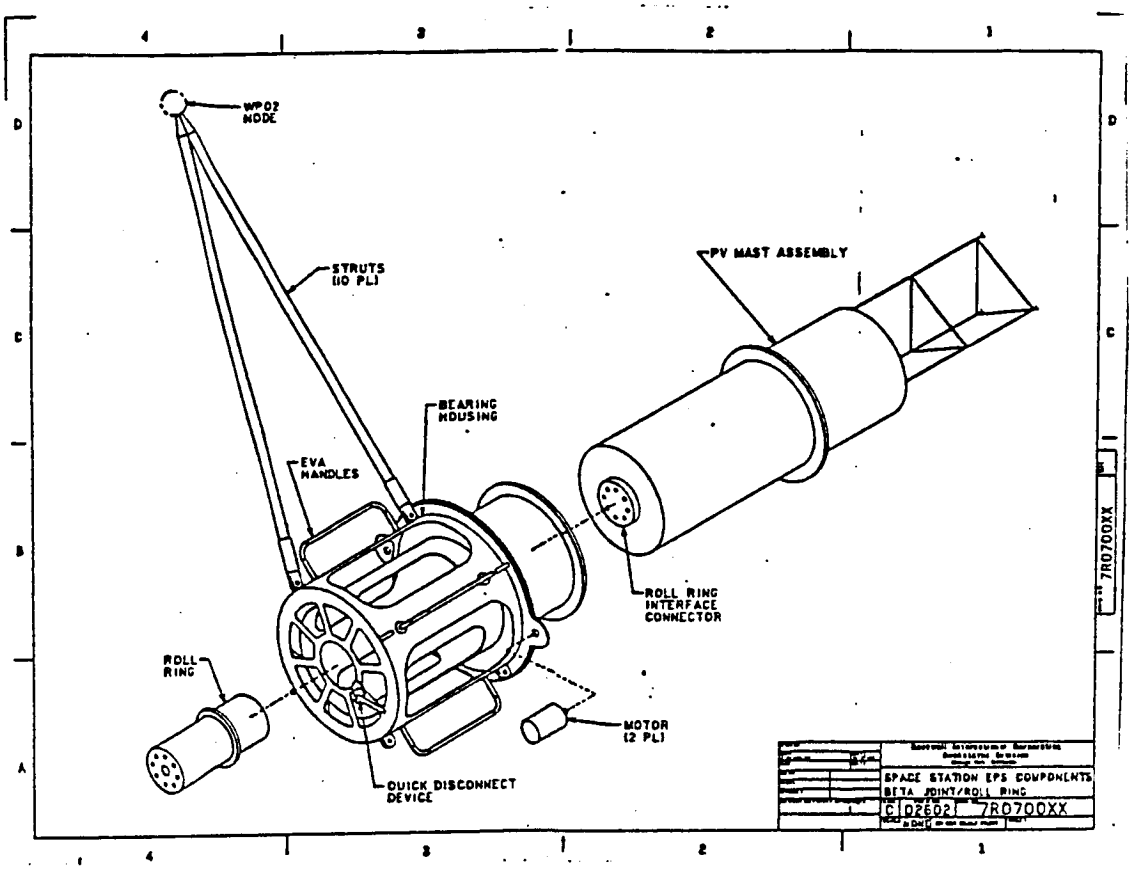

ORIGINAL PAGE IS
OF POOR QUALITY

Figure 3.5-2 Station Beta/Platform Alpha Joint Exploded View

Table 3.5-1

STATION BETA/PLATFORM ALPHA JOINT MASS/JOINT BREAKDOWN [kg (lbm)]

ITEM	SD STATION	PV STATION	PV CO-ORB PLATFM.	PV POLAR PLATFM.
Bearing Subassembly				
Bearing	inc.	inc.	inc.	inc.
Inner Bearing Support	inc.	inc.	inc.	inc.
Outer Bearing Support	inc.	inc.	inc.	inc.
Subassembly Hardware	inc.	inc.	inc.	inc.
Mounting Hardware	inc.	inc.	inc.	inc.
Subtotal	160 (352)	160 (352)	160 (352)	160 (352)
Drive Mechanism Subass. (2 ea.)				
Drive Motors	inc.	inc.	inc.	inc.
Speed Reducers	inc.	inc.	inc.	inc.
Pinion Gears	inc.	inc.	inc.	inc.
Drive Mounts	inc.	inc.	inc.	inc.
Subtotal	44 (97)	44 (97)	44 (97)	44 (97)
Transition Structure				
Struts			*	*
Type A	inc.	inc.	inc.	inc.
Type B	inc.	inc.	inc.	inc.
Type C	inc.	inc.	inc.	inc.
Strut I/F Fitting	inc.	inc.	inc.	inc.
Subtotal	20 (44)	20 (44)	20 (44)	20 (44)
Controls and Instruments				
Sun Sensors (2 ea)	3 (7)	3 (7)	3 (7)	3 (7)
Motor Controllers (2 ea.)	9 (20)	9 (20)	9 (20)	9 (20)
Insolation Meters (2 ea.)	1 (4)	1 (4)	1 (4)	1 (4)
Subtotal	13 (29)	13 (29)	13 (29)	13 (29)
Roll Ring Subassembly				
Power Module	inc.	inc.	inc.	inc.
Signal Module	inc.	inc.	inc.	inc.
Module Lock	inc.	inc.	inc.	inc.
Stator Connector	inc.	inc.	inc.	inc.
Rotor Connector	inc.	inc.	inc.	inc.
Position Resolver	inc.	inc.	inc.	inc.
Subtotal	38 (84)	38 (84)	38 (84)	38 (84)
TOTAL MASS	275 (605)	275 (605)	275 (605)	275 (605)

* Estimate Only, Transition Structure Requirements Not Yet Defined

V2-335/4

3.5.3 Joint Performance

Table 3.5-2 lists for each joint the functional and physical requirements.

Table 3.5-2
STATION BETA/PLATFORM ALPHA JOINTS REQUIREMENTS SUMMARY

ITEM	STATION SD	STATION PV	PLATFORM PV
CONFIGURATION	ROTARY	ROTARY	ROTARY
PHYSICAL INTERFACE	FLANGE	FLANGE+	FLANGE+
MAXIMUM ELECTRICAL TRANSFER LOAD, kWe	33.8	24.7	16.5
MAXIMUM CURRENT, AMPS	<200	160	105
MAXIMUM VOLTAGE, VOLTS	208-440 AC	160, DC	160, DC
ROTATIONAL RANGE, OPERATIONAL, DEGREES	±55	± 55	360 CONT.
ROTATIONAL RANGE, MAINTENANCE, DEGREES	± 180	± 90	± 90
SLEW RATE, DEGREES/MINUTE	± 60	± 0.9	± 0.9
ANGULAR ACCELERATION, DEG./SEC.^{2}	± 0.1	± 0.01	± 0.01
3 SIGMA POINTING ACCURACY, DEGREES	2.0	2.0	2.0
COMMONALITY	100%	100%	<100%*
STIFFNESS			
TORSIONAL, FT-LBS/RAD	8.975 E7	<SD	<SD
VERTICAL, LBS/FT	2.006 E6	<SD	<SD
LATERAL, LBS/FT	3.538 E7	<SD	<SD
LONGITUDINAL, LBS/FT	3.538 E7	<SD	<SD
LOADS			
BENDING, IN-LBS	50,000	50,000	<50,000
SHEAR, LBS	300	300	300
TORSIONAL, LBS	50,000	50,000	<50,000
AXIAL, LBS	300	300	300
LAUNCH, G	4.5	4.5	4.5
ASSEMBLY METHOD	EVA	EVA	EVA
CONTINGENCY ROTATION CAPABILITY	MANUAL	MANUAL	MANUAL
ROTATIONAL AXIS INERTIA, SLUG-FT^2	27,600	10,500	10,500
DESIGN LIFE, YEARS	20	20	20
MTBF, HOURS	TBD	TBD	TBD
MTTR, HOURS	TBD	TBD	TBD

+ PV MAST CANISTER SHALL NEST INSIDE BEARING ID.
* TRANSITION STRUCTURE CANNOT BE COMMON DUE TO PLATFORM CONFIGURATION.

V2-335/5

A summary of the estimated performance capabilities of the joints is shown in Table 3.5-3.

TABLE 3.5-3

STATION BETA/PLATFORM ALPHA JOINT ESTIMATED PERFORMANCE

ITEM	PARAMETER
CONFIGURATION	ROTARY
PV OR SD PHYSICAL INTERFACE	CIRCULAR FLANGE
MAXIMUM ELECTRICAL TRANSFER LOAD, kWe	>33.8
ROTATIONAL RANGE, PV, DEGREES	360
ROTATIONAL RANGE, SD, DEGREES	360
ROTATIONAL RANGE, PV PLATFORM, DEG.	360 CONTINUOUS
SLEW RATE, DEGREES/MINUTE	a) ± 0.9 b) ± 60
ANGULAR ACCELERATION, DEG./SEC./SEC.	a) ± 0.01 a) ± 0.1
3 SIGMA POINTING ACCURACY, DEGREES	0.01*
COMMONALITY	SD = PV

a) STATION AND PLATFORM PV PERFORMANCE
b) STATION MODULE PERFORMANCE
* EXCLUSIVE OF TRANSVERSE BOOM FLEXURE

3.5.4 Assembly Definition

Aside from the transition structure, the station beta and platform alpha joints have identical elements and components. The bearing, drive, roll ring, and control and instrument subassemblies are interchangeable. However, Control software requirements for the different types of joints are unique. The transition structures differ only in the required angle at which the bearing subassembly must be supported with respect to the transverse boom or platform spacecraft.

The reference station beta/platform alpha joint features a single wire race bearing of sufficient inside diameter and stiffness to: support the station or platform PV mast canisters nesting inside the bearing, which reduces

the station transverse boom or platform spacecraft inertia; or attach the SD module to the interface flange. Figure 3.5-1, the layout drawing of the joint, illustrates a PV mast canister installation, however, the joint concept is the same for an SD module installation.

The common station/platform joint configuration was selected on the basis of minimum total program cost as well as reasonable development risk and low moment of inertia, a major GN&C stability driver.

The station beta/platform alpha joint is comprised of five subassemblies: bearing, transition structure, drive, roll ring, and controls and instruments. The total mass of one assembly is 275 kg (605 lbm). The assembly deployed envelope of a station joint is 5 m long by 5 m wide by 1.65 m deep.

A detailed description of the beta joint subassemblies is located in section 2.1.3 of the December issue of DR02.

V2-335/7

3.5.5 ORU Description

The station beta/platform alpha joint ORU, Master Equipment and Initial Spares List is shown in Table 3.5-4.

Table 3.5-4
STATION BETA/PLATFORM ALPHA ORUs/MASTER EQUIPMENT/INITIAL SPARES

Item	Number Per Joint	Approximate Dimensions+ (L x W x D) (m)	Estimated Mass+ [kg (lbm)]
Bearing Subassembly	1	1.65 x 1.2 OD	160 (352)
*Drive Mechanism Subassem.	2	0.3 x 0.3 OD	44 (97)
Transition Structure	1	3.0 x 0.18 x 0.25	20 (44)
*Sun Sensor	2	0.5 x 0.1 OD	1 (2.2)
*Motor Controller	2	0.3 x 0.1 x 0.1	2.3 (5.1)
*Insolation Meter	2	0.5 x 0.06 OD	0.5 (1.1)
Roll Ring Subassembly	1	0.78 x 0.29 OD	38 (84)

* Initial spares.
\+ Excludes Launch Cradles

V2-335/8

3.6 INTERFACE CONTROL DOCUMENT (ICD)

3.6.1 Objectives

The WP-04 EPS ICD external interfaces were developed with the following objectives to be accomplished:

- Identify the interfaces
- Describe the interfaces to the extent the available design permits
- Establish responsibility and scope for the work packages involved, and
- Minimize the number of different interfaces and total interfaces.

3.6.2 Approach and Assumptions

3.6.2.1 Interfaces at WP-04 ORU Level

Considerations of OUR definition combined with the need to clearly identify the hardware performances responsibility, plus the goal of performing the verification activities in the most efficient and cost effective way, resulted in the decision to have all the external interfaces of WP-04 at the ORU level. This should benefit life cycle cost in the areas of spares and maintenance.

3.6.2.2 Type of Interfaces Addressed

Physical and functional external interfaces are addressed for the following:

- The hardware is in orbit and installed for operation.
- The hardware has a structural connection with another WP.

Other external interfaces shall be dealt with later, specifically:

- Interfacing with the NSTS
- Interfacing of spares on orbit in stowed position
- Interfacing of the hardware with man/machine during installation and maintenance.

Interfacing with the natural environment will be addressed as design requirements.

3.6.2.3 Interfaces Description

The interface description for the preliminary design consists of:

- Write-up describing the function of the interfacing ORU
- Block diagram depicting scope of responsibilities, see Figure 3.6-1, and
- Presentation of the quantitative and configurational information available for both, the functional and physical aspects of the interface (example Figures 3.6-2 & 3.6-3).

3.6.3 Status

3.6.3.1 Overview

Table 3.6-1 provides an overview of the WP-04 external interfaces. The table provides the interfacing ORUs, the interfacing WPs, interfacing hardware and location, and the nature of each interface.

3.6.3.2 Station

3.6.3.2.1 PV Module

The PV module interfaces with WP-02 supplied truss at the PV beta joint and the PV equipment box. Both are located outboard of the alpha joints.

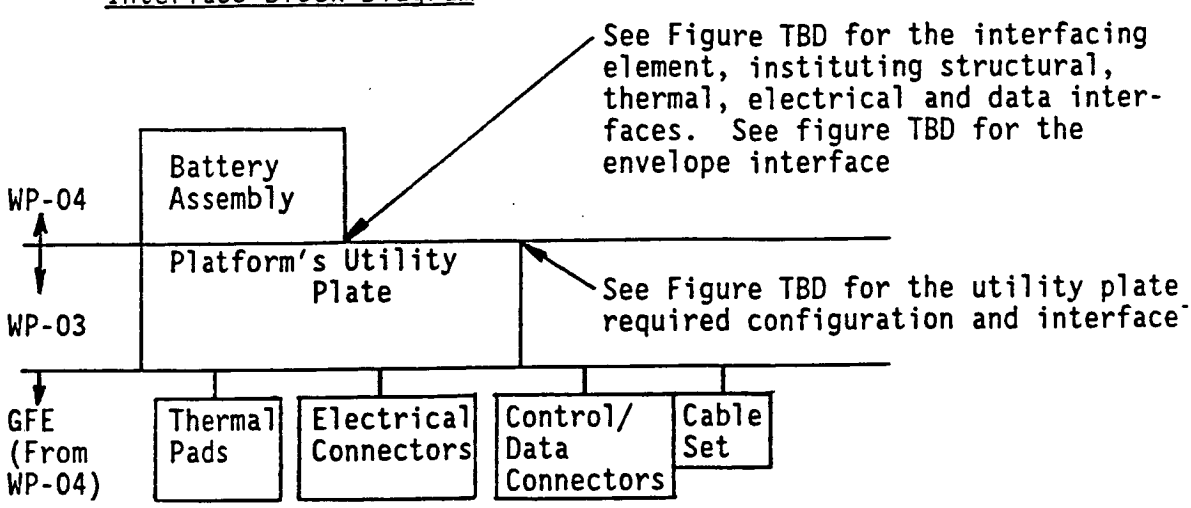

Figure 3.6-1 Sample - Interface Block Diagram

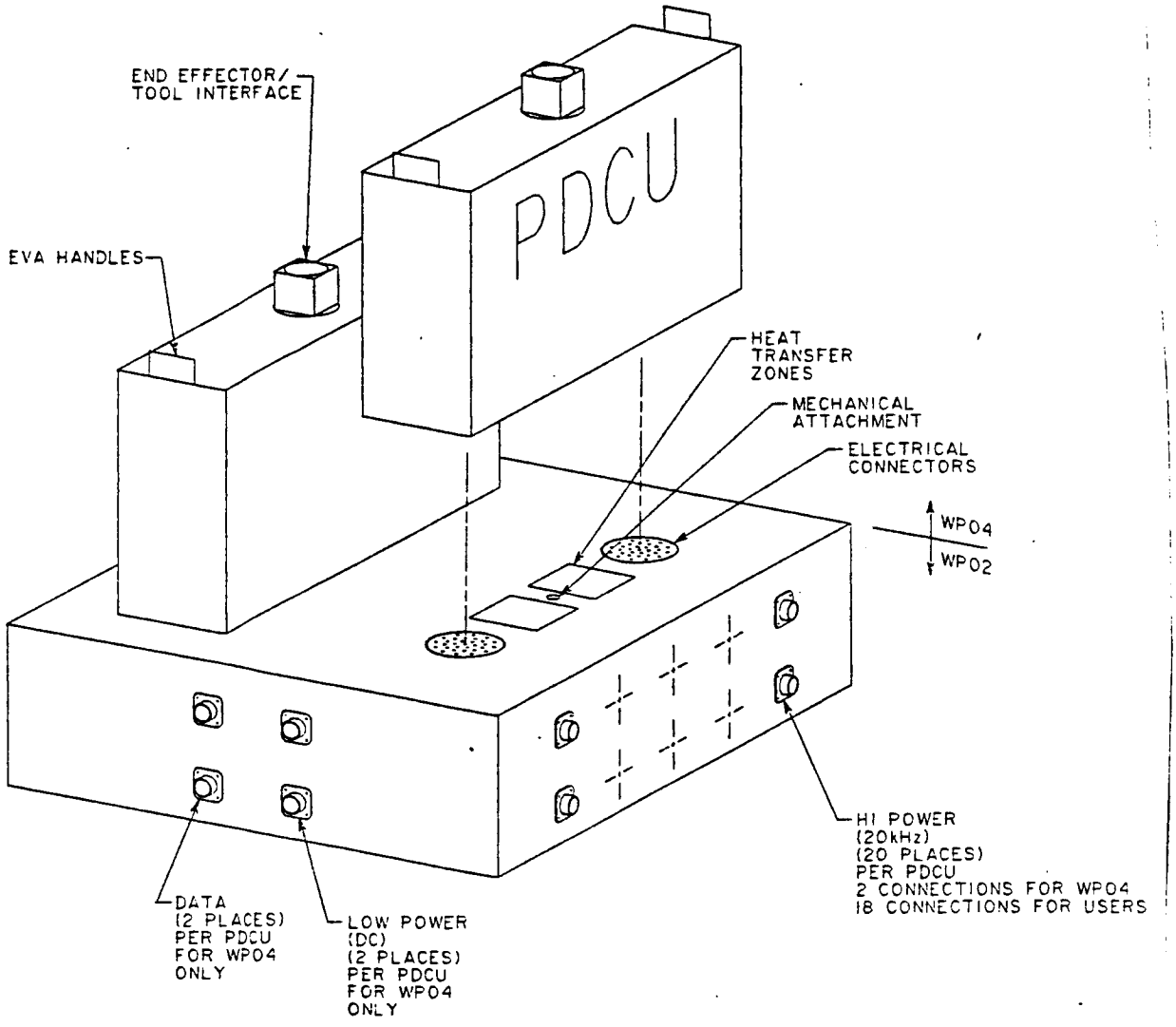

Figure 3.6-2 Sample - IC Drawing

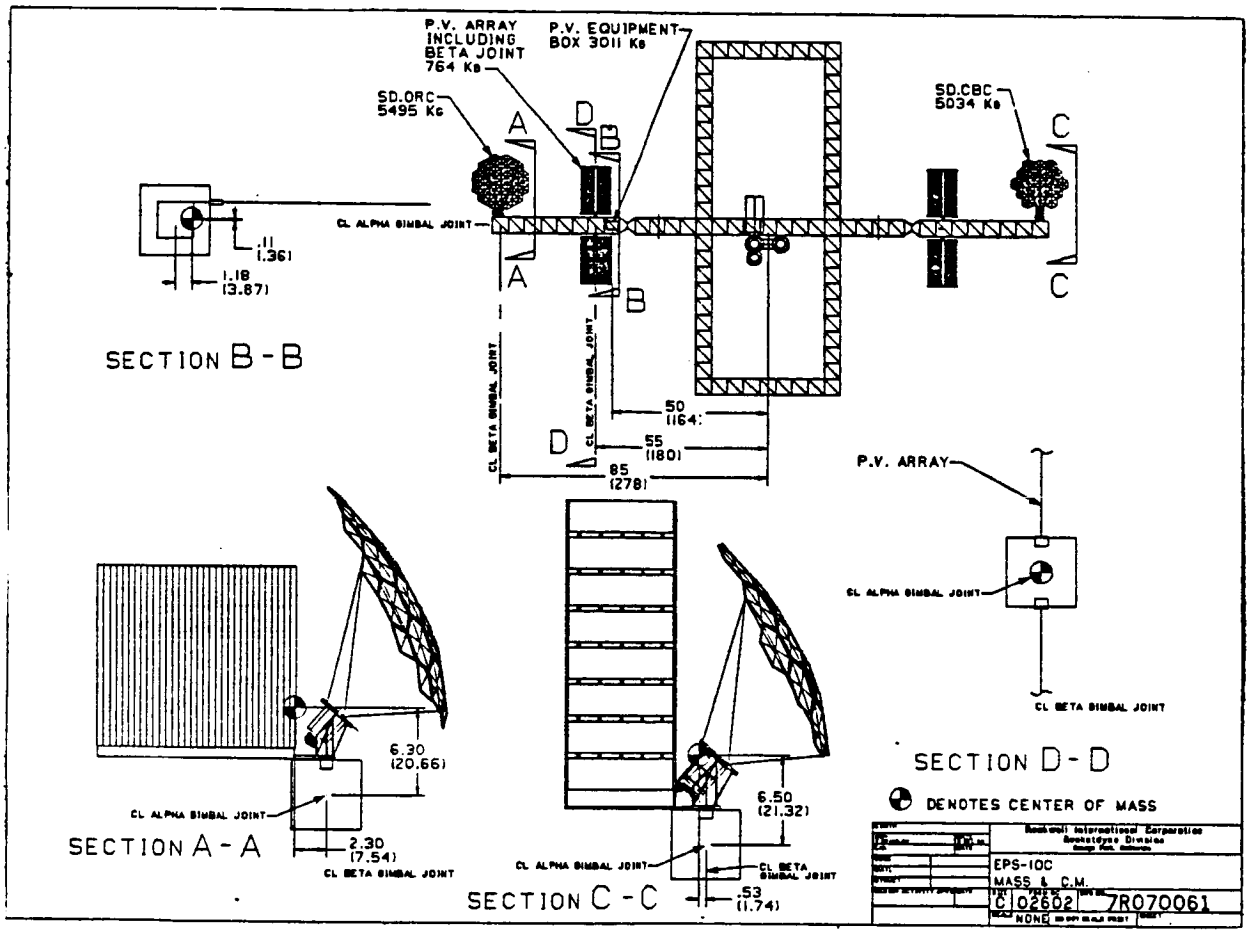

Figure 3.6-3. Sample-Interface Control Drawing

		ELECTRICAL POWER SYSTEM EXTERNAL-INTERFACES	INTERFACING WP	INTERFACING WP: HARDWARE & LOCATION	NATURE OF INTERFACE			
					MECHANICAL/ STRUCTURAL	ENVELOPE	MAN-MADE ENVIRONMENTAL	ELECTRICAL/ DATA
SPACE STATION	DISTRIBUTED PMAD	• MAIN BUS SWITCHING UNIT (MBSU)	2	UTILITY PLATE-INBOARD TRUSS	S,T	M,SS	D,EM,F	A,DC,DS
		• POWE DISTRIBUTION & CONTROL UNIT TRUSS MOUNTED (PDCU-T)	2	UTILITY PLATE-INBOARD TRUSS	S,T	M,SS	D,EM,F	A,DC,DS
		• PDCU-M (M=MODULE/NODE)	2	ELEC. RACK - PRESSURIZED NODE	S,T	SS,	D,EM,I	A,DC,DS
		• TRANSFORMER	2	UTILITY PLATE-INBOARD TRUSS	S,	M,SS	D,EM,F	A,DC
		• POWER MANAGEMENT CONTROLLER (PMC)	2	UTILITY PLATE-INBOARD TRUSS	S,T	SS	D,EV	A,DC,DS
		• NSTS POWER CONVERTER	2	UTILITY PLATE-INBOARD TRUSS	S,T	M,SS,	D,F,	A,DC,DS
		• CABLE SET	2	CABLE TRAYS, UTILITY PLATES, NODES, & ELECTRIC. RACKS-INBOARD	S,	M,	EM,EV,I	A,DC,DS
	PV MODULE	• BETA JOINT TRANSITION STRUC.	2	OUTBOARD TRUSS	S,	M,	D,EV	
		• PV EQUIPMENT BOX STRUT SET	2	OUTBOARD TRUSS	S,	M,	D,EV,	
		• CABLE SET	2	CABLE TRAYS & CONDUITS-OUTBOARD	S,	M,	EM,EV,	A,DC,DS
	SD MODULE	• BETA JOINT TRANSITION STRUC. (IDENT. TO THE PV BETA JOINT)	2	OUTBOARD TRUSS	S,	M,	D,EV	
		• CABLE SET	2	CABLE TRAYS & CONDUITS-OUTBOARD	S,	M,	EM,EV	A,DC,DS
POLAR PLATFORM & COORBITING PLATF.	PMAD SUBSYSTEM	• BATTERY CHARGE/DISCHARGE	3	UTILITY PLATE	S,T	M,	D,EM,F	A,DC,DS
		• DC/AC INVERTER	3	UTILITY PLATE	S,T	M	D,EM,F	A,CD,DS
		• PHOTOVOLTAIC CONTROLLER	3	UTILITY PLATE	S,T	M,	D,EM,F	A,DC,DS
		• PHOTOVOLTAIC CONTROL UNIT	3	UTILITY PLATE	S,T,	M,	D,EM,F	A,DC,DS
		• DC SWITCH UNIT	3	UTILITY PLATE	S,T,	M,	D,EM,F	A,DC,DS
		• AC SWITCH UNIT	3	UTILITY PLATE	S,T	M,	D,EM,F	A,DC,DS
		• PDCU-T	3	UTILITY PLATE	S,T	M, —	D,EM,F	A,DC,DS
		• PMC-T (T=TRUSS)	3	UTILITY PLATE	S,T	M	D,EM,F	A,DC,DS
		• NSTS-POWER CONVERTER	3	UTILITY PLATE	S,T	M	D,EM,F	A,DC,DS
		• CABLE SET	3	CABLE TRAYS, UTILITY PLATES	S,	M,	EM,EVA	A,DC,DS
	PV-SUB-SYSTEM	• BATTERY ASSEMBLY (PP & COR.P)	3	UTILITY PLATE	S,T	M,	D,F	DC,DS
		• PP ALPHA JOINT TRANS. STRUCT	3	PLATFORM STRUCT.	S,	M,	D,EV	
		• COR. P. ALPHA JOINT TRANS. STRUC	3	PLATFORM STRUCT.	S,	M,	D,EV	

ABBREVIATIONS — NATURE OF INTERFACE

MECHANICAL/STRUCTURAL:
- S = STRUCTURAL CONNECTION
- T = THERMAL CONNECTION

ENVELOPE:
- M = MAINTAINANCE ROOM
- SS = SPARE STOWAGE (ON ORBIT)

ENVIRONMENTAL:
- D = DYNAMIC
- EM = ELECTRO-MAGNETIC INTERFERENCE (EMI)
- EV = EXTRA-VEHICULAR ACTIVITY (EVA)
- F = FLIGHT TELEROBOTIC SERVICER (FTS) / MOBILE SERVICE CENTER (MSC) ARM END EFFECTOR
- I = INTRA-VEHICULAR ACTIVITY (IVA)

ELECTRICAL/DATA:
- A = 20 KHz POWER CONNECTION
- DC = ELECT. DIRECT CURRENT (DC) CONTROL CONNECTION
- DS = DATA/SIGNAL

External Interfaces

TABLE 3.6-1

The interface is through struts connecting the beta joints and the PV equipment box to the outboard truss. The struts shall be specified by WP-04 and are GFE from WP-02. The ICD in DR-02 provides conceptual description of the struts, no detail design is available as yet.

An additional interface is the dynamic loading imposed on the assemblies in the PV module, as well as the dynamic loading imposed on the rest of the station by the mass of the assemblies, and in the case of the solar array, the movement of the beta joints and the vibration of the solar array. The preliminary conclusion for the analysis performed is that a dynamic interaction is not expected to present a stability problem from either structural stability or pointing and tracking points of view. The moments of inertia of the alpha joint as well as its stiffness were also identified in the analysis.

3.6.3.2.2 SD Module

The interface of the SD module with Work Package 02 is at the struts connecting the SD beta joint to the outboard truss. The struts are identical to those used for the PV beta joints. The interface, for both the PV and SD design is governed by the SD requirement since it is subjected to higher inertial loads than the PV beta joint. The struts are designed to be identical for commonality.

In the case of the SD module the issue of dynamic stability and interaction with the truss is more significant than that of the PV module in light of the required accuracy of pointing and tracking of the concentrator. The preliminary analysis performed indicates that with properly designed support structure within the SD module, dynamic instability should not be a problem. This will be further studied considering growth and more accurate model of the whole outboard truss.

3.6.3.2.3 Distributed PMAD

As shown in Table 3.6-1 the PMAD ORU's constitute the most extensive external interfaces in WP-04. In order to enhance commonality a trade-off study dedicated to the ORU's packaging was performed, see DR-02, "ORU's Std. Packaging Trade Off Study".

V2-35/6

The PMAD boxes utilize the same interfacing element, which constitutes structural connection, thermal interface, and electrical and data interface. The same interfacing element is the device interfacing with robotics or the astronaut performing EVA. The design does not preclude replacement of components within an ORU. See Figure 3.6-4

The expected mass and thermal characteristics of each of the interfacing ORU's are submitted as well.

The subject of cables and connections is addressed in the ICD in DR-02 to the extent of identifying responsibilities and scope of supply, specifically:

- All cables and connections within PMAD outboard of the alpha joint are by WP-04
- Cables and connections inboard of the alpha joint, among the PMAD ORU boxes are supplied by WP-04 to WP-02 as GFE.
- Cable trays and conduits any where in the station, with the exception of outboard of the beta joints, are by WP-02.

The PMAD cables outboard of the alpha joint interface with the alpha joint roll rings.

3.6.3.3 Platforms

WP-04 provides the photovoltaic power generation system and the PMAD to the platforms. Commonality of components between the platforms and the station was employed to the extent possible.

3.6.3.3.1 PV Subsystem

The PV subsystem interfaces in the platforms are at the alpha joints and the battery assemblies. The platforms alpha joints are identical to the station's beta joints, except for the transition structures utilized on the platforms, reflecting the platforms different structure.

V2-35/7

ORIGINAL PAGE IS
OF POOR QUALITY

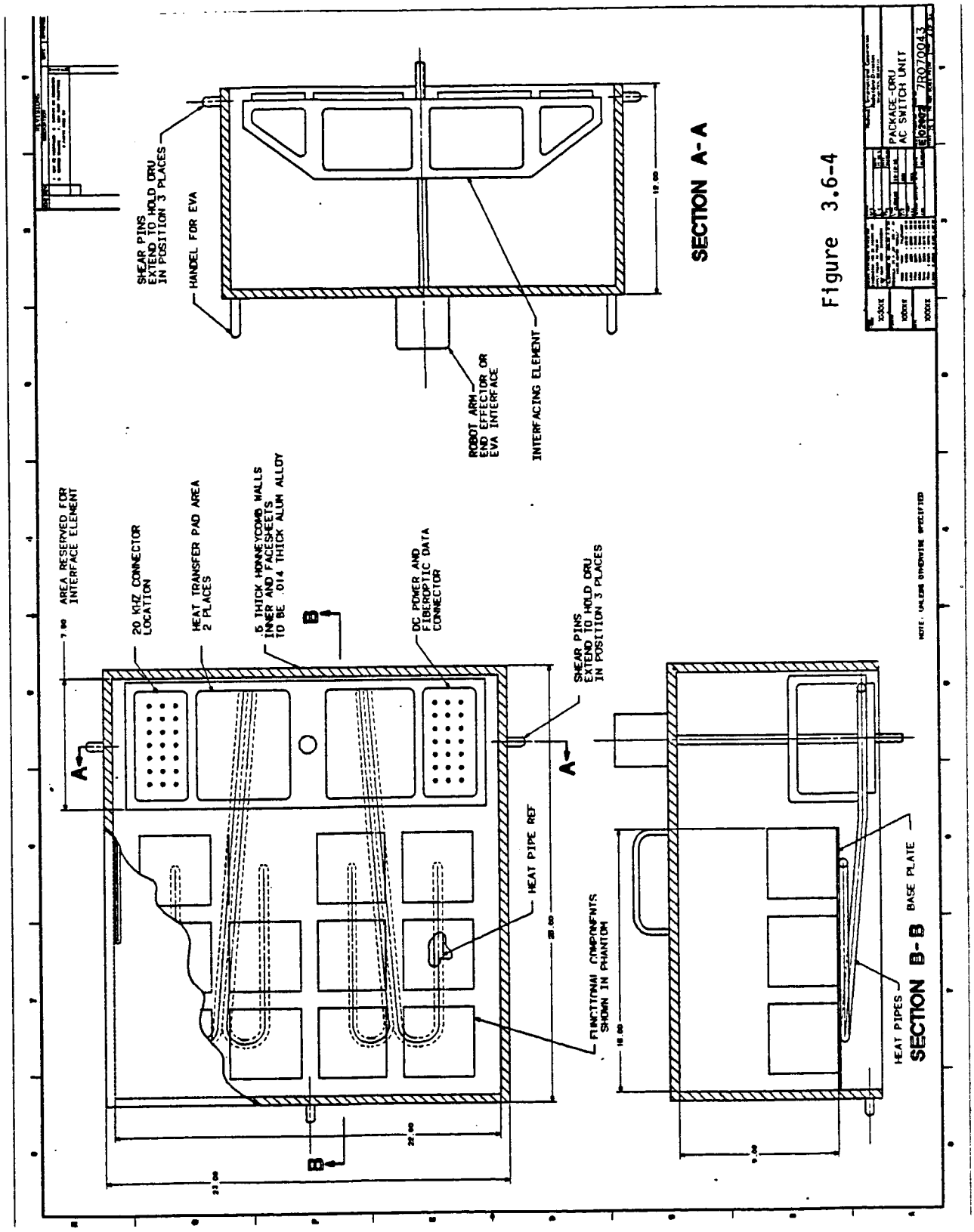

Figure 3.6-4

The alpha joint transition structure is different for the polar platform than that used for the co-orbiting platform, neither are shown due to lack of information regarding the platforms.

The battery assembly interfaces are of the same nature as the PMAD boxes (see Section 3.6.3.2.3).

3.6.3.3.2 PMAD Subsystem

A description of the interface for the PMAD on the platforms is similar to that shown in Section 3.6.3.2.3. Cables and their connections which connect the various PMAD boxes and the PV ORUs, are supplied as GFE to WP-03 from WP-04.

V2-35/9

3.7 CONTRACT END ITEM SPECIFICATIONS

During the Phase B contract, Rocketdyne has prepared and submitted two sets of preliminary Part I CEI specifications. The initial submittal, dated 24 June 1986, was directed by NASA-LeRC to consists of five contract end item specifications, as follows:

1) Station PV Module
2) Station SD Module
3) Station PMAD Subsystem
4) Platform PV Subsystem
5) Platform PMAD Subsystem

The second submittal, dated 19 January 1987 represented an updated set of CEI specifications reflecting the final pre-CETF baseline configuration for the EPS.

The complete preliminary Part I CEI specifications are included in DR-03.

V2-36/1

3.8 TEST AND VERIFICATION

Test and Verification activities were undertaken at several levels during the the phase B effort at Rocketdyne. Specific requirements were identified for; CEI subsystems, external to -WP-04 interfaces identified by Rocketdyne, and general program activities imposed by Level B CE+IS (Combined Elements and Integrated Systems).

Figure 3.8-1 Shows the major interfaces of the Solar Power Module identified to data. In addition to these, distributed PMAD ORU's will also have major physical interfaces with other Wps as discusses in FR-02.

Verification activities planned by Rocketdyne will begin at the individual piece part and component level and progress to subassemblies, assemblies, subsystems, and finally integrated systems.

DR-02 outlines the work package level interfaces between the Electric Power System (EPS) and the other Space Station work packages. Also considered addressed are interfaces with other key program elements including ground support equipment (GSE), the NSTS, and the Space Station crew. Interfaces of both a physical and functional nature, and hardware and software, are discusses. Rocketdyne's planned approach to verification of physical, functional, and software interfaces, and the use of the interface control document (ICD), formalized plans, and master gauges are discussed. The use of process simulators for functional and software interface verification is proposed.

SOLAR POWER MODULE EXTERNAL INTERFACES

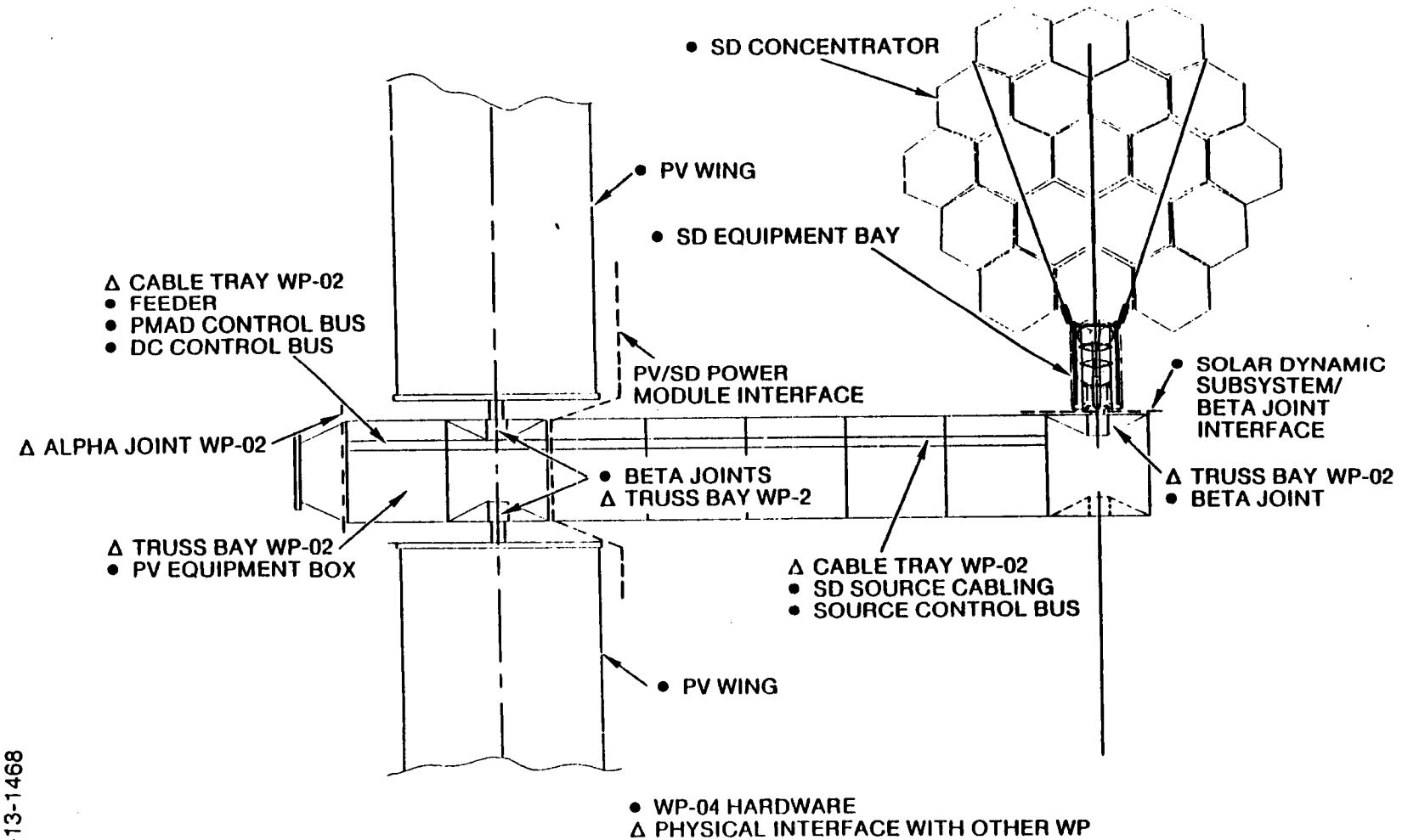

86D-13-1468

Rockwell International
Rocketdyne Division

Figure 3.8-1 Solar Power Module External Interfaces

Preliminary planning for various Test and Verification activities are contained in the following reports:

No.	Content
DR-02 Section 5	Verification of on-order operations WP-04 external interfaces developed for the ICD
DR-03 Section 4	Development and qualification requirements for subsystems developed from CEIS specifications.

Figure 3.8-2 depicts the total verification process during the various stages of the SS program. Verification requirements will be integrated and controlled to assure compliance with all program requirements.

V2-37/3

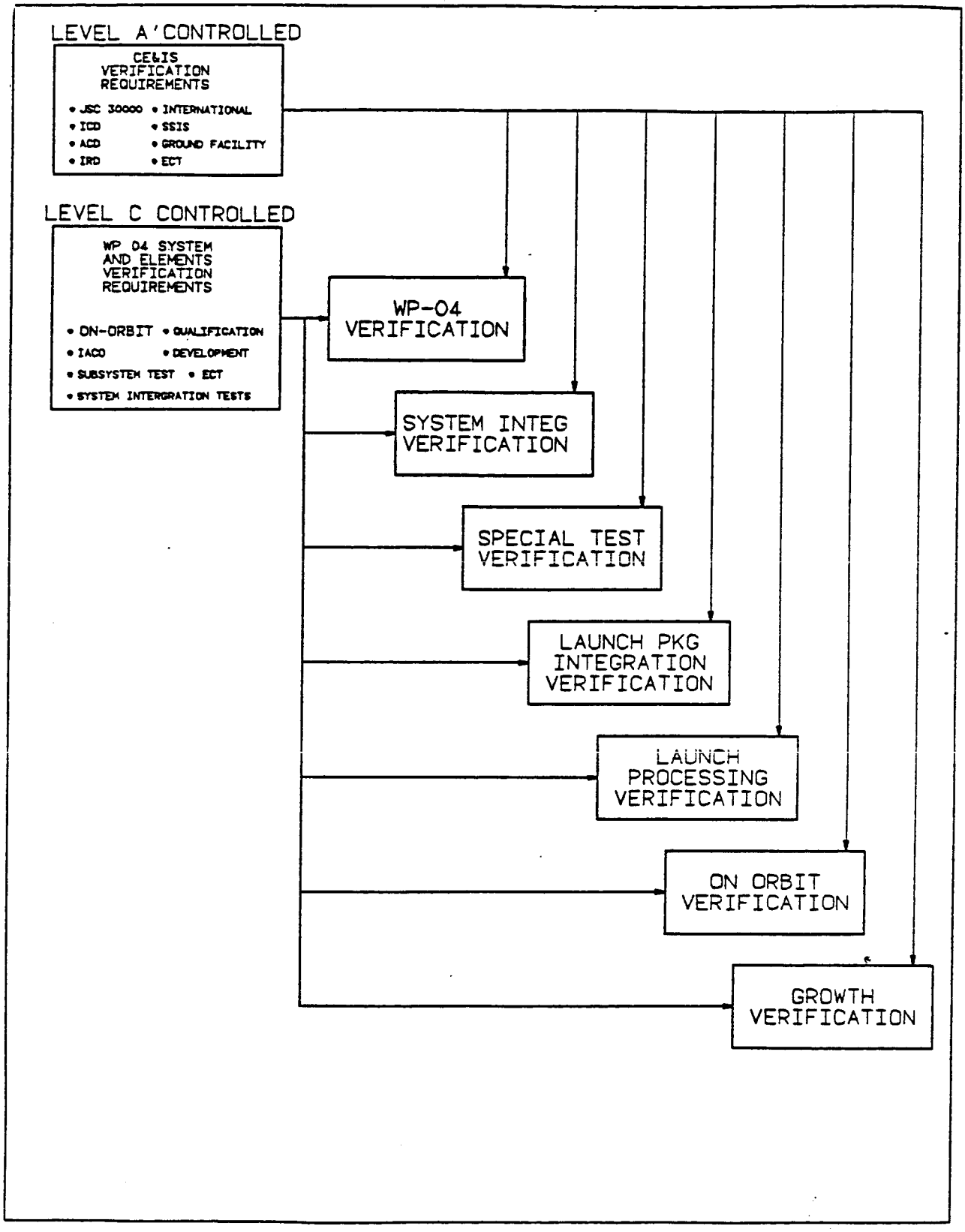

Figure 3.8-2 Verification Process Flow

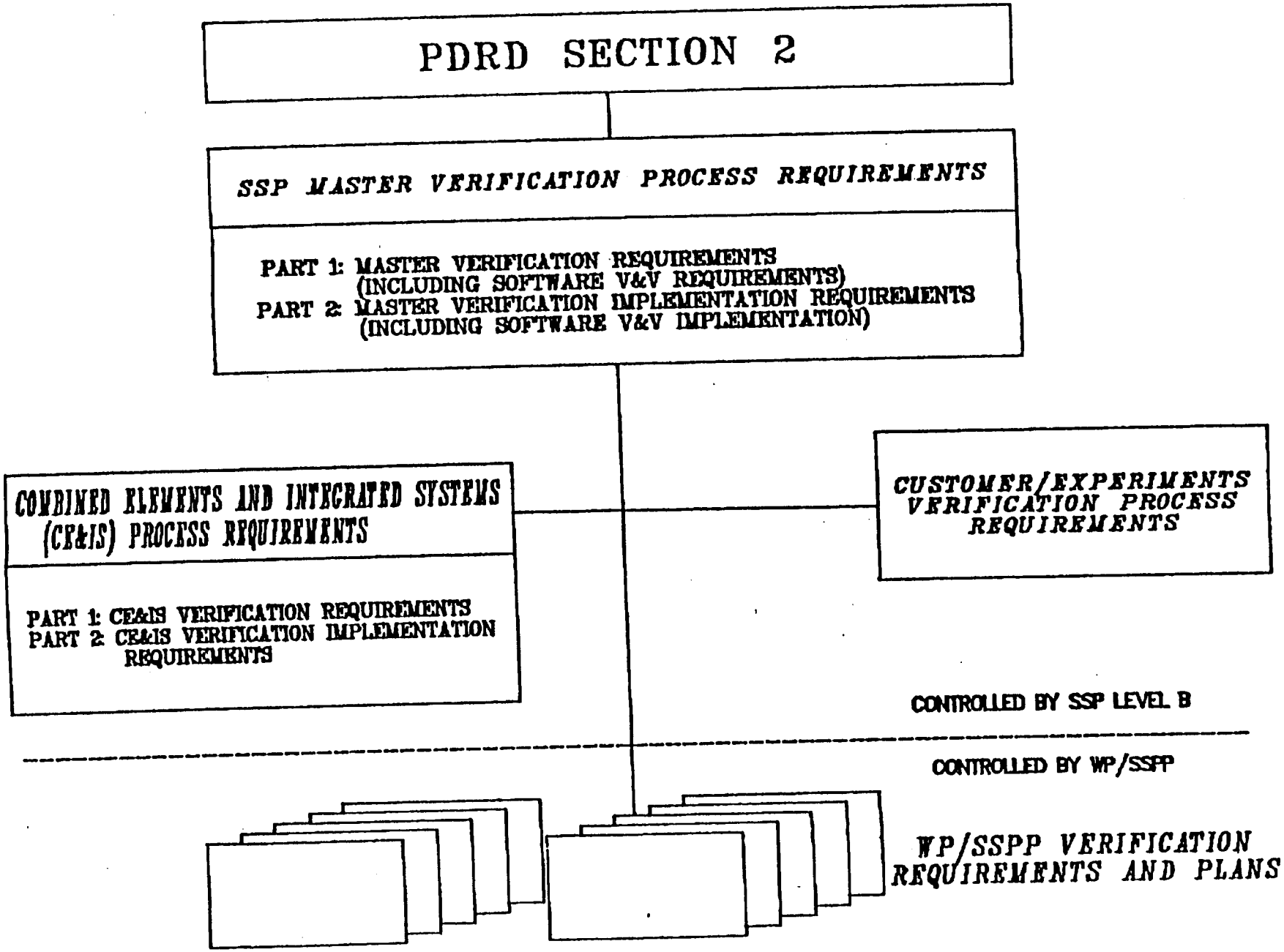

Figure 3.8-3 Hierarchy of Program Verificaiton Documents

Review of the following level B documents as effected through participation in the verification working group convened at several locations.

PDRD JSC 30000 Section 2

- o SSP Master Verification Process Requirements

  Part 1 Master Verification Requirements

  Part 2 Master Verification Implementation Requirements

- o Combined elements and Integrated Systems

  Process Requirements

  Part 1 CE+IS Verification Requirements

  Part 2 CE+IS Verification Implementation Requirements

The above requirements lead to specific WP-04 verification requirements and planning activities to be accomplished during plan C/D.

The hierarchy of Program documents is shown in Figure 3.8-3. Specific WP-04 verification requirements and plans will be built on during Phase C/D.

V2-37/5

Review of the following level B documents as effected through participation in the verification working group convened at several locations.

PDRD JSC 30000 Section 2

- o SSP Master Verification Process Requirements

  Part 1 Master Verification Requirements

  Part 2 Master Verification Implementation Requirements

- o Combined elements and Integrated Systems

  Process Requirements

  Part 1 CE+IS Verification Requirements

  Part 2 CE+IS Verification Implementation Requirements

The above requirements lead to specific WP-04 verification requirements and planning activities to be accomplished during plan C/D.

The hierarchy of Program documents is shown in Figure 3.8-3. Specific WP-04 verification requirements and plans will be built on during Phase C/D.

3.9 EXTERNAL THERMAL ENVIRONMENT DATA BASE

The External Thermal Environment Data Base (ETEDB) consists of a geometric mathematical model and a passive thermal mathematical model of the Space Station Electrical Power System. The development of these models were performed under an add-on to the WP-04 Phase B contract. The TRASYS computer program was used for the geometric math model, and the SINDA computer program was used for the thermal math model. The baseline IOC configuration and the man tended configuration (25 kw of photovoltaic power only) were analyzed. Models were developed for beta angles of 0, 52, and -52 degrees. The geometry reflected in the models is that which was current in May of 1986 when the modeling was started.

The geometric math models were used to calculate the thermal radiation environment of all Space Station power system components as a function of both orbital position and beta angle. This included reflected energy from the earth and other components, as well as the incident solar energy. The results of these analyses were heat fluxes that were then used as inputs to the thermal math models. The temperatures of the components were also calculated as a function of orbital position and beta angle. The size of these models was limited, because they were later integrated into the geometric and thermal math models of the entire Space Station. Details of the analyses and results are contained in the final report, External Thermal Environment Data Base", RI/RD86-234, 29 July 1986.

V2-37/6

4.0 ADVANCED DEVELOPMENT

A number of technology issues associated with the Space Station EPS were identified early in Phase B. A number of these were allocated to the contract Advanced Development program. Others were addressed using team member IR&D resources. The contract tasks fall into three major categories: These were addressed respectively by Garrett, Sundstrand and Harris. A complete list of referenced reports is contained at the end of this section.

Descriptions of the complimentary IR&D activities performed by the contract team have been provided in the quarterly related activities report and are not described in this section except, where specific results affected the approaches taken on the contract activity.

All effort required by DR-05 was completed. The AD-XX designator refers to the tasks described in DR-05 "Advanced Development Plan."

AD-1A	Resolution of issues associated with the CBC receiver/thermal storage concept (Garrett)
AD-1B	Demonstration of feasibility to design and fabricate an ORC receiver incorporating thermal energy storage and a heat pipe (Sundstrand)
AD-2A	Characterization of Solar Dynamic Concentrator kinematics (Harris)
AD-2B	Evaluation of Solar Dynamic Concentrator Materials (Harris)

4.1 AD-1A CBC

There were three specific CBC receiver activities undertaken by the Garrett Corporation::

A. Characterization of LiF-MgF_2 and LiF-CaF_2 eutectic phase change materials.

B. High temperature vacuum sublimination tests of candidate receiver materials.

C. Thermal cycling of a LiF - filled thermal energy storage device.

4.1.1 Phase Change Material Characterization

Departure from the thermal energy storage phase change material (PCM) characterizations, originally planned and defined in GPSD reports 41-5040-3 and 41-5040-4, occurred early in the program. The well characterized, single-compound LiF salt originally selected as the baseline PCM was supplanted by the lower-temperature LiF-MgF_2 eutectic salt for which physical property data was either lacking or exhibited wide variation. A basic research effort was initiated to establish the LiF-MgF_2 eutectic physical property data required to properly design the closed Brayton cycle (CBC) solar receiver and thermal energy storage (TES). Results of this testing are provided below.

Based upon the measured and observed characteristics of the LiF-MgF_2 eutectic salt, it was concluded that the production of bulk quantities to fill test article TES devices required a new, dedicated LiF-MgF_2 eutectic fill facility and the development of carefully controlled procedures.

A second eutectic salt, LiF-CaF_2, was also characterized for latent heat release using the same procedures developed for the LiF-MgF_2 salt.

LiF-MgF_2 Characteristics

A study of the LiF-MgF_2 system, which was the initial candidate eutectic material was completed. The eutectic composition is 32.0 $\pm$ 0.3 m % and it melts at 724.8 $\pm$ 1°C. The apparent phase diagram is strongly affected by maximum heating temperature and cycling rate. Likewise, the recoverable energy at the eutectic composition shifts due to differences in phase precipitation and separation. It ranges from 160-285 BTU/lb with an average of 223 BTU/lb. The average energy agrees with theoretical predictions made for LiF-MgF_2: 231 BTU/lb for an ideal solid-nonideal liquid situation. The initial heat capacity and thermal conductivity measurements on 31.1 m % MgF follow the rule of mixtures. Thermal expansion measurements from 25-700°C on 30.2 m % MgF_2 show good reproductivity and follow the rule of mixtures up to *ca.* 500°C. Beyond 500°C, the thermal expansion measured is greater than predicted from the individual constituents.

No stress corrosion cracking was found in a 140 hours test of INCO 625 at 750°C immersed in salt. The extent of corrosion was minimal as evidenced by chemical analysis of salt following the corrosion test.

Differential thermal analysis (DTA) was utilized as a method of rapidly defining PCM heat release during phase change. It has proven very effective in showing that kinetics of phase separation due to slow temperature cyclic rates preclude the use of LiF-MgF_2 or eutectics with similar phase diagrams for energy storage/recovery. Because the samples required for DTA are quite small, 5-30 mg, multiple samples can be analyzed from 1 g preparations of near eutectic and eutectic mixtures. As DTA is used mostly qualitatively, some method development work was necessary for its use in quantifying energy releases. Because of its rapid sample cycle rate, we have now an equivalent methods/information base in the energy recovery area. The DTA is method used primarily to screen energy storage candidates and concepts.

A series of DTA runs begun Sept. 1985 to Oct. 1985 were used to a) outline the general characteristics of ΔH_m and ΔH_f *vs.* m % MgF_2 and b) show the need for temperature-time data in preparing salt mixtures used for final measurements of the phase diagram. The DTA runs involved ~10mg of carefully mixed combinations of LiF & MgF_2 (Alfa Puratronic Grade). The data were obtained on mixtures maintained at 875 ± 8°C for 10 minutes. Figure 4.1-1 shows the 2nd cycle energies plotted *vs.* m % MgF_2. Clearly, the maximum energy recovered is near the eutectic composition of ~30 m % MgF_2. The reasons 875°C was chosen are: a) It is slightly above the m.p. of LiF, b) LiF has a significant vapor pressure ($4x10^{-2}$ torr) at its m.p., which means unless a means exists to condense it or the surface/volume ratio is low, LiF will volatilize away at unacceptable rates at higher temperatures, and c) 875°C is an industrially feasible temperature using common containment vessels for fluorides, ie., Ni could be used in scaleup. All heat values are electronically integrated.

To obtain a well mixed sample of LiF-MgF_2, the salt must be heated to 800-825°C or approximately 2/3rd of the way between the eutectic temperature of 725.2°C and 844.0°/cm the m.p. of LiF. The lowest predicted heat of fusion, 230 BTU/lb, for an ideal solid and nonideal liquid is exceeded only when the mixture is not allowed to cool below ~675°C. The reasons for this

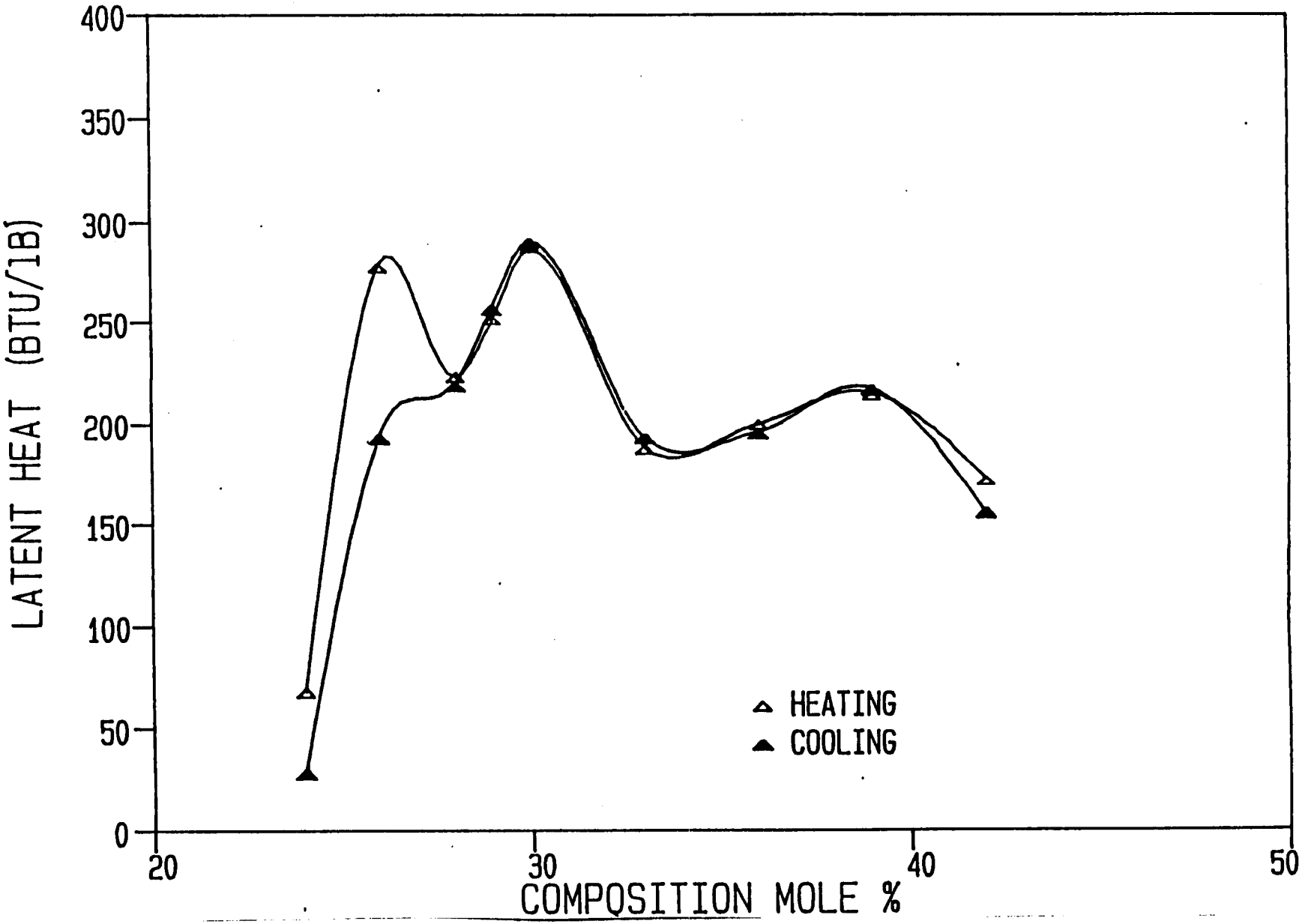

FIGURE 4.1.-1

LATENT HEAT OF LiF-MgF_2 PCM

are not clear. The difference in solidification kinetics of the various phase branches leading from the eutectic composition contribute to the problem.

The projected usage of this eutectic is for energy storage on the Space Station, where expected temperature cycling range is $\sim\pm75^{o}C$ from the eutectic temperature. Two series of temperature cycling experiments at 5, 2, and $1^{o}C$/min. were carried out, from $675^{o}C$ to $800^{o}C$; and from 700 to $825^{o}C$ using a new sample. The primary difficulty in carrying out this experiment out by DTA is the volatility of LiF; therefore, the upper temperature was limited to $\sim825^{o}C$. Results were obtained for the series for a high purity (Puratronic) 31.27 m % MgF_2 mixture prepared at the 1.2 g level and using a new DTA sample scanned from 700-$825^{o}C$. Results from earlier work obtained on a scaleup study sample, 31.06 m % MgF_2, agree closely to those obtained.

Stress Corrosion Cracking

A stress corrosion cracking experiment on INCO 625 was carried out with a 0.065 inch thick sheet.

After 36 hours of heating at $875^{o}C$, under Ar, the temperature of the salt sump was lowered to $750^{o}C$ and by applying Ar pressure to the top of the molten salt via closure of the gas outlet valve, the eutectic mixture (30.2%m MgF_2) was pumped up into the corrosion test vessel. The first attempt wasn't completely successful because the vent area around the Ni rod clogged with salt.

The venting on the next test was done through the gas outlet port on the corrosion test vessel. Although metallographic examination of the stress corrosion coupon at 50 to 1000 X showed no evidence of cracking or intergranular attack, a thin, uniform, layer of corrosion product was evident. This indicates that different metals cannot be joined together without attention to galvanic corrosion.

LiF-CaF_2 Characteristics

The preliminary design PCM is the LiF-CaF_2 eutectic. This selection is a change from the conceptual design specification of the LiF-MgF_2 eutectic. The LiF-CaF_2 system is a simple eutectic with good reproducibility in

thermodynamic properties. (These data was measured by Rocketdyne). The LiF-MgF_2 system, on the other hand, forms conjugate solid solutions, exhibiting a liquescent minimum melting point, rather than a true eutectic point. Measured thermodynamic properties have proven to be less reproducible than those for the LiF-CaF_2 eutectic.

The LiF-CaF_2 thermophysical properties of interest are listed in Table 4.1-1. The latent heat of fusion, measured at Rocketdyne, is in good agreement with theoretical calculations including non-ideal mixing effects. The selected PCM has a high heat of fusion and melts at a temperature appropriate for a high-efficiency CBC while allowing use of conventional superalloy containment materials in the receiver.

Because of interest in LiF-CaF_2 for comparison to LiF-MgF_2 in regard to energy recovery and the ability to cycle better with fewer problems, it was examined briefly. The published phase diagram for LiF-CaF_2 is simpler and is more clearly defined than the LiF-MgF_2 system. Similar procedures to those used in Lif-MgF_2, that is, grinding the CaF_2 (Fisher Scientific 99.95% pure material) and physically mixing it with Puratronic LiF, were employed for Lif-CaF_2. The physical mixture of 10-15 mg was heated in a Pt DTA cup for 10 minutes at 875$\pm$ 8^0 under Ar. Both cycles used the same temperature scan rates as used previously, 20 and 2^{0}C/min, respectively. The scan range used in the 2nd cycle was from 735 to 810^0 rather than 675-800^{0}C because the melting temperature 762.3^{0}C is 37^0 hotter than the LiF-MgF_2 eutectic, yet trying to minimize LiF vaporization losses.

4.1.2 High Temperatures Vacuum Sublimation Testing of Candidate Receiver Materials

The tube and PCM containment material selected for the CBC receiver is a cobalt based alloy, Haynes 188, a high-strength alloy which has extensive fabrication and joining experience. Haynes 188 was selected primarily for its creep rupture characteristics since the stress analyses performed for the conceptual design identified creep damage as the major life-limiting factor.

Sublimation of volatile components (mostly chromium) from superalloys at high temperatures over long periods of time has been considered a matter of

TABLE 4.1-1

PROPERTIES OF EUTECTIC $LiF-CaF_2$ MIXTURE[a]

Parameter	Value
Composition	80.5 pct LiF - 19.5 pct CaF_2 (by mole)
Melting Temperature, F	1416
Latent Heat of Fusion, Btu/lb	340
Solid Density (Melting Point), lb/ft^3	167
Liquid Density (Melting Point), lb/ft^3	131
Liquid Coefficient of Volumetric Expansion[b]	$1.5F \times 10^{-4}-1$
Solid Heat Capacity (Melting Point), Btu/lb-F	0.440
Liquid Heat Capacity (Melting Point), Btu/lb-F	0.471
Solid Thermal Conductivity (Melting Point), Btu/hr-ft-F[b]	3.4
Liquid Thermal Conductivity (Melting Point), Btu/hr-ft-F[b]	1.0

(a) Rocketdyne Data and Theoretical Analysis
(b) Based on pure LiF

concern. Recent data accumulated by the Signal Research Center have indicated that sublimation is not a problem at the temperatures of interest. Although Haynes 188 was not one of the tested materials, the alloys tested had chromium compositions similar to that of Haynes 188. For example, the weight loss for Inconel 625, which has a chromium content of approximately 22 percent (similar to Haynes 188), extrapolates to 30 mg-cm^2 of surface in 30 years at the lowest temperature measured, 1600F. Assuming all of the weight loss is chromium, a maximum depth of penetration, or effective chromium gradient of 0.01 cm (0.006 inch) can be readily calculated. Higher temperature data indicate that the sublimation rate is very temperature-dependent. The time-average maximum wall temperature at any location on the receiver is approximately 1500F. At this temperature, the sublimation penetration depth should be considerably less than 0.006 inch. The wall thickness of the exposed Haynes 188 surface (sidewall of canister) is 0.60 inch. (The canister outer wall is a nickel liner.)

Figure 4.1-2 shows that the weight loss upon vacuum heat treatment for the three alloys tested follows a power law time-dependence of the form:

$$\Delta W = At^b \qquad \text{Equation (1)}$$

where A and b are constants; ΔW = weight loss in mg/cm^2; t = time in hours. These plots can be used, under the appropriate conditions, to predict the time necessary to evaporate a given quantity of material from the various alloys. Inversely, with a known service life, the weight loss can be predicted.

Based on sublimation testing results, the following conclusions were reached:

- MA 754 experienced the lowest weight loss under vacuum heat treatments at 925 and 1000C.

- Weight loss for the three tested alloys follows a power law time dependence. Calculation of an activation energy for overall weight loss and extrapolation of data indicates a 10 mg/cm^2 weight loss for MA 754 after 30 years of exposure to a temperature of 870C.

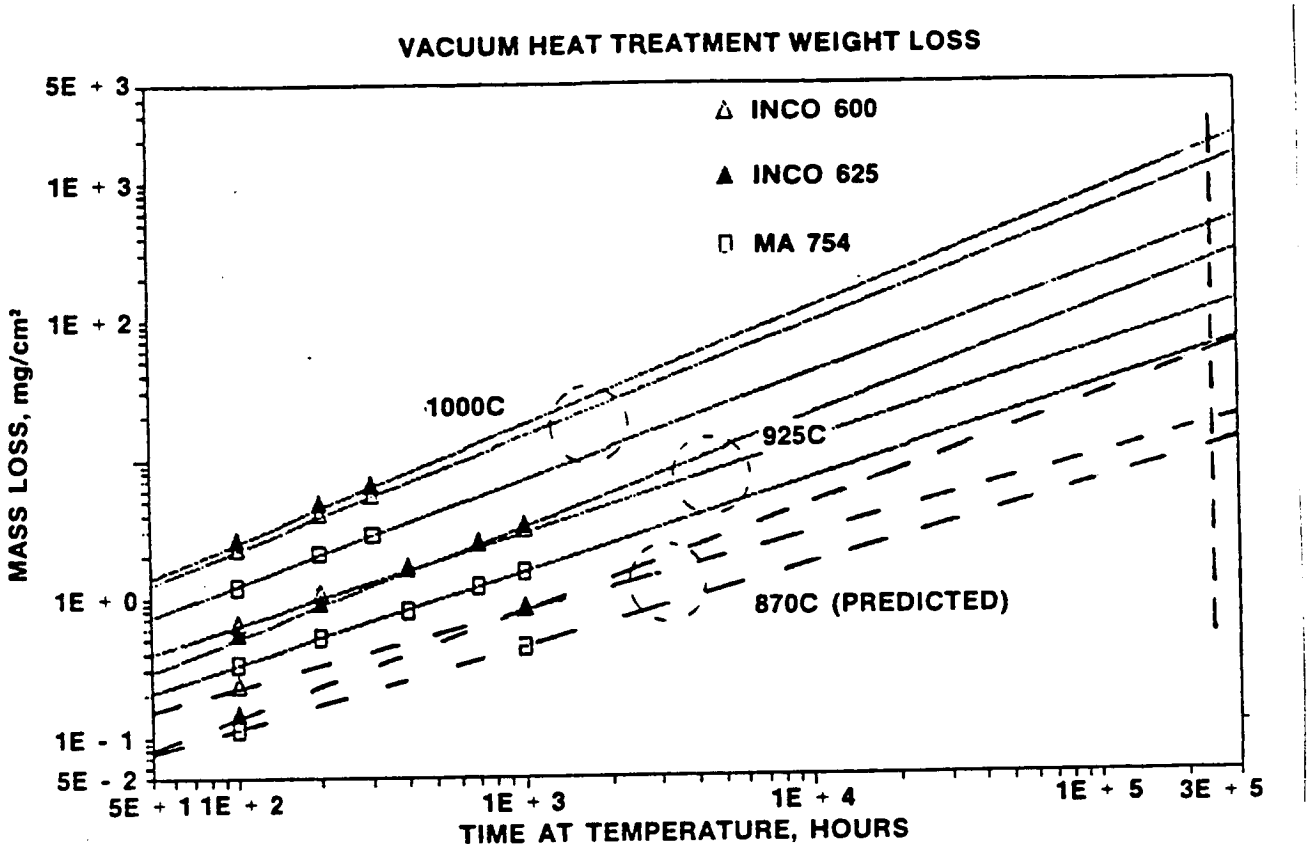

FIGURE 4.1-2

VACUUM HEAT-TREATMENT WEIGHT LOSS FOLLOWS
ΔW-Atb POWER LAW TIME DEPENDENCE

V2-4A/9

- o Grain boundary grooving is experienced by all three alloys tested.

- o Chromium is lost preferentially in all three alloys.

- o The bulk diffusivity of chromium in MA 754 is higher than for Inco 600 and Inco 625. This characteristic, coupled with its low weight loss under vacuum heat treatments, implies that bulk diffusivity is not the controlling factor in MA 754 sublimation.

- o The stability of the microstructure of MA 754 is maintained after 300 hours at 925C. This result is in contract to the dramatic grain growth in Inco 600 and Inco 625.

- o A network of grains high in molybdenum and niobium remains on the surface of Inco 625 after preferential sublimation of chroynium and iron.

- o Inco 600 and MA 754 surfaces sublimate uniformly with no apparent buildup of higher vapor-pressure species.

- o The high-temperature vacuum sublimation of chromium from the three alloys tested does not appear to be a problem at the temperature of 825^{o}C projected for the Space Station CBC power system.

4.1.3 Cyclic testing of LiF-filled phase change material heat exchanger.

The testing was conducted to determine the effect of cyclic melting-solidification of the LiF salt upon the heat exchanger. A secondary purpose for this testing was to establish the approximate heat-transfer characteristics of the heat exchanger when used as a thermal energy storage device.

Signal Research Center, Inc. filled the heat exchanger section, shown in Figure 4.1-3 with 114.54 grams of 99.999-percent-pure LiF salt at 1610 as reported in GPSD report 41-5637. The LiF fill weight and calculated liquid volume at 1610F matched the volume of the heat exchanger within 0.5 percent which indicated a complete fill. Twenty-four type-K thermocouples were attached to the inner and outer cylindrical surfaces and the the ends of the

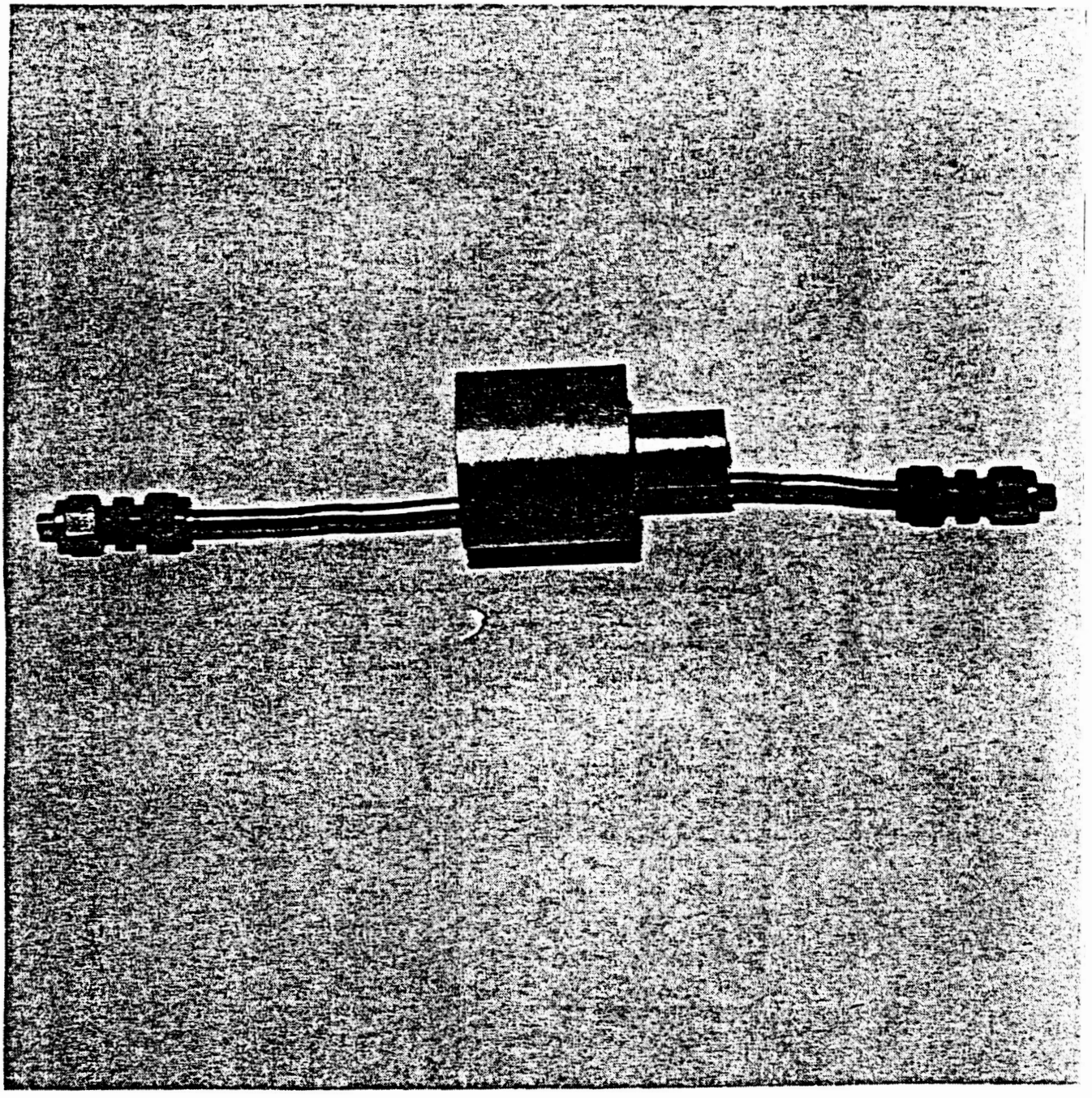

FIGURE 4.1-3

HEAT EXCHANGER FILLED WITH LiF PCM

V2-4A/13

heat exchanger. Four additional thermocouples were added to the inlet and exhaust flanges of the heat exchanger adapters. Two thermocouples were mounted in the inlet and exhaust tubing to measure air temperatures of the cooling gas flow.

The heat exchanger and adapters were installed in a 900-watt clam-shell electrical heater. Insulation was added between the heater and the inlet and exhaust tubing. The discharge tubing was insulated while the inlet tubing was not. This action created an axial thermal gradient that would ensure directional solidification and melting of the PCM.

Two thermocouples, located midway in the axial length of the heat exchanger, were used to control the cyclic operation of the furnace. One thermocouple was attached to the outside cylindrical surface, while the second thermocouple was attached to the inner tube. The thermocouple output was averaged and used to switch the heater on and off. Heater set points were established at 1630F off and 1460F on to allow complete solidification and melting of the LiF PCM. Cooling air flow was initiated when the heater wasswitched off at 1630F and was stopped when the heater was switched on at 1460F. This procedure was required in order to establish a reasonable cycle period for testing.

A typical melting-solidification cycle is shown in Figure 4.1-4. The changes is slope at Points A and B indicate the beginning and end of the latent-heat phase change of the LiF. The steeper slopes of the curve indicate the sensible heat portions associated with the solid and liquid phases. the latent-heat portion of the curve between Points A and B is not shown as isothermal due to the temperature measurements being taken on the metallic portions of the heat exchanger which of necessity, required varying differential temperature gradients to achieve a complete melting of the PCM. The changes of slope, however, accurately reflect the beginning and end of the latent-heat period.

The thermal characteristics of the heat exchanger during a typical melting-solidification cycle is plotted in Figure 4.1-5. The cooling air for the cycle was turned on approximately 13 minutes into the cycle, as shown in Figure 4.1-6. Cooling air flow was 0.05 ppm. As in the plots shown previously, the change in curve slope indicates the onset of a phase change.
V2-4A/11

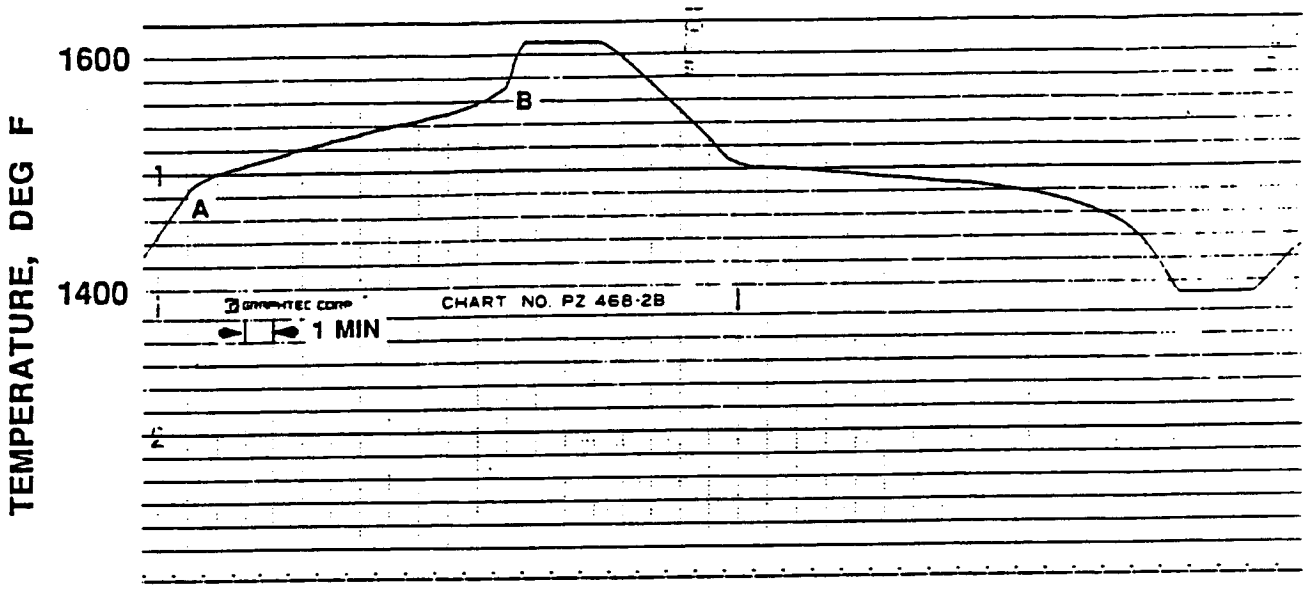

FIGURE 4.1-4
TYPICAL MELTING - SOLIDIFICATION CYCLE

V2-4A/14

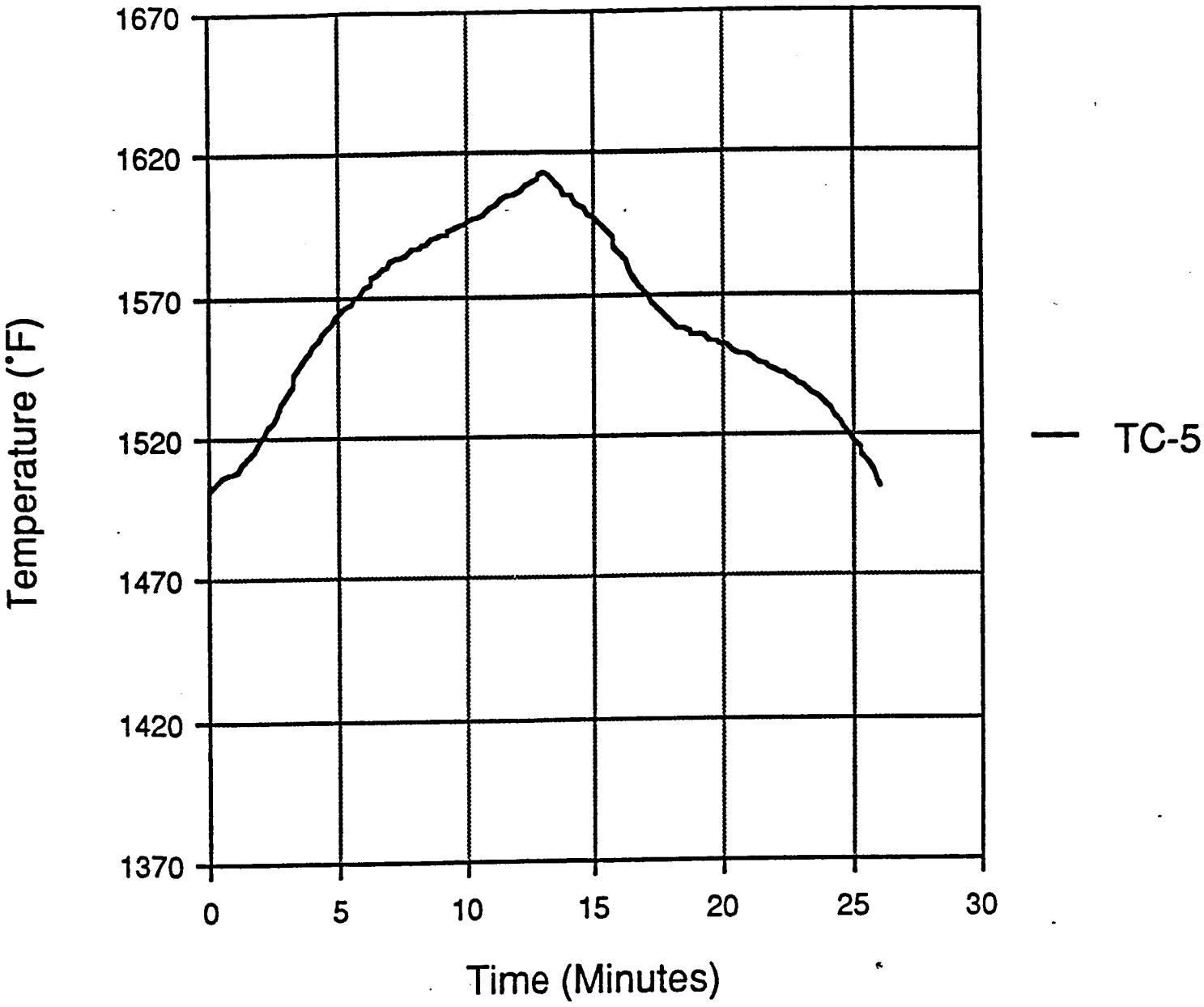

FIGURE 4.1-5

DATA FROM THERMOCOUPLE NO. 5

V2-4A/15

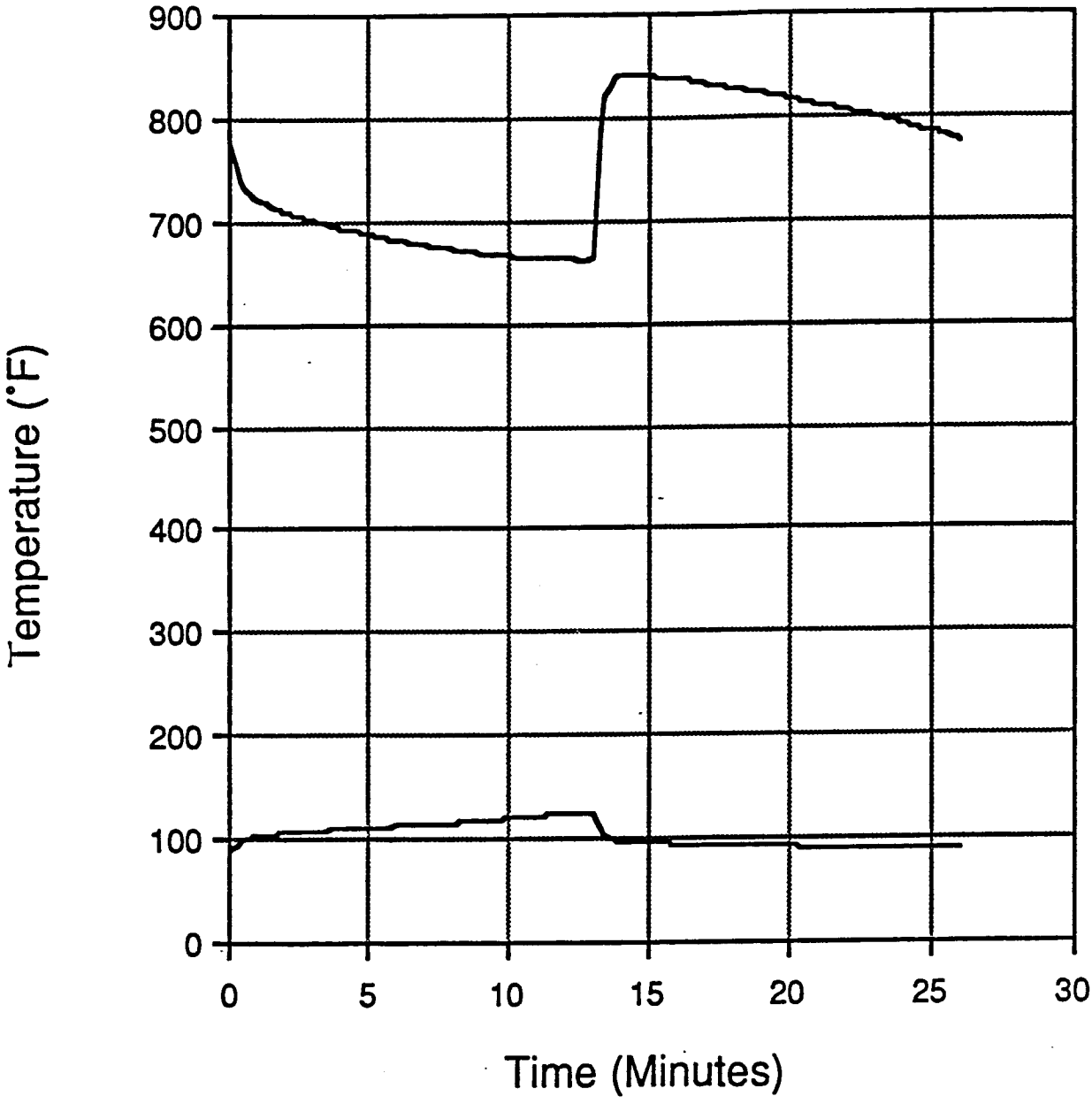

FIGURE 4.1-6

DATA FROM THERMOCOUPLES NOS. 29 AND 30

V2-4A/16

The heat exchanger PCM thermal behavior, several cycles after LiF leakage, is shown in Figure 4.1-7. The condition of the heat exchanger after the LiF leakage showed a black deposit (scale) resulting from the fluxing reaction between the molten LiF and hastelloy B material in the presence of air. Visual inspection of the heat exchanger indicated that the braze alloy was relatively unaffected by the LiF in comparison to the Hastelloy container material.

It was necessary to pinpoint the locations of the liF leakage for metallographic examination of the heat exchanger. This proved to be a difficult task to accomplish. When high-temperature LiF leakage occurs in the presence of air, the resulting scale tends to seal the leak and to obscure the precise location. Since concentrated sulfuric acid was ineffective in removing the scale, a sandblasting procedure was employed. Several apparent pinholes were identified under low-power microscopic examination; however, leak checks using helium gas applied to one fill tube were unable to confirm the apparent holes as sources of the leaks. Subsequent acid cleaning and dye-penetrant examination identified the location of one additional pinhole in the braze joint between the heat exchanger inner tube and the end plate. Cross sectioning and metallographic examination would be required to determine if the pinholes penetrate the heat exchanger walls into the LiF cavity.

The cause of the LiF leaks is not evident from any test data, test procedure, or visual inspection currently available. All inspection data gathered during the initial heat exchanger fabrication, pre-LiF fill inspection, fill, and subsequent 25 melting-solidification cycles indicated the heat exchanger to be leak-free. While the cause of the leaks has not yet been identified, it must be associated with the materials and cyclic testing under which the leakage developed. Radiographic and metallographic evaluation was required to establish the cause of the leakage.

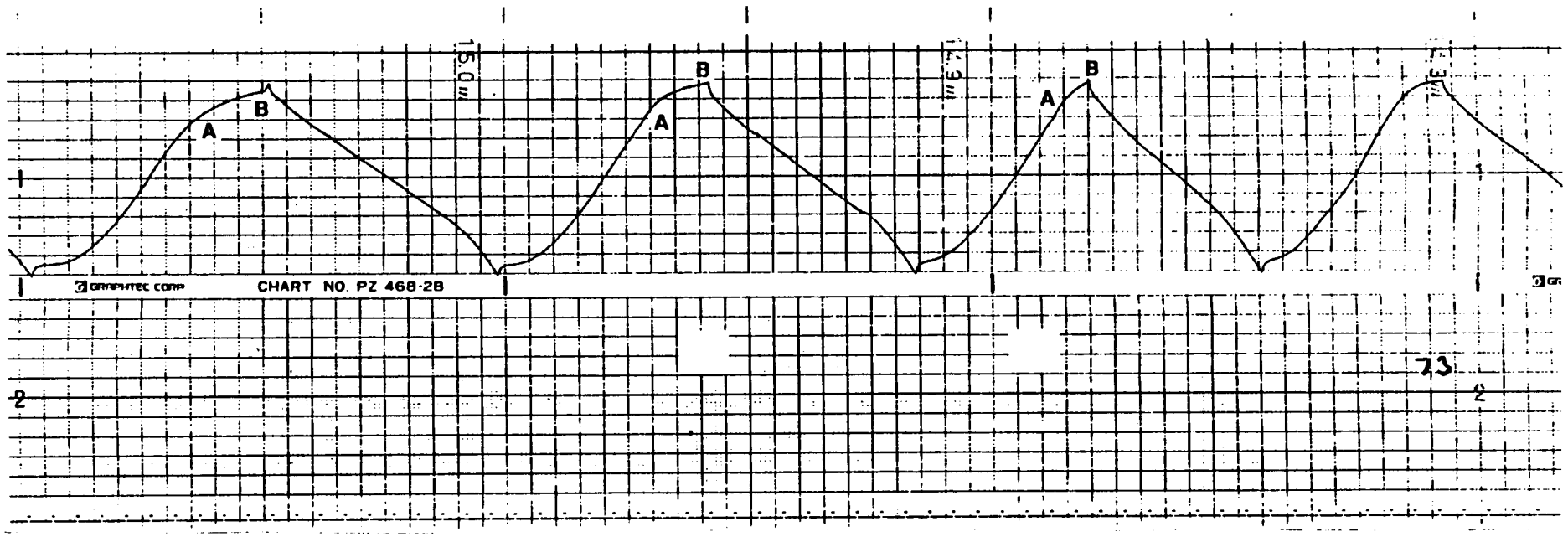

FIGURE 4.1-7

HEAT EXCHANGER PCM THERMAL BEHAVIOR, SEVERAL CYCLES AFTER THE LiF LEAKAGE

Metallurgical Evaluation of LiF-Filled Phase Change Material Heat Exchanger

Post-test of the heat exchanger after the cyclic testing indicated that a number of LiF leaks developed in the braze joints between the 1/4-inch diameter fill tube and heat exchanger end plate, as well as leaks in the joints fluxing action of the high-temperature LiF in the presence of air on the end cap material had obscured the cause of the leaks. Non-destructive penetrant inspection after sand blasting and sulfuric acid etching did not reveal the cause of the leaks.

A metallurgical evaluation was performed to determine the cause for the LiF leakage. A secondary purpose of the evaluation was to determine the effects of thermal cycling on the braze joint between the internal fins and the concentric tubes.

Results of the effort are described below.

- LiF which developed in the braze joint between the 1/4-inch fill tube and heat exchanger end plate during testing were found to be attributable to a fractured braze joint. A 0.002-inch-wide maximum size gap was found in the braze joint between the 1/4-inch fill tube and the heat exchanger and plate.
- LiF leaks which developed in the braze joint between the outside tube and the heat exchanger end plate were found to be due to a defective braze joint. The braze joint contained rounded and linear defects which allowed LiF leakage from the container.
- Internal fins brazed to the outer tube were found to have separated. The separation was attributable to the fracturing of the braze joint. No separation of the internal fins brazed to the inner tube was observed.
- LiF leakage caused a fluxing of the Hastelloy B container material. Corrosion of the 300-series stainless steel fill tube by LiF was evident. Nickel-base braze alloy was relatively unaffected by the LiF in comparison to the hastelloy B container material and the 300-series stainless steel fill-tube material. Nickel fins were relatively unaffected by the LiF.

4.2 AD-1B ORC

There were three specific full scale axial heat pipe tasks undertaken by the Sundstrand Corporation:

A. A specification was generated for an axial heat pipe transport requirements compatible with thermal energy storage and the organic working fluid requirements.

B. Design and analysis was performed to meet these requirements.

C. Fabrication and assembly of the heat pipe, was completed.

4.2.1 Specification for Axial Heat Pipe

Based upon a 37.5 kWe receiver under consideration in August 1985, the following specification shown in Table 4.2-1 and Figure 4.2-1 was generated and provided to Los Alamos National Laboratory.

4.2.2 Analysis and Design

The design requirements imposed on the solar receiver heat pipe are similar to a conventional heat pipe but with some differences in the operational characteristics. The solar flux varies from end to end with a peak of approximately 7.5 w/cm^2. The design required a 100% design margin, i.e. 15 w/cm^2. The temperature in the vapor space is limited to 537^oC so as to provide minimal toluene degradation during the 30 year lifetime. Each heat pipe thermal input is approximately 4.8 kW during insolation at normal operation with a 5.7 kW power maximum possible from concentrator misalignment. Potassium is the heat pipe working fluid. The envelope is 5 in. OD x .050 in wall (347 SS) x 75 in. long. Three layers of 100 mesh screen are tack welded to the envelope ID and to the TES canister and simulated vaporizer OD. Five arteries of 100 mesh screen, .125 inch diameter, closed down to .020 inch diameter on the ends provide liquid axial return flow. Details of the gas-gap 304 CRES simulated vaporizer are shown in Figure 4.2-2. A picture of a TES canister is shown in Figure 4.2-3. There are four canisters 2" OD x .065 wall, x 36" lg., Ni-200 material. Thermal heat transfer enhancement is provided by stamped fins of Ni-200 0.14 inch thick.

The operating requirements and internal flow patterns for the heat pipe vary widely depending on the mode of operation. Figure 4.2-4 shows radial flow during insolation and during eclipse. During insolation there is axial transport as dictated by the axial flux variation along the length of the pipe. During eclipse, the flow is essentially radial from the TES canisters to the vaporizer.

TABLE 4.2-1

RECEIVER PARAMETERS

o Life	10 years (55,000 thermal cycles) (later changed to 30 years)
o Normal operating Temperature	930 - 1000°F
o Total Solar Incident Energy Onto Cavity	288.9 KW
o Thermal Energy Storage (TES) material	LiOH (878°F melt temp)
o Vapor delta T Limits	55° - 100°F max
o Orbit time	94.3 min
o Eclipse Time	35.3 min maximum
o No. of Heat Pipes	40 used
o Receiver I>D>	50 inches
o Heat Pipe Design Weight (without thermal energy storage units)	15.0 lbs.
o Vaporizer	Fluid: Toluene; h = 800 B/Ft^2/Hr/°/F Temp Inlet 467°F Temp Outlet 750°F Mass flow; .658 lb/sec 690 psia inlet pressure
o Environment	Space shuttle launch vibration, shock, acoustic Micrometeoroids Cosmic Radiation Atomic Oxygen Space Vacuum Solar Flux 1-g Earth Testing
o Interfaces	TES Cansiters Circumferential Heat Pipes Vaporizer Assembly

o Nominal axial insolation flux Per Figure 4.2-1

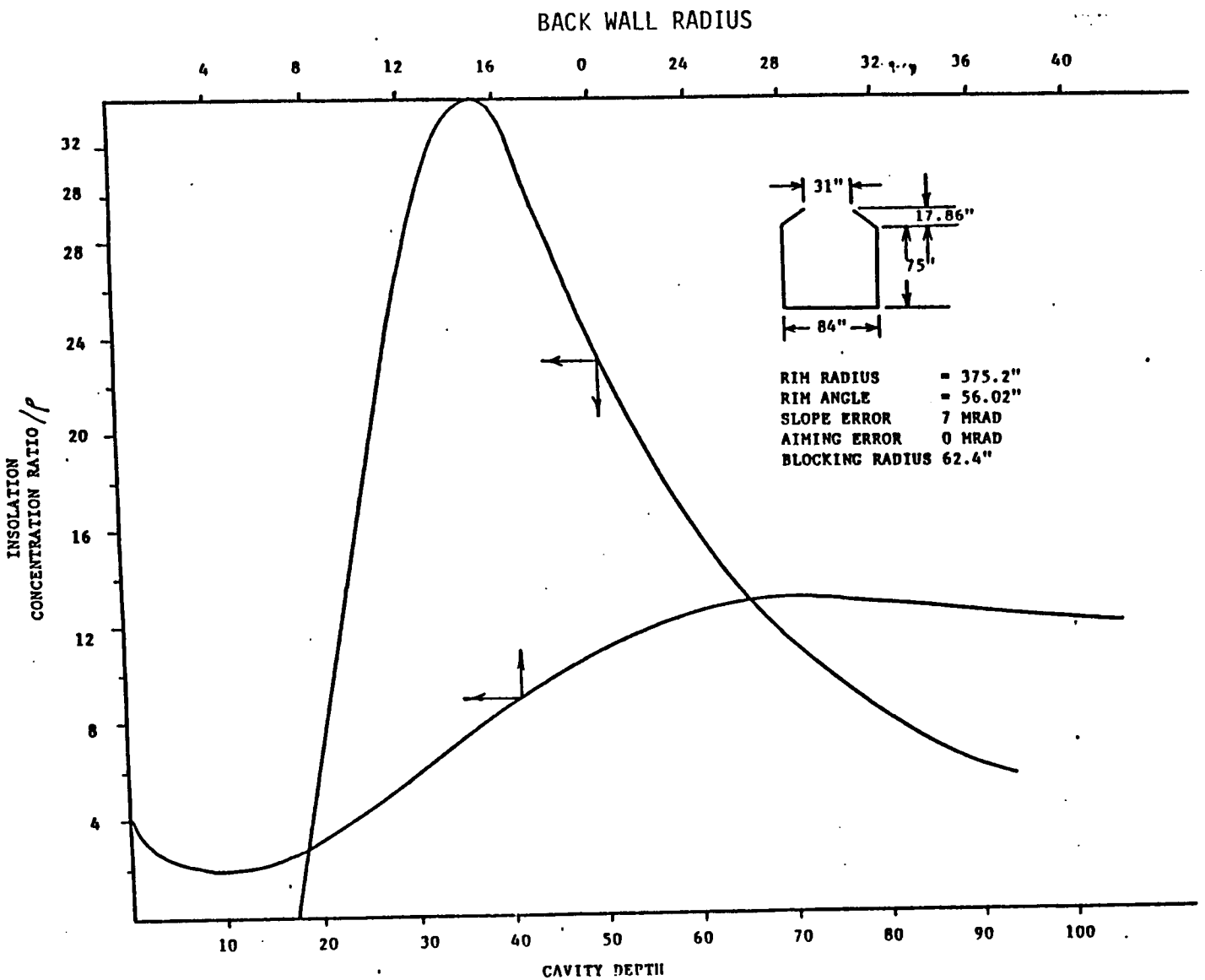

FIGURE 4.2-1

RECEIVER PARAMETERS

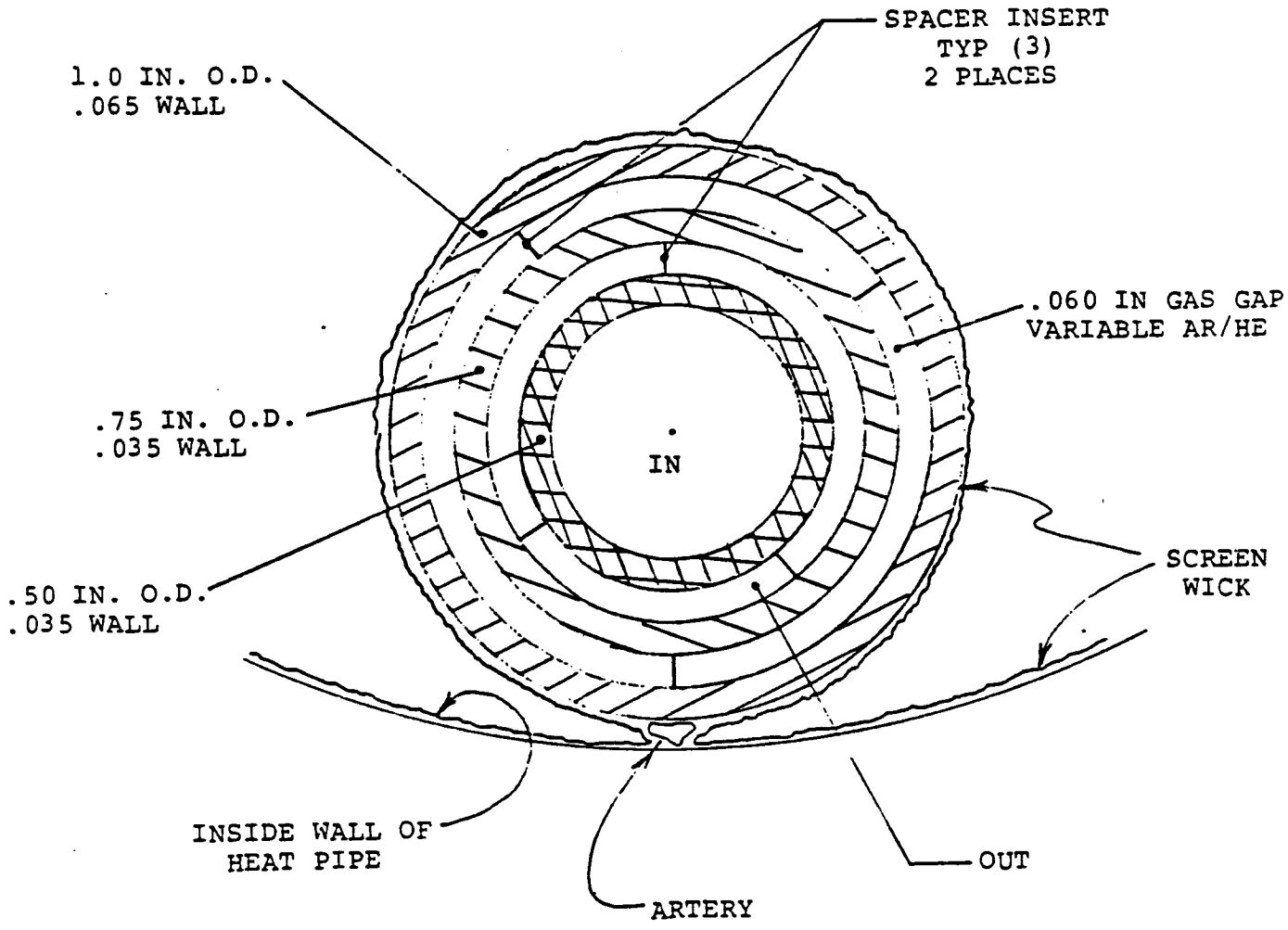

ADVANCED HEAT PIPE VAPORIZER

CROSS-SECTION WITH GAS-GAP

FIGURE 4.2-2

V2-4A/23

Advanced Axial Heat Pipe TES Canister Showing Internal Fin Details

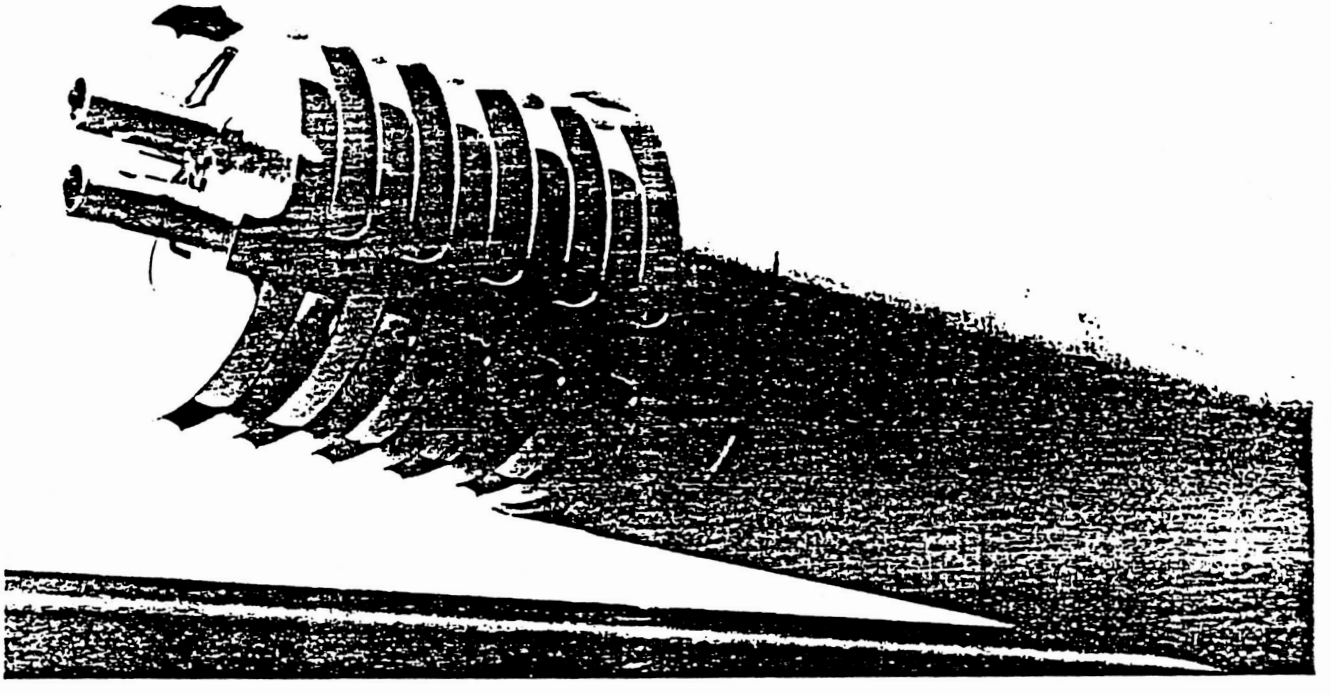

- Fins Enhance Heat Transfer Into PCM to Minimize Orbital Temperature Variations

FIGURE 4.2-3

Heat Pipe Operation

- SCREEN WICK STRUCTURE TRANSPORTS LIQUID POTASSIUM TO HP VAPORIZING SURFACES BOTH RADIALLY AND AXIALLY

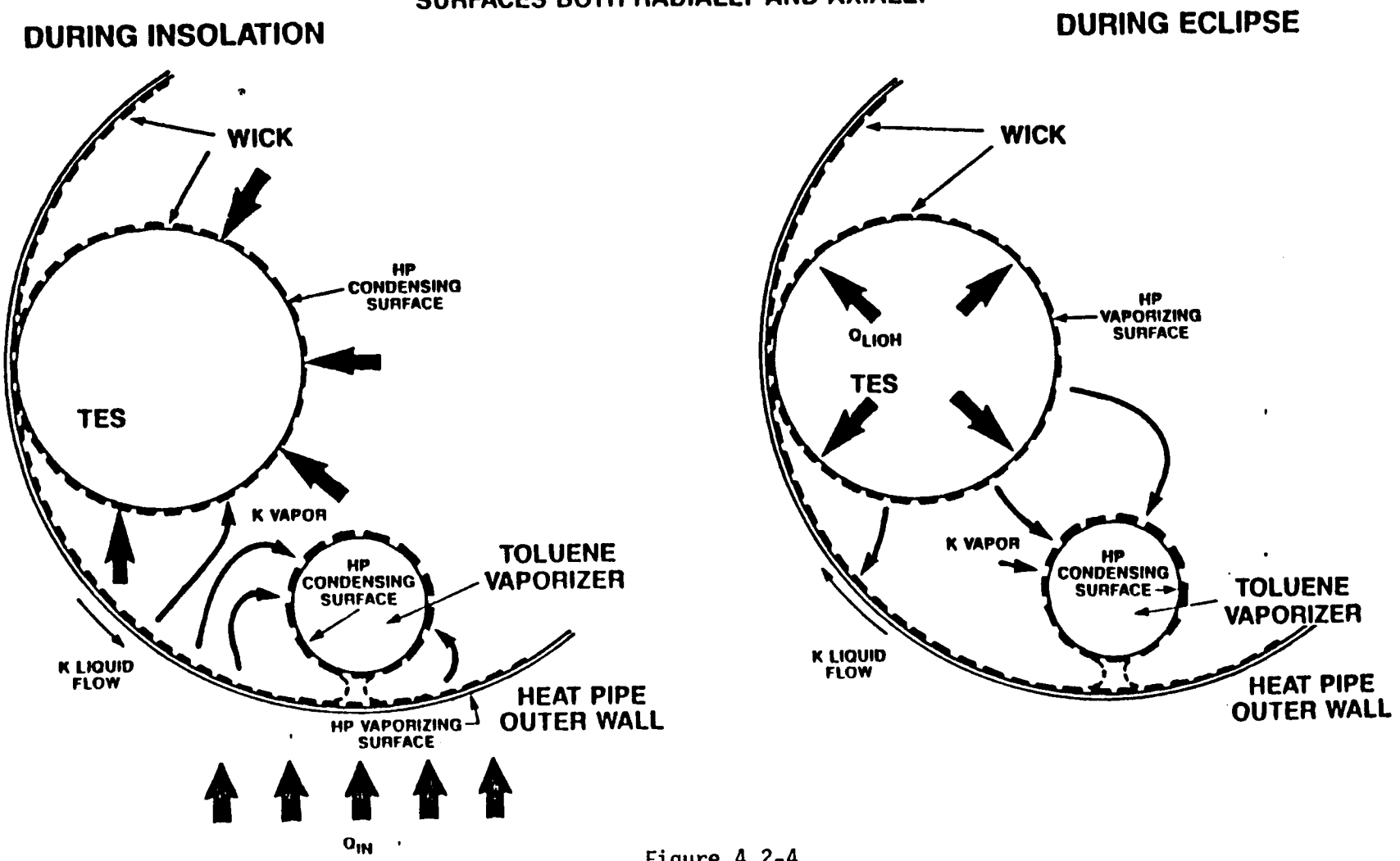

Figure 4.2-4

The design meets the functional requirements of: (1) abosrbing the solar energy reflected by the concentrator, (2) transporting the energy to the ORC vaporizer, (3) providing thermal storage for the eclipse phase, and (4) allowing uniform discharge from all TES elements to the vaporizer.

This heat pipe design, with its internal heat removal surfaces and unusual geometry, does not conform to standard heat pipe computer models, therefore, specific design calculations were performed. To insure an adequate capillary structure for condensate return to the evaporating surface, liquid and vapor pressure drops were calculated on the basis of an anticipated worse case power level or thermal distribution during the insolation/eclipse cycle. Phenomena which might be responsible for heat pipe failure or performance limitations, specifically, sonic vapor velocities, liquid entrainment and boiling, were also investigated. A heat pipe design was chosen which would accommodate these extreme conditions. Successful heat pipe operation requires that the available capillary head equal or exceed the total working fluid pressure drop during its cyclic evaporation and condensation cycle.

The relationships governing this are:

$$\Delta P_{C,\,max} \geq \Delta P_{\ell} + \Delta Pv$$

with

$$\Delta P_{C,\,max} = 2\sigma/r$$

where

$P_{C,\,max}$ is maximum capillary pumping pressure assuming full wetting of the wick,

σ is the liquid surface tension,

r is the wick pore radius,

ΔP_{ℓ} is the pressure drop in the liquid phase,

and

ΔP_v is the pressure drip in the vapor phase.

Because the liquid pressure drop depends upon the chosen wick structure, the usual design approach is to choose a wick on the basis of experience, analyze heat pipe performance and modify the wick design as necessary based on the predicted performance. A wick structure thus chosen for the ORC-SDPS heat

pipes incorporates three layers of 100 mesh stainless steel screen and 5 axial arteries, 1/8 inch diameter. A screen pore radius of 0.083 mm, based on 1/2 the screen mesh size (3.5 mil dia. wire), provides a maximum capillary pressure of 1952 Pa. Potassium fluid properties for this and the following calculations were taken at 502^{o}C.

Heat transfer into the ORC-SDPS heat pipe working fluid is from the solar heated surfaces during insolation and from the storage canisters during eclipse. The nonuniform energy flux during insolation and eclipse which arise due to a nonuniform vaporizer tube temperature must be accommodated. A counter-flowing vaporizer tube arrangement, wherein the toluene passes first through a small diameter tube and then returns down the annulus created by a larger diameter concentric tube, is used to minimize this axial thermal gradient. Both the insolation and eclipse periods were analyzed by neglecting the thermal gradients associated with either the vaporizer tube or the TES tubes.

Insolation during normal operation results in a total power incident on each heat pipe of 4.8 kW. Flux asymetry from the offset concentrator and slight misalignment of the solar reflector could result in a heat pipe load of 5.7 kW. This higher power level was assumed constant in the analysis.

Pressure Drop During Insolation

During solar insolation the incident heat energy is nonuniform over the heat pipe surface which constitutes the receiver surface. Rather than accurately modeling this flux distribution, a suitably conservative model for pressure drop calculations is based on assuming that 100% of the power is evenly distributed over the first 0.5 m of heat pipe length. The peak heat flux was used to evaluate the boiling limit of the working fluid.

During the period of solar heating (59 minutes of the 94.3 minute cycle), some fraction of the power must go into storage so that a steady rate of power removal via the vaporizer tube can be maintained during the eclipse period. With 5.7 kW total power, 2.15 kW is stored in the salts and 3.55 kW is removed by the vaporizer. the potassium flow path during insolation is assumed to be as follows: (1) evaporation occurs over a 0.5 meter long section of the semi-cylindrical surface which is exposed in the receiver cavity, (2) the vapor

leaves that surface and condenses uniformly over the vaporizer tube and TES tube surfaces in the power proportions stated in the preceding paragraph. (3) the condensate flows circumferentially into the nearest artery and down that artery as required to the evaporating surface, (4) the evaporating surface is resupplied by circumferential flow from the arteries. Pressure drops were calculated using Darcy's law for porous medial in the wick, laminar tube flow in the arteries and laminar vapor flow, and the low Reynolds numbers of the flow. No dynamic pressure recovery in the vapor was assumed (dynamic head is negligible). Vapor pressure drop was based on a hydraulic radius determined by the ratio A/P, where A is the cross sectional area of the vapor passage and P is the wetted perimeter. A wick permeability of 2.0×10^{-10} was assumed based on reference values for similar screen structures. The working fluid loops to the vaporizer tube and to the TES tubes were treated as independent paths. The results are summarized in Table 4.2-2.

Pressure Drop During Eclipse

During eclipse, the heat pipe working fluid circulation is from the TES tubes to the vaporizer with little axial flow. The maximum power level is 3.55 kW. The potassium flow is distributed evenly over the entire heat pipe length. This results in a low liquid pressure drop due to the low fluid velocities and short flow paths. The only appreciable pressure drop is in the circumferential liquid flow. In this analysis the heat pipe wall was treated as an adiabatic surface. Results for the eclipse period pressure drop are summarized in Table 4.2-2. Eclipse period pressure drops are quite low; a significant adjustment for axial flow to accommodate thermal nonuniformities in the thermal storage medium could be tolerated.

Pressure Drop Summary

The largest pressure drop occurs in the heat pipe to vaporizer tube loop during insolation. This pressure drop is 376 Pa, much less than the capillary capacity, 1952 Pa. The heat pipe capillary structure is therefore suitably conservative for this application.

TABLE 4.2-2

Tabulation of Heat Pipe Pressure Drops

During Insolation and Eclipse

Condition	Pressure Drop (Pa)* Insolation Heat Pipe to Vaporizer Tube	Insolation Heat Pipe to TES	Eclipse TES to Vaporizer Tube
Vapor phase	16.	10.	0.
Liquid circumferential flow	285.	116.	196.
Liquid axial flow (arterial).	75.	11.	0.
Total P	376.	137.	196.

* Available capillary pressure is 1952 Pa.

Other Power Limits

When operating at 5.7 kW, vapor velocities as high as 8.0 m/s are possible in the radial flow through the constriction between the two TES tubes. This is much less than the 488 m/s sonic velocity limit of potassium at the design temperature.

Heat pipes may also be limited by entrainment of the liquid phase by the counterflowing vapor, however this phenomena also occurs at high vapor velocities which do not occur in this heat pipe.

Another principal consideration in the heat pipe design is boiling of the liquid in the wick or arteries. Boiling in the wicks or arteries may result in local dryout of the heat pipe surface with consequent problems in rewetting, particularly with liquid metal working fluids. For this reason the arteries in this heat pipe design are not in contact with the high flux surfaces.

Boiling in the wick structure on the insolation surfaces is still a concern and was considered in the design.

The required superheat to boil is given by:

Temperature difference, $T = 2\sigma T_s/(\rho v h_{fg} r_p)$,

where T_s is the saturation temperature, r is a nominal nucleation site size, taken as 2.5×10^{-5}m, h_{fg} = evaporizational (phase change) enthalpy for potassium, and v = vapor density. At 502°C the limiting boiling point superheat of potassium is 27.3°C.

The existing superheat is determined as the sum of the temperature drops across the wick/working fluid matrix and the liquid/vapor interface. The temperature drop through the matrix is calculated from

$$T = \delta_w q/k_w,$$

where k_w is an effective working fluid/wick conductivity, and w = goove depth. k_w is difficult to characterize accurately for screen mesh, but a good approximation is:

$$k_w = \frac{\beta - \epsilon}{\beta + \epsilon} k,$$

where k is the working fluid conductivity, E is the volume fraction of the solid phase (wick) and

$$\rho = (1 + (k_s/k_\ell))/(1 - (k_s/k_\ell))$$

with k_s equal to the screen mesh thermal conductivity. With stainless steel screen and an assumed - 0.6, this temperature drop is 3.73°C.

The temperature drop associated with the liquid/vapor interface is calculated from

$$\Delta T = (2\pi RT_s)^{.5} RT_s^2 q/(Ph_{fg}^2)$$

where R is the gas constant for potassium, P = pressure and q is the maximum design heat flux.

The total existing superheat during maximum flux is -268.2°C, much less than the 27.3 C superheat required to boil.

Pressure Drop In Gravity Field

Gravity force has two effects on the heat pipe performance. First, it adds, at most, (ρ g h) to the total pressure drop. A 900 PA adjustment to the above calculations, assuming orizontal orientation, proper artery operation and folar flux on the surface to which the vaporizer tube is attached. This addition is about on half the available head and significantly affects the margin. However, conservative assumptions in the above calculations, coupled with the fact that, regardless of orientation in the gravity field, some flows will be assisted by gravity, it is reasonable to expect the heat pipe to operate. To justify the statement that there will always be some degree of gravity assist, consider the orientation with the vaporizer tube up and solar flux down. The condensate return along the vaporizer tube is up hill, but the circumferential rewetting of the heat pipe wall is down hill.

Circumferential rewetting is still uphill from the TES, but condensate flow along the TES is, on the average, gravity free; half is with and half is against gravity. At any point in time or space the available head is greater than the sume of all the pressure drops.

A second concern is that if any of the arteries are higher than the artery pumping height, referenced to the lowest point in the heat pipe, those arteries will not self-prime or self-fill. The test pipe design artery is closed down to 0.20 inches, resulting in a wicking height of 9 cm (3.5 inches). This is high enough to insure that at any time some or all of the arteries will be working.

With the vaporizer tube down and solar insolation on that surface, all the arteries will operate, so the effect of gravity is less than adding 900 Pa, and the heat pipe should operate.

With the vaporizer tube up and solar insolation on that surface, the vaporizer tube arteries cannot be expected to remain full. The path of least resistance for the condensate returning from the vaporizer tube surface will be simply down the heat input surface over the heated zone but in the low flux

zone most of the condensate will flow down to the TES arteries, down those arteries and up the heat input wick surfaces. The pressure drip without gravity effects in this case is 605 Pa with Pa gravity drop the total pressure drop is 1505 Pa, still below the available head of 1952 Pa.

On the basis of these calculations, the heat pipe should operate in any orientation if the heat flux is on the side with the vaporizer tube.

Performance Limit Summary

The heat pipe design allows for condensate return to the high temperature surfaces under the most extreme anticipated conditions. The design safety averts conditions conducive to heat pipe failure or limitations due to excessive pressure drop, sonic vapor velocities, liquid entrainment or liquid boiling and log operation.

4.2.3 Fabrication and Assembly

Four Ni-200 tubes were machined to accept end caps which were electron beam welded to the tubes. (Nickel-200 is not the material selected for long term use, due to problems associated with its high carbon content. It was used because of availability and success with it in rectangular canisters used in a demonstration heat pipe which had accumulated over 500 hours at that time. The demonstration heat pipes were built and tested y Sundstrand as part of their complimentary IR&D activity.) The canisters were filled in an inert atmosphere (N_2 room with argon purge of the furnace) at Rocketdyne, using the same method as they used to fill several hundred 1" diameter canisters. The existing furnace limited the length of a canister to be filled to 4 feet. Since the heat pipe was just over 6 feet long, the canister length was made 3 feet. Two canisters were connected in series with a welded stud to make the equivalent of a 6 foot canister. After filling with LiOH, the closure end cap was electron beam (EB) welded. A proof thermal cycle test was performed of Rocketdyne. After this test is was discovered that three of the four canisters leaked through the first EB weld. it was decided to remove all end caps, from both ends, and weld new caps by gas tungsten arc welding (GTAW). This was done using an argon purge chamber. This method required a small .042 in. vent hole to allow the heated expanding gas inside the canister to escape. The vent hole was then welded shut. On one of the four, the vent hole was contaminated with

LiOH during the welding making the weld suspect. It was decided to proceed with three filled LiOH canisters. A dummy canister was fabricated and installed in the heat pipe. Failure analysis determined that the Ni-200 tubing, while within specification (ASTM B160) contained four times the normal amount of silicon and about two and one half times the normal amount of sulfur. Energy dispersive X-ray analysis (EDAX) indicated that failed grain boundaries were exceptionally high in silicon and sulfides. It was therefore concluded that a tighter specification is needed to control chemistry of pure nickel for the space station application.

The heat pipe is 75 in. in length, with an outside diameter of 5.1 in. and a wall thickness of .035 in. Stainless steel was selected as the heat pipe material for the heat pipe test assembly based on availability, fabricability and desirable coupling characteristics for high frequency radiant heating. Three-layers of 100 mesh screen were placed against the inner wall of the heat pipe for circumferential fluid distribution. The first two layers of screen were each wrapped on bias over a mandrel and resistance welded wire-to-wire to form a screen tube. These screen tube layers were individually inserted into the heat pipe container tube, expanded and resistance welded to the inside of the heat pipe. Three layers of 100 mesh screen will also be placed over the TES canisters to collect the condensate during the thermal storage cycle and to provide for evaporation of the potassium during the eclipse cycle. The screen on the TES containers was wrapped on the bias directly onto the TES canisters a layer at a time and resistance welded to itself. Three layers of 100 mesh screen were used on the vaporizer tube to collect the condensate during operation. Two of these layers were formed in the same fashion as the screen on the TES units. The third layer was arranged to form a pedestal, which provides a fluid path from the vaporizer tube to the distribution wick and forms the final layer of the circumferential fluid distribution wick. This final layer of screen is resistance welded to the first two layers. Axial fluid distribution is accomplished by five arteries, two between each of the TES units and the inner wall of the heat pipe and one double artery between the vaporizer tube and the screen pedestal which connects the vaporizer tube to the distribution wick. The TES containers and vaporizer tube are positioned internally and held in place by end cap supports and an internal stainless steel skeletal support.

Processing

All internal heat pipe parts were solvent cleaned and then high-vacuum fired at 825°K for 2 hours prior to assembly. The end caps were TIG welded in place and the assembly vacuum fired. Prior to potassium charging, the heat pipe assembly was high-vacuum fired at 552°C. A schematic diagram showing the heat pipe arrangement during high vacuum firing and ready for vacuum distillation shown in Figure 4.2-5. The distillation chamber and the stainless steel tubing connecting the distillation chamber to the heat pipe were high-vacuum fired before they were assembled and welded as a unit. The set-volume chamber was attached to a high purity potassium reservoir at one side and to the distillation chamber at the opposite side. The outlet of the distillation chamber was attached to the heat pipe with an extension for vacuum pumping. A chilled heat sink was placed on the tubing just below the set-volume chamber to act as a valve to prevent the liquid metal from draining out of the set-volume chamber during loading and as a valve during distillation.

The total operation of transferring the working fluid from the resevoir to the set-volume chamber to the distillation chamber and finally into the heat pipe was as follows:

- o A vacuum was pumped in the total system while the set-volume chamber, the transfer lines and distillation chamber heated above the melting point of the working fluid and the reservoir to 201°C.

- o The potassium reservoir was pressurized and the set-volume chamber loaded.

- o Heat sink No. 1 was removed and the top side of the set-volume chamber pressurized forcing the potassium into the distillation chamber.

- o Heat sink No. 1 was reactivated, the heat pipe and transfer line between the heat pipe and the distillation chamber was heated above the melting point of potassium. The liquid metal pool in the distillation chamber was increased to 452°C for distillation.

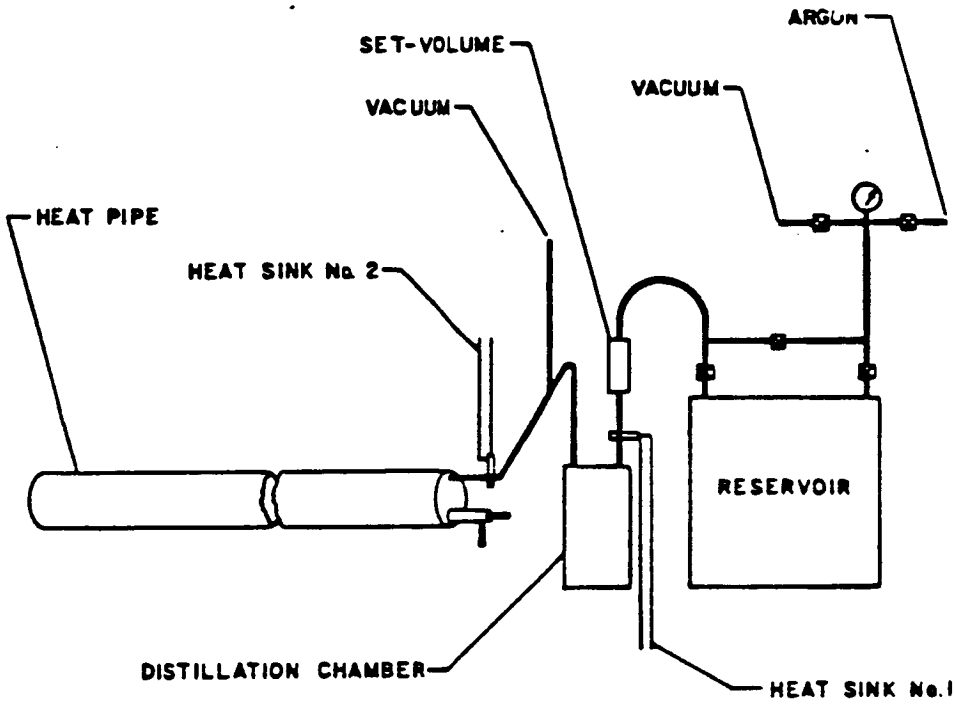

POTASSIUM DISTILLATION APPARATUS

USED FOR FILLING HEAT PIPE

FIGURE 4.2-5

V2-4A/35

Distillation was completed when a rise in temperature was observed in the distillation chamber as a sign of depleted potassium and a decrease in temperature was observed at the transfer line as an indication that vapor was not longer being moved through the line. The distillation chamber was allowed to cool down.

- Heat sink No. 2 was activated, the heat pipe heated to 100 degrees above the melting point of potassium and tilted, allowing the liquid to drain by gravity head into the fill stem, forming a metal freeze plug.

- The heat pipe was removed from the distillation set-up at the freeze plug, capped and was then ready for wet-in and subsequent testing.

After filling, the heat pipe was positioned horizontally and heated over its entire length to distribute the potassium charge uniformly and ensure complete wetting of the interior surfaces and filling of the arteries. Filling of the arteries is accomplished by positioning the heat pipe with one set of arteries at the bottom side of the heat pipe thus allowing the arteries to fill by gravity. This procedure was repeated for each set of arteries.

This completed the fabrication and assembly of an advanced heat pipe, and the heat pipe was ready for testing.

4.3 AD-2 Concentrator

There were two (2) specific tasks undertaken by the Harris Corp.

A. Characterization of this kinematics of the concentrator concept.

B. Evaluation of substrates, reflective coatings, and protective coatings for possible use on the concentrator.

4.3.1 Concentrator Kinematics

The solar dynamic power system uses 19 full hexagonal panels to serve as the concentrator surface. Hexagons were chosen because they are the highest order polygon that can form a plane surface without gaps. High order polygons fit within the circular cargo bay with little wasted space. The objective of this study was to conceptualize, develop, and fabricate the mechanisms necessary for deployment and retraction of the precision hexagonal reflector. The repeatable and reliable deployment mechanisms must support the requirement of a 3 milliradian surface error for the closed Brayton cycle receiver.

Harris had previously performed an antenna design study for Extreme Precision Antenna Reflectors (EPAR) for NASA Lewis Research Center. Kinematic joints recommended for the precision hexagonal panel antennae served as the data base for the precision solar concentrator. In this concept, each panel is connected to the panel above it by a deployment joint designed to supply both rotation and translation. One motor per joint rotates the panels out of the stack. As the panel drops down, the cone and trough fittings settle onto precision spherical fittings mounted to the core panel. The downward motion of the panel causes the lock mechanism to trip and the spring loaded linkage snaps over center to form a preloaded connection.

Panel Description

During the initial design of the kinematic joints for the concentrator, the rotating/translating joints provided high mechanical packing efficiency for the dished hexagonal panels. The folding hinge design was not volume-efficient due to the volume penalty associated with folding dished surfaces in a "cup up" facing "cup down" configuration. The panel innovation selected alleviates this volume penalty by providing flat rather than curved panels.

The selected approach, decoupling the stiffness and surface requirements for a single relatively large structure, makes use of a faceted secondary surface technique and produces flat hexagonal panels. This design incorporates a graphite beam framework to supply the support structure for the graphite/epoxy spherically curved mirror facets (see Figure 4.3-1) that are adjustable at three points to the surface. Since preserving phase integrity is not a design requirement for a solar collector the facets can be translated from the true parabolic surface. The panel height required for the facets is determined by the slope and size of each facet.

Rotating/Translating Joint

The rotating/translating joint is a candidate solution to the deployment of dished panel modules. The deployment sequence of the 19 panel collector is shown in Figure 4.3-2. The rotating/translating joint is located between hex corners. Each panel is connected to the panel above it by the deployment joint designed to supply both rotation and translation. The first deployment rotates the stack of 18 panels 180^{o} relative to the center "core" panel, then translates the stack until the bottom panel on the stack is flush with the 'core' panel. The second deployment rotates the stack of 17 panels, etc. designed to carry radial loads. The nut is free to rotate within the nut housing and is retained by two Kaydon slim ball bearings. The nut housing is attached to the lower panel and provides easily accessible release bolts to allow manual deployment, should the motor fail. The upper release bolts to allow manual deployment, should the motor fail. The upper driven gear is rigidly connected to the nut, and the lower driven gear is attached to the shaft. The gearmotor assembly drives both gears to provide 180 rotation to

TRUSS HEX CONCENTRATOR PANEL MODULE

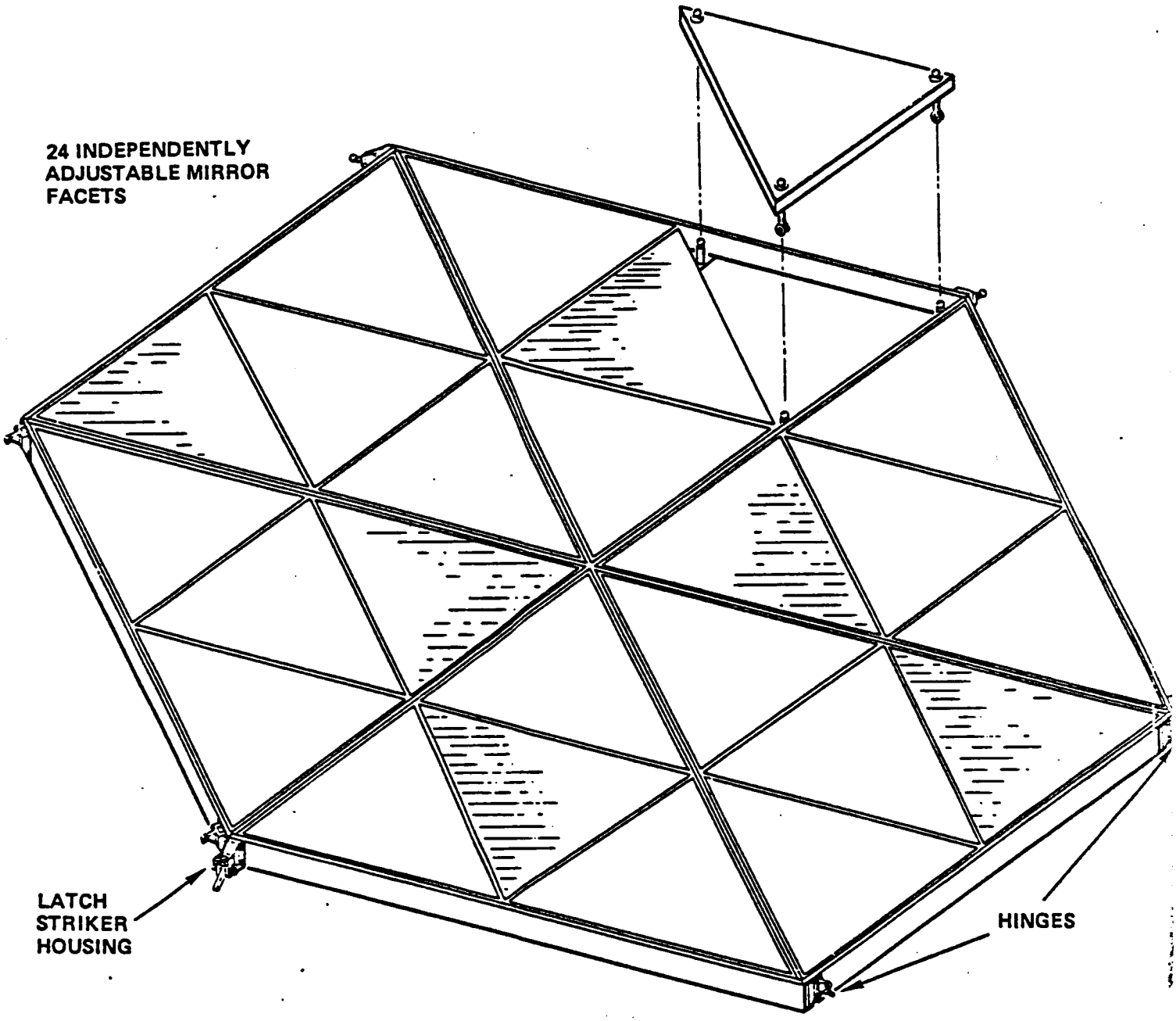

FIGURE 4.3-1 Common flat hexagonal panel modules incorporate a graphite beam framework to supply the support structure for the 24 graphite/epoxy spherically curved mirror facets.

V2-4B/40

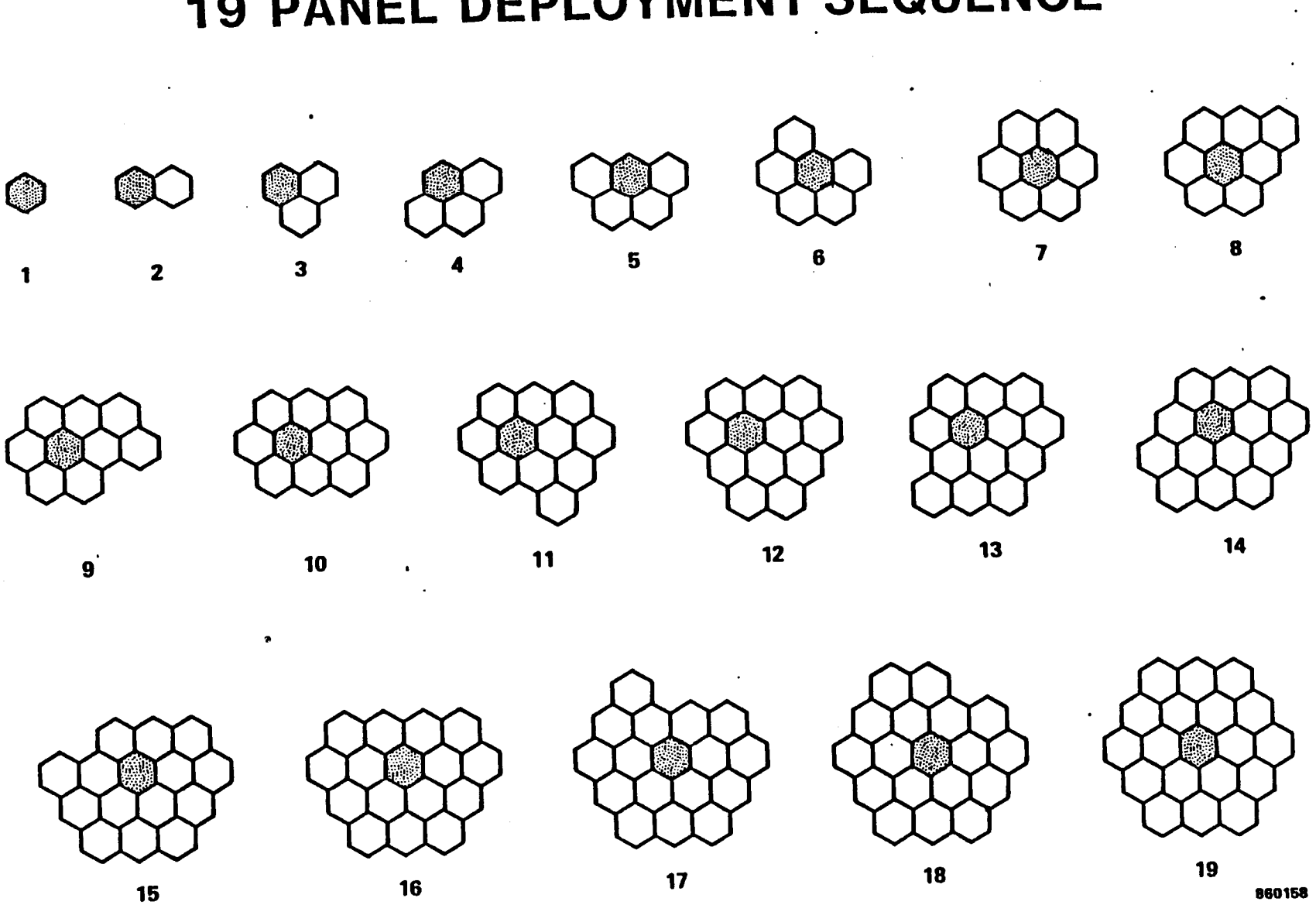

Figure 4.3-2. The deployment sequence is common for both the rotating/translating deployment, and hinge deployment methods. The deployment forms successive rings around the center panel.

the stack of panels until a mechanical stop on the top panel contacts a mechanical stop on the bottom panel. Five degrees prior to the mechanical stop engagement the lower gear (half gear) disengages and the upper gear (coupled with the nut) continues to drive, thus translating the upper panel down, flush with the lower panel. Final alignment is achieved by panel latches. Motor redundancy can be accomplished by dual armature motors. The designed gear motor assembly weighs 1.05 lb.

While deploying a rotating/translating design in a 1-G environment, bending loads will be distributed across the power nut/screw interface. Power screw and nut manufacturers do not have data on the effects of these bending loads on the torque required to rotate the nut, or the effects of the bending moment on the life of the nut and screw. To aid in motor selection a study was performed to determine the torque required to rotate the nut with an applied bending moment. First parametric equations were derived to relate the torque required to rotate the nut as a function of parameters such as bending moment applied, shaft diameter, nut length, nut efficiency, and friction coefficient. The derived torque is shown in Table 4.3.-1. A mechanical model was built to supply empirical data to verify the derived results (see Figure 4.3-3). The mechanical model tested a 3/4 inch and a 1 inch diameter nut/shaft assembly with various applied loads. The forces on the ends of the threaded shaft transmit a bending moment through the restrained nut. The double universal joint assured no force interaction from the torque wrench. A special Nook Industries power screw was tested since conventional acme screws with axial and radial clearances bind when bending loads are applied. The mechanical model tests correlated well with the predicted theoretical results with bending loads as high as 450 in-lb.

V2-4B/38

TABLE 4.3-1 ROTATING/TRANSLATING TEST RESULTS

	Test 1	Test 2	Test 3	Test 4
BENDING MOMENT (IN-LB)	300	450	300	450
SHAFT DIAMETER (INCH)	.75	.75	1.0	1.0
SHAFT LEAD (INCH)	.1	.1	.2	.2
NUT EFFICIENCY	.044	.044	.069	.069
NUT LENGTH (INCH)	1.25	1.25	1.5	1.5
FRICTION COEFFICIENT	1.25	.125	.125	.125
DERIVED TORQUE (IN-LB)	43	65	48	72
TESTED TORQUE (IN-LAB)	55	67	47	77

Single Fold Hinge Deployment

The hinged deployment is made possible by utilizing the flat faceted panels. Flat panels can fold without incurring a 'cup up' against 'cup down' volume penalty. The deployment sequence for the hinged deployment is shown in Figure 4.3.-2.

There are several methods of deploying the panels with the hinged design. One method is to supply each hinge with a torque motor. The first deployment would rotate the stack of 18 panels from the center panel, the second deployment rotates 17 panels, etc. The first deployment cycle, rotating 18 panels from the center core panel, requires a locking hinge to position the stack, all other 34 common hinges are standard non-locking hinges. The final rotated position of each panel is determined by the latch engagement to the adjacent panel.. Motor redundancy can be accomplished with dual armature motors, leaving one hinge free to rotate, and one powered hinge per panel.

ROTATING/TRANSLATING MECHANICAL MODEL

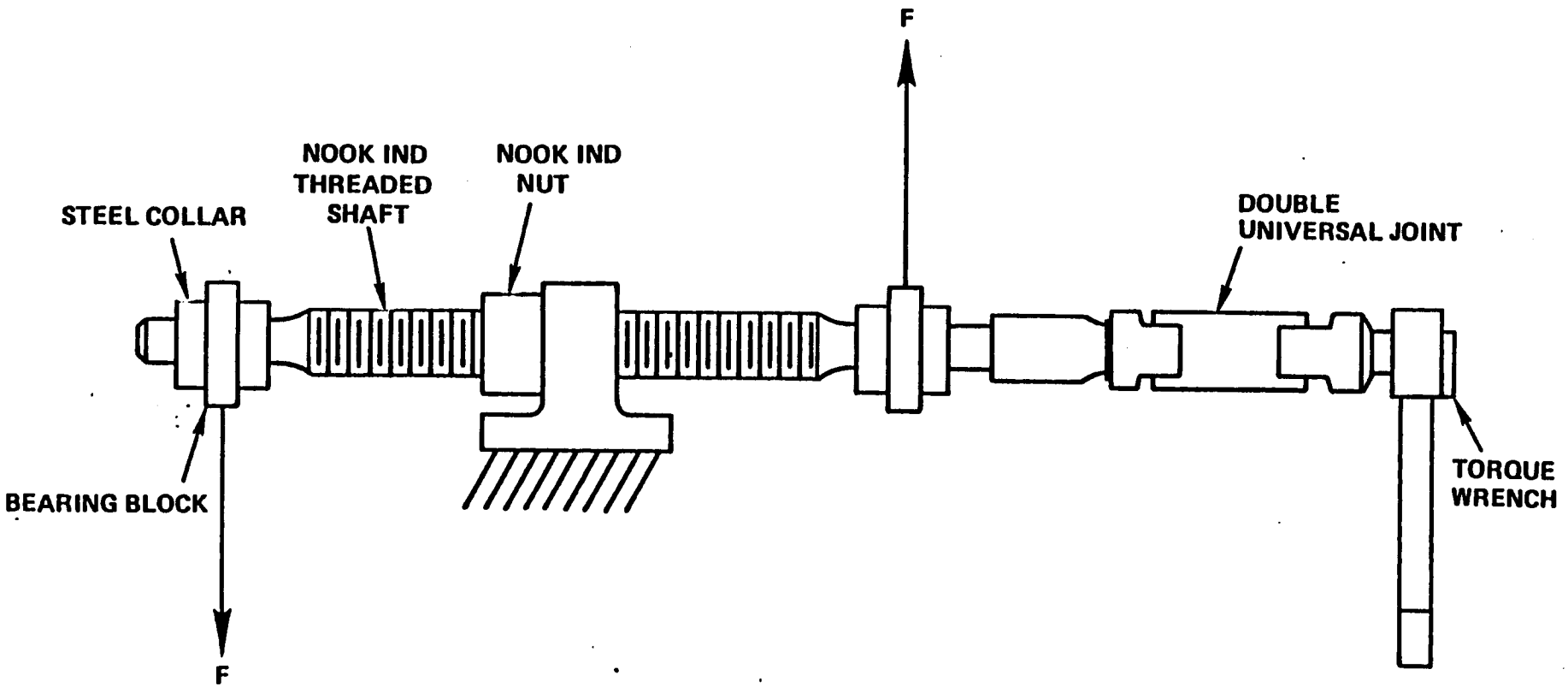

FIGURE 4.3-3 To assist in motor selection for the rotating/translating joint a mechanical model was built to provide empirical data.

V2-4B/42

A powered hinge was designed and fabricated to support the hinge fold deployment. A motor is attached to the stationary panel with the output spline attached to the deploying panel. To insure hinge repeatability the inner race/retainer nut is retained by precision needle bearings and is preloaded against the splined shaft connection. Axial translation are prevented by the parallel mounted, non-powered hinge. The locking hinge (required for the first panel deployment) is similar to the non-locking hinge with the exception of the mechanical stop provided by an adjustment screw. The stop designed for the three panel model prevents rotation in one-direction only, rotation in the other direction is prevented by gravity. A flight version must restrain rotations in both directions.

An externally driven hinge design that reduces the development and recurring cost associated with the drive motors uses a single drill motor operated by an astronaut to rotate the panels. Each hinge would have a splined hole through which the drill-motor could supply the torque necessary to deploy each panel. A detent on the drill motor and hinge would ensure that torque loads are not transmitted to the astronaut.

Another option that offers lower development cost is to deploy the panels by hand (Figure 4.3.4). An astronaut could exert a force through a handle supplied on the stack of panels (A 10 lb force exerted for 5 seconds is sufficient to deploy the first stack of panels in less than one minute). This design requires minimal development cost. No electrical wiring would be required within the panels. The hand deployable approach appears to be the most repeatable and reliable.

A precision hinge designed for this study (Figure 4.3-5) can be used with the manual deployment option, or as the unrestrained rotating hinge in the automated deployment, or can be modified for the externally driven hinge. Repeatability is successfully achieved with hinge pins that are a slight interference fit with extra precision needle bearings. The bearings are pressed into the bearing housing. Axial repeatability is provided by peel shim thrust bearings between the blade and clevis that are lightly pressed into position.

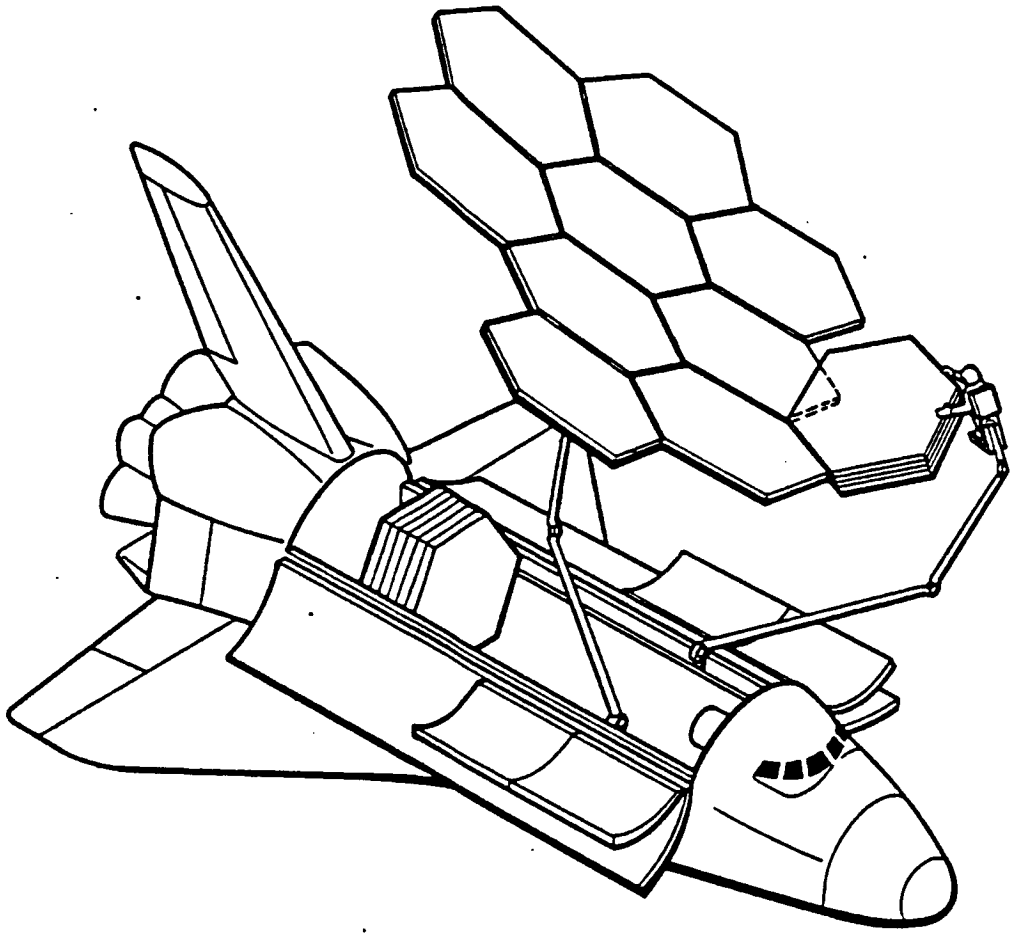

FIGURE 4.3-4 The astronaut assisted manual erection option.

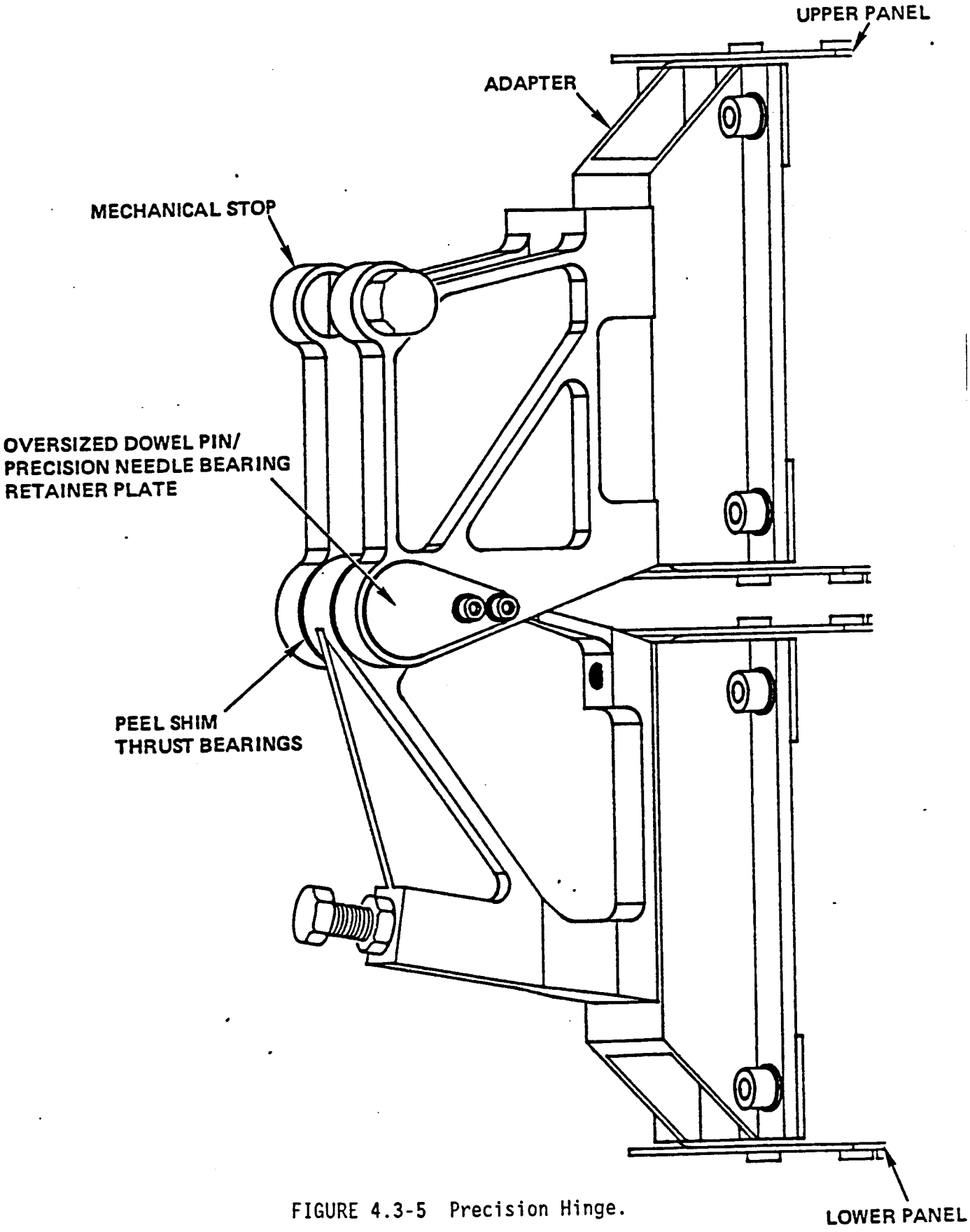

FIGURE 4.3-5 Precision Hinge.

The hinged deployment concept may require some latches to be positioned such that deploying panel latches do not interfere with latches on already deployed panels. The interference can be alleviated by staggering the latches, or providing pins to temporarily remove the latch before an interference occurs. Another solution is to stagger the latches and deploy the 19 panels in two assemblies. This solution would reduce the number of latches at an interference location.

Latch Mechanisms

The latch mechanism design is driven by surface stiffness, thermal distortions, reliability and repeatability issues. A 19 panel finite element model (FEM) evaluated the locations and degrees of restraint of the latch required to support a surface structural frequency of 1 Hz. or greater. The FEM assumed a 60 ft. diameter collector weighing 1030 lb. with a 24 ft. mounting bolt diameter and pin-pin mounting fixity. A F/D ratio of .5 and a 4 in. panel depth were assumed. The objective of this effort was to determine the minimum number of joints and degrees of restraint required to meet surface stiffness requirements. This approach reduces structural redundancy while improving deployment reliability.

Two joints located at each three panel interface appeared to be the most structurally efficient method of restraining the surface. A third joint at each interface has little or no effect on surface stiffness. Several runs were used to determined the effect of varying the latch degrees of restraint on the surface stiffness. One case carried bending and force loads across the latches; the second case transmitted only forces. The six-degree-of-restraint (Six-Dor) case offered only 12% higher surface frequencies than the three-DOR case. However the six-DOR latch would produce redundant structural load paths that are intolerant of slight misadjustments and thermal warping. The reduction of structural redundancy offered by the three-DOR joints helps significantly to assure that repeatible latch-up occurs. A minimum of three translational degrees of restraint is required to assure that misadjustments and thermal warping distortions do not accumulate during successive panel deployments.

The translational restraint latch designed and fabricated on this study accepts a 1/2 inch misalignment (see Figure 4.3-6). The latch consists of a 3/4 inch sphere mounted on one panel, and a conical receptacle and latch pawl on the adjacent panel. As the panel drops into position the conical receptacle places the panel in the precise position. The spherical ball loads the torsion spring on the latch pawl. Once the pawl is released the cam drives the ball into the receptacle which provides four discrete points of contact; the bottom surface, the two side faces, and the latch pawl. Each contact point is separated by a 120^{o} angle. Any relative motion near the end of travel serves to seat the ball more securely.

Two types of translational restraint latches are required to assure distortions do not prevent latch-up. A regenerative latch that relies on panel movement to store energy within the spring, and a powered latch that contains stored energy (loaded spring). The powered latch is similar to the regenerative latch with the exception of the powered pawl. As the panel sphere approaches the receptacle, the trip drives the linkage over-center and releases the stored energy within the spring. The spring driven pawl pulls the sphere down to activate the regenerative latch, which restrains the panel. The powered latch is utilized when a panel latches to two panels concurrently, the stored energy is required to pull the fully restrained panel into position after the first latch is activated. Since distortions make it impossible to determine which of the two latches will engage first, both panel latches must be powered. Panels will engage first, both panel latches must be powered. Panels 7, 10, 12, 14, 16, 18 and 19 required two powered latches each.

The faceted panel modules offer many advantages over the curved graphite/epoxy sandwich panel. The faceted approach offers: lower manufacturing cost; surface adjustment for flux tailoring; high stiffness to weight ratio; replaceability at the facet level due to micrometeoroid impact or monoatomic oxygen degradation; and permits on-orbit deployment.

The rotating/translating joint, powered hinge, externally driven hinge, and manual deployment methods are all potential solutions of deploying hexagonal panels. The non-powered hinge design (externally driven deployment and manual deployment) offers high repeatibility and reliability, and low development cost and lowest weight.

REGENERATIVE TRANSLATIONAL RESTRAINT LATCH DESIGN

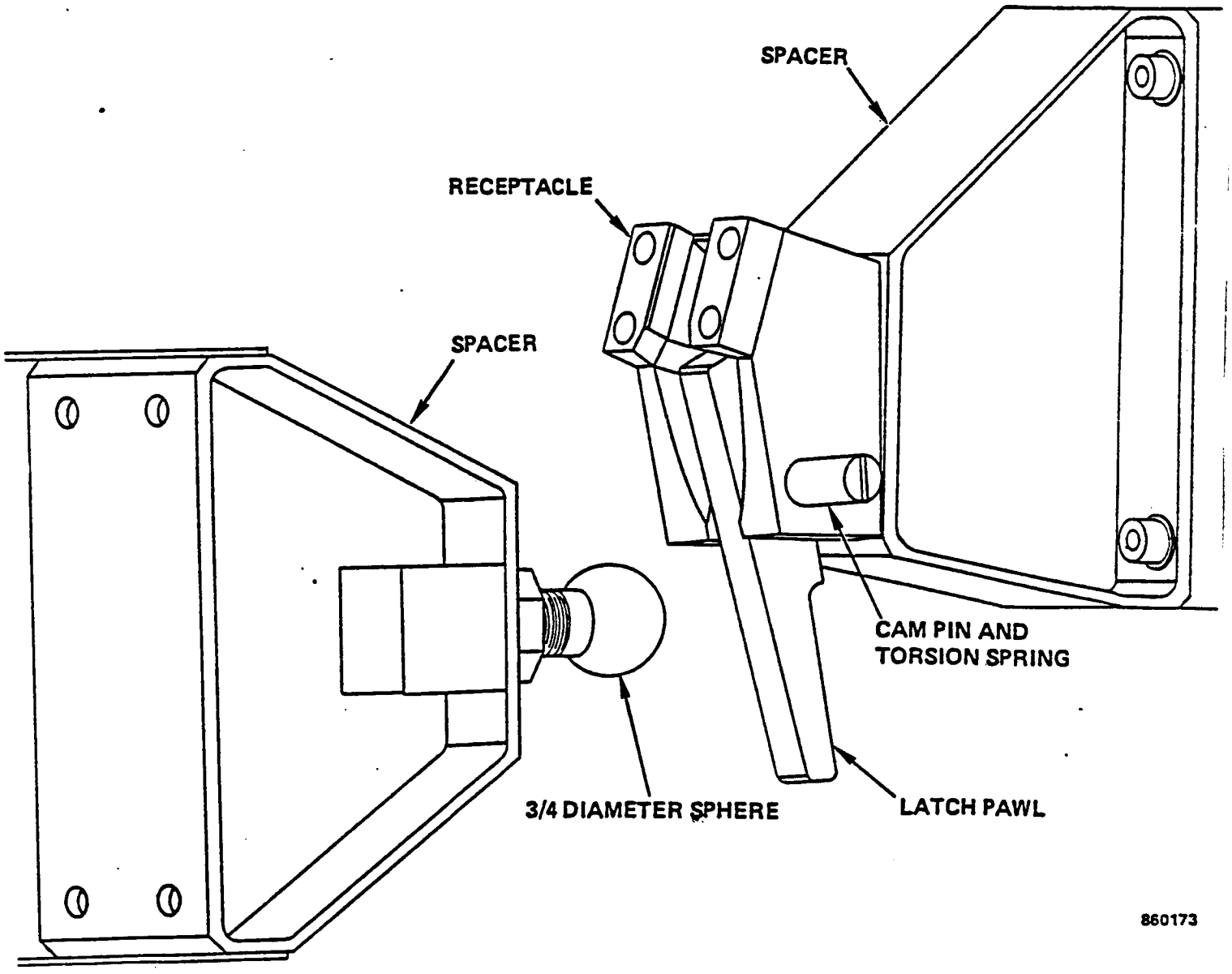

FIGURE 4.3-6 The reduction of structural redundancy offered by the three degree of restraint latch helps significantly to assure that repeatable latch-up occurs. The regenerative latch can be used with all the deployment methods.

Provided the deployment mechanisms are compliant in our of plane rotational stiffness, panel surface accuracies are more dependent on the latch design than the deployment design. The non-powered hinge has no out of plane rotational stiffness, therefore it is the most repeatable method of deployment. The motor driven deployment designs can be as repeatable as the non-powered hinge design at the expense of higher development cost.

Due to the absence of 18 drive motors the non-powered hinge is more reliable and has lower productin/qualification cost. Finally, the non-powered hinge deployment design has substantially lower weight due to the weight associated with the drive motors and telemetry.

The translational restraint regenerative latch is the best solution to the repeatability, reliability, thermal, and stiffness issues as discussed, and was selected as the baseline design in a latch - only configuration for manual on-orbit construction.

The regenerative latch (Figure 4.3-7), powered hinge (Figure 4.3-8), and precision hinge (Figure 4.3-9) are full scale; however a heavier flight surface may necessitate more design work in the areas of strength and compliance. This hardware was ultimately incorporated into a three panel model built under IR&D funding and tested for latchup repeatability (Figure 4.3-10).

4.3.2 Materials Evaluation

The primary objectives of the Phase B materials study effort were to identify candidate reflective and refractive materials and to determine the effects of atomic oxygen impingement on their optical performance. As a result, the test program discussed below centered on sample fabrication, atomic oxygen environment simulation, and pre- and post-exposure optical property measurements.

Environmental concerns at the low earth orbit which the Space Station solar dynamic concentrator will be exposed to include:

Vacuum
Ultraviolet radiation
Protons

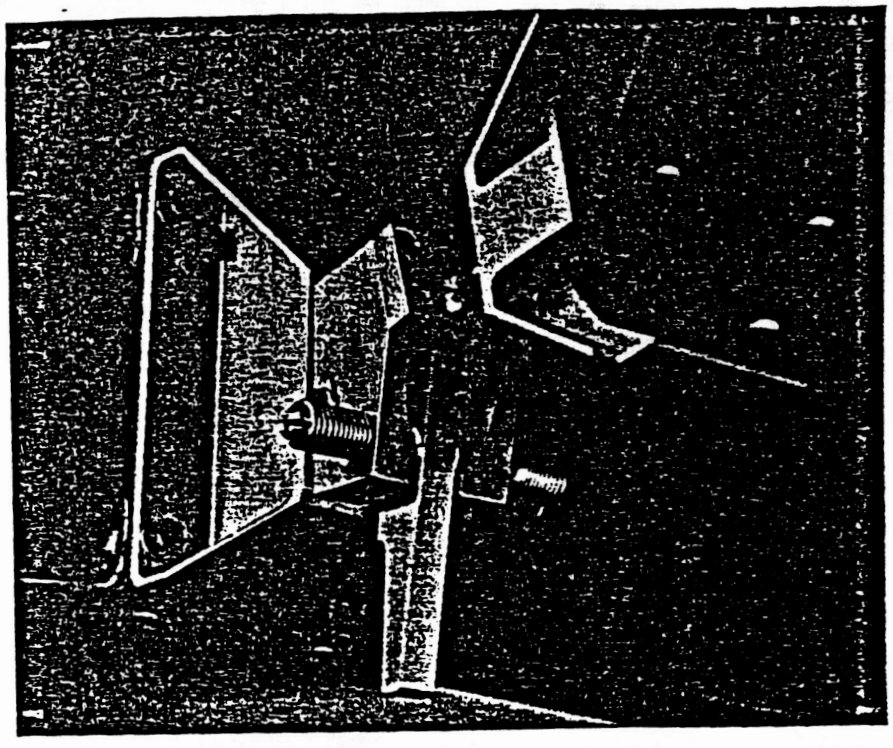

FIGURE 4.3-7 The regenerative translational restraint latch designed for the three panel model is full scale of a flight latch.

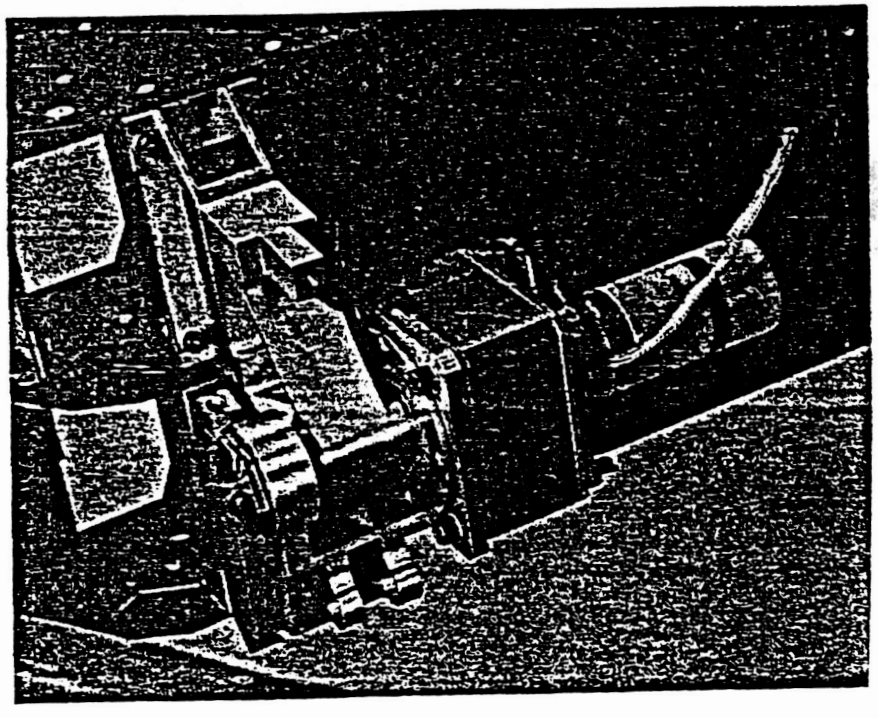

FIGURE 4.3-8 The powered hinge designed for the three panel model demonstrates the automated deployment method.

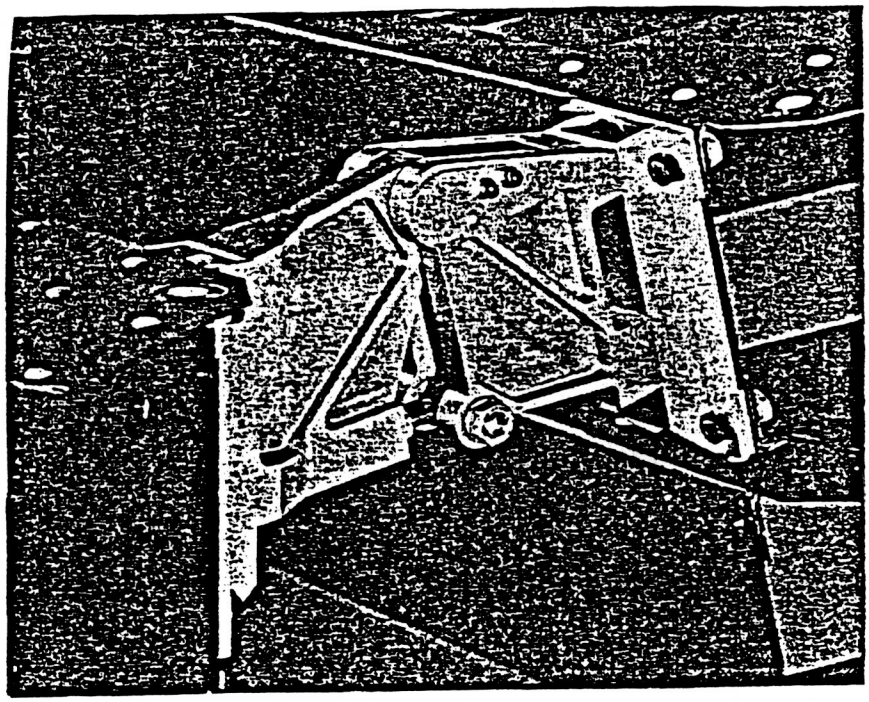

FIGURE 4.3-9 The precision hinge designed for the three panel model demonstrated repeatability during deployment tests.

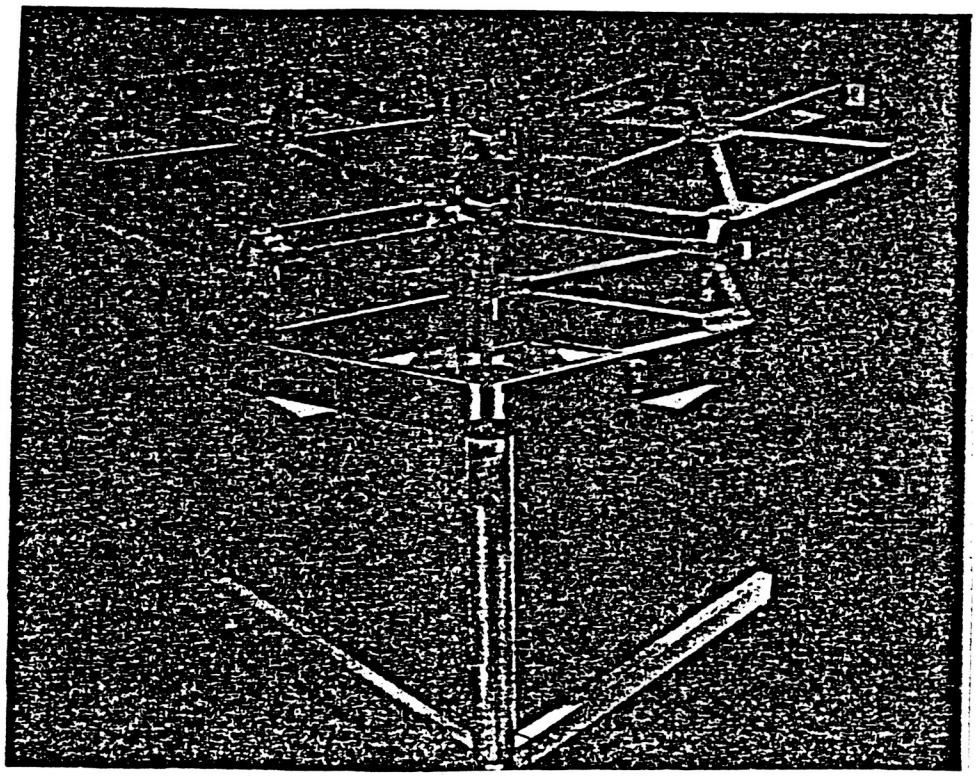

FIGURE 4.3-10 Panel modules are 1/4 scale of flight panels which are 14 feet from flat to flat. The 4 inch model panel thickness is representative of flight panels. The hinges and latches were developed under phase B contract.

Electrons
Temperature cycling
Atomic oxygen
Micrometeoroid debris

Each of these factors, individually and in combination must be addressed to ensure the required service life of the concentrator's reflective surface.

Recent STS flights have demonstrated that some materials degrade rapidly at the altitudes of interest. The observed mass loss and thermo-optical property changes were attributed to atomic oxygen interactions with exposed surfaces.

Atomic oxygen is the predominant atmospheric species at shuttle orbital altitudes. Although the number density is not very high, being on the order of 10^9 cm^{-3}, the high velocity of the spacecraft (8 km/sec) produces high fluxes on ram facing surfaces.

Dedicated atomic oxygen experiments were flown on STS-5[3] and STS-8[4-6] to document the effects of atomic oxygen impingment on a wide variety of materials, The primary effect noted for susceptible materials was surface erosion and associated mass loss. As a result, changes in from surface erosion and associated mass loss. As a result, changes in from surface optical properties were noted for thermal control blankets and coatings. Surface mass loss was also noted for epoxy matrix composites indicating that structural components will also require protection from the atomic oxygen flux.

Finally, it should be noted that the fluence (integrated flux) experienced by a given surface is a function of several factors, including: a) orbital altitude and inclination, b) solar activity, c) impingement angle, and d) spacecraft geometry. Thus a material may experience different mass loss rates depending on its orientation to the ram directions and its location on the spacecraft.

Sample Fabrication and Test Approach

Reflective samples - Test samples for atomic oxygen exposure were fabricated on both glass and graphite reinforced epoxy substrates. This

approach was taken for several reasons. First, the glass substrates would give in indication of the required surface smoothness necessary to maximize total specular reflectance. Second, experimenting with the composite material would give an initial indication as to whether or not this post atomic oxygen mass loss would give an indication of what was being lost from the surface and what was due to outgassing of volatiles from the composite matrix. Each reflective sample consisted of three layers; the substrate, the reflective surface, and the protective coating. The reflective surface was put down via resistive heating vapor deposition. In all samples the reflective surface was 3000 A $\pm$ 100 A thick. Where possible, the protective coating was also put down via vapor deposition. However, some coatings selected could only be deposited using Ion beam sputtering. Protective coatings were 1000 A, + 200 A thick.

Reflective and protective materials selected for evaluation are summarized in Table 4.3-2. Reflective candidates were selected based on their reflectivity over the wavelength range 200-2500 nanometers. This portion of the solar spectrum contains 98 percent of the available incident solar energy. The best candidate from a reflectivity standpoint appeared to be silver followed by aluminum and copper.

Refractive samples- Candidate refractive lens materials were identified based on the optical requirements of the system and limited STS flight data. Several silicones were tested including RTV 615, 655, and 670 produced by GE, and DC 93-500 produced by Dow-Corning. Each of these materials is space qualified. Teflons (fluorinated ethylene polymers) also have shown good resistance to atomic oxygen degradation and were selected for additional testing. Silicone samples were cast onto glass slides and cured out per the manufacturer's instructions. Typical sample thicknesses were on the order of .020 inches + .002 inches. Teflon samples exposed ranged from .005 to .010 inches thick, and were tested as received from the manufacturer. Refractive lens materials tested are summarized in Table 4.3-3.

Atomic Oxygen Exposure - Samples were exposed to atomic oxygen using two different approaches. One set of samples was exposed in a Structure Probe, Inc. Plasma Prepp 11 plasma reactor at NASA Lewis Research Center. This device creates a simulated atomic oxygen environment by passing a carrier gas (in this case, air) over the sample and then exciting the oxygen molecules with

approximately 100 W of continuous RF power at 13.56 MHz. The resulting environment is composed of a number of species including atomic oxygen, molecular oxygen, and oxygen radicals. The operating pressure for all tests was kept at 50 microns. While it is difficult to calculate the resultant atomic oxygen flux accurately, estimates have been made based upon kapton erosion data from the asher and STS experiments that 16 asher hours approximate one year in LEO. Thus the asher provides a means for generating accelerated test data in a relatively short time.

Similar samples exposed in atomic oxygen test facility at the University of Toronto Institute for Aerospace Studies. This approach utilizes an oxygen seeded carrier gas (argon or hellum) released into a quartz tuning cavity in which microwave energy partially dissoclates the oxygen. The monoatomic oxygen is then passed into an evacuated sample chamber where it impinges on the sample at a normal angle of incidence. The microwave generator was run at 2450 MHz and 20-200 W resulting in an approximate flux of 10^{15} atoms/cm^2-sec at and average velocity of 1.2 km/sec with atom translational energies on the order of 0.14 eV. Although the flux is representative of that at shuttle altitudes, the energy is lower than the actual 4.2 eV on orbit.

Reflective Surfaces	Protective Coatings
Aluminum	Magnesium Fluoride
Silver	SiO_x
Copper	Indium Tin Oxide
Platinum	Al_2O_3
Rhodium	Si_3N_4
	RTV Silicone

TABLE 4.3-2 Summary of reflective and protective materials evaluated.

V2-4B/54

Silicones	Teflon	Acrylic
RTV 615	FEP(A)	UVA - 11
655		Polycarbonate
670		
DC 93-500		Lexan 9034 - 112

TABLE 4.3-3 - Fresnel lens material selected for evaluation.

Reflectance and transmittance measurements - Special reflectance and transmittance measurements were made using a Perkin-Elmer Lambda 9 UV/VIS/NEAR IR spectrophotometer equipped with a 60 mm diameter $BaS)_4$ coated integrated sphere. The wave length range evaluated extended from 200 to 2500 nanometers. Specular reflectances were obtained and solar reflectance calculated.

Reflective Samples Testing Results

Reflective samples - Table 4.3-4 summarizes total and specular reflectance as a function of exposure time for selected aluminum and silver reflective surface samples. Data are shown for samples on both glass and graphite reinforced epoxy substrates. Aluminum and silver were selected as the baseline reflective surface due to their excellent reflectance over the majority of the solar spectrum. Silver drops off considerably in the UV region (less than 300 nanometers), however, this does not significantly affect the total solar reflectance since this part of the spectrum is a very small percentage of the total available energy. Aluminum suffers from a dip in its reflectance curve around 800 nanometers, but remains highly reflective in the UV region. Cooper, rhodium and platinum were also considered, however, each had a total solar reflectance value less than that for silver and aluminum.

As expected, the condition of the substrate surface is critical in determining the specular reflections characteristics of the sample. Thus, for identical samples (in terms of reflective and protective coatings) glass substrates typically show higher total and specular reflectance. Data

				REFLECTANCE*			
SUBSTRATE	R	P	ASHER HOURS	START TOTAL	START SPECULAR	FINISH TOTAL	FINISH SPECULAR
GLASS	Ag	SiOx	634	0.978	0.972	0.958	0.937
GLASS	Ag	SiOx/MgF2	634	0.978	0.970	0.943	0.927
Gr/Ep	Ag	SiOx/MgF2	180	0.955	0.940	0.930	0.915
Gr/Ep	Ag	SiOx	180	0.975	0.945	0.945	0.910
Gr/Ep	Ag	MgF2	180	0.955	0.930	0.955	0.925
Gr/Ep	Ag	RTV 655	151	0.965	0.940	0.905	0.840
GLASS	Al	SiOx	634	0.912	0.891	0.904	0.879
GLASS	Al	SiOx/MgF2	634	0.906	0.882	0.859	0.834
Gr/Ep	Al	SiOx	180	0.875	0.868	0.858	0.851
Gr/Ep	Al	MgF2	180	0.945	0.925	0.940	0.910
Gr/Ep	Al	RTV 655	151	0.935	0.905	0.850	0.805

*MEASURED OVER 200 NM TO 2500 NM

R - REFLECTIVE SURFACE

P - PROTECTIVE COATING

RTV 655 GE SILICONE

Gr/Ep - GRAPHITE REINFORCED EPOXY

TABLE 4.3-4 Total and specular reflectance for silver and aluminum samples protected with different coatings as a function of atomic oxygen exposure time. (NASA Lewis plasma asher)

generated as part of this study indicate, however, that composite substrates can be fabricated with surfaces very near those available with glass. Composite substrates for this study were initially fabricated by two methods: prepreg lay-ups and wet (fabric) lay-ups. Use of composite prepreg tape to form the substrate yields poor results. Surfaces adequate for optical applications could not be produced as a result of the fiber surface being readily visible. However, excellent surfaces were obtained using a woven cloth impregnated with resin. This approach allowed the formation of a resin rich layer on the surface of the composite which enabled the deposition of a highly reflective metal layer. Glass was used as the mold surface to ensure the resin rich layer was as smooth as possible.

Table 4.3-5 summarizes mass loss for samples protected with various coatings exposed to atomic oxygen at the University of Toronto facility. In general very small changes in total sample mass are observed for the graphite reinforced epoxy substrates. Equivalent samples on glass show virtually no mass loss indicating the the graphite epoxy samples are undergoing some outgassing in the vacuum of the sample chamber. Separate samples were sent to NASA Goddard for outgassing of volatiles testing which confirmed that the mass loss was due to desorption of volatile species and not due to erosion of the protective coatings.

Samples tested at the University of Toronto showed very small changes in reflectivity following atomic oxygen exposure. Figure 4.3-11 shows total solar reflectance as a function of wavelength for a silver surfaced sample protected with SiO_x and MgF_2 following an exposure time of 167 hours. Above 600 nanometers the curves are indistinguishable. A slight decrease is observed below 600 nanometers, however it is one the order of 1-2 percent which is within the measurement error of the Instrument. A similar curve for an aluminum sample on graphite epoxy coated with MgF_2 showed the post exposure reflectance curve to be slightly higher than the pre-exposure curve. This behavior is associated with the removal of surface contaminants by the oxygen flux. The average reflectance remains high, however, in the 88-90 percent range.

Accelerated testing of reflective samples was performed in the plasma asher facility at NASA Lewis. Samples were exposed for times ranging from 634 hours

MASS LOSS DATA FOR REFLECTIVE CONCEPTS

SAMPLE	EXPOSED MATERIAL	EXPOSURE TIME (HRS)	INITIAL MASS LOSS (g)	FINAL* MASS LOSS (g)
GRE/Ag/MgF_2	GRE	168	1.78×10^{-3}	1.102×10^{-3}
GRE/Ag/SiO_2	SiO_2	167	1.192×10^{-3}	4.51×10^{-4}
GRE/Ag/MgF_2	MgF_2	168	7.62×10^{-4}	1.78×10^{-4}
GRE/Ag/RTV655	RTV655	167	1.014×10^{-3}	9.47×10^{-4}
GRE/Al/RTV655	RTV655	169	1.248×10^{-3}	0.738×10^{-3}
GRE/Al/MgF_2	MgF_2	168	1.119×10^{-3}	0.57×10^{-3}
PEEK	PEEK	167	5.2×10^{-4}	2×10^{-4}
GLASS/Al/SiO_2	SiO_2	167	6.0×10^{-5}	6.0×10^{-5}
GLASS/Al/SiO_2/MgF_2	MgF_2	167	0	0
GLASS/Al/SiO_2/MgF_2	MgF_2	162	0	0

TABLE 4.3-5 Mass loss data for samples tested at the University of Toronto.

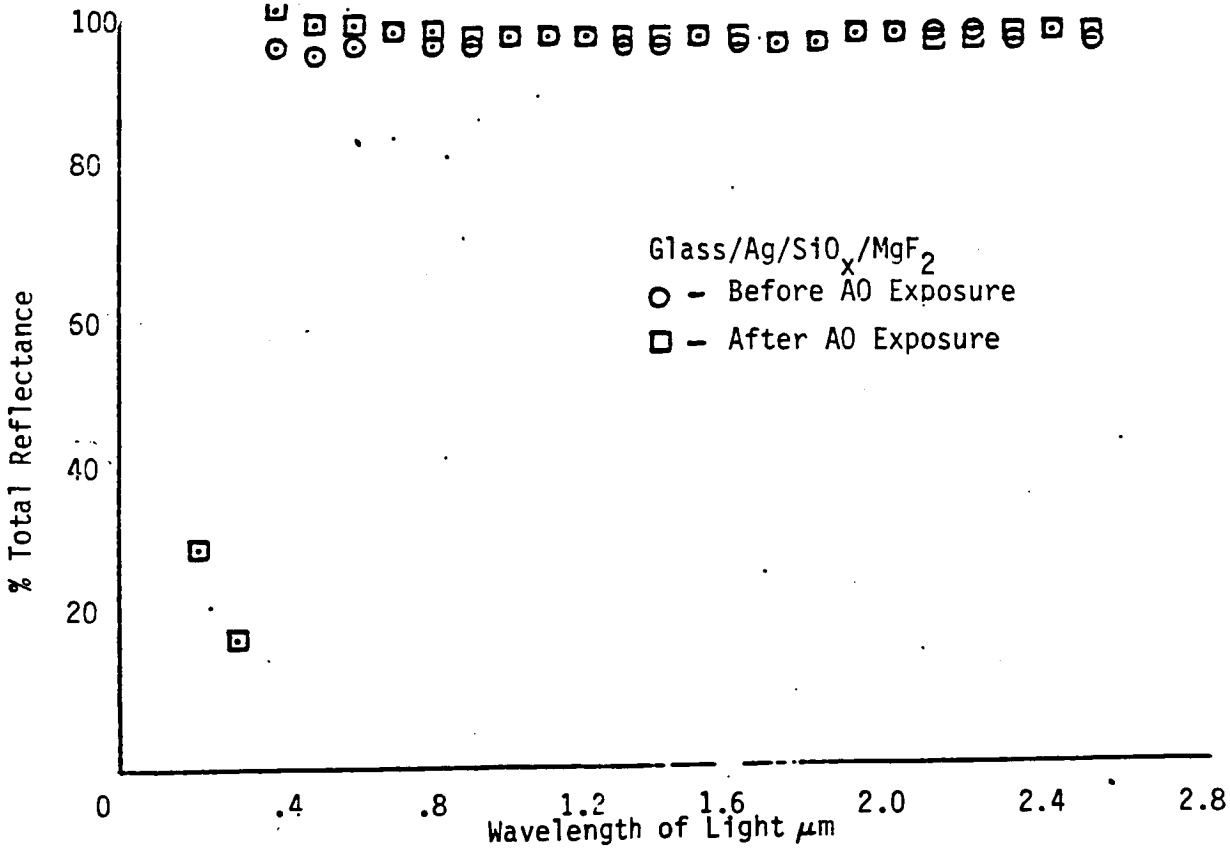

FIGURE 4.3-11 - Total reflectance as a function of wavelength for a silver sample coated with SiO_s and MgF_2 on glass. Exposed 167 hours at the University of Toronto.

to 151 hours, where 16 hours in the asher equate to approximately on year in LEO. Representative curves are shown in Figures 4.3-12 and 4.3-13 for silver surfaces samples. These curves show both specular and total reflections as a function of exposure time.

A comparison of total and specular reflectance as a function of exposure time to two silver samples protected with SiO_x on glass and graphite reinforced epoxy, was made. The sample on the glass substrate was exposed for a total of 634 hours and the sample on the graphite/epoxy substrate was exposed for a period of 180 hours. Although the total reflectance values are very similar prior to exposure, the specular value for the graphite/epoxy sample is only .950 compared with .978 for the glass substrate. Although this difference is small, it remains fairly constant through the post exposure data. The important point, however, is that high specular reflectance values can be achieved on graphite epoxy and maintained following atomic oxygen bombardment.

Each of the reflectance versus exposure time curves exhibits the same general characteristics independent of the protective coating(s) applied. The exception is RTV 655 which is discussed later. Both total and specular reflectance show a gradual decrease up to approximately 150 hours. The curve then levels out and undergoes little or no change up to 400 hours. For samples exposed longer, no change or a small decrease is observed for the remaining time. This behavior is illustrated in Figures 4.3-12 and 4.3-13 for silver on glass and graphite/epoxy protected with a dual coating of SiO_x and MgF_x.

The behavior of samples fabricated with aluminum as the reflective surface behave in a similar fashion. A gradual decrease in both specular and total reflectance is initially observed which continues to about fifty total hours of exposure. The curves then remain essentially flat for the remaining exposure time.

RTV silicones were also considered for protective coating applications. The behavior of an aluminum sample coated with RTV 655 silicone exposed for a total of 151 hours in the plasma asher showed 93 percent at the start of the test to 88 percent after 151 hours. The specular reflectance curve undergoes a very sharp drop in the first five hours from 90 to 71 percent and then recovers at 10 hours to slightly above eight percent where it stayed for the remainder

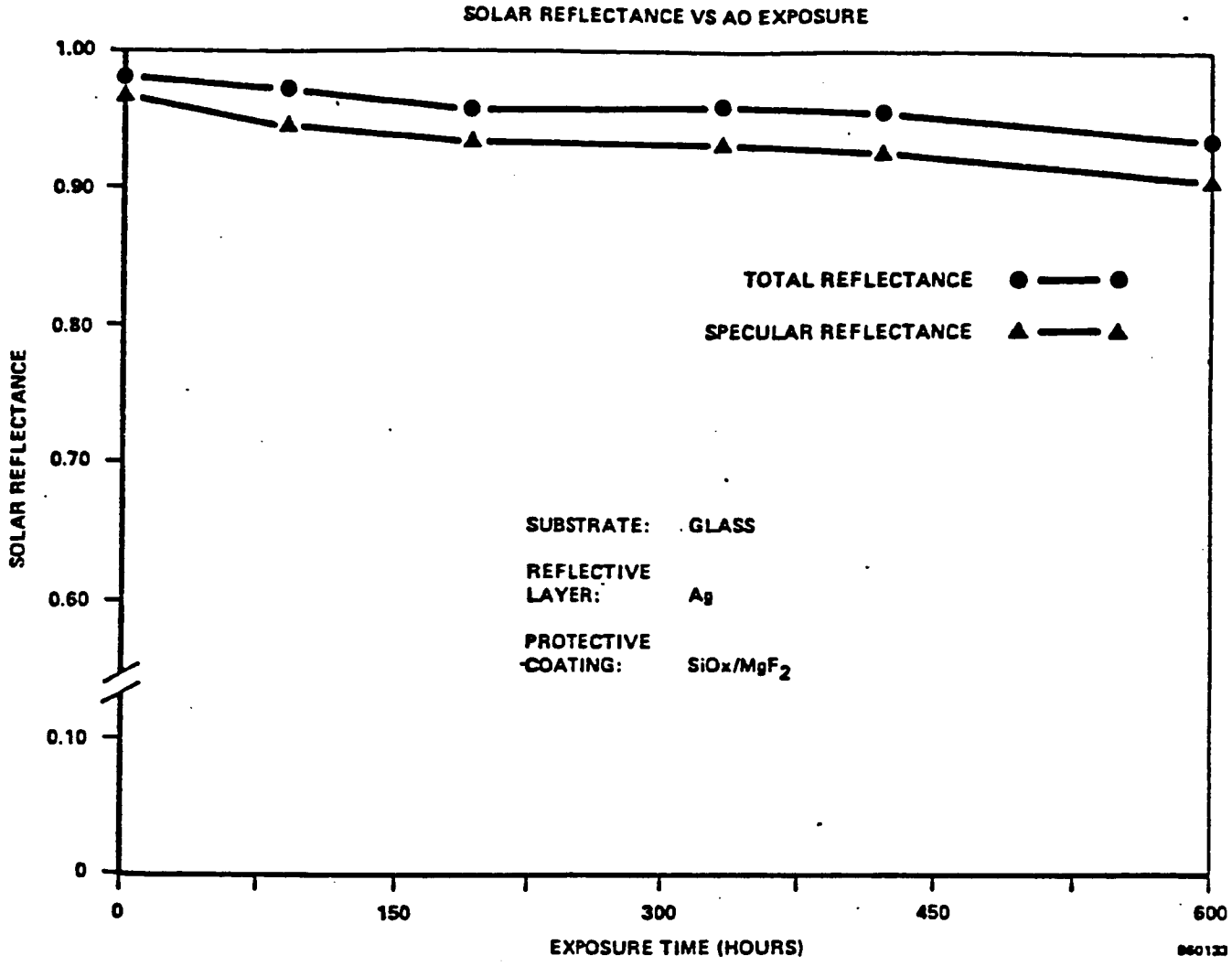

FIGURE 4.3-12 Total and specular reflectance as a function of exposure time for Silver protected with SiO_x and MgF_2 on a glass substrate. Exposed at NASA 634 hours.

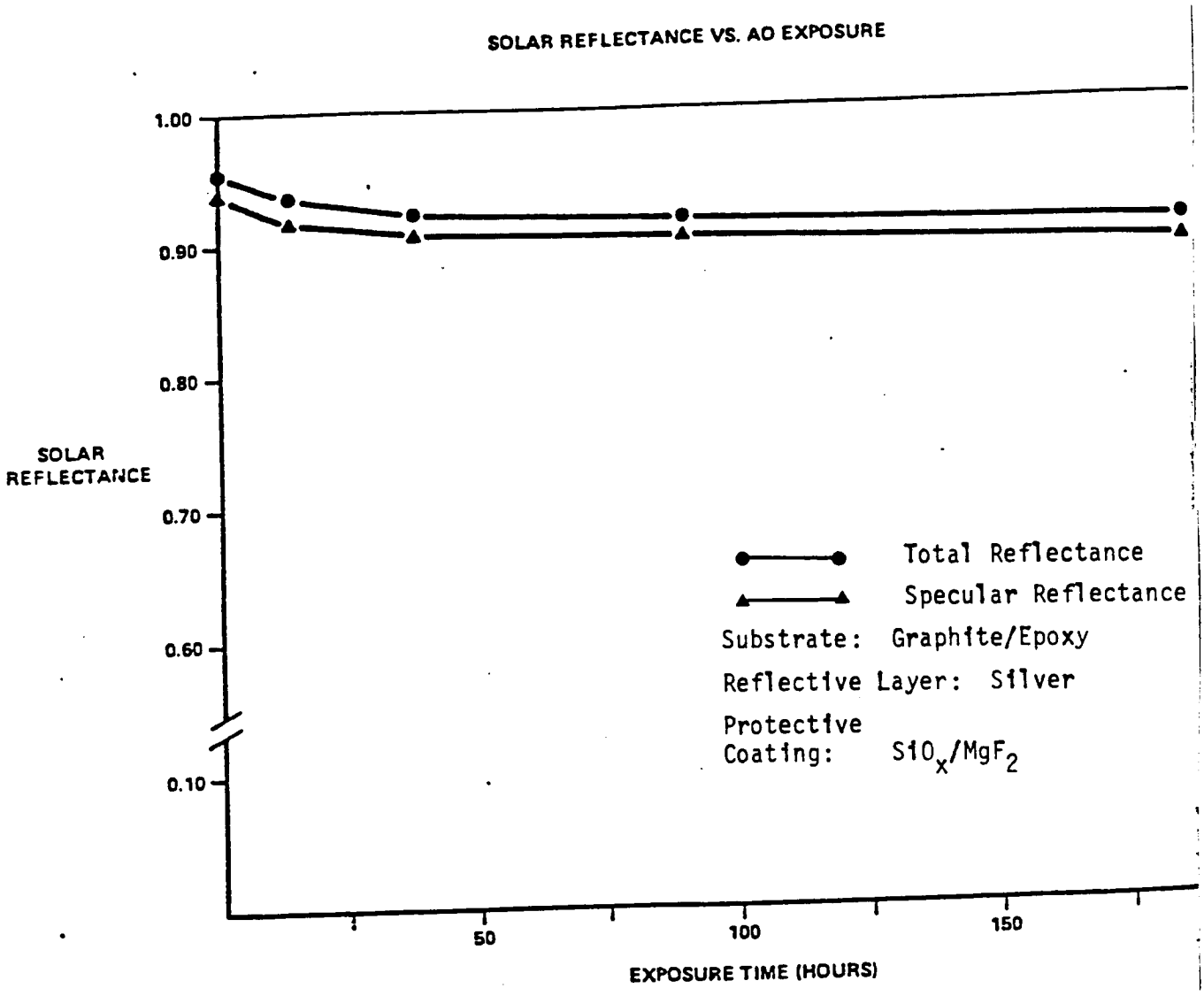

FIGURE 4.3-13 Total and specular reflectance as a function of exposure time for silver coated with SiO_x and MgF_2 on a graphite/epoxy substrate Exposed at NASA Lewis 180 hours.

of the experiment. A sample with silver as the reflective surface protected with RTV 655 showed the same behavior. Scanning electron microscopy of sample surfaces following exposure revealed the presence of numerous cracks and considerable roughening of the surface which accounts for the sharp decrease in specular reflectance.

A summary of of transmission data for materials evaluated for Fresnel lens applications is contained in Table 4.3-6. Four silicones were exposed to atomic oxygen in the asher in addition to a space qualified fluoropolymer (FEP-A), a UV stabilized polycarbonate, and an acrylic, UVA-11. The silicones showed the highest resistance to atomic oxygen degradation followed by the teflon. In both cases, however, samples experienced considerable mass loss and surface erosion during exposure in the asher.

Transmittance as a function of exposure time for two silicones, RTV 670 and DC 93-500, respectively, are very similar and represent the behavior of all silicone samples tested. A gradual decrease is observed in total transmittance which levels out after approximately 50 hours slightly above 80 percent. The specular curves show a more rapid loss up to fifty hours and then also maintain a relatively constant value for the remainder of the exposure time. This behavior is associated with the degradation of the surface as a result of the impinging atomic oxygen flux.

Both the Lexan PC and UVA-11 acrylic were observed to degrade rapidly when exposed to the atomic oxygen flux. The acrylic sample was removed from the plasma chamber following 21.5 hours because of the rapid loss in transmission. The sample has become quite opaque due to the atomic oxygen flux, especially in the high energy visible wavelength range. The Lexan sample at first appeared to be very stable in the plasma; however measurements after 117 hours of exposure indicated that the sample had lost 50 percent of its initial thickness and over 70 percent of its initial mass. The mass loss was uniform over the surface of the sample resulting in a fairly stable specular transmittance curve. thus, although the specular transmittance for this material remains fairly good during exposure to atomic oxygen, the associated mass loss makes it unacceptable for lens applications in LEO.

MATERIAL	ASHER HOURS	START TOTAL*	START SPECULAR*	FINISH TOTAL*	FINISH SPECULAR*
SILICONES					
RTV 615	214	0.910	0.845	0.830	0.640
RTV 655	214	0.910	0.850	0.840	0.635
RTV 670	214	0.880	0.810	0.840	0.725
DC 93-500	214	0.890	0.780	0.830	0.650
FEP (A)	151	0.937	0.900	0.952	0.602
LEXAN PC	117	0.825	0.825	0.842	0.728
UVA-11 ACRYLIC	21.5	0.845	0.838	0.872	0.393

*TRANSMITTANCE VALUES MEASURED OVER 200 NM TO 2500 NM

TABLE 4.3-6 Total and specular tranmittance data for selected Fresnel lens materials exposed to atomic oxygen.

Aluminum and silver are the best candidates for the reflective surface. Both have high reflectance over the wavelength range of interest (200 to 2500 nanometers) and can be vapor deposited in uniform thin layers. Silver has a slightly higher total reflectance, but is more susceptible to degradation and is transparent in the UV region of the spectrum. This could promote decohesion at the substrate silver interface or accelerated degradation of the composite.

Both magnesium fluoride (MgF_2) and silica (SiO_x) provide excellent protection against atomic oxygen degradation, individually or in combination, RTV silicones were found to provide poor protection and degraded significantly in the atomic oxygen flux. Other coatings considered but not discussed in this report were Indium tin oxide, calcium fluoride , aluminum oxide, and silicon nitride. The best and most repeatable results were obtained with magnesium fluoride and silica.

Samples fabricated on glass substrates yielded the best specular reflectance data, however careful fabrication of composite substrates using a glass mold surface produced comparable results. The best substrates were fabricated using woven cloth impregnated with resin as oppossed to panels fabricated with prepreg.

Materials evaluated for Fresnel lens applications proved very susceptible to degradation resulting from exposure to monoatomic oxygen. Of the materials tested the silicones appeared to have the highest Intrinsic resistance to damage from the oxygen flux but still showed significant surface erosion and mass loss. The asher, however, produces a much higher flux than that present in LEO at shuttle altitudes and thus produces different mass loss rates for the same material when compared directly with samples flown on shuttle experiments. Thus one must be careful in extending asher data to predicting actual on-orbit performance. Materials that survive the asher with no visible degradation typically survive in LEO.

REFERENCES

1. Garrett Fluid Systems Company Final Report 41-5842, "Space Station Phase B Study", September 26, 1986.

2. Garrett Pneumatic Systems Division Final Report 41-5637, "Phase-Change Material Characterization LiF-MgF_2 and LiF-CaF_2 Eutectics," June 2, 1986.

3. Garrett Pneumatic Systems Division Final Report 41-5586A, "High Temperature Vacuum Sublimation Testing of Candidate Space Solar Receiver Materials," September 22, 1986.

4. Garrett Pneumatic Systems Division Final Report 41-5706, "Cyclic Testing of LiF-Filled Phase Change Material Heat Exchanger," June 27, 1986.

5. Garrett Pneumatic Systems Division Final Report 41-9190, "Metallurgical Evaluation of Li-Filled Phase-Change Material (PCM) Heat Exchanger, Supplement to Report 41-5706," October 27, 1986.

6. Sundstrand Energy Systems, "Final Study Report DRD 396B, DR55-A-377 Phase B SD-ORC," September 1986.

7. Harris Corporation, "Final Draft, Advanced Development Final Report, DR-55-T-289," June 1986.

5.0 CUSTOMER ACCOMMODATIONS

5.1 DESIGN APPROACH

Work package 04 has the responsibility of providing utility power to all customers (housekeeping loads and payloads). Details of Work package 04 Electrical power system design is presented in Section 3.4.

All electrical loads are served from the Power Distribution and Control Assemblies (PDCA) which are located throughout the station. Each PDCA contains Remote Power Controllers (RPC) that function as the electrical interface with each load. Three sized (75 amp, 25 amp and 5 amp) of RPCs are provided to the user. Connection to more than one RPC is required for fault tolerant operation. The user can chose to connect the load as a critical load which requires three RPCs, essential load which requires two RPCs or as a non-essential load requiring only one RPC.

Work package 04 will supply power to work package 02 utility ports and work package 01 equipment racks as well as work package 03 utility ports. Utility ports and rack locations will be determined by other work packages.

5.2 RESOURCES

Work package 04 generates power resources for the Space Station and Platform. Table 5.2-1 list EPS design considerations and design approaches used to accommodate the customer.

EPS/Customer interface is at the PDCA. All PDCAs on the Space Station and Platform delivers utility power of the same voltage, frequency and other characteristics shown in Table 5.2-2. This allows payloads to be moved from one station or platform location to another without modification. There are 22 PDCAs located on the Space Station as shown in Figure 5.2-1. A total of ten PDCAs are located throughout the truss structure at regular intervals to support truss mounted loads. Loads within manned modules are serviced by 12

CONSIDERATION	APPROACH
CUSTOMER SECURITY	EPS DESIGN DOES NOT POSE A CUSTOMER SECURITY PROBLEM
EASE OF PAYLOAD INTEGRATION	WP-04 PROVIDES USER LOAD CONVERTERS AND A 20 KHZ 208 VAC GSE POWER SOURCE FOR PRE-ORBIT PAYLOAD CHECKOUT
EASE OF PAYLOAD CONFIGURATION	EPS PAYLOAD DATA BASE CAN BE UPDATED AT WILL VIA DMS COMMANDS. 802 CUSTOMER CONNECTION POINTS LOCATED THROUGHOUT THE STATION
EASE OF PAYLOAD SERVICING	POWER CAN BE DE-ENERGIZED TO PAYLOAD AT WILL BY THE EPS VIA DMS COMMANDS
EASE OF PAYLOAD PACKAGING	WP-04 NOT INVOLVED IN PAYLOAD PACKAGING
DEGREE OF TRANSPARENCE OF PAYLOAD OPERATIONS	CUSTOMER OPERATION IS COMPLETELY INDEPENDENT OF PAYLOAD OPERATION
INDEPENDENCE OF PAYLOAD OPERATION	AS LONG AS LOAD IS ALLOCATED POWER BY THE DMS (NOT A PART OF WP-04), CUSTOMER PAYLOADS OPERATE IN COMPLETE INDEPENDENCE OF THE EPS.
RESOURCES PROVIDED	SEE TABLE 6.2-2
PAYLOAD ENVIRONMENT	WP-04 DOES NOT EFFECT PAYLOAD ENVIRONMENTS

DESIGN CONSIDERATIONS
TABLE 5.2-1

- POWER SOURCES (STATION)
  - 75 KW AVERAGE POWER AT IOC
  - 100 KW PEAK POWER AT IOC
  - 300 KW AVERAGE POWER AT GROWTH
  - 350 KW PEAK POWER AT GROWTH

- POWER SOURCES (PLATFORM)

	POLAR	CO-ORBIT
AVERAGE POWER AT IOC	8 KW	6 KW
PEAK POWER AT IOC	16 KW	6 KW
AVERAGE POWER AT GROWTH	15 KW	23 KW
PEAK POWER AT GROWTH	18 KW	23 KW

- UTILITY POWER CHARACTERISTICS
  - PDCA MAXIMUM POWER (25) kWe
  - FREQUENCY 20 kHz $\pm$ 2%
  - VOLTAGE 208 VRMS, SINGLE PHASE $\pm$ 2.5%
  - MINIMUM POWER FACTOR .9
  - HARMONIC DISTORTION < 3% TOTAL
  - VOLTAGE DROPOUT DURATION, 50 MSEC. MAXIMUM
  - TRANSIENT VOLTAGE, $\pm$ 10% MAXIMUM FOR 250 msec.
  - GROUND LINE CURRENT, < 15 MA NOMINAL (FULL LOAD)

POWER RESOURCES TO CUSTOMERS

TABLE 5.2-2

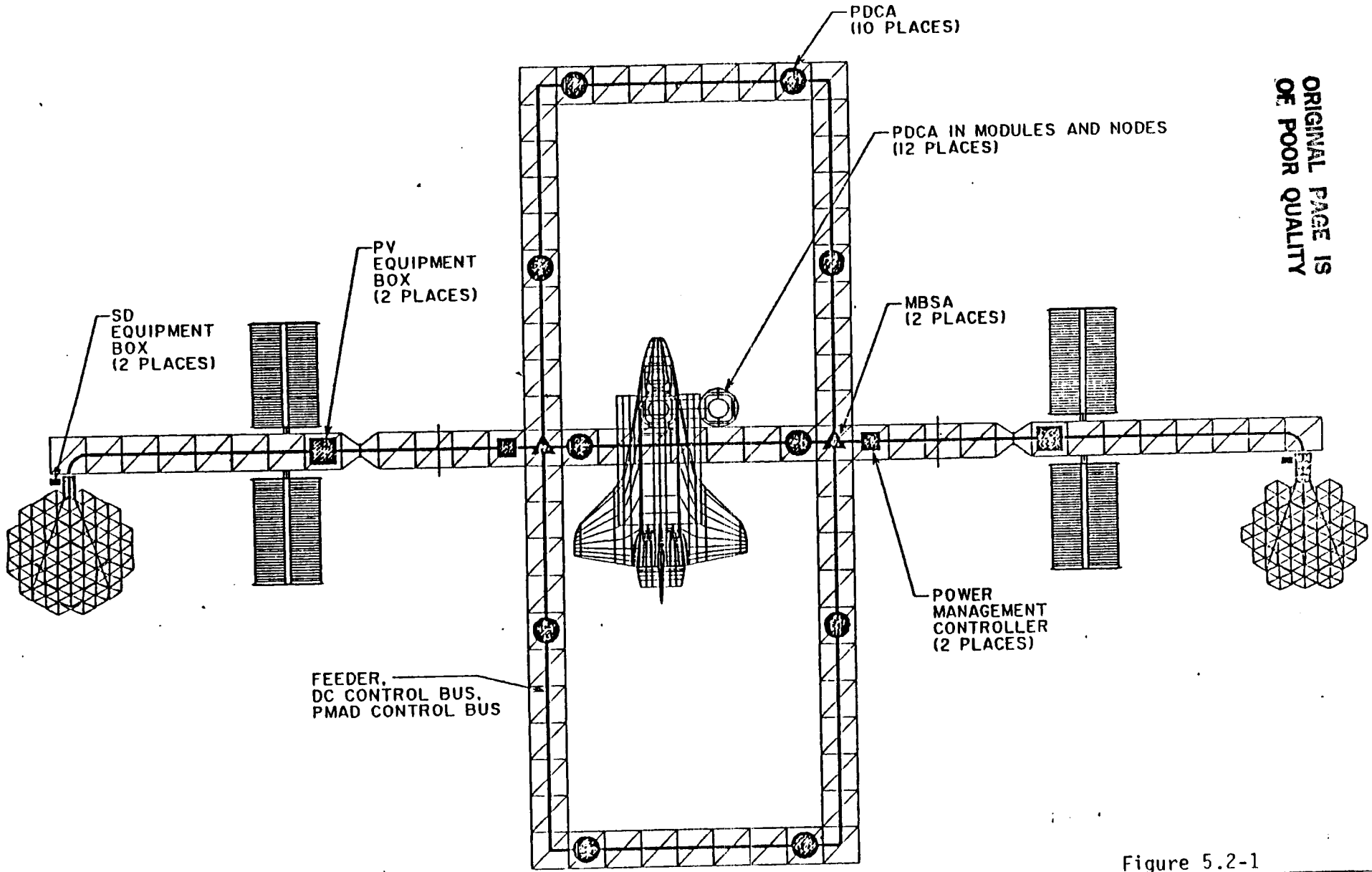

Figure 5.2-1

Rockwell International Corporation
Rocketdyne Division
Canoga Park, California

SPACE STATION EPS COMPONENT LOCATIONS

SIZE C | FSCM NO. 02602 | DWG NO. 7R070021

SCALE NONE | DO NOT SCALE PRINT | SHEET

PDCAs. Table 5.2-3 lists the number of PDCAs serving a feeder segment or pressurized module. This table also includes the number of customer connections (RPC interfaces) and maximum power capacity.

The power management and distribution system of the platform is nearly identical to that of the station. Because of the platforms' smaller size, only two PDCAs (one housekeeping and one payload) are used. Electrically and mechanically, the platform's user interfaces maintain a high degree of commonality with that of the station. Payloads are attached to PMAD system the same way as on the station.

Total power for both co-orbit and polar orbit platforms are shown in Table 5.2-2.

FEEDER/MODULE	NUMBER OF PDCA	NUMBER OF CUSTOMERS CONNECTIONS	MAXIMUM CAPACITY (KW)
UPPER RING	5	180	25
LOWER RING	5	180	25
HAB MODULE	5	180	50
LAB MODULE	5	180	50
JEM MODULE	0	4	50
ESA MODULE	0	4	50
PRESSURIZED PAYLOAD	0	2	50
NODES	2	72	50
TOTALS	22 (3)	802 (2)	(2)

NOTE 1 Each PDCA contains: (10) 5 AMP RPC, (8) 25 AMP RPC and (18) 75 AMP RPC.

NOTE 2 Total station power capacity is limited to 75 KW at any one time.

NOTE 3 See Figures 5.2-1 for PDCA locations.

UTILITY POWER CONNECTIONS

TABLE 5.2-3

A review of the Space Station Mission Data Base and NASA Data Book indicates that customer loads will fall into ten general categories of voltage and power levels. Work package 04 will design, qualify, and produce a family of ten load converters which will satisfy most customer needs. For commonality and ease of integration, all space station customers can use this family of load converters thus lowering payload development costs. Table 5.3-1 lists the ten load converts along with some design data.

LOAD CONVERTER DATA BASE

LOAD CONVERTER	VOLTAGE	FREQ (Hz)	PHASE	POWER (watts)	REG (%)	MASS (lbs)	LENGTH (in)	WIDTH (in)	HEIGTH (in)	THERMAL (watts)	EFF (%)	LOAD DESCRIPTION
LOAD CONVERTER #1	120	400	3	200	5	12	10	4	4	20	90	LIGHTS, SMALL MOTORS
LOAD CONVERTER #2	208	400	3	500	5	25	10	5	5	45	91	PUMPS, MOTORS
LOAD CONVERTER #3	TBD	VAR	1	1000	10	40	15	6	6	80	92	INDUCTION HEATING DEVICES
LOAD CONVERTER #4	TBD	VAR	1	500	10	25	10	6	6	45	91	HEATING DEVICES
LOAD CONVERTER #5	5	DC	-	200	2	5	5	3	3	40	80	ELECTRICAL PROCESSORS AND CONTROLS
LOAD CONVERTER #6	+/-15	DC	-	1000	2	40	15	5	5	150	85	ELECTRICAL/INSTRUMENTATION DEVICES
LOAD CONVERTER #7	50	DC	-	500	5	20	10	5	5	85	83	CONTROLS, DEVICES
LOAD CONVERTER #8	28	DC	-	1000	10	40	15	5	5	150	85	CRITICAL DEVICES
LOAD CONVERTER #9	150	DC	-	200	2	10	6	3	3	30	85	BATTERY PROCESSES
LOAD CONVERTER #10	400	DC	-	500	5	5	10	5	5	70	86	TRANSMITTERS

LOAD CONVERTERS

TABLE 5.3-1

5.4 INTERFACE REQUIREMENTS

Some Work Package 04 customer interfaces have been identified. These interfaces are EPS power characteristics and customer load characteristics. Exact details of the EPS/customer interface will be covered in an Interface Control Document (ICD). A preliminary list of parameters covered in this ICD are shown in Table 5.4.1. As the design matures, values, specifications and part numbers will be added to the control document.

TABLE 5.4-1

PRELIMINARY WP-04/CUSTOMER INTERFACE REQUIREMENTS

EPS POWER CHARACTERISTICS:	Voltage Frequency Phase Polarity Power quality EMI/EMC
CUSTOMER LOAD CHARACTERISTICS:	Power Power Factor Impedance EMI/EMC Grounding Priority Classification (crew critical, station critical, payload critical, deferrable and non-essential) Load Location
MECHANICAL:	Power Connector Pin Functions Wire Gauge Size

6.0 OPERATIONS PLANNING

6.1 OVERVIEW

Rocketdyne supported the iterative process of revising the JSC operations & logistics plans, i.e., JSC 30201 Flight Operations Plan, JSC 30202 Prelaunch/Post Landing Operations Plan, JSC 30203 On-Orbit Maintenance Plan, and JSC 30207 Integrated Logistics Support. This support was given directly to the following listed working groups through a series of meetings held at the NASA centers:

Assembly Sequence Working Group

Integrated Logistics Support (ILS) Working Group

Logistics Support Analysis (LSA) Working Group

On-orbit Maintenance Working Group

Prelaunch Operations Working Group

Flight Operations Working Group

Verification Working Group

6.2 PRE-LAUNCH & POST-LANDING OPERATIONS

A Prelaunch/Post-Landing Operations Plan was developed to ensure that the EPS elements were correctly configured for delivery to orbit, and that their ability to function properly on-orbit has been verified prior to launch. Further, the plan describes the processing of elements on their return from orbit. The plan emphasizes functional verification rather than full performance testing and the use of built-in self test functions to verify operational readiness.

Launch packages and manifests for both PV and SD power modules were developed.

Table 6.2-1 and Fig. 6.2-1 present the PV manifest and launch packaging while Table 6.2-2 and Fig. 6.2-2 illustrate CBC module manifest & launch packaging with Table 6.2-3 and Fig. 6.2-3 presenting the same for an ORC module.

ORU flow from failure detection on-orbit through replacement and return to earth for processing was developed and is illustrated in Fig. 6.2-4.

PV Launch Manifest

Launch	Launch Package	Description	Qty.
1 & 2		Array Blanket Assy (Right)	2
		Array Blanket Assy (Left)	2
		PV Mast/Canister	2
		Beta Joint (Incl. Roll Ring)	2
		Beta Joint Drive Motor	4
		NiH2 Battery Assy (4 Assy/Batt)	24
		Battery/PMAD Heat Exchanger	1
		Wiring Harness	2
		PV Controller	2
		Sequential Shunt Unit	2
		DC-AC Inverter	2
		Power Control Unit	2
		Battery Charge/Discharge Converter	6
		Power Distribution & Control	1
		Battery/PMAD Radiator	8
		Alpha Joint/Roll Ring (Set)	1
		Main Bus Switching Assy	1
		Power Management Processor	1
		Power Distribution & Control Assy	2
		Node Bus Switching Assy	2
		NSTS Power Converter	1

TABLE 6.2-1

ORIGINAL PAGE IS
OF POOR QUALITY

EPS PACI .S FOR FLIGHT
PV LAUNCH PACKAGE

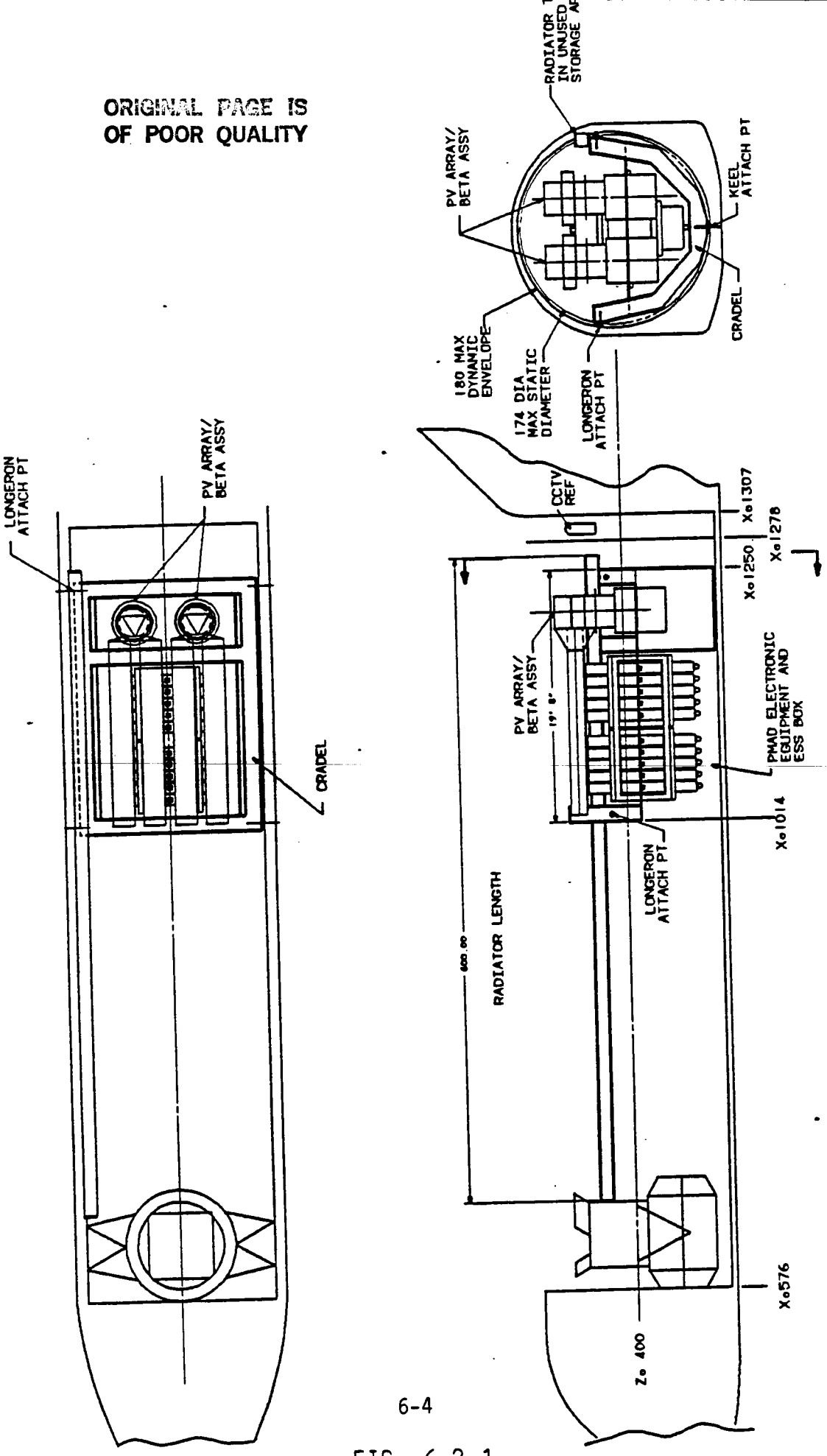

FIG. 6.2-1

SD [CBC] MODULE LAUNCH MANIFEST

Launch	Launch Package	Description	Qty.
9	1	Receiver/PCU [CBC]	2
		PCU Controller	2
		Radiator Panel Set	2
		Coolant Mgt. System	2
		Insolation Meter	4
		SD Interface Structure	2
		Parasitic Load Controller	2
		Parasitic Load Radiator	2
		Radiator Connecting Lines	4
		Wiring Harness	2
		SD Controller	2
		SD Instrumentation	2
		Frequency Converter	2
	2	Linear Actuator/Strut	4
		Fixed Strut	2
	3	Deployable Concentrator (Starboard)	1
		Concentrator Support Structure	1
		Sun Sensor Sub-assemblies	2
	4	Deployable Concentrator (Port)	1
		Concentrator Support Structure	1
		Sun Sensor Sub-assemblies	2
	5	Beta Joint (Incl. Roll Ring)	2
		Beta Joint Drive Motor	4

TABLE 6.2-2

EPS PACKAGING FOR FLIGHT
TWO 25-kW SOLAR DYNAMIC MODULES

'CBC

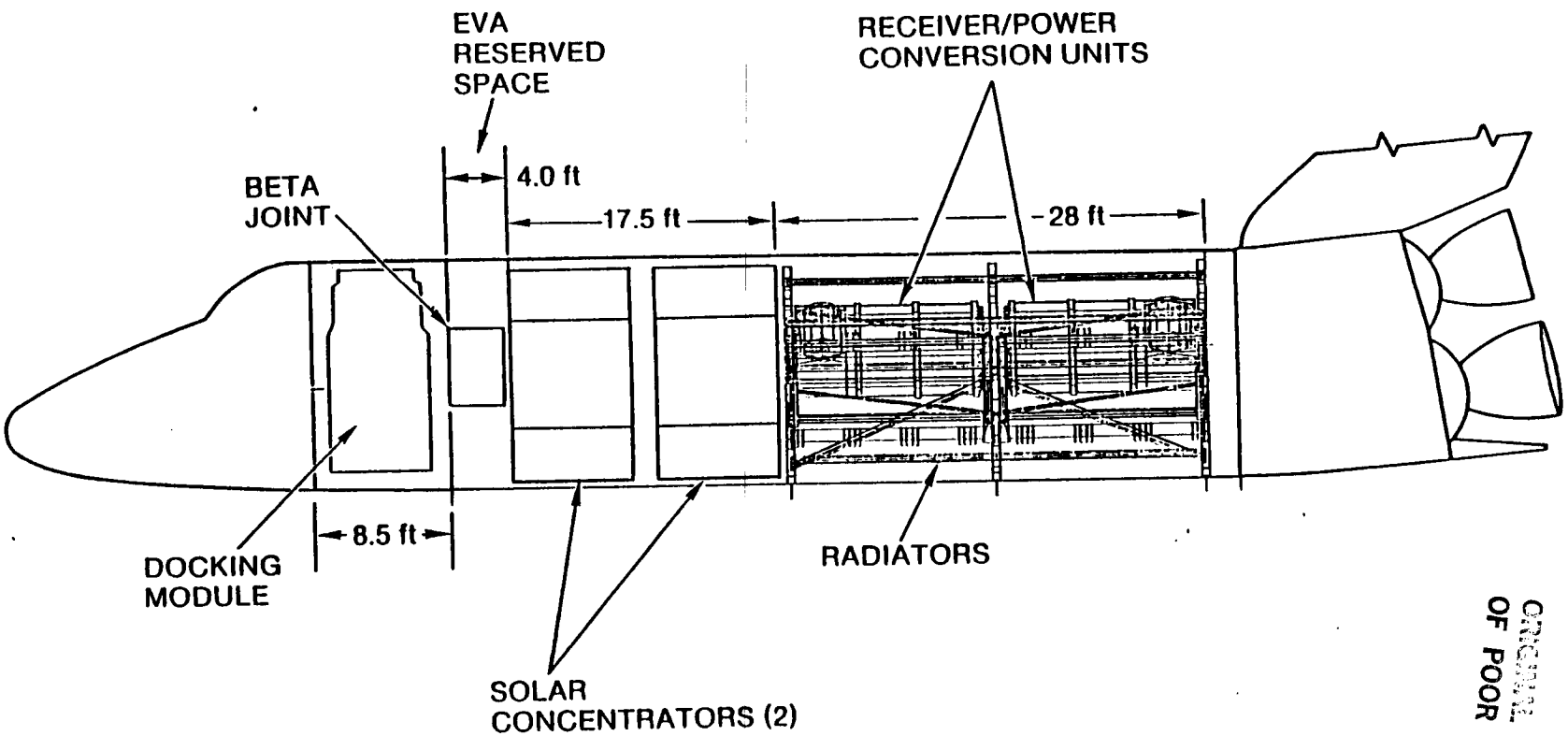

FIG. 9.2-2

9-6

86D-13-795B

Rockwell International
Rocketdyne Division

SD [ORC] Module Launch Manifest

Launch	Launch Package	Description	Qty.
9	1	Deployable Concentrator (Starboard)	1
		Concentrator Support Structure	1
		Sun Sensor Sub-assemblies	2
	2	Deployable Concentrator (Port)	1
		Concentrator Support Structure	1
		Sun Sensor Sub-assemblies	2
	3	Receiver/PCU (Starboard) (ORC)	1
		PLR	1
		PC/PUR Controller	1
		SD Controller	1
		Wiring Harness	1
		Plumbing	1
		Interface Structure	1
	4	Receiver/PCU (Port) (ORC)	1
		PLR	1
		PC/PUR Controller	1
		SD Controller	1
		Wiring Harness	1
		Plumbing	1
		Interface Structure	1
	5	Beta Joint & Roll Ring	2
		Beta Joint Drive Motor	4
	6	Linear Actuators/Struts	4
		Fixed Strut	2
		Condenser	2
		Contact Heat Exchanger	2
		Heat Pipe Panels	64

TABLE 6.2-3

EPS PACKAGE FOR FLIGHT
TWO 25KW SOLAR DYNAMICS MODULES
ORC

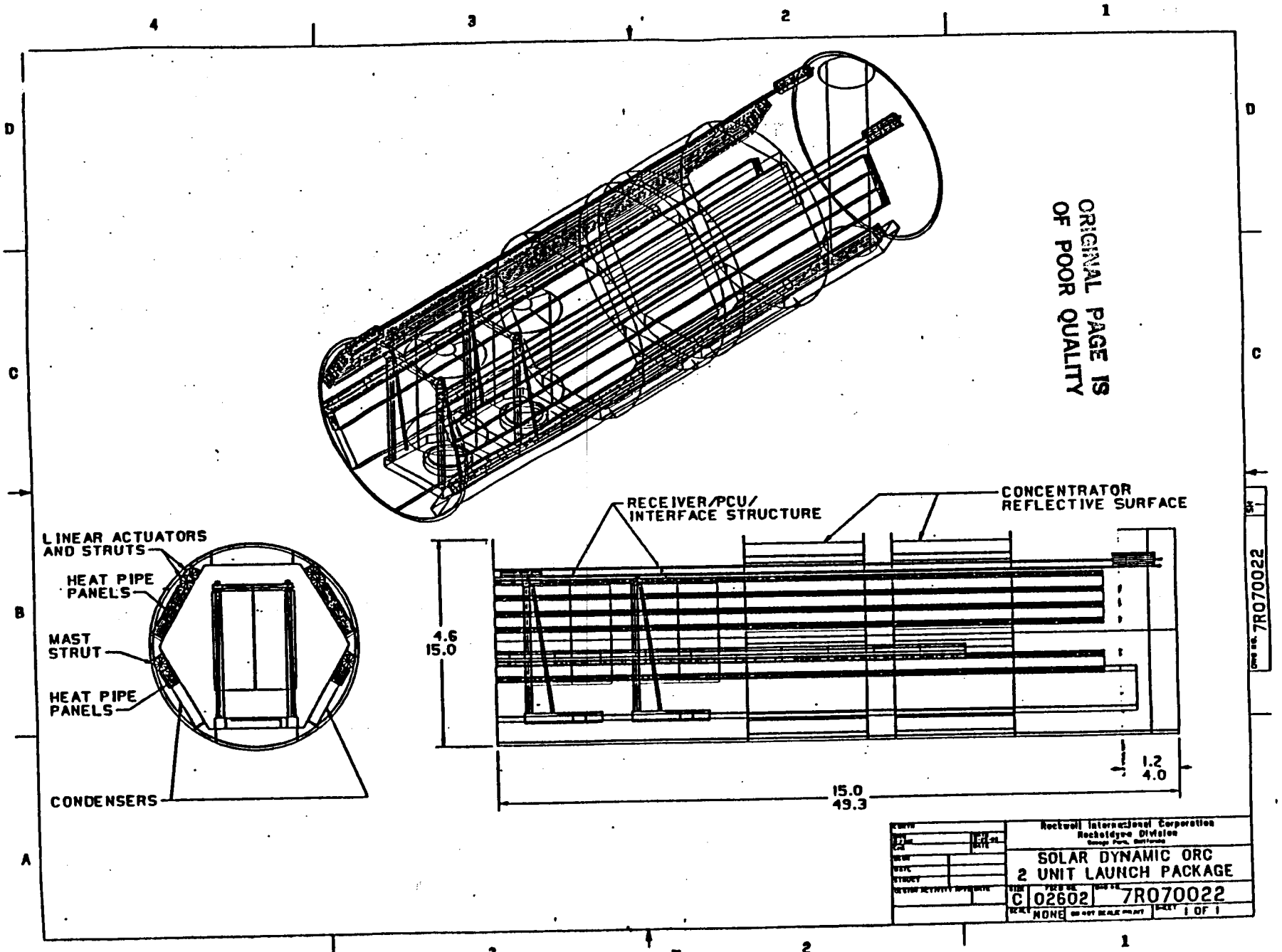

FIG. 6.2-3.

ORU FAULT ISOLATION AND REPLACEMENT

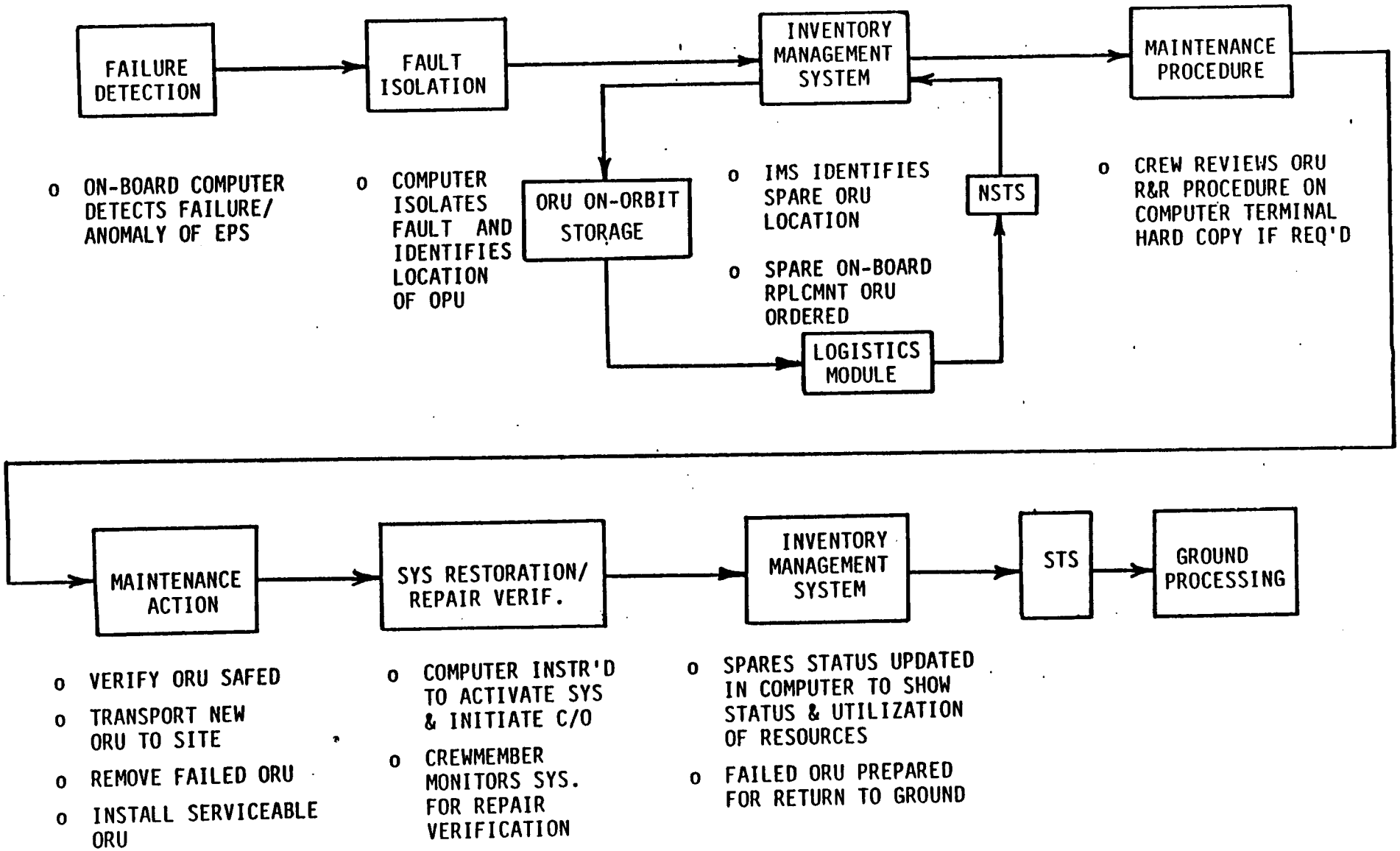

FIG. 6.2-4

6.3 ORBITAL OPERATIONS

The Flight Operations Plan was developed to define the functional elements and related procedures to support EPS operations on-orbit. It sets forth the methods and rationale for determining operational support requirements and describes the systems that will implement the Operations Plan.

Individual sections of the plan describe on-orbit operations philosophy, assembly and operations procedures (including start-up) for both station and platforms, the maintenance approach and resources, ORU replacement procedures, training, safety, and data management. The plans have been updated from time to time during Phase B to reflect the results of ongoing studies and analysis.

The Flight Operations Plan is intended to ensure that the EPS elements are delivered to orbit and assembled in the most timely and cost effective manner utilizing the minimum number of flights and minimum amount of EVA. Checkout, verification, and continuous EPS operation is to be as autonomous as possible using available technology and yet remain cost effective.

Trade studies were conducted of erectable vs. deployable elements to identify the most practical yet cost effective method of assembly.

Assembly sequence studies were conducted to determine the most effective launch packaging and sequencing. It is currently anticipated that the PV power modules will be launched on flights 1 and 2, while the two SD modules, either CBC or ORC, will both be launched on space station assembly flight 9.

EPS autonomous operation frees the crew for other station work. The crew is advised of problem areas or potential problem areas on an exception basis although the crew can interrogate the EPS status at any time.

Studies of NSTS have determined that its use will consist of its being the platform from which station construction begins, use of its RMS for assembly operations, being the electrical power source and control for PV module deployment and activation, and use as a habitation module during man tended phase.

The Flight Operations Plan defined the assembly functions, methods, and EVA/IVA timelines.

The EPS start-up, operation, and shutdown procedures for PV and SD modules were developed and included in the operations plan.

6.4 LOGISTICS & RESUPPLY

A preliminary Integrated Logistics Support (ILS) Plan has been developed to provide a cost-effective program for determining EPS support requirements and to define the means to acquire resources and implement the program to support Space Station schedules and goals.

An Operations Analysis and Logistics Support Analysis will provide a single, coordinated source for identification of support resources. Feedback from these analyses to EPS design will ensure that the EPS is supportable.

Techniques for monitoring schedules and technical performance are defined in the plan as are procedures for controlling & monitoring technical documentation, subcontracting, field operations, quality assurance, and system safety.

Candidate Spares were identified for both PV and SD (ORC & CBC) together with recommended quantities and storage location, i.e., on-orbit or on-ground. Table 6.4-1 lists these candidate spares. Figure 6.4-1 illustrates the Deliverable Spares Acquisition System developed to provide timely availability of EPS spares.

CANDIDATE SPARES

PMAD

ORU	INITIAL SPARES
SEQUENTIAL SHUNT UNIT	2
PV CONTROL UNIT	2
BATTERY CHARGE/DISCHARGE UNIT	2
DC SWITCH UNIT	1
DC-AC INVERTER (2 ICU/ORU)	2
FREQ CONVERTER L(6 ICU/ORU)	2
PV CONTROLLER	2
AC SWITCH UNIT	1
POWER SOURCE CONTROLLER	2
SD CONTROLLER	2
MAIN BUS SWITCHING UNIT	1
PDCUE (TRUSS)	4
PDCUI (MODULE)	3
POWER MANAGEMENT CONTROLLER	2
TRANSFORMER	1
NODE BUS SWITCHING UNIT	1
STS POWER CONVERTER	1
FEEDER/CONNECTOR/CABLING	0
PMAD CONTROL BUS	0
DC CONTROL POWER BUS	0
STATION LOAD CONVERTERS	1
PLATFORM LOAD CONVERTERS	1

TABLE 6.4-1 (Sheet 1 of 4)

CANDIDATE SPARES
SD MODULE (CBC)

ORU	INITIAL SPARES
REFLECTIVE SURFACE SUBASSY	1
SD LINEAR ACTUATOR	1
SD STRUCTURE	
INTERFACE STRUCTURE	0
STRUT SET	0
2-AXIS CONC GIMBAL SUBASSY	1
SUN SENSOR SUBASSY	4
INSOLATION METER SUBASSY	4
UTILITY PLATE	0
RECEIVER/PCU	
RECEIVER/PCU	1
VALVE ACTUATOR	1
PARASITIC LOAD RADIATOR	1
ENGINE CONTROLLER	4
RADIATOR	
RADIATOR/DEPLOY MECH	1
FLUID MGMT UNIT	1
HOT INTERCONNECT LINES	1
COLD INTERCONNECT LINES	1

TABLE 6.4-1 (Sheet 2 of 4)

CANDIDATE SPARES

SD MODULE (ORC)

ORU	INITIAL SPARES
REFLECTIVE SURFACE SUBASSY	1
SD LINEAR ACTUATOR	2
SD STRUCTURE	
INTERFACE STRUCTURE	0
STRUT SET	0
2-AXIS CONC GIMBAL SUBASSY	2
SUN SENSOR SUBASSY	4
INSOLATION METER SUBASSY	4
UTILITY PLATE	0
RECEIVER/PCU	
RECEIVER	1
PCU	1
PARASITIC LOAD RADIATOR	1
ENGINE CONTROLLER	4
RADIATOR	
CONDENSER/IF STRUCTURE SUBASSY	0
PRESSURIZATION UNIT	1
GN2 CANISTER	8
RADIATOR PANEL	2

TABLE 6.4-1 (Sheet 3 of 4)

CANDIDATE SPARES
PV MODULE

ORU	INITIAL SPARES
PV ARRAY WING (STATION)	
PV ARRAY BLKT & BOX (R)	1
PV ARRAY BLKT & BOX (L)	1
DEPLOYABLE MAST & CANISTER	1
PV ARRAY WING (PLATFORM)	
PV ARRAY BLKT & BOX (R)	1
PV ARRAY BLKT & BOX (L)	1
DEPLOYABLE MAST & CANISTER	1
BATTERY ASSY	2
PV THERMAL CONTROL	
CONDENSER/IF SUBASSY	1
RADIATOR PANEL	2
UTILITY PANEL	0
ITC PUMP UNIT	1
PRESSURIZATION UNIT	1
GN2 CANNISTER	4
EQUIPMENT BOX	0
STATION BETA JOINT	
TRANSITION STRUCTURE	0
ROLL RING ASSY	1
BETA JOINT SUBASSY	1
DRIVE MOTOR ASSY	1

TABLE 6.4-1 (Sheet 4 of 4)

SPARES SELECTION AND ACQUISITION PROCESS

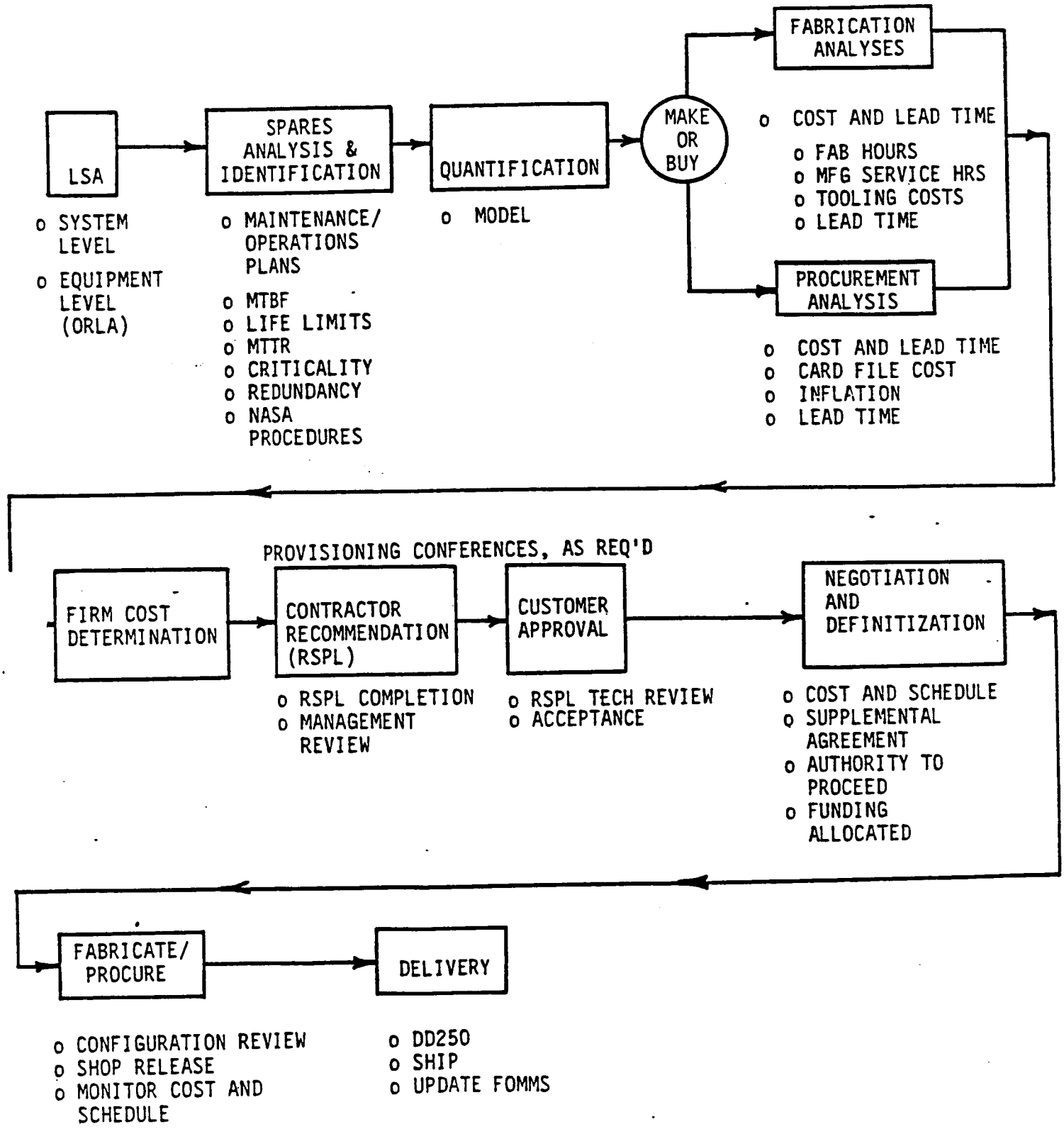

FIG. 6.4-1

Preliminary plans have been developed by NASA for the major elements of ILS identified in the appendices to the Level B ILS Plan, JSC 30207. These plans were reviewed and are identified below:

1) LSA Plan
2) Technical Data & Documentation Plan
3) Personnel Training Plan
4) Maintenance Plans
5) Supply Support Plan
6) Packaging, Handling, & Transportation Plan
7) Support Equipment Plan
8) Logistics Information System Plan
9) On-orbit Logistics Support Plan
10) Field Site Support Plan
11) Facilities Plan
12) Logistics Management Responsibility Transfer Plan

6.5 ON-ORBIT MAINTENANCE

Phase B studies resulted in an on-orbit maintenance philosophy of ORU replacement together with limited on-orbit repair of selected ORU's and replenishment of consummables. There is no scheduled servicing, checkout, adjustment, repair, or inspection of EPS elements after initial on-orbit verification is complete. Visual inspections of solar array panels, radiator elements, and EPS structural elements will be performed during the course of EVA activities but will not be scheduled. There are no hard-time replacements of EPS ORUs.

ORU's have been identified and timelines for EVA/IVA activity involved with their replacement have been defined. The ORUs are listed in Table 6.5-1. Criticality levels have also been defined for each of the ORU's in accordance with the Preliminary Hazards Analysis, DR-11.

An EPS element health monitoring system will be utilized as the basis for performing corrective maintenance on-orbit. No preventive maintenance is required on the EPS.

The Flight Operations Maintenance Management System (FOMMS) is the system used to coordinate and control all information and data concerning on-orbit maintenance.

EVA is a limited resource, consequently it must be used judiciously and its use has been minimized in EPS maintenance planning.

Spare parts support is managed as an element of the Supply Support Plan of the ILS.

Tools & equipment to be used for maintenance operations have been identified as those in the standard SSP Tool Kit, JSC 20466.

ORUs IDENTIFIED

PMAD

ORU	# OF FLIGHT UNITS	MTBR (YR)	MTTR (HR) IVA	MTTR (HR) EVA
SEQUENTIAL SHUNT UNIT	8	10	0.2	-
PV CONTROL UNIT	8	10	0.2	-
BATTERY CHARGE/DISCHARGE UNIT	20	10	0.2	-
DC SWITCH UNIT	8	10	0.2	-
DC-AC INVERTER (2 ICU/ORU)	10	10	0.2	-
FREQ CONVERTER L (6 ICU/ORU)	2	10	0.2	-
PV CONTROLLER	8	5	0.2	-
AC SWITCH UNIT	8	10	0.2	-
POWER SOURCE CONTROLLER	4	5	0.2	-
SD CONTROLLER	4	5	0.2	-
MAIN BUS SWITCHING UNIT	4	10	0.2	-
PDCUE (TRUSS)	32	10	0.2	-
PDCUI (MODULE)	24	10	0.2	-
POWER MANAGEMENT CONTROLLER	6	5	0.2	-
TRANSFORMER	10	15	0.2	-
NODE BUS SWITCHING UNIT	8	10	0.2	-
STS POWER CONVERTER	6	10	0.2	-
FEEDER/CONNECTOR/CABLING	54	80	0.2	-
PMAD CONTROL BUS	72	80	0.2	-
DC CONTROL POWER BUS	72	80	0.2	-
STATION LOAD CONVERTERS	1	10	0.2	-
PLATFORM LOAD CONVERTERS	1	10	0.2	-

TABLE 6.5-1 (Sheet 1 of 4)

ORUs IDENTIFIED
SD MODULE (CBC)

ORU	# OF FLIGHT UNITS	MTBR (YR)	MTTR (HR) IVA	MTTR (HR) EVA
REFLECTIVE SURFACE SUBASSY	2	25	2.0	2.5
SD LINEAR ACTUATOR	4	10	-	1.0
SD STRUCTURE				
INTERFACE STRUCTURE	2	80	-	-
STRUT SET	2	80	-	-
2-AXIS CONC GIMBAL SUBASSY	2	80	-	0.5
SUN SENSOR SUBASSY	2	25	-	0.2
INSOLATION METER SUBASSY	2	25	-	0.2
UTILITY PLATE	2	80	-	-
RECEIVER/PCU				
RECEIVER/PCU	2	20	4.0	4.0
VALVE ACTUATOR	2	25	-	0.2
PARASITIC LOAD RADIATOR	2	10	-	1.0
ENGINE CONTROLLER	2	10	-	0.3
RADIATOR				
RADIATOR/DEPLOY MECH	2	20	1.0	1.0
FLUID MGMT UNIT	4	15	-	1.5
HOT INTERCONNECT LINES	4	30	-	0.4
COLD INTERCONNECT LINES	4	30	-	0.4

TABLE 6.5-1 (Sheet 2 of 4)

ORUs IDENTIFIED
SD MODULE (ORC)

ORU	# OF FLIGHT UNITS	MTBR (YR)	MTTR (HR) IVA	MTTR (HR) EVA
REFLECTIVE SURFACE SUBASSY	2	25	2.0	2.5
SD LINEAR ACTUATOR	4	10	-	1.0
SD STRUCTURE				
INTERFACE STRUCTURE	2	80	-	-
STRUT SET	2	80	-	-
2-AXIS CONC GIMBAL SUBASSY	2	80	-	0.5
SUN SENSOR SUBASSY	2	25	-	0.2
INSOLATION METER SUBASSY	2	25	-	0.2
UTILITY PLATE	2	80	-	-
RECEIVER/PCU				
RECEIVER	2	30	2.5	2.5
PCU	2	20	3.0	3.0
PARASITIC LOAD RADIATOR	2	10	-	1.0
ENGINE CONTROLLER	2	10	-	0.3
RADIATOR				
CONDENSOR/IF STRUCTURE SUBASSY	2	30	-	-
PRESSURIZATION UNIT	68	20	-	0.5
GN2 CANISTER	68	20	0.2	-
RADIATOR PANEL	68	30	0.3	-

TABLE 6.5-1 (Sheet 3 of 4)

ORUs IDENTIFIED

- PV MODULE

ORU	# OF FLIGHT UNITS	MTBR (YR)	MTTR (HR) IVA	MTTR (HR) EVA
1. PV MODULE				
PV ARRAY WING (STATION)				
PV ARRAY BLKT & BOX (R)	4	15	-	1.5
PV ARRAY BLKT & BOX (L)	4	15	-	1.5
DEPLOYABLE MAST & CANISTER	4	15	-	4.0
PV ARRAY WING (PLATFORM)				
PV ARRAY BLKT & BOX (R)	4	15	-	1.5
PV ARRAY BLKT & BOX (L)	4	15	-	1.5
DEPLOYABLE MAST & CANISTER	4	15	-	4.0
BATTERY ASSY	80	5	0.3	-
PV THERMAL CONTROL				
CONDENSER/IF SUBASSY	2	30	4.0	1.0
RADIATOR PANEL	16	30	0.3	-
UTILITY PANEL	16	80		
ITC PUMP UNIT	4	30	-	0.5
PRESSURIZATION UNIT	16	20	-	0.5
GN2 CANISTER	16	20	0.2	-
EQUIPMENT BOX	2	30	-	-
STATION BETA JOINT				
TRANSITION STRUCTURE	6	80	-	-
ROLL RING ASSY	6	10	-	0.3
BETA JOINT SUBASSY	6	15	2.0	2.0
DRIVE MOTOR ASSY	12	10	-	0.2

TABLE 6.5-1 (Sheet 4 of 4)

7.0 PRODUCT ASSURANCE

7.1 PRODUCT ASSURANCE OVERVIEW

Product Assurance activities during Phase B focused upon the reliability and safety requirements of J840001, Product Assurance Requirements for the Space Station culminating in the publication of the Preliminary Safety Analysis (DR-11) and the Failure Modes and Effects Analysis (DR-12). Full implementation of all of the Product Assurance requirements therein was limited, however, due to the preliminary nature of the Phase B effort.
described below:

a) The preliminary Space Station maintainability approach and maintainability guidelines issued by NASA were utilized in selecting ORU candidates, in formulating logistics plans, prompting the preparation of in-house maintainability guidelines, and fostering an attitude of designing for ease of maintenance;

b) The acquisition and management of EEE parts was examined. In the later stages of the Contract, the concept of each Work Package manager procuring all of the EEE parts and providing them to the individual hardware fabricators was proposed by NASA as a potentially significant cost-saving technique. Preliminary discussions with the major subcontractors indicated that the concept could be made to work;

c) Formal Quality Control activities were restricted since the hardware and software were experimental and investigative, thus not supporting a rigorous QC program. However, J8400001 was reviewed by the Quality Control organization and comments were provided in DR-02. It is expected that no major difficulties will be encountered during Phase C/D.

d) The development of software product assurance plans was limited to the pursuit of defining NASA's specific requirements and objectives. It is anticipated that software product assurance will require a major effort during subsequent EPS design and fabrication activities.

7.2 PRODUCT ASSURANCE REQUIREMENTS REVIEW

The original product assurance requirements for the Space Station were delineated in J8400001, Product Assurance Requirements for the Space Station. A formal review of the document was performed and the comments presented in data item DR-02 which was submitted in accordance with Contract requirements in November 1985. No significant problems were identified; however, some clarifications and restatements of specific requirements were suggested in the

interest of eliminating future misunderstandings. A new product assurance requirements document (Section 9 of JSC 30000, Space Station Program Definition and Requirements Document) was issued which incorporated some of Rocketdyne's comments and, presumably, comments from other Work Package Contractors and NASA reviewers.

Beginning in March 1986, a series of Space Station-wide coordination meetings and reviews of Section 9 were conducted to develop a document which would provide the optimum product assurance requirements for the Space Station. Section 9 was baselined in October 1986.

The product assurance requirements invoked for the Space Station Program are typical of product assurance requirements with which Rocketdyne has frequently complied. Although specifically tailored for the Space Station, the underlying objectives, proceedings and reporting requirements do not represent a substantive change from other Rocketdyne-supported, NASA-directed programs.

7.3 SAFETY ANALYSIS

During the concept selection process, the potential hazards of each concept were evaluated in representative groupings: environment (meteorites, solar radiation, etc.), chemical (compatibility, corrosion, etc.), human factors (maneuverability, EVA suit penetrations, etc.) mechanical (pressures, leaks, ruptures, etc.), control operations (sequencing, cabling, instructions, etc.) and electrical anomalies (sparks, EMI, over/under voltage, etc.). Table 7.3-1 is representative of four hazard matrixes prepared for and submitted in data item DR-19 (DP 4.3) in September 1985 which addressed the opportunity for occurrence of each of these hazards during the four main actvivation and operation phases of the SS: Launch, Deployment, Operation, and Maintenance.

A sequel to these matrixes, presenting the relative severity of the anticipated hazards, was presented in DR-19, DP 4.4, in November 1985. Explosion/rupture and missile generation were concluded to be the worst potential hazards. However, competent design techniques (e.g., material selection and structural analyses) should eliminate explosion/rupture as a real concern. To guard against shrapnel, the use of barricades will be investigated during the early stages of Phase C/D.

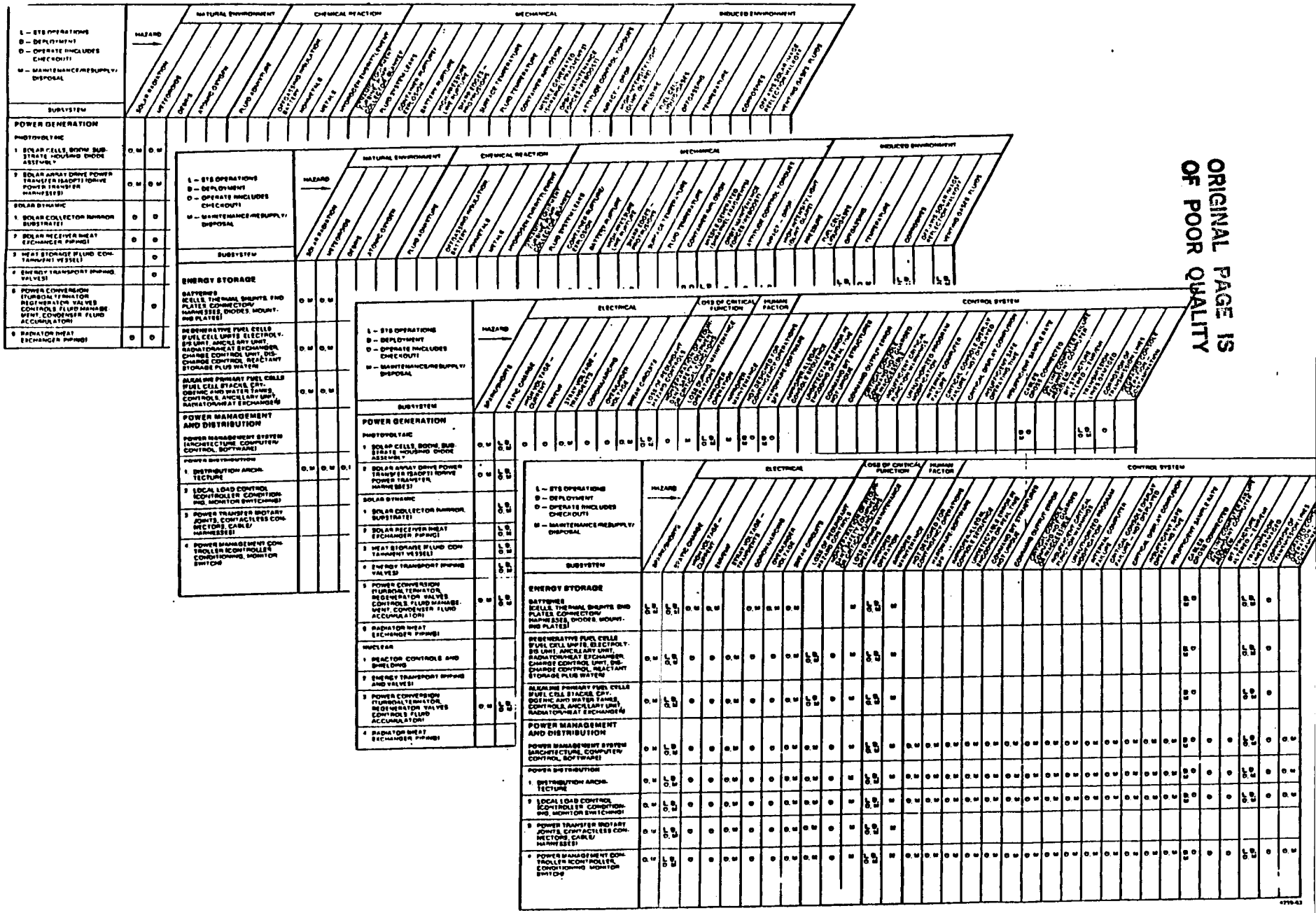

ORIGINAL PAGE IS
OF POOR QUALITY

Table 7.3-1

EPS Preliminary Hazard List

A preliminary evaluation of potential and actual EPS safety hazards was conducted on the selected concept and the results submitted in July 1986 as DR-11. The analysis centered on inherent materal properties, material compatibilities, routine operation, maintenance actions, secondary failures, and handling operations. It was concluded that, as the EPS design evolves and operational maturity progresses, all of the anticipated hazards will be eliminated, controlled or judged to be acceptable risks. All identified hazards were listed as being "open" (i.e., unresolved) pending formal documentation/demonstration that all changes or controls have been implemented or that formal acceptance of the risk has been obtained.

The hazards were classified into the following categories:

LEVEL	CATEGORY	DESCRIPTION
I	Catastrophic	Death or major system destruction
II	Critical	Severe injury, severe occupational illness, or major porperty damage
III	Minor	All other negligible hazards

The quantity of hazards, by severity levels,are:

Category	PV	SD-ORC	SD-CBC	BATTERY	PMAD	TOTAL
I	1	1	1	2	3	8
II	2	7	6	1	4	20
III	0	4	5	2	0	11

The Category I hazards are the result of :

a) unsafe test procedure, inadvertant equipment operation
b) sustained presence of non-controlled, focused heat flux
c) high voltage electric shock
d) fire inside personnel habitat
e) equipment explosion (batteries - 2)
f) structural failure due to fatigue or material defect
g) concentrator off-pointing.

For each hazard, the primary causes have been identified and the controls implemented/recommended are listed in the body of the Hazard Analysis.

The industrial health and safety concerns of the SS program have been addressed to the extent that hardware utilization during Phase B warranted intervention. The PMAD test laboratory installed at Rocketdyne has been certified in accordance with the requirements of the Rockwell International, Rocketdyne Division Health and Safety Program Plan (R-8218) which invokes and enforces Federal, State, and local laws, codes, and ordnances.

The original facility construction plans were reviewed to assure that the site provided adequate fire protection, hazardous material storage, personnel exits and protective devices, etc. Prior to facility activation, a walk-through was conducted by Engineering, Fire Prevention, System Safety and Health, Safety and Environment Personnel. The review uncovered a few minor discrepancies which were promptly resolved.

7.4 FAILURE MODES AND EFFECTS ANALYSIS

In accordance with Contract requirements, a Failure Modes and Effects Analysis (FMEA) was prepared as data item DR-12. The first submittal, in December 1985, defined the style, scope, and format to be used in performance of the analysis. The items analyzed were those ORUs which were representative of the EPS design at the time the analysis began. When significant changes occurred to the ORU list, the scope of the analysis changed accordingly. The first completed analysis was submitted to NASA in July 1986.

The primary benefit gained from performing the analysis during Phase B was the early identification of equipment failure modes to permit the incorporation of system design changes prior to embarking on Phase C/D. Direct involvement of the SD and PV major subcontractors (Ford, Garrett, etc.) in the preparation of the analysis report provided the additional benefit of early supplier awareness of the impact which their respective products have on the successful operation of the EPS.

Secondly, the need for an effective fault isolation and detection system is suggested to translate the malfunction signals generated by the EPS into warning, alarm and status indications. Identification of the specific modes of failures and their respective failure signatures provides the foundation for a health monitoring system which can alert an EPS readiness system to actual or incipient failures, provide for orderly electrical switching in the event of a malfunction and support the performance of maintenance actions.

Lastly, the FMEA provides for the identification of critical items and provides a focus on specific problems for which resolution must be achieved either through equipment redesign, special test/inspection considerations or the acceptance of waivers to program requirements.

For the FMEA, criticality categories are assigned similar to those used in the safety analysis. However, these incidents focus on functional failures relating to the power generating capabilities of the EPS rather than the safety of personnel and/or equipment. Additionally, built-in redundancy, which is not pertinent to an inherent safety hazard, provides a mitigating effect for functional failures.

Five Category 1 failure modes, all dealing with SD rotating machinery, are identified. Each represents a structural failure which would immediately remove a power generating source from operation. There are sixty-four (64) Category 2 failure modes which would result in degraded power output or eliminate a redundancy provision; and thirty-nine (39) Category 2R failures which would result in a recundancy provision being exercised. All of these occurences are individually identified as Critical Items for which resolution is required.

Figures 7.4-1 and 7.4-2 are samples of a typical analysis page and a Critical Item evaluation sheet excerpted from DR-12.

ITEM NO: CB-5	ITEM NAME: COMPRESSOR COOLER	PART NO: TBD	DATE: 7/25/86
1) PHASE 2) FUNCTION	3) FAILURE MODE 4) DETECTION METHOD 5) REACTION TIME	6) DESCRIPTION OF EFFECTS 7) EFFECT ON EPS 8) STATION EFFECT	9) POSSIBLE CAUSE 10) CRITICALITY CATEGORY 11) HAZARD ANALYSIS REF
1) OPERATION 2) TRANSFER HEAT FROM COMPRESSOR INLET TO RADIATOR LOOP	13.1) COOLER TUBE LEAKAGE FROM FATIGUE 14.1) COMPRESSOR INLET TEMP SENSOR, COMPRESSOR DISCHARGE PRESSURE SENSOR, RADIATOR LOOP PRESSURE SENSORS 15.1) PROGRESSIVE - WEEKS TO MONTHS	16.1) COOLANT ENTERS GAS LOOP 17.1) LOSS OF ALTERNATOR OUTPUT 18.1) MAY PRECIPITATE LOAD SHARING	19.1) VIBRATION INDUCED FATIGUE, THERMAL CYCLING 110.1) MINOR/CRITICAL (2) 111.1) TBD
	13.2) COOLER EXTERNAL LEAKAGE 14.2) SAME AS 4.1 15.2) HOURS TO DAYS	16.2) CYCLE GAS DEPLETION, OUTPUT POWER LOSS 17.2) ELECTRICAL POWER REDUCTION TO COMPLETE LOSS OF POWER OUTPUT. 18.2) MAY PRECIPITATE LOAD SHARING.	19.2) VIBRATION INDUCED FATIGUE, THERMAL CYCLING 110.2) CRITICAL (2) 111.2) TBD
PREPARED BY:	ORGANIZATION:	APPROVED BY: DESIGN: SAFETY:	MAINT:

Figure 7.4-1 Typical SD Element FMEA

EPS CRITICAL ITEMS LIST.
RATIONALE FOR RETENTION
(SINGLE FAILURE POINTS - CRITICALITY CATEGORY 2)

ITEM NAME: Compressor Cooler

ITEM NUMBER: CB-5 (3.2)

STATION EFFECT: May precipitate load-sharing

FAILURE DESCRIPTION

Failure Mode — External leakage of cooler heat transfer fluid

Possible Cause — (a) vibration induced fatigue
(b) thermal cycling

Effect — Reduced or complete loss of alternator power output

RATIONALE FOR RETENTION DESIGN

DESIGN

TBD

TEST/INSPECTION

TBD

FAILURE/APPLICATION HISTORY

TBD

Figure 7.4-2 Typical SD Critical Item Evaluation

8.0 DESIGN AND DEVELOPMENT PHASE PLANNING

8.1 WORK BREAKDOWN STRUCTURE

Three versions of the Work Breakdown Structure (WBS) and WBS Dictionary have been submitted to NASA-LeRC for review and approval. Each submittal provided the basis for estimating in the subsequent DR-09 submittals. Most recent is the version submitted on 28 May 1986 which was based on direction provided by NASA-LeRC for the 15 May 1986 submittal of DR09, Design, Development, and Operations Cost Document. The WBS was expanded from the Level 5 elements provided by NASA-LeRC.

8.2 PROGRAM COST ESTIMATES

The Design, Development, and Operations Cost Document (DR09) was submitted six times during the Phase B program. A chronology detailing the submittal dates and groundrules is provided in Figure 8.2-1.

8.3 MANAGEMENT COMMUNICATIONS AND DATA SYSTEM

The current Technical Management Information System (TMIS) consists of a personal computer local area network providing shared computer resources for programming, modeling, spreadsheets, financial planning, scheduling, database management, word processing, electronic mail, and access to corporate mainframe and subcontractor computing facilities. As displayed in Figure 8.3-1, shared network hardware consists of twenty IBM PC's, XT's, and AT's, high speed dot matrix and letter quality printers, 248 megabytes of disk storage, 2400 baud asynchronous modems, a pen plotter, and three tape back-up units.

Several of the TMIS capabilities have been demonstrated during the Phase B program. GTE Telemail links Rocketdyne, its subcontractors and NASA-LeRC via an electronic mail system providing communication as well as the ability to imbed native application files, such as Lotus 123 worksheets, within a message. TMIS has demonstrated the ability to convert and transfer files from IBM PC (Multimate) to Rocketdyne Wang, and from Rocketdyne Wang to NASA Wang.

DR-09 DESIGN, DEVELOPMENT, AND OPERATIONS COST DOCUMENT

CHRONOLOGY

DATE SUBMITTED	GROUNDRULES
3 JUNE 1985	STATION/PLATFORM • 75kW / 8kW • PV / PV • RFC / NiCd • FIRST LAUNCH 4-92
26 JUNE 1985	• SAME AS 3 JUNE EXCEPT LOWER EARLY FUNDING • SLIP 3 YEARS
6 DECEMBER 1985 (ADVANCE SUBMITTAL)	STATION/PLATFORM • PV / PV • FIRST LAUNCH 4-92 • NO OPERATIONAL COST
19 DECEMBER 1985	• PV, SD, HYBRID STATIONS - 75 kW • 400 Hz • FIRST LAUNCH 4-92 • 37 1/2 kW PV, 37 1/2 kW SD ON HYBRID
15 MAY 1986	• HYBRID STATION • 25 kW PV, 50 kW SD • 400 Hz • FIRST LAUNCH 1-93
15 NOVEMBER 1986 (ADDED BY MOD 14)	• CETF CONFIGURATION • HYBRID STATION • 37 1/2 kW PV, 50 kW SD • 20 kHz • FIRST LAUNCH 1-93

FIGURE 8.2-1

SPACE STATION ...NER – PHASE B
TMIS CO...IGURATION

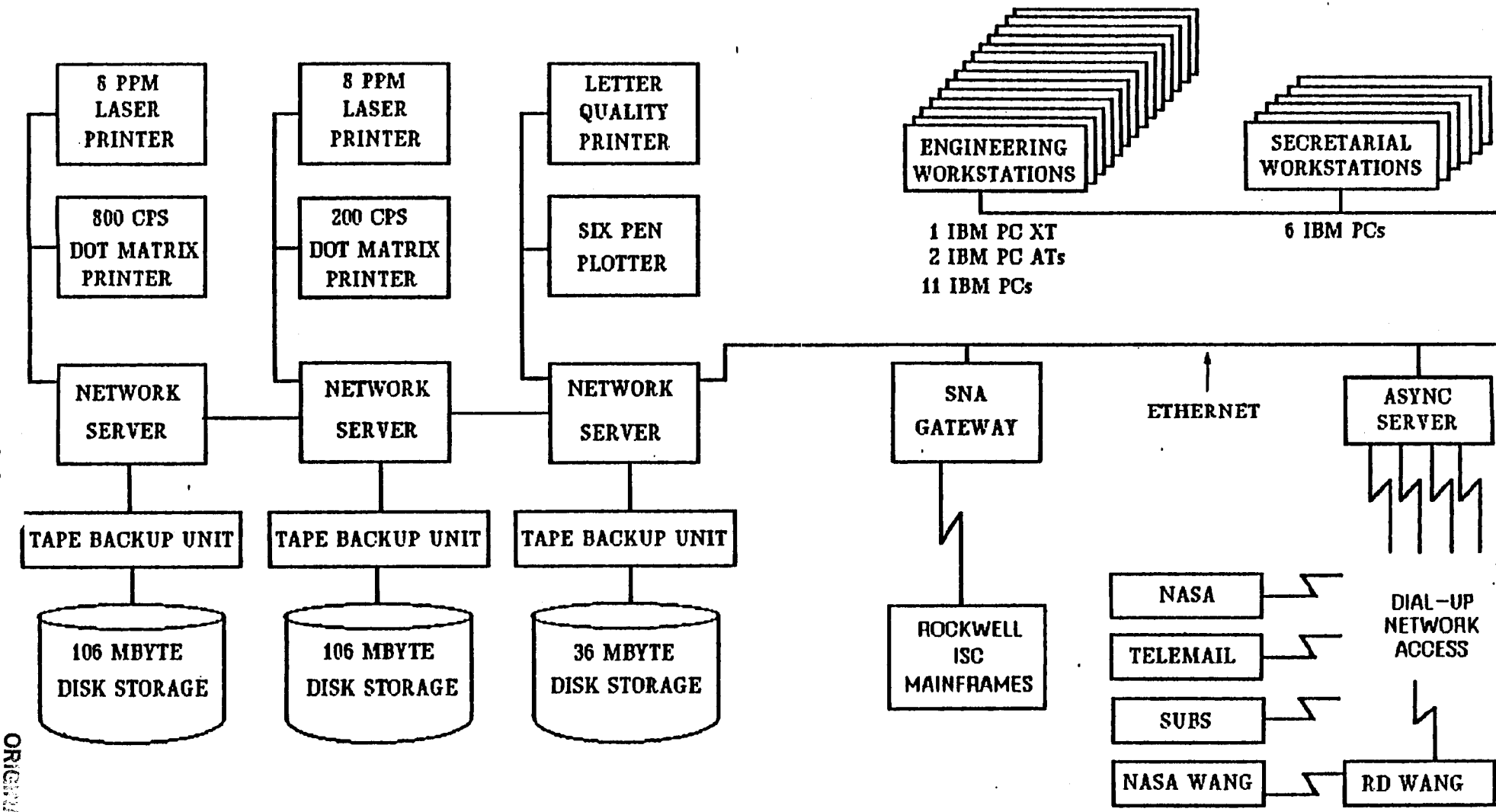

FIGURE 8.3.1

Access to Rocketdyne's corporate computing network allows TMIS the means to utilize subcontractor Fortran source files. Subcontractor data tapes are loaded and transferred from the local IBM 4381 to the corporate mainframe system. These files are downloaded to the TMIS PC's for use by the engineering staff.

Rocketdyne's current TMIS configuration and the experience gained using the system during Phase B have become the foundation from which the Phase C/D system will evolve.

8.4 PROJECT IMPLEMENTATION PLAN
PROJECT RISK ASSESSMENT

8.4.1 Introduction

The project implementation risk assessment plan of the electrical power system (EPS) WP-04 is based on the preliminary design configuration. The schedule assessment is determined for the first launch date in January 1993. A detailed risk assessment of the EPS can be found in the Project Implementation Plan DR10, 1 June 1986 and is updated for individual subsystems in DR02 December 1986.

The technical risk is the risk of obtaining poorer than expected operational performance due to problems encountered during design, development, test and verification. When technical performance becomes unacceptable and requires additional resources, the risk factor contributes to:

1) Cost Risks
2) Schedule Risks

Generally the higher the level of technical maturity the lower the risk. Table 8.4-1 defines the eight levels of technical maturity.

Various trade studies were conducted by Rocketdyne that utilized a decision criteria considering risk assessment. It consists of three elements:

1) Go/No Go Constraints - Limits that include the system's ability to meet the IOC schedule.

2) Objective Measurements - Costs: Initial, growth, operation and life cycle.

3) Supplemental (Subjective) Ratings - Technology readiness

These efforts, together with advance development/internal research and development activities formed our evaluation process and recommendations.

TABLE 8.4-1

NASA LEVELS OF TECHNOLOGICAL MATURITY

LEVEL	TECHNOLOGICAL MATURITY
1	Basic Principles Observed and reported
2	Conceptual design formulated
3	Conceptual design tested analytically or experimentally
4	Critical function breadboard demonstration
5	Component or brassboard model tested in relevant environment
6	Prototype or engineering model tested in relevant environment
7	Engineering model tested in space
8	Baselined into production design

8.4.2 Risk Assessment

A risk assessment was conducted for each of the subsystems that comprise the Electric Power System. This document will summarize the conclusions of the assessment for the photovoltaic, solar dynamic, beta joint and PMAD subsystems and the overall EPS system.

8.4.2.1 Photovoltaic Subsystem Risk Assessment

The solar array system is described fully in DR02. Table 8.4-2 shows the technology readiness of the solar array assemblies. Table 8.4-3 shows the overall technical and cost/schedule risk of the photovoltaic subsystem components.

8.4.2.2 Solar Dynamic Subsystem Risk Assessment

The solar dynamic system is described in DR02. Table 8.4-4 outlines the technical and cost/schedule risk of the various solar dynamics subsystem components.

TABLE 8.4-2

TECHNOLOGY READINESS--SOLAR ARRAY, Si

Description	Maturity Level
Solar Array Wing (Planar)	6
Blanket Assembly	6
Panel	6
Solar cell, 8- by 8-cm (3.15-by 3.15-in) silicon transparent	5[a]
Diode, Flat Pack or Integral	6[b]
Substrate Material	5[c]
Harness	6
Container/Cover Assembly	6
Stowed Blanket Tension System	6
Deployed Blanket Tension System	6
Mast Assembly	6
Boom	6
Canister	6
Drive Assembly	6
Control Electronics	6
Wing Positioner Assembly	d

a Environmental effects tested on 5.9 by 5.9-cm cells; dimensional scale-up only; expected upgrade to 6 in early 1987.
b Baselined for flight on Space Telescope and Olympus
c NASA-LeRC reported results of STS tests indicated 27-year life capability with atomic oxygen protective coating; manufacturing methods scale-up only.
d Noncritical item deferred to Phase C/D, probably deleted from design

TABLE 8.4-3
PV SUBSYSTEM RISK ASSESSMENT

Component	Technical Risk	Cost/Schedule
P.V. Component	Not expected to be a high risk area. NASA Safe experiments/history (no major problems).	Recurring activities, development non-recurring activities, production effort.
	Vast amount of testing material studies/evaluation being conducted by NASA/Boeing/Lockheed. Results in early 1987.	Total factored risks to the PV System: a) Based on cost b) Success probability c) Potential schedule input.
	Material maturity to be increased to Level 6. No PV technical risks to SSP.	Very little impact.
Energy Storing Battery growth	Development program. Not high risk. NASA maturity level 6/7.	For confidence factor based on probability of no new technical problem or human-error problem. Very little impact.
Integrated Thermal Control	Low risk due to commonality and has an alternative. (Fall back position) Maturity level 5/7.	No to very little impact.

V2-84/3

TABLE 8.4-4

SOLAR DYNAMIC SUBSYSTEM RISK ASSESSMENT

Component	Technical Risk/Maturity Level	Schedule/Cost Risk
Concentrator	Concentrator Assembly -- 4/5 Structure Subassembly -- 7 Mechanism -- 6 Control and Subassembly- 6(AV.)	All solar dynamics components have high probability of meeting current time frame for delivery of subsystem to KSC.
Organic Rankine Cycle	PCU Assembly -- 6 Receiver Assembly -- 4/5 Radiator Assembly -- 5 Risk Area / Risk Two phase fluid flow -- Moderate LIOH Tes -- Moderate Receiver Life -- Moderate	Modules schedule 10/1/92.
Closed Brayton Cycle	PCU Assembly -- 6 Receiver Assembly -- 3/4 Radiator Assembly -- 6/7 Risk Area / Risk CBC -- Moderate LiF-CAF2 TES -- Moderate Receiver Performance -- Low/Moderate Receiver Life -- Moderate	Modules schedule 10/1/92.

8.4.2.3 Beta Joint Risk Assessment

The technical risk associated with the beta joint for any given set of performance requirements is expected to be low. Each of the components is an extension of existing space technology but an interpolation of existing terrestrial technology. Table 8.4-5 shows the technology readiness of the beta joint parts.

TABLE 8.4-5

Station Beta/Platform Alpha Joint Assembly Technology Readiness

DESCRIPTION	MATURITY LEVEL
Station Beta/Platform Alpha Joint	4
Bearing Subassembly	4
Bearing	4
Inner Bearing Support	5
Outer Bearing Support	5
Subassembly Hardware	3*
Mounting Hardware	3*
Drive Mechanism Subassembly	6
Drive Motors	7
Speed Reducers	6
Pinion/Spur Gear	7
Drive Mounts	7
Transition Structure	7
Struts	7
Strut Interface Fitting	7
Controls and Instruments	5
Sun Sensor	7
Insolation Meter	7
Motor Controller	7
Roll Ring Subassembly	6
Power Module	6
Signal Module	6
Module Lock	6
Stator Connector	6
Rotor Connector	6
Position Resolver	6

* Noncritical Item Deferred to Phase C/D.

No schedule risk has been identified for this assembly. However, there are potential risks which could be imposed on this assembly due to requirements imposed externally. Examples of such externally driven requirements include: GN&C stability, structural/controls interaction limits and changes to interface locations and definitions. At this time no risks in these areas have been identified.

8.4.2.4 PMAD Risk Assessment

Technical issues associated with PMAD subsystems have been identified by Rocketdyne and its subcontractors. Rocketdyne will be verifying the design of the basic PMAD building blocks by various tests conducted at Rocketdyne, Ford, General Dynamics and NASA Lewis facilities. The tests will verify the adequacy of the design to meet critical functional requirements. Table 8.4-6 delineates the issues and risks.

TABLE 8.4-6

PMAD SUBSYSTEM RISK ASSESSMENT

ISSUES	TECHNICAL RISKS	SCHEDULE/COST RISK
Radiation Effects	Alternate solutions exist. Risks are minimal by added shielding. Redundancy built into the system.	Slight extra cost due to added precautions. Schedule remains the same.
Electromagnetic Compatibility	PMAD will meet MIL-STD-461B. Extra shielding will be provided for plasma interaction.	No significant cost or schedule risks expected.
Interface Controls	ICD's to be defined early in Phase C/D to insure interface compatibility.	No significant cost/ schedule/program risks expected.
High Frequency Cable and Termination	NASA-LeRC initiated development of low loss cable. Testing will be started to increase maturity level.	Some potential risk on cable termination design. 24 Month PMAD design/development time allocated for test cycle. Some parallel design will be pursued. Slight schedule/cost risk.
Power Components	Though low maturity level, General Dynamics development program with 20kHz test bed in place. Tests show high DC-AC efficiencies. Additional tests by R.D., G.D., & NASA continuing.	No schedule/cost risk expected.
DC Fault Isolator	Potential DC hybrid switch design being developed by Westinghouse to be tested by Rocketdyne PMAD test bed.	No schedule/cost program risk expected.

V2-84/6

PMAD Schedule/Cost

It is not expected that the hardware for the PMAD subsystem will become an IOC schedule restraint. Any PMAD technical risks are being minimized by advance development and IR&D efforts to generate engineering solutions to potential problem areas.

PMAD will use many standard parts and long lead/non-standard items will be identified early in the design. Parallel component studies will also be made. No specific cost inputs have been determined or identified at this time.

Software Risks

Software Support Environment Readiness

A major point of risk in the EPS software development effort will be the dependence that WP04 will have upon the readiness of the software support environment (SSE) provided by WP02.

Since there is a possibility that certain support software may not be available in the early stages of the program it may be necessay for Rocketdyne to initiate/develop interim SSE tools which can be utilized until the full SSE is subsequently available and can be phased in. Possible increased costs and schedule slippage will be a function of the number of personnel working, coding, debugging and testing the local, interim SSE software. Additional schedule costs will be incurred if the target processors (which are also to be provided by work package 2) are not ready for integration test 22 months into the program.

EPS Control Bus Architecture

The following table delineates the risks of the station data management system (DMS) for global power system control.

Technical Risks	Schedule/Cost Risks
Lack of EPS Security--Interference from other systems	Risks can be reduced by adding software safe-guards and code/protection resulting in increased development cost.
More DMS interface units, which requires increased hardware and power, making the EPS more vulnerable to equipment failure.	Increasing redundacy requirements to reduce equipment failure risks causes power consumption problems. Some impact on cost risks.
High DMS traffic load and crucial EPS recovery commands might be delayed. Power loss to station/ critical hardware.	Establishment of EPS command priority on the DMS network with WP04, to set these priorities will result in some cost/ schedule impact.

A dedicated bus would be a lower risk option for the station, but the disadvantages have been fully addressed in DR19 DP4.4 and DR10.

The availability of portions of the SSE required for integration testing will impact final integration of the EPS software as a part of the distributed system whether it uses the DMS or a dedicated bus system. This will influence both cost and schedule.

8.4.3 Overall System Technical Risk

The overall system technical risk arises from the fact that the EPS will not be fully assembled and tested as a complete system in an orbit environment prior to launch.

To minimize the risks the following approach is being taken:

a) Extensive use of high fidelity mock-up and simulators to checkout and test EPS component/assembly/subsystems.

b) Detailed system analytical modeling and simulation for both steady state and transient conditions.

8.4.4 Overall System Schedule Risk

Although no schedule risks have been identified at this time. Rocketdyne has several management tools to identify and control these risks. They are as follows:

a) Artemis schedule analysis -
   Perform critical path analysis.
   Evaluate interrelated milestones.

b) Performance Measurement System (PMS) -
   Identify/Control effort by each WBS
   work package for cost/schedule compliance.

c) Variance thresholds - Variance exceeding
   establish criteria brought to management's attention for
   corrective action.

d) Rocketdyne's PMS schedule to be developed to be compatible with key government established milestones.

8.4.5 Overall System Cost Risk

Major risks associated with program cost estimates.

a) Relative maturity of hardware definition.

b) Phase C/D planning.

c) Cost to depth of imposed program requirements.

Several iterations of cost estimates have been completed and reported in the DR09 submittals. Reduction in cost risk has been attained with the increased maturity of the design and cost estimation detail.

8.5 APPLICABLE DOCUMENT REVIEW

The "J" series applicable documents were reviewed and is hereby shown in Table 8.5-1 with their pertinent reference numbers, documents title and location for further discussions on abstract/comments.

The documents reviewed, focused on enhancing the cost effectiveness to the Space Station Program (SSP) and applicability to phase C/D of the electric Power System (EPS).

The listings in Table 8.5-1 encompasses those applicable documents which were reviewed and discussed in SSP WP04 Power Systems, publication DR02 and DR10. An in-depth discussion can be found in these DR's.

TABLE 8.5-1 Applicable Document Review (Page 1 of 6)

Reference	Title	Abstract/Comment
J8400001 2241MA DN084-80	Product Assurance requirements for the SSP	DR02
JB400002 NHB 1700-7A	Safety Policy and requirements for payloads using STS	DR10
J8400003 NHB B060.18	Flammability, Odor, and Offgassing Requirements Procedures for Materials in Environments that support combustion.	DR10
J8400004 JSC 08060	Space Shuttle system pyrotechnic Specification	Dr10
J8400005 JSC 07700	Space Shuttle System Payload Accommodations Handbook	DR10
J8500006 ISO/TC 108/SC4N	Guide to the Evaluation of Human Exposure to Vibration and Shock in Buildings	DR10
J8400007 ISO 2531-1978	Guides for the Evaluation of Human Exposure to Whole-Body Vibration	DR10
J8400008 RP 1026	Anthropometric Source Book, Volume I, II, III	DR10R
J8400009 MSFC STD 512A	Man/System Requirements for Weightless Environments	DR10
J8400014 DOD-D-1000B	Military Specification-Drawings, Engineering and Associated Lists	DR10
J8400015 ICD-GPS-200	Navstar GPS Space Segment/Navigation User Interfaces	DR10
J8400016 SE-R0006C	General Specification, NASA JSC Requirements for Materials and Processes	DR10
J8400020 JSC 19649	Space Station Fracture Control Plan	DR10
J8400021 JSC20001	Orbital Debris Environment for Space Station	DR10
J8400022 NASA SP-7012	The International System of Units	DR10

Reference	Title	Abstract/Comment
J8400026 STDN 101.2	Tracking and Data Relay Satellite (TDRSS) User's Guide	DR10
J8400030 FED. STD. 595	Colors	DR10
J8400031 MSC-SC-M-0003A	Functional Design Requirements for Manned Spacecraft and Related Flight Crew Equipment, Markings, Labeling and Colors	DR10
J8400032 MIL STD 14720	Human Engineering Design Criteria for Military Systems, Equipment and Facilities	DR10
J8400034 JSC 16888	Shuttle Transportation System Microbial Contamination Control Plan	
J8400036	Standard Work Breakdown Structure for Space Systems	DR10
J8400037 JSC 19517	Crew Interface Panel Space Station Habitability Requirements Document	DR10
J8400038 JSC 17543	Payload Integration Plan Space Transportation System and System Test Vehicles	DR10
J8400039 None	Space Station Program Missions Requirements	DR10
J8400040 NASA-TM-82585	Natural Environment Design Criteria for the Space Station Program Definition Phase	DR10
J8400041 MSFC-STD-5068	Standard Materials and Processes Control	DR10
J8400042 SPOR-00022A	General Spec. -- Vacuum Stability Requirements of Polymeric Material for Spacecraft Application	DR10
J8400043 MSFC-SPEC-522A	Design Criteria for Controlling Stress Corrosion Cracking	DR10
J8400044 MSFC-HDBK-505	Structural Strength Program Requirements	DR10
J8400045 JSCK-8080	Manned Spacecraft Criteria And Standards	DR10
J8400058 TM-86652	Book 7, Space Station Program Plan	DR10

Reference	Title	Abstract/Comment
J8400059 None	Space Station Advanced Development Program	DR10
J8400062 None	Space Station System Operational Requirements	DR10
J8400063 NBSIR 82-2631	Initial Graphics Exchange Specification (IGES)	Dr10
J8400064 None BCS RIM	Relational Information Management System Version 6.0 User Guide	DR10
J8400065 8-1-4-PB-01242	Orbital Maneuvering Vehicle RFP-DMV Requirements Document, Part V, Attachment A	DR10
J8400066 8-1-3-PP-01259	OTV Phase A RFP Statement of Work	DR10
J8400067 JSC-19946	Space Station Operation Plan	DR10
J8400068 PT-SSO-001	Space Station Prelaunch Operation Plan	DR10
J8400069 TBD	Space Station Program Customer Services Handbook	DR10
J8400070 MDC H1300	Space Station Mission Data Books and Customer Accommodation Plans for Early Missions (Volumes I-V)	DR10
J8400071 FT-LMO-001	Space Station System Integrated Logistics Support Plan	DR10
J8400073 PT-SSO-002	Space Station Security Requirement Plan	DR10
J8400074 None	Earth Observing System (EOS) Polar Platform Resource Module Interface Requirements	Dr10
J8400079 9BE3-6-4-27P	STS/Space Station Human Productivity Study RFP	DR10
J8400080 JSC-SC-L-0002	Functional Design Requirement for Lighting, Manned Spacecraft and Related Flight Crew Equipment	DR10

TABLE 8.5-1 (Page 4 of 6)

Reference	Title	Abstract/Comment
J8400081 NASA TM-82390	Steering Law for Parallel Mounted Double-Gimbaled Control Moment Gyros	DR10
J8400082 None	Systems Test and Verification Plan Content Guide	DR10
J8400083 TBD	Space Station Lexicon	DR10
J8400084 JSC 10615	STS EVA Description and Design Criteria	DR10
J8400085 RFP BE272437P	Statement of Work for Advanced EVA System Design Requirements Study	DR10
J8400086 NASA TM 82473	Terrestrial Environment (Climatic) Criteria Guidelines for Use In Aerospace Vehicle Development	DR10
J8400087 NASA TM 82478	Space & Planetary Environment Criteria Guidelines for Use in Space Vehicle Development	DR10
J8400088 MM8070.2	Specifications and Standards Approved Baseline List	DR10
J8400089 SE-0-0104	Req. for Flight and Flight Prototype Liquid & High Pressure Oxygen Components and Systems	DR10
J8400090 JSC-09604	Materials Selection List and Materials Documentation Procedures	DR10
J8400091 JSC-02681	Nonmetallic Materials Design Guidelines & Test Data Handbook	DR10
J8400093 MM8020.6	MSFC Cost/Schedule Performance Criteria (C/SPC) with Implementing Provisions	DR10
J8400094 MM8020.8	MSFC Technical Performance Criteria (TPC) with Implementing Provisions	DR10
J8400096 JPL D-1414	Guidelines for Space Station Data Systems Standardization	DR10
J8400097 JPL D-1737	Space Station Information System (SSIS) Final Study Report	DR10
J8400098 JSC-09535	Translation Modes and Bump Protection, Bulletin No. 1	DR10

TABLE 8.5-1 (Page 5 of 6)

Reference	Title	Abstract/Comment
J8400099 JSC-09536	Architecture Evaluation for Airlock, Bulletin No. 2	DR10
J8400100 JSC-09537	Architectural Evaluation for Sleeping Quarters, Bulletin No. 3	DR10
J8400101 JSC-09538	Design Characteristics of the Sleep Restraint, Bulletin No. 4	DR10
J8400102 JSC-09539	Inflight Maintenance as a Viable Program Element; Bulletin No. 5	DR10
J8400103 JSC-09540	Space Garments for IVA Wear, Bulletin No. 6	DR10
J8400104 JSC-09541	An Overview of IVA Personal Restraint Systems, Bulletin No. 7	DR10
J8400105 JSC-09542	Cleansing Provision within the Waste Management Compartment, Bulletin No. 8	DR10
J8400106 JSSC-09543	Foot Restraint Systems, Bulletin No. 9	DR10
J8400107 JSC09545	Personal Mobility Aid, Bulletin No. 11	DR10
J8400108 JSC-09546	Temporary Equipment Restraints, Bulletin No. 12	DR10
J8400109 JSC-09547	Tools, Tests Equipment, and Consumables Required to Support Inflight Maintenance, Bulletin No. 13	DR10
J8400110 JSC-09548	Personal Hygiene Equipment, Bulletin No. 14	Dr10
J8400111 JSC-09549	Cable Management in Zero-G, Bulletin No. 15	DR10
J8400112 JSC-09551	Neutral Body Posture in Zero-G, Bulletin No. 17	DR10
J8400113 JSC-09552	Evaluation of Skylab IVA Architecture, Bulletin No. 18	DR10
J8400114 JSC-09553	Food System, Bulletin No. 19	DR10

Reference	Title	Abstract/Comment
J8400115 JSC-09560	The Methods and Importance of Man-Machine Engineering Evaluations in Zero-G, Bulletin No. 26	DR10
J8400116 JSC-09561	Personnel and Equipment Restraint and Mobility Aids (EVA), Bulletin No. 27	DR10
J8400117 TM-86652	Book 1, Introduction and Summary, Space Station Program Description Document	DR10
J8400118 TM86652	Book 2, Mission Description Document	DR10
J8400119 TM-86652	Book 3, System Requirements and Characteristics, Space Station Program Description Document	DR10
J8400120 TM-86652	Book 4, Space Station Advanced Development Program, Space Station Program Description Document	DR10
J8400121 TM-86652	Book 6, System Operations	DR10
J8400131 MIL-STD-461B	Electromagnetic Emission and Susceptibility Requirements for the Control of Electromagnetic Interference	DR10
J8400132 408SS03020001	Satellite Servicing from the Space Station	DR10
J8400133 JSC-20054	Space Station White Papers	DR10
J8400134 NMI 2410.6	NASA Software Management Requirements For Flight Projects	DR10
J8400135	Human Capabilities in Space	DR10

8.6 INTERNATIONAL SYSTEMS OF UNITS IMPACT STUDY

As part of the Project Implementation Plan (PIP), Rocketdyne conducted a study to assess and evaluate the impact of adopting the S.I. Standard on Work Package 04 of the Space Station. The study which encompasses both literature and subcontractor survey ascertained that some subsystems can be specified in metric terms without undo input, while others would be significantly effected.

A summary of the study showed the following:

Company	System/ Component	S.I. Impact	Comments
Ford Lockheed	Photovoltaic power generation system	1-6 month schedule delay 0-5% cost increase	Example of items not presently in metric units: steel leaf spring; helical springs; hinge pins; Kapton substrate; copper interconnects; honeycomb panel gores; extension mast; gears; drive motors.
Sundstrand	Organic Rankine Cycle	15% cost increase 0-small schedule delay	Presently all parts in customary units.
Garrett	Closed Brayton Cycle	10-20% cost increase 0-moderate schedule delay	Present design in customary units.
LTV	Radiator	No Impact	
Harris	Solar Concentrator	0-small impact on cost and schedule	
Rocketdyne	Power Management and Distribution	Moderate impact on cost and schedule	Example of items not presently in metric units: material and plating standards for printed wiring board; pin fields of integrated circuit packages; card connectors; many standards.

Companys	System/ Component	S.I. Impact	Comments
IFC Life Systems	Regenerative fuel cells	10% cost and schedule increase	
Ford Yardney	Nickel Hydrogen Batteries	No Impact	

The majority of second and lower tier vendors do not currently have a metric fabrication capability so that the flexibility in selecting suppliers and consequent limitation of competition would also have a program impact which is difficult to quantify.

It is therefore recommended that the power system metrication requirement be limited to items of potential interface portions of the Space Station. This will continue to allow access to the largest number of potential U.S. suppliers and assure the most cost-effective power system program.

An in-depth discussion on the S.I. impact study can be found in DR10.

1. Report No.	2. Government Accession No.	3. Recipient's Catalog No.
NASA CR-179587		

4. Title and Subtitle	5. Report Date
Space Station WP-04 Power System Final Study Report DR-15 Volume 1 and 2	1-19-87
	6. Performing Organization Code

7. Author(s)	8. Performing Organization Report No.
G. J. Hallinan	None
	10. Work Unit No. 485-40-02

9. Performing Organization Name and Address	11. Contract or Grant No.
Rockwell International Rocketdyne Division 6633 Canoga Avenue Canoga Park, Ca. 91304	NAS3-24666
	13. Type of Report and Period Covered Contractor Report Final

12. Sponsoring Agency Name and Address	14. Sponsoring Agency Code
National Aeronautics and Space Administration Lewis Research Center Cleveland, Ohio 44135	

15. Supplementary Notes

Project Manager, Jim Faddoul
Project Control Office
NASA Lewis Research Center

16. Abstract DR-15 Abstract

This document describes the Space Station Electrical Power System preliminary design, which resulted from the 21 month phase B study contract, and supporting analyses. The study contract was performed by the Rocketdyne Division of Rockwell International and its team members: Ford; Garrett; General Dynamics; Harris; and Sundstrand. Included herein are the configuration and subsystems preliminary design of the Space Station photovoltaic, solar dynamic, and power management and distribution subsystems including the co-orbiting and polar orbit platforms. The station design is a hybrid approach which provides user power of 25 kWe from the photovoltaic subsystem and 50 kWe from the solar dynamic subsystem. The electric power is distributed to users as a "utility" service, single phase at a frequency of 20 kHz and voltage of 440VAC. The solar array of NiH_2 batteries of the photovoltaic subsystem are based on commonality to those used on the co-orbiting and polar platforms.

In addition this ducument contains an update of the System Test and Verification Plan (DR-04) and the Customer Accommodation Report. (DR-06)

17. Key Words (Suggested by Author(s))	18. Distribution Statement
Space Power Photovoltaics, Solar Dynamic Power, Heat Engines, Organic Rankine Cycle, Brayton Cycle, Power Management, Power Distribution, Solar Arrays, Nickle Hydrogen Batteries, Space Station, Solar Collectors.	Unclassified - Unlimited Star Category- B-20

19. Security Classif. (of this report)	20. Security Classif. (of this page)	21. No. of pages	22. Price*
Unclassified	Unclassified		

*For sale by the National Technical Information Service, Springfield, Virginia 22161